UNIVERSITE MONTPELLIER 2
SCIENCES ET TECHNIQUES DU LANGUEDOC

T H E S E

pour obtenir le grade de

DOCTEUR DE L'UNIVERSITE MONTPELLIER 2

Discipline : Mécanique et Génie Civil

Ecole Doctorale : Information, Structures et Systèmes

présentée et soutenue publiquement

par

Paulo Ricardo GHERARDI HEIN

Le 16 juin 2011

Titre :

GENETIC AND ENVIRONMENTAL CONTROL OF MICROFIBRIL ANGLE ON *Eucalyptus* WOOD: ITS EFFECTS ON WOOD TRAITS AND IMPLICATION FOR SELECTION

JURY

M. xxxxxxxx	Président
M. Joseph GRIL	Directeur de Thèse
M. Philippe ROZENBERG	Rapporteur
M. Jean-Michel LEBAN	Rapporteur
M. Gilles CHAIX	Examinateur
M. Loic BRANCHERIAU	Examinateur
M. José Tarcísio LIMA	Examinateur
M. Bruno CLAIR	Examinateur
M. Kambiz POURTAHMASI	Examinateur

PREFACE

This thesis is based on research done at the "Bois Tropicaux" unit of research (UR40) of the PERSYST department and at the "Amélioration génétique et adaptation des plantes" unit of research (UMR AGAP) of the BIOS department of the *Centre de Coopération Internationale en Recherche Agronomique pour le Développement* (CIRAD, France); at the "Laboratoire de Mécanique et Génie Civil" of the *Université de Montpellier 2* (UM2, France) and at the "Laboratório de Ciência e Tecnologia da Madeira" of the *Universidade Federal de Lavras* (UFLA, Brazil).

The trees used in this study were provided by the *Centre de Recherche sur la Durabilité et la Productivité des Plantations Industrielles* (CRDPI, Republic of Congo) and by *Celulose Nipo-Brasileira S.A.* (CENIBRA, Brazil).

I would like to thank many people who have assisted me to achieve this accomplishment, through encouragement and help along the way during my doctoral thesis at University of Montpellier 2. Financial support for the study was provided by CENIBRA, CIRAD and CNPq (*Conselho Nacional de Desenvolvimento Científico e Tecnológico*, Brazil). My scholarship was granted by CNPq through the process no. 200970/2008-9. Thanks also to the staff of the CIRAD teams *Bois Tropicaux* and *Amélioration génétique et adaptation des plantes* for technical, experimental and scientific support. Thanks to *Departmento de Ciências Florestais*, *Universidade Federal de Lavras*, Brazil, for experimental support. Thanks for Paulo Fernando TRUGILHO and José Reinaldo Moreira da SILVA for critical reading of my project proposal in 2008, when I submit it for evaluation at CNPq.

I wish to thank my Thesis directors Dr. Joseph GRIL and co-advisors Dr. Gilles CHAIX, Dr. Loic BRANCHERIAU and Dr. José Tarcísio LIMA for their helpful, precise guidance. Special thanks to Bruno CLAIR, Tancrede ÁLMERAS and Bernard THIBAUT for their passion, their fruitful tracks and advice. Thanks to Isabelle CHALON and Roselyne LANNES for their helpful assistance.

Thanks to the members of my advisory committee: Dr. Philippe ROZENBERG, Dr. Jean-Michel LEBAN, Dr. Jean-Marc BOUVET, Dr. Bruno CLAIR, Dr. Bernard THIBAUT, Dr. Alfredo NAPOLI, Dr. Gilles CALCHERA and Dr. Jean GÉRARD, whose insights and knowledge guided this process. Special thanks to my advisory committee chair, Dr. xxxxxxx, whose experience steered me in the right direction during this endeavour. Thanks also to Dr. José Tarcísio LIMA for helping to find wood, his valuable insights, and dedication to the scientific process and Dr. Jean Marc BOUVET and Dr. Marie DENIS for their statistic assistance.

To all of my colleagues, I am truly grateful for the support, assistance, and inspiration during my stay at Montpellier, France. I realize that so many individuals helped me, that I cannot name them all. However, special recognition is given to: Luc MARTIN and Cecílio FROIS.

To my parents who have encouraged me over the years. Agradeço aos meus pais, minhas tias e tios, minhas irmãs e irmãos pelos seus conselhos e apoio ao longo dos últimos anos.

Finally, I would like to thank my mate Aline for her patience, love and understanding.

"For scientists, wood remains a fascinating adventure. On the one hand, solutions used by nature to solve its mechanical problems are fully up to date: nano structured materials, smart structures, light and low energy materials... Understanding more and more both the 'making of wood' and the wood properties will surely be very profitable for the progress of man-made materials and structures. On the other hand, humanity will have in future to deal with the struggling problem of avoiding 'troublesome' energy solutions, for the making of materials for example. Wood is a striking demonstration of making a useful material using very simple and renewable factors: solar energy, water and carbon dioxide.

We can try to copy this system for producing 100% man-made materials. We can also try to harvest with care these marvellous gifts from nature that trees are, and use them the best we can, like generations of genius craftsmen did before us, through the making of structures, furniture, musical instruments and so on. If so, the first thing to do is to restore to wood its proper rank among other materials (data bank, material selection software, material teaching...), and admit that diversity is a treasure, not a pledge, for smart engineers".

(B THIBAUT, J GRIL and M FOURNIER, 2001)

CONTROLE GENETIQUE ET ENVIRONNEMENTAL DE L'ANGLE DES MICROFIBRILLES DANS LE BOIS D'*Eucalyptus* : EFFETS SUR LES PROPRIETES DU BOIS ET IMPLICATION POUR LA SELECTION

Le contrôle génétique et l'environnemental de l'angle des microfibrilles (MFA), les corrélations génétiques du MFA avec d'autres caractères du bois et de croissance, et par conséquent les implications pour la sélection sont très peu documentés pour les *Eucalyptus*. Les objectifs de cette étude étaient d'établir la variation spatiale du MFA, de la densité du bois (ρ) et de sa rigidité (E); de déterminer les relations entre MFA et propriétés du bois et enfin d'estimer le contrôle génétique et environnemental des caractères du bois et de la croissance dans le cadre de tests clonaux et de test de descendances d'*Eucalyptus* au Brésil et au Congo. Méthodes classiques, résonance, diffraction des rayons-X et la spectroscopie proche infrarouge ont été combinées pour évaluer les propriétés du bois. La variation du MFA représente 44% de la variation du module spécifique (E/ρ) du bois. La densité du bois est le principal déterminant de la rigidité et de la résistance du bois alors que le MFA joue un rôle secondaire. Les estimations de l'héritabilité sont de modéré à élevées pour le MFA, ρ, E, la lignine de Klason (KL) et les caractères de croissance, selon la position spatiale et le dispositif expérimental. Le contrôle génétique du MFA, ρ et E et leurs corrélations génétiques avec KL et la circonférence à 1.3 mètre des arbres varient avec l'âge. Les résultats suggèrent que les arbres à forte croissance sont génétiquement plus aptes à produire du bois de faible densité et un MFA plus faible pour assurer la rigidité du bois nécessaire à leur développement. La plupart des propriétés du bois sont génétiquement corrélées négativement avec la croissance, bien que corrélations génétiques favorables entre propriétés du bois sont observés. Les corrélations génétiques et environnementales sont parfois de signes opposés selon les caractères considérés. Ceci peut s'expliquer par l'effet pléiotropique des gènes et/ou par le déséquilibre de liaison. Les conséquences de ces résultats sur les stratégies de sélection sont discutées selon l'usage final du bois d'*Eucalyptus*.

GENETIC AND ENVIRONMENTAL CONTROL OF MICROFIBRIL ANGLE ON *Eucalyptus* WOOD: ITS EFFECTS ON WOOD TRAITS AND IMPLICATION FOR SELECTION

The genetic and environmental control of microfibril angle (MFA), the genetic correlations with other wood and growth traits, and therefore the implications for selection are poorly documented for *Eucalyptus*. Thus, the objectives of this study were to determine the spatial variation of the MFA, wood density (ρ) and stiffness (E); to determine the relationship between MFA and wood traits and finally to estimate the genetic and environmental control of wood and growth traits from clonal and progeny tests of *Eucalyptus* in Brazil and Congo. Conventional methods, resonance, X-ray diffraction and spectroscopy were combined to evaluate the wood properties. MFA variation accounted for 44 percent of the variation in specific modulus (E/ρ) of wood. The ρ was the prime determinant on wood stiffness and strength while the MFA played a secondary role. The heritability estimates were moderate to high for the MFA, ρ, E, Klason lignin (KL) and growth traits according to the spatial position and the experimental design. Genetic control of the MFA, ρ and E and their genetic correlations with KL and circumference of 1.3 meters of trees varied with age. The results suggest that tree with potential to grow fast are genetically more likely to produce low ρ and also to decrease the MFA for ensuring stiffness required for their development. Most wood properties were genetically negatively correlated with growth, although favorable genetic correlations between many wood traits were observed. Genetic and environmental correlations were sometimes of opposite signs according to the considered trait. This can be explained by the pleiotropic effect of genes and / or linkage disequilibrium. The implications of these findings for selection strategies are discussed according to the final use of *Eucalyptus* wood.

DISCIPLINE
Mechanical and Civil Engineering

MOTS-CLES
Wood, quality, stiffness, microfibril angle, breeding, quantitative genetic, genetic control, genotype by environment interaction, Clonal propagation, progeny trails

CIRAD - Production and Processing of Tropical Woods TA B-40/16 - 34398 - Montpellier
CNRS - Laboratoire de Mecanique et Genie Civil - 34090 - Montpellier

CONTENTS

PREFACE 3
CONTENTS 9
EXPANDED SUMMARY 11
RÉSUMÉ ÉTENDU 15
Matériel végétal 16
Stratégie de la recherche 16
Phénotypage des propriétés du bois 16
Les modèles SPIR 17
Approches en génétique quantitative 18
Résultats principaux 19
Considérations finales 20
LIST OF NOTATIONS 21
LIST OF WOOD TRAITS 21
LIST OF PAPERS 23
1 INTRODUCTION 25
1.1 BACKGROUND 25
1.2 *Eucalyptus* as a timber source 26
1.2.1 Problems of *Eucalyptus* wood 27
1.2.2 What is wood quality? 29
1.2.3 Selecting traits for wood improvement 30
1.2.4 MFA controls wood quality 31
1.3 *Eucalyptus* breeding programs 36
1.3.1 Quantitative genetic of wood 38
1.3.2 *Eucalyptus* breeding programs 39
1.3.3 Challenges 42
1.3.4 Strategies for wood phenotyping 43
1.4 Scientific strategy 48
1.4.1 Lacks of knowledge 48
1.4.2 Hypothesis of this study 51
1.4.3 Purposes of this study 51
1.4.4 Strategy of this study 53
2 MATERIAL AND METHODS 57
2.1 Origin of the material 57
2.1.1 Progeny test 57
2.1.2 Clonat test 57
2.2 Sampling preparation 59
2.2.1 Progeny test 59
2.2.2 Clonal test 60
2.3 Methods for phenotyping 62
2.3.1 Sonic resonance 62
2.3.2 Static bending test 64
2.3.3 Basic density and shrinkage of wood 65
2.3.4 X-ray diffraction 66
2.3.5 Wet-lab chemistry 67
2.3.6 NIR spectroscopy 67
2.3.7 Resume of wood traits measurements 68
2.4 STATISTICAL ANALYSIS 69
2.4.1 Descriptive statistics and correlations 69
2.4.2 Developing NIR spectroscopy models 69

2.4.3 Genetic parameter estimation ... 71
3 RESULTS AND DISCUSSION ... 75
3.1 Growth traits ... 75
3.2 Wood phenotyping of progeny tests ... 76
3.2.1 Wood chemical composition ... 76
3.2.2 Microfibril angle and wood density ... 77
3.2.3 Effect of wood chemical components on MFA ... 79
3.3 Phenotyping the wood of clonal tests ... 79
3.3.1 Kiln-dried scantlings ... 79
3.3.2 Wood specimens from scantlings ... 81
3.3.3 Small wood samples ... 83
3.3.4 Correlations among wood traits of *Eucalyptus* from clonal test ... 87
3.4 Near infrared spectroscopic models ... 91
3.4.1 NIR spectra ... 91
3.4.2 Reference data ... 92
3.4.3 NIRS-based calibrations and validations ... 93
3.5 Genetic studies from progeny test ... 99
3.5.1 Heritability of growth and wood traits ... 99
3.5.2 Genetic and residual correlations ... 101
3.5.3 Age trends of additive genetic, residual and phenotypic correlations ... 103
3.5.4 Implications for selection ... 105
3.6 Genetic studies from clonal test ... 106
3.6.1 Growth traits ... 106
3.6.2 Genetic studies from the kiln-dried scantlings ... 108
3.6.3 Genetic studies from NIR-predicted data of wood discs ... 109
3.6.4 NIR spectral heritability estimates ... 123
4 CONCLUDING REMARKS ... 127
4.1 Spatial variation of wood traits ... 127
4.2 Influence of MFA on wood traits ... 128
4.3 Combining techniques for assessing wood traits ... 129
4.3.1 Resonance ... 129
4.3.2 NIR spectroscopy calibrations ... 129
4.4 Genetic and environmental control of wood traits ... 131
4.4.1 Genetic studies from the progeny tests ... 131
4.4.2 Genetic studies from the clonal tests ... 132
5 PERSPECTIVES ... 135
6 ANNEXES ... 137
6.1 Phenotyping the air-dried scantlings of clonal tests ... 137
6.2 Correlations between wood traits of air- and kiln-dried scantlings ... 138
6.3 Environmental and radial position effect on MFA and its correlation with wood traits ... 140
6.4 Comparing 3- and 4-points bending tests ... 141
6.5 Genetic approaches from resonance on air-dried scantlings ... 142
6.6 Spatial variation of heritability estimates ... 144
7 REFERENCES ... 147
LIST OF TABLES ... 161
LIST OF FIGURES ... 165

EXPANDED SUMMARY

The first studies on genetics of *Eucalyptus* were carried out in order to determine the suitability of species and provenances for particular environments and to estimate genotype by environment interactions in a range of trials. Afterwards, the studies on genetics of *Eucalyptus* started to concentrate on tree growth, survival, stem straightness and branch quality because the forest industry was focused mainly on achieving gains in growth and form. Thus, the continuity of forestry research on *Eucalyptus* over the past several years has allowed some companies to reached productivity notably higher than those of the first generations. As a result, plantations are producing merchantable trees at faster growth rate with trees harvested at a younger age.

However, the progress in wood production leads to two main concerns. Increasing the growth rate can favour the occurrence of growth stress while shortening the rotation causes an increase in the proportion of juvenile wood within the stem. Growth stress is a major cause of degrade and processing problems (warping and splitting of logs and boards). Juvenile wood has lower density, thinner cell walls, shorter fibres and higher microfibril angles when compared to mature wood. Lower densities and reduced fibre dimensions, higher MFA and low stiffness of juvenile *Eucalyptus* wood are expected to produce a poorer quality product. As a result, these defects affecting wood quality and product yield are the main obstacles for greater market acceptance of fast grown *Eucalyptus* wood as a higher value sawn timber product. Trees develop growth stresses as they grow and this phenomenon manifests itself when the tree is felled, cut into logs and converted into boards. Growth stress is a problem difficult to solve in *Eucalyptus* plantations since it is a natural mechanism of tree for surviving. On the other hand, any reduction of juvenile wood or genetic improvement in the quality of juvenile wood could have broad economic implications for the forest industry. For these reasons, wood traits have begun to receive more attention in *Eucalyptus* breeding programs.

So much knowledge about the wood has been gathered over the past decades and numerous studies are making valuable contributions in wood science and technology. Thus, many traits are known to be important in determining the value of *Eucalyptus* wood as sawn timber including its basic density, wood stiffness and strength, juvenile wood proportion and the microfibril angle (MFA), the preferable angle of the cellulose microfibril within its cell walls. Previous studies investigating the relationship between microfibril angle, basic density (ρ) and wood stiffness showed that MFA was the prime determinant of both the modulus of elasticity (E) and the specific modulus (E/ρ) in *Eucalyptus* wood. These wood traits seem to be important in improving overall products quality in *Eucalyptus* wood. Thus, breeding programs for *Eucalyptus* should include them as selection criteria. While the heritability estimates for wood density have been exhaustively reported for many Eucalypt species, the genetic control over microfibril angle was neglected in breeding strategies for improving wood quality. In short, the genetic and environmental control of microfibril angle (MFA), its genetic correlations with other wood and growth traits and implications for selection are still not well established in *Eucalyptus*.

Thus, the aims of this study were: i) to establish the spatial variation of ρ, E and MFA within the trees; ii) to determine the influence of MFA on wood traits and iii) to determine genetic control over circumference at breast height (C), tree height (H) of MFA, ρ, E, Klason lignin (KL) content, syringyl to guaiacyl (S/G) ratio and growth traits, their variation from pith to cambium and their genetic correlations.

This thesis makes an effort to understanding how genetic and environmental factors control the wood properties variation and how *Eucalyptus* trees adapt their wood traits in order to continuously grow up and at the same time maintains upright even when they are constrained by bending movements in response to wind and gravity. To attend its purposes, this study falls into two parts. The first consisted on phenotyping wood traits and the second on the quantifying the genetic parameters of wood traits.

The parts of the study are valued in the form of publication, but in this thesis the main results were combined along the text in order to make a logical and coherent manuscript.

Wood traits, heritability and correlations were assessed in a progeny test represented by 340 control-pollinated progenies of 14-year-*Eucalyptus urophylla* S.T. Blake and in a clonal test represented by 150 6-year-*Eucalyptus urophylla* x *grandis* hybrids growing at contrasting sites.

In order to provide experimental data to perform such analyses, indirect methods and techniques such as sonic resonance, X-ray diffraction and near infrared (NIR) spectroscopy were combined for assessing MFA and wood stiffness in a large sampling of *Eucalyptus* wood. Traditional methods and indirect methods such as sonic resonance, X-ray diffraction were used in order to provide an experimental data set. Hence, near infrared spectroscopic models were developed based on experimental data for estimating such wood traits from NIR spectra recorded at various radial and longitudinal positions.

The relationships among wood traits investigated in 6-year-*Eucalyptus* wood from clonal test have shown that MFA variation accounted for only 44 percent of the variation in specific modulus in *Eucalyptus* wood. The basic density wood was the prime determinant of both modulus of elasticity and modulus of rupture while the MFA played a secondary role on stiffness and strength of wood from fast growing plantations.

High heritability were found for MFA (h^2=0.65), ρ (h^2=0.61), LK (h^2=0.72) and S/G (h^2=0.71) for 14-years-*Eucalyptus* from the progeny test. The genetic control of ρ and MFA and the genetic and residual correlation between chemical and growth traits varied with age. The genetic correlation C x ρ was always strongly negative (r<-0.88) while the correlation ρ x MFA remained constant and positive in the juvenile wood (r=0.7), decreasing considerably in the mature wood (r=0.3). This could mean that trees with a strong potential to grow fast are genetically programmed to produce low-density woods and also to decrease the microfibril angles for ensuring stiffness (the negative correlation MFA x C). Variations in MFA and KL in the mature wood are also genetically controlled. The low microfibril angle compensating low wood density and fast growth and the changes in KL content can be functionally explained by gene pleiotropic effect or statistically by linkage disequilibrium induced by sampling. From a biological point of view, the correlation MFA x density is strategic for tree survival, maintaining them ever-growing and in upright position even under winds that induces constantly bending movements. In conclusion, the genetic correlations MFA x ρ and MFA x KL acting together reveal a smart biological strategy for the survival of the tree. The underlying principles of the interaction of stiff cellulose fibrils embedded in a pliant matrix would be utilized to adjust mechanical properties. From a technological point of view, these findings allow discussing the impact on breeding strategies for pulpwood, fuelwood and timber wood production. As forestry industries are mainly searching for adequate density woods, such unfavourable correlations between growth and wood traits are of critical importance.

Low to moderate levels of broad-sense heritability (H^2) estimates were found for basic density, wood stiffness and microfibril angle of 6-year-*Eucalyptus* clones. The findings clearly revealed that heritability estimates for E and MFA exhibited opposite patterns of radial variation in the bottom of the tree, and

similar trends towards the top. For density, higher H^2 estimates were found in the higher regions of the tree, especially at the intermediate zone.

Genetic parameters were calculated directly from NIR spectra recorded on the wood. Variations in specific ranges of NIR spectra are related to variation in lignin and cellulose and hemicelluloses contents, and other wood traits. The findings clearly revealed that the variations on these specific ranges of the NIR spectra were controlled by genetic factors. The assignments of absorption bands were useful to identify which wood components presents higher broad-sense heritability estimates from NIR spectroscopic data. Some ranges of the spectra presented H^2 estimates greater than 50%. Considering NIR spectra is countless source of information concerning many wood traits, the analysis of genetic parameters from them appears to be an efficient and promising way to evaluate the genetic control over various wood traits at once.

Most wood properties were unfavourably genetically correlated with growth, although favourable genetic correlations were observed between many *Eucalyptus* wood traits. Because of these unfavourable genetic correlations between wood and growth, selection for increasing density and stiffness or reducing MFA in the absence of selection for growth will result in a reduction (genetic loss) in volume production. Therefore, breeders, forest managers and wood producers will have to strike a balance between overall wood and growth traits, and geneticists should develop breeding strategies to deal with such negative, unfavourable genetic correlations in *Eucalyptus* plantations.

Keywords: Wood, quality, stiffness, microfibril angle, breeding, quantitative genetic, genetic control, genotype by environment interaction, clonal propagation, progeny trails

RÉSUMÉ ÉTENDU

Les premières études sur la génétique des *Eucalyptus* ont porté sur la détermination de l'aptitude en comportement et en croissance des espèces et des provenances pour des environnements particuliers, ainsi que sur l'estimation des interactions génotype environnement dans une série d'essais. Elles se sont ensuite concentré sur la croissance des arbres, la survie, la forme des tiges et la branchaison, car les objectifs de l'industrie forestière sont basés essentiellement sur les gains en termes de volume de bois produit et de forme des arbres. Ainsi la recherche forestière sur les *Eucalyptus* au cours des dernières années, par la production de variétés améliorées, a apporté aux industriels des gains importants par rapport aux variétés des premières générations. Il en a résulté des plantations produisant plus et plus vite et permettant des récoltes à des âges plus précoces.

Toutefois, les progrès réalisés dans la production de bois conduit à deux préoccupations principales. L'augmentation de la vitesse de croissance peut favoriser l'apparition de contraintes de croissance, tandis qu'en réduisant la durée de rotation la proportion de bois juvénile dans la tige est plus élevée. Les contraintes de croissance sont une cause majeure de dévalorisation des produits et de problèmes rencontrés lors de la première transformation (déformations et fentes en bout au moment de l'abattage quand les contraintes sont libérées). Les caractéristiques du bois juvénile par rapport au bois mature sont les suivantes : faible densité, parois cellulaires plus minces, fibres plus courtes et angles de microfibrilles plus élevés. La densité plus faible, la réduction de la longueur des fibres et une rigidité moindre du bois d'*Eucalyptus* entrainent une réduction de la qualité technique et marchande. En conséquence, ces défauts affectant la qualité du bois et le rendement du produit sont les principaux obstacles à une plus grande acceptation par le marché du bois d'*Eucalyptus* à croissance rapide en bois de sciage. Les contraintes de croissance sont un problème difficile à résoudre dans les plantations d'*Eucalyptus*, car ce sont les conséquences d'un mécanisme naturel de l'arbre pour croître et s'adapter à l'environnement. D'un autre côté, la réduction de bois juvénile ou l'amélioration génétique de la qualité du bois juvénile pourrait avoir d'importantes répercutions économiques pour l'industrie forestière. Pour ces raisons, les programmes de sélection des *Eucalyptus* se mobilisent de plus en plus sur la qualité des bois.

De nombreuses connaissances sur le bois ont été recueillies au cours des dernières décennies et de nombreuses études en science des bois apportent une contribution précieuse. Ainsi, plusieurs propriétés des bois sont connues pour jouer un rôle important dans la détermination de la valeur du bois d'*Eucalyptus* : densité basale (ρ), module d'élasticité (E), proportion de bois juvénile et angle des microfibrilles (MFA) de cellulose cristalline dans les parois cellulaires. Des études antérieures sur la relation entre MFA, ρ et E ont montré que le MFA serait le principal facteur déterminant à la fois du module d'élasticité et du module spécifique (E/ρ) du bois d'*Eucalyptus*. Ces propriétés deviennent donc importantes pour l'amélioration de la qualité globale des bois d'*Eucalyptus*, et les programmes de sélection pour les *Eucalyptus* cherchent à les inclure dans les critères de sélection. Le contrôle génétique de la densité du bois est largement rapporté pour de nombreuses espèces d'*Eucalyptus*, par contre pour le MFA ce n'est pas le cas. En bref, le contrôle génétique et environnemental du MFA, ses corrélations génétiques avec les autres propriétés du bois, les caractères de croissance et les implications pour la sélection n'ont pas été encore abordées pour *Eucalyptus*.

Ainsi, les objectifs de cette étude sont les suivants: i) décrire la variabilité intra-arbre de la densité (ρ), le module (E) et l'angle des microfibrilles (MFA); ii) déterminer l'influence du MFA sur les propriétés du bois et iii) déterminer le contrôle génétique de la circonférence à hauteur de poitrine (C), la hauteur des

arbres (H), le MFA, ρ, E, la lignine de Klason (LK), le ratio syringyl sur guaiacyl (S/G) et les caractères de croissance, leur variation de la moelle au cambium et leurs corrélations génétiques.

Cette thèse s'efforce de comprendre comment les facteurs génétiques et environnementaux contrôlent la variabilité des propriétés du bois et comment les arbres d'*Eucalyptus* adaptent ces propriétés afin de croître, s'adapter à l'environnement propre aux plantations forestières intensives et résister aux contraintes telles que vent, terrain en pente, etc.

Chaque partie de l'étude est valorisée sous la forme de publications, mais le choix a été fait de rédiger ce manuscrit reprenant dans leur totalité les travaux effectués, afin de rendre compte des résultats de façon logique et cohérente.

Matériel végétal

Wood traits, les corrélations et l'héritabilité ont été évaluées a partir d'un test de descendances représenté par 340 descendants issus de pollinisation contrôlée d'*Eucalyptus urophylla* ST Blake de 14 ans (Table 4, p. 57) et a partir de trois tests clonaux échantillonnés par 150 *Eucalyptus grandis* x *urophylla* hybrides de 6 ans sur des sites contrastés (Table 5, p. 58).

Stratégie de la recherche

Pour répondre aux objectifs, cette étude se divise en deux parties. La première concerne le phénotypage des propriétés du bois et la seconde l'estimation des paramètres génétiques de ces propriétés avec la croissance. La stratégie de cette étude est décrite comme suit. Un résumé de tous les travaux menés est donné, y compris les procédures de préparation des échantillons et mesures des caractères du bois, ainsi que les principales analyses. La description détaillée de chaque élément est fournie dans Matériel et Méthodes, Résultats et discussion des différents articles.

Phénotypage des propriétés du bois

Une étude détaillée sur les propriétés du bois pour différents types d'échantillons a été réalisée en utilisant le bois de d'un essai de descendances et de tests clonaux. La Figure 12 (p. 80) résume les caractéristiques de croissance et du bois étudié dans les deux modèles expérimentaux.

Afin de fournir des données expérimentales pour effectuer les analyses génétiques, des méthodes directes et indirectes comme la résonance acoustique, la diffraction des rayons X et la spectroscopie proche infrarouge (SPIR) ont été combinées pour évaluer le MFA et la rigidité du bois pour un nombre important d'échantillon de bois d'*Eucalyptus*. Les modèles en SPIR ont été développés à partir des données de références et ont été utilisés pour estimer la qualité du bois à partir de spectres mesurés selon les positions radiales et longitudinales.

Dispositif 1 : Test de descendances du Congo

Les propriétés des bois des arbres issus d'un plan de croisement ont été étudiées à partir des disques de bois récolté à 1,3 mètre. Tout d'abord, les disques ont été coupés en deux quartiers opposés ; 2 bandes radiales exemptes de nœuds et défauts en ont été extraites. Les spectres ont été enregistrés sur la face radiale des quartiers à trois positions radiales (1, 2 et 3) de la moelle à l'écorce. Ensuite, à partir des bandes radiales différents échantillons on été débités selon le type de mesure, tandis que les spectres PIR ont été obtenus sur tous les échantillons (solides et poudre). Ces spectres PIR ont été utilisés pour les prédictions

(Figure 14, p. 59). Les bandes radiales ont été divisées en petits échantillons (20 x 20 x 30 mm) pour les mesures de densité du bois et en sections tangentielles (2 x 20 x 30 mm) pour les mesures du MFA. Les spectres PIR ont été mesurés sur les faces transversales, radiales et tangentielles, des petits échantillons et sur les deux côtés des sections tangentielles. Par la suite, trois valeurs *T* ont été enregistrées par diffraction des rayons X en trois points sur 175 sections tangentielles et la densité du bois a été mesurée sur les petits échantillons. L'article **3** présente la variation radiale du MFA et de la densité du bois, la corrélation entre eux et l'influence de l'âge de formation du bois sur ces relations dans le bois *Eucalyptus urophylla* de 14 ans.

Dispositif 2 : Tests clonaux du Brésil

150 arbres ont été récoltés à partir de 3 tests clonaux. Un billon de 2,4 mètres et 5 disques de bois ont été débités à 0, 25, 50, 75 et 100% de la hauteur commerciale pour chaque arbre. Des bandes diamétrales ont été découpées à partir des disques. Les bandes ont été poncées et les spectres PIR ont été mesurés. Ces spectres PIR ont été utilisés pour les prédictions. Les billes ont été sciées en planches centrales, et un total de 410 carrelets (45 x 60 x 2100 mm) dénommés «scantlings» ont été extraits des planches (Figure 15, p. 60). Les carrelets ont été séchés à l'air libre pendant 90 jours. Une première série de carrelets ne présentant pas de défaut a été sélectionnée avec des dimensions variables (en moyenne, 1,54 mètres de longueur, variant de 0,645 m à 2.080 m et d'épaisseur moyenne comprise entre 60 et 43 mm). Les échantillons ont été soumis à des tests de vibrations transversales et longitudinales (BING). Par la suite, les carrelets ont été séchés dans des conditions douces au séchoir à 14% d'humidité (nominale) pendant deux semaines. De nouveaux tests de vibrations transversales et longitudinales ont été effectués sur les carrelets. Enfin, des petits échantillons sans défauts (25 x 25 x 41 mm) appelés « specimens » ont été découpés à partir des carrelets et soumis à des tests de vibrations transversales et longitudinales. La masse et les dimensions de chaque spécimen ont été mesurées et la densité de poids de chaque pièce de bois a été calculée. Les propriétés dynamiques de ces bois sont discutées dans **l'article 1**, tandis que les approches génétiques obtenues à partir de ces résultats sont rapportés dans **l'article 9**.

Ensuite, ces échantillons de bois ont été testés en utilisant une machine d'essai universelle. Les essais statiques en flexion 3 et 4 points ont été effectués afin de déterminer le module de rupture (MOR). De chaque carrelet, un ou plusieurs échantillons jumeaux ont été débités : quand au moins deux spécimens jumeaux étaient obtenus, le premier était testé en flexion 4 points et le second en flexion 3 points. Cette procédure a permis de comparer les deux types d'essais de flexion sur des échantillons appariés. Ces résultats sont présentés dans la section des annexes (item 6.4, p. 141).

Par la suite, un échantillon de bois mesurant 25 mm × 25 mm × 25 mm a été découpé de ces specimens afin de mesurer la densité basale et le retrait au séchage. Les retraits ont été mesurés à partir de deux mesures, à l'humidité d'équilibre (EMC) et un état au dessus du point de saturation des fibres. Enfin, une section de 2 mm radiale a été découpée à partir de chaque petit échantillon pour les mesures de l'angle des microfibrilles. Ces différentes étapes de mesure nous ont fourni une gamme complète d'informations sur les propriétés physiques, mécaniques et anatomiques de ces échantillons de bois. **L'article 2** évalue les relations entre angle des microfibrilles, densité, rigidité et résistance, module de cisaillement et retrait pour les clones d'*Eucalyptus*.

Les modèles SPIR

Cette partie de l'étude est consacrée à l'élaboration de modèles SPIR afin d'évaluer une gamme de propriétés du bois. L'objectif était également d'examiner et d'expliquer pourquoi la spectroscopie NIR

pourrait être utilisée pour prédire les propriétés dynamiques du bois et l'AMF. Le Table 3 (p. 55) présente un résumé des principales statistiques des étalonnages SPIR.

Pour les bois issus de l'essai descendance, les étalonnages SPIR ont été élaborés pour évaluer les principaux composants chimiques de bois, y compris la teneur en lignine Klason (KL), la teneur en lignine soluble dans l'acide (LAS) et le ratio syringyl et guaiacyle (S/G). Ces calibrations SPIR pour les propriétés chimiques du bois sont décrites dans **l'article 4**, où l'influence de la préparation des échantillons et son effet sur la performance du modèle sont discutés. Dans la présente étude, la lignine soluble dans l'acide n'a pas été présentée. Ensuite, les étalonnages SPIR sont élaborés pour les propriétés physiques et ultrastructurelles des échantillons de bois provenant des bandes diamétrales. **L'article 5** rapporte les modèles SPIR pour la densité basale. La démarche démontre la robustesse des modèles établis par la validation indépendante. **L'article 6** présente les modèles SPIR d'estimation de l'angle des microfibrilles et explique pourquoi la spectroscopie SPIR peut être utilisée pour prédire cette propriété ultrastructurale des parois cellulaires du bois d'*Eucalyptus*.

Pour le bois à partir des test clonaux, les étalonnages SPIR ont été élaborés pour évaluer les propriétés mécaniques du bois, tels que la densité à l'air sec et la densité du bois, le module d'élasticité dynamique, le module de cisaillement et de frottement interne, ainsi que leur première fréquence de résonance. **L'article 7** rapporte les modèles SPIR d'estimation des ces propriétés du bois. Ces modèles sont basés sur les échantillons de bois issus des billes récoltées sur chacun de 150 arbres. Ils ont été utilisés pour prédire ces propriétés à partir des spectres sur les 750 disques de bois afin de cartographier la variation des propriétés du bois dans les tiges.

Approches en génétique quantitative

Les variations génétiques et environnementales des propriétés du bois ont été évaluées. Les calibrations SPIR ont été appliqués sur le bois permettant l'estimation des propriétés sur un grand nombre d'échantillons de bois issus des essais de descendances et de clones. Ces estimations nous ont permis de déterminer les variations spatiales, les corrélations entre les propriétés et le degré du contrôle génétique et environnemental des propriétés du bois.

Dispositif 1 : Test de descendances du Congo

Les valeurs prédites par SPIR pour les caractères du bois des arbres du test de descendance (Figure 33, p. 94) ont été utilisées pour évaluer le niveau du contrôle génétique et environnemental sur une gamme de propriétés du bois, avec un accent particulier sur le MFA et sa corrélation avec d'autres traits. Par ailleurs, les corrélations génétiques et environnementales entre les propriétés du bois et la croissance ont été évaluées à des âges différents afin d'améliorer nos connaissances sur les aspects fonctionnels de la formation du bois chez *Eucalyptus*. Le degré du contrôle génétique et l'environnemental de l'AMF, de la densité, de la teneur en lignine, sa structure et les caractères de croissance a été présenté et une série d'implications pour la sélection a été discutée dans **l'article 8**.

Dispositif 2 : Tests clonaux du Brésil

Les valeurs prédites par SPIR pour les caractères du bois des arbres à partir des tests clonaux (Figure 34, p. 95) ont été utilisées pour évaluer les paramètres génétiques et la variabilité intra arbre de la densité de base, la rigidité du bois et de l'AMF en bois d'*Eucalyptus*. **L'article 10** rapporte ces résultats. La variation entre les clones et les sites des propriétés élastiques mesurées sur l'échantillonnage par la technique de résonance a été présentée et discutée dans **l'article 9**. A partir de ces constatations, nous espérons être en

mesure d'indiquer quels sont les génotypes les plus appropriés pour la production de bois d'œuvre provenant des plantations d'*Eucalyptus*.

Résultats principaux

Influence de l'angle des microfibrilles pour la rigidité et retraits au séchage du bois

Les relations entre les propriétés du bois sur les clones d'*Eucalyptus* de 6 ans ont montré que la variation du MFA n'expliquait que 44 % de la variation du module spécifique (Figure 30, p. 88). La densité du bois basale est le principal déterminant du module d'élasticité et du module de rupture alors que le MFA joue un rôle secondaire sur la rigidité et la résistance du bois provenant de plantations à croissance rapide (Table 21, p. 89). L'angle des microfibrilles de cellulose dans la paroi cellulaire n'explique pas les retraits radial et tangentiel au séchage.

Contrôle génétique

Des héritabilités élevées ont été enregistrés pour le MFA (h^2=0,65), ρ (h^2=0,61), LK (h^2=0,72) et S/G (h^2=0,71) pour les *Eucalyptus* de 14 ans du test de descendance (Table 28, p. 100). Le contrôle génétique de ρ et MFA et leurs corrélations génétiques avec la composition chimique et la croissance varient avec l'âge de formation du bois (Figure 36, p. 104). La corrélation génétique C x ρ est fortement négative (r<-0,88), tandis que la corrélation ρ x MFA est constante et positive dans le bois juvénile (r=0,7), en diminuant considérablement dans le bois mature (r=0,3). Cela pourrait signifier que les arbres avec un fort potentiel de croissance rapide sont « génétiquement programmés » pour produire des bois de faible densité et avec de faibles angles des microfibrilles pour assurer la rigidité. Les variations du MFA et de LK dans le bois mature sont également génétiquement contrôlées. Le faible angle des microfibrilles compense la diminution de la densité, et la croissance rapide avec les changements de la teneur en KL peut s'expliquer fonctionnellement par les effets pléiotropes des gènes ou par le déséquilibre de liaison induit par l'échantillonnage. D'un point de vue biologique, la corrélation MFA x densité est stratégique pour la survie des arbres, leur maintien en position verticale et les conséquences des vents induisant constamment des mouvements de flexion. En conclusion, les corrélations génétiques MFA x densité et MFA x LK agissent de concert et révèlent une stratégie biologique liée à la survie de l'arbre. Le mécanisme sous-jacent à l'interaction de la cellulose cristalline noyée dans une matrice souple serait utilisé pour ajuster les propriétés mécaniques. D'un point de vue technologique, ces résultats permettent de discuter de l'impact sur les stratégies de sélection pour le bois de pâte à papier, le bois énergie et la production de bois massif. Comme les industriels forestiers sont à la recherche de bois selon leur besoin, la connaissance de ces corrélations entre les caractères de croissance et les propriétés du bois sont d'une importance cruciale.

Des niveaux faibles à modérés de l'héritabilité au sens large (H^2) ont été obtenus pour la densité basale, la rigidité du bois et de l'angle des microfibrilles des clones d'*Eucalyptus* de 6 ans (Figure 45, p. 119). Les résultats ont clairement révélé que l'estimation de l'héritabilité pour E et MFA présente des variations selon la position radiale et longitudinale. Pour la densité, la plus élevée des estimations de H^2 ont été trouvées dans les régions supérieures de l'arbre, en particulier dans la zone intermédiaire.

Héritabilité spectrale

Les paramètres génétiques ont été calculés directement à partir des spectres PIR mesurés sur le bois (Figure 46, p. 123). Les variations de zones spécifiques des spectres PIR sont liées aux variations de lignine, cellulose et hémicelluloses contenues et par conséquent corrélées aux propriétés du bois. Les résultats ont clairement montré que les variations sur ces zones spécifiques des spectres PIR sont

contrôlées par des facteurs génétiques. Les attributions des bandes d'absorption sont utilisées pour identifier les composantes du bois qui présentent les héritabilités au sens large les plus élevées à partir des données spectrales. Certaines zones du spectre présentent des H^2 de plus de 50%. Considérant les spectres PIR comme une source d'informations importantes liées aux propriétés du bois, l'analyse des paramètres génétiques pour les variables des spectres semble être un moyen efficace et prometteur pour évaluer le contrôle génétique de plusieurs propriétés du bois à la fois. Ceci est d'autant plus important que la prise de spectres est très rapide et donc peu couteuse pour un grand nombre d'échantillons.

Considérations finales

Notre étude montre que la plupart des propriétés du bois sont génétiquement corrélées négativement avec la croissance, bien que les corrélations génétiques observées entre les propriétés du bois d'*Eucalyptus* soient positives. En raison de ces corrélations génétiques négatives entre le bois et la croissance, la sélection pour augmenter la densité et la rigidité ou la réduction du MFA en l'absence de sélection pour la croissance se traduira par une réduction (perte génétique) dans la production de volume. Par conséquent, les planteurs, les gestionnaires forestiers et les producteurs de bois devront trouver un équilibre entre le bois et les caractères de croissance, et les généticiens devraient élaborer des stratégies d'amélioration en tenant compte de ces résultats.

Mots-clés: qualité bois, rigidité, densité basale, angle des microfibrilles, génétique quantitative, contrôle génétique, le génotype de l'interaction environnement, la propagation clonale, test de descendance

LIST OF NOTATIONS

BING - Beam Identification by Non-destructive Grading®

BLUP - Best Linear Unbiased Prediction

LV - latent variable

NIRS - Near Infrared Spectroscopy

PLS-R - Partial Least Squares Regression

R^2_C - Coefficient of determination of calibration between lab-measured and NIR-predicted values

R^2_{CV} - Coefficient of determination of cross-validation between lab-measured and NIR-predicted values

R^2_P - Coefficient of determination of prediction between lab-measured and NIR-predicted values

REML - Restricted Maximum Likelihood

RMSEC - Root mean square error of calibration

RMSECV - Root mean square error of cross-validation

RMSEP - Root mean square error of prediction

RPD - ratio of performance to deviation

SEE - standard error of estimation

SNV - Standard Normal Variate

SPIR - Spectroscopie proche infrarouge

XRD - X-ray Diffraction

LIST OF WOOD TRAITS

D - Basic density of wood from progeny trees estimated by NIRS

E - Modulus of elasticity estimated by sonic resonance (E_F for Flexural modulus of elasticity and E_L for longitudinal modulus of elasticity)

E' - Specific modulus (E/ρ)

f_1 - First resonance frequency

Fmax - Force at fracture point

KL - Klason lignin

MFA - Microfibril angle (MFA_C for MFA estimated by Cave's (1966) method, $MFA_{Y(RS)}$ for MFA estimated from radial strips and $MFA_{Y(S)}$ for MFA estimated from specimens)

MOR - Modulus of rupture

S to G ratio - Syringyl to Guaiacyl (S/G) ratio

tan δ - internal friction or loss tangent

δ - shrinkage tangential (tg) or radial (rd)

ρ - basic density of wood (ρ14 for kiln-dried at 14% density of wood, ρad for air-dried density of wood, ρs for basic density of small samples and ρsp for air-dried density of entire specimens)

LIST OF PAPERS

Papers concerning wood traits

Paper 1 - Hein PRG, Brancheriau L, Lima JT, Gril J and Chaix G (2011) Resonance of structural timbers indicates the stiffness even of small specimens of *Eucalyptus* from plantations. **Wood Science and Technology** DOI: 10.1007/s00226-011-0431-1 (*in press*)

Paper 2 - Hein PRG (2011) Relationships between microfibril angle and wood traits in *Eucalyptus* from fast-growing plantations. **Holzforschung** (submitted)

Paper 3 - Hein PRG and Brancheriau L (2011) Correlations between microfibril angle and wood density with age in 14-year-old *Eucalyptus urophylla* S.T. Blake wood. **BioResources** (submitted on July 1st 2010)

Papers concerning NIRS calibrations

Paper 4 - Hein, PRG, Lima JT and Chaix G. (2010) Effects of sample preparation on NIR spectroscopic estimation of chemical properties of *Eucalyptus urophylla* S.T. Blake wood. **Holzforschung**, Berlin, v.64, p.45-54

Paper 5 - Hein PRG, Lima JT and Chaix G (2009) Robustness of models based on near infrared spectra to predict the basic density in *Eucalyptus urophylla* wood. **Journal of Near Infrared Spectroscopy**, Chichester, v.17, n.3, p.141-150

Paper 6 - Hein PRG, Clair B, Brancheriau L and Chaix G (2010) Predicting microfibril angle in *Eucalyptus* wood from different wood faces and surface qualities using near infrared spectra. **Journal of Near Infrared Spectroscopy**, Chichester, v.18, n.6, p.455-464

Paper 7 - Hein PRG, Brancheriau L, Trugilho PF, Lima JT and Chaix G (2010) Resonance and near infrared spectroscopy for evaluating dynamic wood properties. **Journal of Near Infrared Spectroscopy**, Chichester, v.18, n.6, p.443-454

Papers concerning genetic studies of wood traits

Paper 8 - Hein PRG, Bouvet JM Mandrou E, Vigneron P and Chaix G (2011) Genetic control of growth, lignin content, microfibril angle and specific gravity in 14-years *Eucalyptus urophylla* S.T. Blake wood. **Annals of Forest Science** (submitted on April 21th 2011)

Paper 9 - Hein PRG, Brancheriau L, Lima JT, Rosado AM, Gril J and Chaix G (2010) Clonal and environmental variation of structural timbers of *Eucalyptus* for growth, density, and dynamic properties. **Cerne**, v.16, suplemento, p.74-81

Paper 10 - Hein PRG, Brancheriau L, Chaix G (2011) Clonal and environmental variation of specific gravity, stiffness, microfibril angle in *Eucalyptus* plantations. **Silvae genetica** (*in the pipeline*)

1 INTRODUCTION

1.1 BACKGROUND

Wood has an important role in the world as an environmentally responsible and sustainable material. The deforestation of natural forests causes serious economic and environmental problems, not only locally but also globally while sustainable management of forests is an urgent necessity. The establishment of forest plantations to supply the raw material for pulp and paper, energy and wood products industries was a key to the reduction of deforestation of natural forests. According to Meder et al. (2010), plantation forest globally covers 140 millions ha providing a sustainable approach to ensuring the continued supply of traditional building materials and, with the advent of emerging technologies, developing novel fuels, speciality chemicals and nano-crystaline cellulose, all of which will play a vital role in shaping our future society and economy.

Worldwide, forest and forest products play a major economic role in the world with global gross domestic product (GDP) topping US$63 trillion in 2010 and this is projected to grow by 3.2 percent per annum reaching US$117 trillion by 2030 (FAO 2011). The Brazilian forest sector has played an important role as a source of income for the national economy, generating products for direct consumption or for export, generating taxes and jobs to people and also working in conservation and preservation of natural resources. According to Tonello et al. (2008) this sector accounts for 3% of the GDP, totalling more than $ 30 billion. In 2008 the roundwood production of *Eucalyptus* reached an estimate of 174.6 million m³ whereas a total of 114 million m³ were consumed (ABRAF 2010). Brazilian exports of wood products from planted forests reached US$ 6.8 billion which represents 3% of total Brazilian exports in 2008. The most representative products in the export agenda for 2008 were pulp (57.4%) and paper (28.1%) in total exports of planted forest products. The export share of other products is low compared to pulp and paper because most of its production is oriented to the domestic market.

Over last years, plantation forests expand ~2.0-2.5 million ha by year meeting an increase proportion of global demand of wood (FAO 2006). *Eucalyptus* is one of the most widely cultivated hardwood genera in tropical and subtropical regions of the world. Nowadays the total area of *Eucalyptus* plantations in world covers about 19.5 million hectares (Iglesias-Trabado and Wilstermann 2008) representing ~0.131% of the total land of the earth surface. In Brazil, the *Eucalyptus* plantation surface covers around 4,515,730 ha (ABRAF 2010). This success largely reflects the adaptability of this genus to a variety of climatic and edaphic conditions, its fast growth and the flexibility and usefulness of its wood for industrial applications (Santos et al. 2004). Originally from Australia, *Eucalyptus* was introduced in Brazil between 1865 and 1870 and in 1904 some *Eucalyptus* species were selected in order to obtain trees which would produce the highest economic return by unity area of wood for poles, railway sleeper and fuel for steam locomotives (Berti Filho 1997).

Many countries have verified significant advances in intensive clonal silviculture with remarkable differences on parameters of growth and development between species clones and hybrids of *Eucalyptus*. As a pioneer species, *Eucalyptus* grows even under thin and poor quality soils with few nutrients. Brazil has highly favourable climate and soil conditions for development of commercial plantations of fast growing species. *Eucalyptus grandis* presents growth at high rates while the *E. urophylla* is a robust species being able to growth under a range of conditions (poor soils, low precipitation) and to resist against diseases. Thus, the most common species in Brazil are *E. grandis* and *E. urophylla* and the hybrid

E. urograndis. Massive plantations of genetically uniform monocultures have moved *Eucalyptus* silviculture into the domain of classic sustainability issues from agriculture: genetic uniformity, pests and pathogens, and environmental impacts of intensive land management (Binkley and Stape 2004).

As a fast-growing and short-rotation source of wood, *Eucalyptus* plantations are the basis for several industries, such as pulp and paper and iron and steel producers. The continuity of forestry research over the past several years has allowed Brazilian companies to reached high productivity for *Eucalyptus* (40.5 $m^3\ ha^{-1}\ yr^{-1}$), notably higher than those of Australia (25 $m^3\ ha^{-1}\ yr^{-1}$), South Africa (18 $m^3\ ha^{-1}\ yr^{-1}$) and Portugal (12 $m^3\ ha^{-1}\ yr^{-1}$) for hardwood plantations (ABRAF 2010). Some Brazilian pulp and paper industries, such as Fibria Celulose, for instance, has recorded yields superior to 70 $m^3\ ha^{-1}\ yr^{-1}$ with *Eucalyptus* hybrids growing under favourable conditions.

The wood produced by these *Eucalyptus* plantations principally attends the demand of three main industrial needs: pulp and paper (37.3%), energy (37.6%) and timber production (18.8%). Table 1 presents the distribution of *Eucalyptus* and *Pinus* forest plantations in Brazil by industrial segment in 2009.

Table 1 - Distribution of *Eucalyptus* and *Pinus* forest plantations in Brazil by industrial segment in 2009

Segment	Roundwood consumption (1,000 m³) - 2009		
	Eucalyptus	*Pinus*	Total
1. Pulp and Paper	52,545 (47.3%)	8,086 (15.7%)	60,631 (37.3%)
2. Industrial Fuelwood	32,363 (29.1%)	9,347 (18.2%)	41,710 (25.7%)
3. Charcoal	19,388 (17.4%)	0 (0%)	19,388 (11.9%)
4. Timber Industry	3,093 (2.8%)	27,463 (53.4%)	30,556 (18.8%)
5. Reconstituted wood panels	2,872 (2.6%)	6,520 (12.7%)	9,392 (5.8%)
6. Others	895 (0.8%)	7 (0%)	902 (0.6%)
TOTAL	111,156	51,423	162,579

(Source: ABRAF 2010)

Pulp and paper industry is the main industrial segment consumer absorbing around 47.3% of the roundwood production from the *Eucalyptus* plantations. Just over a quarter of the roundwood production (29.1%) is consumed as fuelwood while the pig iron and steel industry, in turn, consumed 17.4% (charcoal). Only a small part of roundwood production is directed toward to the timber industry (2.8%) and to the manufacture of engineering wood products (2.6%). In the other hand, 53.4% of the *Pinus* roundwood production is destined for the timber industry and 12.7% for wood panels industry. Given this scenario, it is important to think why only ~5% of the *Eucalyptus* roundwood production has been employed as raw material for furniture, flooring, structural material and engineered wood products industry.

1.2 *Eucalyptus* as a timber source

Since the concept of multiple uses of tree logs to increase the yield of the forest enterprises has been introduced (Arango and Tamayo 2008), numerous companies are changing their focus. In many parts of the world there is a move to the use of smaller logs and there has been a growing need and interest in establishing plantations for sawnwood production, as log supplies from natural hardwood forests are likely to decrease in future (Yang 2007). For example, most of *Eucalyptus* plantations in Australia are being grown for pulpwood, but increasing numbers are being managed for sawlogs (Pelletier et al. 2008). In South Africa, small pine logs (such as those with small-end diameter as small as 10 cm, from plantation thinning), which were also previously sent to pulp mills, are now being used for solid wood products

(Verryn 2008). Yang and Waugh (1996a; 1996b) have evaluated the potential of plantation-grown *Eucalyptus* for structural sawn products. The knowledge that has been established over decades for the natural forests must now be coupled with new knowledge for the plantation forest (Meder et al. 2010). In current wood processing and manufacturing operations, knowledge about wood traits, its co-variation within the stem and their relationships are essential to ensure optimal utilization.

1.2.1 Problems of *Eucalyptus* wood

Although wood from *Eucalyptus* breeding programs presents an optimal performance to pulp and energy, its performance in the timber industry is usually not satisfactory. The properties required of *Eucalyptus* wood put to traditional uses in Brazil (pulp and paper and charcoal production) are not the same as those required of solid wood, where in particular mechanical properties are of importance (Lima et al. 1999). Thus, it is widely recognized that most species have many wood quality characteristics which can have adverse impacts on effective and efficient conversion, product processing and product quality (Shield 2007). The greater proportion of juvenile wood presented in this wood, long time ago indicated by Wilkes (1988) as a critical factor, and the growth stress expression (Jacobs 1945; Boyd 1950; Archer 1986) are probably the most frequently referenced characteristics in an abundant literature detailing often severe problems arising in the course of conversion and processing. The potential of *Eucalyptus* wood for higher value products such as solid wood products, especially appearance-grade sawn timber is influenced by numerous factors. Some of these problems are discussed as following.

Growth stress

High levels of growth stress in *Eucalyptus* are undoubtedly the most serious growth phenomenon affecting wood quality, product yield and product dimensions. Growth stress is a problem difficult to solve in *Eucalyptus* plantations since it is a natural mechanism of tree for surviving and for supporting external forces, such as prevailing winds, thunderstorms and its own weight. According to Alméras and Fournier (2009), the tensile longitudinal stress in the periphery of the stem allows the tree to stay upright and optimizes the resistance of wood against bending forces such as wind. Growth stress result from the superposition of two kinds of stress: (i) support stress, that is, an elastic response to the increasing load of wood and shoots supported by the tree, and (ii) maturation stress, which appears spontaneously inside wood during its formation (Clair et al. 2006).

Growth stress is a major cause of degrade and processing problems, especially in fast-growing *Eucalyptus* wood inducing warping and splitting of logs and boards (Panshin and De Zeeuw 1980). Bamber et al. (1982) have evaluated the effect of fast growth on *Eucalyptus* wood properties. Severe splitting develops in log ends following cross-cutting while further splitting and distortion takes place during conversion into sawn boards (Malan 1995). A reduction in stress levels in tree stems would certainly be by far the most important improvement that can be made regarding many eucalypt species, as the impact on the wood processing industry will be impressive.

Tension wood

Tension wood is a particular kind of wood formed during wood formation on the upper side of the leaning stem and associated to a large longitudinal tensile stress. It occurs frequently in plantation-grown *Eucalyptus* at the stem periphery (Washusen et al. 2005) causing high variations on wood traits within the trees. According to Wardrop (1956), this tissue is an anatomical manifestation of various regulatory processes associated with the maintenance of tree form and movements of orientation in response to environmental changes. Tension wood is associated to the formation of a peculiar layer of the fiber wall,

the gelatinous or G-layer (Clair et al. 2006) which is characterized by its large thickness and its low MFA and lignin (Chaffey 2000). Tension wood of broadleaves such as *Eucalyptus* usually presents high specific longitudinal modulus of elasticity, so that the strongly negative maturation strains (shrinkage) lead to high level of tensile stress in the new layer, without requiring necessarily a compensating material production (Thibaut et al. 2001). Tension wood occurs also in wood of intermediary regions of the stem since it is formed during the wood formation and its localization changes as the tree grows over the years. Normal or opposite wood also can have a low MFA. For instance, Washusen et al. (2001) investigated tension and normal wood in the sapwood and heartwood in 10-year-old *Eucalyptus globulus* Labill finding very low MFA in normal wood, where most tension wood was found.

Tension wood occurrence brings other problems for wood quality. The cells of the stem periphery are in state of tension while the central parts of the stem are under compressive forces (Thibaut et al. 2001). When theses cumulative effects exceeds the maximum crushing strength of wood, numerous slip planes and compression failures take place generating a common problem experienced especially by hardwood saw millers known as "brittle heart" (Malan 1995). The presence of this defect has a very significant effect on the quality and yield of the end product.

Juvenile wood

Eucalyptus plantations have been harvested before their wood reach maturity for reasons of economic efficiency. Hence, an important factor in fast growing stands is the quality in the juvenile wood. *Eucalyptus* stems with high proportion of juvenile wood led to inferior performance as sawn wood. Juvenile wood is characterized by large microfibril angles, short fibres with thin walls and lower density contributing to the lower quality of juvenile wood products (Zobel and Van Buijtenen 1989).

Short rotation ages results in large proportions of juvenile wood, deteriorating even further in future generations as trees are bred to grow faster. As the logs from plantations are often younger and smaller diameter, this problem can be solved by waiting the tree reach their maturity before harvesting or selecting trees with better juvenile wood traits.

Grain angle

Spiral grain is the tangential inclination angle of wood fibers from the vertical stem axis and the variation in grain angles is great among tree species and individual trees (Harris 1989) and it can be caused by winding or spiral growth of wood fibers about the bole of the tree instead of vertical growth. Trees develop spiral grain to adapt themselves to various mechanical constraints; for instance, to withstand stem under forces induced by wind (Skatter and Kucera 1997). However, this adaptive mechanism is an undesirable phenomenon since gives rise to severe problems in sawn timber. It is well known that spiral grain reduces both strength and stiffness of sawn wood (Skatter and Kucera 1997). For instance, Green et al. (1999) showed that the grain slope has strong effect on some wood traits. Moreover, a large amount of spiral grain in the wood causes shrinkage and warping along the longitudinal plane of boards and planks (Eklund and Säll 2000) and also decreases the strength of timber. Brémaud et al. (2011) have investigated the dependence on grain angle on the visco-elastic properties of wood.

Collapse shrinkage

Shrinkage and swelling may occur in wood when the moisture content is changed (Stamm 1964). It occurs as moisture content decreases, while swelling takes place when moisture content increases. Collapse is an abnormal shrinkage encountered in wood of certain trees species in the process of drying (Wu et al. 2005). It results from the physical flattening of fibres to above the fibre saturation point and is thus not a form of

shrinkage anisotropy. Collapse can be defined as the difference between the total shrinkage of a specimen and the shrinkage in the same structural direction of an end-matched cross-section of 1 mm thickness in the fibre direction (Kauman 1961, from Ilic and Hillis 1986). Collapse shrinkage can often be recovered by reconditioning with live steam, but collapse induced checking is a permanent for of degrade (Innes 1996). Some *Eucalyptus* species are prone to collapse during drying contributing to split problems. Thus collapse shrinkage is an important issue in the context of wood drying.

Knots presence

Knots are a major defect factor in plantation grown logs, even those of excellent form and apparently sound. Knots do not only directly contribute to defect in converted products, they are often associated with other defects such as grain deviation and decay. Decay enters through branch stubs which, in Eucalypts, do not become filled with protective resins as is the case with conifers. This signals a caution for pruning *Eucalypts* which is otherwise to be strongly recommended as minimising the defects associated with knots (Shield 2005).

Because of short rotations (6-7 years for pulp and paper, and energy and 12-15 years for sawntimber, in Brazil), logs from *Eucalyptus* plantations are often younger, smaller diameter and of greatly differing wood properties. For these reasons, in many regions of the world *Eucalypts* plantations do not have a good image as sawnwood provider or as their equivalents for rotary peeling. Shield (2007) claims that "the scarcity of the most fundamental requirement for success - prudent and patient investors - leads to poor silviculture, poor sawlog quality, poor sawmilling, poor lumber quality and, unsurprisingly, poor lumber prices".

1.2.2 What is wood quality?

Savidge (2003) presents some interesting concepts about wood quality. According to him, wood quality has to do with its degree of excellence in relation to some application. Because quality assessment is multi-faceted and depends on the intended application, there is no absolute measure. Quality assessment by the woodsmen who fell and process the trees and by the mill workers who decide how logs should be used involves experienced observation and snap-judgment integration of particular features, based largely on subjective experience.

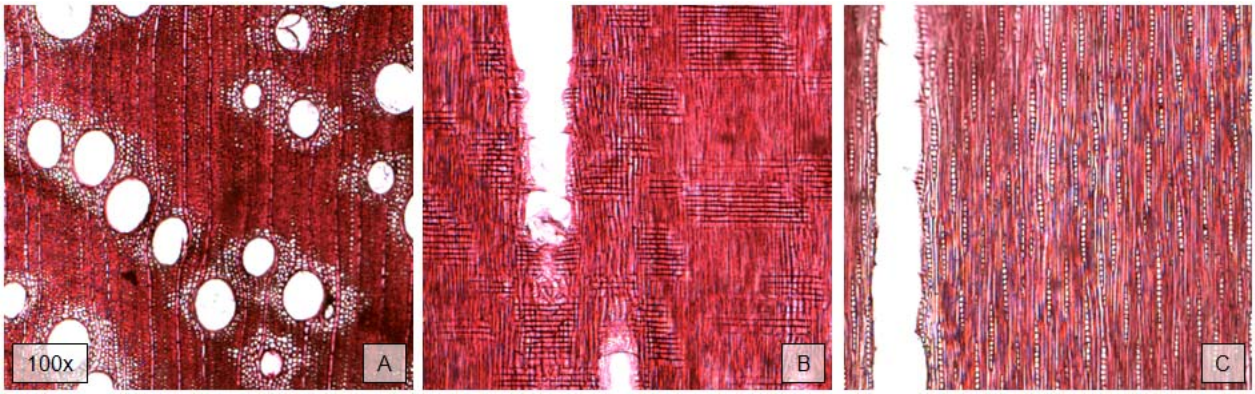

Figure 1 - Transversal (A), radial (B) e tangential (C) sections of 6-year-old *Eucalyptus* wood (source: personal image)

Savidge (2003) affirms that some aspects of the wood quality, such as its density and its amount of cellulose, lignin or extractive can be repeatedly analyzed and quantitatively expressed with high accuracy and precision (it depends of the method accuracy and technician ability). However, other measures such as

fibre length, cell wall thickness, microfibril angle, and percentages of the various types of anatomical elements coexisting in a wood are more problematic. Upon repeated random sampling and measurement of the same preparation, a Gaussian distribution is predictably obtained, and the magnitude of the standard deviation may provide equally or more important information than the mean value. However, that information essentially is no more than a confirmation of what can be readily observed when viewing a wood section in the compound light microscope (Figure 1): large variation exists within wood.

1.2.3 Selecting traits for wood improvement

Many wood traits are known to be important in determining the value of *Eucalypts* wood as sawn timber including its basic density, mechanical properties, grain angle, knots and resin pockets, juvenile wood proportion and the microfibril angle (MFA), the preferable angle of the cellulose microfibril within the cell walls. Most wood properties are age related and co-vary with one another (Zobel and Van Buijtenen 1989) and the correlations between wood traits can be high, leading a positive or adverse effect for industrial applications. Selection of any favourable characteristic has benefits for a number of wood properties, with the overall gain depending on the characteristic sought for improvement (Walker and Butterfield 1995) and its effect on all wood properties.

Due to the ease of measurement and because basic density of wood present high genetic control and correlation with other properties, there are numerous statements that density is the most important characteristic in determining the properties of wood. Hence, a considerable number of studies were conducted for investigating the wood density in *Eucalyptus* breeding in the last decades (Whittock et al. 2007; Hamilton and Potts 2008; Hamilton et al. 2008; Kien et al. 2008; Pelletier et al. 2008; Volker et al. 2008; Wey and Borralho 1997; Kube et al. 2001; Greaves et al. 1997a; Poke et al. 2006; Apiolaza et al. 2005).

Although the density is a desirable characteristic for many industrial applications (Zobel and Jett 1995; Zobel and van Buijtenen 1989), selection according to density does not appear to be a very effective method for identifying better structural timber conifers species (Walker and Butterfield 1995) because density is a kind of measure of the "quantity" of matter in a piece of wood. In the case of some softwood, especially in *Pinus*, the intrinsic characteristic whose improvement is likely to yield the greatest economic benefits is the microfibril angle (Walker and Butterfield 1995), because MFA is a kind of measure of the "quality" of the material in the cell wall. Lindström et al. (2004) claimed that the use the stiffness rather than wood density as a selection criterion will also benefit from the fact that modulus of elasticity is a composite function of MFA and wood density.

Specific modulus is wood trait consisting of the elastic modulus per wood density. The utility of specific modulus is to find varieties of woods which will produce structures with minimum weight. Wood presenting high specific modulus has wide application in which minimum structural weight is required such as large wood structures, bridges, furniture, roof structures etc. Specific modulus is an interesting property because it represents two important traits at once.

According to Verryn (2008), it is suggested that the breeder and wood specialists invest in very careful consideration of which traits are of key importance, and will still be of such importance in years to come (target deployment and harvesting time). The commercial importance of MFA for wood quality is well established for softwoods, but is less clear for hardwoods (Donaldson 2008). In *Pinus*, the MFA is known to be the best indicator of its stiffness (Cave 1968; Barnett and Bonham 2004; Walker and Butterfield 1995). In *Eucalyptus*, few studies have exanimate the influence of the MFA on wood stiffness (Evans and

Ilic 2001; Yang and Evans 2003; Evans 2006) and the relationship between MFA and wood stiffness remains unclear reserving a deeper investigation.

1.2.4 MFA controls wood quality

Microfibril angle (MFA) is a structural characteristic of the cell wall of wood fibres and tracheids, which is made up of millions of strands of cellulose called microfibrils (Fang et al. 2006). This ultrastructural cell wall property represents the orientation of crystalline cellulose along the fiber axis (Andersson et al. 2000). In the secondary cell walls of xylem, the fibres or tracheids typically have three layers, an outer S_1 with transversely oriented microfibrils, a thick S_2 layer with axially oriented microfibrils, and an inner S_3 layer also with transversely oriented microfibrils, in a S-Z-S helical organization (Donaldson 2008). Figure 2 presents the arrangement of cellulose microfibrils in the secondary cell wall of a fibre.

Each layer has its own particular arrangement of cellulose microfibrils, which determine the mechanical and physical properties of the wood in that cell. These cellulose microfibrils may be aligned irregularly (as in the primary (P) cell wall), or at a particular angle to the cell axis (as in layer S_1, S_2, and S_3). The middle lamella (ML) ensures the adhesion between cells (Figure 2). Because S_2 layer is generally much thicker than the other layers is therefore considered to dominate the physical and chemical properties of the cell wall (Donaldson and Xu 2005).

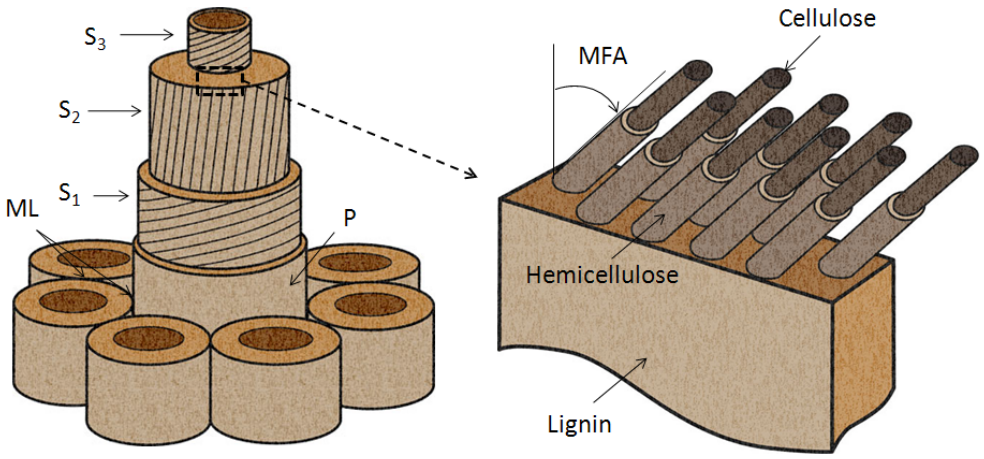

Figure 2 - Three-dimensional structure of the secondary cell wall of a fibre

Plants are able to control the orientation of cellulose fibrils during deposition in the cell walls. Therewith they manifest a powerful tool at the nanoscale to create anisotropy of the cell wall (Burgert and Fratzl 2009). Barnett and Bonham (2004) stated the biological and mechanical role of MFA and its variation in the living trees: “Tracheids or fibres with a high MFA in the centre of the tree, which were produced when the tree was a sapling, endow the wood with a low modulus of elasticity (stiffness). This enables the sapling to bend in a high wind without breaking. As the tree enlarges, the stem has to become stiffer to support the increasing weight of the stem and crown. The lower MFA of the outer wood means that it has a higher modulus of elasticity to enable it to fulfil this role”.

The importance of MFA for wood quality is well established for softwoods, but is less clear for hardwoods (Donaldson 2008). In conifers is well known that MFA decreases with height (Megraw et al. 1998) and varies from pith to bark being large near the pith and declining gradually from pith to cambium (Walker and Butterfield 1995). Relatively few hardwoods have been characterized, so there is a need to extend the range of species and ecotypes to be investigated (Donaldson 2008). Specifically in the genus *Eucalyptus*,

the MFA variation within the trees and its effects on wood properties other than mechanical ones are rarely reported in the literature (Lima et al. 2004).

1.2.4.1 Correlation of MFA with wood traits

Over the past decade, lots of scientific contributions were dedicated on investigation of the microfibril angle of the S_2 layer of the wall in woody plants. MFA has also long been known to have major effects on two key properties of wood: its stiffness and shrinkage. Furthermore, microfibril angle has long also been known to present from moderate to strong, however sometimes none, correlation with fibre or tracheids length (Hirakawa and Fujisawa 1995; Kibblewhite et al. 2005; Tsutsumi et al. 1982), lignin content (Hori et al. 2003; Jungnikl et al. 2008), spiral grain (Cown et al. 2004), growth stress occurrence (Washusen et al. 2001), and other factors. However, the relationship of MFA with wood properties at what Kretschmann et al. (1998) have classified as "macroscopic level" is not fully understood and this is an area of active research. Some of these relationships are described above, but most of studies were based on softwoods.

MFA x stiffness

The curvilinear relationship between MFA and longitudinal stiffness (modulus of elasticity or Young's modulus) has been repeatedly demonstrated in the literature for a range of species. Cave (1968) demonstrated that a reduction in MFA from 40° in the corewood to 10° in the outerwood correspond to the increase of the longitudinal modulus of elasticity fivefold (from 5,000 to 1,000 kg mm^{-2}). This finding was confirmed by Via et al. (2009) who reported a fourfold increase in stiffness of longleaf pine when the microfibril angle dropped from 40° to 5°. Donaldson (2008) lists several studies addressing to this issue in many species and environmental conditions.

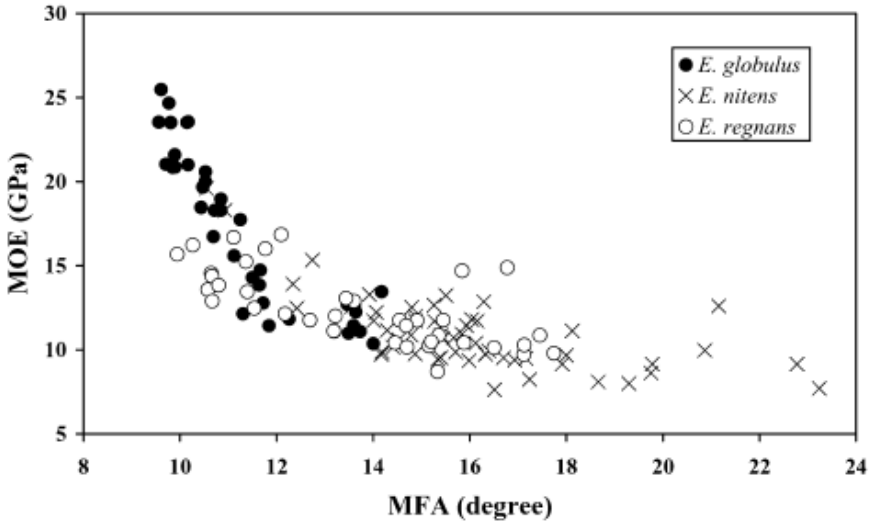

Figure 3 - Relationship between MFA and modulus of elasticity (MOE) of *E. globulus*, *E. nitens* and *E. regnans* wood between 15 and 33 years of age (from Yang and Evans 2003)

In *Eucalyptus*, Evans and Ilic (2001) and Yang and Evans (2003) have investigated the relationship between microfibril angle, basic density and wood stiffness in *Eucalyptus* wood. Figure 3 presents the relationship between MFA and wood stiffness in three *Eucalyptus* species. It is important to note that the stiffness decreased ~3.5 times while MFA increased twofold (from ~9° to 18°). Investigating these relationships in 104 *E. delegatensis* wood samples, Evans and Ilic (2001) have concluded that MFA was the major determinant of specific modulus, while density could not be used as selection criteria for stiffness in tree improvement programs. Yang and Evans (2003) have reported that MFA alone accounted

for 87 percent of the variation in E, while density alone accounted for 81 percent. Together, MFA and density (as Density/MFA) accounted for 92 percent of the variation in E. The above studies indicated that MFA was the prime determinant of both the modulus of elasticity (E) and the specific modulus (E/ρ). If their conclusions can be generalized, MFA measurements should make possible the evaluation of the wood quality.

MFA x shrinkage

The MFA has also long been known to influence dimensional changes in wood with changes in moisture content (Meylan 1968; Yamamoto et al. 2001; Barnett and Bonham 2004). Donaldson (2008) stated that MFA is one of the dominant parameters affecting shrinkage. As water bound to cellulose and hemicelloses moves out of the cell wall during drying of timber, these molecules move closer to each other and the wall shrinks (Barnett and Bonham 2004). As a result, cell walls with very low MFA tend to have greater tangential shrinkage, while cell walls with very high MFA tend to have greater longitudinal shrinkage (Donaldson 2008). Figure 4 presents a theoretical model explaining the influence of cellulose microfibril orientation on shrinkage anisotropy. Shrinkage anisotropy is responsible for some degrade on drying; especially crook (Walker and Butterfield 1995).

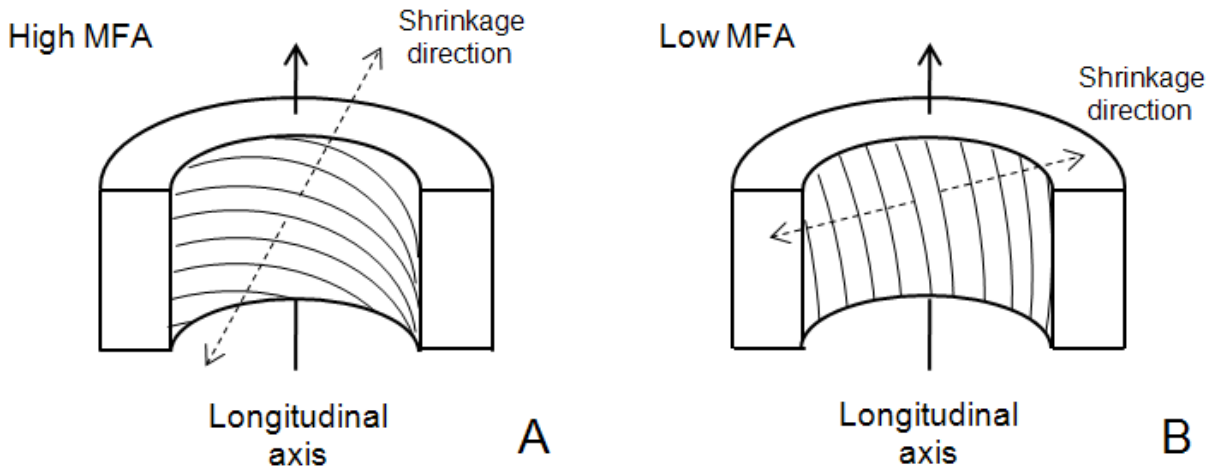

Figure 4 - Theoretical model explaining the influence of high microfibril angle (A) and low microfibril angle (B) on longitudinal and transversal components of shrinkage and swelling

In *Eucalyptus*, Wu et al. (2006) explored the relationships of the main anatomical features with shrinkage in *Eucalyptus urophylla*, *E. grandis*, and *E. urophylla* × *E. grandis*, planted in South China demonstrating that the main factors affecting unit shrinkage were cell wall proportion, microfibril angle, and cell wall thickness and that factors playing an important role in total shrinkage were cell wall proportion, ray parenchyma proportion, and MFA. Changes in moisture content may affect the cellulose crystallite width. For instance, Washusen and Evans (2001) have examined the correlations between tangential shrinkage and cellulose crystallite width in 11-year-old *Eucalyptus globulus*. Their results showed that cellulose crystallite width was closely associated with tangential shrinkage suggesting that cellulose crystallite width is an important predictor of shrinkage. As crystallite width increased, shrinkage also increased. The correlation between tangential shrinkage and crystallite width was strongest in the lower 5% of tree height.

Experimental data showing the relationship between anisotropic shrinkage and MFA is demonstrated in Figure 5. The small black squares (gray path) represent samples of *Pinus jeffreyii* wood from Meylan (1968) while the black and write circles represent *Sugi* wood samples from Yamamoto et al. (2001) in transversal (T-direc.) and longitudinal (L-direc.) shrinkages.

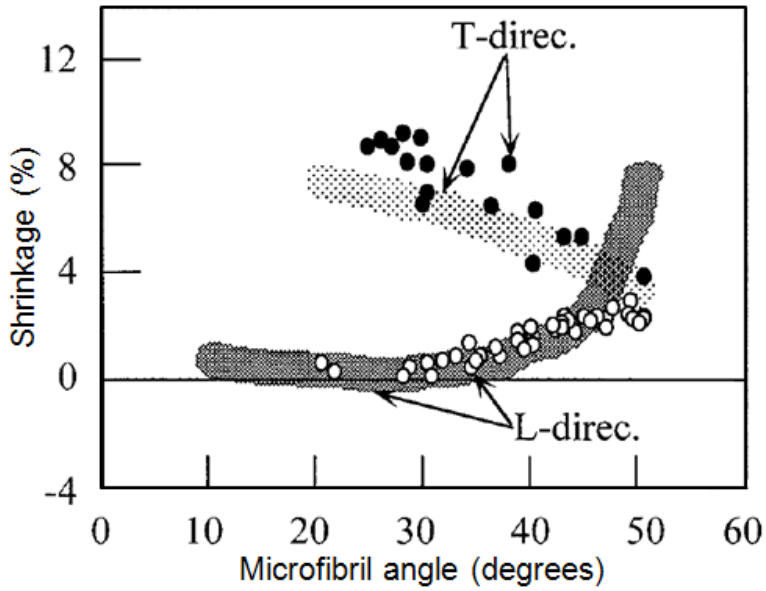

Figure 5 - Relationship between anisotropic shrinkage (from green to oven-dried) and MFA (from Yamamoto et al. 2001)

MFA x density

MFA shows a variable relationship with wood density (Donaldson 2008). Fang et al. (2004) reported significant correlation between MFA and wood density (r=-0.45) for *Populus.* On the other hand, Bergander et al. (2002) found no correlation between fiber morphology (i.e., average length, width, density) and mean fibril angle in wood samples of 100-year old Norway spruce (*Picea abies* L. Karst.). Similarly, Lin and Chiu (2007) studied such wood traits in 20-year-old Taiwania (*Taiwania cryptomerioides*) trees reporting no significant relationship between microfibril angle and wood density by linear regression analysis.

In *Eucalyptus*, Evans et al. (2000) compared MFA and density of 29 *Eucalyptus nitens* wood finding good local relationships between MFA and density but the whole tree average MFA and density yielded no correlation. Washusen et al. (2001) evaluated such traits in 10-year-old *Eucalyptus globulus* reporting strong linear relationship (r=-0.70) between density and MFA. The findings of Washusen et al. (2001) suggest that fibre wall thickening primarily due to thickening of the S_2 (hence increasing density) is the main factor contributing to decreasing MFA. However, Donaldson (2008) pointed out that any relationship between MFA and density is entirely coincidental since MFA is not related to fibre wall thickness. However, the amount of juvenile and mature wood might be responsible for relationships in some cases since both MFA and density are related to these factors. Is important to note that these two characteristics of wood vary from pith towards the bark and this systematic trend may play a role in part of the correlation, when it exists.

1.2.4.2 MFA implication on wood uses

While orientation of cellulose microfibril seems to be an important strategy for tree development and survival, the MFA has important, but sometimes adverse impacts in industrial applications. For sawn timber, a piece in which the MFA is large has a low stiffness and it is therefore suitable only for low-grade use, reducing its value as a raw material and its economic value. This problem was not too serious in the past when trees were allowed to reach maturity before being harvested. Increasing demand for timber,

pulp and wood products is driving the forest industry towards short-rotation cropping of fast-growing species (Barnett and Bonham 2004). Thus, trees with high contents of juvenile wood are used by industry resulting in loss of quality of the end product. According to Barnett and Bonham (2004) the real industrial problem, however, arises in a piece of wood containing partly normal wood with a small MFA, and a proportion of reaction wood with a large MFA can be a problem for industrial uses. From a technological point of view, this problem always existed: such pieces will distort during drying owing to the differential shrinkage occurring as a result of the difference in MFA. Differential shrinkage in pieces of normal timber, which incorporate both juvenile and mature wood, can also lead to distortion or cracking on drying.

When using fibres for paper production, microfibril angle and fibre length significantly affect pulp and paper properties (Thamarus et al. 2004). In wood of *Pinus*, for instance, low MFAs are associated with high tensile strength in paper, while high MFAs are associated with greater stretch and tear indices (Donaldson 1993). In the present study, the implications of the variation in MFA on wood traits and products are examined in *Eucalyptus*.

1.2.4.3 Methods for MFA measurement

MFA can be determined by two types of measurement: from individual tracheids or fibres using microscopy-based techniques and from a bulk wood samples using X-ray diffraction and near infrared (NIR) spectroscopy.

Optical methods

Microscopy-based techniques are divided into those that rely on the optical properties of crystalline cellulose, employing variations on polarised light techniques, and those that directly or indirectly visualise the orientation of the microfibrils themselves. Such methods include confocal reflectance microscopy, fluorescence microscopy, micro-Raman spectroscopy, scanning electron microscopy (SEM), transmission electron microscopy (TEM), iodine precipitation and other biological, chemical or physical treatments. These techniques are detailed described in Donaldson (2008) who presented a detailed review on MFA, its measurement, variation and relationships.

X-ray diffraction

It is likely that X-ray diffraction is currently the most popular method for measuring MFA. It is a fast and reliable technique, but X-ray diffraction is an indirect method and authors should provide the measurement uncertainty. This technique is a direct estimation of cellulose microstructure in the wood, but it needs a model to obtain the microfibril angle estimation from the diffraction pattern called the *T* parameter. Thus, X-ray diffraction provides only a relative figure for the MFA since the estimative comes from an interpretation of the *T* parameter.

The relationship of *T* to the true angle must be determined by other techniques. Thus, numerous studies have proposed models to estimate MFA from *T* parameters. First, Cave (1966) proposed that microfibril angle is 0.6 *T*. Then, Meylan (1967) determined microfibril angle to be $0.612T + 0.843$ for radiata pine. Yamamoto et al. (1993) proposed a formula of determining the MFA over a wide range using two gymnosperms and two angiosperms species whose normal wood shows thin fibre cell walls and tension wood does not show G-layer. According to Yamamoto et al. (1993), their formula improved the Cave's method giving better results, especially for reaction wood. Latter, Megraw et al. (1998) showed microfibril angle to be $0.93T + 10.71$ for loblolly pine with slightly differing equations for early and latewood

samples. Ruelle et al. (2007) proposed formulas for estimating MFA from *T* parameter using three tropical species (*Eperua falcata*, *Laetia procera* and *Simarouba amara*) in order to verify if the existing formulas could provide good estimations for microfibril angle in tropical species with G layer and/or with thick fibre cell walls. Figure 6 shows two examples of converting *T* parameter into MFA measured by other techniques. The blue line (Figure 6 B) represents the estimates by Cave' formula (1966) while the dotted line represents the estimates by Yamamoto' approach (1993).

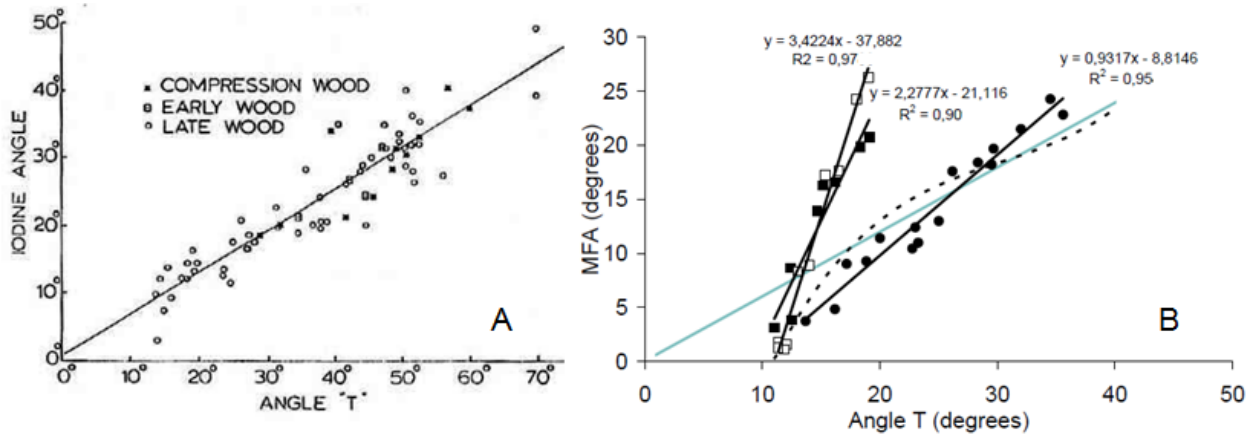

Figure 6 - The relationship between the angle T derivated from the X-ray intensity variation and the mean microfibril angle measured by iodine staining (A, from Meylan 1967) and by Field-Emission Scanning Electron Microscopy (B, from Ruelle et al. 2007)

In this study the formula proposed by Yamamoto et al. (1993) was used in most of cases because the interesting point is to know the relative value of the characteristic between trees or regions of the stem, its variation or stability within the logs. These MFA estimates can be useful for selection of candidate genotypes or commercial clones in forestry industries from a large wood sampling.

NIR spectroscopy

Near infrared spectroscopy technique relies on calibrating multivariate regressions that relates the NIR spectra recorded from wood samples to their known properties, for example lignin content. This NIR-based model is then applied on the NIR spectra of further samples in order to estimate their lignin content. This method has been mainly used for a range of chemical properties of wood. Mechanical and physical properties of wood have been also successfully evaluated by NIR spectroscopy models. Recently, many studies have been proposed NIR spectroscopy as a new tool for estimating microfibril angle in wood samples. NIR spectroscopy do not respond to MFA *per si* (only to chemical composition) but MFA can be correlated to chemistry and physical aspects and these indirect correlation makes possible to assess MFA from NIR spectra in some cases. These issues are discussed in more details within the item 1.3.4.4 (pg. 46).

1.3 *Eucalyptus* breeding programs

Forest genetics principles are central to tree improvement programs that develop genetically improved varieties for plantation systems around the world. Genetically improving the yield, health and product quality of these plantations directly enhances the economic and social value of the plantations (White et al. 2007). Advances in tree breeding and management practices are making significant gains. Forest sectors demand higher productivity and quality, and a faster adaptation of their varieties to rapid changes (Verryn 2008). Hence, the determination of the genetic factors contributing to quantitative trait variation of wood

properties is essential for tree breeders (Raymond 2002; Apiolaza 2009). This thesis focuses on verifying in which extent the MFA, stiffness and wood density are controlled by genetic and environmental factors in *Eucalyptus* plantations.

Selection and mating are key activities in breeding programs. The objective of breeding is to produce new generations or varieties of trees by mating trees with good characteristics in order to adequately meet the requirements of the industry and society. Thus, selecting potential trees from large populations and mating them with each other is expected to produce offspring that potentially will have superior (or inferior) mean phenotypes for the target features. According to Hardwood et al. (2001), selection and mating activities accumulate genes, which influence yield and adaptation, increasing over successive generations the frequency of superior trees. Mating can be done by open pollination or controlled pollination, carefully minimising the potential of inbreeding, which has been shown to be strongly deleterious in *Eucalyptus*.

Figure 7 illustrates an ideal situation where trees having traits of interest were selected from the initial population and artificially mated with each other. Thus, in this new generation (improved population) the frequency of the phenotypic value of interest is increased producing an improved population for such characteristic. The mean of the phenotype value increased from 62 to 72 in the second generation population. The genetic gain is indicated by the gray narrow. However, parents pass on their genes and not their genotypes on their progeny (Falconer 1993). It is therefore the averaged affects of the parent's genes that determine the mean genotypic value of their progeny. The value of an individual, jugged by mean value of its progeny, is called *breeding value* of the individual (Falconer 1993).

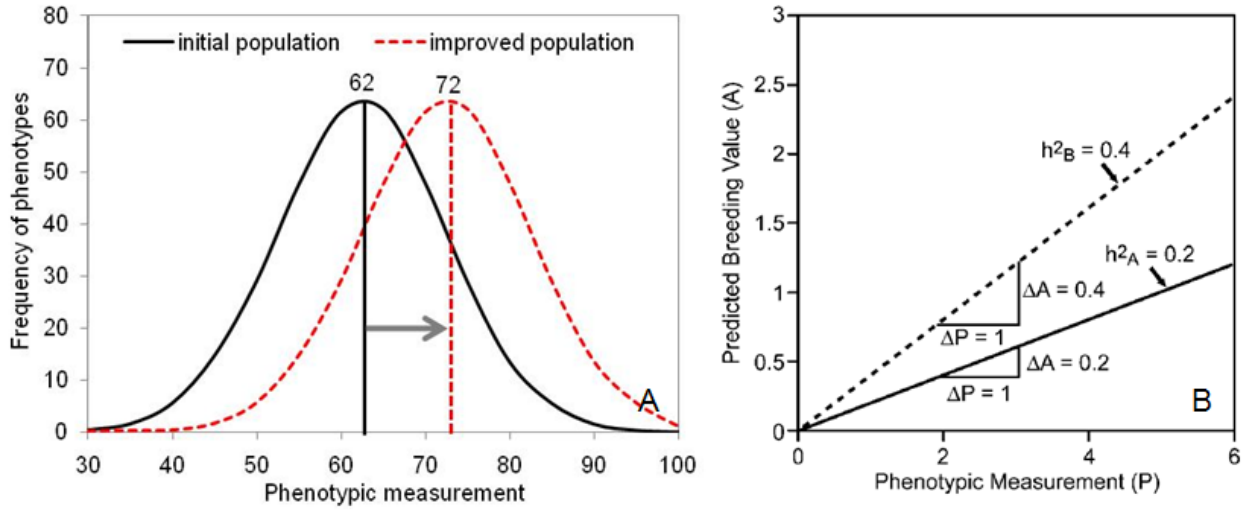

Figure 7 - Genetic gain from tree breeding programs (A, personal source) and graphs of the regression lines of breeding values on phenotypic values for two hypothetical traits, A and B, with h^2_A=0.2 and h^2_B=0.4 (B, from White et al. 2007)

Every successful breeding strategy, therefore, requires efficient methods of selecting superior material including the progeny tests in which the selection is carried out, appropriate measurement techniques and selection technology (Hardwood et al. 2001). In summary, to improve a characteristic of wood, we should be able to accurately measure it by means of a reliable and repeatable method or technique, and such wood property needs to be variable and genetically controlled (inherited). Most wood properties exhibit continuous variation and as such are viewed as quantitative traits influenced by multiple genetic factors and the environment (Zobel and Jett 1995).

1.3.1 Quantitative genetic of wood

Resemblance between relatives with respect to a given wood trait is a basic genetic phenomenon; the degree of resemblance determines the amount of additive genetic variance (Falconer 1993). The causes of resemblance in trees and their wood properties are related to genetics and environment factors (Zobel and Jett 1995). Therefore, the phenotypic value of the growth or wood trait is the sum of genetic and environmental effects.

The genetic of a wood properties centres round the study of its variation, for it is in terms of variation that primary genetic questions are formulated. The basic idea in the study of variation is its partitioning into components attributable to different causes. The relative magnitude of these components determines the genetic properties of the population, in particular the degree of resemblance between relatives.

In genetic approaches, the amount of variations in wood properties are measured and expressed as the variance. According to Falconer (1993) the components into which the variances are partitioned are the genotypic variance (the variance of the genotypic values) and the environmental variance (the variance of the environmental deviations). The total variance of each wood property is the phenotypic variance, or the variance of the phenotypic (measured) values, and is the sum of the separate components. Table 2 lists the components of variance and the values whose variance they measure.

Table 2 - Components of variance of growth and wood traits (from Falconer (1993))

Variance component	Symbol	Value whose variance is measured
Phenotypic	σ^2_P	Phenotypic value
Genotypic	σ^2_G	Genotypic value
Additive	σ^2_A	Breeding value
Dominance	σ^2_D	Dominance deviation
Interaction	σ^2_I	Interaction deviation
Environmental	σ^2_E	Environmental deviation

According to Falconer (1993) the total variance is then, with certain qualification, the sum of the components, thus:

$$\sigma^2_P = \sigma^2_G + \sigma^2_E \quad \text{Eq. (1)}$$

$$\sigma^2_P = \sigma^2_A + \sigma^2_D + \sigma^2_I + \sigma^2_E \quad \text{Eq. (2)}$$

The qualifications are, first, that genotypic values and environmental deviation may be correlated, in which case σ^2_P will increase by twice the covariance of G with E; and, second, there may be interaction between genotypes and environments, in which case the will be an additional component of variance attributable to the interaction.

Most wood characteristics controlling wood quality, such as density, stiffness, lignin etc. are influenced by genetic and environment factors (Zobel and Jett 1995) and can be modified or improved by means of tree breeding programs (Raymond 2002).

Figure 7 contains a hypothetical situation where the offspring from selected parents have improved the target wood property. However, the successful of the genetic gain mainly depends on the heritability level of such trait. The contribution of the genetic variation on the genetic gain (the amount of increase in performance that is achieved through breeding programs) is also of particular importance. When the

characteristic present high heritability estimates (h^2, hereafter called as genetic control) high genetic gains can be achieved. Falconer (1993) states a clear definition of heritability, as well as their applications:

"Heritability of a wood trait is one of its most important properties. It expresses the proportion of the total variance that is attributable to differences of breeding values, and this is what determines the degree of resemblance between relatives. The most important function of heritability in breeding programs is its predictive role, expressing the reliability of the phenotypic values as a guide to the breeding value. Only the phenotypic values of wood traits can be assessed, but it is the breeding value that determines their influence on the next generation. Therefore if the breeder or experimenter chooses individuals to be parents according to their phenotypic values, his success in changing the characteristics of the population can be predicted only from acknowledge of the degree of correspondence between phenotypic values and breeding values. This degree of correspondence is measured by the heritability".

Heritability estimates of two hypothetical traits, A and B, are presented in Figure 7 B. Note that phenotypic values are closer in magnitude to the underlying breeding value for trait B with its higher heritability. Two trees that are different by one unit in their phenotypic value are expected to have breeding values that differ by 0.2 and 0.4 units for traits A and B, respectively. Selection of outstanding phenotypes for trait B is more likely to result in trees that have higher breeding values and therefore, produce better-performing offspring (White et al. 2007).

Therefore, the relative importance of heredity in determining phenotypic values is called the heritability of the wood property. There are, however, two distinctly different meanings of 'heredity' and heritability, according to whether they refer to genotypic values or to breeding values Falconer (1993). Broad-sense heritability estimates (H^2), is the ratio of the entire genetic variance to the total phenotypic variance while narrow-sense heritability estimates (h^2) is the ratio of additive genetic variance to total phenotypic variance (White et al. 2007). In short, the heritability expresses the reliability of the phenotypic values as a guide to the breeding value, or the degree of correspondence between phenotypic values and breeding values (Falconer 1993).

Progeny tests allow the determination of genetic additive variance σ^2_A providing the narrow-sense heritability estimates (h^2) while the Clonal tests allow the determination of the genotypic variance (σ^2_G) providing the broad-sense heritability estimates (H^2). Therefore, it is valuable to have estimates of genetic parameters, such as heritability estimates of the important properties when developing breeding strategies. In the present study, a progeny test and a clonal test were assessed in order to estimate genetic parameters.

1.3.2 *Eucalyptus* breeding programs

The first studies on genetics of *Eucalypts* were carried out to determine the suitability of species and provenances for particular environments (Turner et al. 1983). Thus progeny trials were established in order to evaluate the potential of many progenitors, to estimate genetic parameters and to detect genotype by environment interactions (Wang et al. 1984; Malan 1988). In the past, wood processors tended to demand absolutely straight logs for sawnwood and any deviation from straight logs would translate into lost timber production. Then, the studies on genetics of *Eucalyptus* started to concentrate on tree growth, survival, stem straightness and branch quality because the forest industry was focused mainly on achieving gains in growth and form (Raymond 2002; Dungey et al. 2006). In modern times, the sawing and drying technologies have advanced to the point where stem straightness may not be as important any more (Verryn and Hettasch 2006).

Currently, the purpose of growing plantations is to produce wood, not only in quantity but also in quality, in order to provide a range of wood processing sectors with materials possessing physical, mechanical and chemical properties that match their required qualities. Thus, the need for technological interventions goes beyond productivity gains. In addition to volume, it is important to increase raw materials (wood and fiber) quality and optimize chemical composition contents, pulp yield (for pulpwood), caloric power (for fuelwood), wood density, stiffness and other characteristics of interest of each wood processing sector.

Most of breeding programs of *Eucalyptus* are focusing on important traits to pulp and paper and bioenergy production. The improvements achieved in the last years by the tree breeders for wood quality traits have showed the importance of research in wood anatomy and technology along the genetic improvement program (ABRAF 2010).

Genetic control over growth and wood traits

Numerous studies have addressed to the genetic control of growth traits (Greaves et al. 1997; Wei and Borralho 1997; Kube et al. 2001; Costa e Silva et al. 2004; Volker et al. 2008; Kien et al. 2009; Costa e Silva et al. 2009) reporting variable heritability estimates for these traits in *Eucalyptus* trees. The genetic control for growth traits are lower than those for wood traits, because growth is a polygenic trait strongly influenced by the environment.

Many wood traits have been found to have moderate to high heritability estimates in a range of genera including *Eucalpyptus* (Raymond 2002), *Picea* (Rozemberg and Cahalan 1997) and *Pinus* (Apiolaza and Garrick 2001). Thus, breeding for wood quality traits alone would be effective because heritability for wood quality traits such as wood density, microfibril angle and modulus of elasticity were usually high and there are broad genetic variations (Baltunis et al. 2007). Identification of the genetic factors contributing to quantitative trait variation is an important step in many tree breeding programs.

Genetic control for wood density has been exhaustively reported for many Eucalypt species. It ranges from h^2=0.6 (Kien et al. 2008) to h^2=0.71 (Wey and Borralho 1997) in *E. urophylla*; from h^2=0.51 (Kube et al. 2001) to h^2=0.73 (Greaves et al. 1997) in *E. nitens*, from h^2=0.24 (Poke et al. 2006) to h^2=0.44 (Apiolaza et al. 2005) in *E. globulus* and of h^2=0.17 (Raymond et al. 1998) in *E. regnans*. These examples show that the heritability estimates of such trait exhibit variable magnitudes. Hamilton and Potts (2008) presented a review of the genetic parameters of *Eucalyptus nitens*, reporting that heritability estimates of 12 independent studies ranged from 0.11 to 0.96 presenting mean value of 0.51 for the same species. Despite the large number of studies on this issue, there is no global trend concerning the genetic control over wood density.

The genetic control of the chemical components of wood has been relatively less studied. Gominho et al. (1997) reported high heritability estimates (h^2=0.83) for lignin content in *E. globulus* clones. Poke et al. (2006) evaluated open-pollinated families of *E. globulus* reporting narrow-sense heritability estimates of h^2=0.13±0.2 and family means of h^2=0.42± 0.19. Apiolaza et al. (2005) examined 188 open-pollinated progenies of 11-year-old *E. globulus* reporting high narrow-sense heritability estimates for cellulose content (h^2=0.84±0.27) and moderate ones for pulp yield (h^2=0.44±0.24). Costa e Silva et al. (2009) evaluated *E. globulus* progenies finding moderate heritability estimates (h^2=0.42±0.14) for pulp yield.

Few studies have reported genetic parameters for shrinkage and anatomical features, but these traits are known to be partially under genetic control. For instance, Pelletier et al. (2008) have investigated the genetic variation in linear shrinkage of 152 open-pollinated families of *Eucalyptus pilularis* reporting moderate heritability estimates (h^2=0.36±0.1) for tangential shrinkage but not significant for radial shrinkage (h^2=0.1±0.09) or the ratios of the two. Raymond et al. (1998) examined the genetic control fibre

length and coarseness in 10-year-old *E. regnans* finding low estimates of heritability for fibre coarseness (h^2=0.15) and moderate for fibre length (h^2=0.36). Apiolaza et al. (2005) reported low (and not significant) heritability estimates for fibre length (h^2=0.16±0.17) in 11-year-old *E. globulus*.

The genetic control over microfibril angle was seldom reported for *Eucalyptus*. Apiolaza et al. (2005) used increment cores from 188 open-pollinated progenies of 11-year-old *E. globulus* reporting h^2_{MFA}=0.27±0.24 while Lima et al. (2004) reported broad-sense heritability estimates ranging from 0.13 to 0.36 in 8-year-old clones of *E. grandis* x *E. urophylla*.

Genetic and residual correlations

An observed phenotypic correlation between two wood traits may be due to genetic or environmental causes, their interaction and also to ontogenic factors (age etc) inside the tree. Just as with phenotypic variances, there is a need to understand these underlying components that give rise to a phenotypic correlation (White et al. 2007). Genetic correlation can be defined as the ratio of genetic covariance and the product of the genetic standard deviations of two traits and can be thought of as the correlation of the breeding values (Falconer and Mackay 1996).

Two mechanisms can play a major role on genetic correlations: (i) pleiotropic (manifolds) effects of genes and (ii) linkage disequilibrium (non-random associations of alleles) between loci affecting different characters (Falconer 1993). When pleiotropy occurs this implies that a given gene locus influences the expression of more than one trait (Mode and Robinson 1959). When linkage disequilibrium occurs this means that the genes controlling these traits can be statistically associated, but there is no functional relationship between them.

An observed phenotypic correlation between two traits may also be caused by an underlying environmental (or residual) correlation (r_E) if environmental effects that influence one trait also influence the second trait (White et al. 2007). For example, consider a hypothetical conifer stand in which favorable microsites in the stand (e.g. locations with moister, deeper soils) lead to faster spring stem diameter growth. That is, the amount of spring wood is increased on favorable sites, but growth later in the season is unaffected (and therefore, the amount of late wood is similar on all microsites). Trees on these favorable microsites tend to have faster diameter growth and lower wood specific gravity, since they have a larger fraction of spring wood, which has lower specific gravity than late wood. In this case, there is a negative environmental correlation between diameter growth and wood specific gravity (faster diameter growth associated with lower specific gravity). This does not imply any relationship between the gene loci affecting the two traits, and there may or may not be a genetic correlation.

Genetic and environmental correlations are equally important in estimating the correlated response to selection in breeding programs (Falconer and Mackay 1996). Adverse genetic correlations can curtail breeding progress as, for example, a negative genetic correlation between growth and wood density would make it more difficult to select concurrently for improvement in both traits. Thus, estimating genetic correlations between traits of interest is necessary in proposing the basis for setting up breeding populations and selecting environmentally stable genotypes (Kien et al. 2009).

Genotype by environment interactions

According to White et al (2007) the essence of genotype x environment interaction is a lack of consistency in the relative performance of genotypes when they are grown in different environments. This may mean that the relative rankings of genotypes change in the different environments (called rank change interaction) or that, even in the absence of rank changes, differences in performance are not constant in all

environments (called scale effect interaction). Lima et al. (2000) states that "following a study of interactions it may be possible to identify genotypes with high general adaptability (for example, genotypes which produce wood with high basic density on a range of sites) and others which perform better on particular sites".

According to Muneri and Raymond (2000), genotype by environment interaction may be caused by two factors: different variances between the sites, or changes in the ranking of genotypes across sites. Thus, determining the size and practical importance of genotype by environment interactions is critical for designing tree breeding programs and making decisions about plantation establishment (Muneri and Raymond 2000).

Many *Eucalyptus* forests are planted over a wide range of climatic and edaphic conditions because the pulpwood producers may have extremely large surfaces of plantations for supplying wood to attend their ever-increasing demand for pulp and paper. While some clones have wide amplitudes in terms of the areas where they grow and perform well, other varieties have narrower limits. This is an important concern for wood industry.

Which traits to breed for?

Currently, tree breeders are faced with a growing "shopping list" of traits for which to breed, and in a shorter time period. This is a perilous situation, because, as the list of selection criteria increases, so too does the size of the breeding effort increase, or alternatively, the breeder may have to reduce the level of improvement in the traits (Verryn 2008). A range of key traits to breed for each industrial need was suggested by Raymond (2002). According to her, for pulp and paper industry, the main characteristics are basic density, pulp yield, and cellulose content and fibre length. For sawn timber production, the traits of importance probably are basic density and gradient, microfibril angle, strength and stiffness, dimensional stability, shrinkage and collapse, tension wood, knot size, incidence of decay, spiral grain and end splits. The wood colour is also an important characteristic. For composites manufacturing, the key traits are suggested to be basic density and lignin, extractive and cellulose contents. For bio-energy purposes, wood may have high basic density and lignin content and superior mechanical properties (Brito and Barrichelo 1977).

Breeding strategies for different industrial application are not the same because the processing technologies require different, changing, and sometimes opposing, wood properties. For instance, lignins are undesirable compounds for pulp and paper production, because the delignification process requires energy and reagent consumption (Chang and Sarkanen 1973). Thus varieties of trees growing for pulpwood production should present lignin content as low as possible. On the other hand, the wood for bio-energy applications (charcoal production) may contain high lignin content (Brito and Barrichelo 1977) since wood with high lignin content is known to provide charcoal with high caloric power (Chen et al. 1997).

1.3.3 Challenges

The great difficult for improving wood by means of breeding programs is the high cost involved on wood phenotyping. Indeed, the difficulty and cost of measuring such wood traits in large samplings have limited the efforts from wood specialists in understanding the genetic and environmental contribution on wood variation. As genetic studies require large dataset, producing them is very expensive and can make the implementation of the project impracticable.

A challenge for tree breeders and wood quality researchers of today is to respond appropriately to a complex environment demanding more productivity, higher quality, and a quicker adaptation of their crops to rapid changes (Verryn 2008). In this context, it is essential to know the variability, the inheritance, the genetic and environmental control of the wood traits (in particular, the orientation of the microfibrils in the S_2 layer of cell wall) of *Eucalyptus* wood and its implications with others properties. Hence, the use of new available methods and tools, model plant systems, molecular biological and genetic techniques can make a significant contribution to understand how and why microfibril angle changes in wooden plants (Donaldson 2008).

Considering the great silvicultural advantages of *Eucalyptus* and the low volume of wood managed towards to sawmills in Brazil, researches on *Eucalyptus* wood quality are required in order to verify if this wood specie can be an alternative for sawn timber industry.

1.3.4 Strategies for wood phenotyping

In tree breeding programs, knowledge of wood traits and their measurement are essential to generate reliable findings. The development of rapid, accurate and industrially feasible methods becomes therefore necessary for characterization and classification of raw material in the forestry-related industry, including pulp and paper or steel production (charcoal), since these companies require methods that will cover a large number of samples. In order to accurately measure the wood traits, there is the need to have systems capable of evaluating the wood properties rapidly, precisely, without altering its end-use capabilities and at low cost. Among the current techniques, sonic resonance, X-ray diffraction and near infrared (NIR) spectroscopy are emerging technologies that could provide large data set of wood measurements.

According to Ross and Pellerin (1994), the techniques and methods for evaluating wood differ greatly from those for homogeneous, isotropic materials such as metals, plastics, and ceramics. In such non wood-based materials, whose mechanical properties are known and tightly controlled by manufacturing processes, the techniques for evaluation are used only to detect the presence of discontinuities, voids, or inclusions. However, in wood, these irregularities occur naturally and may be further induced by degradative agents in the environment. Therefore, sonic resonance, x-ray diffraction and near infrared (NIR) spectroscopy could be applied in wood to measure how genetic and environmental factors induces variation in a woods.

1.3.4.1 Methods for assessing standing trees

Nowadays a range of techniques has been proposed for generating a large data set in order to evaluate phenotypic, genetic and environmental parameters for a range of wood properties. Some non-destructive techniques, such as Resistograph (Rinn 1994; Rinn et al. 1996) and Pilodyn wood tester (Rozenberg and Van de Sype 1996; Raymond and MacDonald 1998) have been extensively used because they make possible the evaluation of trees in field. Figure 8 shows the two portable devices for evaluating living *Eucalyptus* trees in field conditions.

The Pilodyn instrument consists of a spring-loaded pin device that drives a hardened steel pin into the wood (Ross and Pellerin 1994). Originally, it was developed to measure of degree of degradation by means the depth of pin penetration (Hoffmeyer 1978), but nowadays this parameter is used as criteria for selection of trees by the density of their wood. For instance, Greaves et al. (1996) used Pilodyn for the indirect selection of basic density in *E. nitens* in field conditions. Then, a range of similar studies were done in order to evaluate genetic parameters in *Eucalyptus* (Rosado et al. 1983; MacDonald et al. 1997;

Kien et al. 2008; Volker et al. (2008), *Pinus* (Klein 1995; Wang et al. 1999; Koch and Fins 2000) and *Picea* plantations (Rozenberg and Van de Sype 1996; Hansen and Roulund 1996).

Resistograph was originally developed to evaluate the health condition of trees and wooden poles (Costello and Quarles 1999); however, it has been suggested as a promising technique for estimating wood density and its genetic parameters in many wooden species. Many studies have used this portable instrument for generating data set for genetic studies on *Eucalyptus* (Lima et al. 2007; Rodrigues et al. 2008), *Pinus* (Gantz 2002; Isik and Li 2003) and *Pseudotsuga* (Chantre and Rozenberg 1997) genera, among other.

Figure 8 - Evaluating standing trees with Resistograph (A) and Pilodyn (B). Dotted lines shows in detail the pine penetration (source: personal image)

Indeed, these field portable equipments are able to estimate wood density in standing trees producing large data base in situ. Their advantage is their relatively low cost for purchasing and maintenance. Whilst they are attractive for real-time assessment of forests, their performance has had contradictory acceptance. While some studies reports clear correlation between density and pine penetration, other studies had shown indicative results. Pilodyn, for instance, is able to assess only the wood of the external portion of the stem providing a local inspection. It is not possible to assess how the wood density varies inside the tree or stem. According to Raymond (2002), the use of a pilodyn is not recommended for indirect assessment of basic density in breeding programs due to the low heritability of pine penetration. The resistograph results are strongly affected by wind because the tree swings altering the tension on the outer stem. Moreover, there may be mechanical problems resulting from intensive use of equipment.

Ultrasonic tomography has been used for evaluating the internal condition and decay on living trees using sound waves (Nicolotti et al. 2003; Gilbert and Smiley 2004; Deflorio et al. 2008). In short, a series of sensors are installed around the tree for sending or receiving sound waves. The distances between the measuring points are measured and recorded. Then, sound waves are generated by a hammer tapping on one of the sensors and the time of flights of sound waves between the sending point and the other receivers are measured. Finally, the apparent sonic velocities (distance/time) are calculated and a "velocity" or "density" map of the tree is plotted by combining the measured tree geometry with sonic data recorded during the assessment (Figure 9). The sonic velocity can be correlated with wood densities and therefore with the soundness of the wood. Bucur (2003) lists a range of methods and techniques for non-destructive characterization and imaging of wood and standing trees.

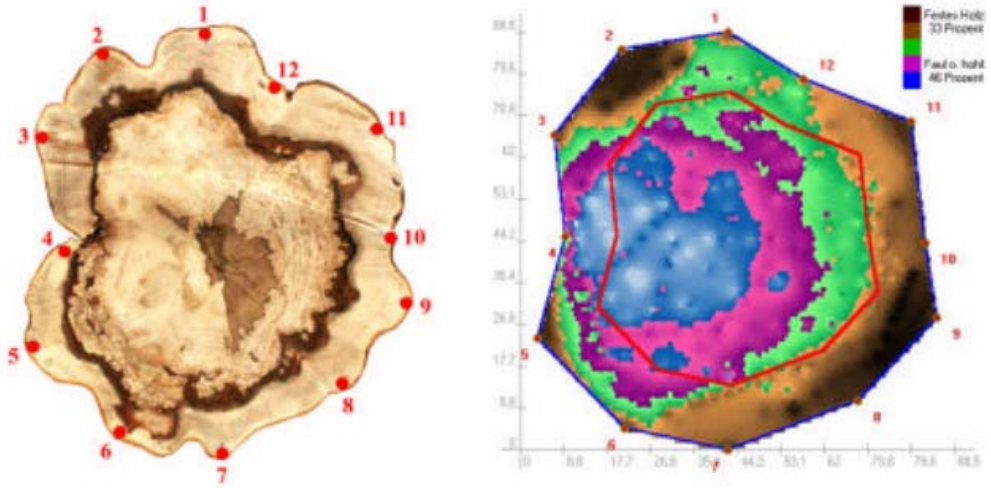

Figure 9 - Example of tomography analysis; a photograph of the disc (diameter: 90 cm) and the corresponding acoustic tomogram showing the decay (blue parts) in a wood disc (from Rabe et al. (2004))

1.3.4.2 X-ray densitometry

Radiation densitometry is a commonly used technique for assessing density characteristics of wood samples. Most of applications have used variations of the Polge (1963) method, i.e., production of a negative image of a wood sample by exposure of the wood and a film to X-rays generated electrically. The films must be developed under carefully controlled conditions and analysed in some form of optical densitometer to give analog or digital output of wood density variations (Cown and Clement 1983). The X-ray system gained widespread acceptance for evaluating variations of wood density (Walker and Dodd 1988). Decoux et al. (2004) have compared optical anatomical measurements to wood density variations assessed by X-ray densitometry within annual rings in softwoods. In *Eucalyptus*, Tomazello et al. (2008) have shown the application of X-rays for evaluating wood density changes across radial samples.

1.3.4.3 Sonic Resonance

Natural vibration analysis is a simple and efficient way of characterizing the mechanical properties of many materials, including wood (Bucur 1995; Brancheriau and Baillères 2002). Using various species of wood, sample dimensions and growth conditions, several studies have shown a strong linear correlation between dynamic and static modulus of elasticity (Ross et al. 1991; Wang et al. 2001; Green et al. 2004; Biblis and Carino 1999; Biblis et al. 2004). For instance, Ilic (2001) obtained strong correlations between static test and longitudinal (r=0.95) or flexural (r=0.99) elastic modulus using short specimens (20 mm x 20 mm x 300 mm) of *Eucalyptus delegatensis* R. Baker. Using larger pieces, Brancheriau and Baillères (2002) reported good correlation between Young's modulus in four-point bending and the flexural vibration modulus of elasticity on 76 beams of *Dicorynia guianensis* Amsy.

Dynamic tests based on the resonance frequency have been applied successfully in order to assess the dynamic modulus of elasticity of small, clean specimens (or clearwood) at the laboratory scale (Haines et al. 1996; Ilic 2003; Brancheriau and Baillères 2003; Ohsaki et al. 2007), as well as of structural timber (Haines et al. 1996; Burdziak and Nkwera 2002; Liang and Fu 2007; Jiang et al. 2010) and logs (Ouis 1999; Wang et al. 2002; Grabianowski et al. 2006).

BING (Beam Identification by Non-destructive Grading) is a portable, simple and low-cost system developed at CIRAD (http://www.xylo-metry.org/fr/bing.html) allowing precise, reliable material

characterization (Figure 10). Based on resonance frequency of vibrating beams measured by this system, it is possible to calculate the modulus of elasticity, shear modulus and internal damping in a range of materials, with various cross-sections, such as wood, metals, plastic, and ceramics.

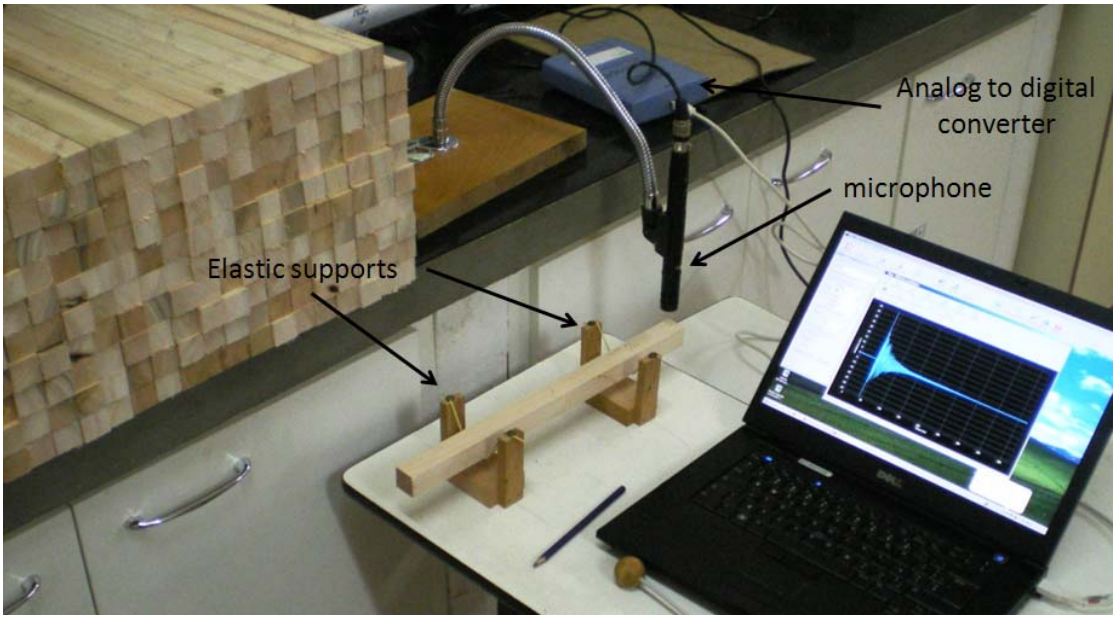

Figure 10 - Portable device for estimating dynamic elastic properties of wood based on sonic resonance frequency (source: personal image)

1.3.4.4 Near infrared spectroscopy

Near infrared spectroscopy (NIRS) is a fast, non-destructive technique (one minute or less) applicable to any biological material, including on-line processes, demanding little or no sample preparation (Pasquini 2003). It is based on vibrational spectroscopy which measures the interaction between light and the material (Næs et al. 2002). Bokobza (1998) and Pasquini (2003) reviewed the basic theory of NIR spectroscopy and its applications presenting the concepts that make a near infrared spectrum understandable. The simple physical principles of the spectrometer are presented in Figure 11. This NIR spectrometer device that operates in transmittance mode, however, there are also spectrometers equipped with sensors that measure the amount of light absorbed or reflected by the material.

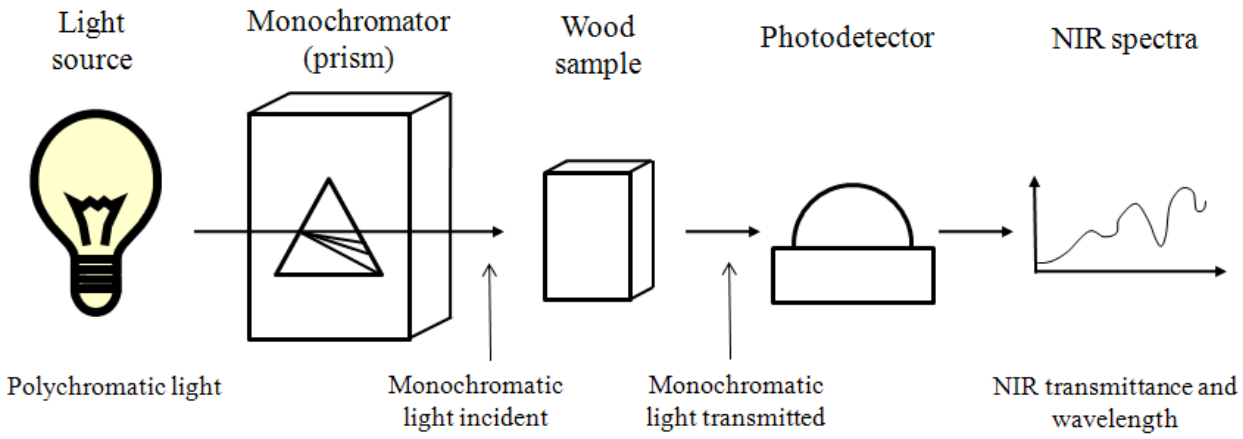

Figure 11 - Schematic of NIR spectrometer readings

In resume, the technique relies on developing a calibration that relates the NIR spectra of a large number of wood samples to their known chemical constitution, for example pulp yield or cellulose content (Raymond 2002). This NIR-based calibration is then used to predict, for instance, the pulp yield or cellulose content of further samples.

The first works that used the NIR spectroscopy technique to assess wood concentrated on properties directly related to wood chemistry and were based on milled chips obtained from composite whole-tree samples. Birkett and Gambino (1989), Easty et al. (1990), Wright et al. (1990) and Wallbacks et al. (1991) presented the first results concerning NIR spectra and chemical properties of the wood, especially its cellulose content. Later, NIR spectroscopy approach has been also extended to assess non-chemical characteristics of solid wood samples showing that NIRS is capable to also estimate physical, mechanical, and anatomical features. The first study involving NIR spectra and wood density probably was presented by Thygesen (1994). She used shavings and solid wood of Norway spruce *Picea abies* (L.) Karst. demonstrating that the technique could be used to estimate the dry matter content and density of wood. Afterward, Hoffmeyer and Pedersen (1995) used NIR spectroscopy in solid wood samples of the same specie to evaluate dry density (dry weight per dry volume). They stated that NIRS could be used to predict wood density, compression and bending strength of dry wood. Since then, NIR spectroscopy has been widely used to evaluate many wood traits covering a wide range of applications. Tsuchikawa (2007) presented a complete review article where recent technical and scientific reports concerning the main NIR spectroscopy application in the wood are discussed. NIR spectroscopy models are especially attractive for tree breeders and genetic programs because it is possible to quickly provide estimates of many wood traits from a single NIR spectrum, if a NIR-based calibration is available. Since measuring NIR spectra is a simple operation, large data set can be rapidly produced at relatively low cost.

1.4 Scientific strategy

To understand the processes that govern the growth of the tree and to optimize the use of wood as a raw material in many industrial applications, numerous research activities are directed to cover different aspects of the structure and properties of wood (Peura 2007). Hence, much knowledge about wood structure, its properties and its performance in industrial applications has been accumulated over the years. However, many questions concerning wood properties, the methods of their measurement, and the analyses made from them remains still unclear. Moreover, the strategy that trees uses to change the MFA, stiffness and density of their wood in order to survive and to respond to specific needs (wood more or less dense, stiff etc) and the interactions between the growing tree and its environment is not well established.

1.4.1 Lacks of knowledge

Knowledge concerning wood, its properties, its variability and its performance in various applications are continuously increasing. However, a series of questions concerning these issues are raised.

1.4.1.1 Wood traits, its variation and relationships

Eucalyptus is the main genera for forestry in Brazil, where the plantations were target for pulp and paper production and bio-energy applications. The forest companies plant their genetically improved varieties of *Eucalyptus* trees on lands of all type, from drastic conditions (sloped terrain, hydric stress, strong winds, poor fertility etc) to optimal conditions (plan fields, light winds, good fertility etc) and they have the hard goal of producing homogeneous products from variable raw material. In this regard, the tree breeder and wood processors have to be aware of some important aspects.

How do wood traits vary within trees?

From an evolutive point of view, the variation of wood traits is vital for tree survival. Trees change their wood in order to respond to specific needs. For instance, if prevailing winds occur, the tree produces a kind of flexible wood (high MFA and low E/ρ) to resist to the bending forces induces by winds. Thus, the microfibril angles and lignin content drastically decrease while cellulose content increases when trees produce tension wood. This wood is stiffer making the tree able to withstand wind action. Such mechanism is well known in the literature; however, the genetic control of this phenomenon is unknown.

On the other hand, knowing how the key traits vary longitudinally and radially within the stem is of key importance for processors. Information about how the wood traits change within the stem in *Eucalyptus* clones planted on contrasting sites are unknown and would be useful in order to increase its economic value. The spatial variation of microfibril angle, elastic modulus and density, as well their relationships along the stem are not well known in *Eucalyptus* trees and are issues that deserve further studies. This kind of knowledge would be valuable to determining the best position for sampling, for instance.

What are the traits of key importance?

Breeders and processors should work on the traits of key importance for controlling the wood and end-product quality. While the importance of the microfibril angle for wood quality is well established for softwoods (Donaldson 2008), the relationship between MFA and wood quality traits remains unclear in *Eucalyptus* wood reserving further studies. Moreover, the effects of some environmental conditions (such as plantations on sloped terrains) on growth rate and wood quality are not well established for fast-

growing plantations. This issue is of particular concern, at least in Brazil, where plantations are grown in variable conditions and regions.

Besides increasing volume production and kraft pulp or calorific value yield, breeders and growers should be alert to biological and mechanical requirements for trees survival. Trees may be stiff enough to support the bending movements in response to wind without breaking and maintaining its erect habit. Hence, MFA and its relationships with density, wood stiffness and strength of woods from fast-growing plantation can be a critical subject deserving deeper investigation.

How to manipulate wood quality

Wood specialists may know in which extent key traits control the wood quality**.** The extent in which the microfibril angle controls the stiffness in *Eucalyptus* wood is not well established. Indeed, the papers by Evans and Ilic (2001) and Yang and Evans (2003) who exploring the relationship between MFA, ρ and E in *Eucalyptus* wood have demonstrated that MFA was the prime determinant of both the E and the specific modulus (E/ρ). However, their data come from Silviscan device (aparattus developed and presented by Evans 1999), which is a powerful instrument for MFA measurement for the one who can access to one of the three apparatus in the world. Indeed, the relationships between MFA and wood stiffness were still not verified in *Eucalyptus* by studies based on non-Silviscan data. If their conclusions can be generalized, selection of trees by MFA should make possible the improvement of the wood quality.

1.4.1.2 Questions concerning techniques for assessing wood traits

In order to phenotyping wood, there is a need to have systems able to precisely, rapidly, and at low cost evaluate them. The techniques employed in this thesis (sonic resonance, near infrared spectroscopy and x-ray diffraction) are used for wood characterization since long time ago. For instance, the relationship between modulus of elasticity and vibration frequency is known to nearly 150 years. Specifically for wood, early studies involving the resonance technique started more than 50 years (Jayne 1959). NIR spectra were used to investigate relationships between water and gelatine (Ellis and Bath 1938) more than 70 years ago. In wood, it is likely that Birkett and Gambino (1989) were the first to report findings involving NIR spectra and wood characteristics. X-rays were discovered in 1895 and used as a technique for producing interesting images of all kind. Then, X-ray diffraction patterns has been used to determine the preferred angle of the cellulose microfibrils of cell walls after the initial studies reported by Preston (1934) who analyzed single tracheids of Sequoia and *Abies nobilis*. Nowadays, these techniques are currently used in science and technology of wood and a sizable body of literature exploring such techniques are available; however, many methodological aspects still need to be better clarified. Some of these specific aspects are raised below.

What is the relationship between the characteristics obtained from laboratory tests and those of the material working in real situations?

In wood science and technology, much knowledge about the wood strength and flexibility has been accumulated over the years. In this regard, the dynamic tests based on the resonance frequency has played a major role since the technique have been applied successfully in order to analyze the dynamic modulus of elasticity of wood samples of any dimensions, from small specimens at the laboratory scale to logs.

Most studies have been done in order to evaluate the mechanical properties of pieces of wood with variable dimensions from large to small specimens. Few studies have been compared the mechanical properties obtained on large pieces of wood and on small specimens sampled from them. The relationships

between the mechanical properties of large and small wood samples are not still well established, especially for *Eucalyptus* wood. These findings would be useful in explaining the scale effect observed on mechanical behaviours of small clear specimens (as they are tested at the laboratory) and structural size material (as they would be really employed). This issue deserves deeper investigation since *Eucalyptus* wood is becoming a potential source as building material.

In order to provide the best estimates of chemical traits of wood, the NIR spectra should be measured in which conditions of sample preparation?

Numerous studies have reported the effects of varying wood surfaces on the NIR spectra (Tsuchikawa et al. 1992; Gierlinger et al. 2004) and their influence on model performance (Thumm and Meder 2001; Schimleck et al. 2003; Jones et al. 2006). However, the influence of the milling procedure, particle size, and solid wood surface quality on NIR-based calibrations for chemical traits is unknown, especially in *Eucalyptus* wood. Thus, wood specialists do not know precisely how they should prepare their samples in order to extract the maximum of information from them. This issue deserves further investigation.

Why NIR spectroscopy is able to estimate non-chemical wood traits, such as wood density, elastic properties and anatomical features?

Although the feasibility of NIR spectroscopy has been shown for numerous wood traits, it is still unclear how this technique can evaluate physical, mechanical traits and anatomical features of wood on the basis of vibrational spectroscopic analysis. In this context, many aspects need to be clarified by validating NIR-models, and analysing and interpreting coefficient regressions.

The association of near infrared spectroscopy, sonic resonance (for estimating elastic properties), x-ray diffraction (for estimating microfibril angles) and multivariate analysis would be a useful, rapid and reliable tool for phenotyping wood. NIR calibrations for dynamic elastic properties based on resonance technique were rarely reported. It is likely that Fujimoto et al. (2008) were the first team to report findings in regard to this issue.

Concerning MFA prediction by NIR spectroscopy, most of studies have been based on reference data provided by SilviScan measurements. NIR calibrations for MFA based on polyvalent X-ray difractometer and NIRS devices are rarely reported. Schimleck et al. (2007), Kelley et al. (2004) and Huang et al. (2008) used softwoods to build their NIRS calibrations for MFA based on measurements made on polyvalent XRD apparatus. There is no report that the association of XRD and NIR would yield good calibrations for more complex wood, such the hardwoods species.

How accurate NIR-based models can predict wood traits in unknown samples?

Several works have used independent test sets to validate their NIR-based calibration for wood traits (Fujimoto et al. 2008; Schimleck et al. 2001; Via et al. 2003; Via et al. 2005; Cogdill et al. 2004; Gierlinger et al. 2002; Mora et al. 2008). These studies were carried out on a sampling systematically divided in two groups and the regressions were performed with one group and validated with the other. These approaches do not adequately simulate a real situation where the properties of unknown samples may be predicted by established NIR models. Few studies have been addressed to verify the robustness of the predictive models using external and independent sample sets (Souza-Correia et al. 2007; Rodrigues et al. 2006). The NIR spectroscopy ability of predicting wood traits on unknown samples from pre-established models is still not fully demonstrated and then, this issue requires further simulations.

1.4.1.3 Lack of information on Genetics of Eucalyptus wood

A number of wood traits, including wood density, stiffness and microfibril angle were identified as worthy of attention for *Eucalyptus* tree improvement (Raymond 2002). Recent studies have centered on the heritability of stiffness and MFA in softwoods (Dungey et al. 2006; Baltunis et al. 2007; Wu et al. 2007), but the degree to which stiffness and MFA are heritable and their genetic relationship with other traits in *Eucalyptus* has been poorly reported. It is likely that there is only one study reporting narrow-sense heritability (Apiolaza et al. 2005) and one study providing broad-sense heritability (Lima et al. 2004) of MFA in *Eucalyptus*. Moreover, genetic and environmental correlations among MFA, elasticity, density, lignin, S/G ratio and growth traits are unknown in *Eucalyptus*. Hence, the extent in which the microfibril angle, stiffness and density are regulated by additive genetic and environmental effects; how are the relationship of MFA and E with the other physico-chemical and growth traits, and how these relationships vary within the tree are still not well established in *Eucalyptus*. Finally, the means through which trees control changes in MFA, density, wood stiffness in response to developmental and environmental influences are poorly understood.

Indeed, the difficulty and cost of measuring such wood traits in large samplings have limited the efforts from wood specialists in understanding the genetic and environmental contribution on wood variation. If high throughput phenotyping tools exist, and make possible obtaining large dataset from a range of experimental dispositive, these issues are able to be answered, at least partially.

1.4.2 Hypothesis of this study

The present study has tested three hypotheses:

1) MFA controls the wood stiffness even in juvenile wood of *Eucalyptus*;

2) MFA and wood stiffness are heritable traits and could be tampered by mating in *Eucalyptus* breeding programs by combining the most favourable genes (allelic forms) and

3) MFA and wood stiffness, in addition to the commonly used wood traits (growth traits and wood density), could be used as target properties in current breeding programs for *Eucalyptus* in order to produce phenotypes exploitable for a wide range of processing needs, allowing effective response to the rapidly changing market, technological, and natural environments.

1.4.3 Purposes of this study

This study was undertaken in order to meet three main objectives, namely:

[i] to establish the radial and longitudinal variation of the microfibril angles, wood stiffness and basic density within *Eucalyptus* trees;

[ii] to provide information about the effective influence of MFA on *Eucalyptus* wood traits;

[iii] to generate a better understanding about the genetic and environmental control over MFA, wood stiffness, basic density and chemical properties of *Eucalyptus* wood.

To attend the main goals of this study, two experimental designs were investigated, namely:

Progeny test: factorial design represented by 35 full-sib families of 14-year-*Eucalyptus urophylla* coming from mating between 16 parents (8 mothers and 8 fathers) conducted by the "Centre de Recherche sur la Durabilité et la Productivité des Plantations Industrielles" (CRDPI) in Pointe Noire, Republic of Congo;

Clonal test: experimental design represented by 10 clones of 6-year-*Eucalyptus* hybrids (*E. urophylla* and *E. grandis*) from tests managed for pulp and paper production by "Celulose Nipo-Brasileira S.A" (CENIBRA), in Belo Oriente, Minas Gerais State, Brazil.

Specific objectives

The specific objectives concerning wood and its variation of this study were: **(i)** to understand the effect of environmental factors on the variation patterns of microfibril angle, wood stiffness and wood density and **(ii)** to establish the correlation between the stiffness of scantlings and small specimens of *Eucalyptus* wood. These findings would be useful in explaining the scale effect observed on mechanical behaviours of wood of different dimensions.

Concerning the methods and techniques for phenotyping wood, polyvalent techniques such as X-ray diffraction and sonic resonance were combined with near infrared spectroscopy in order to obtain precise information from the wood. Then, multivariate data analyses were applied for extracting information about physical, mechanical, and chemical characteristics and also anatomical features of the wood. The specific objectives concerning the NIR spectroscopic models were: **(i)** to evaluate the influence of the milling procedure, particle size, and solid wood surface quality on the predictive power of NIR spectroscopy models for chemical properties of *Eucalyptus* wood; **(ii)** to evaluate the robustness of the predictive models based for wood basic density in *Eucalyptus* wood using two totally independent sample sets; **(iii)** to build NIR spectroscopy models for estimating modulus of elasticity and visco-elastic traits in *Eucalyptus* wood using reference values obtained from dynamic tests; **(iv)** to develop NIR spectroscopy models for estimating MFA traits in *Eucalyptus* wood using reference values obtained by X-ray diffraction.

The genetic studies of the present thesis were performed from two distinct trials, the clonal and the progeny test. Genetic approaches of the clonal test were made using dataset obtained from dynamic tests of large pieces of wood, and from NIR-based estimates of MFA, wood stiffness and density across the discs. Thus, the specific objectives concerning the genetic studies of the clonal test were: **(i)** to investigate the clonal and environmental variation of the elastic properties on large pieces of 6-year-old *Eucalyptus grandis* x *urophylla* wood by means of sonic resonance technique and **(ii)** to explore the variations of the genetic control over basic density, stiffness and microfibril angle of wood within clones of 6-year-old *Eucalyptus grandis* x *urophylla* stem. The genetic approaches of the progeny test were done using dataset obtained from NIR-based estimates of chemical component contents, wood density and MFA values along the discs. Therefore, the specific objectives of the study of progeny test were: **(i)** to determine the level of genetic control over MFA in control-pollinated progeny families of 14-year-old *Eucalyptus urophylla* wood; **(ii)** to determine the genetic and environmental correlations among microfibril angle, wood density, lignin content, syringyl to guaiacyl ratio and growth traits and **(iii)** to investigate the age trends of these genetic parameters.

Knowledge about the variations in wood density, modulus of elasticity and microfibril angle of commonly deployed clones can better describe genetic gains made by each clonal variety. Thus**,** this thesis hopes to be able to respond/indicate how variable are the wood traits in *Eucalyptus* plantations; if the woods from these trials can be improved and how much; and which are the most appropriate genotypes for timber production to future *Eucalyptus* plantations in Brazil.

1.4.4 Strategy of this study

To attend its purposes, this study falls into two parts. The first consisted on phenotyping wood traits and the second on the quantifying the genetic parameters of wood traits. The strategy of this study is described below. It presents a resume of all activities of this study, including procedures for sample preparation and measurements of wood traits, as well the main analysis. The detailed description of each item is provided within Material and Methods, and Results and Discussion sections.

1.4.4.1 Phenotyping wood traits

A detailed investigation about wood characteristics of many kinds of samples (from larger samples to small specimens) was carried out using the wood from the progeny and clonal tests. Figure 12 sums up the growth and wood traits under examination in the two experimental designs.

Progeny test

The wood of the trees of the progeny test were investigated from wood discs. First, the discs were cut into two opposite wedges and radial strips (free of knots and defects). NIR spectra were recorded on the radial surface of the wedges on three radial positions (1, 2 and 3) from pith to bark. Then, the wedges were grounded and NIR spectra were obtained from the wood powders. These NIR spectra were used for predictions. The radial strips were divided in small samples (20 x 20 x 30 mm) for wood density measurements and tangential sections (2 x 20 x 30 mm) for MFA measurements. NIR spectra were recorded on transversal, radial and tangential surfaces of small samples and on two sides of tangential sections. Afterwards, three *T* values were recorded by X-ray diffraction at three points on 175 tangential sections and basic density of wood was measured on the off-cut small samples. **Paper 3** reports the radial variation of MFA and wood density, the correlation between them and the influence of age on such relationships in the 14-year-*Eucalyptus urophylla* wood.

Clonal test

One-hundred fifty trees were harvested from Clonal tests. A log measuring 2.4 meters and 5 wood discs were cut at 0, 25, 50, 75 and 100% of the commercial height were cut from each tree. Diametrical strips were cut from the discs. The diametrical bands were sanded and NIR spectra were recorded. These NIR spectra were used for further predictions. The logs were cut into central boards, and a total of 410 pieces of wood with nominal sizes of 45 x 60 x 2,100 mm (hereafter referred to as scantlings) were taken from the central boards. Subsequently, a pile of scantlings was set up for air-drying under protected exterior conditions (shed of the wood processing sector at UFLA, Brazil) during 90 days. After air-drying process the scantlings presented defects such as small cracks, checks and splits in their ends and, therefore, were trimmed to variable dimensions, depending of the extension of their defects. The clean scantlings had, on average, 1.54 meters of length, varying from 0.645 m to 2.080 m and the averaged width and thickness were 60 and 43 mm, respectively. The scantlings were submitted to flexural and longitudinal vibration tests. Subsequently, the air-dried (unseasoned) scantlings were kiln-dried at 14% (nominal) of moisture content under soft condition during two weeks. Thus, new flexural and longitudinal vibration tests were performed on the kiln-dried scantlings. Finally, small, clean specimens measuring 25 x 25 x 41 mm were cut from the scantlings and submitted to transversal and longitudinal vibration tests. The mass and dimension of the scantlings and the small, clear specimens were measured and the air-dried density of each piece of wood was calculated. The dynamic properties of these woods are discussed in the **paper 1** while the genetic approaches obtained from these results are reported in **paper 9**.

Progeny test (14 years)
Eucalyptus urophylla x E. urophylla

Density of plantation: 4 m x 4 m
Origin: Republic of Congo
Sampling: 348 wood discs (9-10 by family)

Traits: circumference and height, klason lignin, Syringyl to guaiacyl ratio, basic density and microfibril angle

Clonal test (6 years)
Eucalyptus urophylla x E. grandis

Density of plantation: 3 m x 2 m
Origin: Brazil
Sampling: 750 wood discs (10 clones x 3 sites x 5 repetitions x 5 longitudinal positions)
Traits: circumference and height, wood density, modulus of elasticity, specific modulus, modulus of rupture, shear modulus, loss tangent, shrinkage and MFA

Figure 12 - Wood discs from the the progeny and clonal tests and the growth and wood traits under examination in this study (source: personal image)

Subsequently, these wood specimens were tested using a universal testing machine. Static tests in 4-point and 3-point bending tests were performed to determine the modulus of rupture (MOR). From each beam one or more twin specimens were cut, so when two twin specimens were removed from the same scantling, the first was tested in a 4-point bending while the second was tested in a 3-point bending. Similarly, when three or more specimens were removed from the same beam, the first and third specimens were tested in a 4-point bending, and the second (and the fourth, if exists) was performed in a 3-point bending. This procedure was used to compare the two types of bending tests on twin specimens. These findings are presented in the Annexes section (item 6.4, pg. 141).

Afterward, a small wood sample measuring 25 mm × 25 mm × 25 mm was removed from the intact wood in order to measure the basic density and the linear shrinkage of wood. The shrinkage of wood was measured in two situations: from over-dried to equilibrium moisture content (EMC) condition and from EMC to above of saturation point, or green condition. Finally, a 2 mm radial section was cut from each small sample for microfibril angle measurements. This procedure provided a complete range of information about the physical, mechanical and anatomical features of these wood samples. **Paper 2** have evaluated the relationships between microfibril angle, density, wood stiffness and strength, modulus of shear and shrinkage in *Eucalyptus* clones.

NIR-based models

This part of the study was dedicated to developing NIR-based models in order to estimate a range of wood traits and improving the methodology. The objective was also to examine and explain why NIR

spectroscopy could be used for predicting dynamic wood traits and microfibril angles. Table 3 lists a summary of the main statistics of the NIR-based calibration.

Table 3 - Resume of the main statistics of the NIR-based calibration for estimating wood traits of progeny and clonal tests and the corresponding paper

Test	Trait	R²p	RMSEP	LV	Outliers	RPD	Paper
Progeny	KL	0.85	0.53	6	5.00%	2.58	4
	S/G	0.86	0.13	7	5.00%	2.68	4
	ρ	0.85	30	3	2.10%	2.70	5
	MFA	0.59	1.36	6	-	1.57	6
Clonal	ρ_{sp}	0.67	34.78	4	0.90%	1.75	7
	ρ_{s}	0.8	22.88	3	2.60%	2.32	-
	MFA	0.75	1.31	5	6.60%	2.10	-
	E_L	0.81	1149	5	1.20%	2.34	7
	E'_L	0.76	1.62	5	-	1.41	7
	f_1	0.72	215.3	6	-	1.92	7
	E_F	0.74	1219	4	0.60%	2.01	7
	E'_F	0.7	1.69	6	0.30%	1.88	7
	$\tan\delta_L$	0.38	0.81	5	1.40%	1.84	7

For wood from the progeny test, NIR-based calibrations were developed for assessing the main chemical components of wood, including klason lignin content (KL), acid-soluble lignin content (ASL) and syringyl and guaiacyl ratio (S/G). These NIR-based calibrations for wet-chemistry wood traits were reported in **paper 4**, where different procedures for sample preparation and its effect on model performance were discussed. In the present study, the acid-soluble lignin was not presented. Afterwards, NIR-based calibrations were developed for physical and ultrastructural features for wood samples from diametrical bands. **Paper 5** reports the NIR-based models for basic density estimates demonstrating the robustness of the established models by validating them with different sets of samplings, bringing insight to the real external, independent validation approach. **Paper 6** presents the NIR-based models to estimate microfibril angle and explains why NIR spectroscopy could be used to predict this complicated ultrastructural feature of the cell walls in *Eucalyptus* wood.

For wood from Clonal tests, NIR-based calibrations were developed for assessing the mechanical properties of wood, such as air-dry density and basic density of wood, dynamic modulus of elasticity, shear modulus, and internal friction of the specimens, as well as their first resonance frequency. **Paper 7** reports the NIR-based models for estimating such wood properties. These models were based on the wood of the first log of the trees: the samples came from the scantlings, which came from the central boards. These models were applied on the NIR spectra measured on the 750 wood discs in order to predict a range of wood traits making possible to propose the cartography of wood variation within the stem.

1.4.4.2 Quantitative genetic approaches

The genetic and environmental variations of wood traits were assessed. The NIR-based calibrations were applied on the woods enabling the assessment of many wood traits in the progeny and clonal tests. These predictions permitted the determination the patterns of spatial variation, the correlations between traits and degree of genetic and environmental control of wood traits. These findings provided new elements for generating a comprehensive knowledge about patterns of variation in heritability estimates and on the traits themselves within the *Eucalyptus* trees.

Progeny test

The NIR-predicted values of the wood traits of the trees from the progeny test were used to assess the level of genetic and environmental control over a range of wood traits, with special focus on MFA and its correlation with other traits. Moreover, genetic and like-environmental correlations among those traits were assessed at different ages improving our knowledge on the functional aspects of wood formation in *Eucalyptus*. The degree of genetic and environmental control over MFA, ρ, lignin content and its structure and growth traits were presented and a series of implications for selection were discussed in **Paper 8**.

Clonal test

The NIR-predicted values of the wood traits of the trees from the clonal tests were used to assess the genetic parameters and the spatial variation of basic density, wood stiffness and MFA in *Eucalyptus* wood. **Paper 10** reports such results. The variation between clones and sites of elastic properties measured on the scantlings by resonance technique were presented and discussed in **paper 9**. From these findings, we hope to be able to indicate what are the most suitable and environmentally stable genotypes for future timber production from *Eucalyptus* plantations.

As a final point, I hope the findings of this PhD thesis helps us to obtain a deeper understanding about the genetic and environmental control, and the clonal variation of a range of wood traits in *Eucalyptus* wood from plantations. The correlations between growth and wood traits in *Eucalyptus* plantations were also investigated. I expected to bring new element to understand how trees adapt their wood traits in order to maintain their erect habit even when they are constrained by bending movements in response to wind and gravity.

2 MATERIAL AND METHODS

2.1 Origin of the material

2.1.1 Progeny test

348 disks taken in breast height of 14-year-old *Eucalyptus urophylla* S.T. Blake trees coming from progeny test established in the Republic of the Congo in the experimental area of research centre UR2PI "Unité de Recherche sur les plantations Industrielles du Congo" (04°45' S, 12°00' E, alt 50 m) were used in this study. The climate is tropical humid with a mean annual temperature of 24°C, a mean annual rainfall of 1,200 mm and a dry season from May to October. This progeny trial was composed by 35 full-sib families produced by controlled pollination (Table 4). These families provided from an un-complete factorial mating design (8 x 8) with *E. urophylla* (16 genitors originated from two provenances). The families were planted in a randomized design and density of plantation was 625 trees/ha (4 x 4 m spacing).

Seeds obtained by controlled pollination were sown in the nursery in the Republic of the Congo from July to September of each year in poly-bags (20 cm high, 10 cm diameter) containing adequate media (one third sand, one third forest soil and one third compost). Five to six months after sowing, the seedlings were planted in a field trial. The full-sib families were planted in a 4x4 m spacing (625 trees/ha). Within each field trial, the experiment was a complete block design with a 16-tree square plot in four replicates. To minimize the impact of borders, two border lines were planted around the field trials.

Table 4 - Arrays of parents in the incomplete factorial mating design under controlled crosses

BRG project		*E. urophylla* (male)							
		14-130	14-135	14-137	14-142	14-132	14-146	14-147	14-148
E. urophylla (female)	14-128		F9	F8	F10		F12		
	14-133	F15	F14				F16	F17	
	14-138	F5		F35	F6	F36			F7
	14-144	F2	F1		F3			F4	F33
	14-136						F20	F21	F22
	14-140		F24	F23		F25	F26	F27	
	14-149				F39	F32			F37
	14-152	F28				F29		F30	F31

Nine to ten trees were harvested from each family, resulting in a total of 348 trees. Breast height wood disk (30 mm thick) was obtained from each tree and transported to the CIRAD in Montpellier, France. Circumference at breast height (C) and commercial height (H) were measured before harvesting.

2.1.2 Clonat test

One hundred and fifty (150) *Eucalyptus grandis* x *urophylla* hybrids with 6 years-old from clonal tests managed for pulp and paper industry (Cenibra Nipo-Brasileira S.A.) established in Brazil (19°17' S, 42°23' W, alt 230-500 m) were used in this study. Ten (10) hybrids coming from three clonally replicated trials established in contrasting site (Table 5) were investigated.

Table 5 - Description of the environmental information of the clonal tests

Clonal test	Location	Slope of terrain	Type of soil	Mean Temp. (°C)	UR (%)	Precip (mm)	Hidric deficit (mm)	Vapor pressure déficit (hPa)	Global radiation (MJ m^{-2} day^{-1})]	Effectiv radiation (mmol m^{-2} s^{-1})	Wind speed (m s^{-1})
303	Brejo	0°	LVd1	24.5	70.5	1,230	299	4.8	17.7	33,442	0.9
301	Guanhães	20°	CXbd9	21.3	65.7	1,182	150	4.0	15.8	33,158	3.2
302	Coruja	40°	RUbd5	24.5	70.5	1,230	299	4.8	17.7	33,442	0.9

The type of climate is Aw (Tropical Savanna Climate), according to the classification of Köppen (Peel et al. 2007), with mean annual rainfall of around 1,200 mm, mean annual temperature of around 23.5 °C and the average annual humidity is around 70%. Sites 302 and 302 present similar meteorological conditions, but the terrain slope was very contrasting. The location of these two clonal tests is close. The Clonal test 301 is around 100 kilometers distant from others and their weather condition is different.

Figure 13 - Differences of field conditions between clonal tests (source: personal image)

Table 6 - Information about the clones' origin describing their relatives and species

Clone	Mother	Species	Father	Species
4426	89	*E. grandis*	6	*E. urophylla*
4494	7	*E. grandis*	5	*E. urophylla*
4514	9	*E. grandis*	12	*E. urophylla*
4515	3	*E. grandis*	5	*E. urophylla*
4535	48	*E. grandis*	2	*E. urophylla*
4541	53	*E. grandis*	13	*E. urophylla*
4557	24	*E. grandis*	8	*E. urophylla*
4579	89	*E. grandis*	6	*E. urophylla*
4588	97	*E. grandis*	10	*E. urophylla*
4609	10	*E. urophylla*	26	*E. grandis*

Five individuals per clone were sampled in each clonal test, totalizing 150 trees (10 clones x 3 sites x 5 individuals). Trees were selected among those upright, healthy, without fork and out of embroidery and harvested at 72 months (6 years). Circumference at breast height (C) and commercial height (H) were measured before harvesting. Figure 13 illustrates the difference in slope of terrain between sites. The

clones were planted at 2003 in a randomized design and density of plantation was 1,667 trees/ha (3 m x 2 m spacing).

2.2 Sampling preparation

2.2.1 Progeny test

A pith to bark radial strip and a clean wedge (knot-free) were cut by a vertical bandsaw machine from each disc. These wood strips have variable height and length (depending of the circumference and thickness of each wood disc), but their width was fixed at 30 mm.

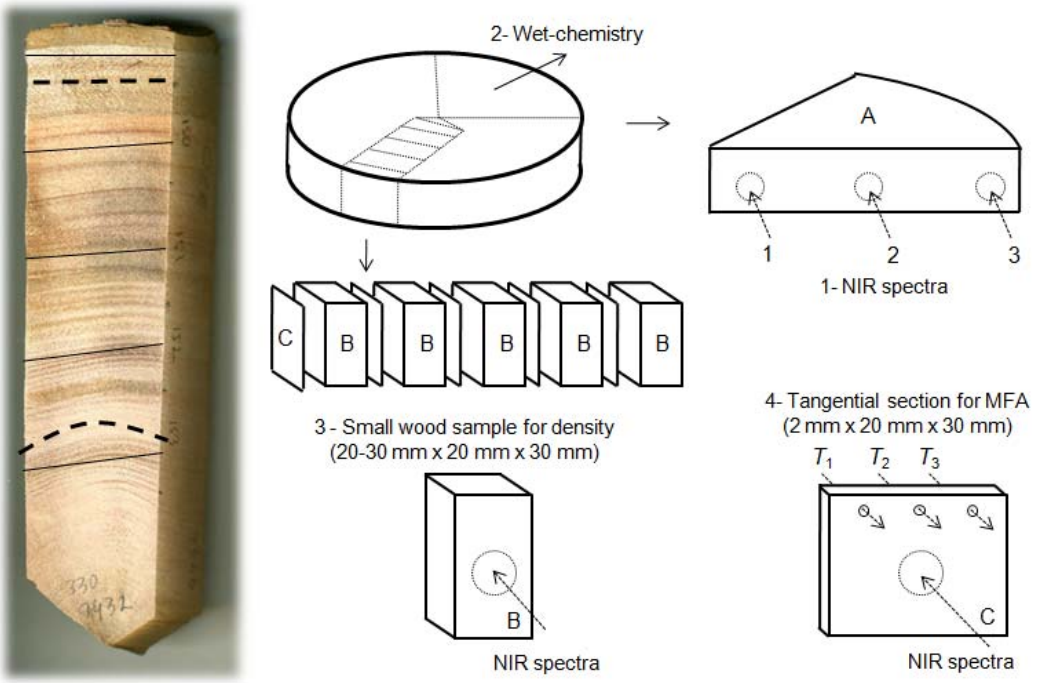

Figure 14 - Strategy of wood sampling and wood measurements of the progeny test

The radial surfaces of the radial strip were sanded with 300-grit sandpaper for approximately 30 seconds. Tangential sections (2 mm x 20 mm x 30 mm), as parallel as possible, to the growth rings angle and wood samples (~15 mm x 20 mm x 30 mm) were cut for microfibril and wood density measurements, respectively.

Wood powder was produced from wedges which were ground in a Retsh ultra-centrifugal mill (ZM 200). The particle sizes of wood meals obtained were less than 0.5 mm and were designated “0.5 mm” for NIRS. 60 wood meals samples were selected according to their representatives from principal component analyses and were submitted to chemical analysis. Figure 14 sums up the strategy of sampling and measurements of the wood from progeny test.

All samples (solid samples and the milled samples) were kept in a conditioned room with 60% relative humidity and temperature of 20°C before analysis. Under these conditions, the equilibrium moisture content was 12%.

2.2.2 Clonal test

2.2.2.1 Wood from logs

Scantlings

A total of 410 pieces of wood (Figure 15 C) with nominal sizes of 45 mm x 60 mm x 2,100 mm (hereafter referred to as 'scantlings') were taken from 150 central boards (Figure 15 B). As the scantlings were removed systematically at each 45 mm of the boards (60 mm in thick), naturally, some parts of the scantlings contained pith, knots and other features inherent to wood. Subsequently, a pile of scantlings was set up for air-drying under protected exterior conditions during 90 days.

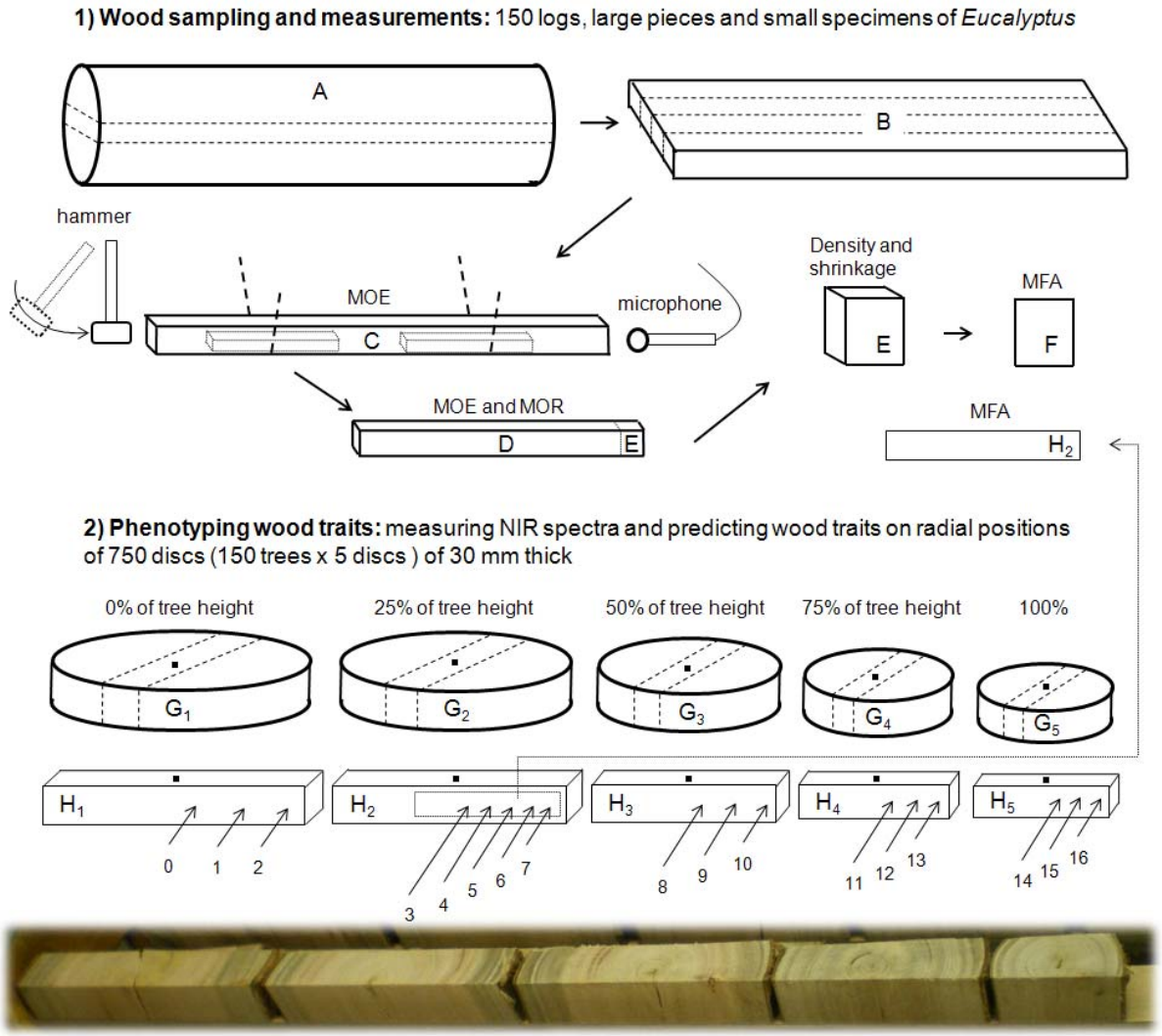

Figure 15 - Strategy of wood sampling and wood measurements of the clonal test and reference of codes relative to radial and longitudinal positions for NIR spectroscopic and genetic analysis

After air-drying process the scantlings presented defects such as small cracks, checks and splits in their ends and, therefore, were trimmed to variable dimensions, depending of the extension of their defects. The clean scantlings had, on average, 1.54 meters of length, varying from 0.645 m to 2.080 m (COV=16.9%) and the averaged width and thickness were, 60 mm and 43 mm, respectively, fluctuating slightly (COV=5.7% for width and COV=2.8% for thickness). Thus, all pieces were free of large fissures,

biological affections, defects produced in the saw mill as severe reduction of width or thickness, but they presented knots and small cracks as well. In the second step, the unseasoned scantlings were kiln-dried at 14% (nominal) under soft condition during two weeks. Therefore, new transversal and longitudinal vibration tests were performed on the kiln-dried scantlings. Figure 15 presents the strategy for preparing wood samples.

Specimens and small wood samples

160 scantlings were selected among the best ones (i.e. annual rings well oriented, free of large cracks etc) and surfaced on the plane machine; beams were cut from them and trimmed to nominal cross-section of 25 mm x 25 mm using a circular saw machine. Finally, clearwood specimens measuring 25 mm x 25 mm x 41 mm (Figure 15 D) were cut from the beams, according to the standard D 143-94 (ASTM 2007). Twin small wood samples (25 mm × 25 mm × 25 mm) were removed from the intact clearwood specimens (Figure 15 E) for wood density and shrinkage measurements;

Wood sections and radial strips

Radial sections (50 mm x 20 mm x 2 mm) were cut from the small wood samples (Figure 15 F) for microfibril angle measurement. Radial strips (50-150 mm x 30 mm x 2 mm) were cut from the discs at 25% of the height (Figure 15 H2) for microfibril angle measurement.

2.2.2.2 Wood from discs

Diametrical strips measuring ~30 mm of width were cut from wood discs. The strips of the trees coming from sloping grounds were removed in the sense of the inclination of sites. Thus, the upslope portion of the strip possibly contains tension wood and those from down slope portions probably contains opposite wood. This procedure was done in most of discs; however, there were some samples presenting cracks and slits and the strip was cut perpendicular to slope to obtain "normal wood". In these regions (Site 301 and 302) the prevailing wind can neutralize the supposed tension wood occurrence due to the sloping grounds. The company's field technicians reported that when high winds occurs breaking trees, the trees topple on top of the hill, in the wind direction.

Table 7 - Reference of codes relative to radial and longitudinal positions

Code	Relative height	Radial position	Code	Relative height	Radial position
0		inner HW^0	8		HW^8
1	0%	outer HW^1	9	50%	inner SW^9
2		SW^2	10		outer SW^{10}
3		inner HW^3	11		inner SW^{11}
4		middle HW^4	12	75%	middle SW^{12}
5	25%	outer HW^5	13		outer SW^{13}
6		inner SW^6	14		outer SW^{14}
7		outer SW^7	15	100%	outer SW^{15}
HW means heartwood while SW means sapwood.			16		outer SW^{16}

The radial surface of each diametrical strip were sanded using a sanding machine in order to produce a homogeneous surface quality. Figure 15 presents the strategy for preparing the radial bands and measuring

NIR spectra from discs, including the reference of codes relative to radial and longitudinal positions for NIR spectroscopic analysis. Table 7 lists the reference of codes relative to radial and longitudinal positions. The main results on genetics of clonal test are presented using these reference codes.

The author is aware that 6-year-old trees still do not produce mature wood or heartwood. This nomenclature has been proposed to facilitate data interpretation and explanation of findings.

2.3 Methods for phenotyping

2.3.1 Sonic resonance

The dynamic tests used to evaluate the elastic properties of wood samples were based on sonic resonance (Brancheriau and Baillères 2002; 2003). The scantlings and clear wood specimens were placed on elastic supports so as to generate free vibrations. An exciting impulse was produced by lightly striking the scantlings with a hammer at the opposite side of the output transducer (acoustic microphone). The transverse vibration was induced by an edgewise impact and the longitudinal vibration by an impact along the bound. The output signals were transmitted via a low-pass filter to an acquisition card on a computer and recorded as described in Brancheriau and Baillères (2003).

2.3.1.1 Equations of motion

The theoretical model used to describe the motion of a uniform prismatic beam that transversally vibrates freely was proposed by Timoshenko (1921) as follow:

$$E_F I_{Gz} \frac{\partial^4 v}{\partial x^4} - \rho I_{Gz}\left(1 + \frac{E_F}{KG_{XY}}\right)\frac{\partial^4 v}{\partial x^2 \partial t^2} + \frac{\rho^2 I_{Gz}}{KG_{XY}}\frac{\partial^4 v}{\partial t^4} + \rho A \frac{\partial^2 v}{\partial t^2} = 0 \qquad \text{Eq. (3)}$$

where E_F is the modulus of elasticity; I_{GZ} is the moment of inertia; v is the transversal displacement; ρ is the density; G_{XY} is the shear modulus; K is a constant which depends of the geometry of the section (For rectangular section, K=5/6); x is the distance along the axis of the beam; A, cross-sectional area of the beam; t is the time. Using the Bordonné´s (1989) solution for this differential equation, the shear effect is taken it account, but the support effects are ignored. The elastic (E_X) and shear modulus (G_{XY}) were calculated according to the follow equation, described in Brancheriau and Baillères (2002):

$$\frac{E_F}{\rho} - \frac{E_F}{KG_{XY}}\left[QF_2(m)4\pi^2 \frac{AL^4}{I_{Gz}}\frac{f_n^{\,2}}{P_n}\right] = 4\pi^2 \frac{AL^4}{I_{Gz}}\frac{f_n^{\,2}}{P_n}[1 + QF_1(m)] \qquad \text{Eq. (4)}$$

where f_i is the resonance frequency of the order i and P_n is the coefficient associated with the solution of Bernoulli (rank n). Parameters Q, F_1, F_2, m and θ are calculated as follows:

$$Q = \frac{I_{Gz}}{AL^2} \qquad \text{Eq. (5)}$$

$$F_1(m) = \theta^2(m) + 6\theta(m) \qquad \text{Eq. (6)}$$

$$F_2(m) = \theta^2(m) - 2\theta(m) \qquad \text{Eq. (7)}$$

$$\theta(m) = m\frac{\tan(m)\tanh(m)}{\tan(m) - \tanh(m)} \quad \text{Eq. (8)}$$

$$m = \sqrt[4]{P_n} = (2n+1)\frac{\pi}{2},\ n \in N^* \quad \text{Eq. (9)}$$

Parameters m, P_n, $F_1(m)$ and $F_2(m)$ are calculated on the basis of index n, and are used in practical applications to calculate the value of the modulus E_X and that of the shear modulus G_{XY}.

In practice, the first frequencies are those that are least influenced by the viscosity of the material; these are theoretically those that give the modulus nearest to the static modulus conventionally obtained by a static bending test (Cilas et al. 2006).

In longitudinal vibrations, the theoretical model used to describe the motion of a uniform prismatic beam that vibrates freely was given in Brancheriau and Baillères (2002) as follow:

$$E_L \frac{\partial^2 u}{\partial x^2} - \rho \frac{\partial^2 u}{\partial t^2} = 0 \quad \text{Eq. (10)}$$

where u is the longitudinal displacement. The first vibration mode can be used in order to estimate its dynamic longitudinal modulus of elasticity (E_L), which represents its stiffness under compressive stress, by means the formula:

$$E_L = 4L^2 \rho f_1^2 \quad \text{Eq. (11)}$$

A deep discussion about different theoretical models of motion, their approximate solutions and their respective hypotheses in longitudinal and transversal vibrations; and the effects of the elastic support was provided in Brancheriau and Baillères (2002).

To extract relevant parameters from acoustic sounds, the concept of additive synthesis was applied (Brancheriau et al. 2006). Each temporal signal $s(t)$ was then considered as a sum of exponentially damped sinusoids as follow:

$$s(t) = \sum_{i=1}^{\infty} \beta_i \exp(-\alpha_i t)\sin(2\pi f_i t + \varphi_i) \quad \text{Eq. (12)}$$

Where s is the radiated signal as a function of time t and φ_i is the phase shift. The parametric method of Steiglitz and McBride (1965) was used to simultaneously determine the first resonance frequency f_1, the amplitude β_1, and the temporal damping α_1 associated with f_1. Only the first frequency was considered because of its high energy.

Vibrations are dampened by internal friction (tg δ), a property of solid materials that transforms mechanical energy to heat when subjected to cyclical stress (Brancheriau et al. 2010). The internal friction was calculated associated with the complex modulus concept with respect to transverse vibrations (Aramaki et al. 2007) according to the equation given by Brancheriau et al. (2006):

$$tg\delta = \frac{\alpha_1}{\pi f_1} \quad \text{Eq. (13)}$$

2.3.1.2 Parameters of vibration tests

The analysis of the signal, the selection of the natural frequencies of vibration and the estimates of the E_F, G, E_L and tg δ were performed using the software BING ® (CIRAD, Montpelier, France, version 9.1.3). The sampling frequencies of the signal were 78,125 Hz and 39,062 Hz for longitudinal and flexural vibration, respectively. The spectral acquisition was carried out by using 32,768 points for each test.

2.3.2 Static bending test

The modulus of rupture (MOR) of the clearwood specimens were tested using an electromechanical universal testing machine (Adamel Lhomargy, model DY 36), of 100 kN capacity in traction-compression.

For 4-point bending test, the specimens were tested in a according to an adaptation of the procedure ASTM D143-94 of the (ASTM 2007) standard. The span between lower supports was 320 mm; the distance between two loading points was 160 mm (1 free and 1 fixed); the diameter of roller bearings was 60 mm; and the test was conducted at a rate of 0.08 mm/s. Figure 16 presents the schema for four-point statistic bending test. The proportional limit, ultimate load, and deflection were obtained from load-deflection curves; and the MOR was calculated as follows:

$$MOR_{4p} = \frac{3 \times F \times (L - a)}{2 \times b \times d^2} \qquad \text{(Eq. 14)}$$

where F is the load (force) at the fracture point, L is the length of the support span, a is the distance between the 2 loading points, b is the width and d is the thickness of the wood specimen.

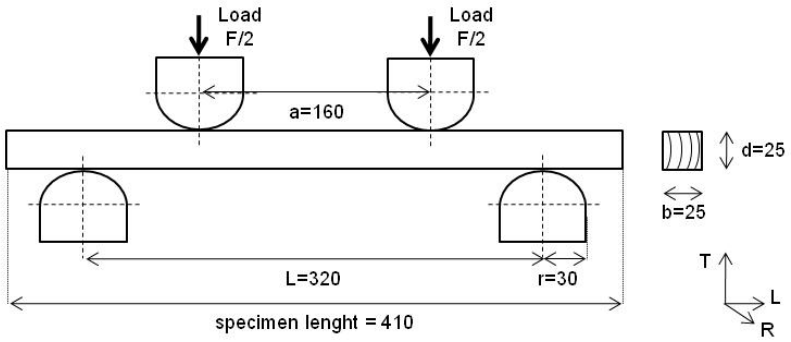

Figure 16 - Schema for four-point statistic bending test

For 3-point bending test, the specimens were tested in a according an adaptation of the procedure ASTM D143-94 of the (ASTM 2007) standard. The proportional limit, ultimate load, and deflection were obtained from load-deflection curves; and the MOR was calculated as follows:

$$MOR_{3p} = \frac{3 \times F \times L}{2 \times b \times d^2} \qquad \text{(Eq. 15)}$$

where F is the load (force) at the fracture point, L is the length of the support span, b is the width and d is the thickness of the wood specimen. Figure 17 presents the schema for three-point statistic bending test.

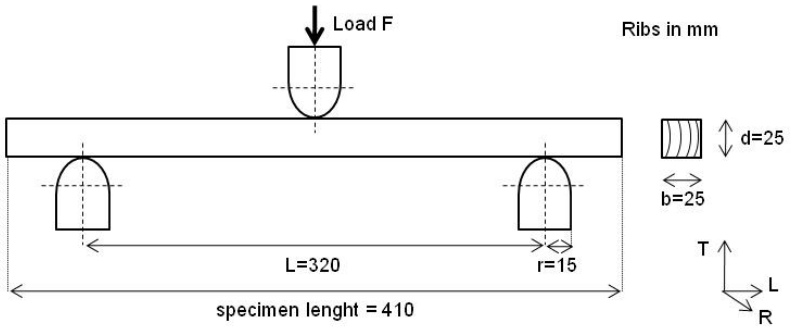

Figure 17 - Schema for three-point statistic bending test

2.3.3 Basic density and shrinkage of wood

The basic density and the shrinkage of the wood samples were measured simultaneously. The small wood samples (in most of cases measuring 25 mm × 25 mm × 25 mm) were removed from the intact wood of the specimens used in bending tests. These small wood samples were used for basic density (ρ) and shrinkage (δrd) measurements, which was determined by the ASTM D2395 (ASTM 2002) procedures. The formulas for calculating the basic density and shrinkage are given as follows:

$$\rho = \frac{\text{oven - dried weight}}{\text{green volume}} \qquad \text{(Eq. 16)}$$

$$\delta = \frac{\text{initial length - final length}}{\text{final length}} x100 \qquad \text{(Eq. 17)}$$

The green volume of a piece of wood was determined by water displacement according to the principle of Archimedes. The samples were first soaked in water to ensure that water is not taken up during the immersion process. An experimental dispositive was used for measuring the green volume of the samples (Figure 18 A).

Figure 18 - Experimental dispositive for measuring the green volume of the samples (A) and the sample dimensions (B) (source: personal image)

Then, a digital dispositive (Figure 18 B) was used for precisely measuring the sample dimensions of the saturated samples immediately after measuring the green volume. After determining the green volume, the samples were oven-dried at 103°C. The time necessary for drying depends on the size of the samples and also on the capacity of the oven. The digital dispositive was used again for precisely measuring the sample

dimensions of the oven-dried samples immediately before measuring their dry weight. Radial (δrd) and tangential (δtg) shrinkage was determined in three conditions: (i) from the oven-dry (0%) condition to equilibrium moisture content - EMC (~14%); (ii) from the EMC to the green (100%) condition and iii) from oven-dried to green condition.

2.3.4 X-ray diffraction

All X-ray diffraction data were collected on a diffractometer (Gemini-S, Agilent Technologies, Yarnton, UK) with CuK α radiation (Figure 19). Images were integrated between 2θ = 21.5° and 23.5° along the whole 360° azimutal interval to plot the intensity diagram of the (200) plane. An automatic procedure allowed the detection of the 200 peaks and their inflexion points. The *T* parameter, as defined by Cave (1966), was measured as the half distance between intersections of tangents at inflexion points with the baseline. The results are given as the mean of values obtained for the two 200 peaks. As shown by Cave (1966), *T* parameter is affected by the cross-sectional shape of the cells. Thus, as also reported by Yamamoto et al. (1993) and latter Ruelle et al. (2007), the corrective factor proposed by Cave (1966) cannot be used for all species but need to be calibrated specie by specie; However, their works show that the *T* parameter allows comparison within a specie which is the purpose of our study. In this thesis, the cross-sectional shape of the cells was considered to remain constant enough from pith to bark allowing comparison with a single *T* parameter within the species.

Figure 19 - X-ray diffractometer device with CuK α radiation used for measuring XRD patterns (A), detail of the specimen holder (B) and the mini-circular machine used for cutting samples (C) (source: personal image)

Two methods were applied in order to estimate the MFA´s based on their X-ray diffraction pattern, namely: (*i*) MFA_C for the values estimated by the Cave (1966) formula and (*ii*) MFA_Y for estimations using formula proposed by Yamamoto et al. (1993) These formulas give an estimation of the mean MFA of woods based on their *T* value and are given by:

(*i*) $MFA_C = 0.6 \times T$ (Eq. 18)

(*ii*) $MFA_Y = 1.575 \times 10^{-3} \times T^3 - 1.431 \times 10^{-1} \times T^2 + 4.693 \times T - 36.19$ (Eq. 19)

Three X-ray diffraction profiles were recorded on three points of each sample (Figure 14). The MFA estimates using these two formulas had a correlation of 0.97. The error of the measure of *T* parameter was estimated at 3%.

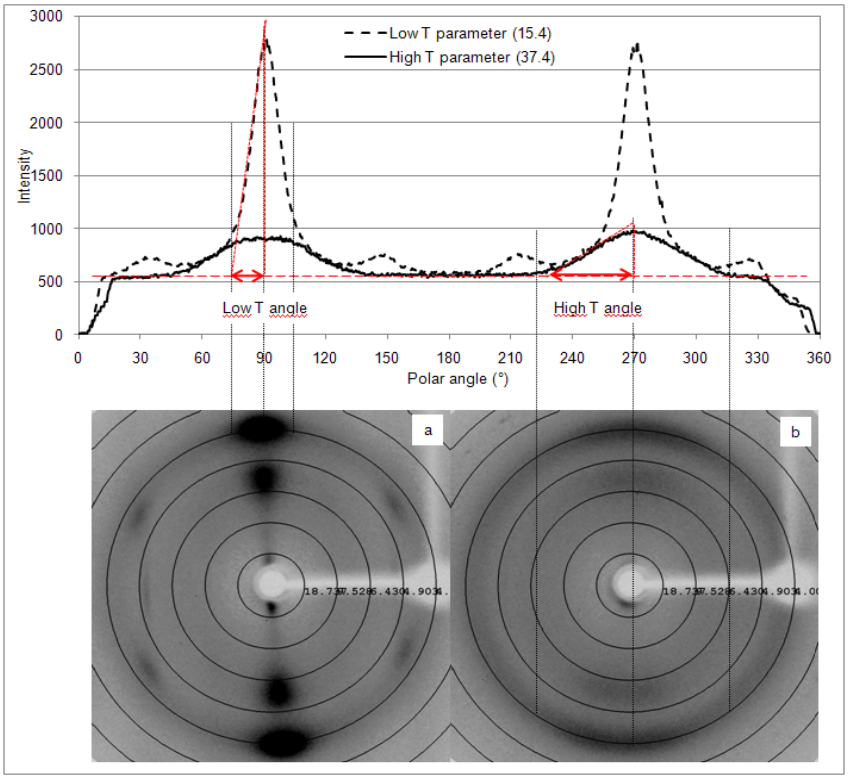

Figure 20 - X-ray scattering patterns recorded in 2 mm tangential sections of *Eucalyptus* samples with low (a) and high (b) *T* parameter

2.3.5 Wet-lab chemistry

The chemical analyses were conducted by the Biological Chemistry Laboratory at INRA-Agro ParisTech. All the samples were subjected to an exhaustive extraction in a soxhlet apparatus with toluene:ethanol (2/1, v/v) ethanol, and then water in order to eliminate all the extractives that could interfere with the lignin analyses. The Klason lignin (KL) and acid-soluble lignin (ASL) were determined from the extractive-free dried material (300 mg of "fine" powder which particle size less than 0.5 mm) according to the standard method (Dence 1992). The ratio between syringyl (S) and guaiacyl (G) units was performed on the extractive-free dried material by thioacidolysis, whereupon the method previously described by (Lapierre et al. 1995). Chemical analyses were performed in duplicate for the 60 samples.

2.3.6 NIR spectroscopy

Bruker spectrophotometer (model Vector 22/N, Bruker Optik GmbH, Ettlingen, Germany) was used in the diffuse reflectance mode (Figure 21). This Fourier transform spectrometer is designed for reflectance analysis of solids with an integrating sphere which measures the diffuse reflected light on a 150 mm² spot. This integrating sphere collects light from all angles; thus, the effects of wood texture and other non-homogeneities are minimized. It also practical that the sphere is "upward looking", with a window on top of the sphere. A sintered gold standard was used as background. NIR spectral analysis was performed within the 12,500-3,500 cm^{-1} range at 8 cm^{-1} resolution (each spectrum consisted of 2,335 absorption values).

Each spectrum was obtained with 32 or 64 scans and then means were calculated and compared to the standard in order to obtain the absorption spectrum of each sample. Thus, one spectrum is the mean of 32 or 64 scanning. In some cases, more than one spectrum was measured per sample and they were averaged into a single NIR spectrum. For solid woods, NIR spectra were recorded directly on the transversal and/or longitudinal wood surfaces while for wood meals, NIR spectra were also collected using a 50 mm spinning cup module (Figure 21 B).

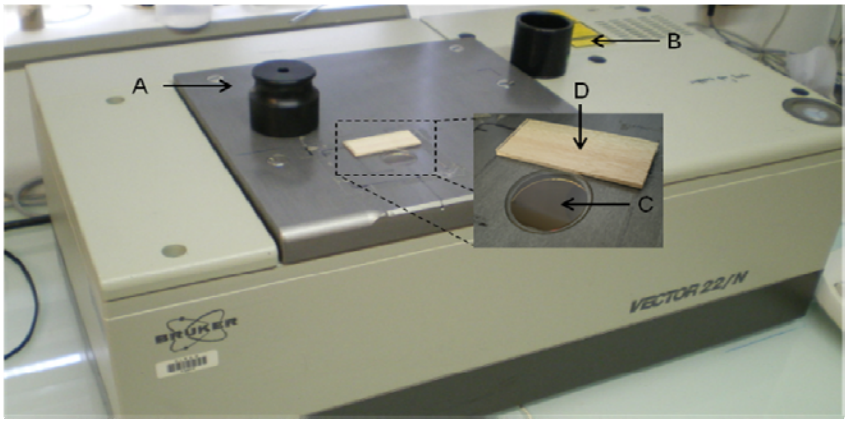

Figure 21 - NIR spectrophotometer used for measuring diffuse reflectance of wood samples showing the sintered gold standard (A), cup module for measuring NIR spectra from grounded wood (B), window for NIR spectra scanning - 10 mm of diameter (C) and 2-mm radial section of wood (D) (source: personal image)

2.3.7 Resume of wood traits measurements

Table 8 and Table 9 list the growth and wood traits measurements, the methods used for determine them, the dimension of the samples and the number of observations for each trait of the trees and wood samples.

Table 8 - Resume of growth and wood traits measurements, methods, sample dimension and number of observations of the trees from Clonal test

Trait	Method	Samples	N
C	Tape-measure in field	Tree (at 1.3 m)	150
H	Tape-measure in field	Tree	150
ρsp	Caliper / balance	Specimen (410 mm x 25 mm x 25 mm)	327
f_{1L}sp	Resonance	Specimen (410 mm x 25 mm x 25 mm)	334
$E_L$sp	Resonance	Specimen (410 mm x 25 mm x 25 mm)	334
E'_Lsp	Resonance	Specimen (410 mm x 25 mm x 25 mm)	334
tg $\delta_F$sp	Resonance	Specimen (410 mm x 25 mm x 25 mm)	141
f_{1F}sp	Resonance	Specimen (410 mm x 25 mm x 25 mm)	334
$E_F$sp	Resonance	Specimen (410 mm x 25 mm x 25 mm)	334
E'_Fsp	Resonance	Specimen (410 mm x 25 mm x 25 mm)	334
$G_F$sp	Resonance	Specimen (410 mm x 25 mm x 25 mm)	334
MOR4p	Static test	Specimen (410 mm x 25 mm x 25 mm)	224
MOR3p	Static test	Specimen (410 mm x 25 mm x 25 mm)	137
ρs	Balance (immersion)	Small sample (25 mm x 25 mm x 25 mm)	225
Shrinkage	Caliper	Small sample (25 mm x 25 mm x 25 mm)	225
MFA	X-ray diffraction	Radial section (25 mm x 25 mm x 2 mm)	165 + 225

Table 9 - Resume of growth and wood traits measurements, methods, sample dimension and number of observations of the trees from Progeny test. Chemical properties were done in duplicate

Trait	Method	Samples	N
C	Tape-measure in field	Tree (at 1.3 m)	348
H	Tape-measure in field	Tree	348
KL	Klason lignin	Wood powder 0.5 mm	60 (x 2)
S/G	Thioacidolysis	Wood powder 0.5 mm	60 (x 2)
D (ρ)	Balance (immersion)	Wood sample (15 mm x 20 mm x 20 mm)	190
MFA	X-ray diffraction	Tangential section (30 mm x 20 mm x 2 mm)	175

2.4 STATISTICAL ANALYSIS

2.4.1 Descriptive statistics and correlations

The descriptive statistic, bivariate correlations, analysis of variance and the comparison between means were performed using SPSS statistics software (SPSS Inc., version 17.0, Chicago, IL). The parameters of each analysis are given in the corresponding Tables.

2.4.2 Developing NIR spectroscopy models

Principal component analysis (PCA) and Partial least squares (PLS) regression analyses were performed using the Unscrambler software (CAMO AS, version 9.7, Norway).

The main advantage of PLS method is their ability to compress the relevant spectral information into a few latent variables; the orthogonality between these variables ensures the stability of the obtained model (Jouan-Rimbaud et al. 1996). In order to analyze NIR spectra information, PLS regression is of particular interest because it can analyze the data strongly collinear (correlated), with noise, with many X-variables (NIR spectra), and also, simultaneously, several variables can shape-response Y (Wold et al. 2001). PLS-R analyses were used to describe the relationship between the data sets obtained from NIR spectra and wood properties. First derivatives (13-point filter and a second order polynomial) and second derivatives (25-point filter and a third order polynomial) were applied on the NIR spectral data by the Savitsky and Golay (1964) algorithm to enhance the quality of the calibrations. In many cases, the NIR spectra were treated using standard normal variate (SNV) transformations. The PLS-R calibrations were performed in full cross-validation mode with a maximum of twelve latent variables (LV). The final number of LVs adopted for each model corresponded to the first minimal residual variance and the outlier samples were indentified from the Student residuals and leverage value plot analyses. The Martens' uncertainty test (Westad and Martens 2000) was used to select the wavenumbers with regression coefficients significally different of zero in order to develop more robust and reliable PLS models. To compare calibration and validation, the following statistics were examined: (**i**) Coefficient of determination of calibration set (R^2c), cross-validation set (R^2cv) or prediction set (R^2p); (**ii**) Root mean square error of calibration (RMSEC), cross-validation (RMSECV) or prediction (RMSEP); (**iii**) Ratio of performance to deviation (RPD) and (**iv**) Number of latent variables (LV). The general formulas for RMSEC, RMSECV and RMSEP are given in Burns and Ciurczak (2008) and can be calculated as follows:

$$RMSEC = \sqrt{\frac{\sum_{i=1}^{N} (\hat{y}_i - \hat{y}_i^{\,2})}{N - A - 1}} \quad \text{Eq. (20)}$$

$$RMSECV = \sqrt{\frac{\sum_{i=1}^{N} (\hat{y}_{CV\,i} - \hat{y}_i^{\,2})}{N}} \quad \text{Eq. (21)}$$

$$RMSEP = \sqrt{\frac{\sum_{i=1}^{Np} (\hat{y}_i - \hat{y}_i^{\,2})}{Np}} \quad \text{Eq. (22)}$$

where the y_i's are obtained by testing the calibration equation directly on the calibration (or cross-validation - y_{cv}) data, A is the number of latent variable, N is the number of samples of calibration set, N_p is th number of samples of the prediction set. RMSEC, RMSECV or RMSEP should be as low as possible whereas coefficient of determination should be high. The RMSEC statistic is a useful estimate of the optimal accuracy obtainable for a given set of wavelengths used to develop a calibration equation, while the calculation of RMSECV is a method useful for determining the "best" number of latent variables to use in building a calibration equation by cross-validation and it is an estimate of the RMSEP. The cross-validation (CV) method is based on an iterative (repetitive) algorithm that selects samples from a sample set population to develop the calibration equation and then predicts on the remaining unselected samples (Workman and Weywer 2007). RMSEP allows the comparison between NIR-observed predicted values and laboratory values (reference values) during the validation test with independent sample set.

The RPD value is the ratio of the RMSECV or RMSEP to the standard deviation (Sd) of the cross-validation or validation sample set and can be calculated as follows:

$$RPD = \frac{Sd}{RMSE} \quad \text{Eq. (23)}$$

This statistic provides a basis for standardizing the RMSECV (Williams and Sobering 1993) and makes possible a comparison of different calibration parameters such as spectral information obtained from different wood faces. According to Fujimoto et al. (2008), the higher the RPD index the more reliable is the model.

2.4.3 Genetic parameter estimation

2.4.3.1 Progeny test

Quantitative genetic analysis was performed with ASReml version 2.0 (Gilmour et al. 2005). Growth, lignin content, syringyl to guaiacyl ratio, wood density and microfibril angle were normally distributed. Each trait was analyzed independently (univariate analysis) to estimate the variance components by using an individual (animal) model proposed by Mrode (2005). The following mixed linear model was considered:

$$y = X.b + Z.a + e \quad \text{(Eq. 24)}$$

where y is the vector of observations, b is the vector of fixed effects (in our case the mean value of the trait in the population), a is the vector of genetic effects (individual additive genetic values), e is the vector of residuals and X and Z are the incidence matrices linking observations to the effects.

The random effect fits a normal distribution whose parameters were

$$E\begin{bmatrix} a \\ e \end{bmatrix} = \begin{bmatrix} 0 \\ 0 \end{bmatrix} \text{ and } \quad Var\begin{bmatrix} a \\ e \end{bmatrix} = \begin{bmatrix} G & 0 \\ 0 & R \end{bmatrix} \quad \text{(Eq. 25)}$$

The variance-covariance matrices were defined as follows:

$$G = A.\sigma^2_A \quad \text{(Eq. 26)}$$

$$R = I.\sigma^2_e \quad \text{(Eq. 27)}$$

where A is the additive genetic relationship matrix computed from a pedigree file that takes into account all the relationships between the individuals, I is the identity matrix, σ^2_A the additive genetic variance and σ^2_e the residual variance. The variances associated to random effects were estimated by restricted maximum likelihood (REML method) using ASReml (Gilmour et al. 2005). As the variances are assumed to be independent, the total phenotypic variance σ^2_P was calculated as follows:

$$\sigma^2_P = \sigma^2_A + \sigma^2_E \quad \text{(Eq. 28)}$$

Because, full-sib families were not replicated in the experimental design (the measurements were done in a single block), dominance and micro-environmental effects were confounded and cannot be properly estimated with this experimental design.

The narrow-sense heritability estimates were calculated as follows:

$$h^2 = \frac{\sigma^2_A}{\sigma^2_P} \quad \text{(Eq. 29)}$$

Variances are not independent of the scale and the mean of the respective traits (Sokal and Rohlf 1995). Therefore, to compare the genetic and phenotypic variances of the different traits, a parameter measuring the genetic (CV_A) and phenotypic (CV_P) coefficient of variation was calculated as:

$$CV_{Aj} = \frac{100 \times \sigma_{Aj}}{\bar{x}} \text{ and } CV_{Pj} = \frac{100 \times \sigma_{Pj}}{\bar{x}} \quad \text{(Eq. 30)}$$

where CV_{Aj} is the coefficient of additive genetic variation; σ_{Aj} is the square root of the additive genetic variance for the trait; CV_{Pj} is the coefficient of phenotypic variation; σ_{Pj} is the square root of the phenotypic variance for the trait and x is the population mean for trait.

CV_{Aj} or CV_{Pj} expresses the genetic or phenotypic variance relative to the mean of the trait of interest and gives a standardized measure of the variance relative to the mean of the trait. The higher the coefficient of variation for a trait, the higher is its relative variation.

To estimate phenotypic (r_P), residual (r_E) and genetic additive (r_A) correlations between two traits (X and Y), were performed from a bi-variate analysis using the same individual model as for univariate analysis. r_P, r_E and r_A were estimated as follows:

$$r_P = \frac{Cov_P(x,y)}{\sqrt{\sigma^2_{Px}.\sigma^2_{Py}}} \quad \text{(Eq. 31)}$$

$$r_E = \frac{Cov_E(x,y)}{\sqrt{\sigma^2_{Ex}.\sigma^2_{Ey}}} \quad \text{(Eq. 32)}$$

$$r_A = \frac{Cov_A(x,y)}{\sqrt{\sigma^2_{Ax}.\sigma^2_{Ay}}} \quad \text{(Eq. 33)}$$

Standard errors of h^2, σ^2_A, σ^2_P, r_P, r_E and r_A were calculated with ASReml using a standard Taylor series approximation (Gilmour et al. 2005).

2.4.3.2 Clonal test

Quantitative genetic analysis was performed with R statistical software version 2.8.1 (R Development Core Team 2008). Circumference and height, wood density, modulus of elasticity and microfibril angle values were normally distributed. Each trait was analyzed independently (univariate analysis) to estimate the variance components by using an individual mixed linear model as following:

$$y = \mu + Clone + Site + Clone \times Site + \varepsilon \quad \text{(Eq. 34)}$$

where μ is the mean value, *Clone* is the random genetic effect, *Site* is the fixed environmental effect, $Clone \times Site$ is random interaction effect and ε is the residual. The variances associated to random and fixed effects were estimated by restricted maximum likelihood (REML) analysis using the "nlme" package of R software (R Development Core Team 2008). As the variances are assumed to be independent, the total phenotypic variance was calculated as follows:

$$\sigma^2_P = \sigma^2_G + \sigma^2_{GxE} + \sigma^2_E \quad \text{(Eq. 35)}$$

$$\sigma^2_P = \sigma^2_G + \sigma^2_E \quad \text{(Eq. 36)}$$

where σ^2_P is the phenotypic variance, σ^2_G is the clonal variance, σ^2_{GE} is the clone by site interaction variance and σ^2_E is the environmental (error) variance. The broad-sense heritability estimates were calculated as follows:

$$H^2 = \frac{\sigma^2_G}{\sigma^2_G + \sigma^2_{GxE} + \sigma^2_E} \quad \text{(Eq. 37)}$$

$$H^2 = \frac{\sigma^2_G}{\sigma^2_G + \sigma^2_E} \quad \text{(Eq. 38)}$$

The choice of model (Eq. 27 or Eq. 28) was based on BIC values (Burnham and Anderson 2004). The model which yielded the lower BIC value was chose. In short, the wood traits were analyzed by the Equation 27 while the growth traits by the Equation 28.

NIR spectral heritability

NIR spectra were recorded from 12,500 to 3,500 cm^{-1} range at 8 cm^{-1} resolution. The NIR range from 8,910 from 5,350 containing 1,400 absorption values was selected. Each NIR spectrum was reduced along its wavenumber by a reduction factor of 5 producing a NIR spectrum containing 280 absorption values. As the NIR spectrum consisted of 280 wavenumbers, the same number of broad-sense NIR spectral heritability estimates was performed using the equation 37.

Surface plots

The 2-D plots presenting the spatial variation of wood traits and heritability estimates (Figure 39, Figure 40, Figure 41, Figure 45, Figure 46 and Figure 47) were developed using the library “grayplot” of the Scilab software (v.5.3.1). As NIR spectroscopic models were used to estimate wood traits on specific points along the tree stem. Thus, data were interpolated in order to create estimates in a whole tree making possible to build the cartography of wood traits.

Scripts for calculating genetic parameters using R

```
Data <- read.table("CNB150predNIR.csv", dec=".", sep=",", header=T)
Data$Site <- as.factor(Data$Site)
Data$Clone <- as.factor(Data$Clone)

## Estimating variance components
Resume <- NULL
Resume1 <- NULL
for (i in 4:124){
Y <- Data[,i]
lme <- lme(Y~ 1 + Site, random=~1|Clone, data=Data, method="REML")
lme1 <- lme(Y~ 1 + Site, random=~1|Clone/Site, data=Data,
method="REML")
Resume <- c(Resume, list(lme))
Resume1 <- c(Resume1, list(lme1))}
Resume
Resume1

## For calculating BIC
Selection <- NULL
Selection1 <- NULL
for (i in 4:124){
Y <- Data[,i]
lme <- lme(Y~ 1 + Site, random=~1|Clone, data=Data, method="ML")
lme1 <- lme(Y~ 1 + Site, random=~1|Clone/Site, data=Data,
method="ML")
Selection <- c(Selection, list(lme))
Selection1 <- c(Selection1, list(lme1))}
Selection
Selection1

## To display BIC results
Resultat <- NULL
for (i in 1:121){ lme0 <- Selection[[i]]
lme1 <- Selection1[[i]]
Resultat <- c(Resultat, list(anova(lme0, lme1)))}
Resultat
```

3 RESULTS AND DISCUSSION

3.1 Growth traits

Circumference at breast height (C) and commercial height (H) were measured before harvesting the trees. Table 10 show the descriptive statistics of growth traits in 14-year-old *Eucalyptus urophylla* from progeny trial (BRG) in the Republic of Congo and in 6-year-old *Eucalyptus grandis* x *urophylla* from three clonal tests (CNB) established in Brazil.

Table 10 - Descriptive statistics of growth traits in 14-year-old *Eucalyptus urophylla* from progeny test and in 6-year-old *E. urograndis* from clonal test, including circumference at 1.3 meter height (C) and total height (H) by site and considering all samples

	Progeny test		Clonal test							
			Site 303 (0°)		Site 301 (20°)		Site 302 (40°)		Overall	
	C (cm)	H (m)	C (cm)	H (m)	C (cm)	H (m)	C (cm)	H (m)	C (cm)	H (m)
Mean	52.8	21.2	67.3	23.1	60.8	23.6	57.4	20.4	61.8	22.4
Sd	11.26	3.67	11.63	3.25	5.87	1.87	8.71	3.28	9.89	3.2
Min	24.0	7.8	45.0	16.1	49.5	17.3	42.0	14.8	42.0	14.8
Max	84.0	29.6	96.0	28.3	75.0	27	81.0	28.5	96.0	28.5
CV (%)	21.3	17.3	17.3	14.0	9.7	7.9	15.2	16.1	16.0	14.3
N	340	340	50	50	50	50	50	50	150	150

The range of variation for growth traits of the trees from progeny test (CV=21.3%) was higher than those from clonal tests (CV=16%). This result was expected because the genetic variation of a progeny test (where offspring of a range of progenitors are evaluated) is larger than the genetic variation of a clonal test (where the best offspring are vegetatively propagated). The environment effect on the growth rate of the trees from the clonal tests is presented in Figure 22.

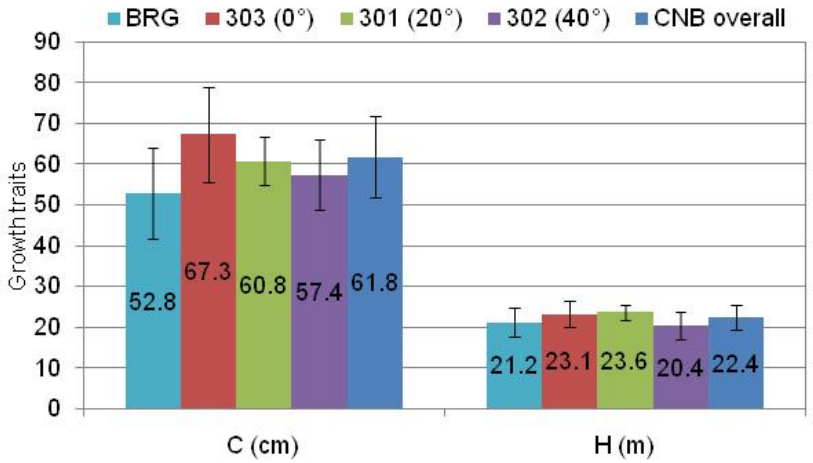

Figure 22 - Mean and standard deviation of circumference at breast height (C) and commercial height (H) for each site and considering all samples

While trees growing under optimal conditions (in this case, no terrain slope) produce biomass at high growth rates, trees grow up relatively slower at sites with high inclination (40°). The site 301, with 20° of inclination, presented the lower standard deviation while the site 303 (0°) had the higher variability in the growth traits. Multiple range tests for mean circumference and height by clone and by site are presented and discussed in the genetic studies section (Table 31, pg. 107).

On average, the *E. urophylla* trees from progeny trial (BRG) presented a mean circumference at 1.3 meters of 52.8 cm and 21.2 meters of height. The circumference of these trees were much lower than those reported by Cruz (2006) who evaluated 16-year-old *Eucalyptus urophylla* from Paraopeba (Brazil) with a mean circumference of around 110 cm and mean height of around 32 meters.

3.2 Wood phenotyping of progeny tests

3.2.1 Wood chemical composition

Table 11 shows the statistical summary of wet-chemistry analysis including the mean, minimum (Min) and maximum (Max) values of the results, and the coefficient of variation (CV) of wood of sixty *Eucalyptus urophylla* from progeny test. Analyses were performed in duplicate and had good reproductive values. The duplicates never showed differences at the 5% significance level.

Table 11 - Descriptive statistic for Klason lignin (KL); acid-soluble lignin (ASL) and total lignin content (TL); syringyl to guaiacyl ratio (S/G); and extractive content (EXT) in 14-year-old *Eucalyptus urophylla* wood

	KL (%)	ASL (%)	TL (%)	S/G	EXT (%)
Mean	28.5	1.63	30.1	2.4	14.6
Sd	1.37	0.22	1.33	0.35	2.15
Min	25.1	1.14	26.95	1.7	11.2
Max	31.95	2.12	33.25	3.04	19.6
CV (%)	4.8	13.2	4.4	14.5	14.7
N	60	60	60	60	60

Because the delignification process requires energy and reagent consumption, trees presenting high lignin content are undesirable in plantations for pulp and paper. On the other hand, wood may have high lignin content for bioenergy purposes. Here, Klason lignin content varied from 25.1 to 31.95 percent but the coefficient of variation was small (4.8%). Acid-soluble lignin content varied in higher magnitude presenting CV of 13.2 percent and the S to G ratio ranged from 1.7 to 3.04. These results are compatible with those reported in similar studies on *Eucalytus* genus. For intance, Brito and Barrichello (1977) investigated 7-year-old *E. urophylla* from Rio Claro (Brazil) with Klason lignin content of 23.6% and 11-year-old *E. urophylla* from Timor with 29.8 percent of Klason lignin content. Carvalho and Nahuz (2001) studying hybrids of 7-year-old *E. grandis* and *E. urophylla* reported woods with an averaged KL content of 22.4%. Alencar et al. (2002) found averaged levels of KL of 27.38% in 7-year-old *E. grandis* x *E. urophylla* hybrids. Gomide et al. (2005) reported total lignin content ranging from 27.5 to 30.5 percent, and acid-soluble lignin from 3.1 to 5.1% in *E. grandis* and *E. urophylla* clones.

The S/G ratio is an important parameter for tree breeders. High S/G is advantageous for pulping (Rodrigues et al. 1999) since every unit increase in the lignin S/G ratio would roughly double the rate of lignin removal (Chang and Sarkanen 1973). Here, the mean S/G was of 2.42 ranging from 1.67 to 3.13

(Table 11). The varation range is in agreement with those reported in the literature. For instance, Gomide et al. (2005) studied 7-year-old *Eucalyptus* reporting S to G ratio ranging from 2.1 to 2.8. Silva (2006) studied *E. grandis* and *E. urograndis* reporting averaged S/G values of 2.1 and 2.5, respectively and Yamada et al. (2004) investigated transgenic trees presenting mean S/G ratio of 2.8.

3.2.2 Microfibril angle and wood density

Microfibril angle and wood density were investigated. Tangential sections (2 mm of thickness) of wood were used to evaluate the MFA by X-ray diffraction technique (Cave 1966) and small samples were cut between tangential section were use for wood density measurements. Figure 14 sums up the procedure of sample preparation and measurements. The samples taken close to the pith presents a "curvature effect" while the tangential sections taken near the bark, parallel to the growth ring, showed little or no "curvature effect". The curvature effects are illustrated by dotted lines in Figure 23. This procedure was used to verify the influence of the curvature effect on the repeatability of the XRD measurements. The findings concerning these issues were presented and discussed in Hein and Brancheriau (2011) **(paper 3)**.

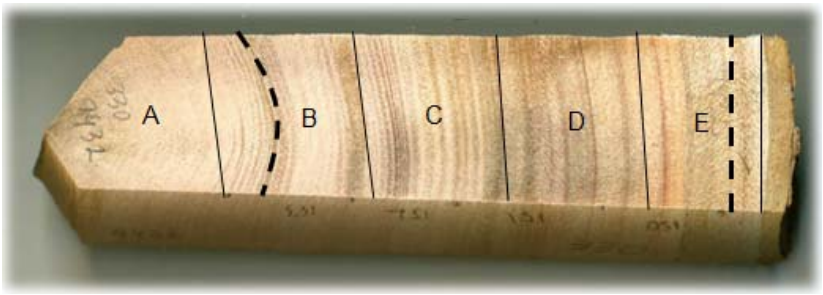

Figure 23 - Radial strips showing curvature effect by dotted lines and classes by continuous lines

The approach for conversion of the X-ray diffractometer pattern to microfibril angle was based on the *T* parameter and on Yamamoto's formula (Yamamoto et al. 1993). Table 12 presents the descriptive statistics for wood basic density, *T* parameter and microfibril angle determinations in *Eucalyptus* wood. The variation range of wood density (CV of ~14%) and microfibril angle (CV of ~17%) are crucial for *Eucalyptus* breeding programs whereas the tree breeders are interested in selecting progenies or clones presenting the most appropriate phenotype.

Table 12 - Descriptive statistics, including average, standard deviation (Sd), minimum (Min), maximum (Max) and coefficient of variation (CV) for basic density (ρ), *T* parameter and microfibril angle (MFA) measurements in 14-year-old *Eucalyptus urophylla* wood

	Average	Sd	Min	Max	CV (%)	N
ρ (kg m^{-3})	547	79	372	742	14.4	175
T parameter (°)	19.7	2.87	14.6	28.7	14.6	175
MFA (°)	12.5	2.14	7.7	19.7	17.1	175

The samples were ranked by radial position in ascending order of their relative radial position. The variation on MFA and density as a function of the relative distance from the pith to bark for 14 radial strips is given in Figure 24. The samples from class B (from 20 to 40% of radial distance) represent the wood formed at the 4^{th} to 6^{th} years while samples from class E (from 80 to 100%) correspond to the wood developed at approximately the 12^{th}, 13^{th} and 14^{th} years. Due to the small dimension of some radial strips, only two or three tangential sections for MFA, and small wood samples for density were removed and these data were not presented in Figure 24.

The patterns of radial variation of these wood traits are in accordance with those reported in the literature, ie, MFA decrease from juvenile wood to mature wood in *Eucalyptus*. For instance, Evans et al. (2000), reported variation in MFA from 20° at the pith to 14° at the bark in 15-year-old *Eucalyptus nitens*. Lima et al. (2004) investigated 8-year-old *E. grandis* × *E. urophylla* clones reporting that its MFA decreased slightly from pith to bark. The radial variation of these wood traits is important, because such properties are targeted in breeding programs to distinguish improved varieties according to their variance; however, frequently, the within-tree variability is higher than the between-trees variability.

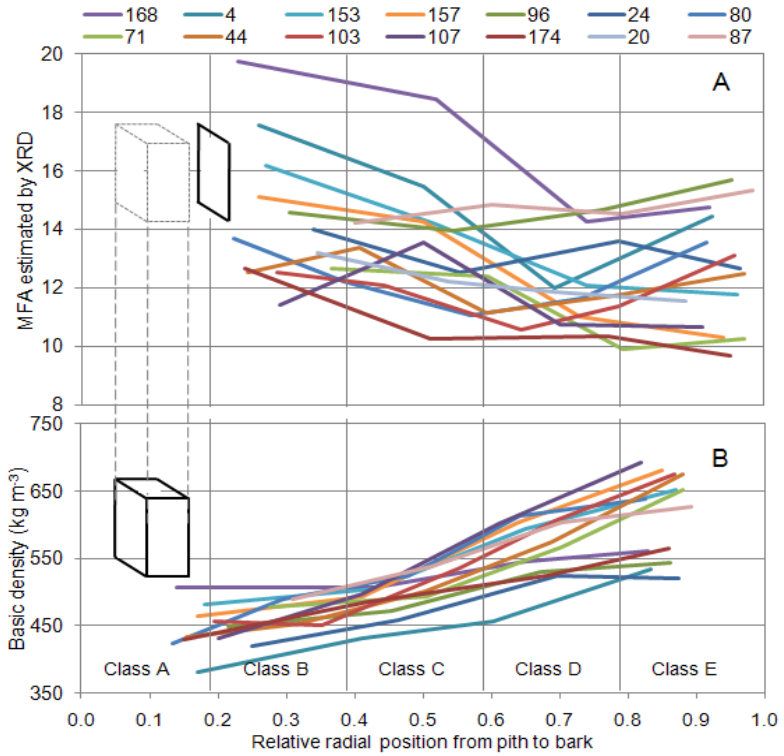

Figure 24 - Radial variation of MFA (A) and basic density (B) in 14-year-*Eucalyptus urophylla* wood for radial strips (N=14)

The mean MFA values of each class (B to E) were not statistically different by the Tukey test at $p>0.01$ while the mean basic density of wood significantly increased in a linear way from pith to bark (Table 13). Thus, the radial variation of MFA in *Eucalyptus* wood is not statistically evident, because the large MFA variability between trees results in a large standard deviation within each class (for instance, in class B the MFA ranged from ~11° to ~19°).

The trends in radial variation of MFA and density (Table 13) are in accordance to those of Lima et al. (2004), who reported that the microfibril angle of 8-year *Eucalyptus* seemed to decrease slightly from pith to bark in a non-linear fashion, but not statistically significant. However, a decrease of MFA values from pith to bark can be clearly observed when each radial strip was analysed. Figure 24 reveals that, on average, the microfibril angles appears to be higher near the pith of the discs (Class B), decreasing radially towards to the bark (Class E). Such pattern of MFA variation occurred most frequently, but among the various strips we used (40), different trends could be observed. For instance, the MFA of samples 80, 87, 96, 103 and 153 slightly increased near to the bark. For basic density of wood, a linear increase from pith to bark was found (Figure 24), even if the variability of density between trees was taken into account.

Table 13 - Description of tangential sections from the radial wood strips, their influence on the *T* parameter measurements and the radial variation of MFA and basic density in 14-year-old *Eucalyptus urophylla* wood. The relative radial position is presented in squared brackets while the range of variation of traits is presented in parentheses

Classes	A [0-20]	B [21-40]	C [41-60]	D [61-80]	E [81-100]
Curvature effect	very strong	strong	moderate	weak	none
T_1	-	20.3[a] (16-27)	19.0[a] (16-24)	19.1[a] (15-26)	19.3[a] (15-25)
T_2	-	20.3[a] (16-26)	19.5[a] (16-25)	19.3[a] (15-28)	19.4[a] (15-24)
T_3	-	19.5[a] (16-22)	19.4[a] (16-27)	19.6[a] (15-29)	19.4[a] (15-25)
ρ	-	450[a] (370-520)	507[b] (430-620)	564[c] (420-740)	622[d] (520-700)
% of samples	-	16.6	26.9	26.3	30.3

Means followed by the same letter are not significantly different at 1% level by the Tukey test.

3.2.3 Effect of wood chemical components on MFA

Based on studies on hardwood and softwood tissue reaction, which possess special features in cell wall composition, one may assume that cellulose MFA and lignin content in the S_2 layer could be generally related to each other (Jungnikl et al. 2008). In softwoods, Via et al. (2009) showed that MFA and lignin content are associated, at least in some way. In hardwoods, this relationship has been observed in a range of wood species (Barnett and Bonham 2004) both in reaction and normal wood, but some studies have reported no correlations between MFA and chemical components. For instance, Baillères et al. (1995) investigated hybrids of *Eucalyptus* clones from Congo demonstrating clearly that decreases in microfibril angles of cellulose are linked to the decrease in lignin content and increase in syringyl to guaiacyl ratio. On the other hand, Jungnikl et al. (2008) examined this correlation in *Picea abies* tissues finding any correlation, neither for the individual tissue types nor for the compiled data of all tissues.

In the present study, MFA showed a low coefficient of correlation with lignin content predicted by NIR-based model. We applied our NIR-based model for klason lignin content (Hein et al. 2010d, **paper 4**) in the 175 tangential sections. The correlation between the NIR-based estimates of lignin content and XRD measured microfibril angle values was 0.4. It is important to note that this klason lignin model was calibrated from NIR spectra measured on the transverse face of the wood discs (such discs were surfaced using a plane). Phenotypic, residual and genetic relationships between Klason lignin and microfibril angle are presented and discussed within the item 3.5.3 at page 103.

3.3 Phenotyping the wood of clonal tests

3.3.1 Kiln-dried scantlings

The air-dried scantlings were kiln-dried at 14% (nominal) under soft condition during two weeks. Table 14 lists the descriptive statistics of the kiln-dried density and dynamic properties of the kiln-dried at 14% scantlings of *Eucalyptus* wood.

For kiln-dried scantlings there was no statistically significant difference between averaged values of longitudinal and flexural elastic modulus (Table 14). Flexural vibrations are assumed to be more sensitive to the presence of knots and small cracks in the scantlings than longitudinal vibrations, especially for air-

dried scantlings. Some key factors affecting the transverse vibration were reported by Murphy (2000) and possibly influenced our results. In addition to these factors, according to Burdzik and Nkwera (2002) no elasticity measurement method leads to the calculation of pure modulus of elasticity in bending, due to the presence of a shear component in the deflection of the specimen, except for the region of the specimen between the two loading points of 4-points bending tests. However, in this study, the differences between E_L and E_F did not come about from shear effects on flexural vibration, which could bias the estimation, because the model we used to estimate the elastic modulus takes into account the shear effect. Here, we applied the solution proposed by (Bordonné 1989) to the (Timoshenko 1921) motion equation to the first four vibration modes of the scantlings.

Table 14 - Descriptive statistics of dynamic properties of the kiln-dried scantlings of 6-year-old *Eucalyptus grandis* x *urophylla*, including kiln-dried density (ρ14, kg m^{-3}), first resonant frequency ($f_1$14, Hz), elastic modulus (E14, MPa), specific modulus (E'14, E/ρ), loss tangent (tg δ14, 10^{-3}) and shear modulus (G14, MPa) estimated by longitudinal ($_L$) and flexural ($_F$) vibration tests

	ρ14	f_{1L}14	E_L14	E'_L14	tg δ_L14	f_{1F}14	E_F14	E'_F14	G_F14
Mean	548	1,618	12,825	23.43	7.74	98.27	13,278	24.3	693.69
Sd	65.8	346	2,565	2.98	1.74	49.04	2740	3.32	207.6
Min	383	1,027	7432	15.6	4.45	42.9	6,555	13.8	123
Max	776	3,414	21236	32.5	18.7	441.1	23,941	35.5	1,833
CV (%)	12	21.4	20	12.7	22.4	49.9	20.6	13.7	29.9
N	410	410	410	410	328	410	410	410	378

The wood density of the kiln-dried scantlings varied from 518 to 573 kg m^{-3} according to the site where they come from. As trees from site 303 (no inclination) grew up faster than those from site 302 (40 degrees of inclination), the results presented in Figure 25 lead us to suppose that trees developing at low growth rates produce high wood densities while trees growing at high growth rates will result in low dense woods, at least, from a phenotypic point of view. Thus, the differences in mean wood density between sites reflect the effect of growth conditions on biomass production.

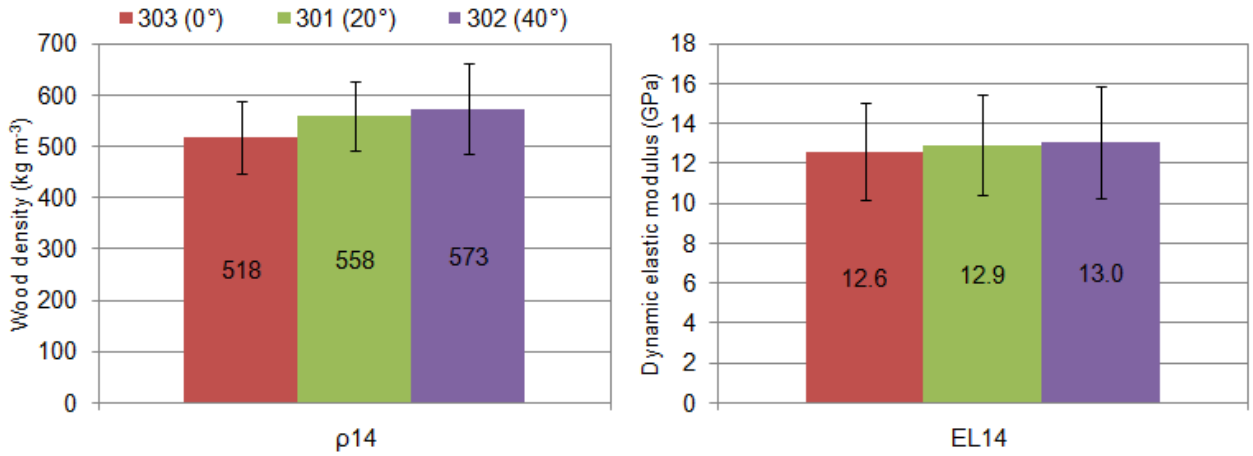

Figure 25 - Mean and standard deviation values of kiln-dried wood density and dynamic elastic modulus in kiln-dried scantlings for each site

The environmental effect on the dynamic elastic modulus on longitudinal vibration test is not clear (Figure 25). Because the elastic properties greatly varied between clones, the standard deviations were high and there were no significant differences between sites according to Tukey test.

Further details are described within the genetic studies section (Table 49, pg. 143) where multiple range tests for density of wood and for dynamic elastic modulus on longitudinal vibration by clone and by site are presented and discussed.

3.3.2 Wood specimens from scantlings

From the 410 scantlings, 160 were selected among the best ones (i.e. annual rings well oriented, free of large cracks etc) and surfaced on the plane machine; beams were cut from them and trimmed to nominal cross-section of 25 mm x 25 mm using a circular saw machine. Then, clean, small specimens measuring 25 mm x 25 mm x 410 mm were cut from the beams. Table 15 lists the descriptive statistics of the dynamic properties and densities of the 334 specimens (sp) of *Eucalyptus* wood. The loss tangent values of the scantlings were calculated from longitudinal test while the loss tangent of the specimens derived from flexural vibrations. As the software alerts us about imprecise estimations, only 141 values for tg $\delta_F$sp were used.

Table 15 - Descriptive statistics of dynamic properties of the clearwood specimens of 6-year-old *Eucalyptus grandis* x *urophylla*, including air-dried density (ρsp, kg m^{-3}), resonant frequency ($f_1$sp, Hz), elastic modulus (Esp, MPa), specific modulus (E'sp, E/ρ), loss tangent (tg $\delta_F$sp, 10^3) and shear modulus (Gsp, MPa) estimated by longitudinal ($_L$) and flexural ($_F$) vibration tests

	ρsp	f_{1L}sp	$E_L$sp	E'_Lsp	tg $\delta_F$sp	f_{1F}sp	$E_F$sp	E'_Fsp	$G_F$sp
Mean	518	6,174	13,391	25.66	7.33	721.69	12,495	24.02	693.68
Sd	59.05	395	2,540	3.52	1.01	42.52	2356	3.082	168.5
Min	362.4	4,918	6522	16.27	5.71	567.4	5,930	14.05	344
Max	708.3	6,945	20785	32.43	10.5	805.9	18,732	30.61	1,499
CV (%)	11.4	6.41	18.97	12.53	13.8	5.89	18.8	12.81	24.3
N	334	334	334	334	141	334	334	334	334

Wood traits of 6-year *Eucalyptus* specimens from Clonal tests strongly varied: coefficient of variation ranging from ~6 (for resonance frequencies) to ~20% (for moduli of elasticity). The air-dried density of the wood specimens ranged from ~350 to ~700 kg m³. Figure 27 presents the air-dried density of the wood specimens (ρsp) and the basic density of the small wood samples taken from specimens (ρs) by site, highlighting the environmental effect on this trait. It appears that trees growing under plan sites produce low density woods, but this pattern of wood density variation seems to be more linked to the growth rate. The results indicate that trees grow up faster in plan sites and their densities are lower. The correlations between these wood traits are presented within the section 3.3.4 (pg. 87).

3.3.2.1 Air-dry density

The effect of growth rate on wood properties, especially on wood density, has been studied intensively (Zobel and Van Buijtenen 1989; Zobel and Jett 1995). According to Zobel and Jett (1995) the growth rate and wood density show little or no meaningful relationship in most of the conifers with dense wood, especially hard pines and in most diffuse-porous hardwoods. However, there were contradictory reports about the relationship between growth rate and wood properties in the hardwoods. A negative relationship between growth rate and wood density has been reported in several softwood genera such as *Picea* (Herman et al. 1998; Dutilleulet al. 1998; Petty et al. 1990) and *Pinus* (Zamudio et al. 2002; Kärenlampi and Riekkinen 2004). Examining the relationships of wood density with growth rate in 16 timber species

(including soft- and hardwoods), Zhang (1995) pointed out that compared with softwoods, and density of hardwoods is remarkably less influenced by growth rate.

For tree breeding programs and industrial applications, the correlation between growth rate and density is of great importance. If increased growth rate results in low-density wood, it also means poor wood quality which limits the suitability of raw material for high quality products. On the other hand, it may also be possible to select trees with both high growth rate and high wood density for breeding.

3.3.2.2 Modulus of elasticity

The flexural vibrations are influenced by the shear effect while the longitudinal ones are affected by the Poisson effect when the length to thickness ratio of the beams is small (Rayleigh 1877). Early studies on dynamic tests of wood (Hearmon 1961; Ilic 2001) showed important differences between E_L and E_F; however, when Ilic (2001) applied the Timoshenko correction, the difference between E_L and E_F varied from 13% (for uncorrected E_F) to 1.1% (for corrected E_F). Table 15 show that average value of $E_L$sp (13,391 MPa) was higher than $E_F$sp (12,495 MPa). In this study, the differences between E_L and E_F did not come about from shear effects on flexural vibration because the model we used to estimate the E_F takes into account the shear effect. Here, the solution proposed by Bordonné (1989) to the Timoshenko (1921) motion equation was applied to the first four vibration modes of the wood beams. The Poisson effect in longitudinal vibrations is negligible because the length to thickness ratio of the scantlings and small specimens was superior to 30 and 15, respectively. Additional factors affecting the flexural vibrations were reported by Murphy (2000).

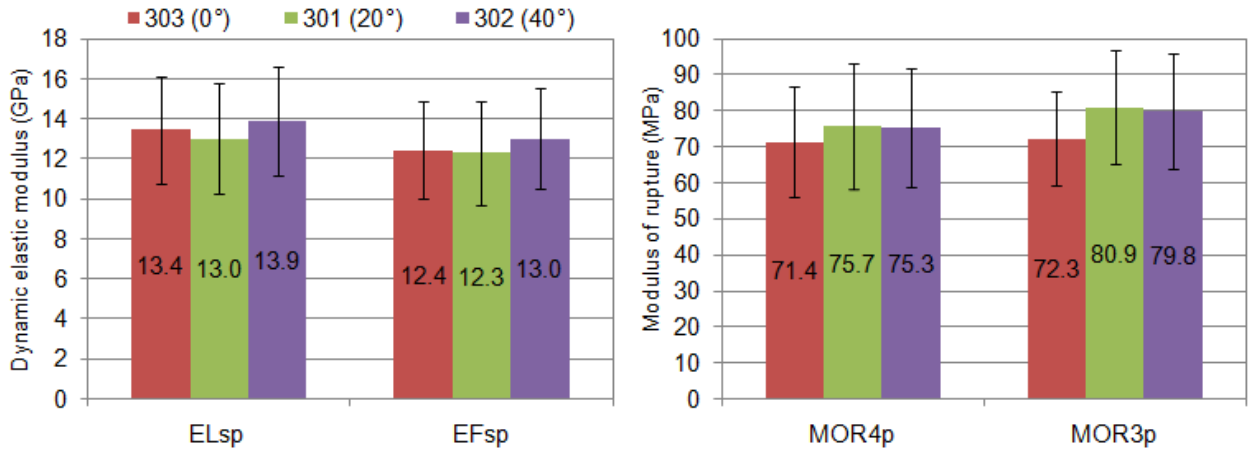

Figure 26 - Mean and standard deviation values of longitudinal and flexural dynamic elastic modulus and 4- and 3-points bending test in small samples of *Eucalyptus* for each site

Figure 26 shows the statistics of longitudinal and flexural dynamic elastic modulus by site and considering all samples. Although the wood stiffness is related with its density, the pattern of variation of elastic modulus according to the site is different than that presented for wood density (Figure 27). Since the standard deviations were high, there were no differences between sites for wood stiffness; however there was significant effect for clones. These findings (Figure 26) are discussed within the genetic studies section (Table 39, pg. 116) where multiple range tests for wood stiffness by radial position, by clone and by site are presented.

3.3.2.3 Modulus of rupture

After the dynamic tests, the twin wood specimens were tested in a 4- and 3-points bending test using a universal testing machine. Table 16 lists the descriptive statistics of the modulus of rupture (MOR) and force at rupture point (Fmax) in 4- and 3-points bending test using 224 and 137 specimens, respectively.

Table 16 - Descriptive statistics of the 4- and 3-points bending test of the specimens of 6-year-old *Eucalyptus grandis* x *urophylla*, including force at rupture point (Fmax, N) and modulus of rupture (MOR, MPa)

	$Fmax_{4p}$	MOR_{4p}	$Fmax_{3p}$	MOR_{3p}
Mean	3,404	73.7	2,129	77.2
Sd	757	16.3	419	15.3
Min	1,207	25.4	1,149	42.3
Max	5,557	119.1	3,528	122.5
CV (%)	22.2	22.1	19.7	19.8
N	224	224	137	137

According to Brancheriau et al. (2002), contrary to 3-points bending, a 4-points loading does not induce a shear effect between the loading points. Moreover the indentation of the supports and the loading head does not influence the deflection measurement.

The results using the twin specimens shows no significant differences between MOR obtained by 4- and 3-points bending tests; However, force at rupture point (Fmax) were significantly higher in 4-points (3,404 N) than in 3-points (2,129 N) bending tests. Figure 26 shows the modulus of rupture in 3- and 4-points bending test by site. Similarly to wood stiffness, there were no differences between sites for modulus of rupture.

3.3.3 Small wood samples

3.3.3.1 Dimensional Stability

Wood is dimensionally stable when moisture content is greater than the fibre saturation point (FSP). Below FSP wood changes dimension as it gains moisture (swells) or loses moisture (shrinks), because volume of the cell wall depends on the amount of bound water (Glass and Zelinka 2010). As an anisotropic material, wood shrinks (swells) most in the direction of the annual growth rings (tangentially) and about half as much across the rings (radially). Here, the radial and tangential shrinkage of wood samples is presented under three conditions: (**i**) from the oven-dried (0%) to the equilibrium moisture content (EMC) condition [0-EMC]; (**ii**) from the EMC to the green (100%) condition [EMC-100] and (**iii**) from oven-dried to green condition [0-100%]. Table 17 shows the descriptive statistics of the basic density and radial and tangential shrinkage of the small wood samples, taken from the wood specimens.

From the oven-dried condition to EMC, the wood samples swell around 1.2% and 1.8% radially and tangentially, respectively (Table 17). From EMC to the green condition, the wood samples swell around 3.5 and 5.9% in radial and tangential sense, respectively. In short, wood swell 4.8% (radially) and 7.8% (tangentially) from oven-dried to above FSP condition. Figure 27 shows the mean and standard deviation values of radial and tangential shrinkage from oven-dried to green conditions for each site. It seems that shrinkage is affected by growth rate or by density (since growth rate and density are correlated and

affected by site); however, the analysis of variance (GLM procedure) shows no difference of shrinkage between sites.

Table 17 - Descriptive statistics of basic density (ρs, kg m^{-3}) and radial and tangential shrinkage (%) of the small samples of 6-year-old *Eucalyptus grandis* x *urophylla*

	ρs	radial shrinkage			tangential shrinkage		
		0-EMC	EMC-100	0-100	0-EMC	EMC-100	0-100
Mean	420	1.21	3.54	4.80	1.79	5.90	7.80
Sd	52.2	0.56	1.18	1.40	0.79	1.54	1.58
Min	288	0.10	1.23	1.75	0.04	1.94	3.24
Max	617	4.02	7.55	10.39	5.76	12.26	13.35
CV (%)	12.4	46.6	33.4	29.2	43.8	26.2	20.3
N	225	225	225	225	225	225	225

The combined effects of radial and tangential shrinkage can distort the shape of wood pieces because of the difference in shrinkage and the curvature of annual rings (Glass and Zelinka 2010). Thus, these dimensional changes are important because can result in warping, checking, and splitting of the wood decreasing utility and economic value of wood products.

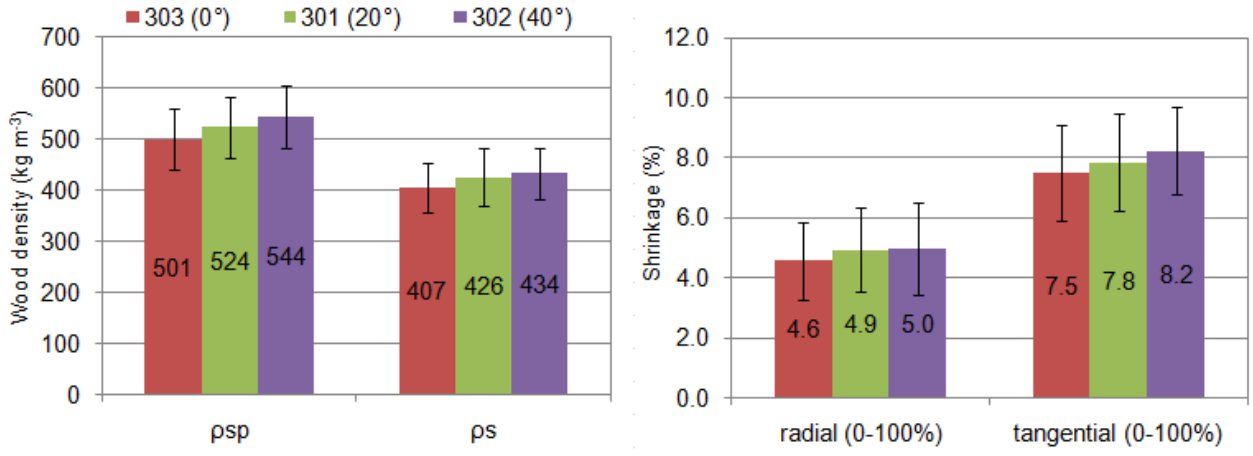

Figure 27 - Mean and standard deviation values of air-dried density of the specimens (ρsp) and of the basic density of the small wood samples (ρs) and radial and tangential shrinkage from oven-dried to green conditions for each

3.3.3.2 Microfibril angle

Microfibril angle of the secondary cell wall were analysed by X-ray diffraction using 2-mm radial sections taken from the specimens and from radial strips. Table 18 lists the descriptive statistics of the *T* parameter obtained by X-ray diffraction and microfibril angle estimated by Cave (MFA_C) and Yamamoto (MFA_Y) formulas from the small wood samples and radial strips of 6-year-old *Eucalyptus grandis* x *urophylla*. Figure 28 exhibits the microfibril angles estimated from X-ray diffraction patterns measured on 2-mm radial sections while Figure 29 shows the MFA's measured on 2-mm radial strips of *Eucalyptus* by clone and by site presenting the radial variation of the microfibril angle in 6-year-old *Eucalyptus* wood. Table 19 lists the statistics of microfibril angle measured on the radial strips according to the year of wood formation by site. The variation in MFA between clones appears to be uniform in the Site 303 (Figure 29 A2) presenting standard deviation of similar magnitude over the radial range (Sd≈1.6°) while the MFA of

samples from Site 301 (Figure 29 B2) clearly varied in higher magnitude in the first years (Sd≈3°) decreasing their variance magnitude towards the cambium (Sd≈0.7°).

Table 18 - Descriptive statistics of the *T* parameter obtained by X-ray diffraction and microfibril angle estimates by Cave (MFA_C) and Yamamoto (MFA_Y) formulas from the small samples of 6-year-old *Eucalyptus grandis* x *urophylla*. Samples were taken from the small wood samples (MFA_{YS}) and from radial strips (MFA_{YRS})

	XRD measures from small wood samples			XRD measures from radial strips		
	T (°)	MFA_C (°)	MFA_{YS} (°)	*T* (°)	MFA_C (°)	MFA_{YRS} (°)
Mean	19.57	11.68	12.11	17.72	10.63	10.33
Sd	3.91	2.25	2.55	3.06	1.83	2.76
Min	15.43	9.37	8.21	12.98	7.79	4.06
Max	41.09	24.66	24.31	33.05	19.83	19.47
CV (%)	20	19.2	21	17.2	17.2	26.7
N	225	225	225	165	165	165

Trees from site 301 (20°) presented, in average, the higher MFA. It is important to note that wind velocity (see Table 5, pg. 58) of this site is higher (3.2 m/s) than other (0.9 m/s) and this factor also can explain why MFA is higher. The radial strips of sites 301 (20°) and 302 (40°) were taken from the region presenting (hypothetically) tension wood because the terrain slope. In *Eucalyptus*, as in many other hardwood species, tension wood is associated to the formation of the gelatinous layer where the microfibril angle is very small (Clair et al. 2006). For this reason, the averaged MFA values of XRD measurements from radial strips (MFA_{YRS}=10.3) are lower than those for small specimens (MFA_{YS}=12.1) in which samples were taken containing opposite, normal, and tension wood. Because these data comes from two independent set of samples (longs and discs), it was not possible to perform multiple range tests to verify if the mean values were significantly different. However, the analysis of variance shows no difference in MFA between sites. In short, as the standard error bars overlap (Figure 28) this implies that the two means were not significantly different. Table 19 shows the radial variation of the MFA mean values measured on the radial strips.

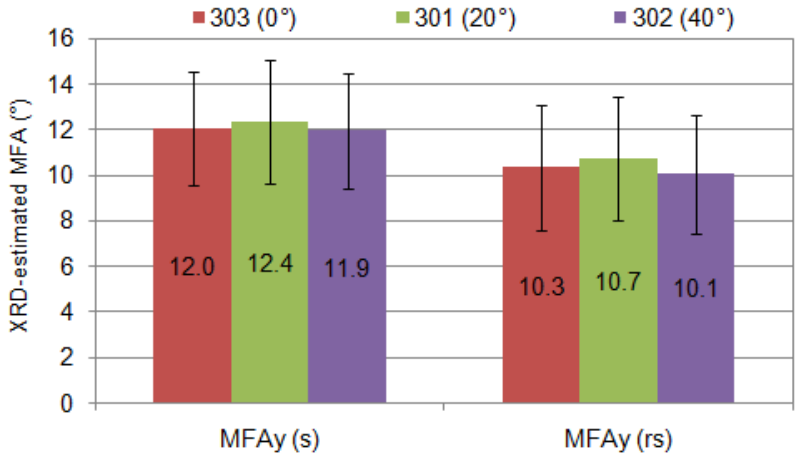

Figure 28 - Mean and standard deviation values of MFA in small wood samples (MFA_{YS}) and radial strips (MFA_{YRS}) of *Eucalyptus* wood for each site and for all samples

X-ray diffraction is fast and reliable technique, but gives only a relative figure for the microfibril angle since the estimative comes from an interpretation of the diffraction pattern called the *T* parameter.

Numerous studies have proposed models to estimate MFA from *T* parameters (Cave 1966; Meylan 1967; Yamamoto et al. 1993; Ruelle et al. 2007). In this study the formula proposed by Yamamoto et al. (1993) was used in most of cases. We did not propose a formula for transforming *T* values into MFA estimates specifically for *Eucalyptus* because the absolute value of the property is of no matter in this study. The interesting point is to know the relative value of the characteristic between trees or regions of the stem, its variation or stability within the logs. These MFA estimates can be useful for selection of candidate genotypes or commercial clones in forestry industries from a large wood sampling. For instance, clones 4557 and 4515 appear to produce the lower microfibril angles.

Table 19 - Mean and standard deviation (in parentheses) of microfibril angle according to the year of wood formation estimated by Yamamoto (MFA_{YRS} in degrees) formulas from radial strips of 6-year-old *Eucalyptus* clones from sites 301, 302 and 303

Site	1st year	2nd year	3th year	4th year	5th year
303 (0°)	14.2 (1.9)	12.0 (1.6)	10.4 (1.3)	8.7 (1.8)	8.4 (1.3)
301 (20°)	13.3 (3.0)	11.3 (2.1)	9.5 (0.8)	8.4 (0.6)	7.9 (0.7)
302 (40°)	14.6 (1.7)	11.3 (1.8)	9.2 (1.9)	8.3 (0.8)	7.9 (1.7)

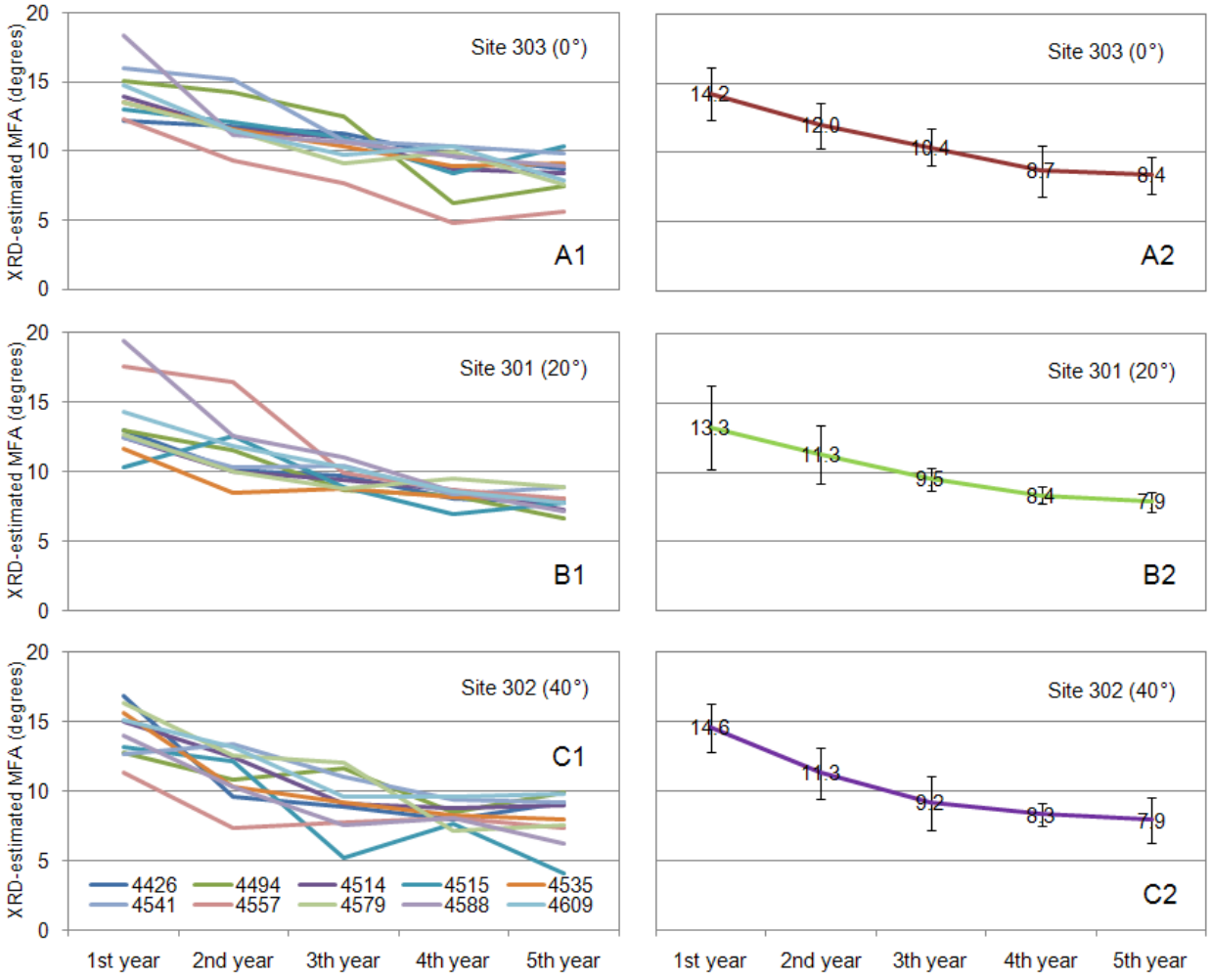

Figure 29 - Radial variation of MFA (estimated by Yamamoto's formula) for wood samples taken from radial strips of 6-year-old *Eucalyptus* clones

The X-ray diffraction data from radial strips were used to develop NIR calibrations while the XRD data from small wood samples provided information about the relationships concerning MFA and other wood traits.

3.3.4 Correlations among wood traits of *Eucalyptus* from clonal test

The correlations among MFA, wood stiffness and strength, density and shrinkage are presented in Table 20. As expected, wood density was found to be well correlated with stiffness (r=0.82) and strength (r=0.68 for MOR_{4p} and r=0.71 for MOR_{3p}) in these *Eucalyptus urophylla* x *grandis*. Early studies have reported correlation between these traits in higher magnitudes. For instance, Evans and Ilic (2001) found higher relationship between density and modulus of elasticity (R^2=0.70) in *Eucalyptus delegatensis*. Yang and Evans (2003) reported strong correlations between wood density and modulus of rupture (R^2=0.80) in wood samples of *Eucalyptus globulus*, *E. nitens* and *E. regnans*.

MFA was negatively correlated to radial (r=-0.24) and tangential (r=-0.33) shrinkage (Table 20). Because the variation ranges of MFA are greater in softwoods, these correlations are lower than those presented by Meylan (1968) for *Pinus* and Yamamoto et al. (2001) for *Sugi.*

Although the range of variation in MFA is narrow in *Eucalyptus* some studies have been demonstrated the influence of microfibril orientation on anisotropic shrinkage. Washusen and Evans (2001) examined the correlations between tangential shrinkage and cellulose crystallite width in 11-year-old *Eucalyptus globulus* showing that cellulose crystallite width was closely associated with tangential shrinkage. According to their results, shrinkage increases as crystallite width increased. Wu et al. (2006) explored the relationships of the main anatomical features with shrinkage in *Eucalyptus* wood demonstrating that the main factors affecting shrinkage were cell wall proportion, microfibril angle, and cell wall thickness.

Table 20 - Correlations between wood traits including wood density (ρ), elastic modulus (E), specific modulus (E'), shear modulus (G), radial (δrd) and tangential shrinkage (δtg), microfibril angle, ρ/MFA parameter and modulus of rupture (MOR). The correlations were statistically significant at $p<0.01$

	ρ	E_L	E'_L	G	δrd	δtg	MFA	ρ/MFA	MOR_{4p}
E_L	0.82	1							
E'_L	-	0.83	1						
G	0.28	-	-0.23	1					
δrd	0.39	0.40	0.28	0.18	1				
δtg	0.43	0.44	0.29	-	-	1			
MFA	-0.40	-0.61	-0.65	0.20	-0.24	-0.33	1		
ρ/MFA	-	0.82	0.60	-	0.36	0.43	-0.84	1	
MOR_{4p}	0.68	0.81	0.66	-	0.29	0.29	-0.47	0.61	
MOR_{3p}	0.71	0.79	0.53	-	0.31	0.29	-0.46	0.60	0.86

Wood density also shows a negative relationship with MFA and positive relationship with shrinkage. According to Donaldson (2008) MFA shows a variable relationship with wood density. Here, we found a moderate, but significant negative correlation between MFA and density (r=-0.40) in *Eucalyptus urophylla x grandis* wood from clonal tests. However, this finding is contrary to that reported in this study for the woods from progeny test, where no correlation between density and MFA were found. Evans et al. (2000) also reported no correlation between MFA and density in *Eucalyptus nitens* wood samples.

Figure 30 shows the correlations of MFA with specific modulus (A), tangential shrinkage (B), and the correlations of ρ/MFA with modulus of elasticity (C) and modulus of rupture (D) in *Eucalyptus* wood. The specific modulus decreased as microfibril angle increased (Figure 30 A) as expected (Evans and Ilic 2001; Yang and Evans 2003; Donaldson 2008). However, MFA variation accounted for only 44 percent of the variation in specific modulus. Thus, microfibril angle controls in low magnitude the wood stiffness in 6-year-old *Eucalyptus*. The correlation (r) between MFA and modulus of elasticity was -0.61. These relationships were lower than those reported in previous studies. For instance, Evans and Ilic (2001) showed that various combinations of MFA and density accounted for up to 96 percent of the variability in modulus of elasticity. Similarly, Yang and Evans (2003) reported that MFA alone accounted for 87 percent of the variation in E, while density alone accounted for 81 percent. Thus, MFA and density accounted together for 92 percent of the variation in wood stiffness. MFA was also negatively correlated to MOR_{4p} (r=-0.47) and MOR_{3p} (r=-0.46) in these wood samples (Table 20). The relationships of modulus of elasticity and modulus of rupture were high (r=0.81 for 4-point and r=0.79 for 3-point bending test).

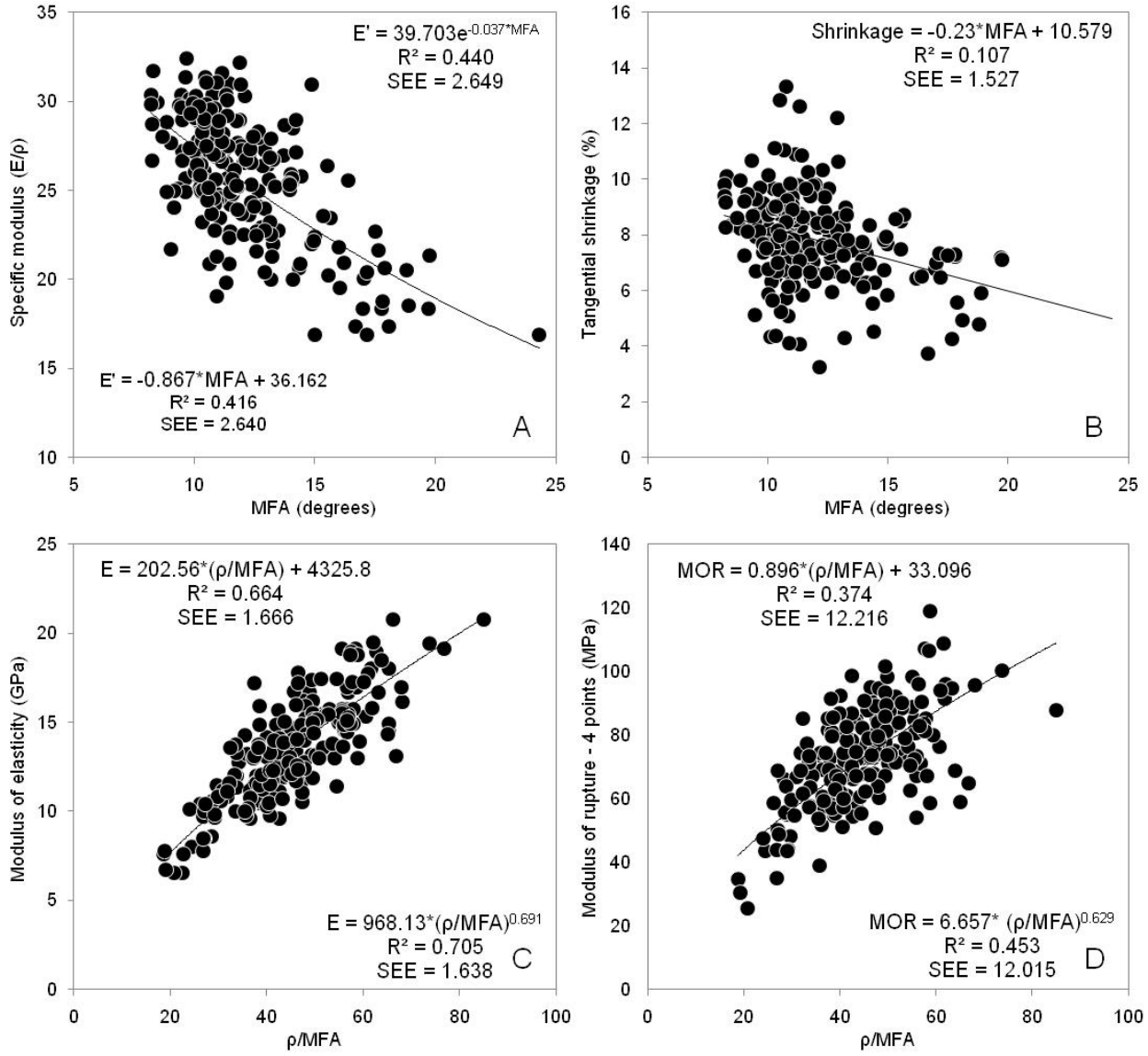

Figure 30 - Relationship between wood traits in *Eucalyptus* wood. SEE is the standard error of estimation

3.3.4.1 Relationships of density and MFA with stiffness and strength

The influence of MFA and/or density on stiffness and strength of these wood samples were better examined. Table 21 presents regression models for predicting modulus of elasticity and modulus of rupture with MFA, density, ρ/MFA and MFA and density together. These findings are particularly useful for understanding the relationships between MFA and stiffness, and strength with and without considering wood density. Because fewer samples were tested in 3-point bending test, only MOR_{4p} was examined in this part of the study.

Evans and Ilic (2001) reported that density variation alone accounted for 70% of the variation in E, while MFA alone accounted for 86% using *Eucalyptus delegatensis* R.T. Baker samples. Thus, the influence of MFA on wood stiffness was significantly greater than that of density for their samples. Afterward, Yang and Evans (2003) found that MFA alone accounted for 87% of the variation in modulus of elasticity. They also reported a strong coefficient of determination (R^2=0.92) between ρ/MFA and E in *Eucalyptus globulus*, *E. nitens* and *E. regnans*.

Table 21 - Regression models for predicting modulus of elasticity in longitudinal (E_L) and flexural (E_F) vibrations and modulus of rupture (MOR_{4p}) with MFA, density, and ρ/MFA

Trait	Intercept	MFA	ρ	ρ/MFA	R^2	SEE
E_L	21427.2	-680.43			0.37	2,281
	-5287.1		35.976		0.68	1,609
	4325.7			202.567	0.67	1,651
	1995.6	-367.61	30.557		0.78	1,349
E_F	20208.6	-634.28			0.38	2,082
	-4606.6		32.940		0.67	1,509
	4170.2			186.068	0.67	1,521
	2441.4	-352.01	27.612		0.77	1,253
MOR_{4p}	110.97	-3.166			0.22	14.10
	-22.17		0.184		0.46	11.72
	33.096			0.896	0.37	12.20
	11.42	-1.660	0.158		0.51	11.12

After the previous studies presented by Evans and Ilic (2001) and Yang and Evans (2003), the parameter ρ/MFA has been used for explaining the stiffness in a range of wood. This parameter (ρ/MFA) is able to predict the modulus of stiffness better than MFA explains variation in specific modulus of wood of a range of genera. For instance, McLean et al. (2010) recently demonstrated that 76% of the variation in E was explained by the factor ρ/MFA in wood samples of Sitka spruce.

Despite these relationships (Figure 30 A and C) involve the same variables (E, ρ and MFA), many studies have systematically reported equivalent findings (Evans and Ilic 2001, Yang and Evans 2003, McLean et al 2010). The arisen hypothesis is that the coefficient of variation of MFA (21.2), E (21.2) and ρ (12.5) played a critical role to explain this trend. In the correlation concerning the parameter ρ/MFA, the numerator represents a quantity varying 12.5 percent while the denominator varies twice as. On the other hand, the correlation concerning specific modulus (E/ρ), the CV of the denominator is 2 times greater than the numerator's CV. There may be also a scale effect since the E values were calculated from entire specimens whereas the ρ and MFA represented only a small portion of them.

Here, the coefficient regressions for longitudinal and flexural elastic modulus are very close (Table 21). These two dependent variables are much correlated and models were performed using the two variables to serve as a sort of validation. Density was the prime factor controlling wood stiffness. The models relating wood density to its stiffness yield coefficient of determination (R^2) of 0.68 (using E_L) and 0.67 (using E_L). MFA variations accounted for around 0.38 percent of the variation in modulus of elasticity. When density and MFA are considered together, variations in modulus of elasticity are better explained (R^2=0.78). The parameter ρ/MFA was also a good predictor of wood stiffness. The relationships of MOR_{4p} with MFA and wood density presented similar patterns. Again, density was the primary factor controlling wood strength (R^2=0.46) but MOR_{4p} is better predicted when density and MFA are considered together (R^2=0.51). The coefficient of determination was high and the standard error of prediction was lower when E or MOR_{4p} were modeled from density and MFA together. These finding are similar to those presented by Lachenbruch et al. (2010) who evaluate these relationships in Douglas fir. **Paper 2** presents and discusses theses issues.

3.4 Near infrared spectroscopic models

3.4.1 NIR spectra

Wood is a complex three-dimensional biopolymer material composed of an interconnected network of cellulose, hemicelluloses, and lignin with minor amounts of extractives and inorganics (Kollmann and Côté 1968). Hence, NIR spectra reflect the energy reflected (or captured) by chemical bonds from different wood components, their contents and interactions. Figure 31 illustrates the untreated NIR spectra measured directly in two contrasting specimens (A and B) of 14-year-old *Eucalyptus urophylla* wood from progeny test. The specimen labeled as "A" exhibits the NIR spectra of the denser or stiffer sample while B represents to the less dense or stiff sample.

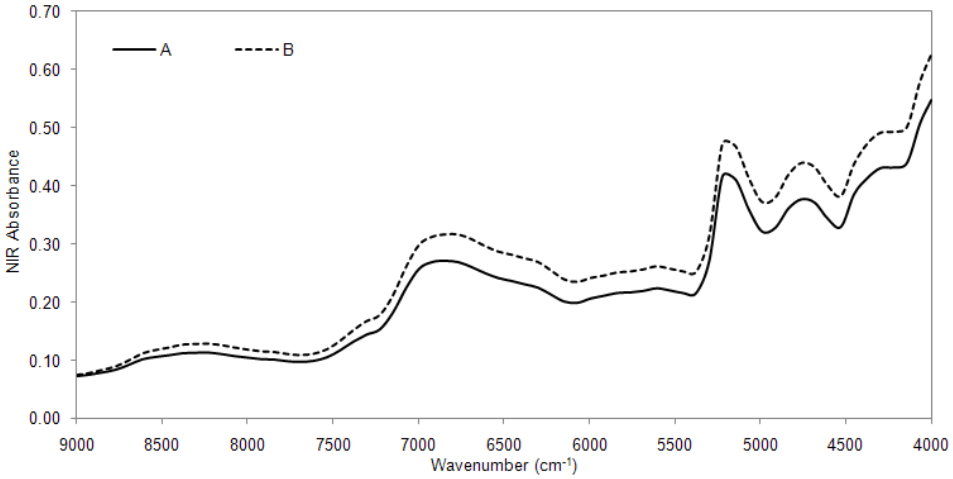

Figure 31 - NIR absorbance versus wavenumber plot for raw (untreated) NIR spectra from 9,000 to 4,000 cm^{-1} range.

Figure 32 shows minutely the NIR absorbance versus wavenumber plot for first and second derivative of the NIR spectra from 8,000 to 5,500 cm^{-1} range spectra of two contrasting specimens (A and B) of 6-year-Eucalyptus wood from clonal test. The scaling factor for first derivatives was of 10^2 and for second derivatives was of 10^3. Bands assigned to chemical compounds are represented by numbers and listed in Table 26. This wavenumber range is important because the differences between the stiffest and the weaker samples can be clearly visualized. The band at 7,092-7,057 cm^{-1} (index 3) is assigned to lignin.

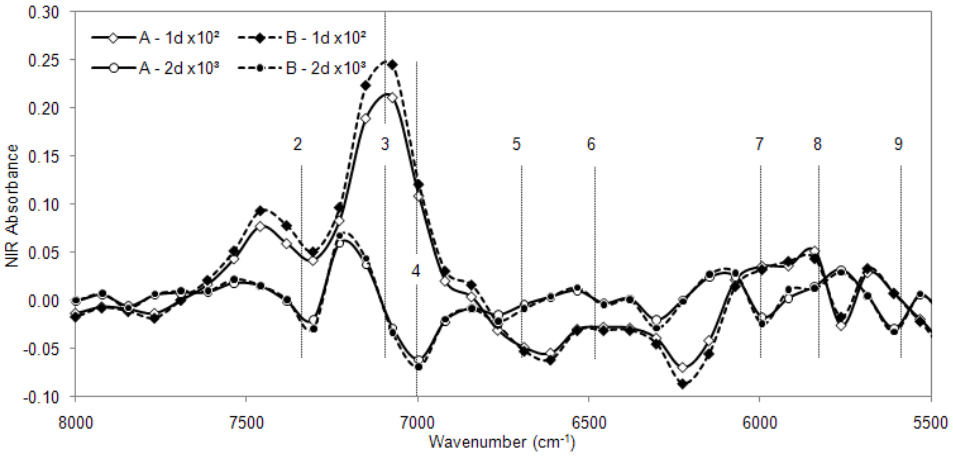

Figure 32 - Absorbance versus wavenumber plot for first and second derivative of the NIR spectra

3.4.2 Reference data

Table 22 and Table 23 list the mean, minimum and maximum values, coefficient of variation and number of samples of the calibration and test sets for a range of *Eucalyptus* wood traits from progeny and clonal tests, respectively. According to Mora and Schimleck (2008) the predictive models must include all possible sources of variation that can be encountered later in real applications because the goal is to estimate values in new samples.

Table 22 - Descriptive statistics of Klason lignin (KL), S to G ratio (S/G), basic density (ρ) and microfibril angle (MFA) of 14-year-old *Eucalyptus urophylla* woods from progeny test

Traits	Average	SD	Min	Max	CV (%)	N
Klason lignin (%)	28.5	1.37	25.4	31.9	4.8	60
S/G ratio*	2.4	0.34	1.7	3.0	14.5	60
ρ (kg m^{-3})	525	82	338	746	15.6	190
MFA (degrees)	12.5	2.14	7.7	19.7	17.1	175

* syringyl to guaiacyl ratio obtained by thioacidolysis

Cross-validation models were performed for KL and S/G because only 60 samples were analysed by wet-chemistry. In the other hand, independent test sets could be used to validate the PLS-R models for density (ρ), MFA and dynamic elastic properties. A range of PLS-R models were developed from calibrations set and validated from the validation set. The subsets were manually selected in order to guarant that the test set of such wood traits had as extreme values as possible. The extreme samples of the validation set were comprehended within the variation interval of the calibrations set.

Table 23 - Statistical summary of the overall, calibration and validation sets for air-dry density, basic density, microfibril angle and a range of dynamic properties of the small, clean specimens of *Eucalyptus* wood from clonal test

	ρsp	ρs	MFA	E_L	E'_L	f_1	E_F	E'_F	$\tan\delta_L$
Mean	517.4	419.8	10.33	13361	25.7	6170	12468	24.0	7.51
sd	58.38	52.21	2.76	2528	3.23	396.5	2331.8	3.07	1.53
min	362.5	287.7	4.06	6522	16.3	4919	5930	14.1	5.18
max	708.4	617.4	19.47	20785	32.4	6945	18732	30.6	15.60
CV	11.3	12.4	26.7	18.9	12.6	6.4	18.7	12.8	20.3
N	327	225	165	326	326	326	327	327	147
Calibration set									
Mean	517.1	418.5	10.20	13333	25.6	6170	12455	24.0	7.52
min	362.5	313.8	4.20	6522	17.9	4919	5930	14.1	5.18
max	708.4	548.9	18.10	20785	29.8	6916	18732	30.6	15.60
COV	11.0	11.0	22.2	18.2	8.2	6.2	18.1	12.5	20.9
N	196	129	98	195	195	195	196	196	80
Validation set									
Mean	517.8	419.6	10.60	13403	25.6	6171	12488	24.1	7.51
min	375.2	331.4	6.24	6715	18.0	5014	6035	15.3	5.66
max	697.1	537.4	19.20	19475	29.7	6945	18176	29.8	13.70
COV	11.8	10.2	28.3	20.0	9.0	6.7	19.6	13.2	19.7
N	131	90	63	131	131	131	131	131	67

3.4.3 NIRS-based calibrations and validations

3.4.3.1 Progeny test

Statistical summaries of the predictive PLS-R models for klason lignin, S to G ratio, density and microfibril angle of the wood from progeny test are presented in the Table 24. The PLS-R models for chemical properties, especially KL and S/G, were previously presented in Hein et al. (2010) (**paper 4**). In regard to the non-chemical wood traits, the PLS-R models for wood density were presented, validated and discussed in Hein et al. (2009) (**paper 5**) while the models for MFA in Hein et al. (2010b) (**paper 6**).

Table 24 - PLS-R models for Klason lignin (KL, %), syringyl to guaiacyl ratio (S/G, no unit), wood basic density (ρ, kg m^{-3}) and microfibril angle (MFA, degrees) used for estimating phenotypic values for 14-year-old *Eucalyptus urophylla*

Trait	Treat	R²c	RMSEC	R²p	RMSEP	LV	Outliers	RPD
KL	none	0.88	0.44	0.85	0.53	6	5.0%	2.58
S/G	2nd der.	0.92	0.01	0.86	0.13	7	5.0%	2.68
ρ	2nd der.	0.89	27.0	0.85	30.0	3	2.1%	2.70
MFA	2nd der.	0.66	1.24	0.59	1.36	6	0.0%	1.57

NIR-predicted versus laboratory-determined values plots for klason lignin (A), syringyl to guaiacyl ratio (B), basic density (C) and microfibril angle (D) of the wood from progeny test are given in Figure 33. The PLS-R models for KL and S/G were based on NIR spectra measured from milled wood at 0.5 mm while the predictive models for density and MFA were developed with NIR spectra measured from radial surface of the wood samples.

3.4.3.2 Clonal test

PLS-R models validated by independent test set

The PLS-R models were built from the untreated and pre-treated NIR spectra data from 9,000 to 4,000 cm^{-1} for ρ, E_L, E'_L, f_{1L}, E_F, E'_F and $\tan\delta_F$ of *Eucalyptus* wood specimens. The statistics associated to the PLS-R models validated by test sets are presented in the Table 25.

Table 25 - PLS-R models for air-dry density (ρ_{sp}, kg m^{-3}), wood basic density (ρ_s, kg m^{-3}), microfibril angle (MFA, degrees), longitudinal and flexural modulus of elasticity (E, MPa), longitudinal and flexural specific modulus (E', MPa/ρ), first resonance frequency (f_1, MHz) and loss tangent ($\tan\delta_L$, 10^3) used for estimating phenotypic values for 6-year-old *Eucalyptus* clones

Trait	Treat	R²c	RMSEC	R²p	RMSEP	LV	Outliers	RPD
ρ_{sp}	2nd der.	0.66	31.44	0.67	34.78	4	0.9%	1.75
ρ_s	snv+1st der.	0.82	21.75	0.80	22.88	3	2.6%	2.32
MFA	snv+1st der.	0.77	1.11	0.75	1.31	5	6.6%	2.10
E_L	1st der.	0.78	1128	0.81	1149	5	1.2%	2.34
E'_L	2nd der.	0.74	1.59	0.76	1.62	5	0.0%	1.41
f_1	2nd der.	0.77	185.6	0.72	215.3	6	0.0%	1.92
E_F	1st der.	0.71	1211	0.74	1219	4	0.6%	2.01
E'_F	1st der.	0.62	1.82	0.70	1.69	6	0.3%	1.88
$\tan\delta_L$	1st der.	0.49	0.71	0.38	0.81	5	1.4%	1.84

While promissory model statistics ($r^2p \geq 0.70$) were obtained for ρ, MFA, E_L, E'_L, E_F, E'_F and f_{1L}, the PLS-R models for air-dry density (ρsp) and loss tangent ($tan\delta_T$) provided low to moderate coefficients of determination ($r^2p=0.67$ and $r^2p=0.38$, respectively) but still acceptable "ratio of performance to deviation" values (RPD=1.75 and RPD=1.84, respectively) for screenings. Specific modulus (E') yielded models with good r^2p, but low RPD values.

NIR-predicted versus laboratory-determined values plot for air-dry density (A), basic density (B), microfibril angle (C), longitudinal elastic modulus (D), first resonance frequency (E) and loss tangent (F) of the woos from clonal test are given in Figure 34.

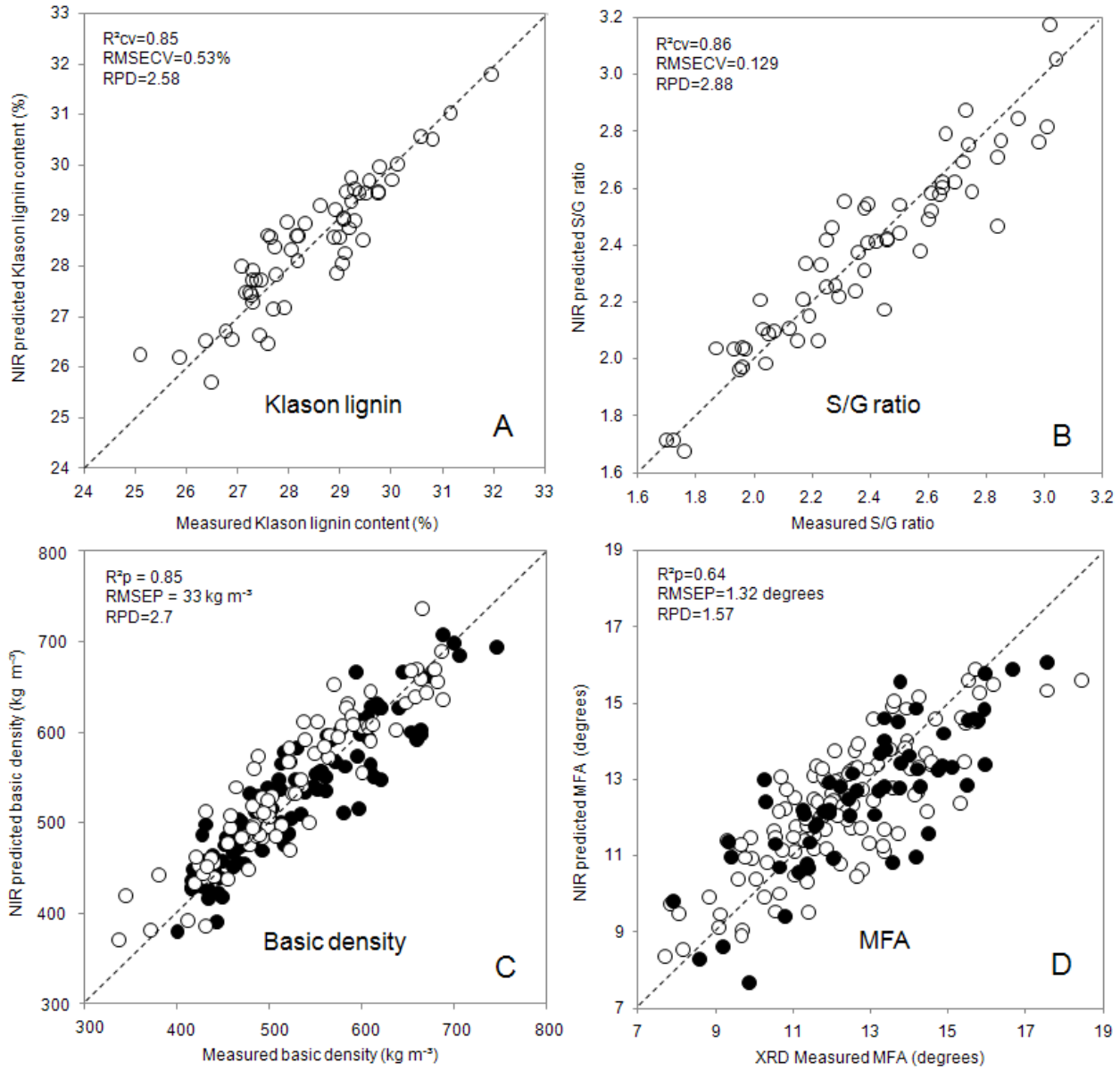

Figure 33 - NIR predicted versus measured values plot for Klason lignin (A), S/G ratio (B), basic density (C) and microfibril angle (D) of wood. The calibration set samples are represented by white circles and the validation set samples are represented by black circles

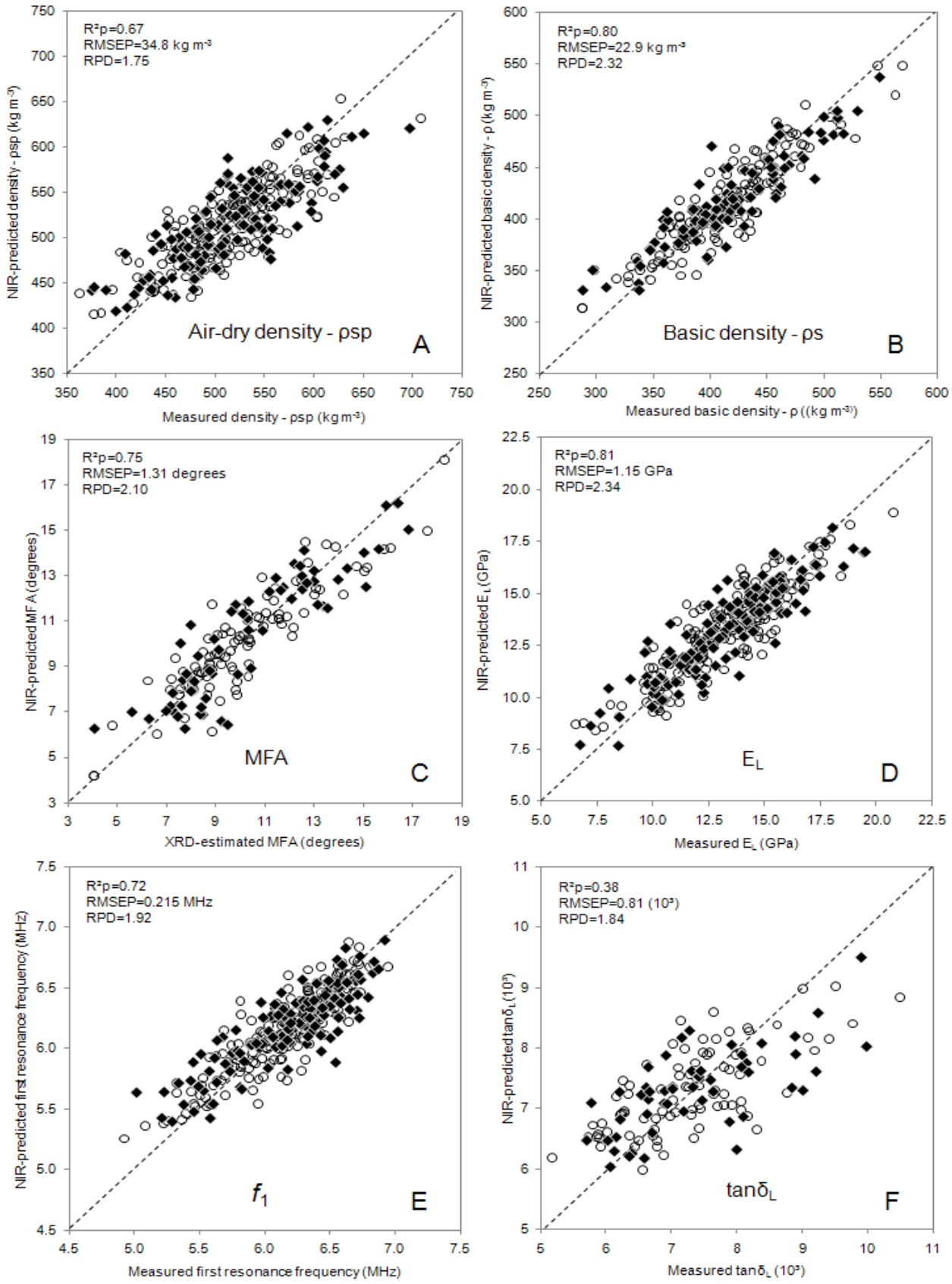

Figure 34 - NIR predicted versus measured values plot for air-dry density (A), basic density (B), MFA (C), dynamic elastic modulus (D), first resonance frequency (E) and loss tangent (F) based on NIR spectra for both training (open circles) and test sets (filled rhombs)

3.4.3.3 PLS-Regression coefficients

The underlying factors controlling wood properties are essentially the result of its chemical composition at three levels: i) chemical features of the molecules that constitute the cell walls (structural components) and those contained within the cellular structure (extractive components); ii) distribution of the chemical components in the cell structure and iii) the relative proportions of the different chemical components in the wood cells and tissues. The specific properties of wood may be traced back to a combination of these aspects, and wood utilization and end-product related quality should thereby link directly to its chemical characteristics (Pereira et al. 2003). For this reason, mechanical, physical, and chemical wood traits are often correlated. For instance, it is known that the influence of density on strength and elasticity of wood is strong (Kollmann and Côté 1968).

Table 26 - NIR absorption bands normally associated to the main wood components (cellulose, hemicelluloses, lignin, and water) contained in the wood specimens

Index	cm^{-1}	Bond vibration	Structure	Ref.
1	8547	2nd overtone asymmetric stretching CH, HC=CH	Lignin	a
2	7353	CH deformation + CH stretching 2nd overtone	CH_3	b
3	7092	OH stretching 1st OT lignin or first overtone of an O-H stretching vibration of phenolic hydroxyl groups	Lignin	c
3	7057	C-H combination, aromatic associated C-H	Lignin	a
4	7003	1st overtone OH stretching (amorphous region in cellulose)	Cellulose	e
5	6711	1st overtone OH stretching	Cellulose	a,d
6	6460	1st overtone OH stretching (crystalline regions in cellulose)	Cellulose	c
7	5981	1st overtone CH stretching	Lignin	e
7	5934	1st overtone CH stretching (aromatic associated CH)	Lignin	a,d
8	5800	1st overtone CH stretching	Hemicellulose	e
9	5618	1st overtone CH_2 stretching	Cellulose	a,d
10	5250	not assigned	-	
11	5050	OH stretching + OH deformation combination band	Water	e,a
12	4800	Asymmetric NH stretching + amide III	-	a
13	4750	not assigned	-	
14	4545	CH stretching and C=O combination	Lignin	a
15	4490	not assigned	-	
16	4375	not assigned	-	
17	4282	CH stretching + CH_2 deformation combination band (and 2nd overtone of CH_2 stretching)	Cellulose	a,c
17	4261	CH (1st overtone CH_2 symmetric stretching and δ CH_2) combination	Cellulose	a,c
17	4252	CH bending and stretching combination band	Cellulose	a
18	4063	CH stretching + CC stretching	Cellulose	a

a: Workman and Weyer (2007); b: Schimleck and Evans (2004); c: Shenk et al. (2001); d: Schimleck et al. (2004) and e: Fujimoto et al. (2008)

The analysis of the loading plots for each calibration is useful to investigate the underlying relationships that have made the estimation of air-dry density and dynamic elastic properties of wood possible by NIR spectroscopy. The assignments of absorption bands indicated in Figure 35 are useful to identify which wood components were important for the PLS-R models. It helps to understanding how NIR spectroscopy

can evaluate wood traits based on resonance analysis. Table 26 lists the NIR absorption bands normally associated to the main wood components (cellulose, hemicellulose lignin, and water) contained in the wood specimens. Numbers assigned to the specific bands and regression coefficients are presented in Figure 35

The lignin content of wood was important for air-dry density PLS-R models, as bands at 7,092-7,057 cm^{-1} (index 3) and 5,081-5,934 cm^{-1} (index 7) yielded high regression coefficients and were assigned to lignin. The high regression coefficient at 4,282 cm^{-1} (Index 18) indicates that cellulose content also played an important role on PLS-R models for air-dry density. Band at 4,490 cm^{-1} (index 15) seems to be important for air-dry density calibration. For dynamic elastic models, the bands at 5,800 cm^{-1} (index 8), associated to the hemicellulose contents; at 4,800 cm^{-1} (index 12) and 4,750 cm^{-1} (index 13) had a strong coefficient regression, but the bands at 4,375 cm^{-1} (index 16) and 4,282 cm^{-1} (index 18) appears to be the most important for stiffness. Schimleck et al. (2002) also reported similar loading plots for air-dry density and for stiffness.

The bands with higher coefficient of regression for first frequency resonance were those associated to hemicellulose (4,750 cm^{-1}) and cellulose (4,282 cm^{-1}) contents, and also the bands at 5,250 (index 10) and 4,750 cm^{-1} (index 13). Cellulose and hemicellulose contents were also important for PLS-R models for loss tangent. High absorptions occurred at 5,800 cm^{-1} (index 8), at 4,750 cm^{-1} (index 13), at 4,375 cm^{-1} (index 16) and at 4,282 cm^{-1} (index 18). In short, combinations of lignin, hemicelluloses and cellulose contents in wood control the elastic properties of wood. The absorptions correspondent to lignin (index 3, 7 and 14), to hemicelluloses (index 8) and to cellulose (index 4, 5, 6, 9, 17 and 18) content were significant to the Martens' uncertainty test (Westad and Martens 2000) for the wood traits, and other important bands (index 10, 13 and 16) seems to be associated or combined to the specific absorptions of the known wood components.

Figure 35 is useful for brings new elements to understand the underlying relationships between wood traits. For instance, density and stiffness are wood traits well correlated. Figure 35 A and D reveals that these properties presented high peaks at the same bands (index 14 and 18), confirming that both cellulose and lignin content variations are closely associated. Similarly, the regression coefficients for MFA and modulus of elasticity have high peaks at bands indicated by index 14 and 16.

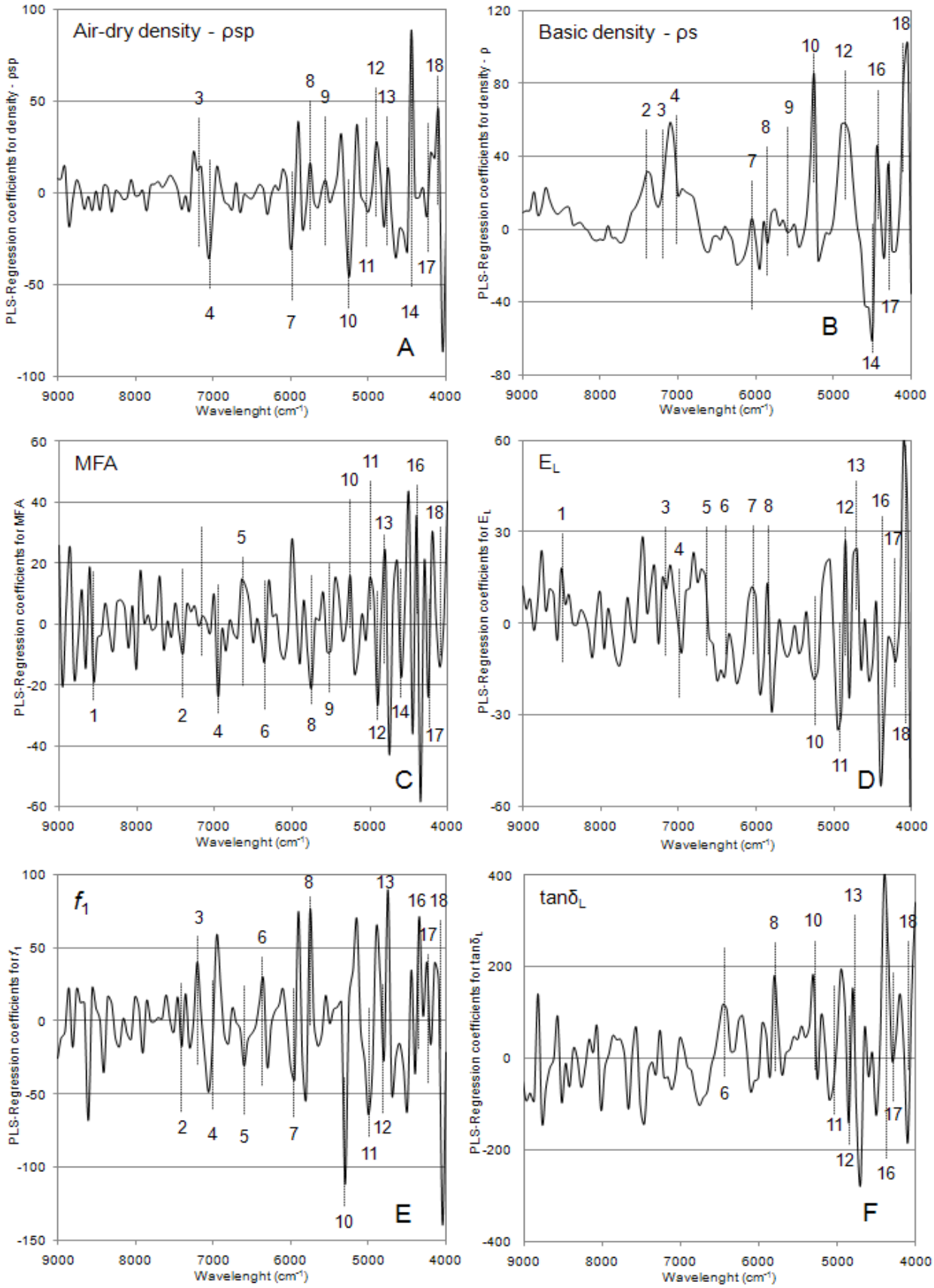

Figure 35 - PLS-regression coefficients for NIR-based model for estimating air-dry density (A), basic density (B), microfibril angle (C), dynamic elastic modulus (D), first resonance frequency (E) and loss tangent (F)

3.5 Genetic studies from progeny test

The descriptive statistics of the wood traits of the 14-year-old *Eucalyptus urophylla* population are listed in Table 27. This phenotypic database was produced from NIR-based estimates for Klason lignin, S to G ratio, basic density of wood and microfibril angle of the cell walls. To take into account the within-tree variation, MFA and D were evaluated at the inner heartwood (point 1), at the outer heartwood (point 2), and at the sapwood (point 3). In this part, the NIR-predicted basic density is designed as "D", in order to avoid confusion with lab-measured values or NIR-predicted densities of wood from clonal tests.

Table 27 - Mean, minimum and maximum values, coefficient of variation and number of observations (N) for measured circumference (C, centimeters) and height (H, meters), and NIR-estimated Klason lignin (KL, %), syringyl to guaiacyl ratio (S/G, no unit), wood density (D, kg m^{-3}) and microfibril angle (MFA, degrees) of the 14-year-old *Eucalyptus urophylla* population

Trait	Mean	Minimum	Maximum	CV (%)	N
C	52.68	24	84	21.17	340
H	21.15	7.8	29.6	17.26	340
KL	28.03	25.1	31.75	4.42	321
S/G	2.29	1.54	3.51	13.54	321
D_1	443	330	607	10.23	274
D_2	522	391	698	8.43	274
D_3	615	480	761	8.11	274
D	526	423	654	7.09	274
MFA_1	18.05	12.7	23.9	10.08	274
MFA_2	15.34	10	21.1	12.39	274
MFA_3	13.32	7.22	19.5	13.89	274
MFA	15.57	11	20	9.76	274

The wood chemical properties (KL and S/G) are comparable to those found in similar studies which have investigated mature *Eucalyptus* wood (Brito and Barrichelo 1977; Poke et al. 2006) and higher than those reported for juvenile wood (Baillères et al. 2002; Gomide et al. 2005).

Patterns in pith to bark variation of these traits have been known for many years; wood density generally increases while MFA decreases from pith to bark (Kollmann and Côté 1968). Here, the microfibril angles were, on average, higher near the pith decreased radially towards the cambium whereas an opposite trend was observed for the basic density of wood (Table 27). The software alerted us about some estimates presenting high deviations. Thus we removed these outliers from the original dataset.

The coefficients of variation were similar to those observed in previous studies on *Eucalyptus* in the Congo (Bouvet et al. 1999). They were higher for growth traits than for wood property traits. Their magnitude showed that the sampling used in this study was representative of a breeding population involved in genetic improvement programs in the Congo (Bouvet et al. 2009).

3.5.1 Heritability of growth and wood traits

While many papers have reported heritability estimates and correlations among growth and density (or pilodyn penetration) in *Eucalyptus* wood, few studies have addressed to genetic parameters of chemical,

mechanical and anatomical properties (Kube et al. 2001; Apiolaza et al. 2005; Poke et al. 2006; Mandrou et al. 2011). This study presents the genetic control for microfibril angle, wood density, klason lignin content, syringyl to guaiacyl ratio of the wood and for circumference and height of the trees and should improve our knowledge on the role on genetic and non-genetic factors on the variation of these kind of traits.

Table 28 presents the additive genetic and residual variance components, genetic (CV_A) and residual (CV_P) coefficient of variance and narrow-sense heritability estimates for various traits, including circumference (C), height (H), microfibril angle (MFA), basic density (D), Klason lignin (KL) and syringyl to guaiacyl ratio (S/G).

Genetic and residual variation was higher for growth traits than for wood property traits as shown by CV_A and CV_E. As expected, the narrow-sense (h^2) estimates were lower for growth traits: h^2=0.30 for height and h^2=0.14 for circumference while moderate to high levels of heritability (from 0.37 to 0.72) were reported for wood traits. The low heritability estimates for growth traits confirms the trends described in previous studies addressing the heritability of growth traits for other Eucalyptus breeding programs (Kube et al. 2001; Costa e Silva et al. 2004; Volker et al. 2008; Kien et al. 2009; Costa e Silva et al. 2009) and more specifically in the Congo (Bouvet et al. 2003, Bouvet et al. 2009).

Table 28 - Additive genetic and residual variance components, genetic and residual coefficient of variance and narrow-sense heritability estimates for various traits

Trait	Additive genetic variance			Residual variance			Genetic control	
	σ^2_A	SE σ^2_A	CV_A	σ^2_E	SE σ^2_E	CV_E	h^2	SE h^2
C	13.62	9.44	7.0	85.61	8.59	17.6	0.14	0.09
H	3.27	1.69	8.6	7.63	6.37	13.1	0.30	0.14
KL	1.11	0.47	3.8	0.43	1.72	2.3	0.72	0.20
SG	0.068	0.069	11.4	0.027	1.770	7.2	0.71	0.20
D_1	8.16	4.11	6.4	13.54	4.95	8.3	0.37	0.16
D_2	8.90	4.02	5.7	11.40	4.40	6.5	0.44	0.17
D_3	13.44	6.12	6.0	12.89	3.67	5.8	0.51	0.18
D	9.22	3.69	5.8	5.51	2.35	4.5	0.61	0.17
MFA_1	1.47	0.68	6.7	1.96	4.75	7.7	0.43	0.16
MFA_2	1.88	0.82	8.9	1.88	3.70	8.9	0.50	0.14
MFA_3	1.58	0.74	9.5	1.96	4.27	10.5	0.44	0.17
MFA	1.57	0.60	8.0	0.84	2.25	5.9	0.65	0.15

σ^2_A - additive genetic variance component; σ^2_E - residual variance component; h^2 - narrow-sense heritability estimates and SE - standard errors. For the estimates of variance components for wood density, the phenotypic values were divided by 10.

Narrow-sense heritability estimate of elevated magnitude was found for MFA (h^2=0.65±0.17) when calculated from the mean values per disc (Table 28). These h^2 estimates were higher than those reported in two previous studies. Apiolaza et al. (2005) used increment cores from 188 open-pollinated progenies of 11-year-old *E. globulus* reporting h^2_{MFA}=0.27±0.24 while Lima et al. (2004) reported mean broad-sense heritability (H^2) of 0.29 in 8-year-old *Eucalyptus* wood. Normally, broad-sense heritability estimates are higher than narrow-sense estimates. The low H^2 estimate of Lima et al. (2004) was expected since they evaluated clones of *E. grandis* x *E. urophylla* for pulpwood so genetic base was narrow. On the other hand, the relatively lower narrow-sense h^2 estimates of Apiolaza et al. (2005) can be attributed to larger environmental variation since their CV_A (8.36%) is close to the CV_A of Table 3 (8%).

Just as the phenotypic values, the genetic control also varied with age. The heritability estimates of the MFA in the inner heartwood (h^2_{MFA1}=0.43±0.16) increased towards the outer heartwood (h^2_{MFA2}=0.50±0.14), decreasing again in the sapwood (h^2_{MFA3}=0.44±0.17). This variation trend with age (Table 28) was similar to the variation pattern reported by Lima et al. (2004) in *Eucalyptus* clones (h^2_{MFA} departing from 0.13, increasing to 0.36 and decreasing to 0.16 towards the cambium). However, the biological significance of these two results is not compatible since the peaks in heritability estimates occurred at different ages.

Comparing these findings requires prudence because the experimental dispositive were different (open- and controlled-pollinated and clonally propagated tests) and the methods for wood phenotyping were distinct: Apiolaza et al. (2005) estimated the phenotypic MFA values of their study by means of the SilviScan device (based on X-ray diffraction); Lima et al. (2004) used polarised light microscopy technique and, here, X-ray-diffraction patterns were associated with NIR spectroscopy to estimate the MFA).

Moderate genetic control was found for mean wood density (h^2=0.62±0.17) and for local wood density measurements. The heritability estimates linearly increased from 0.37±0.16 to 0.51±0.18 towards the sapwood; however this linear trend should be considered with caution since the standard errors (SE) were elevated (~0.17).

Due its relatively easy and simple measurement, the wood density has been extensively investigated in *Eucalyptus* and the heritability of such trait exhibits variable magnitudes: from h^2≈0.6±0.12 (Kien et al. 2008) to h^2=0.71±0.2 (Wey and Borralho 1997) in *E. urophylla*; from H^2=0.51±0.13 (Kube et al. 2001, for all sites) to h^2=0.73 (Greaves et al. 1997, for whole-disk density at 1.3 m across sites) in *E. nitens*; from h^2=0.24±0.26 (Poke et al. 2006) to h^2=0.44±0.22 (Apiolaza et al. 2005) in *E. globulus* and of h^2=0.17 (Raymond et al. 1998) in *E. regnans*. Most of these studies have shown the high heritability of this trait mainly explained by the low environmental rather than by marked genetic variation (see CV's in table 3); our study reinforces these previous results.

Lignin content and S/G ratio were traits shown to be under strong genetic control (Table 28). The high narrow-sense heritability estimates of these chemical traits (h^2>0.7±0.2) indicates that genetic improvement is possible through breeding. The heritability for lignin (h^2=0.72±0.2) were lower than those reported by Gominho et al. (1997) in *E. globulus* clones (h^2=0.83) and higher than those reported by Poke et al. (2006) in *E. globulus* families (narrow-sense h^2=0.13±0.2 and family means h^2=0.42±0.19). As lignin content and its composition are key traits of *Eucalyptus* breeding programs, especially for pulp, paper and bioenergy production the high genetic control of lignin content and syringyl to guaiacyl ratio reported here (Table 28) are of major importance for tree breeders.

Although these estimates are population- and site-specific parameters, these findings are coherent with previous studies and useful for tree breeders since they show that MFA, density, lignin and S to G ratio present a high heritability being susceptible to improvement.

3.5.2 Genetic and residual correlations

Genetic correlation is the ratio of genetic covariance and the product of the genetic standard deviations of two traits and can be thought of as the correlation of the breeding values (Falconer and Mackay 1996). According to Baltunis et al. (2007) a strong genetic correlation may imply that the same genes may be responsible for the two traits (pleiotropy). In tree improvement, genetic correlations are important in describing the extent to which one trait can indirectly be improved by selecting for another trait (Zobel

and Talbert 2003). For instance, strong negative genetic correlation indicates that selection for reducing one trait would lead to gain in another one, and vice-versa.

Estimates of genetic and residual correlations among growth, Klason lignin content, S/G ratio and mean MFA and wood density are shown in Table 29. Here, few relationships (C x H; KL x MFA and KL x SG) presented additive and residual correlation with the same sign. These correlations presenting the same sign indicates pleiotropic gene effect (Falconer 1993). This becomes a problem when selection on one trait favours one specific version of the gene (allele), while the selection on the other trait favours another allele.

Most of correlations (Table 29) presented opposite sign indicating that linkage disequilibrium (non-random associations of alleles) between loci may affect the relationship among different wood traits (Falconer 1993). This means that the genes controlling these traits can be statistically associated, but there is no functional relationship between them. Sampling procedure used in this study could have played a role on linkage disequilibrium, since the 9 or 10 trees of each family were selected among the best ones in growth and stem straightness. According to Villanueva and Kennedy (1990) selection not only produces changes in the genetic variance of the trait directly selected, but genetic variances of and co-variances between other correlated traits are also affected. Moreover, Lande (1984) states that "when two characters under separate genetic control are selected to be highly correlated, in a large randomly mating population with no linkage between loci influencing different characters the genetic correlation maintained is small in magnitude".

Table 29 - Estimated additive genetic (r_A, below the diagonal) and residual (r_E, above the diagonal) correlations for various traits, including circumference (C), height (H), microfibril angle (MFA), basic density (D), Klason lignin (KL) and syringyl to guaiacyl ratio (S/G). Standard errors are shown in parentheses

	C	H	MFA	D	KL	SG
C		0.80 (0.05)	0.07 (0.15)	0.48 (0.27)	0.30 (0.18)	-0.20 (0.17)
H	0.46 (0.32)		0.16 (0.22)	0.41 (0.24)	0.35 (0.29)	-0.41 (0.27)
MFA	-0.50 (0.33)	-0.70 (0.21)		-0.87 (0.00)	0.22 (0.34)	0.63 (0.49)
D	-0.99 (0.18)	-0.56 (0.26)	0.48 (0.16)		-0.35 (0.44)	0.10 (0.43)
KL	-0.16 (0.39)	-0.61 (0.24)	0.58 (0.20)	0.28 (0.28)		-0.24 (0.39)
SG	0.18 (0.39)	0.37 (0.30)	-0.27 (0.28)	-0.65 (0.18)	-0.16 (0.29)	

Our results bring new element to understand the correlation between wood and growth traits. However these results should be considered with caution due to the low accuracy of our estimation (see Table 29). A sizable body of literature exists about genetic correlations between growth traits and wood density; however the findings concerning this issue are inconsistent. Zobel and Van Buijtenen (1989) reviewed a number of studies prior to 1986, reporting contradictory findings for a range of wood species. Recently, Hamilton and Potts (2008) reviewed the studies on genetic parameters in *Eucalyptus nitens* showing genetic correlations between growth and density between -0.79 to 0.08, with a mean correlation of -0.27 for density-diameter from more than 10 studies. In regard to the *Eucalyptus* genus, this issue is still not clear. While numerous papers have reported low genetic correlations between growth traits and wood density (r=-0.20, Greaves et al. 1997; r=-0.11, Kube and Raymond 2005), a range of studies has reported a moderate negative genetic correlations (r=-0.36, and Borralho 1999; r=-0.57, Kube et al. 2001). Moreover, numerous papers have shown contrasting results of correlations between the same traits but

from different sites (Wei and Borralho 1999; Muneri and Raymond 2000; Osorio et al. 2003; Hamilton et al. 2009) outlining the environmental x genotype interaction effect on these correlations.

As expected, the genetic and residual correlation between growth traits was positive. The correlations between growth and wood traits (MFA, D and KL) were negative. Positive residual correlations were obtained for this same group of correlations. Such patterns are different for S to G ratio. The correlations concerning S/G are of low magnitude considering the standard errors (Table 29).

The strong genetic correlation between C and D was investigated by means of the residual scattering analysis (not shown). The point's dispersion revealed that there was no aberrant point, which could favour (stretching) the correlation. The correlation estimates had large standard errors probably due to the small sample size.

3.5.3 Age trends of additive genetic, residual and phenotypic correlations

Age trends of genetic, residual and phenotypic correlations, respectively, between density and circumference (D x C), and between microfibril angle and circumference (MFA x C), klason lignin (MFA x KL) and, density (MFA x D) are shown in Table 30 and Figure 36. The correlation between circumference and wood density remained high during all phases of wood formation, from the first to the last years of development. On the other hand, the correlation between circumference and MFA seems to decrease towards the bark. This kind of linear increase of correlation is also found between MFA and lignin in which there is an increase with age. The correlation between MFA and wood density decreased from juvenile to mature wood.

Table 30 - Variation with age of additive genetic, residual and phenotypic correlations of density with C, and MFA with C, KL and density. Standard errors are in parenthesis

	Inner heartwood (1)	Outer heartwood (2)	Sapwood (3)
		Additive genetic correlation	
D-C	-0.89 (0.24)	-0.99 (0.00)	-0.88 (0.23)
MFA-C	-0.67 (0.28)	-0.53 (0.32)	-0.27 (0.40)
MFA-LK	0.40 (0.27)	0.52 (0.23)	0.74 (0.15)
MFA-D	0.69 (0.22)	0.70 (0.21)	0.30 (0.30)
		Residual correlation	
D-C	0.20 (0.12)	0.34 (0.07)	0.39 (0.16)
MFA-C	-0.06 (0.11)	-0.06 (0.12)	0.24 (0.11)
MFA-LK	0.11 (0.24)	0.16 (0.27)	0.19 (0.25)
MFA-D	-0.79 (0.24)	-0.92 (0.33)	-0.52 (0.22)
		Phenotypic correlation	
D-C	-0.06 (0.07)	0.00 (0.05)	0.01 (0.08)
MFA-C	-0.20 (0.07)	-0.17 (0.07)	0.11 (0.07)
MFA-LK	0.27 (0.09)	0.37 (0.08)	0.50 (0.07)
MFA-D	-0.17 (0.10)	-0.13 (0.11)	-0.13 (0.10)

The residual correlation is of low magnitude, except for the correlation between MFA and D. The phenotypic and additive genetic correlation between C and MFA, and LK and MFA presented the same

trends slightly differing in their magnitude. The phenotypic correlation between circumference and wood density is null while the genetic one is strong. Similarly, the phenotypic correlation between MFA x D is of low magnitude while the residual and genetic ones are considerable. These findings indicate that the phenotypic correlation is not a good predictor of genetic correlation.

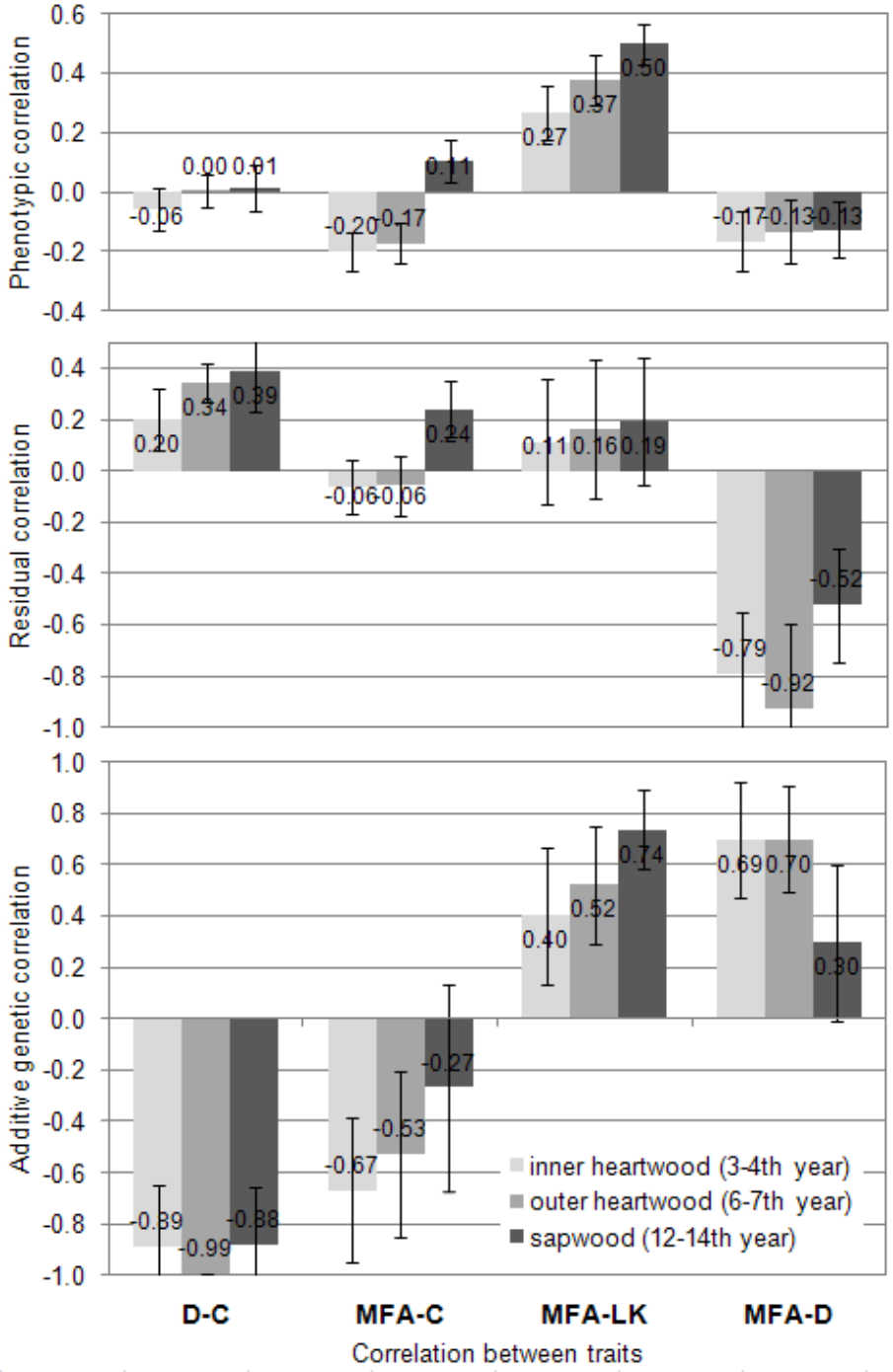

Figure 36 - Age trends of phenotypic, residual and additive genetic correlations of density with C, and MFA with C, KL and density

In general, additive genetic correlations presented higher magnitudes when compared with the residual correlations. Moreover, the radial variations of the values of the genetic relationships were stronger than those for residual or phenotypic correlations.

As the tree grows up, new layers of wood are produced and overlapped in order to withstand the ever-increasing mass of the tree. The variations of the genetic and residual correlations with age may be useful to understanding how one tree adapt the characteristics of its wood to support gravity and bending movements caused by winds. A theoretical view of this issue was provided in Alméras and Fournier (2009).

The narrow-sense heritability estimates for wood density and MFA varied with age (Table 28), as well as their phenotypic values (Table 27). This means that trees adapt both their density, lignin content and MFA to answer to the specific needs of the stems (such as its ever-increasing mass or its vulnerability to wind) and such adaptations are somewhat regulated by genetic factors.

The genetic correlation C x D is always strongly negative while the correlation D x MFA remained constant in the juvenile wood, decreasing considerably in the mature wood (Figure 36). This means that trees with a strong potential to grow fast are genetically programmed to produce low-density woods and also to decrease the microfibril angles for ensuring stiffness. Wood stiffness is partially controlled by the MFA in most wood species, including *Eucalyptus* (Evans and Ilic 2001). Hence, it appears that the trees try to compensate the weakness of its low-density by reducing its MFA, and consequently by increasing the specific modulus of the wood ($r_{A\ (MFA1\ x\ D1)}$ and $r_{A\ (MFA2\ x\ D2)} =\sim 0.7$), especially in the juvenile stage.

When the tree reaches maturity, the stem becomes especially susceptible to prevailing winds because the higher heights and inertia moments. It is known that a reaction wood is typically formed as the tissues of the periphery are held in "tension" (Clair et al. 2006) and in many wood species, tension wood is characterised by the presence of a thick, inner cell-wall layer that consists of highly crystalline cellulose, in which the MFA is close to zero (Thibaut et al. 2001). Moreover, this particular layer (G-layer) is almost invariably unlignified (Du and Yamamoto 2007). Thus, the low lignin content and MFA of the sapwood could be associated to tension wood occurrence and our results indicate that variations in these wood traits are also genetically controlled: the genetic correlation between MFA and KL increases from 0.4 to 0.74 towards the cambium (Figure 36). In conclusion, the genetic correlations MFA x D and MFA x KL acting together reveal a smart biological strategy for the survival of the tree.

It is important to note that the tension wood is distributed tangentially and not radially whereas the lignin content slightly varies with age. Regrettably, there was only a mean, single estimative of Klason lignin content by tree in this study because the NIR calibration was based on powder of the wedge. Here, the hypothesis is that NIR-based models for MFA and KL are sensible to the variations in wood characteristics. Thus the decrease in lignin content should be more important than that of MFA due to tension wood presence. Moreover, another source of co-variation should play a role on these findings, such as the changes in S to G ratio with age within the wood.

3.5.4 Implications for selection

The phenotypic and genetic correlations show opposite patterns for wood traits. While phenotypic correlation between C and D exhibit null magnitudes, the genetic associations between these traits can be prominent. For the correlation MFA x D, the phenotypic values yield no relationships while their genetic or residual estimates indicates that these traits are linked (Figure 36). These findings suggest that the phenotypic value of the trait is not a good predictor of its genetic potential or its consequences. When trees are selected on the base of only their phenotypic values, the characteristics of their offspring can be surprising since the consequences of mixing different allelic forms are unpredictable. Our study allows considering the consequences that these results can have on the genetic improvement strategies.

In the frame of pulpwood production, the objective is to produce tree with important biomass production and reduced lignin content. The negative r_A between growth traits and lignin content (-0.61 for height and r_A=-0.16 for circumference) and MFA and S/G (r_A=-0.27) and the positive correlation between MFA and lignin content ($0.4<r_A<0.74$) are favourable for pulp and paper production since the improvement in all of these traits would be simultaneously possible (Table 30). Lignins are undesirable compounds for pulp and paper production, because the delignification process requires energy and reagent consumption. In regard to its structure, high syringyl to guaiacyl ratio is advantageous for pulping (Rodrigues et al. 1999) since every unit increase in the lignin S/G ratio would roughly double the rate of lignin removal (Chang and Sarkanen 1973).

In the frame of bio-energy production, the positive genetic correlation between lignin and density (0.28) is favourable, despite the low magnitude. However, positive additive correlations between MFA and lignin (Table 30) are unfavourable for bioenergy purposes since decreasing MFA, may result in decreasing lignin content. The problem is that, for energy production, the wood may simultaneously have high lignin content and adequate mechanical properties. Charcoal is used in blast furnace for iron-steel production and has to support the weight charge of the iron feedstock during the steps of oxydo-reduction reactions at elevated temperature (higher to 1500°C) without breaking. As lignin content and its composition are key traits of *Eucalyptus* breeding programs, especially for pulp, paper and bioenergy production the high genetic control of lignin content and syringyl to guaiacyl ratio reported here (Table 28) are of major importance for tree breeders. These issues are presented and discussed in the **paper 8**.

3.6 Genetic studies from clonal test

3.6.1 Growth traits

Understanding the interaction between the genotype and the environment is increasingly becoming a key modelling element for the management of forests (Verryn 2008). Generalized linear model (GLM) was performed to analyze the clonal and environmental variance of growth traits. Results of the analyses of variance for circumference at breast height (C) and commercial height (H) for the trees from the clonal tests (not presented) showed significant ($p<0.0001$) effect for clone, site and clone x site interaction for these growth traits (R^2_C=0.68 and R^2_H=0.51).

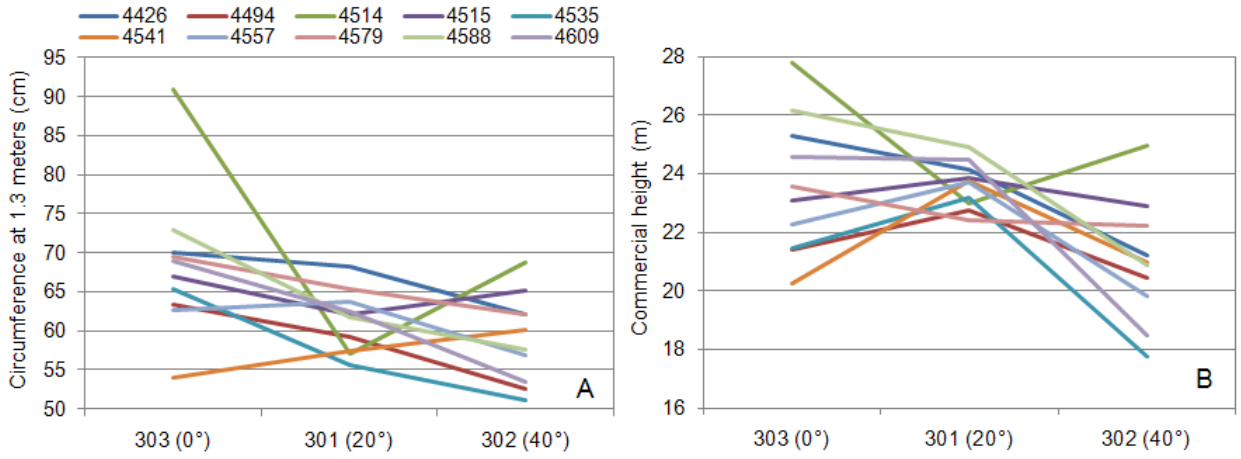

Figure 37 - Clone x site interaction for mean circumference at 1.3 meters (A) and commercial height (B) of the trees from Clonal test

Thus, multiple range tests for circumference at breast height (C) and commercial height (H) by clone and by site where performed (Table 31) in order to classify the clones and sites according to their growth traits. Clone 4514 presented the higher circumference at breast height (77.8 cm) and commercial height (26 meters) while clones 4494, 4535, 4541 and 4557 presented relatively low, but even satisfactory growth rates. The trees grow up faster on site 303 (no slope ground) presenting a circumference of 72 centimeters, on average, an elevated growth rate for trees with only six-years old.

Genotype by environmental interaction for growth traits is of particular concern to tree breeders since it determines critical decisions in developing optimal breeding strategies and realizing genetic gains. Figure 37 presents the clone x site interaction for mean circumference at 1.3 meters (A) and commercial height (B) of the 6-year-old *Eucalyptus urophylla* x *grandis* trees.

Table 31 - Tukey (HSD) multiple range tests for growth traits by clone and by site in 6-year-old *Eucalyptus urophylla* x *grandis* clones

Clone	C (cm)	H (m)
4426	66.8^{B}	23.6^{BC}
4494	59.2^{D}	21.7^{DE}
4514	77.8^{A}	26.0^{A}
4515	64.7^{BC}	23.3^{BCD}
4535	58.3^{D}	21.1^{E}
4541	57.7^{D}	21.8^{DE}
4557	61.5^{CD}	22.2^{CDE}
4579	66.1^{BC}	22.8^{BCD}
4588	64.5^{BC}	24.1^{B}
4609	62.3^{BCD}	22.9^{BCD}
Site	C (cm)	H (m)
301	61.6^{B}	23.7^{A}
302	59.8^{B}	21.2^{B}
303	72.0^{A}	24.3^{A}

Means with the same letter are not significantly different at $\alpha = 0.05$ threshold, using Tukey multiple range tests

Clone 4514 presented the higher genotype by environmental interaction fir circumference. This clone presented optimal performance in growth in the Sites 303 (0 degrees) and 302 (40 degrees) but its circumference is low in site 301. This trend can be explained by possible sampling error. In general, all clones had better performance in the plane site (303), decreasing their growth rate in sloped Sites. The higher the terrain slope, the lower the growth rate, except for clone 4541 that shows an opposite trend.

Taking into account only the growth traits, clones 4514, 4426, 4579 and 4588 are the best ones, presenting superior circumference at 1.3 meters and commercial height. On the other hand, clones 4535, 4494 and 4541 showed the worst performances for growth.

3.6.2 Genetic studies from the kiln-dried scantlings

Table 32 shows the analysis of variance (GLM) for density and dynamic traits in kiln-dried scantlings. Similarly to air-dried scantlings (Table 48), there were significant differences among clones for all traits, and among clones and sites for density and shear modulus.

Table 33 lists the classification of clones and sites for density and dynamic traits of kiln-dried scantlings. Clones 4494, 4515, 4535, 4557 and 4609 presented the higher mean density values and the lower growth rates. On the other hand, clones 4426 and 4588 presented the lower densities, but their growth rates are high. In regards to the elastic modulus of scantlings, clone 4515 produced the stiffest woods while clones 4426 and 4579 produced the less rigid and more flexible woods (this clones presented the higher growth rates).

Table 32 - Analysis of variance for density and dynamic traits in kiln-dried at 14% scantlings of 6-year-old *Eucalyptus urophylla* x *grandis* clones

	ρ14	E_L14	tgδ14	E_F14	G14
Clone	p<0.0001	p<0.0001	p<0.001	p<0.0001	p<0.005
Site	p<0.0001	ns	p<0.001	ns	p<0.03
interaction	p<0.0001	ns	ns	ns	p<0.04
R^2	0.41	0.22	0.18	0.21	0.16

Table 33 - Tukey (HSD) multiple range tests for density and dynamic traits by clone and by site in kiln-dried at 14% scantlings of 6-year-old *Eucalyptus urophylla* x *grandis* clones

Clone	ρ14 (kg m^{-3})	E_L14 (MPa)	tg δ14 (10^3)	E_F14 (MPa)	G14 (MPa)
4426	496.6^{EF}	$11,254^{D}$	7.25^{ABC}	$11,801^{D}$	625.6^{B}
4494	560.2^{ABCD}	$13,636^{ABC}$	8.16^{ABC}	$14,906^{A}$	599.3^{B}
4514	546.9^{BCDE}	$12,934^{ABCD}$	7.82^{ABC}	$13,301^{BCD}$	680.0^{AB}
4515	564.7^{ABCD}	$14,272^{A}$	7.96^{ABC}	$14,639^{AB}$	728.5^{AB}
4535	578.4^{AB}	$13,877^{AB}$	7.07^{BC}	$14,269^{BC}$	778.1^{A}
4541	528.8^{DEF}	$11,959^{CD}$	8.37^{AB}	$12,421^{C}$	742.8^{AB}
4557	586.5^{A}	$14,131^{AB}$	7.88^{ABC}	$14,515^{AB}$	741.5^{AB}
4579	540.2^{CDE}	$11,638^{D}$	8.55^{A}	$12,114^{D}$	689.6^{AB}
4588	518.3^{EF}	$12,451^{BCD}$	6.95^{C}	$12,593^{C}$	678.2^{AB}
4609	568.5^{ABC}	$12,490^{BCD}$	7.58^{ABC}	$12,833^{BC}$	705.2^{AB}
Site	ρ14 (kg m^{-3})	E_L14 (MPa)	tg δ14 (10^3)	E_F14 (MPa)	G14 (MPa)
301	558.5^{A}	$12,930^{A}$	7.56^{B}	$13,528^{A}$	700.1^{AB}
302	573.4^{A}	$13,044^{A}$	8.38^{A}	$13,355^{A}$	742.2^{A}
303	518^{B}	$12,610^{A}$	7.45^{B}	$13,042^{A}$	653.3^{B}

Means with the same letter are not significantly different at $p = 0.05$ threshold, using Tukey multiple range tests

According to Muneri and Raymond (2000), as wood properties are generally under much stronger genetic control than tree growth it may be expected that the magnitude and patterns of genetic by environment interaction for wood traits (Figure 38) may differ from those observed for growth traits (Figure 37). Clone by site interaction for wood density (A) and longitudinal elastic modulus (B) of the kiln-dried scantlings is presented in Figure 38. The more inclined the terrain, the lower the growth rate. Clones 4426 and 4588 grow at fast rates but presented the lower wood density in all sites while the clones 4535 and 4557 grow

slowly producing the denser woods. The lower growth rate implies an increase in wood density and stiffness. This trend can be observed for most clones, except for the 4494, that produced the higher density in the site 303 (0 degrees) compared to densities in site 301 (20 degrees). The higher wind velocity (3.2 m/s) striking the trees from the site 301 (20°) (see Table 5, pg. 58) also can contribute to changes in wood traits.

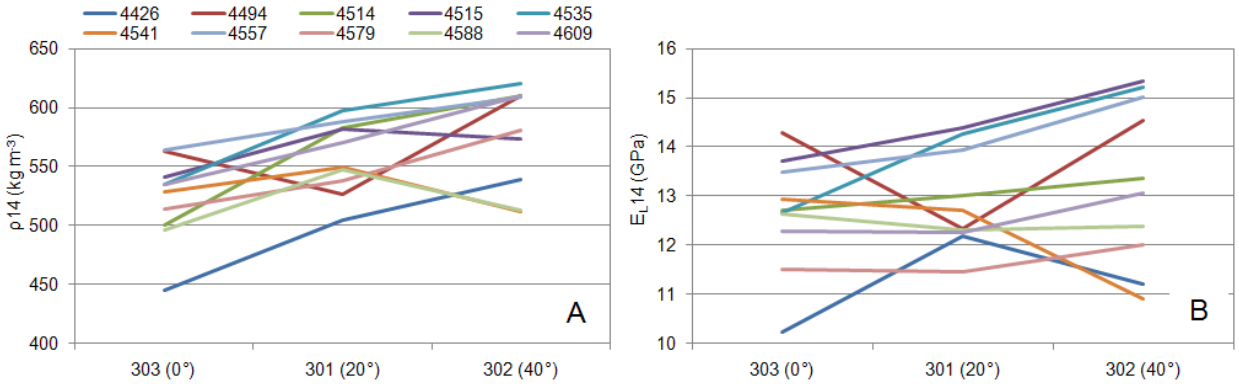

Figure 38 - Clone x site interaction for wood density (A) and longitudinal elastic modulus (B) of the kiln-dried scantlings

Resonance technique was able to simply, rapidly and at such low cost characterize the mechanical properties of these scantlings. The method permitted to rapidly estimate key wood properties (such as the modulus of elasticity, the shear modulus and the loss tangent) of the scantlings even in pieces containing knots, small cracks and also slightly damaged areas. In short, the BING system rapidly provided a large, reliable data set of mechanical wood properties as required for high-throughput phenotyping tool of genetic approaches. These results can be useful for initial classifications, screenings or preliminary selections in breeding programs of *Eucalyptus*. As reported by Burdzik and Nkwera (2002), this method proved to be fast, highly repeatable and does not require heavy equipment, making it the ideal method for on-site determining of wood stiffness at the sawmill, for instance.

3.6.3 Genetic studies from NIR-predicted data of wood discs

This study is of particular interest since very few clonal tests exist across contrasting sites and no study is known to establish the variations of basic density, stiffness and MFA of wood along the tree and to compare these variations among contrasting sites.

3.6.3.1 Spatial variation of wood traits within the tree

NIR-based models develop and presented in the NIR section were used to estimate a large data base (N= 2,550 estimates for each wood trait) of woods from clonal tests. The spatial variation of basic density, modulus of elasticity and microfibril angle along the *Eucalyptus* trees at three contrasting sites are presented in the following Tables and Figures. The codes of radial and longitudinal positions used for presenting these results are listed in Table 7 (pg. 61). Seventeen points of measure within the tree were available and to build the cartography maps, data were linearly interpolated. It is important to note that, at the base of the tree; the comparison is made using wood developed at the first years and at the sixth year while the comparison between wood traits in the top of the tree is based on wood formed exclusively at the sixth and last year of development. Furthermore, as the cylinder of juvenile wood extends from the base (0%) to the top (100%) the proportion of juvenile wood within the stem increases.

Table 34 - Radial and longitudinal variation for wood basic density (kg m^{-3}) in *Eucalyptus* clones at three contrasting sites. The means were compared by the Tukey test at p=0.01 threshold. Small letters are comparisons between radial positions while capital ones compares sites. Values in brackets are coefficients of variation in percentage

Height	Radial	303 (0°)	301 (20°)	302 (40°)	Overall
100%	outer SW^{14}	514.7^{aA}	531.2^{bA}	526.9^{bA}	524.3^{b}
100%	outer SW^{15}	521.6^{aB}	545.9^{abA}	530.6^{abAB}	532.7^{ab}
100%	outer SW^{16}	527.1^{aB}	548.8^{aA}	551.6^{aA}	542.5^{a}
75%	inner SW^{11}	511.4^{cB}	541.7^{bA}	536^{bA}	529.7^{c}
75%	middle SW^{12}	537.8^{bA}	554.8^{bA}	548.3^{bA}	547.0^{b}
75%	outer SW^{13}	558.1^{aB}	598.9^{aA}	582.7^{aA}	579.9^{a}
50%	HW^{8}	482.0^{cB}	511.6^{cA}	503.6^{cA}	499.1^{c}
50%	inner SW^{9}	537.4^{bB}	571.1^{bA}	559.5^{bA}	556.0^{b}
50%	outer SW^{10}	570.7^{aB}	624.0^{aA}	616.0^{aA}	603.5^{a}
25%	inner HW^{3}	467.5^{cB}	496.5^{dA}	461.6^{dB}	475.2^{d}
25%	middle HW^{4}	485.5^{cA}	488.3^{dA}	489.9^{cA}	487.9^{d}
25%	outer HW^{5}	521.8^{bB}	554.5^{cA}	545.0^{bA}	540.4^{c}
25%	inner SW^{6}	563.1^{aB}	598.4^{bA}	603.0^{aA}	588.2^{b}
25%	outer SW^{7}	571.9^{aB}	629.4^{aA}	618.8^{aA}	606.7^{a}
0%	inner HW^{0}	438.7^{cB}	473.8^{cA}	470.2^{cA}	460.9^{c}
0%	outer HW^{1}	521.6^{bB}	579.5^{bA}	557.1^{bA}	552.7^{b}
0%	SW^{2}	566.2^{aB}	615.3^{aA}	614.6^{aA}	598.7^{a}

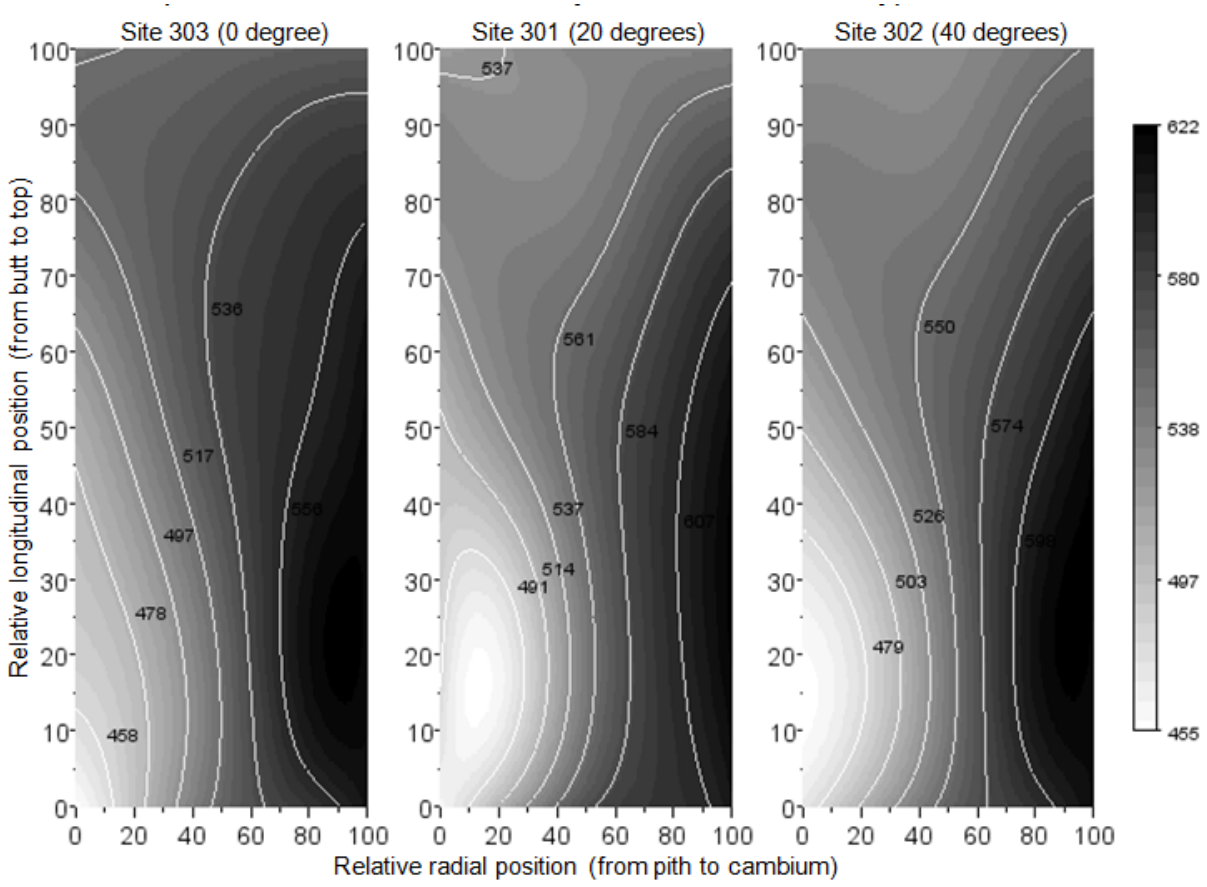

Figure 39 - Spatial variation of wood basic density (kg m^{-3}) in *Eucalyptus urophylla* x *grandis* trees

Table 35 - Radial and longitudinal variation for modulus of elasticity (MPa) in clones of *Eucalyptus* wood at three contrasting sites. The means were compared by the Tukey test at p =0.01 threshold. Small letters are comparisons between radial positions while capital ones compares sites. Values in brackets are coefficients of variation in percentage

Height	Radial	303 (0°)	301 (20°)	302 (40°)	Overall
100%	outer SW[14]	11,514^{bA}	11,058^{cAB}	10,439^{bB}	11,003^{c}
100%	outer SW[15]	12,051^{abAB}	12,189^{bA}	11,178^{bB}	11,806^{b}
100%	outer SW[16]	12,550^{aB}	13,510^{aA}	12,522^{aB}	12,861^{a}
75%	inner SW[11]	11,301^{bA}	11,268^{cA}	10,695^{cA}	11,088c
75%	middle SW[12]	13,211^{aA}	13,858^{bA}	12,416^{bB}	13,162b
75%	outer SW[13]	14,097^{aB}	16,120^{aA}	14,654^{aB}	14,957a
50%	HW[8]	10,642^{cA}	10,904^{cA}	10,522^{cA}	10,689^{c}
50%	inner SW[9]	13,753^{bAB}	14,427^{bA}	13,524^{bB}	13,901^{b}
50%	outer SW[10]	15,442^{aB}	17,075^{aA}	16,428^{aA}	16,315^{a}
25%	inner HW[3]	10,115^{dA}	10,170^{eA}	9,333^{eB}	9,873^{e}
25%	middle HW[4]	11,677^{cA}	11,816^{dA}	10,644^{dB}	11,379^{d}
25%	outer HW[5]	13,656^{bAB}	14,358^{cA}	13,346^{cB}	13,787^{c}
25%	inner SW[6]	15,292^{aB}	16,235^{bA}	15,692^{bAB}	15,740^{b}
25%	outer SW[7]	15,876^{aB}	17,687^{aA}	16,835^{aAB}	16,800^{a}
0%	inner HW[0]	6,599^{cB}	8,098^{cA}	7,832^{cA}	7,509^{c}
0%	outer HW[1]	10,716^{bA}	11,809^{bA}	10,998^{bA}	11,174^{b}
0%	SW[2]	13,198^{aA}	14,006^{aA}	14,214^{aA}	13,806^{a}

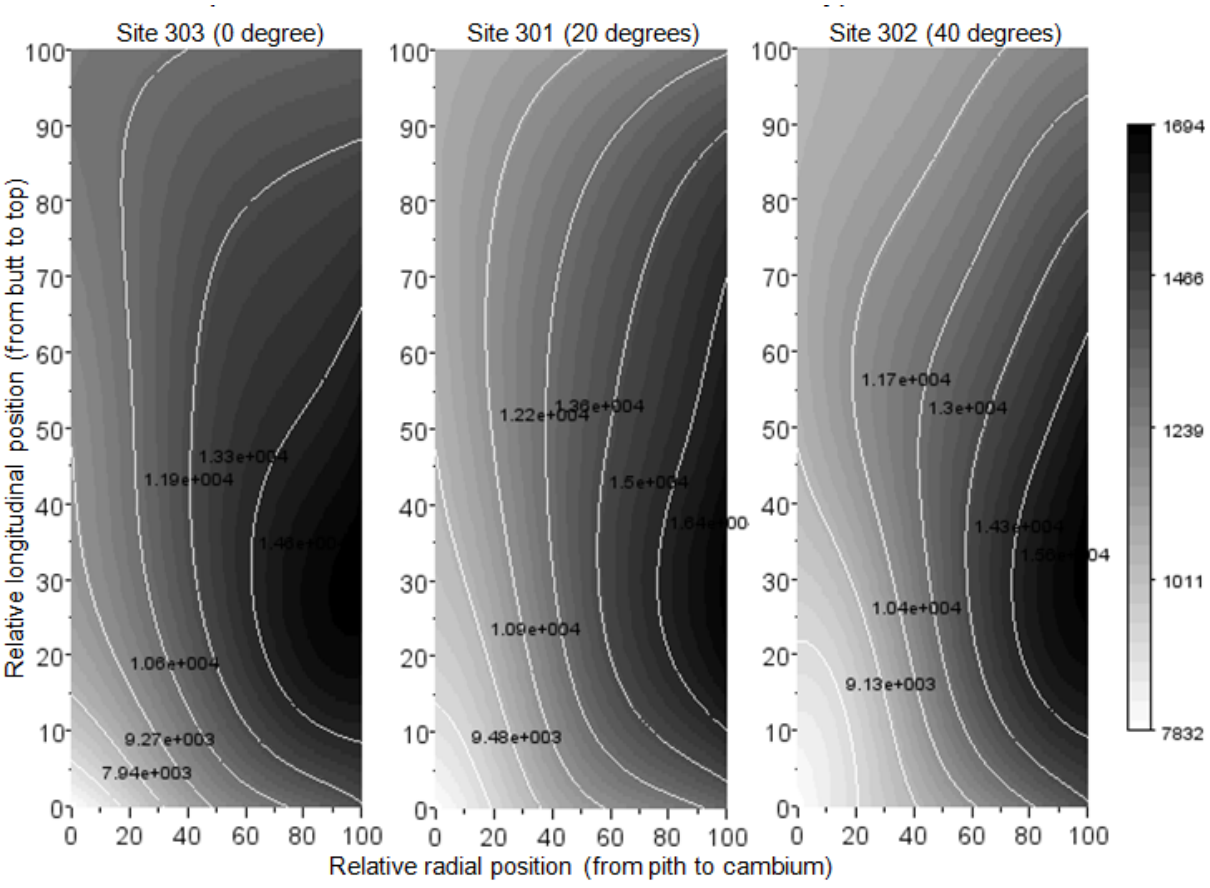

Figure 40 - Spatial variation of modulus of elasticity (MPa) in *Eucalyptus urophylla* x *grandis* trees

Table 36 - Radial and longitudinal variation for microfibril angle (degrees) in clones of *Eucalyptus* wood at three contrasting sites. The means were compared by the Tukey test at p =0.01 threshold. Small letters are comparisons between radial positions while capital ones compares sites. Values in brackets are coefficients of variation in percentage

Height	Radial	303 (0°)	301 (20°)	302 (40°)	Overall
100%	outer SW[14]	12.71^{aB}	13.10^{aAB}	13.33^{aA}	13.05^{a}
100%	outer SW[15]	12.16^{bAB}	11.93^{bB}	12.54^{bA}	12.21^{b}
100%	outer SW[16]	11.45^{cA}	10.67^{cB}	11.59^{cA}	11.24^{c}
75%	inner SW[11]	12.31^{aB}	12.71^{aAB}	12.88^{aA}	12.63^{a}
75%	middle SW[12]	10.66^{bB}	10.38^{bB}	11.21^{bA}	10.75^{b}
75%	outer SW[13]	10.03^{cA}	8.97^{cB}	9.98^{cA}	9.66^{c}
50%	HW[8]	12.55^{aA}	12.29^{aA}	12.33^{aA}	12.39^{a}
50%	inner SW[9]	10.15^{bA}	9.87^{bA}	10.26^{bA}	10.09^{b}
50%	outer SW[10]	9.05^{cA}	8.18^{cB}	8.92^{cA}	8.72^{c}
25%	inner HW[3]	12.53^{aA}	12.96^{aA}	12.53^{aA}	12.67^{a}
25%	middle HW[4]	11.13^{bA}	11.09^{bA}	11.43^{bA}	11.22^{b}
25%	outer HW[5]	9.88^{cA}	9.60^{cA}	9.92^{cA}	9.80^{c}
25%	inner SW[6]	8.92^{dAB}	8.50^{dB}	9.06^{dA}	8.83^{d}
25%	outer SW[7]	8.65^{dA}	7.74^{eB}	8.56^{dA}	8.31^{e}
0%	inner HW[0]	13.18^{aA}	12.93^{aA}	12.84^{aA}	12.98^{a}
0%	outer HW[1]	10.78^{bA}	10.50^{bA}	10.82^{bA}	10.70^{b}
0%	SW[2]	9.54^{cA}	9.12^{cA}	9.31^{cA}	9.32^{c}

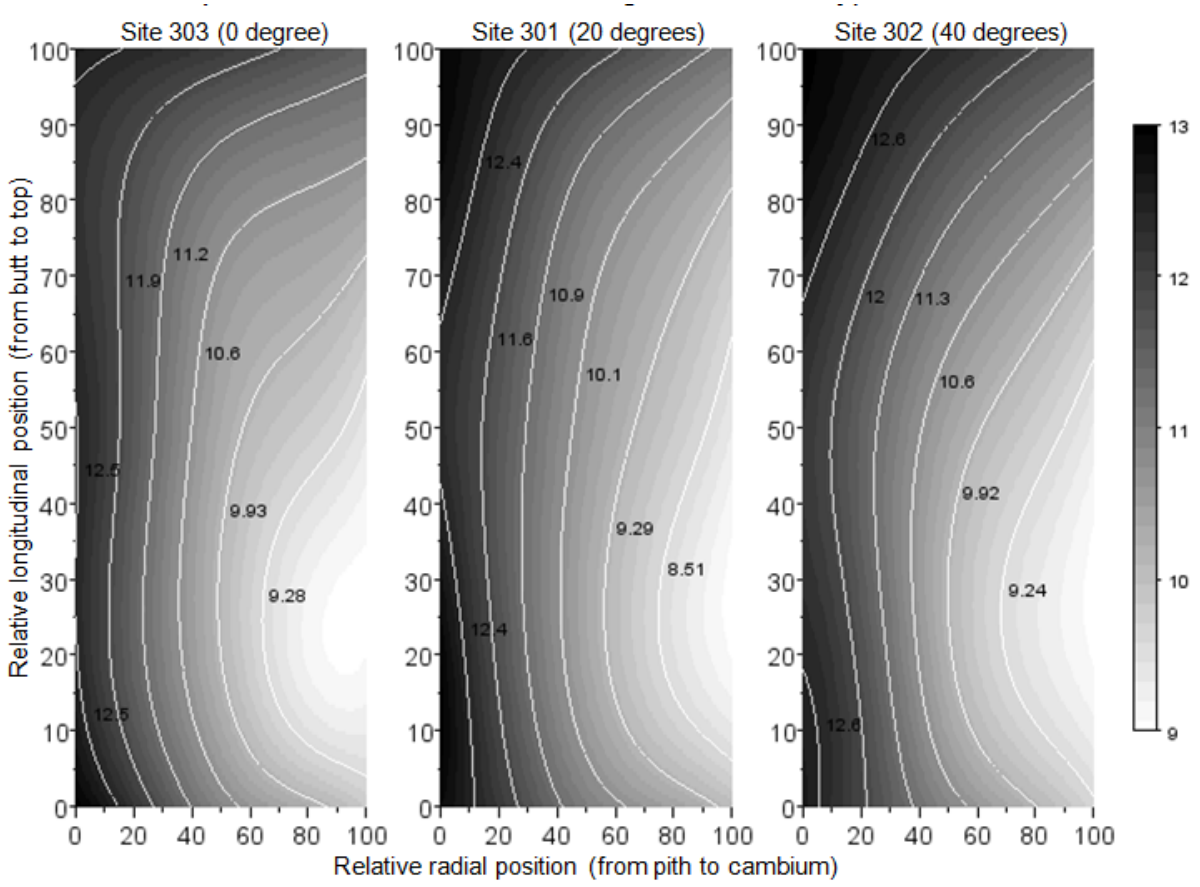

Figure 41 - Spatial variation of microfibril angle (degrees) in *Eucalyptus urophylla* x *grandis* trees.

Table 34 shows the patterns of radial and longitudinal variation in basic density of wood along the *Eucalyptus* trees. Variations in basic density of wood along the stem are less consistent than those in the radial direction (Figure 39), especially in the bottom. Overall, the wood density strongly varied from pith to cambium at the base (~140 kg m^{-3}) and at 25% of stem height (~130 kg m^{-3}). At 50% of height the trait also increased (~104 kg m^{-3}), but in relative low magnitude. The density slightly increased from pith to bark at 75% of height (~50 kg m^{-3}) and at the top of the tree the variation was of lower magnitude (~20 kg m^{-3}).

Figure 39 shows that the pith to cambium variation in wood density was higher in trees from the Site 302 (40°). For instance, at 25%, the radial variation was 104 kg m^{-3} in the site 303 (0°), 133 kg m^{-3} in the site 301 (20°) and 157 kg m^{-3} in the site 302 (40°). The higher the slope of the terrain, the greater the magnitude of variation in wood density.

The spatial variation of the modulus of elasticity within the *Eucalyptus* trees at the three contrasting sites is presented in Table 35 and Figure 40. The patterns of variation in modulus of elasticity and wood density were similar. Again, variations in basic modulus of elasticity along the stem are less consistent than those in the radial direction (Figure 40), especially in the bottom. Overall, the modulus of elasticity strongly increased from pith to bark at the base (~6,300 MPa), at 25% of height (~6,900 MPa), at 50% of height (~5,600 MPa) and at 75% of height (~3,900 MPa). At the top of the tree there was a significant increase (1,800 MPa) but of low magnitude (Table 35). Interestingly, the stiffness at the base and at 25 of height increased in the same magnitude (~6,500 MPa) towards the bark, but the absolute E values at 25% of height were, on average, 2,500 MPa higher. Similarly to the wood density, the variation in the top of the tree was low because these woods were produced recently, some months before the tree be harvested. The trends in spatial variation for modulus of elasticity over the contrasting sites were similar to those for density of wood.

The pith to cambium variation in wood stiffness was lower in trees from the Site 303 (0°) and higher in trees from site 301 (20°) (Table 35). For instance, at 25%, the radial variation was 7.5 GPa in the sites 301 (20°) and 302 (40°) and 5.7 GPa in the site 303 (0°). At 50% and 75% of height, the magnitude of radial variation was higher in trees from site 301 (20°) (Figure 40). These findings are interesting for sawn timber breeders because it is stiffness that is desirable rather than its constituent traits, density and MFA.

Table 36 and Figure 41 show the patterns of spatial variation in MFA of *Eucalyptus* trees. The trends in MFA were inversely similar to those for density and stiffness. The microfibril angle strongly decreased from pith to bark at 25% of height (~4.4 degrees). Similar decrease in MFA was observed at the base and at 50% of height (~3.7 degrees). A decrease in MFA of low magnitude, but significant was obtained at 75% of height (~3 degrees) and at the top of the tree (~2 degrees). In most of the positions, there was no difference between sites in MFA.

The magnitude of radial variations in MFA was higher in trees from Site 301 (20°) while the radial variation of trees from site 303 (0°) was in lower magnitude. This trend was also observed for stiffness and could be partially attributed to the higher wind velocities of Site 301. In short, for wood density, the higher the slope of the terrain, the greater the magnitude of variation in wood density and for stiffness and MFA, trees from site 301 (20°) presented the higher radial variations. These patterns of spatial variation are in accordance of those reported in numerous studies. Patterns in pith to bark variation of the traits themselves have been known for many years; wood density and stiffness generally increases while MFA decreases from pith to bark (Kollmann and Côté 1968). These variations result in wood traits becoming more advantageous for sawn timber production as trees become older.

Here, the patterns of spatial variation for basic density, stiffness and microfibril angle along the *Eucalyptus* stems indicates that variability in stems wood is not negligible, even at six years old. The interesting point of this part of the study is the establishment of the spatial variations of basic density, stiffness and MFA along the *Eucalyptus* tree and the comparison of these variations among contrasting sites.

Analyzing these results requires an important consideration: the aging of the meristematic cells that produces the cambium. At the base, the first growth ring is totally juvenile (meristem and cambium had the same age). On the other hand, the meristem had 6 years while the cambium had some months when the wood was produced in the top of these trees. The cambial juvenility is frequently less pronounced in the top. These issues are discussed in Thibaut et al. (2001). Table 37 presents the pith to cambium variation of wood density (kg m^{-3}), stiffness (GPa) and microfibril angle (degrees) at various relative heights.

Table 37 - Pith to cambium variation of wood density (kg m^{-3}), stiffness (GPa) and microfibril angle (degrees) at various relative heights.

Trait	Height	303 (0°)	301 (20°)	302 (40°)
ρ	100%	12.4	17.6	24.7
	75%	46.7	57.2	46.7
	50%	88.7	112.4	112.4
	25%	104.4	132.9	157.2
	0%	127.5	141.5	144.4
E	100%	1.04	2.45	2.08
	75%	2.80	4.85	3.96
	50%	4.80	6.17	5.91
	25%	5.76	7.52	7.50
	0%	6.60	5.91	6.38
MFA	100%	1.26	2.43	1.74
	75%	2.28	3.74	2.90
	50%	3.50	4.11	3.41
	25%	3.88	5.22	3.97
	0%	3.64	3.81	3.53

Variations in ρ along the stem were less consistent than those in the radial direction, especially in the bottom. The wood density varied 127-144 kg m^{-3} from pith to bark at the base (increasing from ~460 to ~600 kg m^{-3}) and at the top of the tree the variation were of lower magnitude (from 12 to 24 m^{-3}). The higher the slope of the terrain, the greater the magnitude of variation in wood density. Variations in E of wood along the stem were again less consistent than those in the radial direction especially at the base. E varied 5.9-6.6 GPa from pith to bark at the base (increasing from ~7.5 to ~13.8 GPa). The trends in spatial variation for E were similar to those for ρ. The pith to cambium variation in wood stiffness was lower in trees from the Site 303 (0°). However, pith to cambium variations were higher in trees from site 301 (20°) for all heights, except at the base. The MFA decreased 3.5-3.8 degrees from pith to bark at the base and 1.3-2.4 degrees at the top of the tree. The magnitude of radial variations in MFA was higher in trees from Site 301 (20°) while the radial variation of trees from site 303 (0°) was in lower magnitude. This trend was also observed for stiffness.

3.6.3.2 *Clonal by environmental interaction of the wood traits*

Knowledge of possible genotype by environment (G x E) interaction is vital to tree improvement if genotypes are to be planted across different environments (Zobel and Talbert, 2003). For ease of deployment, clonal performance and ranking should be predictable and stable across a range of sites, as G x E interaction can add complexity and cost to a tree improvement program (McKeand et al., 1990). Clone by site interaction for basic density, modulus of elasticity and microfibril angle in the inner heartwood (near to pith) and of the outer sapwood (near to cambium) at 25% of height are presented and discussed. The wood from this region (at 25% of tree height) was chosen because is the zone more interesting from a merchantable point of view. The radial variation of basic density of the wood at 25% of height was analyzed between clones and sites. This longitudinal position (at 25% of the tree height) was chosen because represents the most commercially valuable part of the stem. The means were compared between clones, sites and radial positions by Tukey test and the results are presented in Table 38.

Table 38 - Radial variation at 25% of the stem height for wood basic density (kg m^{-3}) for clones of *Eucalyptus* wood and sites. The means were compared by the Tukey test at p=0.05 threshold. Small letters are comparisons between clones or sites while capital ones compares the radial positions

Clone	inner HW[3]	middle HW[4]	outer HW[5]	inner SW[6]	outer SW[7]
4426	424.1^{dC}	442.5^{dC}	482.5^{dB}	521.8^{cA}	543.6^{bA}
4494	474.3^{bcC}	493.1^{bcC}	548.9^{abcB}	625.7^{aA}	617.0^{aA}
4514	487.0^{abcC}	488.1^{bcC}	537.2^{bcB}	580.1^{abA}	600.3^{abA}
4515	483.3^{abcC}	490.9^{bcC}	541.8^{abcB}	590.6^{abA}	621.3^{aA}
4535	514.6^{aB}	514.7^{abB}	581.9^{abA}	605.5^{abA}	623.9^{aA}
4541	466.7^{cB}	474.3^{cB}	516.3^{cdB}	571.8^{bA}	586.3^{abA}
4557	505.9^{abC}	531.2^{aC}	587.7^{aB}	608.4^{abB}	641.4^{aA}
4579	454.3^{cdC}	473.9^{cC}	526.0^{cdB}	608.7^{abA}	620.1^{aA}
4588	466.8^{dD}	480.7^{cD}	525.7^{cdC}	564.7^{bcB}	591.7^{abA}
4609	474.9^{cdC}	489.6^{bcC}	556.2^{abcB}	604.3^{abA}	621.0^{aA}
Site	**inner HW[3]**	**middle HW[4]**	**outer HW[5]**	**inner SW[6]**	**outer SW[7]**
301	496.5^{aD}	488.3^{aD}	554.5^{aC}	598.4^{aB}	629.4^{aA}
302	461.6^{bD}	489.9^{aC}	545.0^{aB}	603.0^{aA}	618.8^{aA}
303	467.5^{bC}	485.5^{aC}	521.8^{bB}	563.1^{bA}	571.9^{bA}

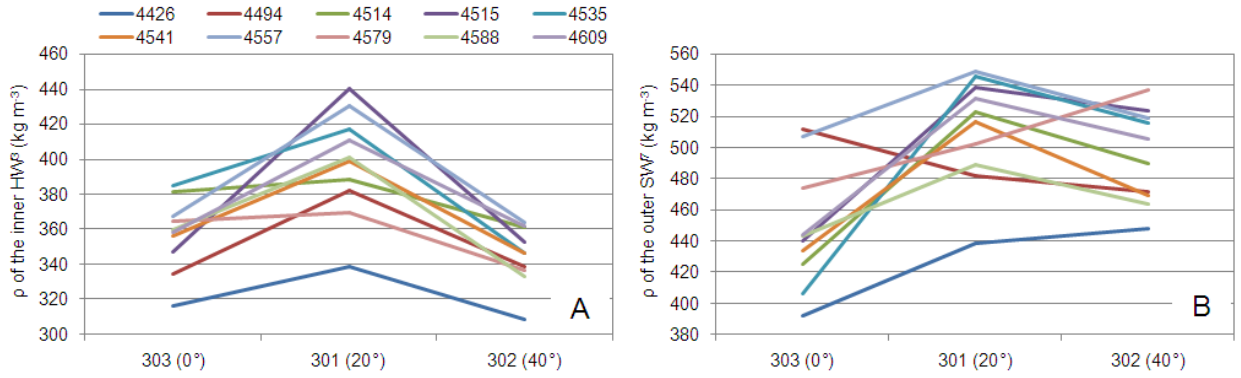

Figure 42 - Clone by site interaction for basic density of the inner heartwood (A) and of the outer sapwood (B) at 25% of height

Estimating genotype by environment interaction is necessary in proposing the basis for setting up breeding populations and selecting environmentally stable genotypes (Kien et al. 2009). Clone by site interaction for basic density of the inner heartwood and of the outer sapwood at 25% of height is presented in Figure 42. Comparing variations in genotype by environment interaction the inner heartwood and of the outer sapwood allows examining how wood traits and ranking clones varies over the years.

First, it is possible to note that, in the most of clones, site 301 (20°) produces the denser wood either at the first year (inner heartwood) or at the sixty year (outer sapwood). Site 302 (40°) produces the wood with lower densities in the inner heartwood. This finding is contrary to those reported for wood scantlings (Figure 38, pg. 109). However, the wood density of the clones from the site 302 (40°) strongly increased at the sapwood. Despite the increase of wood density near to cambium, the patterns observed from the scantlings results are still different. From the NIR-predicted data, clones planted in site 302 produced the denser woods.

The information from NIR-predicted data is more realistic and reliable because the experimental design was equilibrated, ie, each clone had its density estimated by the same NIR-based models, in the same points whereas the scantlings were sampled in a non-uniform way. 411 scantlings were taken form 150 central boards, then, the number of scantlings by site and by clone were not equivalent because of the difficulty of producing "beautiful" pieces of some clones of site 302 (40°), for example.

Second, it is important to note that clones producing the denser woods at the first year continue producing the denser woods at the sixty year (the contrary is also true). For instance, clones 4515, 4557, 4535 produces the wood with the higher densities while the clone 4426 produces lower wood density both at the first and at the last year of development. From this point of view, the findings from scantlings (Figure 38, pg. 109) and NIR-predicted wood density (Figure 42) are similar: the best (4535 and 4557) and the worst (4426) clones are the same.

Table 39 - Radial variation at 25% of the stem height for elastic modulus (MPa) for clones of *Eucalyptus* wood and sites. The means were compared by the Tukey test at p=0.05 threshold. Small letters are comparisons between clones or sites while capital ones compares the radial positions

Clone	inner HW[3]	middle HW[4]	outer HW[5]	inner SW[6]	outer SW[7]
4426	$8{,}279^{cD}$	$9{,}621^{cC}$	$11{,}635^{cB}$	$13{,}073^{bA}$	$13{,}776^{bA}$
4494	$9{,}025^{bcC}$	$10{,}597^{bcC}$	$13{,}808^{abB}$	$16{,}728^{aA}$	$17{,}593^{aA}$
4514	$10{,}302^{abC}$	$11{,}599^{bC}$	$13{,}488^{bcB}$	$15{,}210^{aA}$	$16{,}287^{abA}$
4515	$10{,}875^{aC}$	$12{,}051^{abC}$	$14{,}573^{abB}$	$16{,}419^{aA}$	$17{,}559^{aA}$
4535	$10{,}829^{aC}$	$12{,}095^{abC}$	$14{,}105^{abB}$	$15{,}943^{aA}$	$17{,}151^{aA}$
4541	$9{,}932^{abD}$	$10{,}661^{bcCD}$	$12{,}780^{bcBC}$	$15{,}220^{aAB}$	$15{,}822^{abA}$
4557	$11{,}332^{aD}$	$13{,}533^{aC}$	$15{,}675^{aB}$	$16{,}859^{aAB}$	$18{,}057^{aA}$
4579	$9{,}022^{bcC}$	$10{,}741^{bcC}$	$13{,}677^{bB}$	$16{,}272^{aA}$	$17{,}387^{aA}$
4588	$9{,}023^{bcE}$	$11{,}207^{bcD}$	$13{,}535^{bcC}$	$15{,}229^{aB}$	$16{,}751^{aA}$
4609	$10{,}107^{abD}$	$11{,}686^{bC}$	$14{,}589^{abB}$	$16{,}444^{aA}$	$17{,}613^{aA}$
Site	inner HW[3]	middle HW[4]	outer HW[5]	inner SW[6]	outer SW[7]
301	$10{,}170^{aE}$	$11{,}816^{aD}$	$14{,}358^{aC}$	$16{,}235^{aB}$	$17{,}687^{aA}$
302	$9{,}333^{bE}$	$10{,}644^{bD}$	$13{,}346^{bC}$	$15{,}692^{abB}$	$16{,}835^{abA}$
303	$10{,}115^{aD}$	$11{,}677^{aC}$	$13{,}656^{abB}$	$15{,}292^{bA}$	$15{,}876^{bA}$

The radial variation of wood stiffness at 25% of the tree height between clones and sites was examined and the means between clones, sites and radial positions were compared by Tukey test (Table 39). As the tree ages, it produces stiffer wood. Table 39 shows significant increase in wood stiffness according to the radial positions. Modulus of elasticity ranged from 8 to 12 GPa in the wood near to the pith and from 13 to 20 GPa near to the cambium.

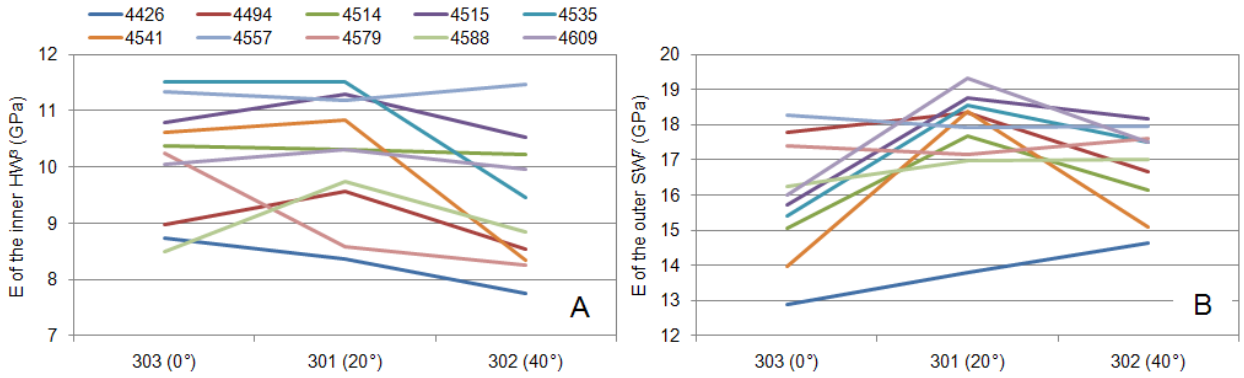

Figure 43 - Clone by site interaction for longitudinal elastic modulus of the inner heartwood (A) and of the outer sapwood (B) at 25% of height

Figure 43 presents the genotype by environment interaction for wood stiffness of the inner heartwood and outer sapwood at 25% of height. Some of the clones (4557, 4609, and 4514) present stable values of elastic modulus independently of the environment where they grow, but the ranking of the most of clones is very confusing at the first year (inner heartwood). Again, the wood of clone 4426 presented the lowest stiffness (and wood density) in the first and last years of development (but grows at fast rates). It is clear that site 301 (20°) favors the production of stiffer (and denser) woods for most of clones. The clones producing the stiffer woods at the first year continues producing the stiffer woods at the sixty year. Similarly to trends in wood density, the results obtained from the scantlings (Figure 38, pg. 109) and NIR-predicted wood density (Figure 43) indicated the same clone ranking: clones 4515, 4535 and 4557 are among the top ones while clone 4426 is again the less stiff. Both resonance and NIR spectroscopy indicates the same classification of clones, however, the ranking indicated by NIR spectroscopy analyses is more consistent.

Table 40 presents the radial variation between clones and sites of microfibril angle at 25% of the tree height. The means between clones, sites and radial positions were compared by Tukey test. As the tree ages, the microfibril angle of the cell wall of its wood significantly decrease towards the bark. For some clones, notably the 4426, 4494, 4514 and 4535, the decrease from pith to bark of microfibril angles is less accentuated.

The genotype by environment interaction for microfibril angle of the inner heartwood and of the outer sapwood at 25% of height is presented in Figure 44. Interestingly, site 302 favors the highest MFA when the trees were young and the lowest MFA when the trees reached six years old. In short, the wood of the clones growing at site 302 presented the highest variability.

This part of the study showed the size and importance of genotype by environment interactions for wood density, stiffness and microfibril angle. As stated by Muneri and Raymond (2000), this is a critical issue for designing tree breeding programs and making decisions about plantation establishment.

Table 40 - Radial variation at 25% of the stem height for microfibril angle (degrees) for clones of *Eucalyptus* wood and sites. The means were compared by the Tukey test at p=0.05 threshold. Small letters are comparisons between clones or sites while capital ones compares the radial positions

Clone	inner HW[3]	middle HW[4]	outer HW[5]	inner SW[6]	outer SW[7]
4426	12.36^{abA}	11.09^{abB}	9.79^{abcC}	9.24^{aC}	9.09^{aC}
4494	12.73^{abA}	11.78^{aA}	9.83^{abcB}	8.56^{abC}	7.95^{abcC}
4514	13.39^{aA}	11.52^{aB}	10.57^{aB}	9.53^{aC}	9.05^{aC}
4515	12.47^{abA}	11.25^{aB}	9.48^{bcC}	8.22^{bD}	7.85^{abcD}
4535	12.55^{abA}	11.20^{aB}	10.35^{abB}	9.27^{aC}	8.43^{abcC}
4541	12.54^{abA}	11.27^{aB}	10.16^{abBC}	9.02^{abCD}	8.90^{abD}
4557	12.06^{bA}	10.10^{bB}	9.06^{cC}	8.10^{bD}	7.49^{cD}
4579	12.62^{abA}	11.01^{abB}	8.96^{cC}	8.13^{bCD}	7.77^{bcD}
4588	13.35^{aA}	11.87^{aB}	10.26^{abC}	9.54^{aC}	8.61^{abcD}
4609	12.66^{abA}	11.09^{abB}	9.54^{abcC}	8.67^{abD}	8.02^{abcD}
Site	inner HW[3]	middle HW[4]	outer HW[5]	inner SW[6]	outer SW[7]
301	12.96^{aA}	11.09^{aB}	9.60^{aC}	8.50^{bD}	7.74^{bE}
302	12.53^{aA}	11.43^{aB}	9.92^{aC}	9.06^{aD}	8.56^{aD}
303	12.53^{aA}	11.13^{aB}	9.88^{aC}	8.92^{abD}	8.65^{aD}

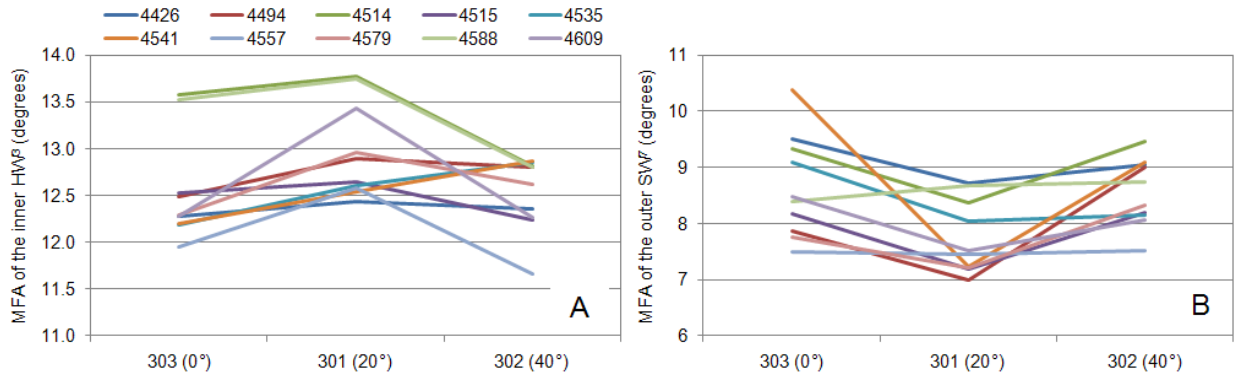

Figure 44 - Clone by site interaction for microfibril angle of the inner heartwood (A) and of the outer sapwood (B) at 25% of height

3.6.3.3 Genetic control over growth and wood traits in Eucalyptus

From the NIR-estimated dataset, the genetic (σ^2_G), residual (σ^2_E) and genetic by residual interaction (σ^2_{GxE}) variance components were estimated by Restricted Maximum Likelihood (REML) method. Thus, broad-sense heritability estimates (H^2) for growth traits and basic density of wood, elastic modulus and microfibril angle at various relative heights and radial positions were calculated. For growth traits, the BIC values of the model with GxE interaction (Eq. 37) were much lower than those from models with interaction indicating that genetic control over growth traits may be evaluated by this Equation altrough the lower estimates. The heritability estimates of wood traits were calculated with the Equation 38, without the variance due to interaction effects. The coefficient of phenotypic variation, the genetic, residual and interaction variance components and broad-sense heritability estimates for growth traits are given in Table 41. Growth traits are under low genetic control in this clonal test

Table 41 - Genetic parameters for growth traits in 6-year-old *Eucalyptus urophylla* x *grandis* clones

Model	Trait	CV (%)	σ^2_G	σ^2_{GxE}	σ^2_E	H^2	SE H^2
$Y = \mu + G + G*E + E$ Eq. 37	C	16.0	2.349	5.428	7.053	0.065	0.082
	H	14.3	0.691	1.335	2.489	0.056	0.071
$Y = \mu + G + E$ Eq. 38	C	16.0	3.749	-	8.304	0.169	0.087
	H	14.3	0.997	-	2.712	0.119	0.073

Y - trait; μ - mean; G - genetic effect; E - environmental (residual) effect and G*E - interaction effect

Estimates of broad-sense heritability (H^2) for basic density of wood, elastic modulus and microfibril angle in various relative heights and radial positions are presented below. The patterns spatial variation in the genetic control over basic density, wood stiffness and microfibril angle within the *Eucalyptus* trees are represented in Figure 45. These plots present the heritability estimates taking into account the genetic by environmental interaction (Eq. 37). The coefficient of phenotypic variation, the genetic, residual and interaction variance components and broad-sense heritability estimates (Eq. 37, with GxE interaction) for basic density, wood stiffness and microfibril angle at various relative heights and radial positions are listed in following Tables.

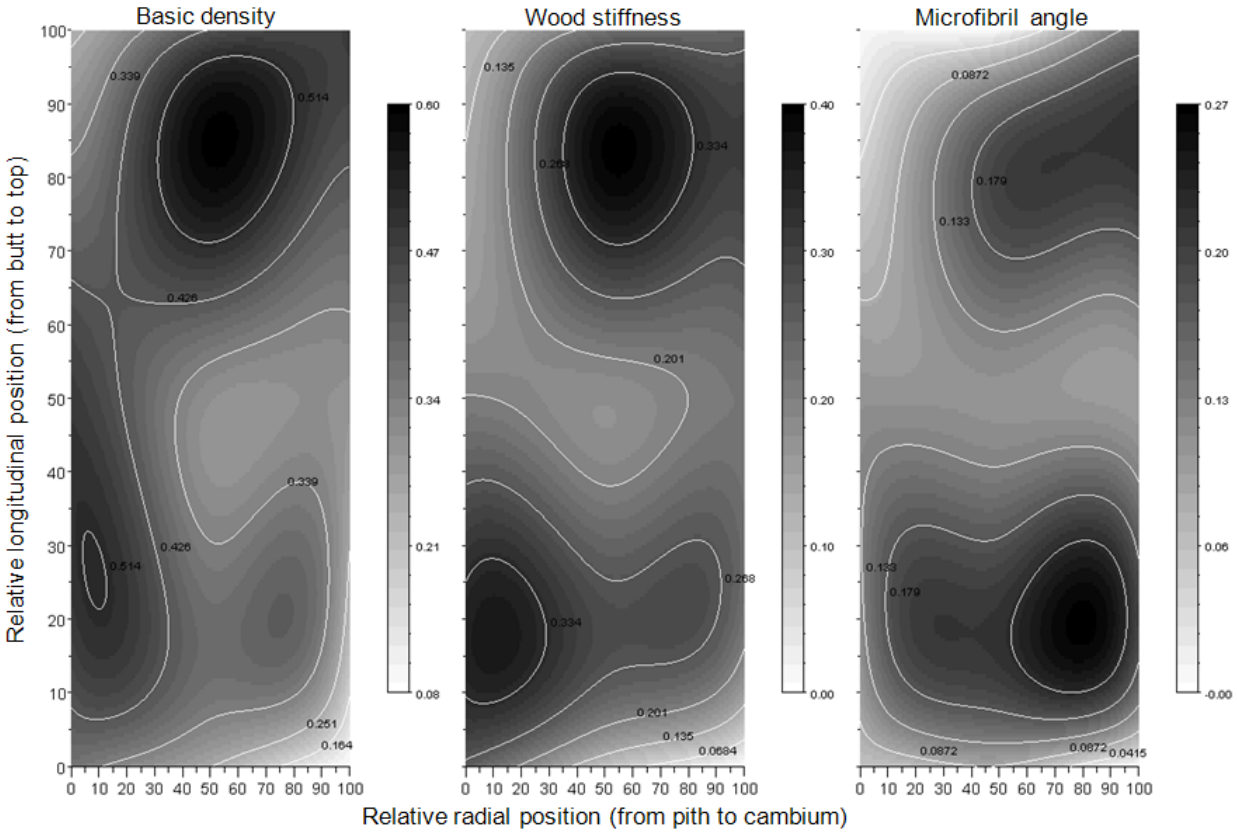

Figure 45 - Spatial variation of heritability estimates over basic density of wood, wood stiffness and microfibril angle within *Eucalyptus* trees

Table 42 - Genetic parameters for basic density of the wood in 6-year-old *Eucalyptus urophylla* x *grandis*

Height	Radial position	CV (%)	σ^2_G	σ^2_{GxE}	σ^2_E	H^2	SE H^2
100%	inner HW[14]	12.5	20.09	11.51	34.13	0.237	0.116
	outer HW[15]	11.9	26.69	14.07	27.38	0.429	0.139
	SW[16]	10.8	26.04	0.01	27.11	0.480	0.128
75%	inner HW[11]	12.8	27.71	4.93	34.80	0.383	0.130
	outer HW[12]	10.8	28.78	1.74	25.90	0.551	0.129
	SW[13]	10.3	24.88	12.86	27.78	0.398	0.134
50%	inner HW[8]	10.8	28.13	14.51	25.19	0.484	0.146
	outer HW[9]	9.7	23.23	15.34	31.39	0.307	0.121
	SW[10]	12.2	23.94	9.89	35.56	0.296	0.119
25%	inner HW[3]	11.2	24.19	10.49	22.07	0.495	0.138
	middle HW[4]	8.8	22.66	7.76	22.89	0.468	0.139
	outer HW[5]	11.3	28.96	9.52	37.16	0.363	0.126
	inner SW[6]	11.3	28.59	3.32	34.70	0.402	0.137
	outer SW[7]	12.6	24.05	15.32	39.91	0.240	0.110
0%	inner HW[0]	10.2	25.52	14.78	30.11	0.367	0.131
	outer HW[1]	12.7	32.86	19.20	53.12	0.253	0.112
	SW[2]	11.7	12.51	20.98	38.18	0.076	0.074

Table 43 - Genetic parameters for dynamic longitudinal modulus of elasticity of the wood in 6-year-old *Eucalyptus urophylla* x *grandis*

Height	Radial position	CV (%)	σ^2_G	σ^2_{GxE}	σ^2_E	H^2	SE H^2
100%	inner HW[14]	19.3	682.5	238.6	1974.9	0.105	0.077
	outer HW[15]	17.1	947.1	849.2	1567.6	0.220	0.112
	SW[16]	15.4	973.2	624.0	1586.4	0.246	0.121
75%	inner HW[11]	17.3	736.5	623.8	1676.2	0.145	0.078
	outer HW[12]	13.1	1001.8	600.8	1182.6	0.363	0.131
	SW[13]	15.0	1145.9	842.0	1573.6	0.292	0.117
50%	inner HW[8]	15.1	734.0	447.8	1385.2	0.203	0.103
	outer HW[9]	12.5	724.3	702.3	1397.5	0.177	0.098
	SW[10]	13.1	959.1	584.0	1735.9	0.215	0.097
25%	inner HW[3]	16.5	934.2	201.1	1304.5	0.334	0.117
	middle HW[4]	15.7	1000.3	260.1	1412.2	0.327	0.121
	outer HW[5]	14.0	995.0	303.5	1608.1	0.270	0.110
	inner SW[6]	12.5	1042.7	0.6	1658.3	0.283	0.119
	outer SW[7]	14.4	1128.7	330.3	2035.3	0.231	0.108
0%	inner HW[0]	27.0	995.7	685.4	1549.9	0.257	0.121
	outer HW[1]	21.8	771.3	806.0	2163.1	0.100	0.073
	SW[2]	16.0	93.8	1086.1	1911.4	0.002	0.055

Table 44 - Genetic parameters for microfibril angle of cell wall of wood in 6-year-old *Eucalyptus urophylla* x *grandis* clones

Height	Radial position	CV (%)	σ^2_G	σ^2_{GxE}	σ^2_E	H^2	SE H^2
100%	inner HW[14]	9.5	0.001	0.107	1.213	0.000	0.000
	outer HW[15]	8.4	0.059	0.477	0.891	0.003	0.048
	SW[16]	9.4	0.378	0.331	0.861	0.144	0.096
75%	inner HW[11]	7.8	0.239	0.289	0.897	0.060	0.059
	outer HW[12]	8.7	0.390	0.350	0.709	0.196	0.102
	SW[13]	12.7	0.507	0.517	0.895	0.194	0.125
50%	inner HW[8]	7.7	0.323	0.178	0.888	0.113	0.079
	outer HW[9]	8.2	0.277	0.183	0.757	0.112	0.072
	SW[10]	12.2	0.322	0.271	0.918	0.101	0.077
25%	inner HW[3]	7.6	0.341	0.000	0.895	0.127	0.080
	middle HW[4]	8.5	0.435	0.101	0.849	0.205	0.104
	outer HW[5]	10.3	0.461	0.326	0.850	0.204	0.096
	inner SW[6]	11.2	0.495	0.323	0.786	0.253	0.112
	outer SW[7]	14.0	0.480	0.370	0.926	0.188	0.106
0%	inner HW[0]	8.7	0.283	0.231	1.072	0.062	0.063
	outer HW[1]	12.3	0.388	0.445	1.189	0.086	0.067
	SW[2]	11.0	0.000	0.521	0.886	0.000	0.000

It is important to note that in the base of stem it is possible to compare genetic effects on wood developed at the first, third and sixth year of development. Then, the temporal difference between each H^2 estimate at the base of the stem is approximately of two years whereas the three H^2 estimates of the top of the tree refer to wood developed at the same year differing only some months.

Low to moderate levels of broad-sense heritability estimates (from 0.07 to 0.55) were found for basic density of wood within the stem of 6-year-old *Eucalyptus* clones (Table 42). The longitudinal variations in H^2 estimates were more consistent than those in radial direction (Figure 45), especially in the highest parts of the stem. The darker the graph, the higher the H^2 estimates. At 25% of tree height heritability estimates is higher near to pith and in the top, but no clear trends of spatial variation could be defined. For instance, the H^2 estimates linearly decreased from 0.37 near the pith to 0.08 near to the cambium in the base of the stem (0% of the commercial height) while the H^2 estimates increased from 0.24 to 0.48 on the top of the tree (Table 42). The higher H^2 estimate was found at 75% of tree height in the intermediate radial position.

The broad-sense heritability estimates for modulus of elasticity strongly varied within the stem (Table 43). Null heritability was found in the sapwood of the base while H^2 of 0.36 was estimated in the outer heartwood at 75% of height. Figure 45 shows that genetic control over stiffness is larger in two regions of the stem: (i) in the inner heartwood region (0-25% of relative radial position) of the lower zones of the tree (10-30% of the relative longitudinal position) (dark and round spot at the bottom of the chart) and (ii) at the top of the tree, a zone localized at 40-80% of relative radial position and at 70-90% of the relative longitudinal position (dark and round spot at the top of the chart). Again, no clear patterns of radial variation were established for H^2 estimates of E_L along the tree. For instance, the heritability of E_L increased from zero to 0.26 towards the cambium at the base of the stem and from 0.10 to 0.24 at the top while the H^2 estimates remains constant at 50% of height (Table 43). A linear decrease (from 0.33 to 0.23) was observed at 25% of height.

Genetic control over MFA exhibits variable patterns of variation presenting values from 0 to 0.25 (Table 44). The heritability estimates is low in the base and in the top of the tree and at 50% of the tree height (H^2=0.11). Figure 45 shows that genetic control over microfibril angle is superior in the sapwood region (60-100% of relative radial position) of the lower zones of the tree (10-30% of the relative longitudinal position) (dark and round spot at the bottom of the chart) and at the higher zones of the stem near to the cambium (dark spot at the top of the chart).

In short, Figure 45 clearly reveals that heritability estimates for D and E_L exhibited similar patterns of radial variation in the bottom of the tree, and similar trends towards the top. MFA shows opposite trends of spatial variation (mirror effect at radial direction). For density and stiffness, higher H^2 estimates were found in the higher regions of the tree, especially at the intermediate zone (dark spot at the top of the chart).

The results of heritability estimates for these wood traits from the Equation 38 (without the genotype by site interaction) are presents in the annexes section (item 6.6, pg.144).

Biological significance

The results have shown that the genetic control of MFA, stiffness and density also changes from pith to bark and from the base to top of the tree. The variation patterns of the genetic parameters in *Eucalyptus* traits have not been often reported. The estimation of genetic parameters at different ages and heights allows observation of variation of genetic control over wood traits with age. This kind of results can also be helpful when defining the optimal selection age for each species of interest.

In the base of stem, heritability estimates of wood density decreased towards the bark. These findings appear to indicate that there is more genetic control in determining the wood density in the first years, whereas the sapwood seems more likely to be controlled by external factors. Despite the low magnitude of the values, this makes biological sense. At the beginning of its development, the trees can easily find water, light and mineral nutrients and the genetic factors are the most important determinant for the tree development. As trees become older, the competition between them for light, water and space begun to take place and thus the environmental conditions increases their influence on the growth of trees at the base of the stem. On the other hand, Figure 45 clearly shows that there is more genetic control in determining the wood density from 50% of the tree height (at six years).

The heritability estimates of wood stiffness decreased towards the cambium in lower zones of the stem (Figure 45) indicating that there is more genetic control in determining the wood stiffness in the beginning of tree growth whereas the sapwood seems more likely to be controlled by external factors. When the tree reaches 5 to 6 years, there is more genetic control in determining the wood stiffness in the top of the tree. As discussed above, the genetic control over microfibril angle show opposite trends in radial variation, indicating that tree genetically controls variations in wood density, wood stiffness and microfibril angle in specific regions of the stem and at different periods (during wood development) in order to adapt the properties of its wood to support the ever-increasing weight of the stem, gravity, and wind forces.

That there exists mechanisms for controlling MFA is evidenced by the beautifully ordered structure of the secondary wall in fibers, the purposeful change from a large MFA conferring flexibility on the young stem to a small MFA conferring stiffness on the older stem, the frequent inverse relationship between cell length and MFA and the ability of the tree to over-ride this relationship in producing reaction wood (Barnett and Bonham 2004). At the same time, trees produce stiffer and denser woods at the stem periphery in order to support the external forces. The trends presented in this study revealed that part of these variations in wood density; wood stiffness and MFA are governed by genetic factors.

3.6.4 NIR spectral heritability estimates

NIR spectra contain a lot of information about wood, this complex three-dimensional biopolymer material composed of an interconnected network of cellulose, hemicelluloses, lignins and extractives. Considering a NIR spectrum as a source of information concerning many wood traits (it is based on chemical content), genetic parameters were calculated from them. The genetic (σ^2_G), residual (σ^2_E) and genetic by residual interaction (σ^2_{GxE}) variance components were estimated by Restricted Maximum Likelihood (REML) method from the NIR spectra data. Thus, broad-sense heritability estimates (H^2) for NIR spectra in radial and longitudinal positions were calculated using the model described within the item.2.4.3.2 (pg. 72). Figure 46 presents the broad-sense NIR spectral heritability estimates at the base (A) and at 25% of the tree height (B) while Figure 47 presents the NIR spectral H^2 estimates at 50% (A), 75% (B) and at 100% (C) of the commercial height. The radial variation of broad-sense heritability estimates of the NIR spectra at the base and at 25% of the tree height is presented by the gradient colors (Figure 46).

The analysis of the NIR spectra heritability estimates by wavenumber plot is useful to investigate the underlying relationships that have made the estimation of genetic parameters possible by NIR spectroscopy. The assignments of absorption bands (Table 26, pg. 96) are useful to identify which wood components presents higher broad-sense heritability estimates from NIR spectroscopic data. It helps to understanding how NIR spectroscopy can evaluate genetic control over wood traits.

Some ranges of the NIR spectra presented heritability estimate greater than 50%. This means that NIR spectra are able to capture the potential genetic of some chemical components and wood traits indirectly. The bands normally associated with cellulosic or lignin type biomolecules may be observed in the near-infrared (NIR) spectra of wood.

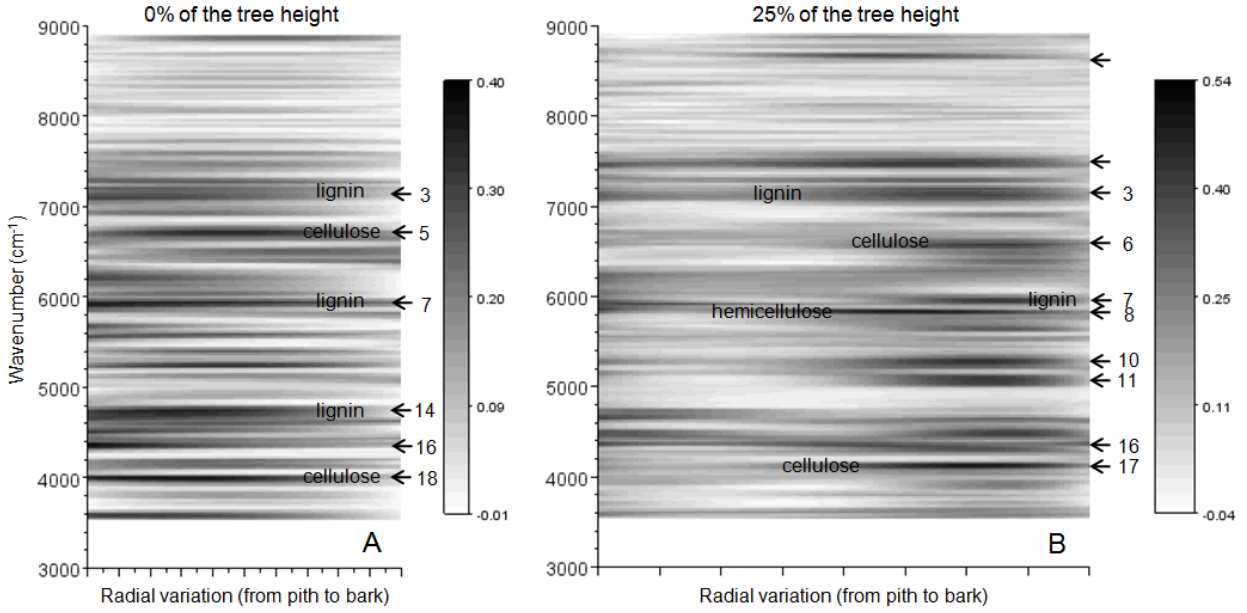

Figure 46 - Spatial variation of NIR spectral broad-sense heritability estimates at the base and at 25% of the tree height. The bands normally associated to cellulose, hemicelluloses and lignin are indicated by numbered narrows (these index are presented in Table 26, pg. 96)

In the base of the stem (Figure 46), variation in the bands around 4,060 (index 18), 4,540 (index 14), 5,950 (index 7) and at 7,085 cm^{-1} (index 3) can be mainly attributed to genetic factors because the high values of H^2 estimates At 25% of height, bands corresponding to index 3, 6, 7, 8 and 17 yielded high NIR spectra

heritability estimates. These bands are normally associated to cellulose and lignin contents, as indicated by numbered arrows within the plot. The bands were assigned to chemical compounds of the wood based on the Table 26 (pg. 96) and these information are also listed in Workman and Weyer (2007). At 50, 75 and 100% of the tree height (Figure 47), NIR spectral heritability estimates are systematically strong at bands around 5,000-5,600 (including index 9, 10 and 11) and 7,000-7,600 (including index 2, 3 and 4).

The band at 6831cm^{-1} (close to the index 5) is associated to O-H polymeric (2νO-H) and is assigned to cellulose type I. The NIR spectral heritability estimates also were high at 5,669 cm^{-1} (close to index 9) and this band is associated to functional grouping CH_2: stretching (2ν) being related to cellulose content (Workman and Weyer 2007). The band 5,553 cm^{-1} is associated to O-H stretching plus 2x C-O stretching combination, and the band at 4,313 cm^{-1} (close to index 16) belongs to functional grouping CH stretching plus CH_2 deformation combination, both related to the cellulose content of the wood.

According to Workman and Weyer (2007) lignin is representative of aromatic natural product compounds. The band at 7,180 cm^{-1} (close to index 3) is associated to C-H (2νCH_2 and δCH_2) and is interrelated to lignin content. The band at 5,940 cm^{-1} (close to index 7) belongs to functional grouping C-H (2ν), ArcC-H: C-H aromatic associated to C-H, also related to lignin content. The NIR spectral heritability estimates also were high at 4,585 cm^{-1} and this band (close to index 14) is associated to C-H stretching and C=O combination related to lignin content of wood (Workman and Weyer 2007).

It appears that variations in the indicated bands (index 5, 6, 9, 17 and 18) can be attributed to variations in genetic control over cellulose content of wood while variations in the indicated bands (index 3, 14 and 17) are attributed to variations in heritability estimates of lignin content of the wood within the stem.

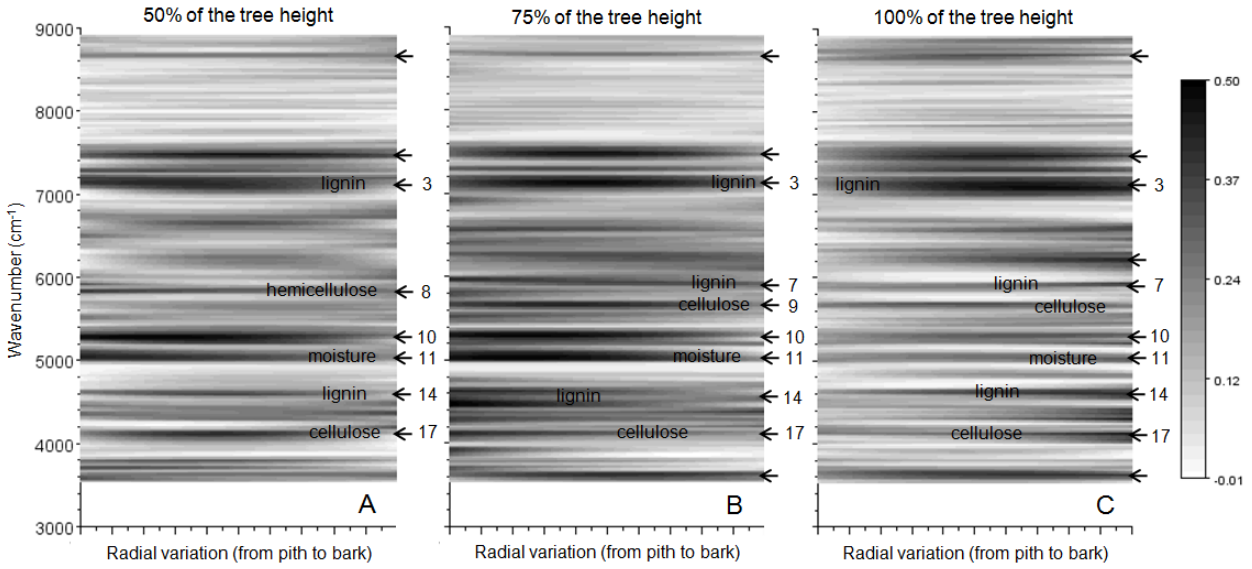

Figure 47 - Spatial variation of NIR spectral broad-sense heritability estimates at 50, 75 and 100% of the tree height. The bands normally associated to cellulose, hemicelluloses and lignin are indicated by numbered narrows (these index are presented in Table 26, pg. 96)

Indeed, Figure 46 and Figure 47 clearly reveal that the variations of some specific ranges of the NIR spectra are controlled by genetic factors. These variations in NIR spectra are supposed to be related to variation in lignin and cellulose and hemicelluloses contents. Complex combination in these specific bands may be related to variation in basic density, modulus of elasticity, MFA and other wood traits, but establishing assumption about the genetic control over these non-chemical wood traits from these NIR spectral heritability estimates is a complicated issue.

However, as NIR spectra is a countless source of information concerning chemical, mechanical, physical and ultrastructural properties of wood indirectly, the analysis of genetic parameters from NIR spectra of wood appears to be an efficient and promising way to indirectly evaluate the genetic control over many wood traits at once.

4 CONCLUDING REMARKS

4.1 Spatial variation of wood traits

In the *Eucalyptus* from **progeny tests**, the basic density of wood increased while MFA decreased towards the bark. The MFA decreased from ~18 degrees near to the pith to 13.3 degrees near to the bark. The basic density of the wood increased from ~440 kg m^{-3} near to the pith to ~615 kg m^{-3} near to the bark. These variations were observed at 1.3 meter of the tree height.

This study established spatial variations of basic density, stiffness and MFA of wood along the tree and compared these variations within trees across contrasting sites in the *Eucalyptus* from **clonal plantations**. The patterns of spatial variation for basic density, stiffness and microfibril angle along the *Eucalyptus* stems indicates that variability in stems wood is not negligible, even at six years old. In general, the basic density and stiffness of wood increased while MFA decreased towards the bark.

In short, for wood density, the higher the slope of the terrain, the greater the magnitude of variation in wood density and for stiffness and MFA, trees from site 301 (20°) presented the higher radial variations. There were significant differences between clones, but general trends could be described as follows:

Wood density: variations in basic density of wood along the stem are less consistent than those in the radial direction, especially in the bottom. The wood density strongly varied from pith to bark at the base (from ~460 to ~600 kg m^{-3}) and at 25% of stem height (from ~450 to ~605 kg m^{-3}). At 50% of height the trait also increased (~500 to ~600 kg m^{-3}), but in relative low magnitude. The density slightly increased from pith to bark at 75% of height (from ~530 to ~580 kg m^{-3}) and at the top of the tree the variation was of lower magnitude (from ~525 to ~540 kg m^{-3}). The terrain slope influenced the variations in wood density. The higher the slope of the terrain, the greater the magnitude of variation in wood density.

Wood stiffness: again, variations in modulus of elasticity of wood along the stem are less consistent than those in the radial direction (Figure 40), especially in the bottom. The elastic modulus strongly increased from pith to bark at the base (from ~7.5 to 13.8 GPa), at 25% of height (from ~9.9 to ~16.8 GPa), at 50% of height (from ~10.7 to ~16.3 GPa) and at 75% of height (from ~11.1 to ~14.9 GPa). At the top of the tree there was a significant increase (from 11 to 12.8 GPa) but of low magnitude. Interestingly, the stiffness at the base and at 25 of height increased in the same magnitude (~6.5 GPa) towards the bark, but the absolute E values at 25% of height were, on average, 2.5 GPa higher. The trends in spatial variation for modulus of elasticity were similar to those for density of wood. The pith to cambium variations in wood stiffness were lower in trees from the Site 303 (0°). However, pith to cambium variations were higher in trees from site 301 (20°) for all heights, except at the base. The higher pith to bark variation at the base was found in trees from the Site 303 (0°).

Microfibril angle: The MFA decreased from pith to bark at the base (from ~13 to ~ 9.3 degrees), at 25% of height (from ~12.7 to ~8.3 degrees) and at 50% of height (from ~12.4 to ~8.7 degrees). A decrease in MFA of low magnitude, but significant was obtained at 75% of height (from ~12.6 to ~9.7 degrees) and at the top of the tree (from ~13 to ~11.2 degrees). In most of the positions, there was no difference between sites in MFA. The magnitude of radial variations in MFA was higher in trees from Site 301 (20°) while the radial variation of trees from site 303 (0°) was in lower magnitude. This trend was also observed for stiffness.

It is important to note that, at the base of the tree, the comparison is made using wood developed at the first year and wood produced at the sixty year while the comparison between densities in the top of the tree is based on wood formed exclusively at the sixty and last year of development. As the cylinder of juvenile wood extends from the base (0%) to the top (100%) the proportion of juvenile wood over the cross-section of the stem increases.

4.2 Influence of MFA on wood traits

The relationships among wood traits were investigated in *Eucalyptus* wood. In the trees from the **progeny tests**, there was no significant correlation between microfibril angle and basic density of wood.

For the trees from the **clonal tests**, there were weak to strong linear relationships between microfibril angle, density, wood stiffness and strength, modulus of shear and shrinkage. For instance, a strong relationship between stiffness and wood density (r=0.82) was found. There were significant relationship of MOR with stiffness (r=0.81), basic density (r=0.68) and MFA (r=-0.47). The parameter D/MFA was well correlated with stiffness (r=0.82) and MOR (r=0.61), but a slight correlation was found with tangential and radial (r=0.29) shrinkage. Basic density was moderately correlated with tangential (r=0.43) and radial (r=0.39) shrinkage while MFA was slightly negatively correlated to tangential (r=-0.33) and radial (r=-0.24) shrinkage. Significant, but of low magnitude relationship was found between shear modulus and wood density (r=0.28) and shear modulus and MFA (r=0.2). This study shows that MFA variation accounted for only 44 percent of the variation in specific modulus in *Eucalyptus* wood from fast growing plantations.

The influence of MFA and /or density on wood stiffness and modulus of rupture (MOR) of wood samples was better examined. Multiple regression analyses showed that wood density was the prime determinant of both modulus of elasticity and modulus of rupture. In this study, MFA variation accounted for only 37% of the variation in E while the basic density variation alone accounted for 68 percent. Acting together, basic density and MFA accounted for 78 percent of the variation in modulus of elasticity. For modulus of rupture, basic density variation accounted for 46%, and MFA for 22% of the variation in wood strength. Basic density and MFA combined accounted for 51% of the variation in modulus of rupture. The parameter “density/MFA” was fine correlated with both modulus of elasticity (R^2=0.7) and modulus of rupture (R^2=0.45) by power models.

In this study, wood density was the prime determinant of both modulus of elasticity and modulus of rupture while the MFA played a secondary role on stiffness and strength of wood from **clonal tests**.

Influence of terrain slope on correlations

In this study, the relationships between MFA and mechanical traits were examined in details for each radial position (internal, near to the pith or external, near to the bark) and contrasting sites (at 0, 20 and 40 degrees of inclination) of the **clonal tests**.

The correlations relating MFA and mechanical traits were lower for outer wood likely due the occurrence of growth stresses, tension wood and grain angle, which are more evident on stem periphery. For instance, MFA were significantly correlated ($0.7<R^2<0.8$) with E for specimens sampled from central zones of stem (near to the pith) while weak E x MFA correlations ($0.2<R^2<0.3$) were found for specimens sampled from external zones of the trunk.

In regard to the effect of terrain slope on wood traits, we found the same trends for the three evaluated sites. The correlation of MFA with ρ, E, E/ρ and MOR were slightly similar for the contrasting sites.

These findings indicate that environmental conditions, at least the terrain slope, did not play a major role on a cellulose microfibril orientation in the secondary cell wall of *Eucalyptus* wood.

Our results are especially useful for forest-based industries which produce their own raw material, such as pulp and paper or pig iron producers. *Eucalyptus* forests planted in sloped zones, for instance, will produce woods with similar mechanic resistance; however, differences in growth rate will be remarkable between trees from different site conditions.

4.3 Combining techniques for assessing wood traits

4.3.1 Resonance

The relationships between the mechanical properties obtained on large pieces of wood (scantlings measuring ~45 mm x ~60 mm x 645-2,080 mm) and on small specimens (measuring 25 mm x 25 mm x 410 mm) of the wood from **clonal test** were investigated. Correlations from 0.68 to 0.75 between the E of scantlings and small specimens of *Eucalyptus* wood were found when the E of the scantling with the averaged E values of the specimens per scantling were compared. When the E_F value of each single specimen was compared with its respective scantling, the coefficient of correlation decreased to 0.64 in the longitudinal tests and to 0.61 in the flexural tests. A roughly linear correlation (r=0.59) between specific modulus and loss tangent was obtained for the small specimens of *Eucalyptus*.

The findings demonstrate that resonance technique is potentially able to characterize the mechanical properties of wood in a simple and rapid way and at low cost. The dynamic tests enabled rapid estimates of the key mechanical properties (such as the Young, the shear modulus and the loss tangent) of the wood even in lumbers containing knots, small cracks and also slightly damaged areas.

Moreover, scantlings of different lengths were used in this study. At the outset, we think that this condition would be a limitation, but the tightness of the correlations confirms that the vibrations tests are suitable for phenotyping wood of any dimensions, with high accuracy and repeatability.

In short, the resonance technique rapidly provided a large accurate data set of mechanical wood properties as required for high-throughput phenotyping in recent genetic studies.

4.3.2 NIR spectroscopy calibrations

NIR models for chemical properties

Satisfactory NIR calibrations were obtained for estimating Klason lignin and acid-soluble lignin contents and syringyl to guaiacyl ratio in *Eucalyptus urophylla* wood from **progeny tests**. The best calibrations were developed using NIR spectra measured on wood powder (RPD from 2.0 to 2.9), but satisfactory calibrations were still developed from NIR spectra measured on solid samples (RPD from 1.7 to 2.2). Accordingly, it was demonstrated that the sample preparation influences strongly the statistics associated with the predictive models. For these *Eucalyptus urophylla* woods, the effect of the sample presentation (solid or milled wood) was stronger than the effect of the particle size (fine and coarse powder). The NIR spectral information acquired from solid wood are sufficient to provide acceptable calibrations to estimate quickly the Klason and acid-soluble lignin contents and the S/G ratio. However, the time-consuming milling operation is strongly recommended for optimum accuracy. In this study, acid-soluble lignin could be predicted from surfaced wood NIR spectra with the same statistical performance when compared to wood powder calibrations. In short, the NIR spectra acquired from coarse wood powder provided

calibrations with strong correlations for Klason lignin (R^2cv=0.86, SECV=0.48% and RPD=2.85) and S/G ratio (R^2cv=0.86, SECV=0.12 and RPD=2.88 for) and so that the extra effort required to produce 0.5 mm wood powder is not warranted.

NIR models for wood density

Promising NIR calibrations were obtained for assessing basic density of wood in *Eucalyptus* trees. The NIR spectra measured on radial surface provided the best regression statistics. These NIR calibrations yielded good estimates for basic density of woods from the **progeny** (R^2p=0.85; RMSEP=30 kg m^{-3} and RPD=2.7) and **clonal tests** (R^2p=0.80; RMSEP=22.9 kg m^{-3} and RPD=2.3). The procedure for validating the NIR models ensures the reliability of the application of this tool in routine analysis for the determination of basic density of wood in breeding programs and *Eucalyptus* plantations.

NIR models for visco-elastic traits

Good NIR models were established for estimating dynamic properties of the wood from **clonal test** using as reference data provided by resonance tests. The NIR models for modulus of elasticity presented good performance and acceptable statistics (R^2=0.81, RMSEP=1.15 GPa and RPD=2.3), showing the robustness of the association NIR-resonance. Models for first resonance frequency (R^2=0.72 and RPD=1.9) and loss tangent (R^2=0.38 and RPD=1.8) were also developed but the estimated values were not used for genetic studies.

NIR models for MFA

NIR calibrations for microfibril angle in *Eucalyptus* wood were developed based on reference values recorded by the X-ray diffraction technique. The NIR model for 100/MFA based on NIR spectra measured on tangential surface presented the best statistics (R^2p=0.72, RMSEP=0.89 degrees and RPD=1.65) while the model based on NIR spectra measured on radial surface was the best for MFA (R^2p=0.64, RMSEP=1.32 degrees and RPD=1.63) in the trees from **progeny test**. Relatively best NIR models for MFA (R^2p=0.75, RMSEP=1.31 degrees and RPD=2.1) were developed for the trees from **clonal test**. With respect to these models for MFA, the reference data based on Yamamoto formula generated better statistics than those based on Cave formula. NIR spectroscopy tool was able to predict MFA of *Eucalyptus* wood, using both different wood faces, and wood quality surfaces.

Associating polyvalent techniques for assessing wood traits

The association NIR spectroscopy with resonance and X-ray diffraction techniques to evaluate wood traits has three substantial advantages: speed, accuracy and low-cost. Considering the small area scanned by X-ray beam or NIR spectra and the high correlations with MFA of wood sections and elastic properties of entire wood specimens, the scale effect was not a source of substantial error.

The association of NIR spectroscopy with resonance and X-ray diffraction techniques seems to be an adequate, low-cost tool for phenotyping woods. This technique associated to motor-driven coring system, allows predicting a range of wood traits, at the same time, in a large (dry) sample set as required by genetic studies. As NIR spectra measured on radial surface of wood are expected to be more informative, the recommendation is to cut the core sample parallel to the fiber orientation allowing the radial face to be measured by the spectrometer.

The idea behind of combining polyvalent techniques is to provide large datasets of key wood properties, sufficiently representative of the properties in parts of the stem, and sufficiently precise in order to be useful for genetic studies. Indeed, the absolute value of the property is of no matter for genetic approaches.

The interesting point is to know the relative value of the characteristic between trees or regions of the stem and its variation or stability within the logs. This thesis supports the premise that the NIR is currently the most powerful high throughput phenotyping tools for tree breeders, making possible the selection of candidate genotypes or commercial clones in forestry industries from large samplings. According to Meder et al. (2010) one often overlooked advantage of NIR is that a single spectrum has the potential to provide predictions for numerous properties once the calibrations are established. This has significant benefit to tree breeders who can potentially access chemical composition, wood density, stiffness, microfibril angle and other traits from a single NIR spectrum. For genetic screening purposes this has immense power, given that traditional methods are specific in nature and only determine a single property at a time.

4.4 Genetic and environmental control of wood traits

Genetic parameters were assessed from two independent trials of *Eucalyptus*. Progeny and clonal test are experiments that allow obtaining useful information for tree breeders. Indeed, each type of test had its advantages and inconvenient. For instance, because the full-sibs of the **progeny test** were not replicated in the experimental design, dominance and micro-environmental effects were confounded, thus family effect was not considered in the model. However, this design allows the prediction of additive genetic values of trees making possible the calculus of narrow-sense heritability estimates and the genetic and environmental correlations. The **clonal tests** were replicated in three contrasting sites allowing the examination of the genetic x environmental interaction for a range of wood and growth traits. However, this design allows the calculus of broad-sense heritability estimates, which is less informative since the additive and non-additive effects are taken into account.

4.4.1 Genetic studies from the progeny tests

MFA was found to be under strong genetic control in *E. urophylla*. While the mean MFA value per tree presented narrow-sense heritability of 0.65 the h^2 estimates increased from 0.43 in the inner heartwood to 0.50 in the outer heartwood but decreasing again to 0.44 in the sapwood. For density, the h^2 was 0.62 for the mean value, increasing from 0.37 (inner heart wood) to 0.51 towards the sapwood. Lignin content and S/G ratio were found to be under strong genetic control ($h^2>0.7$). These high narrow-sense heritability estimates indicate that genetic improvement is possible through selective breeding.

The genetic correlation between height and lignin (r=-0.61) and between MFA and lignin (r from 0.4 to 0.74 towards the bark) are favourable for pulp and paper production since they indicate that increase of one trait leads to decrease of another and vice-versa. On the other hand, these correlations are undesirable for bio-energy purposes.

We found strong negative genetic correlations for circumference and density and for density and S/G ratio and positive genetic correlation between MFA and density. The genetic correlation between wood density and MFA remained constant (r=0.7) in the heartwood, decreasing considerably towards the sapwood. As forestry industries are mainly searching for adequate density woods, such correlations are unfavourable for pulpwood, sawnwood and bio-energy applications.

The genetic correlation among growth and wood traits bring new elements to understanding how trees adapt their wood traits in order to maintain their erect habit even when they are constrained by bending movements in response to wind and gravity. Trees with a strong potential to grow fast are genetically programmed to produce low-density woods, but at the same time they are pre-planned to decrease its microfibril angles in order to ensure stiffness and compensate (by increasing the specific modulus) the

weakness of its low-density. Genetic correlations between MFA and lignin increased with age showing that the decrease in these traits, usually attributed to the occurrence of reaction wood, are genetically controlled.

4.4.2 Genetic studies from the clonal tests

Growth traits

Growth traits of 6-year-old *Eucalyptus* trees are under low genetic control (H^2_C=0.17 and H^2_H=0.12) in this clonal test. There were significant differences between clones and sites for height and circumference of the trees. Taking into account only the growth traits, clones 4514, 4426, 4579 and 4588 are the best ones, presenting superior circumference at 1.3 meters and commercial height while clones 4535, 4494 and 4541 showed the worst performances for growth.

Genetic approaches from large wood pieces

Using the dynamic elastic estimates, significant differences were detected between clones for all traits. No significant differences between sites were detected for dynamic modulus of elasticity. There were significant effect of interaction clone x site for circumference, height, density and shear modulus.

Clones 4494, 4515, 4535, 4557 and 4609 presented the higher mean density values and the lower growth rates. On the other hand, clones 4426 and 4588 presented the lower densities, but their growth rates are high. In regards to the elastic modulus of scantlings, clone 4515 produced the stiffest woods while clones 4426 and 4579 produced the less rigid and more flexible woods (this clones presented the higher growth rates).

In short, the sonic resonance method rapidly provided a large accurate data set of mechanical wood properties as required for high-throughput phenotyping of genetic approaches. These results can be useful for initial classifications, screenings or preliminary selections in breeding programs of *Eucalyptus*. As reported by Burdzik and Nkwera (2002), this method proved to be fast, highly repeatable and does not require heavy equipment, making it the ideal method for on-site determining of modulus of elasticity at the sawmill.

Genetic control over wood traits

This study has established in which extend the radial and longitudinal variations in wood density; wood stiffness and MFA within trees are governed by genetic factors.

Low to moderate levels of broad-sense heritability estimates were found for basic density, wood stiffness and microfibril angle of 6-year-old *Eucalyptus* clones. For wood density, the longitudinal variations in H^2 estimates were more consistent than those in radial direction, especially in the highest parts of the stem. No clear trends of radial variation could be defined.

The findings show that genetic control over density and stiffness is larger in two regions of the stem: (i) in the inner heartwood region (0-25% of relative radial position) of the lower zones of the tree (10-30% of the relative longitudinal position) and (ii) at the top of the tree, a zone localized at 40-80% of relative radial position and at 70-90% of the relative longitudinal position. Again, no clear patterns of radial variation were established for H^2 estimates of E_L along the tree.

Genetic control over MFA exhibits variable patterns of variation. It was shown that H^2 of MFA is superior in the sapwood region (60-100% of relative radial position) of the lower zones of the tree (10-30% of the relative longitudinal position) and at the higher zones of the stem near to the cambium.

The results clearly reveal that heritability estimates for E_L and MFA exhibited opposite patterns of radial variation in the bottom of the tree, and similar trends towards the top. For density, higher H^2 estimates were found in the higher regions of the tree, especially at the intermediate zone.

NIR spectral heritability

This study shows that NIR spectra are able to capture the potential genetic of some chemical components and wood traits. Genetic parameters were obtained directly from NIR spectra. The bands normally associated with cellulosic or lignin type biomolecules may be observed in the near-infrared (NIR) spectra of wood. Thus, variations in specific ranges NIR spectra are related to variation in lignin and cellulose and hemicelluloses contents, and other wood traits. The findings clearly revealed that the variations on these specific ranges of the NIR spectra were controlled by genetic factors. The assignments of absorption bands were useful to identify which wood components presents higher broad-sense heritability estimates from NIR spectroscopic data. It helps to understanding how NIR spectroscopy can evaluate genetic control over wood traits.

Some ranges of the spectra presented heritability estimate greater than 50%. Considering NIR spectra is countless source of information concerning many wood traits, the analysis of genetic parameters from them appears to be an efficient and promising way to evaluate the genetic control over various wood traits at once.

Validity of these findings

As there are only 5 individuals per clone per site involved in the study of clonal tests, and only nine to ten individuals per family involved in the study of progeny tests presented here, these findings should be viewed with caution. Sampling is one of the most expensive steps of the genetic studies. As large samplings are, as accurate results are provided. Here, we could sample a limited number of individuals however it was possible to provide reliable indications of genetic control and genetic correlations. The similarity of the results from the two experimental designs, despite the data sets being so different in structure and representation, suggests that the results may be more generally applicable.

5 PERSPECTIVES

Wood and biomass are now regarded as renewable resources that can partially alleviate reliance on petrochemical for every day needs and at the same time sequester carbon from the atmosphere to reduce atmospheric CO_2 levels (Meder et al. 2010). The *Eucalyptus* plantations have successfully met the demand for raw material of quality required for the pulp and paper, and bioenergy industry. However, the performance in *Eucalyptus* wood as sawn-timber is usually not satisfactory. Selecting trees and improving wood traits seems to be a good strategy for overcoming deficiencies in timber. *Eucalyptus* breeding programs for wood quality may focus on the properties that cannot be manipulated during processing.

Here, we examined the genetic parameters of and correlations between growth traits, wood density, lignin content, wood stiffness and microfibril angle in wood samples from *Eucalyptus* plantations. The findings have shown that wood traits are under moderate to strong genetic control indicating that genetic improvement is possible through breeding. However, most wood properties were unfavorably genetically correlated with growth, although favorable genetic correlations were observed between many *Eucalyptus* wood traits. Because of these unfavorable genetic correlations between wood and growth, selection for increasing density and stiffness or reducing MFA in the absence of selection for growth will result in a reduction (genetic loss) in volume production. Breeders, forest managers and wood producers will have to strike a balance between overall wood and growth traits, and geneticists should develop breeding strategies to deal with such negative, unfavorable genetic correlations, as pointed out by Baltunis et al. (2007) for similar findings in *Pinus*. Indeed, slight reductions in growth may be of little consequence when considering the genetic gains in juvenile wood properties. However, there may be opportunities for selection of correlation breakers for both breeding and deployment, thus improving wood traits without adversely affecting growth traits in *Eucalyptus* plantations. Developing breeding objectives may be the first step in dealing with these unfavorable genetic correlations. If it is possible further understand the genetic basis of these negative genetic correlations using molecular tools (e.g., identifying pleiotropic alleles or genes associated with antagonistically correlated traits), more efficient breeding strategies may be developed to circumvent these antagonistic genetic correlations by crossing genotypes with a desirable suite of alleles.

6 ANNEXES

6.1 Phenotyping the air-dried scantlings of clonal tests

Table 45 lists the descriptive statistics of the density and dynamic properties of air-dried scantlings of *Eucalyptus* wood. Based on early studies on dynamic tests of wood (Hearmon 1961; Ilic 2001; Ilic 2003), we expected to find longitudinal elastic properties higher than the flexural ones. Surprisingly, the flexural elastic moduli were the highest for air-dried scantlings: since the *p*-value of the *t*-test was less than 0.01, there was a statistically significant difference between the mean $E_L$ad and $E_F$ad at the 99% confidence level. The environmental effect on the dynamic elastic modulus on longitudinal vibration test is not clear (Figure 48). Because the elastic properties greatly varied between clones, the standard deviations were high and there were no significant differences between sites according to Tukey test.

Table 45 - Descriptive statistics of dynamic properties of the air-scantlings of 6-year-old *Eucalyptus grandis* x *urophylla*, including air-dry density (ρad, kg m^{-3}), first resonant frequency ($f_1$ad, Hz), elastic modulus (Ead, MPa), specific modulus (E'ad, E/ρ), loss tangent (tg δad, 10^{-3}) and shear modulus (Gad, MPa) estimated by longitudinal ($_L$) and flexural ($_F$) vibration tests

	ρad	f_{1L}ad	$E_L$ad	E'_Lad	tg $\delta_L$ad	f_{1F}ad	$E_F$ad	E'_Fad	$G_F$ad
Mean	596	1,548	12,666	21.2	8.08	101.92	13,292	22.3	652.9
Sd	78	343	2,565	3.0	1.96	47.45	2,697	3.17	170.5
Min	416	984.7	7,237	14.3	2.71	44.1	6,200	12.8	199
Max	827	3,345	20,163	30.7	20.8	366	23,536	32.5	1,419
CV (%)	13.2	22.2	20.2	14.1	24.3	46.5	20.3	14.2	26.1
N	410	410	410	410	339	410	410	410	398

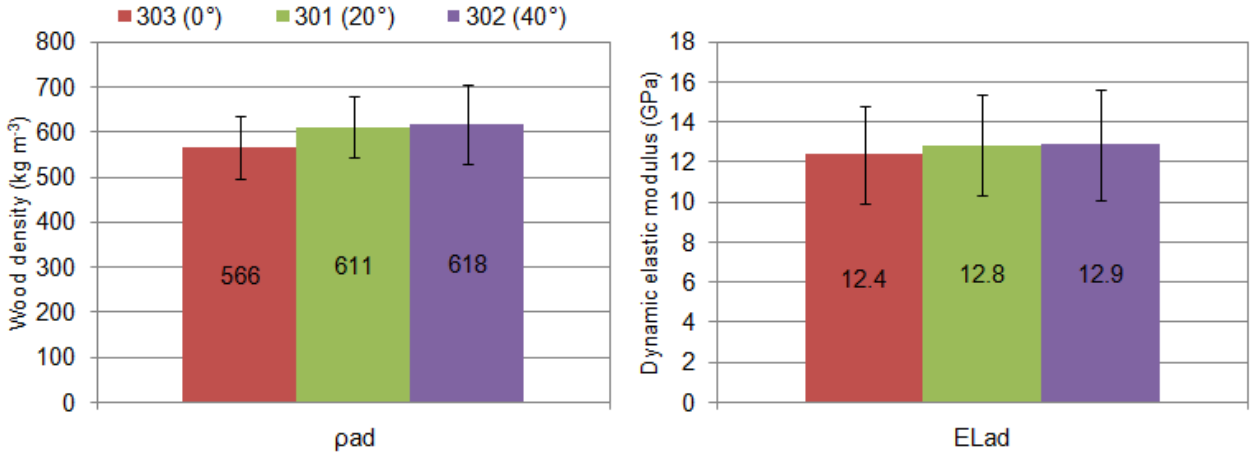

Figure 48 - Mean and standard deviation values of air-dried density and dynamic elastic modulus in air-dried scantlings for each site.

6.2 Correlations between wood traits of air- and kiln-dried scantlings

The correlations among the physical and elastic properties of 395 air-dried and kiln-dried scantlings are presented in Table 46. Correlations between air-dried (ad) and kiln-dried (14) were stronger for both longitudinal and flexural (r=0.99) tests.

Table 46 - Correlations among physical and elastic properties of 395 air-dried and 14% dried scantlings of 6-year-old *Eucalyptus grandis* x *urophylla* wood. The significance level for all relationships was <0.0001

	ρad	ρ14	$E_L$ad	$E_F$ad	E_L14
ρ14	0.91	1			
$E_L$ad	0.72	0.78	1		
$E_F$ad	0.70	0.74	0.94	1	
E_L14	0.71	0.80	0.99	0.94	1
E_F14	0.69	0.76	0.91	0.99	0.91

The moisture content of the air-dried scantlings ranged from 14 to 26% but this variation was not high enough to highlight the moisture content effect on these elastic properties. Hence, it appears that short variation in moisture content did not significantly influence the ability of the dynamic tests to estimate the elastic properties of the unseasoned or seasoned wood beams. Accordingly, further studies are required to show the influence of moisture content of wood on dynamic tests.

The correlation between the modulus of elasticity of the kiln-dried (E_L14) and air-dried ($E_L$ad) scantlings in the flexural test for the all samples (411 scantlings) is detailed in Figure 49 where the fitted linear regression explained 95.4% of the variability in E_L14. The standard deviation of the residuals was 546.5 MPa (Figure 49).

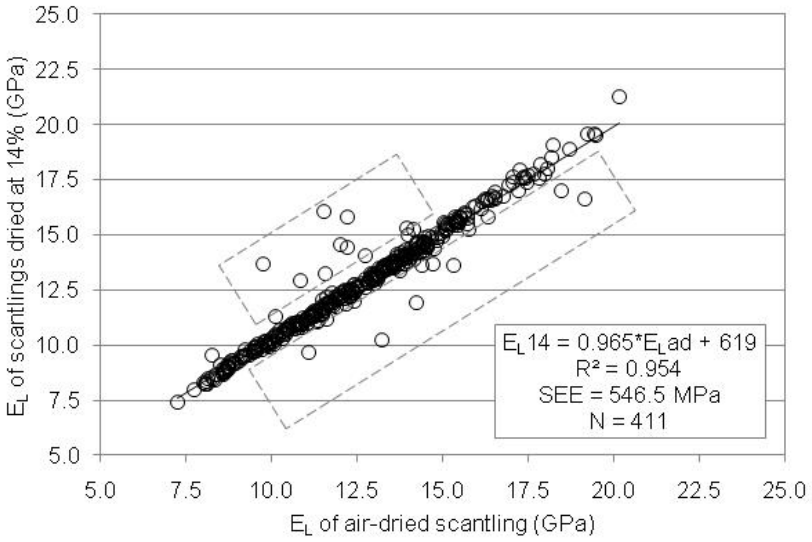

Figure 49 - Correlation between the modulus of elasticity of the kiln- (E_L14) and air-dried ($E_L$ad) scantlings obtained in the flexural test for 411 scantlings of *Eucalyptus* showing the samples presenting problems after drying

After kiln-drying process, fifteen (15) scantlings (3.6% of total sampling) presented small cracks. These defects had a negative effect on the vibration test, notably changing the natural frequency and the Young modulus of the scantling. Hence, we considered them as outliers and they were not included in the calculation of correlations presented in Table 46. Figure 50 shows an even stronger correlation between the modulus of elasticity of the kiln-dried (E_L14) and air-dried (E_Lad) scantlings in the longitudinal test without the 15 outliers (395 scantlings).

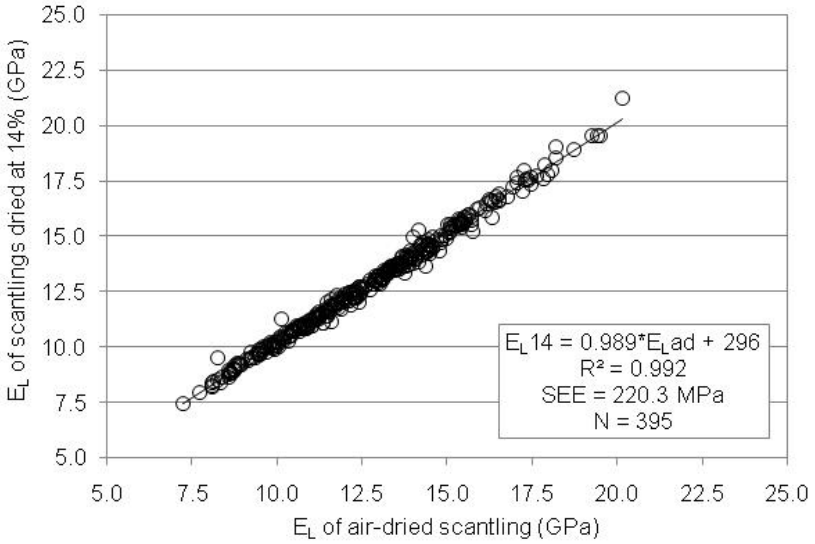

Figure 50 - Correlation between the modulus of elasticity of the kiln- (E_L14) and air-dried (E_Lad) scantlings obtained in the flexural test for 395 scantlings of *Eucalyptus grandis* x *urophylla* wood with 45 mm x 60 mm cross section

From air- and kiln-dried condition, the scantlings lost around 84 litres of water that corresponded to 8.3% of the total mass (1,013 kg). Considering the high coefficients of determination between these two conditions, these findings indicate that when analyzing elastic properties by means of this resonance method, there is no need to dry the wood pieces in a kiln, which can be expensive, apart from the need to own it. This is a very useful finding for those who need to evaluate their wood samples without owning a wood kiln for large pieces.

It is well know that values of the modulus of elasticity increased with increasing wood density (Kollmann and Côté 1968). According to the Table 46, the density of the kiln-dried scantlings showed good correlation (from 0.74 to 0.80) with their elastic properties. The E_L presented higher correlations with density than the E_F, both for air- and kiln-dried scantlings (Table 46). The main raison for this trend is the lower uncertainty of measurement for longitudinal test.

The correlations (not shown) between air- and kiln-dried values were strong for shear modulus (0.73). The correlation between loss tangent on air- and kiln-dried scantling was weak, but statistically significant (0.47). The modulus of shear and loss tangent had no correlation with elasticity, nor density. Ilic (2001) also did not find statistically significant correlations among these properties.

In the present study, scantlings of different lengths were used. At the outset, we think that this condition would be a limitation, but the tightness of the correlations confirms that the resonance technique is suitable for characterizing wood of any dimensions, with high accuracy and repeatability.

6.3 Environmental and radial position effect on MFA and its correlation with wood traits

The environmental and position effect on correlations among *Eucalyptus* wood traits are listed in Table 47. Taking into account the samples taken from central position (near to the pith), all correlations were higher than those calculated with the samples from external position. For correlation involving MFA, the differences between samples from central or external positions were even stronger.

The ρ x E correlations were significant, presenting weak variation according to the sites ($0.81<r<0.86$) or positions ($0.79<r<0.86$) where the samples came from. These results indicate that these traits are not much sensitive to variations in environmental conditions or sampling positions. In other words, the stiffness will be always correlated to the quantity of mass (its density), independently of the sites where the trees were planted or the age at which was considered, at least for these *Eucalyptus* trees. However, for the correlations MFA x ρ and MFA x E, the coefficients increased as the terrain slope increased, and such correlations varied strongly according to the position.

Table 47 - Correlations among *Eucalyptus* wood traits by site and by radial position. All correlations were statistically significant at $p<0.01$

correlations	Site effect			Position effect	
	A (0°)	B (20°)	C (40°)	Central	External
MFA x ρ	-0.35	-0.37	-0.51	-0.52	-0.24
MFA x E	-0.58	-0.65	-0.67	-0.76	-0.49
MFA x E/ρ	-0.68	-0.76	-0.67	-0.82	-0.55
MFA x MOR	-0.53	-0.43	-0.53	-0.68	-0.31
ρ x E	0.86	0.81	0.85	0.86	0.79
ρ x MOR	0.66	0.85	0.62	0.74	0.67
E x MOR	0.83	0.87	0.77	0.86	0.76
ρ/MFA x E	0.85	0.87	0.82	0.92	0.78
ρ/MFA x MOR	0.69	0.70	0.56	0.78	0.57

The lower correlations for the samples from external regions can be explained by the possible occurrence of growth stresses, tension wood and grain angle, which are more evident on stem periphery. This indicates that these traits were somewhat correlated when the trees were young, indicating that trees adapt both their stiffness and MFA of their juvenile wood to respond to the specific needs of the young stems, at least, from a phenotypic point of view. However, these relatively close correlations tend to decrease, or disappear, over the years. When the wood reaches certain degree of maturity, variations of other factors (such as density and lignin content) begin to determine its mechanical properties beyond the microfibril angle. These findings outlined the influence of MFA on *Eucalyptus* wood quality. If trees are planted in drastic conditions (sloped areas) or if they are subjected to changing environmental conditions (winds, storms), the trees start developing complementary mechanisms to adapt themselves to the new situation.

In this study, the main difference between sites was the terrain slope, and the results demonstrated that the variation in correlations among traits was stronger for position (age) than for sites (Table 47). In short, specimens taken from central position presented traits and correlations among traits different than those taken from external position. Perhaps, the genetic effects are stronger than the environmental ones in the inner wood. These issues were discussed within the genetic studies section (pg. 109).

6.4 Comparing 3- and 4-points bending tests

After dynamic tests, the wood specimens were tested using a universal testing machine. The modulus of rupture (MOR) of the twin specimens were obtained from three and four points bending tests. Figure 51 shows the correlations between the dynamic flexural elastic modulus and the MOR obtained by tree and four points bending tests for wood samples of *Eucalyptus urophylla* x *grandis* clones.

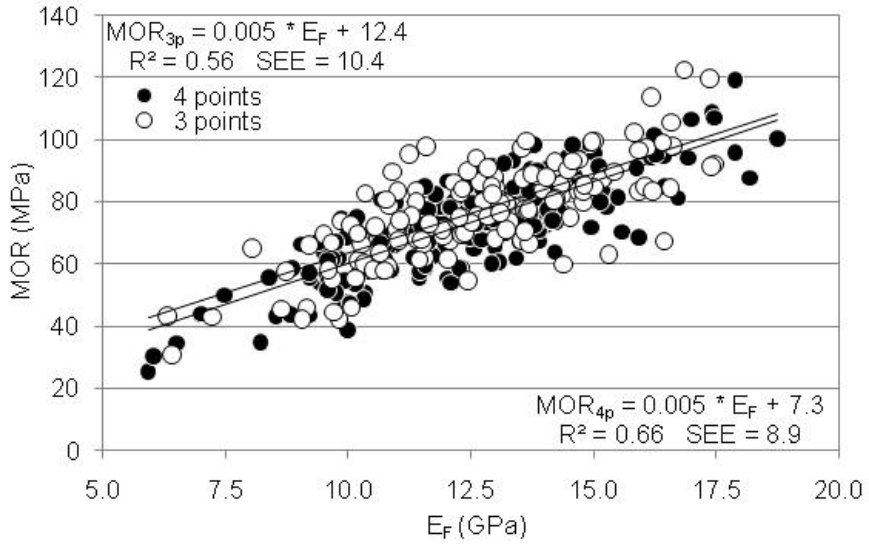

Figure 51 - Linear regression plot between the dynamic flexural elastic modulus and the MOR obtained by tree and four points bending tests using complete sampling of *Eucalyptus* wood. SEE is the standard error of estimation

The correlation between MOR and E_F was higher for four points bending test, while the correlation between MOR and wood density was higher for three points bending test. Two hundred twenty-four (224) samples were considered for correlations concerning MOR_{4p} and 137 specimens were used for three points bending tests. Figure 52 shows the correlations between the wood density and the MOR obtained by tree and four points bending tests for wood samples of *Eucalyptus urophylla* x *grandis* clones.

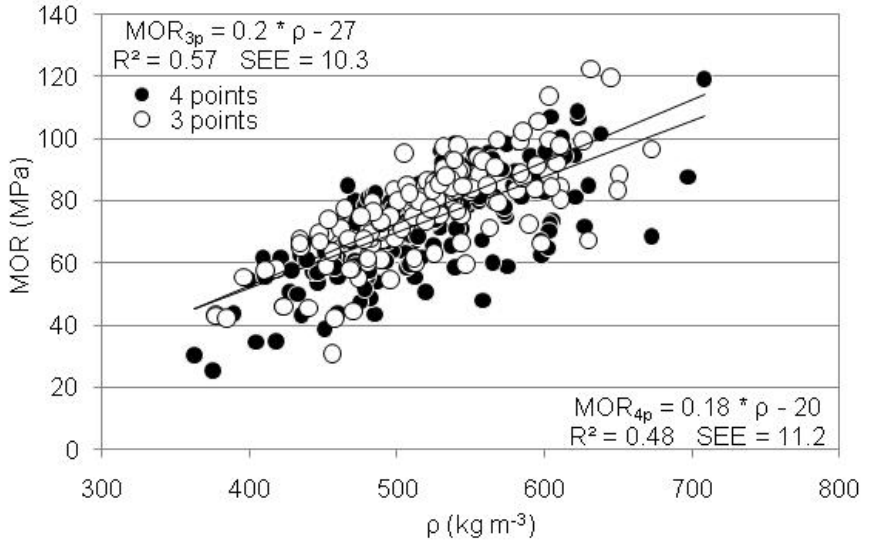

Figure 52 - Linear regression plot between the wood density and the MOR obtained by tree and four points bending tests using complete sampling of *Eucalyptus* wood. SEE is the standard error of estimation

Brancheriau et al. (2002) have compared 3- and 4-point bending tests concerning the longitudinal modulus of elasticity and proposed a crossing analytic formula from a 3-point bending modulus of elasticity to a 4-point bending one, verified by the experimentation. In the present study, an analytic formula for MOR from a 3- to 4-points bending test is proposed: $MOR_{4p}=0.885*MOR_{3p} + 5.38$. Figure 53 exhibit the correlation between the modulus of rupture obtained by 3- and 4-points bending tests using twin specimens of *Eucalyptus* wood. As the more commonly methods used for determining the MOE and MOR are the 3- and 4-point bending tests, these findings can be useful when comparing data obtained by different test methods. According to Brancheriau et al. (2002), the analytical study and the experiences have shown that the supports and loading head indentation effect are not negligible but have the same influence as the shear effect. The indentation is the result of the competition between two physical phenomena which are the wood stiffness and the load level applied on the piece of wood during a bending test.

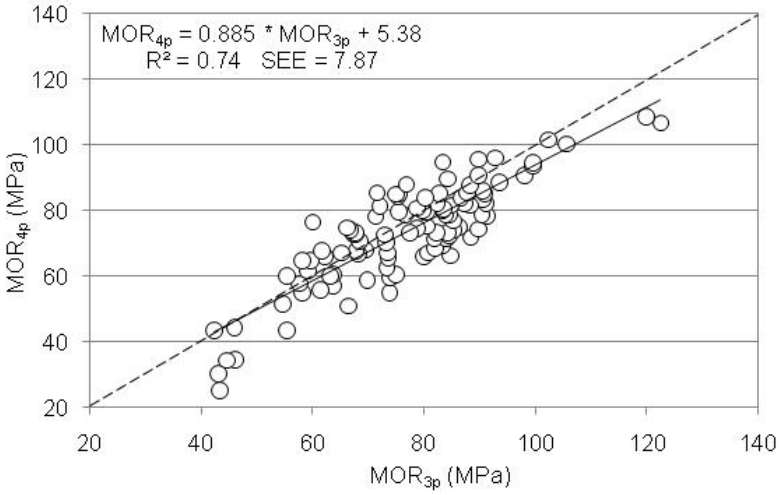

Figure 53 - Linear regression plot between the MOR obtained by tree and four points bending tests. SEE is the standard error of estimation

6.5 Genetic studies from resonance on air-dried scantlings

Table 48 presents the analysis of variance for air-dried density (ρad), elastic modulus (E), loss tangent (tg δ) and modulus of shear (G) in air-dried scantlings of the *Eucalyptus* clones from Brazilian plantations. Significant differences between clones were detected for all traits. There were significant differences between clones for all traits, but only for air-dried density and modulus of shear there were significant differences between sites and clones. No significant differences between sites were detected for dynamic modulus of elasticity.

Table 48 - Analysis of variance for density and dynamic traits in air-dried scantlings of 6-year-old *Eucalyptus urophylla* x *grandis* clones

	ρad	$E_L$ad	tg δad	$E_F$ad	Gad
Clone	p<0.0001	p<0.0001	p<0.01	p<0.0001	p<0.0001
Site	p<0.0001	ns	p<0.03	ns	p<0.0001
interaction	p<0.0011	ns	ns	ns	p<0.04
R^2	0.34	0.20	0.13	0.20	0.20

(* significant at 0.05; ** at 0.01 and *** at 0.001, ns: non-significant)

Table 49 lists the classification of clones and sites for density and dynamic traits of air-dried scantlings. Similarly to Table 33, clones 4494, 4515, 4535, 4557 and 4609 presented the higher mean densities while clones 4426 and 4588 presented the lower densities. For elastic properties, the Tukey (HSD) multiple range tests of air-dried scantlings (Table 49) was less selective than those for kiln-dried scantlings (Table 33). Again, clones 4515 and 4557 produced the stiffest wood samples while clones 4426 and 4579 produced the less stiff ones. Trees growing up on sites 301 and 302 produce the denser woods.

Table 49 - Tukey (HSD) multiple range tests for density and dynamic traits by clone and by site in air-dried scantlings of 6-year-old *Eucalyptus urophylla* x *grandis* clones

Clone	ρad (kg m^{-3})	$E_L$ad (MPa)	tgδad (10^3)	$E_F$ad (MPa)	Gad (MPa)
4426	545.1^{E}	$11{,}100^{D}$	8.28^{AB}	$11{,}650^{D}$	565.4^{C}
4494	614.7^{ABC}	$13{,}493^{ABC}$	8.21^{AB}	$14{,}277^{ABC}$	611.0^{BC}
4514	596.7^{BCD}	$12{,}758^{ABCD}$	8.08^{AB}	$13{,}433^{ABCD}$	660.3^{ABC}
4515	614.8^{ABCD}	$13{,}938^{A}$	7.89^{AB}	$14{,}482^{AB}$	695.8^{ABC}
4535	632.6^{A}	$13{,}646^{AB}$	6.78^{B}	$14{,}259^{ABC}$	731.3^{A}
4541	570.5^{CDE}	$11{,}863^{CD}$	8.17^{AB}	$12{,}556^{CD}$	707.2^{AB}
4557	638.8^{A}	$13{,}836^{AB}$	8.67^{A}	$14{,}576^{A}$	625.4^{ABC}
4579	582.3^{BCDE}	$11{,}597^{D}$	8.87^{A}	$12{,}284^{D}$	664.5^{ABC}
4588	549.7^{DE}	$12{,}191^{BCD}$	7.91^{AB}	$12{,}687^{BCD}$	628.3^{ABC}
4609	629.0^{AB}	$12{,}570^{ABCD}$	7.69^{AB}	$13{,}069^{ABCD}$	670.9^{ABC}
Site	ρad (kg m^{-3})	$E_L$ad (MPa)	tgδad (10^3)	$E_F$ad (MPa)	Gad (MPa)
301	610.5^{A}	$12{,}846^{A}$	7.92^{B}	$13{,}688^{A}$	661.4^{A}
302	617.8^{A}	$12{,}864^{A}$	8.63^{A}	$13{,}322^{AB}$	704.9^{A}
303	566.3^{B}	$12{,}394^{A}$	7.82^{B}	$12{,}952^{B}$	607.0^{B}

Means with the same letter are not significantly different at α = 0.05 threshold, using Tukey multiple range tests

The findings obtained from air-dried scantlings (Table 49) and kiln-dried scantlings (Table 33, pg. 108) were basically the same, confirming the repeatability and reliability of the resonance technique as a tool for rapid and low-cost screening technique. Similarly to the Table 49, trees growing up on sites 301 and 302 produce the denser woods and there were no significant differences among sites for modulus of elasticity.

These findings clearly demonstrated that resonance technique is able to simply, rapidly and at such low cost characterize the mechanical properties of wood. The resonance technique permit to rapidly estimate key mechanical properties (such as the modulus of elasticity, the shear modulus and the loss tangent) of the wood even in lumber containing knots, small cracks and also slightly damaged areas. In short, the BING system rapidly provided a large accurate data set of mechanical wood properties as required for high-throughput phenotyping of genetic approaches. These results can be useful for initial classifications, screenings or preliminary selections in breeding programs of *Eucalyptus*. As reported by Burdzik and Nkwera (2002), this method proved to be fast, highly repeatable and does not require heavy equipment, making it the ideal method for on-site determining of MOE at the sawmill.

6.6 Spatial variation of heritability estimates

From the NIR-estimated dataset, the genetic (σ^2_G) and residual (σ^2_E) variance components were estimated by Restricted Maximum Likelihood (REML) method. Thus, broad-sense heritability estimates (H^2) for growth traits and basic density of wood, elastic modulus and microfibril angle at various relative heights and radial positions were calculated. For wood traits, the estimates from the model without GxE interaction (Eq. 38) were similar than those from models with interaction (Figure 45 at pg. 119). Here, the heritability estimates of wood traits were calculated without the variance due to interaction effects.

The patterns spatial variation in the genetic control over basic density, wood stiffness and microfibril angle within the *Eucalyptus* trees are represented in Figure 54. The coefficient of phenotypic variation, the genetic, residual and interaction variance components and broad-sense heritability estimates (Eq. 38, without GxE interaction) for basic density, wood stiffness and microfibril angle at various relative heights and radial positions are listed in following Tables.

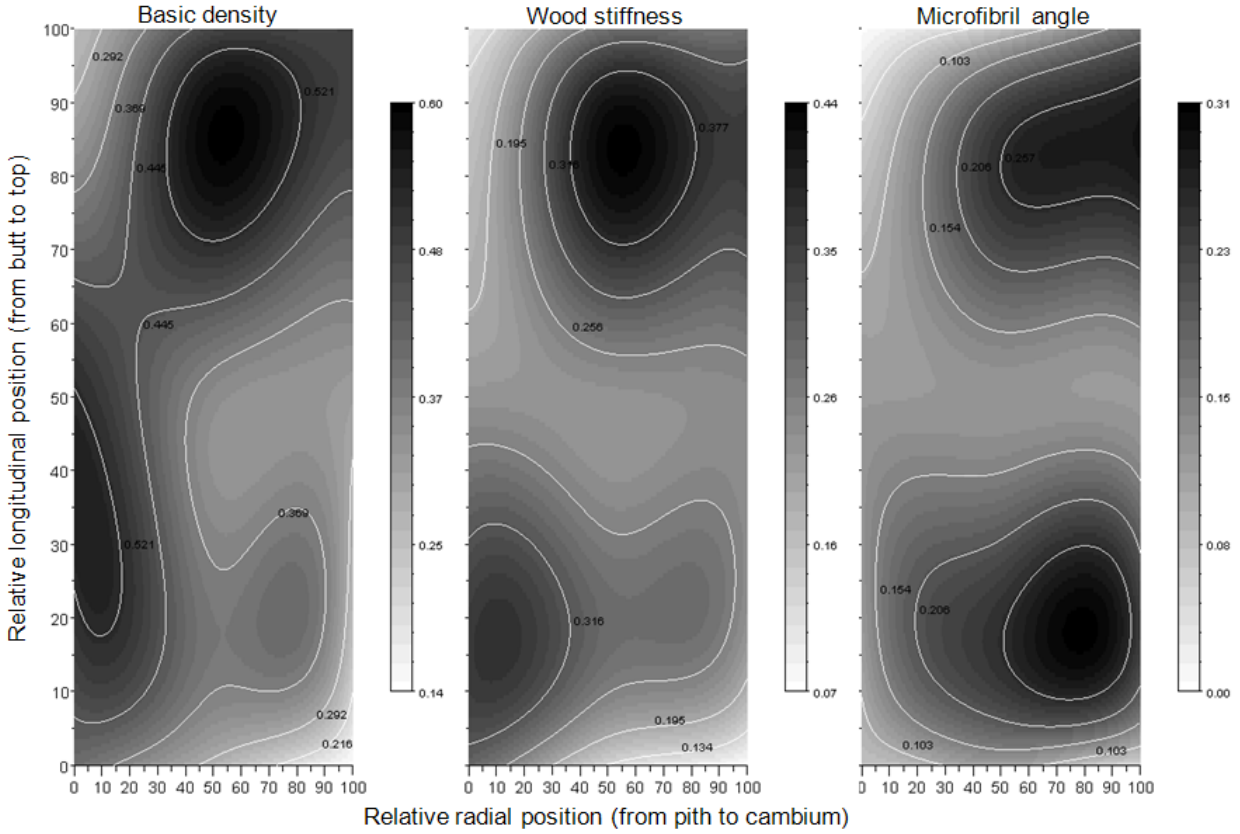

Figure 54 - Spatial variation of heritability estimates over basic density of wood, wood stiffness and microfibril angle within *Eucalyptus* trees (model $y = \mu + G + E$)

Table 50 - Genetic parameters for basic density of the wood in 6-year-old *Eucalyptus urophylla* x *grandis* clones (model $y = \mu + G + E$)

Height	radial position	CV (%)	σ^2_G	σ^2_E	H^2	SE H^2
100%	inner HW[14]	12.5	21.03	35.37	0.261	0.105
	outer HW[15]	11.9	27.75	29.65	0.467	0.135
	SW[16]	10.8	26.04	27.11	0.480	0.129
75%	inner HW[11]	12.8	27.83	35.02	0.387	0.122
	outer HW[12]	10.8	28.80	25.94	0.552	0.139
	SW[13]	10.3	25.83	29.65	0.431	0.121
50%	inner HW[8]	10.8	29.19	27.78	0.525	0.129
	outer HW[9]	9.7	24.66	33.75	0.348	0.111
	SW[10]	12.2	24.52	36.45	0.312	0.118
25%	inner HW[3]	11.2	24.84	23.64	0.525	0.135
	middle HW[4]	8.8	23.04	23.73	0.485	0.135
	outer HW[5]	11.3	29.41	37.95	0.375	0.126
	inner SW[6]	11.3	28.65	34.80	0.404	0.134
	outer SW[7]	12.6	25.43	41.78	0.270	0.112
0%	inner HW[0]	10.2	26.73	32.39	0.405	0.140
	outer HW[1]	12.7	34.45	55.33	0.279	0.104
	SW[2]	11.7	16.86	41.77	0.140	0.080

Table 51 - Genetic parameters for dynamic longitudinal modulus of elasticity of the wood in 6-year-old *Eucalyptus urophylla* x *grandis* clones (model $y = \mu + G + E$)

Height	radial position	CV (%)	σ^2_G	σ^2_E	H^2	SE H^2
100%	inner HW[14]	19.3	694.5	1984.3	0.109	0.069
	outer HW[15]	17.1	1051.7	1711.0	0.274	0.113
	SW[16]	15.4	1029.5	1664.5	0.277	0.122
75%	inner HW[11]	17.3	809.5	1750.2	0.176	0.099
	outer HW[12]	13.1	1052.8	1278.2	0.404	0.130
	SW[13]	15.0	1232.3	1714.2	0.341	0.111
50%	inner HW[8]	15.1	772.6	1431.6	0.226	0.100
	outer HW[9]	12.5	817.0	1508.2	0.227	0.106
	SW[10]	13.1	1009.3	1798.8	0.239	0.092
25%	inner HW[3]	16.5	940.4	1314.6	0.339	0.115
	middle HW[4]	15.7	1010.0	1427.8	0.334	0.117
	outer HW[5]	14.0	1008.3	1626.7	0.278	0.101
	inner SW[6]	12.5	1042.7	1658.3	0.283	0.110
	outer SW[7]	14.4	1142.7	2052.7	0.237	0.099
0%	inner HW[0]	27.0	1061.9	1645.7	0.294	0.113
	outer HW[1]	21.8	885.0	2258.9	0.133	0.079
	SW[2]	16.0	592.2	2103.0	0.073	0.051

Table 52 - Genetic parameters for microfibril angle of cell wall of wood in 6-year-old *Eucalyptus urophylla* x *grandis* clones (model $y = \mu + G + E$)

Height	radial position	CV (%)	σ^2_G	σ^2_E	H^2	SE H^2
100%	inner HW[14]	9.5	0.000	1.217	0.000	0.000
	outer HW[15]	8.4	0.264	0.971	0.069	0.060
	SW[16]	9.4	0.418	0.902	0.177	0.091
75%	inner HW[11]	7.8	0.285	0.927	0.087	0.057
	outer HW[12]	8.7	0.433	0.763	0.244	0.103
	SW[13]	12.7	0.578	0.988	0.255	0.100
50%	inner HW[8]	7.7	0.337	0.899	0.123	0.075
	outer HW[9]	8.2	0.294	0.771	0.127	0.080
	SW[10]	12.2	0.353	0.944	0.123	0.081
25%	inner HW[3]	7.6	0.341	0.895	0.127	0.072
	middle HW[4]	8.5	0.438	0.853	0.209	0.097
	outer HW[5]	10.3	0.493	0.890	0.235	0.102
	inner SW[6]	11.2	0.525	0.828	0.286	0.107
	outer SW[7]	14.0	0.520	0.973	0.222	0.103
0%	inner HW[0]	8.7	0.309	1.088	0.075	0.050
	outer HW[1]	12.3	0.456	1.242	0.119	0.082
	SW[2]	11.0	0.232	0.992	0.052	0.044

It is important to note that in the base of stem it is possible to compare genetic effects on wood developed at the first, third and sixth year of development. Then, the temporal difference between each H^2 estimate at the base of the stem is approximately of two years whereas the three H^2 estimates of the top of the tree refer to wood developed at the same year differing only some months.

In short, Figure 54 clearly reveals that heritability estimates for D and E_L exhibited similar patterns of radial variation in the bottom of the tree, and similar trends towards the top. MFA shows opposite trends of spatial variation (mirror effect at radial direction). For density and stiffness, higher H^2 estimates were found in the higher regions of the tree, especially at the intermediate zone (dark spot at the top of the chart).

7 REFERENCES

1. ABRAF (2010) Associação Brasileira de Produtores de Florestas Plantadas. Statistical Yearbook – Base Year 2009/ ABRAF - Brasília, 127p.
2. Alencar GSB, Barrichelo LEG and Júnior FGSJ (2002) Qualidade da madeira de híbrido de *E. grandis* x *E. urophylla* e seleção precoce. 35° congresso e exposição anual de celulose e papel. Outubro, 2002. São Paulo. Disponível em: http://www.celuloseonline.com.br/imagembank/Docs/DocBank/dc/dc054.pdf
3. Alméras T and Fournier M (2009) Biomechanical design and long-term stability of trees: morphological and wood traits involved in the balance between weight increase and the gravitropic reaction. Journal of Theoretical Biology 256: 370-381
4. Andersson S, Serimaa R, Torkkeli M, Paakkari T, Saranpfifi P and Pesonen E (2000) Microfibril angle of Norway spruce [*Picea abies* (L.) Karst.] compression wood: comparison of measuring techniques. Journal of Wood Science 46: 343-349
5. Apiolaza LA and Garrick DJ (2001) Breeding objectives for three silvicultural regimes of radiata pine. Canadian Journal of Forest Research 31: 654-662
6. Apiolaza LA, Raymond CA and Yeo BJ (2005) Genetic variation of physical and chemical wood properties of *Eucalyptus globulus*. Silvae Genetica 54: 160-166
7. Apiolaza LA. (2009) Very early selection for solid wood quality: screening for early winners. Annals of Forest Science 66: 601
8. Aramaki M, Baillères H, Brancheriau L, Kronland-Martinet R and Ystad S (2007) Sound quality assessment of wood for xylophone bars. J Acoust Soc Am 121 (4): 2407-2420
9. Arango B and Tamayo L (2008) Densidad de la madera en clones de *Eucalyptus* por densitometría de rayos X. Revista Facultad de Ingeniería Universidad de Antioquia 45: 87-99
10. Archer RR (1986) Growth stresses and strains in trees. Springer-Verlag, Berlin. 240p.
11. ASTM - American Society for Testing and Materials (2007) D 143-94 - Standard test methods for small, clear specimens of timber. 32 p. West Conshohocken, PA, USA
12. ASTM - American Standards and Testing Methods (2002) D2395-02 - Standard test methods for specific gravity of wood and wood-based materials, West Conshohocken, PA, USA
13. Baillères H, Chanson B, Fournier M, Tollier MT and Monties B (1995) Structure, composition chimique et retraits de maturation du bois chez les clones *d'Eucalyptus*. Annals of Science Forest 52, 157-172
14. Baillères H, Davrieux F, Ham-Pichavant F. (2002) Near infrared analysis as a tool for rapid screening of some major wood characteristics in a *Eucalyptus* breeding program. Annals of Forest Science 59: 479-490
15. Balturis BS, Wu HX and Powell MB (2007) Inheritance of density, microfibril angle, and modulus of elasticity in juvenile wood of *Pinus radiata* at two locations in Australia. Canadian Journal of Forest Research 37: 3164-2174
16. Bamber RK, Horne R and Graham-Higgs A (1982) Effect of fast growth on the wood properties of *Eucalyptus grandis*. Australian Forestry Research 12(2): 163-167
17. Barnett JR and Bonham VA (2004) Cellulose microfibril angle in the cell wall of wood fibres. Biol. Rev. 79: 461-472
18. Bergander A, Brändström J, Daniel G and Salmén L (2002) Fibril angle variability in earlywood of Norway spruce using soft rot cavities and polarisation confocal microscopy. J. Wood Sci. 48: 255-263
19. Biblis EJ and Carino HF (1999) Flexural properties of lumber from a 50-year-old loblolly pine plantation. Wood and Fiber Science 31(2): 200-203
20. Biblis EJ, Meldahl R and Pitt D (2004) Predicting flexural properties of dimension lumber from 40-year-old loblolly pine plantation stands. Forest Products Journal 54: 109-113

21. Binkley D and Stape JL (2004) Sustainable management of eucalyptus plantations in a changing world. In Borralho et al. (2004) *Eucalyptus* in a Changing World. Proc. of IUFRO Conf., Aveiro 11-15 October 2004.

22. Birkett MD and Gambino MJT (1989) Estimation of pulp kappa number with near infrared spectroscopy. Tappi Journal 9(72): 193-197

23. Bokobza L (1998) Near infrared spectroscopy. Journal of Near Infrared Spectroscopy 6(1): 3-17

24. Bordonné PA (1989) Module Dynamique et Frottement Inte´rieur dans le Bois, Mesures sur Poutres Flottantes en Vibrations Naturelles. Institut National Polytechnique de Lorraine: 109

25. Bouvet JM, Bouillet JP, Vigneron P and Ognouabi N (1999) Genetic and environmental effects on growth and wood basic density with two Eucalyptus hybrids. In: 09/99. Connexion Between Silviculture and Wood Quality through Modelling Approaches and Simulation Softwares, La Londe les Maures, 05 au 12. s.l.: s.n., 2 p. Workshop on Connexion Between Silviculture and Wood Quality Through Modelling Approaches and Simulation Softwares. 3, 1999-09-05/1999-09-12, La Londe-Les Maures, France.

26. Bouvet JM, Saya A and Vigneron P (2009) Trends in additive, dominance and environmental effects with age for growth traits in Eucalyptus hybrid populations. Euphytica 165: 35-54

27. Bouvet JM, Vigneron P, Gouma R and Saya A (2003) Trends in Variances and Heritabilities with Age for Growth Traits in Eucalyptus Spacing Experiments. Silvae Genetica 52: 3-4

28. Boyd JD (1950) Tree growth stresses. I Growth stress evaluation. Australian Journal of Scientific Research B (Biological Sciences) 3: 270-293.

29. Brancheriau L and Baillères H (2002) Natural vibration analysis of clear wooden beams: a theoretical review. Wood Science and Technology 36: 347-365

30. Brancheriau L and Baillères H (2003) Use of the partial least squares method with acoustic vibration spectra as a new grading technique for structural timber. Holzforschung 57(6): 644-652

31. Brancheriau L, Baillères H and Guitard D (2002). Comparison between modulus of elasticity values calculated using 3 and 4 point bending tests on wooden samples. Wood Science and Technology 36: 367-383

32. Brancheriau L, Kouchade C and Brémaud I (2010) Internal friction measurement of tropical species by various acoustic methods. Journal of Wood Science 56(5): 371-379

33. Brémaud I, Gril J and Thibaut B (2011) Anisotropy of wood vibrational properties: dependence on grain angle and review of literature data. Wood Science and Technology. on line first

34. Brito JO and Barrichelo LEG (1977) Correlações entre características físicas e químicas da madeira e a produção de carvão vegetal: I. densidade e teor de lignina da madeira de eucalipto. IPEF 14: 9-20

35. Bucur V (1995) Acoustics of wood. Boca Raton: CRC Press. 284p.

36. Bucur V (2003) Non-destructive characterization and imaging of wood. Springer Series in Wood Science, pp. 181-214.

37. Burdzik WMG and Nkwera PD (2002) Transverse vibration tests for prediction of stiffness and strength properties of full size *Eucalyptus grandis*. Forest Products Journal 52 (6): 63-67

38. Burgert I and Fratzl P (2009) Plants control the properties and actuation of their organs through the orientation of cellulose fibrils in their cell walls. Integrative and Comparative Biology 1–11

39. Burnham KP and Anderson DR (2004) Multimodel inference: Understanding AIC and BIC in model selection. Sociological Methods and Research 33(2): 261-304

40. Burns DA and Ciurczak EW (2008) Handbook of Near-Infrared Analysis, Third Ed., Marcel Dekker, New York

41. Carvalho AM and Nahuz MAR (2001) Valorização da madeira do híbrido *Eucalyptus grandis* x *urophylla* através da produção conjunta de madeira serrada em pequenas dimensões, celulose e lenha. Scientia Forestalis 59: 61-76

42. Cave ID (1966) Theory of X-ray measurement of microfibril angle in wood. Forest Products Journal 16(10): 37-42

43. Cave ID (1968) The anisotropic elasticity of the plant cell wall. Wood Science and Technology 2(44): 268-278

44. Chaffey I (2000) Microfibril orientation in wood cells: new angles on an old topic. Trends Plant Science 5: 360-362

45. Chang HM and Sarkanen KV (1973) Species variation in lignin: Effects of species on the rate of kraft delignification. Tappi Journal 56: 132-143

46. Chantre G and Rozenberg P (1997) Can drill resistance profiles (Resistograph) lead to within-profile and within-ring density parameters in Douglas fir wood? In: Timber management toward wood quality and end-product values. CTIA/IUFRO International Wood Quality Workshop, p 41-47. 1997.

47. Chen G, Yu Q and Sjöström K (1997) Reactivity of char from pyrolysis of birch wood. Journal of analytical and applied pyrolysis, 40(41): 491-499

48. Cilas C, Godin C, Bertrand B and Baillères H. (2006) Genetic study on the physical properties of *Coffea arabica* L. wood. Trees 20: 587-592

49. Clair B, Alméras T, Yamamoto H, Okuyama T and Sugiyama J (2006) Mechanical behaviour of cellulose microfibrils in tension wood, in relation with maturation stress generation. Biophys. Journal 91: 1128-1135

50. Cogdill RP, Schimleck LR, Jones PD, Peter GF, Daniels RF and Clark A (2004) Estimation of the physical wood properties of *Pinus taeda* L. radial strips using least square support vector machines. Journal of Near Infrared Spectroscopy 12: 263-269

51. Costa e Silva J, Borralho NMG, Araujo JA, Vaillancourt RE and Potts BM (2009) Genetic parameters for growth, wood density and pulp yield in *Eucalyptus globulus*. Tree Genetics and Genomes 5(2): 291-305

52. Costa e Silva J, Hardner C and Potts BM (2004) Genetic variation and parental performance under inbreeding for growth in *Eucalyptus globulus*. Annals of Forest Science 67(6)

53. Costello LR and Quarles SL (1999) Detection of wood decay in blue gum and elm: an evaluation of the Resistograph® and the Portable Drill. Journal of Arboriculture 25 (6): 311-318

54. Cown DJ and Clement BC (1983) A wood densitometer using direct scanning with X-rays. Wood Science and Technology 17: 91-99.

55. Cown DJ, Ball RD and Riddell MJC (2004) Wood density and microfibril angle in 10 *Pinus radiata* clones: Distribution and influence on product performance. New Zealand Journal of Forest Science 34: 293-315

56. Cruz CR (2006) Aplicação de ondas de tensão para a estimativa da umidade em madeira de *Eucalyptus*. Tese (Doutorado em Ciências Florestais) - Universidade Federal do Paraná, Curitiba. 72 p.

57. Decoux V, Varcin E and Leban JM (2004) Relationships between the intra-ring wood density assessed by X-ray densitometry and optical anatomical measurements in conifers. Consequences for the cell wall apparent density determination, Annals of Forest Science 61: 251-262

58. Deflorio G, Fink S, and Schwarze FWMR (2008) Detection of incipient decay in tree stems with sonic tomography after wounding and fungal inoculation. Wood Science and Technology 42: 117-132

59. Dence CW (1992) The determination of lignin. In: Methods in Lignin Chemistry. Eds. Lin, S.Y., Dence, C.W. Springer-Verlag, Berlin. pp.33-61

60. Donaldson L (1993) Variation in microfibril angle among three genetic groups of *Pinus radiate* trees. New Zealand Journal of Forest Science 23: 90-100

61. Donaldson L (2008) Microfibril angle: measurement, variation and relationships - a review. IAWA Journal 29(4): 345-386

62. Donaldson L and Xu P (2005) Microfibril orientation across the secondary cell wall of Radiata pine tracheids. Trees 19: 644-653

63. Dungey HS, Matheson AC, Kain D and Evans R (2006) Genetics of wood stiffness and its component traits in *Pinus radiata*. Canadian Journal of Forest Research 36: 1165-1178

64. Dutilleul P, Herman M, Avella-Shaw T (1998) Growth rate effects on correlations among ring width, wood density and mean tracheid length in Norway spruce (*Picea abies*). Canadian Journal of Forestry Research 28: 56-68

65. Easty DB, Berben SA, Dethomas FA, Brimmer PJ (1990) Near-infrared Spectroscopy for the analysis of wood pulp: quantifying hardwood-softwood mixtures and estimating lignin content. Tappi Journal 73(10): 257-261

66. Eklund L and Säll H (2000) The influence of wind on spiral grain formation in conifer trees. Trees 14: 324-328

67. Ellis JW and Bath J (1938) Modifications in the near infra-red absorption spectra of protein and of light and heavy water molecules when water is bound to gelatine. Journal Chem. Phys. 6: 723-729

68. Evans R (1999) A variance approach to the x-ray diffractometric estimation of microfibril angle in wood. Appita J. 52: 283-289

69. Evans R (2006) Wood stiffness by x-ray diffractometry. In: "Characterisation of the Cellulosic Cell Wall", Chapter 11. Proceedings of the workshop 25-27 August 2003, Grand Lake, Colorado, USA. Southern Research Station, University of Iowa and the Society of Wood Science and Technology. D. Stokke and L. Groom, eds. Blackwell Publishing

70. Evans R and Ilic J (2001) Rapid prediction of wood stiffness from microfibril angle and density. Forest Products Journal 51(3): 53-57

71. Evans R, Stringer S and Kibblewhite RP (2000) Variation of microfibril angle, density and fibre orientation in twenty-nine *Eucalyptus nitens* trees. Appita Journal 53: 450-457

72. Falconer DS (1993) Introduction to quantitative genetics, 3rd edn. Longman Scientific and Technical, New York.

73. Falconer DS and Mackay TFC (1996) Introduction to Quantitative Genetics. 4th Edition. Prentice Hall. Essex, England. 464p.

74. Fang S, Yang W and Tian Y (2006) Clonal and within-tree variation in microfibril angle in poplar clones. New Forests 31: 373-383

75. Fang S-Z, Yang W-Z and Fu X-X (2004) Variation of microfibril angle and its correlation to wood properties in Poplars. Journal of Forest Research 15(4): 261-267

76. FAO (2006) Global Forest Resources Assessment 2005. Progress towards sustainable forest management. FAO Forestry Paper: 147p. Rome, Italy

77. FAO. State of the World's forests. Food and Agriculture Organization of the United Nations. Viale delle Terme di Caracalla. Rome, 2011. 164p.

78. Berti Filho E (1997) Impact of *Coleoptera cerambycidae* on *Eucalyptus* forests in Brazil. Scientia forestalis 52: 51-54

79. Fujimoto T, Kurata Y, Matsumoto K and Tsuchikawa S (2008) Application of near infrared spectroscopy for estimating wood mechanical properties of small clear and full length lumber specimens. Journal of Near Infrared Spectroscopy 16: 529-537

80. Gachet C and Guitard (2006) Influence relative de la morphologie cellulaire et de l'angle des microfibrilles sur l'anisotropie élastique tissulaire Longitudinale/Tangentielle du bois sans défaut des résineux. Annals of forest science 63(3): 275-283

81. Gantz CH (2002) Evaluating the efficiency of the Resistograph® to estimate genetic parameters for wood density in two softwood and two hardwood species. Raleigh: University of North Carolina State, 88p.

82. Gierlinger N, Schwanninger M and Wimmer R (2004) Characteristics and classification of fourier-transform near infrared spectra of heartwood of different larch species (*Laris* sp.). Journal of Near Infrared Spectroscopy 12: 113-119

83. Gierlinger N, Schwanninger M, Hinterstoisser B and Wimmer R (2002) Rapid determination of heartwood extractives in *Larix* sp. by means of Fourier transform near infrared spectroscopy. Journal of Near Infrared Spectroscopy 10: 203-214

84. Gilbert EA and Smiley ET (2004) Picus sonic tomography for the quantification of decay in white oak (*Quercus alba*) and hickory (*Carya* spp.). Journal of Arboriculture 30: 277-281

85. Gilmour AR, Gogel BJ, Cullis BR, Welham SJ and Thompson R (2005) ASReml user guide release 2.0, VSN international Ltd, Hemel Hempstead HP1 1ES, UK.

86. Glass SV and Zelinka SL (2010) Moisture Relations and Physical Properties of Wood. Cap. 4: 4.1-4.19. Forest Products Laboratory. 2010. Wood handbook - Wood as an engineering material. General Technical Report FPL-GTR-190. Madison, WI: U.S. Department of Agriculture, Forest Service, Forest Products Laboratory. 508p.

87. Gomide JL, Colodette JL, Oliveira RC and Silva CM (2005) Caracterização tecnológica, para produção de celulose, da nova geração de clones de *Eucalyptus* do Brasil. Árvore 29(1): 129-137

88. Gominho J, Rodrigues J, Almeida MH, Leal A, Cotterill PP, and Pereira H (1997) Assessment of pulp yield and lignin content in a first-generation clonal testing of *Eucalyptus globulus* in Portugal, in: Proceedings of the IUFRO Conference on Silviculture and Improvement of Eucalypts, Salvador, Brazil, August 24-29, 1997, pp. 84-89.

89. Grabianowski M, Manley B and Walker JCF (2006) Acoustic measurements on standing trees, logs and green lumber. Wood Science and Technology 40: 205-216

90. Greaves BL, Borralho NMG, Raymond CA (1997b) Breeding objective for plantation eucalypts grown for production of kraft pulp. Forest Science 43: 465-472

91. Greaves BL, Borralho NMG, Raymond CA and Farrington A (1996) Use of a Pilodyn for the indirect selection of basic density in *Eucalyptus nitens*. Canadian Journal of Forest Research 26: 1643-1650

92. Greaves BL, Borralho NMG, Raymond CA, Evans R and Whiteman PH (1997a) Age-age correlations and relationships between basic density and growth in *Eucalyptus nitens*. Silvae Genetica 46: 264-270

93. Green DW, Gorrnan TM, Evans JW and Murphy JF (2004) Improved grading system for structural logs for log homes. Forest Products Journal 54(9): 59-62

94. Green DW, Winandy JE, Kretschmann DE (1999) Mechanical properties of wood, Chapter 4. In: Wood Handbook – Wood as an Engineered Material, FPL-GTR-113, USDA Forest Service, Forest Products Laboratory, Madison WI, USA

95. Haines DW, Leban JM and Herbe C (1996) Determination of Young's modulus for spruce, fir and isotropic materials by the resonance flexure method with comparisons to static flexure and other dynamic methods. Wood science and technology 30(4): 253-263

96. Hamilton MG and Potts BM (2008) *Eucalyptus nitens* genetic parameters. New Zealand Journal of Forestry Science 38(1): 102-119

97. Hamilton MG, Raymond CA, Harwood E and Potts BM (2009) Genetic variation in *Eucalyptus nitens* pulpwood and wood shrinkage traits. Tree Genetics and Genomes 5: 307-316

98. Hansen JK and Roulund H (1996) Genetic parameters for spiral grain, stem form, pilodyn and growth in 13 years old clones of Sitka Spruce (*Picea sitchensis* (Bong.) Carr.). Silva Genetica 46(2-3): 107-113

99. Harris JM (1989) Spiral grain and wave phenomena in wood formation, Springer-Verlag, Berlin, 214 p.

100. Harwood C, Bulman P, Bush D, Stackpole D and Mazanec R (2001) Australian Low Rainfall Tree Improvement Group: Compendium of Hardwood Breeding Strategies. RIRDC Publication No. 01/100. p.31. Rural Industries Research and Development Corporation, Canberra.

101. Hearmon RFS (1961) An introduction to applied anisotropic elasticity. Oxford: Oxford University Press, 136 p.

102. Hein PRG, Lima JT and Chaix G (2009) Robustness of models based on near infrared spectra to predict the basic density in *Eucalyptus urophylla* wood. Journal of Near Infrared Spectroscopy 17(3): 141-150

103. Hein PRG, Brancheriau L, Lima JT, Rosado AM, Gril J and Chaix G. (2010a) Clonal and environmental variation of structural timbers of *Eucalyptus* for growth, density, and dynamic properties. Cerne 16: 74-81

104. Hein PRG, Brancheriau L, Trugilho PF, Lima JT and Chaix G. (2010b) Resonance and near infrared spectroscopy for evaluating dynamic wood properties. Journal of Near Infrared Spectroscopy 18(6): 443-454

105. Hein PRG, Clair B, Brancheriau L and Chaix G. (2010c) Predicting microfibril angle in *Eucalyptus* wood from different wood faces and surface qualities using near infrared spectra. Journal of Near Infrared Spectroscopy 18(6): 455-464

106. Hein PRG, Lima JT and Chaix G (2010d) Effects of sample preparation on NIR spectroscopic estimation of chemical properties of *Eucalyptus urophylla* S.T. Blake wood. Holzforschung 64: 45-54

107. Hein PRG, Brancheriau L, Lima JT, Gril J and Chaix G (2011) Resonance of structural timbers indicates the stiffness even of small specimens of *Eucalyptus* from plantations. Wood Science and Technology (DOI: 10.1007/s00226-011-0431-1)

108. Hein PRG and Brancheriau L (2011) Correlations between microfibril angle and wood density with age in 14-year-old *Eucalyptus urophylla* S.T. Blake wood. BioResources (submitted)

109. Hein PRG (2011) Relationships between microfibril angle and wood traits in Eucalyptus from fast-growing plantations. Holzforschung (submitted)

110. Hein PRG, Bouvet JM Mandrou E, Vigneron P and Chaix G (2011) Genetic control of growth, lignin content, microfibril angle and specific gravity in 14-years Eucalyptus urophylla S.T. Blake wood. Annals of Forest Science (submitted)

111. Herman M, Dutilleul P and Avella-Shaw T (1998) Growth rate effects on temporal trajectories of ring width, wood density and mean tracheid length in Norway spruce (*Picea abies* (L.) Karst.). Wood Fiber Science 30: 6-17

112. Hirakawa Y and Fujisawa Y (1995) The relationship between microfibril angles of the S2 layer and latewood tracheid lengths in elite sugi tree (*Cryptomeria japonica*) clones. Journal Japanese Wood Research Socociety 41: 123-131

113. Hoffmeyer P (1978) The Pilodyn instrument as a nondestructive tester of the shock resistance of wood. In: Proceedings, 4th nondestructive testing of wood symposium; 1978 August 28-30; Vancouver, WA. Pullman, WA: Washington State University: 47-66

114. Hoffmeyer P and Pedersen JG (1995) Evaluation of density and strength of Norway spruce by near infrared reflectance spectroscopy. Holz als Roh- und Werkstoff 53: 165-170

115. Hori R, Suzuki H, Kamiyama T and Sugiyama J (2003) Variation of microfibril angles and chemical composition: Implications for functional properties. J. Mat. Sci. Lett. 22: 963-966

116. Huang A, Fu F, Fei B and Jiang Z (2008) Rapid estimation of microfibril angle of increment cores of Chinese fir by near infrared spectroscopy. Chin. For. Sci. Technol. 7: 52-56

117. Iglesias-Trabado G and Wilstermann D (2008) *Eucalyptus universalis*. Global cultivated eucalypt forests map 2008. Version 1.0.1 In GIT Forestry Consulting's Eucalyptologics: Information resources on Eucalyptus Cultivation wordwide. Retrieved from [March 23th 2011]

118. Ilic J (2001) Relationship among the dynamic and static elastic properties of air-dry *Eucalyptus delegatensis* R. Baker. Holz als Roh- und Werkstoff 59: 169-175

119. Ilic J (2003) Dynamic MOE of 55 species using small wood beams. Holz als Roh- und Werkstoff 61:167-172

120. Ilic J and Hillis WE (1986) Prediction of Collapse in Dried Eucalypt Wood. Holzforschung 40(2): 109-112

121. Innes TC (1996) Pre-drying of collapse prone wood free of surface and internal checking. Holz als Roh- und Werktoff 54(3): 195-199

122. Isik F and Li B (2003) Rapid assessment of wood density of live trees using the Resistograph® for selection in tree improvement programs. Canadian Journal of Forest Research 33(12): 2426-2435

123. Jacobs MR (1945) The Growth of Woody Stems. Commonwealth Forestry Bureau, Australia, Bulletin No. 28, 67 pp.

124. Jayne BA (1959) Vibrational properties of wood as indices of quality. Forest Products Journal 9(11): 413-416

125. Jiang J, Lu J, Ren H, and Long C (2010) Predicting the flexural properties of Chinese fir (*Cunninghamia lanceolata*) plantation dimension lumber from growth ring width. Journal of Wood Science 56: 15-18

126. Jones PD, Schimleck LR, Peter GF, Daniels RF and Clark III A (2006) Nondestructive estimation of wood chemical composition of sections of radial wood strips by diffuse reflectance near infrared spectroscopy. Wood Science and Technology 40: 708-720

127. Jouan-Rimbaud D, Massart DL and Noord O.E. (1996) Random correlation in variable selection for multivariate calibration with a genetic algorithm. Chemometrics and Intelligent Laboratory Systems 35: 213-220

128. Jungnikl K, Koch G and Burgert I (2008) A comprehensive analysis of the relation of cellulose microfibril orientation and lignin content in the S2 layer of different tissue types of spruce wood (*Picea abies* (L.) Karst.). Holzforschung 62: 475-480

129. Kärenlampi PP and Riekkinen M (2004) Maturity and growth rate effects on Scots pine basic density. Wood Science and Technology 38(6): 465-473

130. Kelley SS, Rials TG, Groom LR and So C-L (2004) Use of Near Infrared Spectroscopy to predict the mechanical properties of six softwoods. Holzforschung 58, 252-260

131. Kibblewhite RP, Evans R, Grace JC and Riddell MJC (2005) Fibre length, microfibril angle and wood colour variation and interrelationships for two radiata pine trees with mild and severe compression wood. Appita J. 58: 316-322

132. Kien ND, Jansson G, Harwood C and Thinh HH (2009) Genetic control of growth and form in *Eucalyptus urophylla* in Northern Vietnam. Journal of Tropical Forest Science 21(1): 50-56

133. Kien ND, Jansson K, Harwood G, Almqvist C, Ha C and Huy T (2008) Genetic variation in wood basic density and pilodyn penetration and their relationships with growth, stem straightness, and branch size for *Eucalyptus urophylla* in northern Vietnam. New Zealand Journal of Forestry Science 38: 160-175

134. Klein JI (1995) Multiple-trait combined selection in jack pine family-test plantations using best linear prediction. Silvae Genetica 44(5/6): 362-375

135. Koch L and Fins L (2000) Genetic variation in wood specific gravity from progeny tests of ponderosa pine (*Pinus ponderosa* Laws.) in northern Idaho and western Montana. Silvae Genetica 49(4): 174-181

136. Kollmann FR and Côté WA (1968) Principles of Wood science and technology. Berlin: Springer-Verlag, 592p.

137. Kretschmann DE, Alden HA and Verrill S (1998) Variations of microfibril angle in loblolly pine: comparison of iodine crystallization and X-ray diffraction techniques. In: Butterfield, B.G., ed. Microfibril angle in wood. New Zealand: University of Canterbury. p.157-176

138. Kube PD and Raymond CA (2005) Breeding to minimise the effects of collapse in *Eucalyptus nitens*. Forest genetics 12: 23-34

139. Kube PD, Raymond CA and Banham PW (2001) Genetic parameters for diameter, basic density, cellulose content and fibre properties for *Eucalyptus nitens*. Forest Genetics 8: 285-294

140. Lachenbruch B, Johnson GR, Downes G and Evans R (2010) Relationships of density, microfibril angle, and sound velocity with stiffness and strength in mature wood of Douglas-fir. Canadian Journal of Forest Research 40: 55-64

141. Lande R (1984) The genetic correlation between characters maintained by selection, linkage and inbreeding. Genetic Research 44: 309-320

142. Lapierre C, Pollet B and Rolando C (1995) New insights into the molecular architecture of hardwood lignins by chemical degradative methods. Res. Chem. Intermed. 21: 397-412

143. Liang S-Q and Fu F (2007) Comparative study on three dynamic modulus of elasticity and static modulus of elasticity for Lodgepole pine lumber. Journal of Forestry Research 18(4): 309-312

144. Lima JT, Breese MC and Cahalan CM (1999) Variation in compression strength parallel to the grain in *Eucalyptus* clones. Proceedings of the Fourth International Conference on the Development of Wood Science, Wood Technology and Forestry, Missenden Abbey, UK, 14 16 July 1999

145. Lima JT, Breese MC and Cahalan CM (2000) Genotype-environment interaction in wood basic density of *Eucalyptus* clones. Wood Science and Technology 34: 197-206

146. Lima JT, Breese MC and Cahalan CM (2004) Variation in microfibril angle in *Eucalyptus* clones. Holzforschung 58: 160-166

147. Lima JT, Sartorio RC, Trugilho PF, Cruz CR and Vieira RS (2007) Uso do resistógrafo para estimar a densidade básica e a resistência à perfuração da madeira de *Eucalyptus*. Scientia Forestalis 75: 85-93

148. Lin C-J and Chiu C-M (2007). Relationships among selected wood properties of 20-year-old Taiwania (*Taiwania cryptomerioides*) trees. Journal of Wood Science 53: 61-66

149. Lindström H, Harris P, Sorensson CT and Evans R (2004) Stiffness and wood variation of 3-year old *Pinus radiata* clones. Wood Science and Technology 38: 579-597

150. MacDonald AC, Borralho NMG and Potts BM (1997) Genetic variation for growth and wood density in *Eucalyptus globulus* ssp. *globulus* in Tasmania (Australia). Silvae genetiva 46: 236-241

151. Malan FS (1988) Genetic variation in some growth and wood properties among 18 full-sib families of South African grown *Eucalyptus grandis*: a preliminary investigation. South African Forestry Journal 146: 38-43.

152. Malan FS (1995) *Eucalyptus* improvement for lumber production. Seminário internacional de utilização da madeira de eucalipto para serraria. 05 e 06 de abril de 1995. IPT, São Paulo, Brazil

153. Mandrou E, Hein PRG, Villar E, Vigneron P, Plomion C and Gion JM (2011) A candidate gene for lignin composition in *Eucalyptus*: Cinnamoyl-CoA Reductase (CCR), Tree Genetics and Genomes (submitted)

154. McKeand SE, Li B, Hatcher AV and Weir RJ (1990) Stability parameter estimates for stem volume for loblolly pine families growing in different regions in the southeastern United States. Forest Science 36(1): 10-17

155. McLean J P, Evans R and Moore J R (2010). Predicting the longitudinal modulus of elasticity of Sitka spruce from cellulose orientation and abundance. Holzforschung 64:495-500

156. Meder R, Trunga T and Schimleck L (2010) Guest editorial: Seeing the wood in the trees: unleashing the secrets of wood via near infrared spectroscopy. Journal of Near Infrared Spectroscopy 18(6): v-vii

157. Megraw RA, Leaf G and Bremer D (1998) Longitudinal shrinkage and microfibril angle in Loblolly pine. In Microfibril Angle in Wood: Proceedings of the IAWA/IUFRO International Workshop on the Significance of Microfibril Angle to Wood Quality (ed. B. G. Butterfield), pp. 27-61. Westport, N.Z. University of Canterbury Press, Canterbury, N.Z.

158. Meylan BA (1967) Measurement of microfibril angle by X-ray diffraction. Forest Products Journal 17: 51-58

159. Meylan BA (1968) Cause of high longitudinal shrinkage of wood. Forest Products journal 18: 75-78

160. Mode CJ and Robinson HF (1959) Pleiotropism and the genetic variance and covariance. Biometrics 15: 518-537

161. Mora CR, Schimleck LR (2008) On the selection of samples for multivariate regression analysis: application to near-infrared (NIR) calibration models for the prediction of pulp yield in *Eucalyptus nitens*. Canadian Journal Forest Research 38(10): 2626-2634.

162. Mora CR, Schimleck LR and Isik F (2008) Near infrared calibration models for the estimation of wood density in *Pinus taeda* using repeated sample measurement. Journal of Near Infrared Spectroscopy 16: 517-528

163. Mrode RA (2005) Linear models for the prediction of animal breeding values. 2nd ed. CAB International, Wallingford, Oxon, UK.

164. Muneri A and Raymond CA (2000) Genetic parameters and genotype-by-environment interactions for basic density, pilodyn penetration and stem diameter in *Eucalyptus globulus*. Forest Genetics 7: 317-328

165. Murphy JF (2000) Commentary on factors affecting transverse vibration using an idealized theoretical equation. Res. Note FPL-RN-0276. Madison, WI: U.S. Department of Agriculture, Forest Service, Forest Products Laboratory. 4 p

166. Næs T, Isaksson T, Fearn T and Davies T (2002) A user-friendly guide to multivariate calibration and classification. Chichester: NIR. 344 p.

167. Nicolotti G, Socco LV, Martinis R, Godio A and Sambuelli L (2003) Application and comparison of three tomographic techniques for detection of decay in trees. Journal of Arboriculture 29: 66-78

168. Ohsaki H, Kubojima Y, Tonosaki M and Ohta M (2007) Vibrational properties of wetwood of todomatsu (*Abies sachalinensis*) at high temperature. Journal of Wood Science 53: 134-138

169. Osorio LF, White TL and Huber DA (2003) Age-age and trait-trait correlations for *Eucalyptus grandis* Hill ex Maiden and their implications for optimal selection age and design of clonal trials. Theoretical and Applied Genetics 106: 735-743

170. Ouis D (1999) Vibrational and acoustical experiments on logs of spruce. Wood Science and Technology 33: 151-184

171. Panshin AJ and De Zeeuw C (1980) Textbook of wood technology. 4.ed. New York: Mc Graw Hill. 722p.

172. Pasquini C (2003) Near infrared spectroscopy: fundamentals, practical aspects and analytical applications. Journal of the Brazilian Chemical Society 14(2): 198-219

173. Peel MC, Finlayson BL and McMahon TA (2007) Updated world map of the Köppen-Geiger climate classification. Hydrol. Earth Syst. Sci. 11: 1633-1644

174. Pelletier MC, Henson M, Boyton S, Thomas D and Vanclay J (2008) Genetic variation in shrinkage properties of *Eucalyptus pilularis* assessed using increment cores and test blocks. New Zealand Journal of Forestry Science 38(1): 194-210

175. Pereira H, Graça J and Rodrigues JC (2003) Wood chemistry in relation to quality" in Wood Quality and its Biological Basis, Ed by J.R. Barnett and G. Jeronimidis, Blackwell Publishing, Victoria, p.226

176. Petty JA, MacMillan DC and Steward CM (1990) Variation of density and growth ring width in stems of Sitka and Norway spruce. Forestry 63: 39-49

177. Peura M (2007) Studies on the cell wall structure and on the mechanical properties of Norway spruce. Report Series in Physics HU-P-D146

178. Poke FS, Potts BM, Vaillancourt RE and Raymond CA (2006) Genetic parameters for lignin, extractives and decay in *Eucalyptus globulus*. Annals of Forest Science 63(8): 813-821

179. Polge H (1963) Une nouvelle méthode de détermination de la texture du bois : l'analyse densitométrique de clichés radiographiques. Annales de Sciences Forestières 20(4): 531-581

180. Preston RD (1934) The organization of the cell wall of the conifer tracheid. Philosophical Transactions of the Royal Society B 224: 131-173

181. R Development Core Team. 2008. R: A Language and Environment for Statistical Computing. Vienna, Austria: R Foundation for Statistical Computing. ISBN 3-900051-07-0. http://www.r-project.org.

182. Rabe C, Ferner D, Fink S and Schwarze FWMR (2004) Detection of decay in trees with stress waves and interpretation of acoustic tomograms. Journal of Arboriculture 28: 3-19

183. Rayleigh JWS (1877) The theory of the sound (Edition of 1945). New York. pp. 243-305

184. Raymond CA (2002) Genetics of Eucalyptus wood properties. Annals of Forest Science 59: 525-531

185. Raymond CA and MacDonald AC (1998) Where to shoot your pilodyn: within tree variation in basic density in plantation *Eucalyptus globulus* and *E. nitens* in Tasmania. New Forests 15: 205-221

186. Raymond CA, Banham P and MacDonald AC (1998) Within tree variation and genetic control of basic density, fibre length and coarseness in *Eucalyptus regnans* in Tasmania. Appita Journal 41(4): 299-305

187. Rinn F (1994) Bohrwiderstandmessungen mit Resistograph®- Mikorbohrungen. Allgemeine Forst Zeitschrift 49(12): 652-654

188. Rinn F, Schweingruber F-H and Schär E (1996) Resistograph and X-ray density charts of wood comparative evaluation of drill resistance profiles and X-ray density charts of different wood species. Holzforschung 50:303-311

189. Rinn F, Schweingruber H and Schar E. (1996) Resistograph and X-ray density charts of wood comparartive evaluation on drill resistance profiles and X-ray density charts of different wood species. Holzforschung 50(4): 303-311

190. Rodrigues EAC, Rosado SCS, Trugilho PF and Santos AM (2008) Seleção de clones de *Eucalyptus* para as propriedades fisicas da madeira avaliadas em arvores no campo. Cerne 14: 147-152

191. Rodrigues J, Alves A, Pereira H, da Silva Perez D, Chantre G and Schwanninger M (2006) NIR PLSR results obtained by calibration with noisy, low-precision reference values: Are the results acceptable? Holzforschung 60: 402-408

192. Rodrigues J, Meier D, Faix O and Pereira H (1999) Determination of tree to tree variation in syringyl:guaiacyl ratio of *Eucalyptus globulus* wood lignin by analytical pyrolysis. Journal of Analytical and Applied Pyrolysis 48: 121-128

193. Rosado SCS, Brune A and Oliveira LM (1983) Avaliação da densidade básica da madeira de árvores em pé. Revista Árvore 7(1): 147-153

194. Ross RJ and Pellerin (1994) Nondestructive testing for assessing Wood members in structures: A review. USDA Forest Service Forest Products Laboratory, General Tech Rep FPL-GTR-70

195. Ross RJ, Geske EA, Larson GL and Murphy JF (1991) Transverse vibration non-destructive testing using a personal computer, Research Paper, FPL-RP-502, Forest Products Laboratory, Forest Service, US Department of Agriculture

196. Rozenberg P and Cahalan C (1997). Spruce and wood quality: Genetic aspects (A review). Silvae Genetica 46: 270-279.

197. Rozenberg P and Van de Sype H (1996) Genetic variation of the pilodyn-girth relationship in Norway spruce (*Picea abies* L. Karst). Annals of Forest Science 53(6): 1153-1166

198. Ruelle J, Yamamoto H and Thibaut B (2007) Growth stresses and cellulose structural parameters in tension and normal wood from three tropical rainforest angiosperms species. BioResources 2(2): 235-251

199. Santos PET, Geraldi IO, Garcia N.G. (2004) Estimates of genetic parameters of wood traits for sawn timber production in *Eucalyptus grandis*. Genetics and Molecular Biology 27(4): 567-573

200. Savidge RA (2003) Tree growth and wood quality" in Wood Quality and its Biological Basis, Ed by J.R. Barnett and G. Jeronimidis, Blackwell Publishing, Victoria, p.226

201. Savitzky A, Golay MJE (1964) Smoothing and differentiation of data by simplified least-squares procedures. Anal Chem 36(8):1627-1639

202. Schimleck L, Jones PD, Peter GF, Daniels RF and Clark III A (2004) Nondestructive estimation of tracheid length from sections of radial wood strips by near infrared spectroscopy. Holzforschung 58, 375-381

203. Schimleck LR and Evans R (2002) Estimation of microfibril angle of increment cores by near infrared spectroscopy. IAWA Journal 23(3): 225-234

204. Schimleck LR and Evans R (2004) Estimation of *Pinus radiata* D. Don tracheid morphological characteristics by near infrared spectroscopy. Holzforschung 58: 66-73

205. Schimleck LR, Evans R and Ilic J (2001) Estimation of *Eucalyptus delegatensis* wood properties by near infrared spectroscopy. Canadian Journal of Forest Research 31: 1671-1675

206. Schimleck LR, Evans R and Matheson AC (2002) Estimation of *Pinus radiata* D. Don clear wood properties by near-infrared spectroscopy. Journal of Wood Science 48: 132-137

207. Schimleck LR, Evans R, Jones PD, Daniels RF, Peter GF, Clark III A (2005) Estimation of microfibril angle and stiffness by near infrared spectroscopy using sample sets having limited wood density variation. IAWA Journal 26(2) 175-187

208. Schimleck LR, Mora C, Daniels RF (2003) Estimation of the physical wood properties of green Pinus taeda radial samples by near infrared spectroscopy. Canadian Journal of Forest Research 33:2297-2305

209. Shenk JS, Workman JJ and Westerhaus MO (2001) Application of NIR Spectroscopy to Agricultural Products". In: Burns DA, Ciurczak EW (eds) Handbook of Near-Infrared Analysis, Marcel Dekker Inc., New York, p. 419

210. Shield ED (1995) Plantation grown eucalypts: Utilisation for lumber and rotary veneers – primary conversion. Seminário internacional de utilização da madeira de eucalipto para serraria. 05 e 06 de abril de 1995. IPT, São Paulo, Brazil

211. Shield ED (2007) Whither eucalypt sawlogs? IUFRO 'Eucalypts and diversity: balancing productivity and sustainability'. Durban, South Africa

212. Silva VL (2006) Caracterização de ligninas de *Eucalyptus* spp. pela técnica de pirólise associada à cromatografia gasosa e à espectrometria de massas. 2006. 85 p. Dissertação - Universidade Federal de Viçosa, Viçosa.

213. Skatter S and Kucera B (1997) Spiral grain - An adaptation of trees to withstand stem breakage caused by wind-induced torsion. Holz als Roh- und Werkstoff 55: 207-213

214. Sokal RR and Rohlf FJ (1995) Biometry: The principles and practice of statistics in biological research. 3rd edition. W.H. Freeman, New York.

215. Sousa-Correia C, Alves A, Rodrigues JC, Ferreira-Dias S, Abreu JM, Maxted N, Ford-Lloyd B and Schwanninger M (2007) Oil content estimation of individuals kernels of *Quercus ilex* subsp. *rotundifolia* [(Lam) O. Schwarz] acorns by Fourier transform near infrared spectroscopy and partial least squares regression. Journal of Near Infrared Spectroscopy 15: 247-260

216. Stamm AJ (1964) Wood and Cellulose Science. Ronald Press, New York. 509p.

217. Steiglitz K, McBride LE (1965) A technique for the identification of linear systems. IEEE Trans Automat Contr 10:461-464

218. Thamarus K, Groom K, Bradley A, Raymond CA, Schimleck LR, Williams ER and Moran GF (2004) Identification of quantitative trait loci for wood and fibre properties in two full-sib pedigrees of *Eucalyptus globulus*. Theoretical and Applied Genetics 109(4): 856-864

219. Thibaut B, Gril J and Fournier M (2001) Mechanics of wood and trees: some new highlights for an old story. Comptes Rendus de l'Academie des Sciences Series IIB Mechanics. 329(9) 701-716

220. Thumm A and Meder R (2001) Stiffness prediction of radiata pine clearwood test pieces using near infrared spectroscopy. Journal of Near Infrared Spectroscopy 9: 117-122

221. Thygesen L (1994) Determination of dry matter content basic density of Norway spruce by near infrared reflectance and transmittance spectroscopy. Journal of Near Infrared Spectroscopy 2: 127-135

222. Timoshenko S (1921) On the Correction for Shear of the Differential Equation for Transverse Vibrations of Prismatic Bars. Philosophical Magazine and Journal of Science XLI - Sixth Series: 744-746

223. Tomazello Fo M, Brazolin S, Chagas MP, Oliveira JTS, Ballarin AW and Benjamin CA (2008) Application of X-ray technique in non-destructive evaluation of *Eucalyptus* wood. Maderas. Ciencia y tecnología 10(2): 139-149.

224. Tonello KC, Cotta MK, Alves RR, Ribeiro CFA and Polli HQ (2008) O desenvolvimento do setor florestal brasileiro. Revista da madeira 112

225. Tsuchikawa S (2007) A Review of Recent Near Infrared Research for Wood and Paper. Applied Spectroscopy Review 42: 43-71

226. Tsuchikawa S, Hayashi K and Tsutsumi S (1992) Application of near infrared spectrophotometry to wood. 1. Effects of the surface-structure. Mokuzai Gakkaishi 38:128-136

227. Tsutsumi J, Matsumoto T, Kitahara R and Mio S (1982) Specific gravity, tracheid length and microfibril angle of sugi (*Cryptomeria japonica* D. Don): Seed grown trees compared with grafts. Bull. Kyushu Univ. For. 52: 115-120

228. Turner CH, Balodis V and Dean GH (1983) Variability in pulping quality of *E. globulus* from Tasmanian provenances. Appita Journal 36(5): 371-376

229. Verryn SD (2008) Breeding for wood quality - a perspective for the future. New Zealand Journal of Forestry Science 38(1): 5-13

230. Verryn SD and Hettasch MH (2006) Synopsis of the "Pine Platform - Global Forest Products Workshop on Pine Tree Traits of Importance in the Solid Wood Value Chain". CSIR, Pretoria, Report Ref. No. CSIR/NRE/FOR/ER/2006/0055/C: 1-40.

231. Via BK, Shupe TF, Groom LH, Stine M and So CL (2003) Multivariate modelling of density, strength and stiffness from near infrared spectra for mature, juvenile and pith wood of longleaf pine (*Pinus palustris*). Journal of Near Infrared Spectroscopy 11: 365-378

232. Via BK, So CL, Shupe TF, Groom LH and Wikaira J (2009) Mechanical response of longleaf pine to variation in microfibril angle, chemistry associated wavelengths, density, and radial position. Composites: Part A 40: 60-66

233. Via BK, So CL, Shupe TF, Stine M and Groom LH (2005) Ability of near infrared spectroscopy to monitor air-dry density distribution and variation of wood. Wood Fiber Science 37: 394-402

234. Villanueva B and Kennedy BW (1990) Effect of selection on genetic parameters of correlated traits. Theoretical and Applied Genetics 80(6): 746-752

235. Volker PW, Potts BM and Borralho NMG (2008) Genetic parameters of intra- and inter-specific hybrids of *Eucalyptus globulus* and *E. nitens*. Tree Genetics and Genomes 4: 445-460

236. Walker JCF and Butterfield BG (1995) The importance of microfibril angle for the processing industries. New Zealand Forestry, November: 35-40.

237. Walker NK and Dodd RS (1988) Calculation of Wood Density Variation From X-ray Densitometer Data. Wood and Fiber Science 20: 35-43

238. Wallbacks L, Edlund U, Norden B and Berglund I (1991) Multivariate characterization of pulp using 13C NMR, FTIR and NIR. Tappi Journal 74(10): 201-206

239. Wang S, Littell RC and Rockwood DL (1984) Variation in density and moisture content of wood and bark among twenty *Eucalyptus grandis* progenies. Wood Science and Technology 18(2): 97-100

240. Wang T, Aitken SN, Rozenberg P and Carlson MR (1999) Selection for height growth and Pilodyn pin penetration in lodgepole pine: effects on growth traits, wood properties, and their relationships. Canadian Journal of Forest Research 29: 434-445

241. Wang X, Ross RJ, Mattson JA, Erickson JR, Forsman JW, Geske EA and Wehr MA (2001) Several nondestructive evaluation techniques for assessing stiffness and MOE of small-diameter logs. (General Technical Report FPL-RP-600).Madison: U.S.D.A Department of Agriculture, Forest Products Laboratory

242. Wang X, Ross RJ, Mattson JA, Erickson JR, Forsman JW, Geskse EA, Wehr MA (2002) Nondestructive evaluation techniques for assessing modulus of elasticity and stiffness of small-diameter logs. For Prod J 52:79-85

243. Wardrop AB (1956) The nature of reaction wood. V. The distribution and formation of tension wood in some species of *Eucalyptus*. Australian Journal of Botany 4: 152-166

244. Washusen R and Evans R (2001) Prediction of wood tangential shrinkage from cellulose crystallite width in one 11-year-old tree of *Eucalyptus globulus* Labill. Australian Forest 64: 123-126

245. Washusen R, Ades P, Evans R, Ilic J and Vinden P (2001) Relationships between density, shrinkage, extractives content and microfibril angle in tension wood from three provenances of 10-year-old *Eucalyptus globulus* Labill. Holzforschung 55: 176-182

246. Washusen R, Baker T, Menz D and Morrow A (2005) Effect of thinning and fertilizer on the cellulose crystallite width of *Eucalyptus globulus*. Wood Science and Technology 39: 569-578

247. Wei X and Borralho NMG (1997) Genetic control of wood basic density and bark thickness and their relationships with growth traits of *Eucalyptus urophylla* in south east China. Silvae Genetica 46(4): 245-250

248. Wei X and Borralho NMG (1999) Objectives and selection criteria for pulp production of Euc*alyptus urophylla* plantation in south east China. Forest genetics 6(3): 181-190

249. Westad F and Martens H (2000) Variable selection in near infrared spectroscopy based on significance testing in partial least square regression. Journal of Near Infrared Spectroscopy 8: 117-124

250. White TL, Adams WT and Neale DB (2007) Forest genetics. CABI Publishing, CAB International, Wallingford, UK.

251. Whittock SP, Dutkowski GW, Greaves BL and Apiolaza LA (2007) Integrating revenues from carbon sequestration into economic breeding objectives for *Eucalyptus globulus* pulpwood production. Annals of Forest Science 64: 239-246

252. Wilkes J (1988) Variations in wood anatomy within species of *Eucalyptus*. IAWA Journal 9(1): 13-23

253. Williams PC, Sobering DC (1993) Comparison of commercial near infrared transmittance and reflectance instruments for analysis of whole grains and seeds. Journal of Near Infrared Spectroscopy 1:25-33

254. Wold S, Sjöström M and Eriksson L (2001) PLS-regression: a basic tool of chemometrics. Chemometrics and Intelligent Laboratory Systems 58: 109-130

255. Workman J and Weywer L (2007) Practical guide to interpretive near infrared spectroscopy. Boca Raton: CRC Press. 332p.

256. Wright JA, Birkett MD and Gambino MJT (1990) Prediction of pulp yield and cellulose content from wood samples using near infrared reflectance spectroscopy. Tappi Journal 73(8): 164-166

257. Wu HX, Powell MB, Yang JL, Ivkovic M and McRae TA (2007) Efficiency of early selection for rotation-aged wood quality traits in radiata pine. Annals of Forest Science. 64(1): 1-9

258. Wu Y-Q, Hayashi K, Liu Y, Cai Y-C and Sugimori M (2006) Relationships of anatomical characteristics versus shrinkage and collapse properties in plantation-grown eucalypt wood from China. Journal of Wood Science 52(3): 187-194

259. Wu Y-Q, Hayashi K, Liu Y, Cai Y-C, Sugimoro M and Luo J-J (2005) Collapse-type shrinkage characteristics in plantation-grown eucalypts: I. Correlations of basic density and some structural indices with shrinkage and collapse properties. Journal of Forestry Research 16(2): 83-88

260. Yamada T, Yeh T-F, Ching H-M, Li L, Kadla FK and Chiang VL (2004) Rapid analysis of transgenic trees using transmittance near-infrared spectroscopy. Journal Near Infrared Spectroscopy 12: 263-269

261. Yamamoto H, Okuyama T and Yashida M (1993) Method of determining the mean microfibril angle of wood over a wide range by the improved Cave´s method. Mokuzai Gakkaishi 39: 118-125

262. Yamamoto H, Sassus F, Ninomiya M and Gril J (2001) A model of anisotropic swelling and shrinking process of wood. Part 2. A simulation of shrinking wood. Wood Science and Technology 35: 167-181

263. Yang JL (2007) Investigation of potential sawlog quality indicators - A case study with 32-year-old plantation *Eucalyptus globulus* Labill. Holz als Roh- und Werkstoff 65: 419-427

264. Yang JL and Evans R (2003) Prediction of MOE of eucalypt wood from microfibril angle and density. Holz als Roh- und Werkstoff 61: 449-452

265. Yang JL and Waugh G (1996a) Potential of plantation-grown eucalypts for structural sawn products. I. *Eucalyptus globulus* Labill. spp. *globulus*. Australian Forestry 59: 90-98

266. Yang JL and Waugh G (1996b) Potential of plantation-grown eucalypts for structural sawn products. II. *Eucalyptus nitens* (Deane & Maiden) Maiden and *E. regnans* F. Muell. Australian Forestry 59: 99-107

267. Zamudio F, Baettyg R, Vergara A, Guerra F and Rozenberg P (2002) Genetic trends in wood density and radial growth with cambial age in a Radiata pine progeny test. Annals of Forest Science 59: 541-549

268. Zhang SY (1995) Effect of growth rate on wood specific gravity and selected mechanical properties in individual species from distinct wood categories. Wood Science and Technology 29(6): 451-465

269. Zobel B and Jett JB (1995) Genetics of Wood Production. Berlin: Springer-Verlag. 336 p.

270. Zobel B and Talbert J (1984) Applied Forest Tree Improvement. The Blackburn Press, Caldwell, NJ, Reprint of First Edition. 505p.

271. Zobel BJ and Van Buijtenen JP (1989) Wood Variation: Its Causes and Control. Springer Verlag, Berlin. 363p.

LIST OF TABLES

Table 1 - Distribution of *Eucalyptus* and *Pinus* forest plantations in Brazil by industrial segment in 200926

Table 2 - Components of variance of growth and wood traits (from Falconer (1993)) 38

Table 3 - Resume of the main statistics of the NIR-based calibration for estimating wood traits of progeny and clonal tests and the corresponding paper 55

Table 4 - Arrays of parents in the incomplete factorial mating design under controlled crosses..... 57

Table 5 - Description of the environmental information of the clonal tests 58

Table 6 - Information about the clones' origin describing their relatives and species 58

Table 7 - Reference of codes relative to radial and longitudinal positions..... 61

Table 8 - Resume of growth and wood traits measurements, methods, sample dimension and number of observations of the trees from Clonal test 68

Table 9 - Resume of growth and wood traits measurements, methods, sample dimension and number of observations of the trees from Progeny test. Chemical properties were done in duplicate 69

Table 10 - Descriptive statistics of growth traits in 14-year-old *Eucalyptus urophylla* from progeny test and in 6-year-old *E. urograndis* from clonal test, including circumference at 1.3 meter height (C) and total height (H) by site and considering all samples..... 75

Table 11 - Descriptive statistic for Klason lignin (KL); acid-soluble lignin (ASL) and total lignin content (TL); syringyl to guaiacyl ratio (S/G); and extractive content (EXT) in 14-year-old *Eucalyptus urophylla* wood 76

Table 12 - Descriptive statistics, including average, standard deviation (Sd), minimum (Min), maximum (Max) and coefficient of variation (CV) for basic density (ρ), *T* parameter and microfibril angle (MFA) measurements in 14-year-old *Eucalyptus urophylla* wood 77

Table 13 - Description of tangential sections from the radial wood strips, their influence on the *T* parameter measurements and the radial variation of MFA and basic density in 14-year-old *Eucalyptus urophylla* wood. The relative radial position is presented in squared brackets while the range of variation of traits is presented in parentheses 79

Table 14 - Descriptive statistics of dynamic properties of the kiln-dried scantlings of 6-year-old *Eucalyptus grandis* x *urophylla*, including kiln-dried density (ρ14, kg m^{-3}), first resonant frequency (f_l14, Hz), elastic modulus (E14, MPa), specific modulus (E'14, E/ρ), loss tangent (tg δ14, 10^{-3}) and shear modulus (G14, MPa) estimated by longitudinal ($_L$) and flexural ($_F$) vibration tests..... 80

Table 15 - Descriptive statistics of dynamic properties of the clearwood specimens of 6-year-old *Eucalyptus grandis* x *urophylla*, including air-dried density (ρsp, kg m^{-3}), resonant frequency ($f_l$sp, Hz), elastic modulus (Esp, MPa), specific modulus (E'sp, E/ρ), loss tangent (tg $\delta_F$sp, 10^3) and shear modulus (Gsp, MPa) estimated by longitudinal ($_L$) and flexural ($_F$) vibration tests..... 81

Table 16 - Descriptive statistics of the 4- and 3-points bending test of the specimens of 6-year-old *Eucalyptus grandis* x *urophylla*, including force at rupture point (Fmax, N) and modulus of rupture (MOR, MPa) 83

Table 17 - Descriptive statistics of basic density (ρs, kg m^{-3}) and radial and tangential shrinkage (%) of the small samples of 6-year-old *Eucalyptus grandis* x *urophylla* 84

Table 18 - Descriptive statistics of the *T* parameter obtained by X-ray diffraction and microfibril angle estimates by Cave (MFA_C) and Yamamoto (MFA_Y) formulas from the small samples of 6-year-old *Eucalyptus grandis* x *urophylla*. Samples were taken from the small wood samples (MFA_{YS}) and from radial strips (MFA_{YRS}) 85

Table 19 - Mean and standard deviation (in parentheses) of microfibril angle according to the year of wood formation estimated by Yamamoto (MFA_{YRS} in degrees) formulas from radial strips of 6-year-old *Eucalyptus* clones from sites 301, 302 and 303 86

Table 20 - Correlations between wood traits including wood density (ρ), elastic modulus (E), specific modulus (E'), shear modulus (G), radial (δrd) and tangential shrinkage (δtg), microfibril angle, ρ/MFA parameter and modulus of rupture (MOR). The correlations were statistically significant at $p<0.01$ 87

Table 21 - Regression models for predicting modulus of elasticity in longitudinal (E_L) and flexural (E_F) vibrations and modulus of rupture (MOR_{4p}) with MFA, density, and ρ/MFA 89

Table 22 - Descriptive statistics of Klason lignin (KL), S to G ratio (S/G), basic density (ρ) and microfibril angle (MFA) of 14-year-old *Eucalyptus urophylla* woods from progeny test 92

Table 23 - Statistical summary of the overall, calibration and validation sets for air-dry density, basic density, microfibril angle and a range of dynamic properties of the small, clean specimens of *Eucalyptus* wood from clonal test 92

Table 24 - PLS-R models for Klason lignin (KL, %), syringyl to guaiacyl ratio (S/G, no unit), wood basic density (ρ, kg m^{-3}) and microfibril angle (MFA, degrees) used for estimating phenotypic values for 14-year-old *Eucalyptus urophylla* 93

Table 25 - PLS-R models for air-dry density (ρ_{sp}, kg m^{-3}), wood basic density (ρ_s, kg m^{-3}), microfibril angle (MFA, degrees), longitudinal and flexural modulus of elasticity (E, MPa), longitudinal and flexural specific modulus (E', MPa/ρ), first resonance frequency (f_1, MHz) and loss tangent ($\tan\delta_L$, 10^3) used for estimating phenotypic values for 6-year-old *Eucalyptus* clones 93

Table 26 - NIR absorption bands normally associated to the main wood components (cellulose, hemicelluloses, lignin, and water) contained in the wood specimens 96

Table 27 - Mean, minimum and maximum values, coefficient of variation and number of observations (N) for measured circumference (C, centimeters) and height (H, meters), and NIR-estimated Klason lignin (KL, %), syringyl to guaiacyl ratio (S/G, no unit), wood density (D, kg m^{-3}) and microfibril angle (MFA, degrees) of the 14-year-old *Eucalyptus urophylla* population 99

Table 28 - Additive genetic and residual variance components, genetic and residual coefficient of variance and narrow-sense heritability estimates for various traits 100

Table 29 - Estimated additive genetic (r_A, below the diagonal) and residual (r_E, above the diagonal) correlations for various traits, including circumference (C), height (H), microfibril angle (MFA), basic density (D), Klason lignin (KL) and syringyl to guaiacyl ratio (S/G). Standard errors are shown in parentheses 102

Table 30 - Variation with age of additive genetic, residual and phenotypic correlations of density with C, and MFA with C, KL and density. Standard errors are in parenthesis 103

Table 31 - Tukey (HSD) multiple range tests for growth traits by clone and by site in 6-year-old *Eucalyptus urophylla* x *grandis* clones 107

Table 32 - Analysis of variance for density and dynamic traits in kiln-dried at 14% scantlings of 6-year-old *Eucalyptus urophylla* x *grandis* clones 108

Table 33 - Tukey (HSD) multiple range tests for density and dynamic traits by clone and by site in kiln-dried at 14% scantlings of 6-year-old *Eucalyptus urophylla* x *grandis* clones 108

Table 34 - Radial and longitudinal variation for wood basic density (kg m^{-3}) in *Eucalyptus* clones at three contrasting sites. The means were compared by the Tukey test at p=0.01 threshold. Small letters are comparisons between radial positions while capital ones compares sites. Values in brackets are coefficients of variation in percentage 110

Table 35 - Radial and longitudinal variation for modulus of elasticity (MPa) in clones of *Eucalyptus* wood at three contrasting sites. The means were compared by the Tukey test at p =0.01 threshold. Small letters are comparisons between radial positions while capital ones compares sites. Values in brackets are coefficients of variation in percentage 111

Table 36 - Radial and longitudinal variation for microfibril angle (degrees) in clones of *Eucalyptus* wood at three contrasting sites. The means were compared by the Tukey test at p =0.01 threshold. Small letters are comparisons between radial positions while capital ones compares sites. Values in brackets are coefficients of variation in percentage 112

Table 37 - Pith to cambium variation of wood density (kg m^{-3}), stiffness (GPa) and microfibril angle (degrees) at various relative heights. 114

Table 38 - Radial variation at 25% of the stem height for wood basic density (kg m^{-3}) for clones of *Eucalyptus* wood and sites. The means were compared by the Tukey test at p=0.05 threshold. Small letters are comparisons between clones or sites while capital ones compares the radial positions..... 115

Table 39 - Radial variation at 25% of the stem height for elastic modulus (MPa) for clones of *Eucalyptus* wood and sites. The means were compared by the Tukey test at p=0.05 threshold. Small letters are comparisons between clones or sites while capital ones compares the radial positions..... 116

Table 40 - Radial variation at 25% of the stem height for microfibril angle (degrees) for clones of *Eucalyptus* wood and sites. The means were compared by the Tukey test at p=0.05 threshold. Small letters are comparisons between clones or sites while capital ones compares the radial positions..... 118

Table 41 - Genetic parameters for growth traits in 6-year-old *Eucalyptus urophylla* x *grandis* clones.... 119

Table 42 - Genetic parameters for basic density of the wood in 6-year-old *Eucalyptus urophylla* x *grandis* 120

Table 43 - Genetic parameters for dynamic longitudinal modulus of elasticity of the wood in 6-year-old *Eucalyptus urophylla* x *grandis*..... 120

Table 44 - Genetic parameters for microfibril angle of cell wall of wood in 6-year-old *Eucalyptus urophylla* x *grandis* clones 121

Table 45 - Descriptive statistics of dynamic properties of the air-scantlings of 6-year-old *Eucalyptus grandis* x *urophylla*, including air-dry density (ρad, kg m^{-3}), first resonant frequency ($f_1$ad, Hz), elastic modulus (Ead, MPa), specific modulus (E'ad, E/ρ), loss tangent (tg δad, 10^{-3}) and shear modulus (Gad, MPa) estimated by longitudinal ($_L$) and flexural ($_F$) vibration tests..... 137

Table 46 - Correlations among physical and elastic properties of 395 air-dried and 14% dried scantlings of 6-year-old *Eucalyptus grandis* x *urophylla* wood. The significance level for all relationships was <0.0001 138

Table 47 - Correlations among *Eucalyptus* wood traits by site and by radial position. All correlations were statistically significant at $p<0.01$ 140

Table 48 - Analysis of variance for density and dynamic traits in air-dried scantlings of 6-year-old *Eucalyptus urophylla* x *grandis* clones 142

Table 49 - Tukey (HSD) multiple range tests for density and dynamic traits by clone and by site in air-dried scantlings of 6-year-old *Eucalyptus urophylla* x *grandis* clones 143

Table 50 - Genetic parameters for basic density of the wood in 6-year-old *Eucalyptus urophylla* x *grandis* clones (model y = μ + G + E)..... 145

Table 51 - Genetic parameters for dynamic longitudinal modulus of elasticity of the wood in 6-year-old *Eucalyptus urophylla* x *grandis* clones (model y = μ + G + E) 145

Table 52 - Genetic parameters for microfibril angle of cell wall of wood in 6-year-old *Eucalyptus urophylla* x *grandis* clones (model y = μ + G + E) 146

LIST OF FIGURES

Figure 1 - Transversal (A), radial (B) e tangential (C) sections of 6-year-old *Eucalyptus* wood (source: personal image) 29

Figure 2 - Three-dimensional structure of the secondary cell wall of a fibre 31

Figure 3 - Relationship between MFA and modulus of elasticity (MOE) of *E. globulus*, *E. nitens* and *E. regnans* wood between 15 and 33 years of age (from Yang and Evans 2003) 32

Figure 4 - Theoretical model explaining the influence of high microfibril angle (A) and low microfibril angle (B) on longitudinal and transversal components of shrinkage and swelling 33

Figure 5 - Relationship between anisotropic shrinkage (from green to oven-dried) and MFA (from Yamamoto et al. 2001) 34

Figure 6 - The relationship between the angle T derivated from the X-ray intensity variation and the mean microfibril angle measured by iodine staining (A, from Meylan 1967) and by Field-Emission Scanning Electron Microscopy (B, from Ruelle et al. 2007) 36

Figure 7 - Genetic gain from tree breeding programs (A, personal source) and graphs of the regression lines of breeding values on phenotypic values for two hypothetical traits, A and B, with h^2_A=0.2 and h^2_B=0.4 (B, from White et al. 2007) 37

Figure 8 - Evaluating standing trees with Resistograph (A) and Pilodyn (B). Dotted lines shows in detail the pine penetration (source: personal image) 44

Figure 9 - Example of tomography analysis; a photograph of the disc (diameter: 90 cm) and the corresponding acoustic tomogram showing the decay (blue parts) in a wood disc (from Rabe et al. (2004)) 45

Figure 10 - Portable device for estimating dynamic elastic properties of wood based on sonic resonance frequency (source: personal image) 46

Figure 11 - Schematic of NIR spectrometer readings 46

Figure 12 - Wood discs from the the progeny and clonal tests and the growth and wood traits under examination in this study (source: personal image) 54

Figure 13 - Differences of field conditions between clonal tests (source: personal image) 58

Figure 14 - Strategy of wood sampling and wood measurements of the progeny test 59

Figure 15 - Strategy of wood sampling and wood measurements of the clonal test and reference of codes relative to radial and longitudinal positions for NIR spectroscopic and genetic analysis 60

Figure 16 - Schema for four-point statistic bending test 64

Figure 17 - Schema for three-point statistic bending test 65

Figure 18 - Experimental dispositive for measuring the green volume of the samples (A) and the sample dimensions (B) (source: personal image) 65

Figure 19 - X-ray diffractometer device with CuK α radiation used for measuring XRD patterns (A), detail of the specimen holder (B) and the mini-circular machine used for cutting samples (C) (source: personal image) 66

Figure 20 - X-ray scattering patterns recorded in 2 mm tangential sections of *Eucalyptus* samples with low (a) and high (b) *T* parameter 67

Figure 21 - NIR spectrophotometer used for measuring diffuse reflectance of wood samples showing the sintered gold standard (A), cup module for measuring NIR spectra from grounded wood (B), window for NIR spectra scanning - 10 mm of diameter (C) and 2-mm radial section of wood (D) (source: personal image) 68

Figure 22 - Mean and standard deviation of circumference at breast height (C) and commercial height (H) for each site and considering all samples 75

Figure 23 - Radial strips showing curvature effect by dotted lines and classes by continuous lines 77

Figure 24 - Radial variation of MFA (A) and basic density (B) in 14-year-*Eucalyptus urophylla* wood for radial strips (N=14) 78

Figure 25 - Mean and standard deviation values of kiln-dried wood density and dynamic elastic modulus in kiln-dried scantlings for each site 80

Figure 26 - Mean and standard deviation values of longitudinal and flexural dynamic elastic modulus and 4- and 3-points bending test in small samples of *Eucalyptus* for each site 82

Figure 27 - Mean and standard deviation values of air-dried density of the specimens (ρsp) and of the basic density of the small wood samples (ρs) and radial and tangential shrinkage from oven-dried to green conditions for each 84

Figure 28 - Mean and standard deviation values of MFA in small wood samples (MFA_{YS}) and radial strips (MFA_{YRS}) of *Eucalyptus* wood for each site and for all samples 85

Figure 29 - Radial variation of MFA (estimated by Yamamoto's formula) for wood samples taken from radial strips of 6-year-old *Eucalyptus* clones 86

Figure 30 - Relationship between wood traits in *Eucalyptus* wood. SEE is the standard error of estimation 88

Figure 31 - NIR absorbance versus wavenumber plot for raw (untreated) NIR spectra from 9,000 to 4,000 cm^{-1} range. 91

Figure 32 - Absorbance versus wavenumber plot for first and second derivative of the NIR spectra 91

Figure 33 - NIR predicted versus measured values plot for Klason lignin (A), S/G ratio (B), basic density (C) and microfibril angle (D) of wood. The calibration set samples are represented by white circles and the validation set samples are represented by black circles 94

Figure 34 - NIR predicted versus measured values plot for air-dry density (A), basic density (B), MFA (C), dynamic elastic modulus (D), first resonance frequency (E) and loss tangent (F) based on NIR spectra for both training (open circles) and test sets (filled rhombs) 95

Figure 35 - PLS-regression coefficients for NIR-based model for estimating air-dry density (A), basic density (B), microfibril angle (C), dynamic elastic modulus (D), first resonance frequency (E) and loss tangent (F) 98

Figure 36 - Age trends of phenotypic, residual and additive genetic correlations of density with C, and MFA with C, KL and density 104

Figure 37 - Clone x site interaction for mean circumference at 1.3 meters (A) and commercial height (B) of the trees from Clonal test 106

Figure 38 - Clone x site interaction for wood density (A) and longitudinal elastic modulus (B) of the kiln-dried scantlings 109

Figure 39 - Spatial variation of wood basic density (kg m^{-3}) in *Eucalyptus urophylla* x *grandis* trees 110

Figure 40 - Spatial variation of modulus of elasticity (MPa) in *Eucalyptus urophylla* x *grandis* trees 111

Figure 41 - Spatial variation of microfibril angle (degrees) in *Eucalyptus urophylla* x *grandis* trees. 112

Figure 42 - Clone by site interaction for basic density of the inner heartwood (A) and of the outer sapwood (B) at 25% of height 115

Figure 43 - Clone by site interaction for longitudinal elastic modulus of the inner heartwood (A) and of the outer sapwood (B) at 25% of height 117

Figure 44 - Clone by site interaction for microfibril angle of the inner heartwood (A) and of the outer sapwood (B) at 25% of height 118

Figure 45 - Spatial variation of heritability estimates over basic density of wood, wood stiffness and microfibril angle within *Eucalyptus* trees 119

Figure 46 - Spatial variation of NIR spectral broad-sense heritability estimates at the base and at 25% of the tree height. The bands normally associated to cellulose, hemicelluloses and lignin are indicated by numbered narrows (these index are presented in Table 26, pg. 97) 123

Figure 47 - Spatial variation of NIR spectral broad-sense heritability estimates at 50, 75 and 100% of the tree height. The bands normally associated to cellulose, hemicelluloses and lignin are indicated by numbered narrows (these index are presented in Table 26, pg. 97) 124

Figure 48 - Mean and standard deviation values of air-dried density and dynamic elastic modulus in air-dried scantlings for each site. 137

Figure 49 - Correlation between the modulus of elasticity of the kiln- (E_L14) and air-dried (E_Lad) scantlings obtained in the flexural test for 411 scantlings of *Eucalyptus* showing the samples presenting problems after drying 138

Figure 50 - Correlation between the modulus of elasticity of the kiln- (E_L14) and air-dried (E_Lad) scantlings obtained in the flexural test for 395 scantlings of *Eucalyptus grandis* x *urophylla* wood with 45 mm x 60 mm cross section 139

Figure 51 - Linear regression plot between the dynamic flexural elastic modulus and the MOR obtained by tree and four points bending tests using complete sampling of *Eucalyptus* wood. SEE is the standard error of estimation 141

Figure 52 - Linear regression plot between the wood density and the MOR obtained by tree and four points bending tests using complete sampling of *Eucalyptus* wood. SEE is the standard error of estimation 141

Figure 53 - Linear regression plot between the MOR obtained by tree and four points bending tests. SEE is the standard error of estimation 142

Figure 54 - Spatial variation of heritability estimates over basic density of wood, wood stiffness and microfibril angle within *Eucalyptus* trees (model $y = \mu + G + E$) 144

Paper 1

Authors: Hein PRG, Brancheriau L, Lima JT, Gril J and Chaix G

Title: Resonance of structural timbers indicates the stiffness even of small specimens of *Eucalyptus* from plantations

Journal: Wood Science and Technology (*in press*)

Resonance of scantlings indicates the stiffness even of small specimens of *Eucalyptus* from plantations

Paulo Ricardo Gherardi HEIN (corresponding author)
CIRAD - PERSYST Department - Production and Processing of Tropical Woods
73 rue Jean-François Breton TA B-40/16
34398 Montpellier, Cedex 5, France
Tél: +33 4 67 61 44 51
Fax: +33 4 67 61 65 60
email: phein1980@gmail.com

José Tarcísio LIMA
Ciência e Tecnologia da Madeira - Departamento de Ciências Florestais
Universidade Federal de Lavras - campus universitário
Lavras, Minas Gerais, Brasil
CEP 37200-000
email: jtlima@dcf.ufla.br

Joseph GRIL
Laboratory of Mechanics and Civil Engineering, CNRS-University of
Montpellier 2, Place E. Bataillon, cc 048
34095 Montpellier Cedex 5, France
email: jgril@lmgc.univ-montp2.fr

Antônio Marcos ROSADO
Celulose Nipo-Brasileira S.A
Rodovia BR 381, Km 172
Belo Oriente, Minas Gerais, Brazil
CEP 35196-000
email: antonio.rosado@cenibra.com.br

Loïc BRANCHERIAU
CIRAD - PERSYST Department - Production and Processing of Tropical Woods
73 rue Jean-François Breton TA B-40/16
34398 Montpellier, Cedex 5, France
email: loic.brancheriau@cirad.fr

ABSTRACT: The aim of this study was to establish the relationship between the stiffness of scantlings, approaching structural size materials, and small specimens of 6-year-old *Eucalyptus urophylla* x *grandis* wood using a resonance technique. The correlation between the elastic modulus (E) of the scantlings in longitudinal vibration and small specimens in flexural vibration was r=75 when we compared the scantling values with the averaged values of the specimens per scantling. However, when the E of each single specimen was compared with its respective scantling, the coefficient of correlation decreased to r=0.64 in the longitudinal tests and to r=0.61 in the flexural tests. A roughly linear correlation (r=0.59) between specific modulus and loss tangent was obtained for the small specimens of *Eucalyptus*. In short, the resonance technique rapidly provided a large accurate data set of mechanical wood properties as required for high-throughput phenotyping in recent genetic studies.

Key-words*: acoustic, dynamic properties, mechanical traits, wood, lumber, Eucalyptus, hardwood*

1. INTRODUCTION

The main objective of *Eucalyptus* breeding programs for the pulp and paper industry is to produce varieties of trees with high levels of cellulose with the least possible amount of lignin. However, trees with these characteristics can be a major problem in the field, because of their fragility that makes them susceptible to breaking.

Natural vibration analysis is a simple and efficient way of characterizing the mechanical properties of many materials, including wood (Brancheriau and Baillères 2002). Using various species of wood, sample dimensions and growth conditions, several studies have shown a strong linear correlation between dynamic and static modulus of elasticity (Ross et al. 1991, Wang et al. 2001; Green et al. 2004; Biblis and Carino 1999; Biblis et al. 2004). For instance, Ilic (2001) obtained strong correlations between static test and longitudinal (r=0.95) or flexural (r=0.99) elastic modulus using short specimens (20 mm x 20 mm x 300 mm) of *Eucalyptus delegatensis* R. Baker. Using larger pieces, Brancheriau and Baillères (2002) reported good correlation between Young's modulus in four-point bending and the flexural vibration modulus of elasticity on 76 beams (60 mm x 155 mm x 3500 mm) of *Dicorynia guianensis* Amsy.

Dynamic tests based on the resonance frequency have been applied successfully in order to analyze among other elastic properties, the dynamic modulus of elasticity of small, clean specimens (or clearwood) at the laboratory scale (Haines et al. 1996; Ilic 2003; Brancheriau and Baillères 2003; Ohsaki et al. 2007), as well as of structural timber (Haines et al. 1996; Burdziak and Nkwera 2002; Liang and Fu 2007; Jiang et al. 2010) and logs (Ouis 1999; Wang et al. 2002; Grabianowski et al. 2006). To our knowledge, few studies have been conducted in order to establish the relationship between the mechanical properties obtained on large pieces of wood and on small specimens sampled from them. For instance, Haines et al. (1996) compared mean values of transverse resonance (13.3 GPa) obtained for wood beams measuring 1 x 5 x 30 mm with mean values from previous static tests (13.6 GPa) reporting differences less than 3%. Ilic (2003) compared dynamic elasticity of specimens measuring 20 mm x 20 mm x 300 mm with small wood

beams (120 x 20 x 1.6 mm) reporting high correlations (R^2=0.96-0.98) for groups of soft- and hardwood. Carter et al. (2006) reported good relationship (R^2=0.86) between dynamic modulus of elasticity in air-dried and green conditions using 42 boards of 24-year *Pinus*. They also showed strong correlation (R^2=0.94) between acoustic properties between logs and boards, however this study uses a small number of samples (6 logs). In effect, the relationship between the mechanical properties of small clear specimens and larger sized samples approaching structural size material is not still well established. Hence, the aim of this study was to establish the correlation between the stiffness of scantlings and small specimens of *Eucalyptus* wood. These findings would be useful in explaining the scale effect observed on mechanical behaviors of wood of different dimensions.

Here, we performed longitudinal and flexural dynamic tests on scantlings and on small specimens of clones of *Eucalyptus grandis* x *urophylla* hybrids using the BING (Beam Identification by Non-destructive Grading) system developed by CIRAD (http://www.xylo-metry.org). The procedure we used for preparing samples, the dimensions and the relationships we established in this study are factors that may help explain part of the mechanical behaviors of wood. We discussed the effect of these factors on over- or under estimating of wood quality on the basis of resonance frequency of large and small specimens. Complementarily, we investigated the effect of the radial position on the resonance frequency of these wood samples.

2. MATERIAL AND METHODS

2.1 Origin and preparation of wood samples

One hundred (100) logs of 6-year old *Eucalyptus grandis* x *urophylla* hybrids coming from a clonal test established in Brazil (19°17' S, 42°23' W, alt 230-500 m) were used in this study. The type of climate is Aw (Tropical savanna climate), according to the classification of Köppen (Peel et al. 2007), with mean annual rainfall of 1205 mm. The mean annual temperature is around 25 °C and the average annual humidity is 67.3%. The trees were planted in a randomized design and density of plantation was 1,667 trees/ha (3 m x 2 m spacing).

A total of 160 pieces of wood with nominal sizes of 45 mm x 60 mm x 2100 mm (hereafter referred to as 'scantlings') were taken from 100 central boards (Figure 1). As the scantlings were removed systematically at each 45 mm of the boards (60 mm in thick), naturally, some parts of the scantlings contained pith, knots and other features inherent to wood. Subsequently, a pile of scantlings was set up for air-drying under protected exterior conditions during 90 days. After air-drying process the scantlings presented defects such as small cracks, checks and splits in their ends and, therefore, were trimmed to variable dimensions, depending of the extension of their defects. The clean scantlings had, on average, 1.82 meters of length, varying from 1.65 m to 2.08 m (COV=13.7%) and the averaged width and thickness were, 60 mm and 43 mm, respectively, fluctuating slightly (COV=5.7% for width and COV=2.8% for thickness). Thus, all pieces were free of large fissures, biological affections, defects produced in the saw mill as severe reduction of width or thickness, but they presented knots and small cracks as well. Finally, the scantlings were

kiln-dried at 14% (nominal) under soft condition during two weeks. The wood samples here investigated contain only juvenile wood.

2.2 Dynamic tests on woods

The pieces of wood were submitted to flexural and longitudinal vibration tests. In flexural vibration, the first four modes of vibration were measured and used for estimating the dynamic transversal modulus of elasticity (E_F) of wood, which represents its stiffness under bending stress; the dynamic shear modulus (G) and the loss tangent (tg δ), also called internal damping. In longitudinal vibrations, the first vibration mode was measured and used for estimating the dynamic longitudinal modulus of elasticity (E_L) of wood, which represents its stiffness under compressive stress, and the tg δ. The theoretical models of motion and theirs solutions used to estimate such elastic properties were deeply detailed in Brancheriau and Baillères (2002). The mass and the dimensions of each wood sample were measured at the moment of the dynamic tests providing the density (ρ) of the wood samples.

This study falls into two sections: First, the masses of the kiln-dried scantlings were measured providing the weight density of the scantlings (ρsc). The scantlings were submitted to dynamic tests providing the information labeled as $E_L$sc, tg δsc, $E_F$sc and Gsc. In the second section, 160 scantlings were selected among the best ones (i.e. annual rings well oriented, free of large cracks, etc) and surfaced on the plane machine; beams were cut from them and trimmed to nominal cross-section of 25 mm x 25 mm using a circular saw machine.

Then, small specimens measuring 25 mm x 25 mm x 410 mm (knot and defects free) were cut from the beams, according to the standard D 143-94 (ASTM 1997). The mass and dimension were measured and the weight density (ρsp) of each specimen was calculated. The small specimens were submitted to vibration tests, which provided the data designed as $E_L$sp, tg δsp, $E_F$sp and Gsp. Before tests, the specimens were conditioned in a room set for 20 °C and 65% relative humidity to maintain the equilibrium moisture content of 14%. The error of measure was 0.1 g and 0.1 mm for mass and dimension, respectively, for the scantlings and 0.001 g and 0.001 mm for the small specimens. Figure 1 sums up the procedure of sample preparation and acoustic measurements.

2.3 Procedure of dynamic tests

The scantlings were placed on elastic supports so as to generate free vibrations. An exciting impulse was produced by lightly striking the scantlings with an instrumented hammer at the opposite side of the output transducer (acoustic microphone). The flexural vibration was induced by an edgewise impact and the longitudinal vibration by an impact along the end. The input and output signals were transmitted via a low-pass filter to an acquisition card on a computer and recorded as described in Brancheriau and Baillères (2003).

2.4 Equations of motion

The theoretical model used to describe the motion of a uniform prismatic beam that vibrates transversely, freely was proposed by Timoshenko (1921) as follow:

$$E_X I_{Gz} \frac{\partial^4 v}{\partial x^4} - \rho I_{Gz}\left(1 + \frac{E_X}{KG_{XY}}\right)\frac{\partial^4 v}{\partial x^2 \partial t^2} + \frac{\rho^2 I_{Gz}}{KG_{XY}}\frac{\partial^4 v}{\partial t^4} + \rho A \frac{\partial^2 v}{\partial t^2} = 0 \qquad \text{Eq. (1)}$$

where E_X is the Young's modulus; I_{GZ} is the moment of inertia; v is the transversal displacement; ρ is the density; G_{XY} is the shear modulus; K is a constant which depends of the geometry of the section (for rectangular section, K=5/6); x is the distance along the axis of the beam; A, cross-sectional area of the beam; t is the time. Using the Bordonné's (1989) solution for this differential equation, the shear effect is taken it account, but the support effects are ignored. The elastic (E_X) and shear modulus (G_{XY}) were calculated according to the follow equation, described in Brancheriau and Baillères (2002):

$$\frac{E_X}{\rho} - \frac{E_X}{KG_{XY}}\left[QF_2(m)4\pi^2 \frac{AL^4}{I_{Gz}}\frac{f_n^{\,2}}{P_n}\right] = 4\pi^2 \frac{AL^4}{I_{Gz}}\frac{f_n^{\,2}}{P_n}[1 + QF_1(m)] \qquad \text{Eq. (2)}$$

where f_i is the resonance frequency of the order i and P_n is the solution of Bernoulli (rank n). Parameters Q, F_1, F_2, m and θ are calculated as follows:

$$Q = \frac{I_{Gz}}{AL^2} \qquad \text{Eq. (3)}$$

$$F_1(m) = \theta^2(m) + 6\theta(m) \qquad \text{Eq. (4)}$$

$$F_2(m) = \theta^2(m) - 2\theta(m) \qquad \text{Eq. (5)}$$

$$\theta(m) = m\frac{\tan(m)\tanh(m)}{\tan(m) - \tanh(m)} \qquad \text{Eq. (6)}$$

$$m = \sqrt[4]{P_n} = (2n+1)\frac{\pi}{2},\ n \in N^* \qquad \text{Eq. (7)}$$

Parameters m, P_n, $F_1(m)$ and $F_2(m)$ are calculated on the basis of index n, and are used in practical applications to calculate the value of the modulus E_X and that of the shear modulus G_{XY}.

In longitudinal vibrations, the first vibration mode can be used in order to estimate its dynamic longitudinal modulus of elasticity (E_L), which represents its stiffness under compressive stress, by means the formula:

$$E_X = 4L^2 \rho f_1^{\,2} \qquad \text{Eq. (8)}$$

A detailed discussion about different theoretical models of motion, their approximate solutions and their respective hypotheses in longitudinal and flexural vibrations; and the effects of the elastic support required by BING system was provided in Brancheriau and Baillères (2002).

To extract the damping parameters from acoustic sounds, the concept of additive synthesis was applied (Brancheriau et al. 2006). Each temporal signal $s(t)$ was then considered as a sum of exponentially damped sinusoids as follow:

$$s(t) = \sum_{i=1}^{\infty} \beta_i \exp(-\alpha_i t) \sin(2\pi f_i t + \varphi_i) \qquad \text{Eq. (9)}$$

Where s is the radiated signal as a function of time t and φ_i is the phase shift. The parametric method of Steiglitz and McBride (1965) was used to simultaneously determine the first resonance frequency f_1, the amplitude β_1, and the temporal damping α_1 associated with f_1. Only the first frequency was considered because of its high energy. The internal friction (tg δ) was calculated associated with the complex modulus concept with respect to flexural or longitudinal vibrations (Aramaki et al. 2007) according to the equation given by Brancheriau et al. (2006):

$$tg\delta = \frac{\alpha_1}{\pi f_1} \qquad \text{Eq. (10)}$$

2.5 Parameter of dynamic tests

The analysis of the spectral signal, the selection of the peaks of the natural frequency of vibration of the wood samples and the estimates of the E_F, G, E_L and tg δ were performed using the software BING ® (CIRAD, Montpelier, France, version 9.1.3). The sampling frequencies of the signal were 78125 Hz and 39062 Hz for longitudinal and flexural vibration, respectively. The spectral acquisition was carried out by using 32768 points for each test. We used an analogical to numeric conversion with 12-bit resolution.

3. RESULTS

3.1 Dynamic properties and densities of the scantlings and specimens

Table 1 lists the descriptive statistics of the dynamic properties and densities of the 160 scantlings (sc) and of the 334 small specimens (sp) of *Eucalyptus* wood. The loss tangent values of the scantlings were calculated from longitudinal test while the tg δ of the specimens derived from flexural vibrations. As the software alerts us about imprecise estimations, we used only 143 values for tg $\delta_L$sc and 141 for tg $\delta_F$sp.

The variation ranges of wood properties for these young *Eucalyptus* (Table 1) are higher than those reported by Ilic (2001), who evaluated mature *E. delegatensis* R. Baker (E_L=18 GPa with COV=25.9% and G=1.32 GPa with COV=30.1%). The comparison of the variation range of these

young wood samples (Table 1) with other young softwoods reveals the high stiffness of the *Eucalyptus* clones. For instance, the elastic modulus of *Pinus radiate* wood clones (4 years) ranged from 2.6 to 6 GPa (Lindström et al. 2004) while this property varied from 6.5 to 20.7 GPa for these *Eucalyptus* clones. In comparison with mature wood of other important species, the mean mechanical properties of these young *Eucalyptus* samples (Table 1) are comparable to those reported by Green et al. (2004) for Teak (ρ=550 kg m^{-3}; E_L=10.7 GPa); by Ilic (2003) for Poplar (E_L= 13.3 GPa and ρ=448 kg m^{-3}) and by Keunecke et al. (2007) for Norway spruce (ρ=400 kg m^{-3}, E_L=13.8 GPa and G=617 MPa).

Figure 2 shows the correlation (r=0.64) obtained between the modulus of elasticity in longitudinal test of the scantlings ($E_L$sc) and the modulus of elasticity in flexural test of the small specimens ($E_F$sp) cut from them. The small specimens presented stiffness lower than the scantlings: the cloud of points is below the dotted line). The $E_L$sc x $E_F$sp plot (Figure 2) reveals that stiffness of small specimens strongly varied along the same scantling. Depending on external factors such as presence, or not, of knots and small cracks, the resonance frequency of wood can under or over-estimate its properties.

To facilitate the understanding, we classified the scantlings cut from the external region (near the bark) as "ext" and represent them by open circles and the scantlings cut from internal region (near the pith) were labeled as "int" and represented by full rhomb in Figures 2, 3 and 4. Figure 2 shows that the scantlings cut from the external portions (open circles) of the logs were stiffer than those sampled from the internal portions (full rhomb).

The number of specimens cut from each scantling was not the same. For instance, the scantling less stiff (labeled as "A") gave only one specimen while the stiffer scantlings (labeled as "B") gave two specimens (Figure 2). It is important to notice that specimens cut from the same scantling present variable properties, especially stiffness. Analyzing the stiffness of the scantling labeled as B_1 ($E_F$sc=21.7 GPa), its specimens presented lower, but closed values for modulus of elasticity (16.2 and 16.4 GPa) while for the scantling B_2 ($E_F$sc=23.5 GPa) its specimens presented lower and spread values of $E_F$sp (16.6 and 18.7 GPa).

3.2 Averaging mechanical properties of small specimens by scantling

In order to minimize the effect of the variability within scantlings, we used the averaged value of the small specimens to correlate them with their respective scantlings. Table 2 shows the coefficient of correlation between each single value of the small specimens with its correspondent scantling (below diagonal), and the correlations between the averaged value of small specimens per scantling with its correspondent scantling (above diagonal).

Figure 3 shows in detail the correlation between E_L of the scantlings and the averaged E_F of the small specimens cut from them. Again, due to the effect of the side of the scantlings where the specimens were removed (near the pith), the averaged stiffness of the specimens was lower than the stiffness of the scantlings that generated them. On average, the size scale effect can be

indicated by the linear coefficient (3.9 GPa) of the regression. We tried to fit these data using a polynomial model but the coefficient of determination was statistically similar to the linear model.

3.3 Loss tangent x specific modulus of specimens

Figure 4 shows the correlation between the loss tangent (tg δ) and the specific modulus (E') of the specimens of *Eucalyptus*. This plot present the loss tangent values and the specific modulus of the 141 specimens obtained from flexural test. The correlation between the specific modulus and loss tangent was roughly linear (r=0.59). The radial position of the samples did not show any particular trend.

4. DISCUSSION

Few studies have compared dynamic properties obtained on wood samples and small specimens obtained from them (Ilic 2003; Haines et al. 1996). Moreover the differences between sample dimensions were small and did not take into account the effect of defects (knots or small cracks). For example, Ilic (2003) compared specimens measuring 300 x 20 x 20 mm with smaller specimens measuring 120 x 20 x 1.6 mm. Here, we compared elastic properties of structural timbers measuring 63 mm x 43 mm of cross-section and from 645 mm to 2080 mm in length with elastic properties of small specimens measuring 410 mm x 25 mm x 25 mm in length.

4.1 Dynamic tests of wood

While flexural vibrations are influenced by the shear effect, the longitudinal vibrations can be affected by the Poisson effect when the length to thickness ratio of the beams is small (Rayleigh 1877). Early studies on dynamic tests of wood (Hearmon 1961, Ilic 2001) showed important differences between E_L and E_F; however, when Ilic (2001) applied the Timoshenko correction, the difference between E_L and E_F varied from 13% (for uncorrected E_F) to 1.1% (for corrected E_F). Table 1 show that average value of E_L was higher than E_F for the scantlings; although, there was no statistically significant difference between elastic modulus values. In this study, the differences between E_L and E_F did not come about from shear effects on flexural vibration because the model we used to estimate the E_F takes into account the shear effect. Here, we applied the solution proposed by Bordonné (1989) to the Timoshenko (1921) motion equation to the first four vibration modes of the wood beams. Moreover, the Poisson effect in longitudinal vibrations is negligible because the length to thickness ratio of the scantlings and small specimens was superior to 30 and 15, respectively. Additional factors affecting the flexural vibrations were reported by Murphy (2000).

The nominal dimension of each fresh cut scantling was 45 mm x 60 mm x 2100 mm, but after air- and kiln drying, the pieces of wood were trimmed to variable dimensions. Thus, we evaluated scantlings of different lengths. At the outset, we think that this experimental condition would be a

limitation of this study; however, the tightness of the correlations show that the system is suitable for characterizing wood of any dimensions, with good accuracy and repeatability.

4.2 Stiffness and density of wood

It is well know that values of the modulus of elasticity increased with increasing wood density (Kollmann and Coté 1968), especially in small specimens. This is also valid for relationships between density and vibrationally deduced elastic constants since a number of studies have demonstrated the linear correlation between static and dynamic tests (Siclair and Farshad 1987; Ilic 2001; Brancheriau and Baillères 2002). Thus, as expected, the density of the scantlings showed good correlation (r=0.79-0.84) with their elastic properties (Table 2). The E_L presented higher correlations with density than the E_F, both for the scantling and for the small specimens. The main raison for this trend is the lower uncertainty of measurement for longitudinal test. The higher correlations with density for E_L are in accordance to the findings of Ilic (2001), who tested small samples of *Eucalyptus delegatensis* R. Baker and found good correlations between air-dried density and longitudinal (r=0.83) and flexural (r=0.81) dynamic elastic modulus. Bektas et al. (2002) showed good relationships between compression strength and air-dry density, static bending strength and oven-dry density, and impact bending strength and oven-dry density; the coefficients of correlation (r) were 0.71, 0.75, and 0.73 for these data, respectively.

4.3 Scale effect on mechanical properties of wood

Jiang et al. (2010) states that compared with the small, clean specimen, a lower relationship among mechanical and/or physical properties could be obtained for the large pieces of wood, due to their defects. However, here it was shown that longitudinal elastic moduli of the scantlings ($E_L$sc) were useful for estimating the flexural elastic modulus of specimen ($E_F$sp). Our results show that vibration analysis of large pieces of wood can be used to estimate the stiffness of small specimens.

The plots presented in Figure 2 and 3 clearly show that the specimens present lower modulus of elasticity than the scantlings where they were sampled. The reason for this trend is explained by the procedure to cut specimens from scantlings. Our technician systematically surfaced the internal side (near the pith) of each scantling with the plane machine and then, he cut the beams from them. Hence, the specimens represent the less stiff portion of the scantlings and the cloud of points remains always below the dotted line. Thus, the resonance frequencies of scantlings can over- or under-estimate the stiffness of specimens, depending of the sampling procedure.

Our results showed that stiffness of wood varied strongly along the same scantling. This observation can be attributed to the existence of factors such as knots, grain slope, and shake that affects the mechanical properties of wood. If the purpose is to use these scantlings as structural timber, this variability can be a major problem.

4.4 Averaged elastic properties of specimens per scantling

The elastic properties of the small specimens were averaged into a single value per scantling (each scantling yielded 1, 2, 3 or 4 specimens). As expected, when the values of the properties of specimens were averaged into a single value of small specimens per scantling the correlations between properties of small and large wood samples were higher (correlations above the diagonal in Table 2). For instance, the correlations between the E_L of the scantlings and the correspondent averaged E_F of the specimens (R^2= 56.8; Figure 3) were better than the relationships presented in Figure 2 (R^2=40.4). Averaging the elastic properties of specimens, the variability within the beam, and the uncertainty of the measurement is minimized. From the last line of Table 2, we can draw some important considerations. First, the average modulus of elasticity of the specimens presents weak correlation with density of the scantlings (r=0.55) while a moderate correlation (r=0.79) was obtained for the density of the specimen. This means that the specimens with high-density are stiffer however, high-density scantlings will not necessarily provide stiffer wood. Second, longitudinal tests on scantlings gave modulus of elasticity adequately correlated with flexural test of small specimens (0.64). The flexural test on the scantlings also provides good correlations with E_F of specimens, but of lesser magnitude (0.61). Using the averaged values of elastic properties, the E_F of the specimens was satisfactorily correlated with the E of the scantlings (0.75) to both vibration modes. These results can be useful for initial classifications, screenings or preliminary selections. As reported by Burdzik and Nkwera (2002), this method proved to be fast, highly repeatable and does not require heavy equipment, making it the ideal method for on-site determining of wood stiffness at the sawmill.

An aspect not covered in this study was the effect of grain slope on transverse vibration modulus. It is well known that spiral grain reduces both strength and stiffness of wood (Skatter and Kucera, 1997) and that the stiffness differs in each of the orthogonal directions of wood (Kollmann and Coté 1968). As the small samples are cut carefully with orthogonal faces, the effect of the grain slope on wood stiffness may play a major role on the scantlings.

4.5 Viscoelastic properties of wood

Internal friction (loss tangent - tg δ - or damping coefficient) is the term used to denote the mechanism that causes energy dissipation when wood is strained (Green et al. 1994). Previous studies involving the loss tangent have demonstrated that there is a relationship between internal friction and specific modulus (E/ρ). For instance, Ono and Norimoto (1984) used a non-linear model to establish the correlation between specific modulus and internal friction on 30 kinds of broad-leaved woods, taking into account the effect of the wood porosity. Obataya et al. (2000) also found a non-linear relationship between E' and tg δ in *Picea sitchensis* Carr.. Most of studies regarding this issue were done for noble woods because of the use of wood for manufacturing musical instruments. According to Ono and Norimoto (1983; 1984), wood having high specific modulus and low loss tangent is suitable for soundboards, for instance. Previous studies have used

this criterion for evaluating the potential of alternative wooden species as substitute materials for violin bows, but some findings indicates that specific modulus and low loss tangent are not the main factors affecting the vibrational properties (Minato et al. 2010).

The correlation between loss tangent and specific modulus for *Eucalyptus* wood is poorly reported by the literature. Moreover, loss tangent is a wood characteristic hard to accurately measure. In *Eucalyptus* from plantations, the basic visco-elastic properties of wood are of interest since they plays a role when attempting to reduce the energy consumption of mechanical pulping in paper and pulp industry (Havimo 2009). In the present study we found a roughly linear correlation (r=0.59) between specific modulus (E/ρ) and loss tangent from flexural vibration for 141 small specimens (Figure 4). This E' x tg δ plot for *Eucalyptus grandis* x *urophylla* was quite similar to the non-linear correlations reported by Ono and Norimoto (1983, 1984, 1985) and Obataya et al. (2000). Figure 4 shows no tendency according to the radial position where the specimens were sampled. In contrast, Yano (1994) reported higher tg δ values for heartwood than for sapwood specimens of *Thuja plicata*. The trends observed by Yano (1994) can be attributed to the extractive presence, which is less evident in juvenile wood such as our 6-year *Eucalyptus* samples. Variations in moisture content also affect the damping properties (Green et al. 1994), although this factor is negligible in this study because the wood samples we used here had the same moisture content.

According to Ona and Norimoto (1984; 1985), the values of elastic modulus and loss tangent of wood are determined in large part by the microfibril angle in the S_2 layers of wood cell. According to these authors, specific modulus decreases and loss tangent increases with increasing average microfibril angle within cell walls.

5. CONCLUSIONS

The relationships between the mechanical properties obtained on large pieces of wood (scantlings measuring ~45 mm x ~60 mm of cross-section and length ranging from 645 mm to 2080 mm) and on small specimens (measuring 25 mm x 25 mm x 410 mm) were investigated. We found correlations from 0.68 to 0.75 between the E of scantlings and small specimens of *Eucalyptus* wood when we compared the E of the scantling with the averaged E of the specimens per scantling. When the E_F value of each single specimen was compared with its respective scantling, the coefficient of correlation decreased to 0.64 in the longitudinal tests and to 0.61 in the flexural tests. A roughly linear correlation (r=0.59) between specific modulus and loss tangent was obtained for the small specimens of *Eucalyptus*.

The findings demonstrate that resonance technique is able to characterize the mechanical properties of wood in a simple and rapid way and at low cost. The dynamic tests enabled us to rapidly estimate key mechanical properties (such as the Young, the shear modulus and the loss tangent) of the wood even in lumbers containing knots, small cracks and also slightly damaged areas. In short, the resonance technique rapidly provided a large accurate data set of mechanical wood properties as required for high-throughput phenotyping in recent genetic studies.

6. ACKNOWLEDGMENTS

The authors express their special thanks to the CENIBRA for providing vegetal material; to the Department of Wood Science and Technology of the Universidade Federal de Lavras (UFLA, Brazil) for supporting the experimental work. We thanks particularly to José Francisco de Sousa, Carlos Henrique da Silva, Heber Alvarenga, and Hernani Alves for their technical support. This project was funded by CENIBRA (Celulose Nipo-Brasileira), CNPq (Conselho Nacional de Desenvolvimento Científico e Tecnológico, Brazil) and CIRAD (UR39 and UR40). P.R.G. Hein was supported by CNPq (process no. 200970/2008-9).

7. CONFLICT OF INTEREST

We have no financial relationship with CENIBRA and CNPq, which sponsored this study. We declare that we have no conflict of interest.

8. REFERENCES

AMERICAN SOCIETY FOR TESTING AND MATERIALS-ASTM. Annual book of ASTM standards. Denvers: 1997. 679 p. D 143-94. Standard methods of testing small, clear specimens of timber. p. 23-53

Aramaki M, Baillères H, Brancheriau L, Kronland-Martinet R, Ystad S (2007) Sound quality assessment of wood for xylophone bars. J Acoust Soc Am 121 (4): 2407-2420

Biblis EJ, Carino HF (1999) Flexural properties of lumber from a 50-year-old loblolly pine plantation. Wood and Fiber Science 31(2): 200-203

Biblis EJ, Meldahl R, Pitt D (2004) Predicting flexural properties of dimension lumber from 40-year-old loblolly pine plantation stands. For Prod J 54:109-113

Bordonné PA (1989) Module Dynamique et Frottement Inte´rieur dans le Bois, Mesures sur Poutres Flottantes en Vibrations Naturelles. Institut National Polytechnique de Lorraine: 109

Brancheriau L, Baillères H (2003) Use of the partial least squares method with acoustic vibration spectra as a new grading technique for structural timber. Holzforschung 57(6):644-652

Brancheriau L, Baillères H, Détienne P, Gril J, Kronland-Martinet, R. (2006) Key signal and wood anatomy parameters related to the acoustic quality of wood for xylophone-type percussion instruments. J. Wood Sci 52(3), 270-274

Brancheriau L, Baillères H. (2002) Natural vibration analysis of clear wooden beams: a theoretical review. Wood Sci Technol 36:347-365

Bucur V (1995) Acoustics of wood. Boca Raton: CRC Press, 284 p

Burdzik WMG, Nkwera PD (2002) Transverse vibration tests for prediction of stiffness and strength properties of full size *Eucalyptus grandis*. For Prod J 52 (6):63-67

Carter P, Chauhan S, Walker J (2006) Sorting logs and lumber for stiffness using Director HM200. Wood Fiber Sci 38(1):49-54

Grabianowski M, Manley B, Walker JCF (2006) Acoustic measurements on standing trees, logs and green lumber. Wood Sci Technol 40:205-216

Green DW, Gorrnan TM, Evans JW, Murphy JF (2004) Improved grading system for structural logs for log homes. For Prod J 54(9):59-62

Green DW, Winandy JE, Kretschmann DE (1999) Mechanical properties of wood, Chapter 4. In: Wood Handbook – Wood as an Engineered Material, FPL-GTR-113, USDA Forest Service, Forest Products Laboratory, Madison WI, USA

Haines DW, Leban JM, Herbe C (1996) Determination of Young's modulus for spruce, fir and isotropic materials by the resonance flexure method with comparisons to static flexure and other dynamic methods. Wood Sci Technol 30(4):253-263

Havimo M (2009) A literature-based study on the loss tangent of wood in connection with mechanical pulping. Wood Sci Technol 43:627-642

Hearmon RFS (1961) An introduction to applied anisotropic elasticity. Oxford: Oxford University Press, 136 p.

Ilic J (2001) Relationship among the dynamic and static elastic properties of air-dry *Eucalyptus delegatensis* R. Baker. Holz Roh Werkst 59:169-175

Ilic J (2003) Dynamic MOE of 55 species using small wood beams. Holz Roh Werkst 61:167-172

Jiang J, Lu J, Ren H, Long C (2010) Predicting the flexural properties of Chinese fir (*Cunninghamia lanceolata*) plantation dimension lumber from growth ring width. J Wood Sci 56:15-18

Keunecke D, Sonderegger W, Pereteanu K, Lüthi T, Niemz P (2007) Determination of Young's and shear moduli of common yew and Norway spruce by means of ultrasonic waves. Wood Sci Technol 41:309-327

Kollmann FR, Coté WA (1968) Principles of Wood science and technology. Berlin: Springer-Verlag, 592 p.

Liang S-q, Fu F (2007) Comparative study on three dynamic modulus of elasticity and static modulus of elasticity for Lodgepole pine lumber. J For Res 18(4):309-312

Lindström H, Harris P, Sorensson CT, Evans R (2004) Stiffness and wood variation of 3-year old *Pinus radiata* clones. Wood Sci Technol 38: 579-597

Minato K, Konaka Y, Bremaud I, Suzuki S, Obataya E (2010) Extractives of muirapiranga (*Brosimun* sp.) and its effects on the vibrational properties of wood. J Wood Sci (2010) 56:41-46

Murphy JF (2000) Commentary on factors affecting transverse vibration using an idealized theoretical equation. Res. Note FPL-RN-0276. Madison, WI: U.S. Department of Agriculture, Forest Service, Forest Products Laboratory. 4 p

Obataya E, Ono T, Norimoto M (2000) Vibrational properties of wood along the grain. J Mat Sci 35 2993-3001

Ohsaki H, Kubojima Y, Tonosaki M, Ohta M (2007) Vibrational properties of wetwood of todomatsu (*Abies sachalinensis*) at high temperature. J Wood Sci 53:134-138

Ono T, Norimoto M (1983) Study on Young's Modulus and Internal Friction of Wood in Relation to the Evaluation of Wood for Musical Instruments. Jpn J Appl Phys 22:611-614

Ono T, Norimoto M (1984) On physical criteria for the selection of wood for soundboards of Musical instruments. Rheol acta 23(6):652-656

457 Ono T, Norimoto M (1985) Anisotropy of dynamic Young's modulus and internal friction in
458 wood. Jpn J Appl Phys 24(8):960-964
459 Ouis D (1999) Vibrational and acoustical experiments on logs of spruce. Wood Sci Technol 33:
460 151-184
461 Peel MC, Finlayson BL, McMahon TA (2007) Updated world map of the Köppen-Geiger climate
462 classification. Hydrol. Earth Syst Sci 11:1633-1644
463 Rayleigh JWS (1877) The theory of the sound (Edition of 1945). New York. pp. 243-305.
464 Ross RJ, Geske EA, Larson GL, Murphy JF (1991) Transverse vibration nondestructive testing
465 using a personal computer, Research Paper, FPL-RP-502, Forest Products Laboratory, Forest
466 Service, US Department of Agriculture
467 Skatter S, Kucera B (1997) Spiral grain - An adaptation of trees to withstand stem breakage caused
468 by wind-induced torsion. Holz als- und Werkstoff 55: 207-213
469 Steiglitz K, McBride LE (1965) A technique for the identification of linear systems. IEEE Trans
470 Automat Contr 10:461-464
471 Timoshenko S (1921) On the Correction for Shear of the Differential Equation for Transverse
472 Vibrations of Prismatic Bars. Philosophical Magazine and Journal of Science XLI - Sixth Series:
473 744-746
474 Wang S-Y, Chen J-H, Tsai M-J, Lin C-J, Yang T-H (2008) Grading of softwood lumber using
475 non-destructive techniques. J Mat Proc Tech 208:149-158
476 Wang X, Ross RJ, Mattson JA, Erickson JR, Forsman JW, Geske EA, Wehr MA (2001) Several
477 nondestructive evaluation techniques for assessing stiffness and MOE of small-diameter logs.
478 Madison: U.S.D.A Department of Agriculture, Forest Products Laboratory, 2001. (General
479 Technical Report FPL-RP-600)
480 Wang X, Ross RJ, Mattson JA, Erickson JR, Forsman JW, Geskse EA, Wehr MA (2002)
481 Nondestructive evaluation techniques for assessing modulus of elasticity and stiffness of small-
482 diameter logs. For Prod J 52:79-85
483 Yano H (1994) The changes in acoustic properties of Western Red Cedar due to Methanol
484 Extraction. Holzforschung 48:491-495
485

9. LIST OF TABLE

Table 1 - Descriptive statistics of dynamic properties of scantlings and of the small specimens of *Eucalyptus grandis* x *urophylla*, including weight density (ρ, kg m^{-3}), resonant frequency (*f*, Hz), elastic modulus (E, MPa), specific modulus (E', MPa m^3 kg^{-1}), loss tangent (tg δ, 10^{-3}) and shear modulus (G, MPa) estimated by longitudinal ($_L$) and flexural ($_F$) vibration tests.

Step 1	Scantlings kiln-dried at 14%								
	ρsc	$f_L$sc	$E_L$sc	E'_Lsc	tg $\delta_L$sc	$f_F$sc	$E_F$sc	E'_Fsc	$G_F$sc
Average	556	1,672	13,673	24.5	7.49	98.76	13,982	25.1	719.30
Sd	69.2	384	2,698	3.20	1.28	42.81	2,654	3.10	193.1
Min	384	1,032	7,944	18.2	4.45	43.1	8,195	14.8	123.0
Max	776	3,414	23,136	44.3	11.2	434.2	21,609	32.3	1,388
COV	12.5	23.0	19.7	13.1	17.1	43.3	19.1	12.7	26.85
N	160	160	160	160	143	160	160	160	154
Step 2	Small specimens sampled from scantlings (moisture content=14%)								
	ρsp	$f_L$sp	$E_L$sp	E'_Lsp	tg $\delta_F$sp	$F_F$sp	$E_F$sp	E'_Fsp	$G_F$sp
Average	518	6,174	13,391	25.66	7.33	721.6	12,495	24.02	693.6
Sd	59.05	395	2,540	3.52	1.01	42.52	2,356	3.082	168.5
Min	362.4	4,918	6,522	16.27	5.71	567.4	5,930	14.05	344
Max	708.3	6,945	20,785	32.43	10.5	805.9	18,732	30.61	1,499
COV	11.4	6.41	18.97	12.53	13.8	5.89	18.80	12.81	24.3
N	334	334	334	334	141	334	334	334	334

493 Table 2 - Correlations among physical and elastic properties of the 160 scantlings and the small
494 specimens. Below the diagonal are the correlations of each single small specimen with its
495 correspondent scantling while above the diagonal are the correlations taking into account the
496 averaged values of small specimens by scantling. All correlations were statistically significant at
497 $P<0.001$.

	ρsc	ρsp	$E_L$sc	$E_F$sc	$E_L$sp	E_F sp
ρsc		0.732	0.824	0.791	0.563	0.578
ρsp	0.720		0.598	0.534	0.845	0.822
$E_L$sc	0.824	0.574		0.920	0.692	0.754
$E_F$sc	0.791	0.518	0.920		0.685	0.733
$E_L$sp	0.538	0.812	0.628	0.619		0.978
$E_F$sp	0.552	0.795	0.636	0.615	0.972	

498
499

10. LIST OF FIGURES

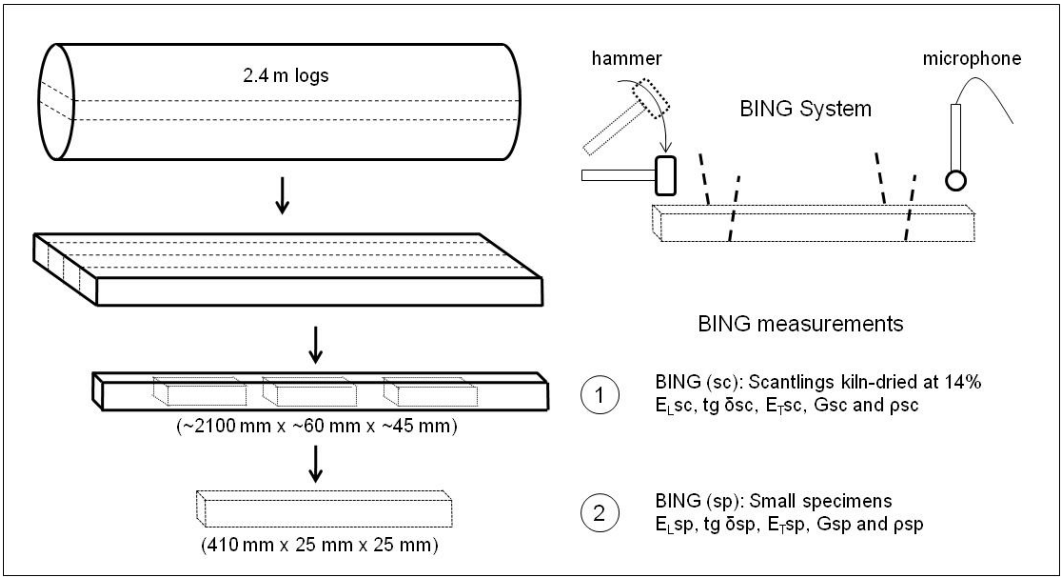

Figure 1 - Procedure of sample preparation and acoustic measurements.

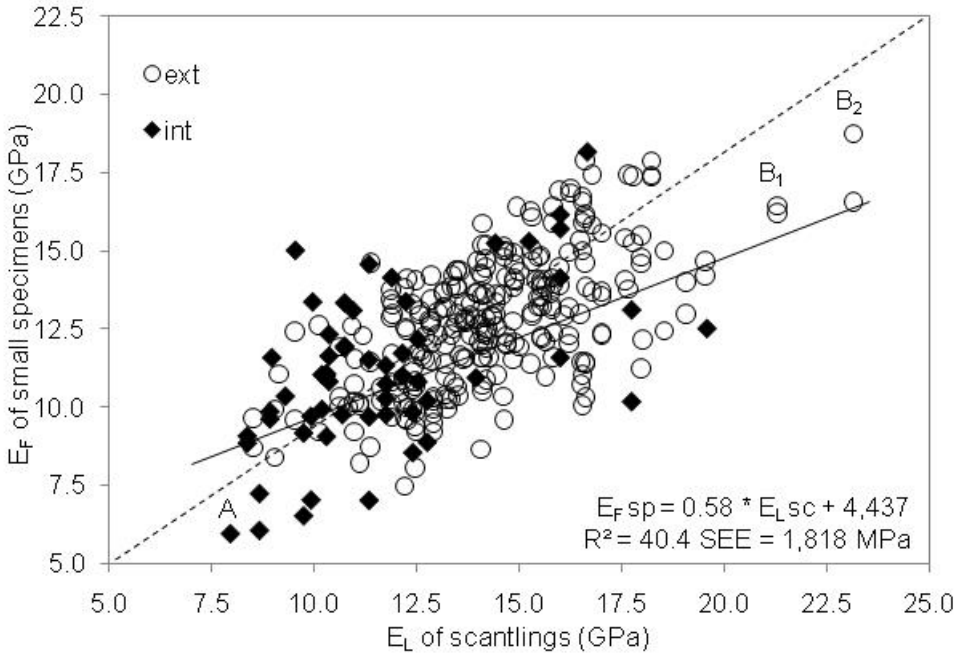

Figure 2 - Correlation between the modulus of elasticity in longitudinal test of scantlings ($E_L$sc) and the modulus of elasticity in flexural test of small specimens ($E_F$sp) of *Eucalyptus grandis* x *urophylla*. The scantlings sampled from extern or intern regions of the logs are represented by open circles and full rhomb, respectively.

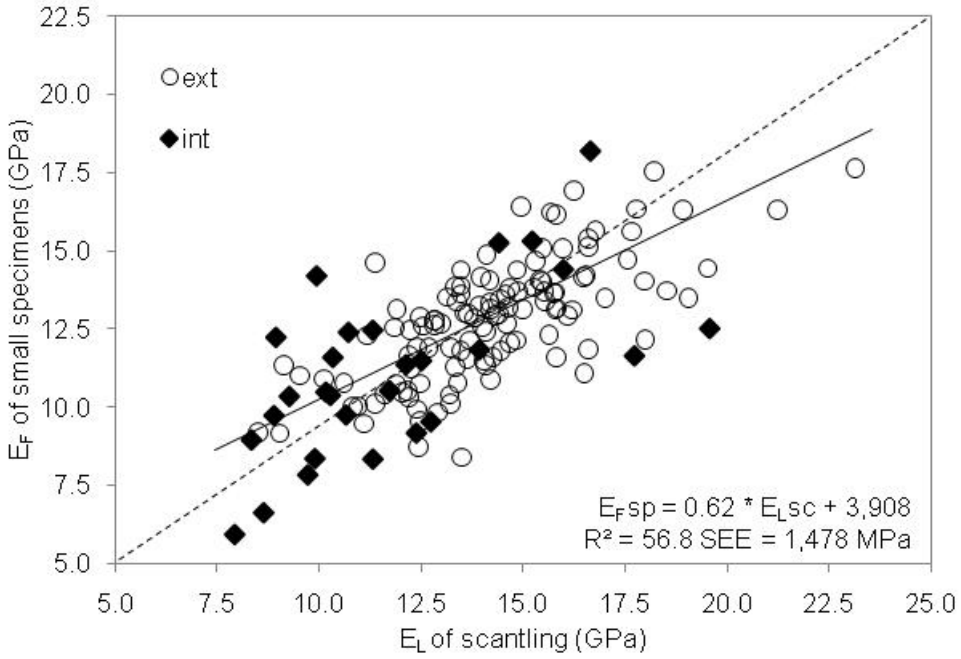

511

512 Figure 3 - Correlation between the modulus of elasticity in longitudinal test of scantlings ($E_L$sc)
513 and the averaged modulus of elasticity by beam in flexural test of small specimens ($E_F$sp) of
514 *Eucalyptus grandis* x *urophylla*. The scantlings sampled from extern or intern regions of the logs
515 are represented by open circles and full rhomb, respectively.

516

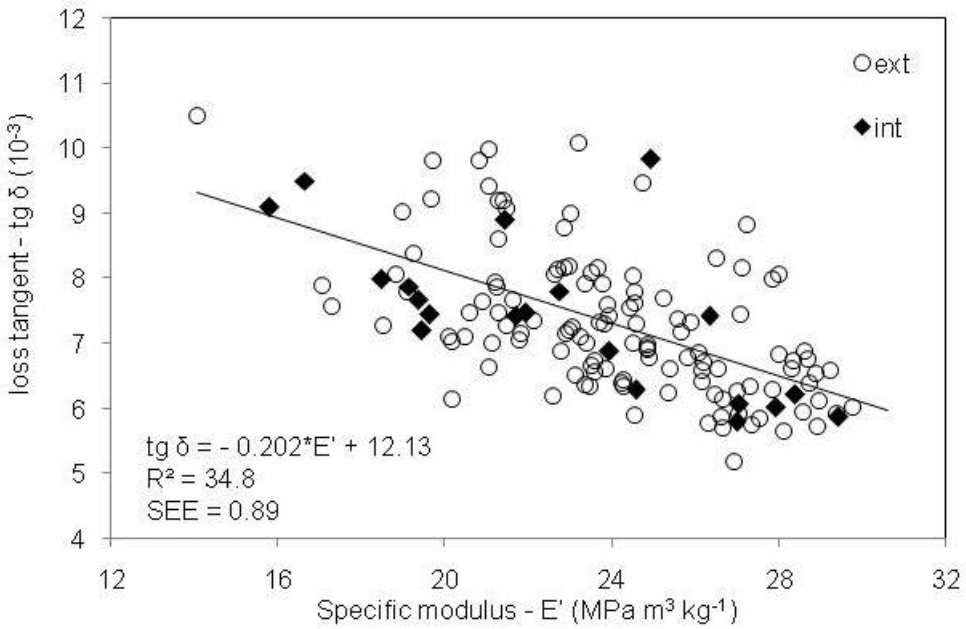

517

518 Figure 4 - Correlation between the loss tangent and the specific modulus of the small specimens of
519 *Eucalyptus grandis* x *urophylla*. The specimens from external or internal regions of the boards are
520 represented by open circles and full rhomb, respectively.

Paper 2

Authors: Hein PRG

Title: Relationships between microfibril angle and wood traits in Eucalyptus from fast-growing plantations

Journal: Holzforschung (*submitted*)

DE GRUYTER Holzforschung - International Journal of the Biology, Chemistry, Physics and Technology of Wood

Relationships between microfibril angle and wood traits in Eucalyptus from fast-growing plantations

Journal:	*Holzforschung - International Journal of the Biology, Chemistry, Physics and Technology of Wood*
Manuscript ID:	Draft
Manuscript Type:	Original Article
Date Submitted by the Author:	n/a
Complete List of Authors:	Hein, Paulo Ricardo; CIRAD, PERSYST
Section/Category:	Technology
Keywords:	Eucalyptus urophylla S.T. Blake , microfibril angle, resonance, X-ray diffraction, wood phenotyping, stiffness, strength, shrinkage, juvenile wood

Relationships between microfibril angle and wood traits in *Eucalyptus* from fast-growing plantations

Running head: Correlations between MFA and wood traits in *Eucalyptus*

Paulo Ricardo Gherardi HEIN*
CIRAD - PERSYST Department - Production and Processing of Tropical Woods
73 rue Jean-François Breton TA B-40/16
34398 Montpellier, Cedex 5, France
Tél: +33 4 67 61 44 51
Fax: +33 4 67 61 65 60
email: phein1980@gmail.com

ABSTRACT

The cellulose microfibril angle (MFA) in the cell wall is known to play major effects on wood stiffness and shrinkage; however, its influence on juvenile wood traits is not fully understood. The aim of this study was to evaluate the relationships among MFA, density (ρ), wood stiffness (E) and strength (MOR), modulus of shear and linear shrinkage in 6-year-old *Eucalyptus grandis* × *urophylla*. MFA was negatively correlated to E (r=-61), MOR (r=-0.47), and radial (r=-0.24) and tangential (r=-0.33) shrinkage. The linear variation on elastic modulus (E) was better explained by the parameter ρ/MFA (r=0.82) than the specific modulus (E/ρ) was explained by MFA (r=-0.65), despite these relationships involve the same variables. Multiple regression analyses showed that the MFA variation accounted for only 37% of the variation in E while the ρ variation alone accounted for 68 percent. Acting together, ρ and MFA accounted for 78 percent of the variation in E. Wood density variation accounted for 46%, and MFA for 22% of the variation in MOR. MFA and ρ combined accounted for 51% of the variation in MOR. In short, MFA played a secondary role on the mechanical traits of 6-year-*Eucalyptus* wood while the density was the prime determinant of wood stiffness and strength.

Keywords: *Eucalyptus urophylla* S.T. Blake / microfibril angle / resonance / x-ray diffraction / wood phenotyping

INTRODUCTION

The orientation of cellulose microfibril (MFA) in the cell wall along the fibre axis is known to play major effects on wood stiffness (Cave 1968) and drying shrinkage (Meylan 1967); and is of key importance for wood quality (Donaldson 2008). In general, wood in which the MFA is large has a low modulus of elasticity (E) and is therefore suitable only for low-grade use, reducing its value as a raw material and its economic value (Walker and Butterfield 1995). Trees with these characteristics can be a major problem in the field, because of their lower stiffness that makes them susceptible to breaking, especially in regions with prevailing windstorms. This concern was not too serious in the past when the forest companies allowed the trees to reach their maturity before harvesting them (Barnett and Bonham 2004).

Eucalyptus is one of the most widely cultivated hardwood genera in tropical and subtropical regions of the world. *Eucalyptus* plantation covers about 19.5 million hectares (Iglesias-Trabado and Wilstermann 2008) of which 4.5 millions are in Brazil (ABRAF 2010). *Eucalyptus grandis* × *urophylla* is an important hybrid for plantation forestry, especially in Brazil, where the plantations were targeted for pulp and paper and also for bio-energy purposes (iron production) and managed on short rotation (~6 years) to maximize the production of raw material (Raymond 2002). Besides increasing volume production and kraft pulp or calorific value yield, breeders and growers should be alert to issues of trees survival. Trees may be stiff enough to support the bending movements in response to wind without breaking and maintaining its erect habit. Hence, MFA and its relationships with wood mechanical traits of trees from fast-growing plantation can be a critical subject.

Few studies have addressed to this issue in hardwoods, so there is a need to extend the range of species that have been investigated (Donaldson 2008). Specifically in the genus *Eucalyptus*, the effects of microfibril angle on wood properties other than mechanical ones are rarely reported in the literature (Lima et al. 2004). Evans and Ilic (2001) and Yang and Evans (2003) have investigated the relationship between MFA, density and stiffness (E) in *Eucalyptus* wood. They demonstrated that MFA was the prime determinant of both the modulus of elasticity and the specific modulus (E/ρ). If their conclusions can be generalized, MFA measurements should make possible the evaluation of the wood quality.

The primary aim of this study was to generate a better understanding about the relationship of the microfibril angle with wood traits. Here, the relationships between microfibril angle with density, wood stiffness and strength, modulus of shear and shrinkage in 6-year-old *Eucalyptus* wood were examined. The influence of MFA and /or density on wood stiffness and strength was investigated.

MATERIAL AND METHODS

Material origin and wood sample preparation

Eucalyptus grandis × *E. urophylla* hybrids (6-year-old) from clonal tests established for pulpwood production in Brazil (19°17’ S, 42°23’ W, and alt 230-500 m) were evaluated. The details of wood sampling are given in Hein et al. (2010). The trees had mean circumference at breast height of 62 centimeters and mean height of 23 meters at seventy-two months.

Two hundred-thirty (230) clearwood test specimens measuring 25 mm (R) × 25 mm (T) × 410 mm (L) were cut from central boards and submitted to dynamic and static tests for obtaining dynamic modulus of elasticity (E) and modulus of rupture (MOR), respectively. Then, a small wood sample (25 mm × 25 mm × 25 mm) was removed from the intact wood for basic density and shrinkage measurements. Finally, a 2 mm radial section was cut from the small wood sample for X-ray diffraction analysis and MFA estimation (Figure 1). Prior to the dynamic and static tests and MFA measurements, the specimens were conditioned in a room set for 20°C and 50% relative humidity to maintain the equilibrium moisture content of 10%.

Dynamic tests on specimens

The dynamic tests used to evaluate the elastic properties of these wood samples were previously described in Hein et al. (2010) and were based on sonic resonance (Brancheriau and Baillères 2002; 2003). In flexural vibration, the first four modes of vibration were recorded for estimating the dynamic flexural modulus of elasticity (E_F) of wood, which represents its stiffness under bending stress and the dynamic shear modulus (G). In longitudinal vibrations, the first vibration mode was measured and used for estimating the dynamic longitudinal modulus of elasticity (E_L) of wood, which represents its stiffness under compressive stress. The specific modulus (E/ρ) was calculated as the ratio between E and basic density of wood (ρ). The analysis of the spectral signal, the selection of the natural frequencies of vibration and the estimates of the E and G were performed using the BING ® software (CIRAD, Montpellier, France, version 9.1.3) according to the parameters proposed in Brancheriau et al. (2010). The maximum relative errors for dynamic E obtained by means of this system are lower than 5%.

Static test

Modulus of rupture (MOR) was obtained using an universal testing machine (Adamel Lhomargy, model DY 36) by means a 4-point bending test. Following the procedure B 51-008 of the French standard (NF 1987), the span between lower supports was 320 mm; the distance between two loading points was 160 mm (1 free and 1 fixed); the diameter of roller bearings was 60 mm; and the test was conducted at a rate of 0.08 mm/s. The proportional limit, ultimate load, and deflection were obtained from load-deflection curves; and the MOR was calculated as follows:

$$MOR = \frac{3 \times F \times (L - a)}{2 \times b \times d^2}$$

where F is the load (force) at the fracture point, L is the length of the support span, a is the distance between the 2 loading points, b is the width and d is the thickness of the wood specimen.

Wood density and shrinkage measurement

The basic density and the shrinkage of the wood samples were measured simultaneously according to the procedures ASTM D2395 (ASTM 2002). The green volume of a piece of wood was determined by water displacement according to the principle of Archimedes. The samples were first soaked in water to ensure that water is not taken up during the immersion process. After determining the green volume, a digital instrument was used for measure precisely the sample dimensions. Subsequently, the samples were oven-dried at 103°C and their dry weight and dimensions were measured again and the basic density and radial and tangential shrinkage of wood were calculated.

Microfibril angle measurement

The 2 mm radial sections were used for microfibril angle measurements. All X-ray diffraction data were collected on a diffractometer (Gemini-S, Agilent Technologies, Yarnton, UK) with CuK α radiation. Images were integrated between 2θ = 21.5 and 23.5 along the whole 360° azimuth interval to plot the intensity diagram of the (200) plane. An automatic procedure allowed the detection of the 200 peaks and their inflexion points. The *T* parameter, as defined by Cave (1966) as the measure of the width of the (200) diffraction arc. Thus, the half distance between intersections of tangents at inflexion points of the 200 peaks with the baseline was measured and the results are given as the mean of values obtained for the two 200 peaks.

Yamamoto's formula (1993) was applied in order to estimate the MFA based on their X-ray diffraction pattern. The formulas give an estimation of the mean MFA of woods based on their *T* value and is given by:

$$MFA = 1.575\times10^{-3}\times T^{3} - 1.431\times10^{-1}\times T^{2} + 4.693\times T - 36.19$$ (Yamamoto et al. 1993)

A single X-ray diffraction profile was recorded on each sample. The estimated error of the repeatability of the *T* parameter measurements was 3%, on average, for *T* ranging from 14° to 29° which correspond to ±0.6 degrees.

Statistic analysis

The descriptive statistics, bivariate correlations and multiple regressions were performed using SPSS statistics software (SPSS Inc., version 17.0, Chicago, IL).

RESULTS AND DISCUSSION

Table 1 presents the statistical summary of *Eucalyptus* wood traits including wood basic density (ρ, kg m^{-3}), dynamic elastic modulus (E, MPa), specific modulus (E', E/ρ), modulus of shear (G, MPa), radial (δrd, %) and tangential shrinkage (δtg, %), microfibril angle (MFA, degrees), ρ/MFA parameter and modulus of rupture (MOR, MPa) of clear specimens.

There are numerous statements that density is the most important characteristic in determining the properties of wood (Walker and Butterfield 1995) since it is related to many mechanical traits including modulus of elasticity and rupture. Specific modulus is a wood trait consisting of the elastic modulus per wood density (Kollmann and Cote 1986) and is an interesting property because represents two important traits at once. The utility of specific modulus is to find varieties of woods which will produce structures with minimum weight. Here, the variation range of wood density and specific modulus (CV of ~13%) were lower than those of elastic modulus, MFA and MOR (CV of ~22%).

The mean value of E_L (13.4 GPa) was significantly ($p<0.001$) higher than E_F (12.5 GPa). It is known that the flexural vibrations are influenced by the shear effect (Rayleigh 1877); however the differences between E_L and E_F did not come from shear effects on flexural vibration because the model we used to estimate the E_F takes it into account. As a consequence, the specific modulus means (E'_L and E'_F) were also significantly different. E_L and E_F values were highly correlated (r=0.97, not shown) as well as the corresponding specific moduli.

Here, wood samples swells 7.8% (tangentially) and 4.8% (radially) from oven-dried to above fiber saturation point condition, confirming that wood shrinks (swells) most in

the direction of the annual growth rings (tangentially) and about half as much across the rings (radially) (Glass and Zelinka 2010).

Considering the age of the trees of this study, the range of variation allows the examination of the relationships among wood traits. Variability within trees can have a negative impact for industrial applications while the variability between trees are crucial for *Eucalyptus* breeding programs where the tree breeders are interested in selecting progenies or clones presenting contrasting phenotype.

Correlations among wood traits

Linear correlations among density wood stiffness and strength, modulus of shear, shrinkage, MFA and ρ/MFA are presented in Table 2. The correlations of longitudinal and flexural elastic modulus or specific modulus with wood traits were closed, thus only the longitudinal ones were presented for simplifying and shortening the discussion.

As expected, basic density was found to be well correlated with wood stiffness (r=0.82) and strength (r=0.68) and high relationships of modulus of elasticity with modulus of rupture (r=0.81) were found confirming the findings in *Eucalyptus globulus*, *E. nitens* and *E. regnans* wood by Yang and Evans (2003). Contradicting these results, Crown et al. 1999 and Ivkavi et al. (2009) found higher correlation of wood density with MOR than with MOE in *Pinus* wood samples. Early studies on *Eucalyptus* wood have reported strong correlations between these traits. For instance, Evans and Ilic (2001) found higher relationship between density and modulus of elasticity (R^2=0.70) in *Eucalyptus delegatensis* while Yang and Evans (2003) reported strong correlations between wood density and modulus of rupture (R^2=0.80) in wood samples of *Eucalyptus*.

Here, MFA was negatively correlated to E (r=-61) and MOR (r=-0.47) in *Eucalyptus* samples (Table 2). These trends seem to systematically occur in *Eucalyptus* woods (Evans et al. 1996; Evans and Ilic 2001; Yang and Evans 2003) as well in other genera. For instance, Crown et al. (1999) and Ivkavi et al. (2009) reported higher correlation of MFA with E than with MOR in *Pinus* and Treacy et al. (2000) also found a linear relationship of MFA with E and MOR in *Picea* wood samples.

According to Donaldson (2008) MFA shows a variable relationship with wood density. Basic density shows a significant negative relationship with MFA (r=-0.40) and positive relationship with shrinkage (Table 2). Evans et al. (2000) reported clear non-linear correlation between MFA and density in *Eucalyptus nitens* using subsets of the same wood section.

Figure 2 shows the relationships of MFA with specific modulus (A) and tangential shrinkage (B), and the correlations of the parameter ρ/MFA with modulus of elasticity (C) and modulus of rupture (D) in *Eucalyptus* wood.

The specific modulus decreased as microfibril angle increased in wood from fast-growing plantations (Figure 2 a) confirming previous studies on mature woods (Evans and Ilic 2001; Yang and Evans 2003; Donaldson 2008). However, MFA variation accounted for only 44 percent of the variation in specific modulus. If the sample presenting the higher MFA (24.3°) is removed, the statistics do not change notably (the R^2 decreases from 0.44 to 0.42) and the trend is maintained.

After the previous studies presented by Evans and Ilic (2001) and Yang and Evans (2003), the parameter ρ/MFA has been used for explaining the stiffness in a range of wood. This parameter (ρ/MFA) is able to predict the modulus of stiffness better than

MFA explains variation in specific modulus of wood of a range of genera. For instance, McLean et al. (2010) recently demonstrated that 76% of the variation in E was explained by the factor ρ/MFA in wood samples of *Picea*. Despite these relationships (Figure 2 A and C) involve the same variables (E, ρ and MFA), many studies have systematically reported equivalent findings (Evans and Ilic 2001; Yang and Evans 2003; McLean et al 2010). In this study, the arisen hypothesis is that the coefficient of variation of MFA (21.2), E (21.2) and ρ (12.5) played a critical role to explain this trend. In the correlation concerning the parameter ρ/MFA, the numerator represents a quantity varying 12.5 percent while the denominator varies twice as. On the other hand, the correlation concerning specific modulus (E/ρ), the CV of the denominator is 2 times greater than the numerator's CV. There may be also a scale effect since the E values were calculated from entire specimens whereas the ρ and MFA represented only a small portion of them.

The linear variation on elastic modulus (E) was explained by the parameter ρ/MFA (r=0.82, Table 2) better than specific modulus (E') was explained by MFA (r=-0.65, Table 2). Figure 2 A and B shows the plots concerning E, ρ and MFA. The potential model (Figure 2 A) yielded a coefficient of determination of 0.44 and the linear one gave a R^2 of 0.42 (r=-65, Table 2). Figure 2 C shows that E and the parameter ρ/MFA are also better fitted by non-linear model. This study indicates that cellulose microfibril inclination explains in low magnitude the specific modulus of juvenile *Eucalyptus* wood (Figure 2 A).

MFA x shrinkage

Microfibril orientation within cell walls influences the anisotropic shrinkage during drying (Kollmann and Cote 1986). When the MFA is small, most shrinkage takes place transversely while as the MFA increases, the longitudinal component of the shrinkage increases in a highly non-linear manner. Such phenomenon is responsible for some degrade on drying; especially crook (Walker and Butterfield 1995).

Because the range of variation in MFA of *Eucalyptus* wood often is narrowed, few studies have been investigated the influence of microfibril orientation on anisotropic shrinkage. Here, MFA was significantly correlated to radial (r=-0.24) and tangential (r=-0.33) shrinkage (Table 2) but in low magnitude. The MFA x shrinkage plot (Figure 2 B) shows no clear trend. Since the variation ranges of MFA are greater in softwoods, these correlations were lower than those presented by Meylan (1968) for *Pinus* and Yamamoto et al. (2001) for *Sugi* wood samples.

Changes in moisture content affect other structural characteristics. For instance, Washusen and Evans (2001) examined the correlations between tangential shrinkage and cellulose crystallite width in 11-year-old *Eucalyptus globulus* showing that cellulose crystallite width was closely associated with tangential shrinkage. According to their results, shrinkage increases as crystallite width increased. Wu et al. (2006) explored the relationships of the main anatomical features with shrinkage in *Eucalyptus* wood demonstrating that the main factors affecting shrinkage were cell wall proportion, microfibril angle, and cell wall thickness.

Influence of MFA and/or density on wood stiffness and strength

The influence of MFA and/or density on stiffness and strength of these wood samples were examined. Multiple regression analyses were performed to search for the optimal

combination of component wood variables to predict wood stiffness and strength. Table 3 presents regression models for predicting E and MOR from MFA, density, ρ/MFA and MFA and density together. These findings are particularly useful for understanding the relationships between MFA and stiffness, and strength with and without considering wood density.

Theoretically, MFA has a predominant effect on wood stiffness (Cave 1966) and numerous studies have supported this argument using experimental data (Donaldson 2008; Walker and Butterfield 1995; Downes et al. 2002). In *Eucalyptus*, Evans and Ilic (2001) reported that density variation alone accounted for 70% of the variation in E in *E. delegatensis* samples, while MFA alone accounted for 86%. Thus, the influence of MFA on wood stiffness was significantly greater than that of density for their samples. Yang and Evans (2003) found similar trend reporting that MFA alone accounted for 87% of the variation in modulus of elasticity.

Here, a contrary trend was obtained. Regression analysis showed that wood density was the prime determinant of both modulus of elasticity and modulus of rupture. The MFA variation accounted for only 37 percent of the variation in E while the basic density variation alone accounted for 68 percent of variation in modulus of elasticity (Table 3). Acting together, basic density and MFA accounted for 78 percent of the variation in modulus of elasticity. For modulus of rupture, basic density variation accounted for 46%, and MFA for 22% of the variation in wood strength. Basic density and MFA combined accounted for 51% of the variation in modulus of rupture.

The parameter ρ/MFA was correlated with both modulus of elasticity (R^2=0.70) and modulus of rupture (R^2=0.45) using power models (Figure 2 C and D) while the

regressions between ρ/MFA and, E and MOR had an R^2 of 0.67 and 0.37 (Table 2). Yang and Evans (2003) reported a stronger coefficient of determination (R^2=0.92) for relationship between ρ/MFA and E in *Eucalyptus globulus*, *E. nitens* and *E. regnans*.

The methods of sampling preparation and measurement may be taken into account for comparing the relationships concerning MFA, ρ and E reported in similar studies. For instance, Evans and Ilic (2001), Yang and Evans (2003) and McLean et al (2010) have employed SilviScan device (Evans et al. 1999) to perform multiple measurements using across a small strip cut from the specimen and obtain the mean MFA. Here, the MFA were measured in a single point of a larger specimen (radial section cut from an intact portion of the sample after dynamic and static test) using a polyvalent X-ray diffractometer. Hence, it is possible that only one measurement does not provide a realistic estimation of the MFA of the entire specimen used for determining the wood stiffness and strength.

There are few studies of this nature with juvenile wood from *Eucalyptus* to compare and validate the findings reported here. The relationships between MFA, wood density, stiffness and strength are important in trees from fast-growing forests because most of the *Eucalyptus* plantations are grown to supply with high quality raw material the pulp and paper industry.

Relationships between wood traits play a major role on functional biology of the tree and on industrial utilization of the wood. Cambial activity may produce stiffer wood to support the ever-increasing stem weight, gravity forces and bending movements induced by winds. Then, changes in cell wall thickness and cellulose microfibril orientation allow the trees to grow and survive under adverse conditions, such as

prevailing winds (Alméras and Fournier 2009). On the other hand, such relationships influence the industrial application of wood. For instance, the mechanical properties of paper are strongly influenced by the strength and stiffness of the fibers from which it is formed (Evans et al. 1996).

CONCLUDING REMARKS

In this study, the relationship between MFA and wood traits was investigated in *Eucalyptus* from fast grown plantations. MFA has been considered as an ultrastrutural characteristic controlling wood stiffness in many wooden species. Theoretical models and experimental data have supported the argument that the inclination of cellulose microfibrils within secondary cell walls has a predominant effect on mechanical properties of wood. This study shows that MFA variation accounted for only 44 percent of the variation in specific modulus of *Eucalyptus* wood from fast-growing plantations. Wood density was the most important trait determining both wood stiffness and strength while the MFA played a secondary role on the mechanical properties of 6-year *Eucalyptus* wood. Density variation accounted for 68 and 46 percent of the variation in E and MOR, respectively. Acting together, basic density and MFA accounted for 78 percent of the variation in wood stiffness and 51 percent in variation in wood strength.

ACKNOWLEDGMENTS

The author expresses his special thanks to the CENIBRA for providing plant material; to the Universidade Federal de Lavras (UFLA, Brazil), CIRAD and CNRS (Montpellier, France) for supporting the experimental work. The author would like to thanks Dr. T. Alméras (LMGC-CNRS) for helping X-ray diffraction measurements and Dr. L. Brancheriau (UPR40-CIRAD) and Dr. J.T. Lima (UFLA) for critical reading of

the manuscript. This project was funded by CENIBRA (Celulose Nipo-Brasileira), CNPq (Conselho Nacional de Desenvolvimento Científico e Tecnológico, Brazil) and CIRAD (UPR40). P.R.G. Hein was supported by CNPq (process no. 200970/2008-9).

REFERENCES

ABRAF (2010) Associação Brasileira de Produtores de Florestas Plantadas. Statistical Yearbook - Base Year 2009/ ABRAF - Brasília, 127p.

Alméras, T., Fournier, M. (2009) Biomechanical design and long-term stability of trees: morphological and wood traits involved in the balance between weight increase and the gravitropic reaction. J. Theor. Biol. 256:370-381.

American Standards and Testing Methods - ASTM, Standard Test Methods for Specific Gravity of Wood and Wood-Based Materials, D2395-02, 2002. American Standards and Testing Methods, West Conshohocken, PA, USA.

Barnett, J.R., Bonham, V.A. (2004) Cellulose microfibril angle in the cell wall of wood fibres. Biol. Rev. 79:461-472.

Brancheriau, L., Baillères, H. (2002) Natural vibration analysis of clear wooden beams: a theoretical review. Wood Sci. Technol. 36:347-365.

Brancheriau, L., Baillères, H. (2003) Use of the partial least squares method with acoustic vibration spectra as a new grading technique for structural timber. Holzforschung 57:644-652.

344 Brancheriau, L., Kouchade, C., Brémaud, I. (2010) Internal friction measurement of
345 tropical species by various acoustic methods. Journal of Wood Science. Online First.
346 DOI: 10.1007/s10086-010-1111-8

347 Cave, I.D. (1966) Theory of X-ray measurement of microfibril angle in wood. For.
348 Prod. J. 16(10):37-42.

349 Cave, I.D. (1968) The anisotropic elasticity of the plant cell wall. Wood Sci. Technol.
350 2(44):268-278.

351 Cown, D.J., Hebert, J., Ball, R. (1999) Modelling radiata pine lumber characteristics.
352 Part 1: mechanical properties of small clears. NZ J For Sci 29(2):203-213.

353 Donaldson, L. (2008) Microfibril angle: measurement, variation and relationships - a
354 review. IAWA J. 29(4):345-386.

355 Downes, G.M., Nyakuengama, J.G., Evans, R., Northway, R., Blakemore, P., Dickson,
356 R.L., Lausberg, M. (2002) Relationship between wood density, microfibril angle and
357 stiffness in thinned and fertilized *Pinus radiata*. IAWA J. 23(3):253-265

358 Evans, R., Stuart, S.A., Van der Tour, J. (1996) Microfibril angle scanning of increment
359 cores by X-ray diffractometry. Appita J. 49(6):411-414.

360 Evans, R., Ilic, J. (2001) Rapid prediction of wood stiffness from microfibril angle and
361 density. For. Prod. J. 51(3):53-57.

362 Evans, R. (1999) A variance approach to the x-ray diffractometric estimation of
363 microfibril angle in wood. Appita J. 52:283-289.

Evans, R., Stringer, S., Kibblewhite, R.P. (2000) Variation of microfibril angle, density and fibre orientation in twenty-nine *Eucalyptus nitens* trees. Appita J. 53:450-457.

Glass, SV, Zelinka, SL. (2010) Moisture Relations and Physical Properties of Wood. In: Wood handbook - Wood as an engineering material. General Technical Report FPL-GTR-190. Madison, WI: U.S. Department of Agriculture, Forest Service, Forest Products Laboratory. pp. 4.1-4.19.

Hein, P.R.G., Brancheriau, L., Trugilho, P.F., Lima, J.T., Chaix, G. (2010) Resonance and near infrared spectroscopy for evaluating dynamic wood properties. J. Near Infrared Spectrosc. 18(6):443-454.

Iglesias-Trabado, G., Wilstermann, D. (2008) *Eucalyptus universalis*. Global cultivated eucalypt forests map 2008. Version 1.0.1 In GIT Forestry Consulting's Eucalyptologics: Information resources on *Eucalyptus* Cultivation wordwide.

Ivković, M., Gapare, W.J., Abarquez, A., Powell, M.B., Ilic, J., Wu, H.X. (2009) Prediction of wood stiffness, strength, and shrinkage in juvenile corewood of radiata pine. Wood Sci. Technol. 43:237-257.

Kollmann, F.R., Côté, W.A. (1968) Principles of Wood science and technology. Berlin: Springer-Verlag, 592p.

Lima, J.T., Breese, M.C., Cahalan, C.M. (2004) Variation in microfibril angle in Eucalyptus clones. Holzforschung 58:160-166.

McLean, J.P., Evans, R., Moore, J.R. (2010) Predicting the longitudinal modulus of elasticity of Sitka spruce from cellulose orientation and abundance. Holzforschung 64(4):495-500.

Meylan, B.A. (1967) Measurement of microfibril angle by X-ray diffraction. For. Prod. J. 17:51-58.

Meylan, B.A. (1968) Cause of high longitudinal shrinkage of wood. For. Prod. J. 18:75-78.

NF (1987) Norme Française B51-008. AFNOR.

Rayleigh, J.W.S. The theory of the sound (Edition of 1945). New York, 1977.

Raymond, C.A. (2002) Genetics of *Eucalyptus* wood properties. Ann. For. Sci. 59(5/6):525-531.

Treacy, M., Dhubha´in, A.N., Evertsen, J. (2000) The influence of microfibril angle on modulus of elasticity and modulus of rupture in four provenances of Irish grown Sitka spruce (*Picea sitchensis* (Bong.) Carr). J. Inst. Wood Sci. 15:211-220.

Walker, J.C.F., Butterfield, B.G. (1995) The importance of microfibril angle for the processing industries. New Zealand For. 35-40.

Washusen, R., Evans, R. (2001) The association between cellulose crystallite width and tension wood occurrence in *Eucalyptus globulus*. IAWA J. 22:235-243.

Wu, Y-Q., Hayashi, K., Liu, Y., Cai, Y., Sugimori, M. (2006) Relationships of anatomical characteristics versus shrinkage and collapse properties in plantation-grown eucalypt wood from China. J. Wood Sci. 52(3):187-194.

Yamamoto, H., Sassus, F., Ninomiya, M., Gril, J. (2001) A model of anisotropic swelling and shrinking process of wood. Part 2. A simulation of shrinking wood. Wood Sci. Technol. 35:167-181.

Yamamoto, H., Okuyama, T., Yashida, M. (1993) Method of determining the mean microfibril angle of wood over a wide range by the improved Cave´s method. Mokuzai Gakkaishi 39:118-125.

Yang, J.L., Evans, R. (2003) Prediction of MOE of eucalypt wood from microfibril angle and density. Holz als Roh- und Werkstoff 61:449-452.

TABLES

Table 1 - Descriptive statistics for ρ (kg m^{-3}), E (MPa), E' (E/ρ), G (MPa), δrd and δtg (%), MFA (degrees), ρ/MFA and MOR (MPa) of clear specimens of *Eucalyptus* wood. CV is the coefficient of variation, given in percent.

	Mean	Minimum	Maximum	CV	N
ρ	520.2	362.5	708.4	12.5	228
E_L	13,438	6,522	20,785	21.2	227
E'_L	25.7	16.9	32.4	13.4	227
E_F	12,530	5,930	18,732	20.9	228
E'_F	23.9	15.3	30.6	13.5	228
G	712.0	434.0	1499.0	26.1	228
δrd	4.81	1.75	10.39	29.1	222
δtg	7.81	3.24	13.35	20.4	221
MFA	12.09	8.20	24.31	21.2	220
ρ/MFA	45.1	18.7	85.0	25.4	219
MOR	72.7	15.1	119.1	22.0	197

Table 2 - Correlations among wood traits in *Eucalyptus* trees. The correlations were statistically significant at $p<0.01$.

	ρ	E_L	E'_L	G	δrd	δtg	MFA	ρ/MFA
E_L	0.82	1						
E'_L	0.38	0.83	1					
G	0.28	-	-0.23	1				
δrd	0.39	0.40	0.28	0.18	1			
δtg	0.43	0.44	0.29	-	-	1		
MFA	-0.40	-0.61	-0.65	0.20	-0.24	-0.33	1	
ρ/MFA	-	0.82	-	-	0.36	0.43	-0.84	1
MOR	0.68	0.81	0.66	-	0.29	0.29	-0.47	0.61

Table 3 - Regression models for predicting modulus of elasticity in longitudinal (E_L) and flexural (E_F) vibrations and modulus of rupture (MOR) with MFA, density, and ρ/MFA.

Trait	Intercept	MFA	ρ	ρ/MFA	R^2	SEE
	21427.2	-680.43			0.37	2,281
	-5287.1		35.976		0.68	1,609
	4325.7			202.567	0.67	1,651
E_L	1995.6	-367.61	30.557		0.78	1,349
	20208.6	-634.28			0.38	2,082
	-4606.6		32.940		0.67	1,509
	4170.2			186.068	0.66	1,521
E_F	2441.4	-352.01	27.612		0.77	1,253
	110.97	-3.166			0.22	14.10
	-22.17		0.184		0.46	11.72
	33.096			0.896	0.37	12.20
MOR	11.42	-1.660	0.158		0.51	11.12

FIGURES

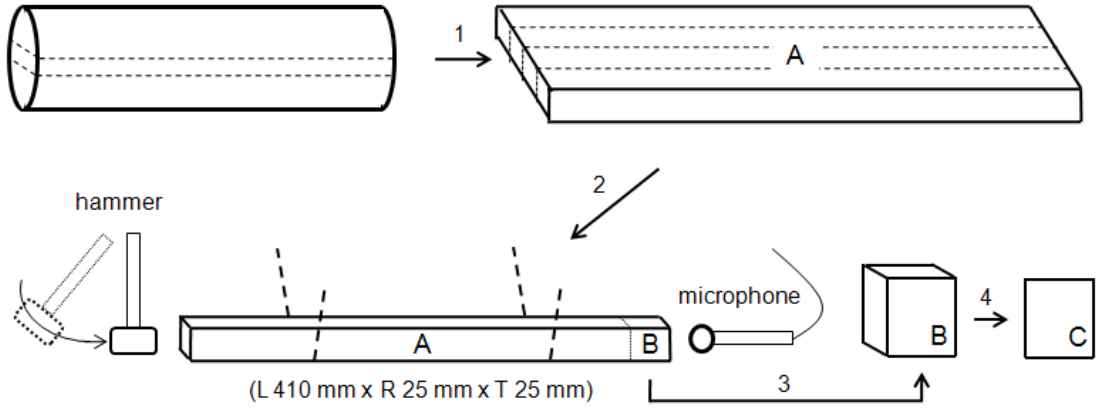

Figure 1 - Procedure of sampling. Clear wood specimens were cut from central boards (A). Dynamic tests for determining E, E/ρ and G followed by static tests for MOR were performed in each specimen. After testing, a small sample measuring 25 mm × 25 mm × 25 mm (B) was removed from intact wood for ρ measurement, and a 2 mm section sample (C) for XRD measurements.

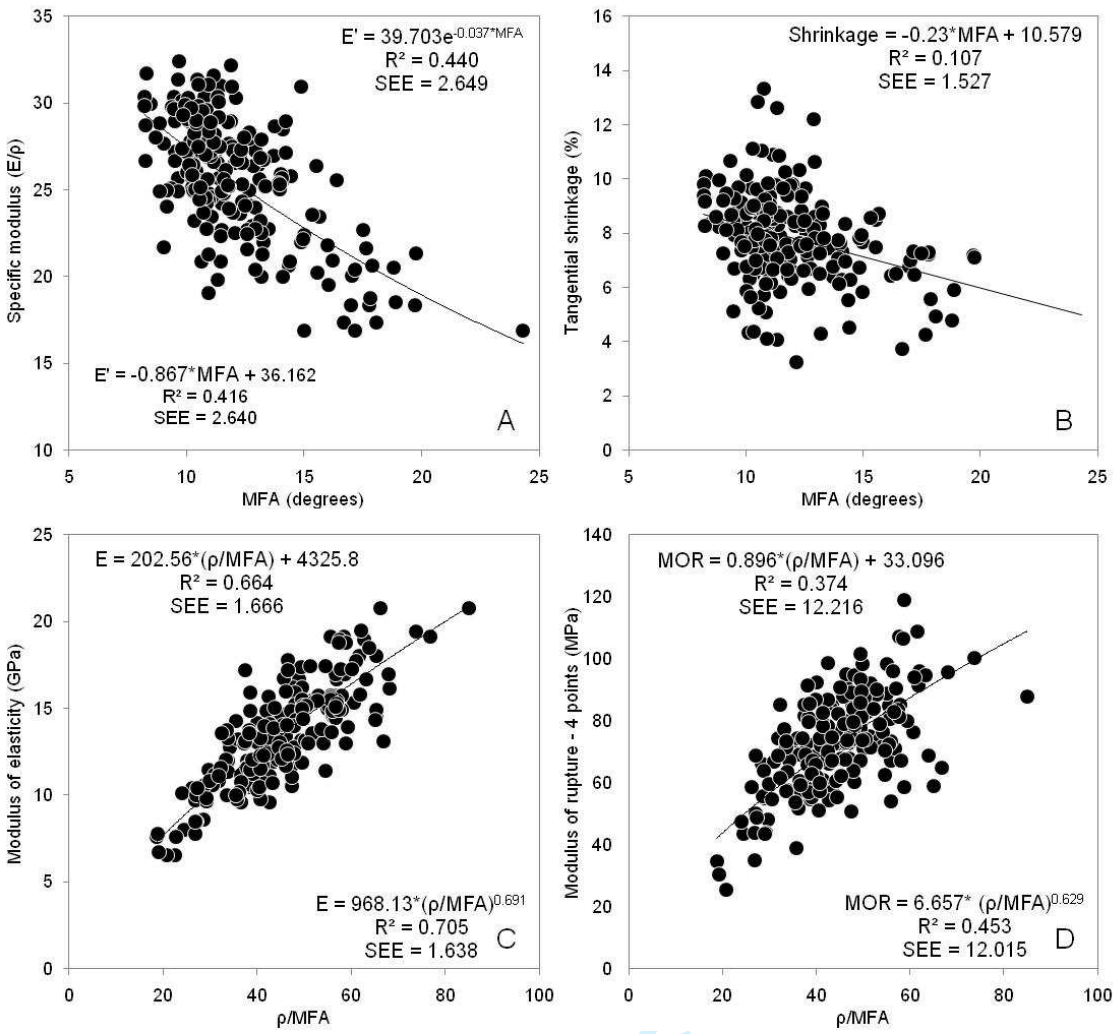

Figure 2 - Relationship between wood traits in *Eucalyptus* wood. SEE is the standard error of estimation

Paper 3

Authors: Hein PRG and Brancheriau L

Title: Correlations between microfibril angle and wood density with age in 14-year-old Eucalyptus urophylla S.T. Blake wood

Journal: BioResources (*submitted*)

RADIAL VARIATION OF MICROFIBRIL ANGLE AND WOOD DENSITY AND THEIR RELATIONSHIPS IN 14-YEAR-OLD *Eucalyptus urophylla* S.T. BLAKE WOOD

Paulo Ricardo Gherardi Hein[a*] and Loic Brancheriau[a]

The orientation of cellulose microfibril in the cell wall along the stem axis has major effects on stiffness and longitudinal shrinkage and is of key importance in wood quality. The aim of this study was to investigate the radial variability of MFA and wood density (ρ) and their relationships in *Eucalyptus urophylla* wood. Three MFA values were estimated by X-ray diffraction at three points of each one of the 175 tangential sections and the basic density was measured. A decrease of microfibril angles from pith to bark can be observed in most samples; however, some radial strips presented different patterns of variation. For basic density, a linear significant increase from pith to bark was confirmed. There was no significant correlation between microfibril angle and density. The relationships among the three MFA estimated on tangential sections of wood were strong. The "curvature effect" due to the growth rings had a negligible effect on the three measurements of tangential sections cut near to the pith. This study showed that a single *T* value measurement by X-ray diffraction, preferably at the centre of the tangential section is precisely sufficient to estimate the mean MFA of *Eucalyptus urophylla* wood.

Keywords: MFA; X ray diffraction; density; ageing; hardwood; wood phenotyping

Contact information: a: CIRAD - PERSYST Department, Research unit: Production and Processing of Tropical Woods, TA B-40/16, 73 rue Jean-François Breton, 34398 Montpellier, France;
**Corresponding author: phein1980@gmail.com*

INTRODUCTION

Wood density and the angle of its microfibrils in the secondary wall are of particular interest for breeding programs (Raymond 2002) since they are the two main factors affecting wood mechanical properties. Microfibril angle (MFA) is a property of the cell wall of wood fibres, which is made up of millions of strands of cellulose called microfibrils (Fang et al. 2006). This elementary wood trait represents the orientation of crystalline cellulose in the cell wall along the stem axis (Andersson et al. 2000). MFA has major effects on two key properties of wood: its stiffness and longitudinal shrinkage. For instance, Cave (1968) demonstrated that a reduction in MFA from 40° in the corewood to 10° in the outerwood increases the stiffness of the cell wall fivefold. This finding was confirmed by Via et al. (2009) who reported a fourfold increase in stiffness of longleaf pine when the microfibril angle dropped from 40° to 5°. The early optical measurements of MFA were extremely tedious, but currently, a wide range of different methods are available to evaluate MFA in wood (reviewed by Donaldson 2008). Among all available techniques only X-ray diffractometry is apt for quick MFA measurements for a large number of samples (Evans et al. 1996; Evans 1999). X-ray diffractometry has been

largely used thanks to the crystalline arrangement of cellulose microfibrils in the wood cell wall; it allows studying not only its organization (like MFA) but also its apparent crystal size (Washusen and Evans 2001) or its mechanical state (Clair et al. 2006).

MFA and wood density presents a variable relationship (Donaldson 2008). For instance, Fang et al. (2004) reported significant correlation between MFA and wood density (-0.45) for *Populus* while no correlation was found in *Picea* by Bergander et al. (2002) and in *Taiwania* by Lin and Chiu (2007). In *Eucalyptus*, Evans et al. (2000) reported no correlation between whole tree average density and MFA in 15-year-old *Eucalyptus nitens*. The radial variation and the correlation between MFA and density is still not clear in Eucalyptus requiring further studies.

Therefore, the aims of this study were: i) to investigate the radial variation of microfibril angle (MFA) and wood density in *Eucalyptus* wood and ii) to generate a better understanding about the correlation between MFA and wood density, and the influence of age on these relationships.

Here, we used 2-mm tangential sections of *Eucalyptus urophylla* wood to evaluate the MFA by X-ray diffraction technique (Cave 1966). Each tangential section was cut as parallel as possible to the growth rings. Thus, the samples taken close to the pith presents a "curvature effect" while the tangential sections taken near the bark, parallel to the growth ring, showed little or no "curvature effect". Hence, an additional objective of this study was to verify the influence of the curvature effect on the repeatability of the XRD measurements.

EXPERIMENTAL

Wood origin

40 breast height wood disks of 14-year-old *Eucalyptus urophylla* S.T. Blake trees from the progeny test in Republic of Congo were used in this study. Hein et al. (2010) presented details of sampling procedure and the chemical composition of the trees from the same progeny trial.

Sampling preparation

From each disc, a pith to bark radial strip was removed by a vertical bandsaw. The radial strips were marked randomly but well distributed along the radial gradient on the strips in order to supply tangential sections, as parallel as possible, to the growth rings for microfibril angle and small samples for wood density measurements (Figure 1). While from the large radial strips it was possible to take 4 or 5 samples (for instance, Fig.1), only two or three samples were removed from radial strips with small dimensions.

The radial strips were classified in five classes (from A to E) depending on their relative radial position. The tangential sections cut from the region close to the pith presented the stronger "curvature effect" while the tangential sections cut near the bark, parallel to the growth ring, showed little or no curvature effect (Figure 1). The samples were sectioned along to the wood strips in the same proportion as well as possible, but no sample was taken from class A because of operational limitations.

Microfibril angle measurement

All X-ray diffraction data were collected on a diffractometer (Gemini-S, Agilent Technologies, Yarnton, UK) with CuK α radiation. Images were integrated between 2θ = 21.5 and 23.5 along the whole 360° azimutal interval to plot the intensity diagram of the (200) plane. An automatic procedure allowed the detection of the 200 peaks and their inflexion points. The *T* parameter, as defined by Cave (1966), was measured as the half distance between intersections of tangents at inflexion points with the baseline. The results are given as the mean of values obtained for the two 200 peaks. As shown by Cave (1966), *T* parameter is affected by the cross-sectional shape of the cells. Thus, as also reported by Yamamoto et al. (1993) and latter Ruelle et al. (2007), the corrective factor proposed by Cave (1966) cannot be used for all species but need to be calibrated specie by specie; However, their works show that the *T* parameter allows comparison within a specie which is the purpose of our study. In our study, we considered that the cross-sectional shape of the cells remain constant enough from pith to bark to allows comparison with a single *T* parameter within the species. Figure 2 illustrates X-ray scattering patterns recorded in 2mm tangential sections of *Eucalyptus* samples with contrasting *T* parameters.

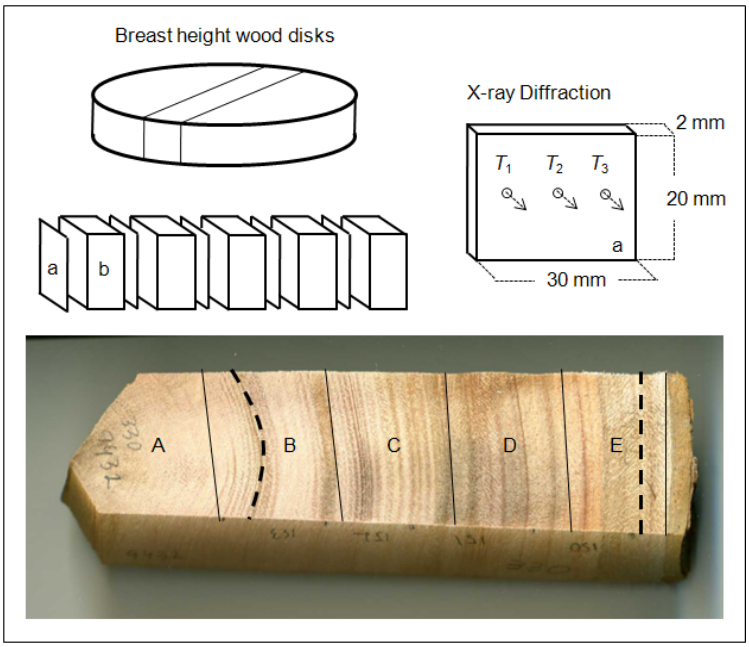

Fig.1. Sampling protocol in 14-year *Eucalyptus urophylla*. Tangential sections for X-ray diffraction measurement (a) and wood samples for basic density measurement (b) taken from the radial strips. Classes from A to E of the radial strips; the dotted lines represent the "curvature effect" on tangential section of wood due to the growth rings.

The method proposed by Yamamoto et al. (1993) was applied in order to estimate the MFA based on their X-ray diffraction pattern. The formula gives an estimation of the mean MFA of woods based on their *T* value and is given by:

$$MFA = 1.575 \times 10^{-3} \times T^3 - 1.431 \times 10^{-1} \times T^2 + 4.693 \times T - 36.19$$

Three X-ray diffraction profiles were recorded on three points, namely T_1, T_2 and T_3, of each sample (Figure 1). The estimated error of the repeatability of the T parameter measurements was 3%, on average, for T ranging from 14° to 29° which correspond to ±0.6 degrees.

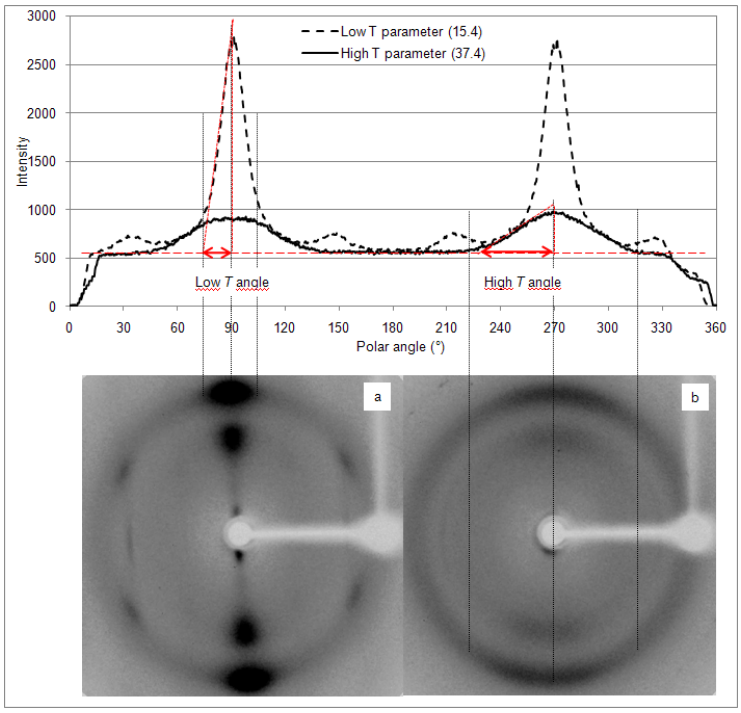

Fig.2. X-ray scattering patterns recorded in 2mm tangential sections of *Eucalyptus* samples with low (A) and high (B) *T* parameter. Lower chart: full diffraction images. Upper chart: 1-D patterns obtained by azimutal integration of the diffraction image near the (200) reflection. Dotted lines show the correspondence between the peak on the integrated pattern and the spot on the diffraction image. For each sample, integration yields two symmetric peaks located at 90° and 270°. The dotted line in red is the base line and the red arrows are the *T* parameter. Sample A shows a narrow peak (*T*=15.4°), corresponding to a low MFA, while sample B shows a wide peak (*T*=37.4°) corresponding to a large MFA.

Wood density measurement

The offcut samples between the tangential sections (Figure 1 b) were used for basic density measurements, which was determined by the ASTM D2395 (ASTM 2002) procedures.

RESULTS AND DISCUSSION

The wood basic density and *T* parameter measurements (Table 1) showed a range of variation of ~14.5%. The approach for conversion of the X-ray diffractometer pattern to microfibril angle is based on the *T* parameter, but the MFA had the higher coefficient of variation (17.1%). The range of variation of the investigated properties is crucial for *Eucalyptus* breeding programs whereas the breeders are interesting in finding significant differences between progenies or clones.

Table 1. Descriptive statistics, including average, standard deviation (SD), minimum (Min), maximum (Max) and coefficient of variation (CV) for basic density (ρ), *T* parameter and microfibril angle (MFA) measurements in 14-year-old *Eucalyptus urophylla* wood.

	Average	SD	Min	Max	CV (%)	No. of samples
ρ (kg m^{-3})	547	79	372	742	14.4	175
T parameter (°)	19.7	2.87	14.6	28.7	14.6	175
MFA (°)	12.5	2.14	7.7	19.7	17.1	175

Radial variability

While data between 20 to 40% of radial distance represent the samples from class B, which correspond to the wood formed at the 4th to 6th year, the data from the last 20% (from 80 to 100%) correspond to the wood developed at approximately the 12th, 13th and 14th years. Figure 3 presents the variation on MFA and density as a function of the relative distance from the pith to bark for 14 radial strips. The samples were ranked by radial position in ascending order from 0.22 to 0.97 of their relative radial position and the mean comparisons were performed for each class (B to E). Due to the small dimension of some radial strips, we removed only two or three tangential sections for MFA, and small wood samples for density from them and these data were not presented in the graphic.

The mean MFA values of each class (B to E) were not statistically different by the Tukey test at P>0.01 while the mean basic density of wood significantly increased in a linear way from pith to bark. Thus, the radial variation of MFA in *Eucalyptus* wood is not statistically evident, because the large MFA variability between trees results in a large standard deviation within each class (for instance, in class B the MFA ranged from ~11° to ~19°). However, a decrease of MFA values from pith to bark can be observed. Figure 3-A) reveals that, on average, the microfibril angles appears to be higher near the pith of the discs (Class B), decreasing radially towards to the bark (Class E). Such pattern of MFA variation occurred most frequently, but among the various strips we used (40), different trends could be observed. For instance, the MFA of samples 80, 87, 96, 103 and 153 slightly increased near to the bark. For basic density of wood, a linear increase from pith to bark was found (Figure 3-B), even if the variability of density between trees was taken into account.

The patterns of radial variation of these *Eucalyptus* wood traits are in accordance with those reported in the literature. For instance, Evans et al. (2000) reported variation in MFA from 20° at the pith to 14° at the bark in 15-year-old *Eucalyptus nitens*. Lima et al. (2004) investigated 8-year-old *E. grandis* × *E. urophylla* clones reporting that its MFA decreased slightly from pith to bark. The radial variation of these wood traits is important, because such properties are targeted in breeding programs to distinguish improved varieties according to their variance; however, frequently, the within-tree variability is higher than the between-trees variability. Regarding to this issue, the fundamental question should be posed: does trees producing low MFA in the first years

of their development continue presenting low MFA over the years? Evans et al. (2000) reported variation patterns in MFA and density in *Eucalyptus*, showing that the trend lines for 29 *E. nitens* tend to be approximately parallel. This means that trees presenting high MFA or density when young will continue to having high MFA or density when mature. In this study, Figure 3 shows the MFA and ρ for all ages providing to the tree breeders clear evidences for ρ, but rough indications for MFA.

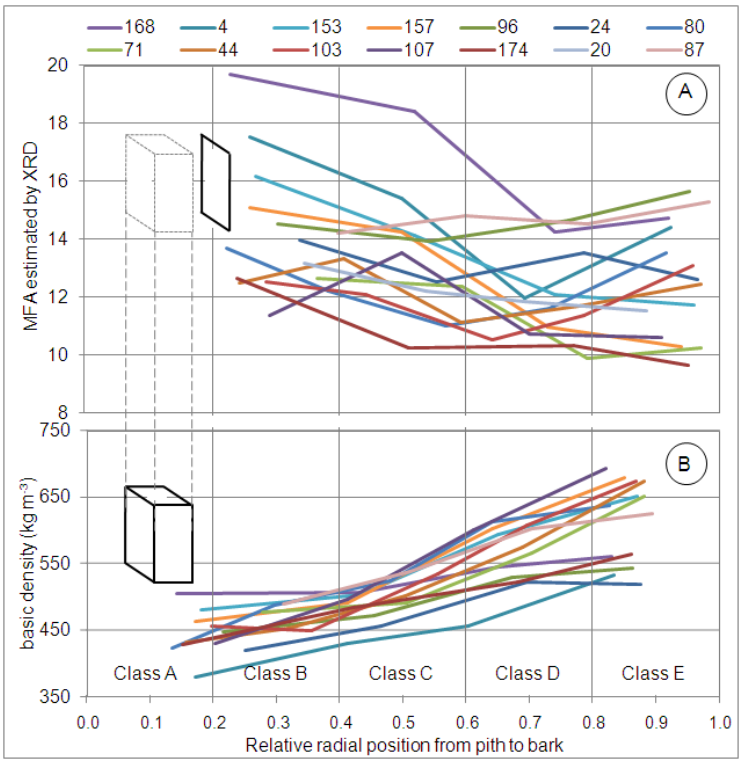

Fig.3. Radial variation of MFA (A) and basic density (B) in 14-year-*Eucalyptus urophylla* wood for fourteen radial strips.

Correlation among MFA estimates

Three X-ray diffraction profiles were recorded on three points of each tangential section (Figure 1). Considering that the measurement at the central point (MFA_2) represents precisely the information of a tangential surface and that the measurement at the external points (MFA_1 and MFA_3) includes tangential information, but also radial (at least partially) information, mainly in samples near to the pith, it is interesting to analyze the correlation among the MFA values according to the points of measurement. The tangential sections cut near to the pith presented the stronger "curvature effect" whereas the samples near to the bark, parallel to the growth ring, showed little or no curvature effect (Figure 1). Thus, at the outset, we expected to find higher deviation between MFA estimates in the samples cut near the pith, since its "curvature effect" is expected to be stronger. No sample was taken from class A because of the technical difficulty and risk of cutting tangential section from the remaining end of the radial strips.

Table 2 presents the correlation among MFA recorded at the three points of each wood section using all samples (Classes B to E). Although it is intuitive, due to the effect

of distance between measurements the correlation MFA_1/MFA_3 (0.82) was slightly lower than those for MFA_1/MFA_2 (0.84) and MFA_2/MFA_3 (0.91). The average between measurements 1 and 3 ($MFA_{1,3}$) were also strongly correlated with local measurements 1 (0.95), 2 (0.93) and 3 (0.96). The correlation between the measurement at point 2 (central) and the three averaged measurements ($MFA_{1,2,3}$) was very strong (0.97). This finding suggested that a single measurement of the *T* value, preferably at the centre of each tangential section, is enough to precisely evaluate the MFA of the tangential section. Three measurements are time-consuming and did not provide additional information on MFA in *Eucalyptus* wood.

Table 2. Above the diagonal: correlation among the MFA estimated at points 1 (MFA_1), 2 (MFA_2) and 3 (MFA_3), the average of points 1 and 3 ($MFA_{1,3}$) and the average of three measurements ($MFA_{1,2,3}$) for all samples. The correlations were statistically significant at 99%. Below the diagonal: the standard error of the estimate.

	MFA_1	MFA_2	MFA_3	$MFA_{1,3}$	$MFA_{1,2,3}$
MFA_1	-	0.84	0.82	0.95	0.93
MFA_2	1.15	-	0.91	0.93	0.97
MFA_3	1.18	0.90	-	0.96	0.96
$MFA_{1,3}$	0.64	0.88	0.62	-	0.99
$MFA_{1,2,3}$	0.79	0.54	0.62	0.33	-

Additionally, we calculated the correlations among MFA recorded at the three points of each wood section according to the classes (B, C, D and E) where they were cut (not shown). The correlations between MFA's were always strong indicating that the X-ray approach is a repeatable method and that the curvature effect plays a negligible role on the repeatability of measurements.

Correlation among MFA and density

The density and MFA shows no significant correlation (r=~0.11) when considering all classes (Table 3). A weak correlation between MFA and density is observed for samples from Class B (r=~-0.18) and Class C (r=~-0.13) but the relationships among these traits disappeared with age.

Table 3. Correlations between ρ with the MFA estimated at point 2 (MFA_2) and the averaged MFA values ($MFA_{1,2,3}$).

	Class				
	B	C	D	E	Overall
ρ-MFA_2	-0.190	0.149	0.091	-0.038	-0.119
ρ-$MFA_{1,2,3}$	-0.181	0.126	0.088	-0.025	-0.115

Evans et al. (2000) compared MFA and density of 29 *Eucalyptus nitens* wood finding good local relationships between MFA and density but the whole tree average

MFA and density yielded no correlation. Bergander et al. (2002) found no correlation between fiber morphology (i.e., average length, width, density) and mean fibril angle in wood samples of 100-year-old Norway spruce (*Picea abies* L. Karst.). Similarly, Lin and Chiu (2007) studied such wood traits in 20-year-old Taiwania (*Taiwania cryptomerioides*) trees reporting no significant relationship between microfibril angle and wood density. Figure 4 shows the relationships between MFA and basic density of *Eucalyptus* wood showing the classes of radial position by colors. While samples from class B (21-40%) are concentrated in the zone of low density, most samples from class E (81-100%) have high densities.

According to Donaldson (2008), it seems likely that any relationship between MFA and density is entirely coincidental since MFA is not related to fiber wall thickness. However, the amount of juvenile wood and latewood might be responsible for relationships in some cases since both MFA and density are related to these factors. The weak correlations between microfibril angle and density found in the present study seem to support such argument.

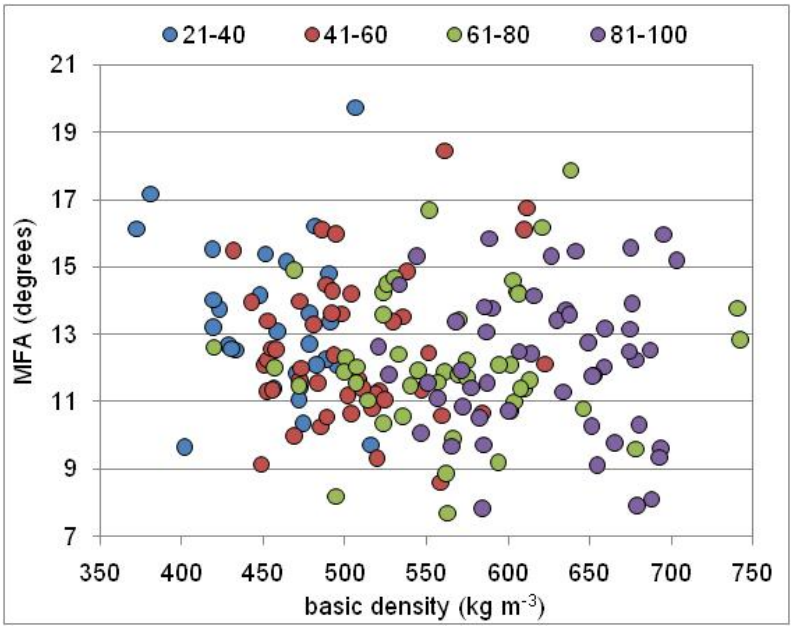

Fig.4. Bi-dimensional plot for $MFA_{1,2,3}$ and basic density according to the age in 14-year-*Eucalyptus urophylla* wood. Colors indicate relative radial positions from pith (0) to bark (100).

The use of X-ray diffraction to evaluate MFA in woods has two substantial advantages: speed and accuracy sufficient for genetic studies. The *T* parameter measurements have an error of ~0.6 degrees (~3%), but they are able to distinguish trees that produce wood with larger or smaller microfibril angles. For genetic studies, the absolute value of the property is of no matter. The interesting point is to know the relative value of the characteristic between trees, its variation within stem and stability. Since phenotyping tools are required in genetic studies and breeding programs, our results can be useful for selection of candidate genotypes or commercial clones in forestry industries from a large wood sampling.

CONCLUDING REMARKS

A decrease of microfibril angles from pith to bark could be verified for some of these 14-year-old *Eucalyptus urophylla* wood; however, some radial strips presented different patterns of variation. Due to the sampling procedure, the radial variation of MFA could not be statistically analyzed. For basic density, a linear significant increase from pith to bark was observed.

There was no significant correlation between microfibril angle and density. The supposed "curvature effect" due to the growth rings had a negligible effect on the three measurements of tangential sections cut near to the pith.

The relationships among the three MFA estimates by X-ray diffraction on each tangential section were strong. The high correlation between the MFA estimated at the central and the three averaged MFA estimates suggests that a single measurement of the MFA value, preferably at the centre of each tangential section, is enough to precisely evaluate this trait.

ACKNOWLEDGMENTS

The authors would like to thank Arie van der Lee from "Institut Européen des Membranes" and the researchers from "Laboratoire de Mécanique et Génie Civil" (CNRS, University of Montpellier 2) for assistance for X-ray diffraction measurements; to CRDPI (Republic of Congo - N. Ognouabi, J. Akana, A. Matsoumbou and E. Vilar) and the "Bureau des Ressources Génétiques" (project: "Un modèle de variabilité fonctionnelle chez les arbres forestiers: le gène CCR d*'Eucalyptus*") for providing material and funding; to UPR39 (JM Gion, P Vigneron) and UPR40 of CIRAD-Montpellier for providing technical support. PRG Hein was supported by the National Council of Technological and Scientific Development (CNPq, Brazil - process no. 200970/2008-9).

REFERENCES

American Society for Testing and Materials. (2002). *ASTM D 2395-02*: *Standard Test Methods for Specific Gravity of Wood and Wood-Based Materials*, West Conshohocken, PA, USA.

Andersson, S., Serimaa, R., Torkkeli, M., Paakkari, T., Saranpfifi, P., Pesonen, E. (2000). "Microfibril angle of Norway spruce (*Picea abies* [L.] Karst.) compression wood: comparison of measuring techniques," *Journal of Wood and Science* 46, 343-349.

Barnett, J.R., Bonham, V.A. (2004). "Cellulose microfibril angle in the cell wall of wood fibres," *Biol. Rev*. 79, 461-472.

Bergander, A., Brändström, J., Daniel, G., Salmén, L. (2002). "Fibril angle variability in earlywood of Norway spruce using soft rot cavities and polarisation confocal microscopy," *J. Wood Sci.* 48, 255-263.

Cave, I.D. (1966). "Theory of X-ray measurement of microfibril angle in wood," *For. Prod. J.* 16(10), 37-42.

Cave, I.D. (1968). "The anisotropic elasticity of the plant cell wall," *Wood Sci. Technol.* 2, 268- 278.

Clair, B., Alméras T., Yamamoto, H., Okuyama T., Sugiyama, J. (2006). "Mechanical behaviour of cellulose microfibrils in tension wood, in relation with maturation stress generation," *Biophys. J.* 91, 1128-1135.

Donaldson, L. (2008). "Microfibril angle: measurement, variation and relationships – a review," *IAWA J.* 29(4), 345-386.

Evans, R. (1998). "Rapid scanning of microfibril angle in increment cores by x-ray diffractometry,".In: Microfibril Angle in Wood. Proceedings of the IAWA/IUFRO International Workshop on the Significance of Microfibril Angle to Wood Quality. University of Canterbury Press, p. 116.

Evans, R. (1999). "A variance approach to the x-ray diffractometric estimation of microfibril angle in wood", *Appita J.* 52, 283-289.

Evans, R., Stringer, S., Kibblewhite, R.P. (2000). "Variation of microfibril angle, density and fibre orientation in twenty-nine *Eucalyptus nitens* trees", *Appita J.* 53, 450-457.

Evans, R., Stuart, S.A., Van der Touw, J. (1996). "Microfibril angle scanning of increment cores by X-ray diffractometry," Appita J. 49(6), 411.

Fang, S-Z., Yang, W-Z., Fu, X-X. (2004). "Variation of microfibril angle and its correlation to wood properties in Poplars," *J. For. Res*. 15(4), 261-267.

Fang, S-Z., Yang, W-Z., Tian, Y. (2006). "Clonal and within-tree variation in microfibril angle in poplar clones," *New Forests* 31, 373-383.

Fujimoto, T., Kurata, Y., Matsumoto K., Tsushikawa, S. (2008). "Application of near infrared spectroscopy for estimating wood mechanical properties of small clear and full length lumber specimens," *J. Near Infrared Spectrosc.* 16, 529-537.

Hein, P.R.G., Lima, J.T., Chaix, G. (2010). "Effects of sample preparation on NIR spectroscopic estimation of chemical properties of *Eucalyptus urophylla* S.T. Blake wood," *Holzforschung* 64, 45-54.

Huang, A., Fu, F., Fei B., Jiang Z. (2008). "Rapid estimation of microfibril angle of increment cores of Chinese fir by near infrared spectroscopy," *Chinese Forestry Science and Technology* 7(1), 52-56.

Jungnikl, K., Koch, G., Burgert, I. (2008). "A comprehensive analysis of the relation of cellulose microfibril orientation and lignin content in the S_2 layer of different tissue types of spruce wood (*Picea abies* (L.) Karst.)," *Holzforschung* 62, 475-480.

Lima, J.T., Breese, M.C., Cahalan, C.M. (2004). "Variation in microfibril angle in *Eucalyptus* clones," *Holzforschung* 58, 160-166.

Lin, C-J., Chiu, C-M. (2007). "Relationships among selected wood properties of 20-year-old Taiwania (*Taiwania cryptomerioides*) trees," *J. Wood Sci.* 53, 61-66.

Raymond, C.A. (2002). "Genetics of *Eucalyptus* wood properties," *Ann. For. Sci.* 59, 525-531.

Ruelle, J., Yamamoto, H., Thibaut, B. (2007). "Growth stresses and cellulose structural parameters in tension and normal wood from three tropical rainforest angiosperms species," *BioResources* 2(2), 235-251.

Tsuchikawa, S. (2007). "A Review of Recent Near Infrared Research for Wood and Paper," *Appl. Spectrosc. Reviews* 42, 43-71.

Via, B.K., So, C.L., Shupe, T.F., Groom, L.H., Wikaira, J. (2009). "Mechanical response of longleaf pine to variation in microfibril angle, chemistry associated wavelengths, density, and radial position," *Composites: Part A* 40, 60-66.

Washusen, R., Evans, R. (2001). "The association between cellulose crystallite width and tension wood occurrence in *Eucalyptus globules*," *IAWA J*. 22, 235-243.

Yamamoto, H., Okuyama, T., Yashida, M. (1993). "Method of determining the mean microfibril angle of wood over a wide range by the improved Cave´s method," *Mokuzai Gakkaishi* 39, 118-125.

Yamashita, S., Yoshida, M., Takayama, S., Okuyama, T. (2007). "Stem-righting mechanism in Gymnosperm trees deduced from limitations in compression wood development," *Ann. Bot*. 99, 487-493.

Article submitted July xx, 2010;

Paper 4

Authors: Hein, PRG, Lima JT and Chaix G

Title: Effects of sample preparation on NIR spectroscopic estimation of chemical properties of Eucalyptus urophylla S.T. Blake wood

Journal: Holzforschung, v.64, p.45-54 (2010)

Holzforschung, Vol. 64, pp. 45–54, 2010 • Copyright © by Walter de Gruyter • Berlin • New York. DOI 10.1515/HF.2010.011

Effects of sample preparation on NIR spectroscopic estimation of chemical properties of *Eucalyptus urophylla* S.T. Blake wood

Paulo Ricardo Gherardi Hein[1,*], José Tarcísio Lima[2] and Gilles Chaix[3]

[1] CIRAD, PERSYST Department, Production and Processing of Tropical Woods, Montpellier, France
[2] Ciência e Tecnologia da Madeira, Departamento de Ciências Florestais, Universidade Federal de Lavras, Lavras, Minas Gerais, Brazil
[3] CIRAD, BIOS Department, Genetic Diversity and Breeding of Forest Species, Montpellier, France

*Corresponding author.
CIRAD, PERSYST Department, Production and Processing of Tropical Woods, 73 rue Jean-François Breton TA B-40/16, 34398 Montpellier Cedex 5, France
Phone: +33-4-67614451, Secretary: +33-4-67596525
Fax: +33-4-67616560
E-mail: phein1980@gmail.com

Abstract

Many studies have successfully applied near infrared (NIR) spectroscopy to estimate important wood traits. Some of them have reported the effects of wood surfaces on NIR spectra information and their influence on the performance of the predictive model. However, limited information is available concerning the effect of sample preparation on the model performance to estimate chemical properties in *Eucalyptus* wood. Hence, the aim of this study was to investigate the influence of the milling procedure, particle size, and quality of the solid wood surface on the performance of the partial least squares regression to predict chemical properties of *Eucalyptus urophylla* wood by NIR spectroscopy. Adequate models were built to predict klason lignin content, acid-soluble lignin content, and syringyl-to-guaiacyl ratio in *Eucalyptus urophylla* wood. Sample preparation strongly influences the ratio of performance to deviation (RPD) of these predictive models. The effect of the sample presentation (solid or milled wood) was stronger than the effect of the particle size difference between thin and thick powder. The best calibrations were developed using NIR spectra measured on wood powder (RDP values from 1.99 to 2.97), but satisfactory calibrations were developed from NIR spectra measured on solid samples (RPD values from 1.68 to 2.16).

Keywords: acid-soluble lignin; *Eucalyptus urophylla*; lignin; near infrared (NIR) spectroscopy; particle size; solid wood; syringyl-to-guaiacyl ratio; wood powder; wood surface.

Introduction

Near infrared (NIR) spectroscopy is a frequent method of choice for the nondestructive analysis of agricultural products or foods (Hart et al. 1962; Ben-Gera and Norris 1968). This method can also be applied for wood characterization (Tsuchikawa 2007). The measurement is fast (1 min or less per sample), requires minimum or no sample preparation and is suitable for online process control. NIR spectroscopy responses to vibrations caused by C-H, NH, S-H, or O-H bonds (Pasquini 2003). In the case of wood, NIR radiation interacts with C-H, C-O, C-O-H bonds, and C=C bonds, but also with water, which is always present in wood (Lestander et al. 2008).

NIR spectra mainly consist of overtone and combination bands of the fundamental stretching vibrations shown above and it contains not only chemical but also physical information about a sample – such as density, particle size and particle shape, porosity, etc. (Burns and Ciurczak 2008). What is time-consuming is the careful collection of NIR spectra of a set of well characterized samples (calibration set), establishing regression equations between known analytical data and NIR spectral characteristics (calibration), and checking the validity of regression equations (validation) for samples, which were not previously in the calibration set (validation set) (Jones et al. 2008).

The pioneers of NIR spectroscopy of wood are Birkett and Gambino (1988), Easty et al. (1990), and Wright et al. (1990). More recent NIR studies of wood are focusing on mechanical properties (Hoffmeyer and Pedersen 1995; Thumm and Meder 2001; Schimleck et al. 2005; Fujimoto et al. 2008), anatomical characteristics (Schimleck and Evans 2004; Alves et al. 2007), physical (Codgill et al. 2004; Mora et al. 2008; Taylor et al. 2008; Hein et al. 2009), and chemical properties (Zahri et al. 2008; Tyson et al. 2009). NIR spectroscopy can also be applied to wood based composites (Campos et al. 2009).

Several procedures can improve predictive model performance. Spectral pretreatment techniques are useful for reducing effects, such as differences in sample thickness and light scattering in diffuse reflectance spectroscopy (Næs et al. 2002). In addition, wavelength selection (Ghasemi et al. 2003) and mathematical treatments (Alsberg et al. 1998) are known to improve reliability of the model. Furthermore, statistical regression models, such as principal component regression (PCR) and partial least square (PLS) regression, employed to eliminate superfluous (abundant) data and to

improve the predictive power of the NIR based analyses (Pasquini 2003) are also very important.

Sample preparation, such as particle size and thickness of the sample (Faix and Böttcher 1992), can influence NIR data. Bull (1991) and Otsuka (2004) also pointed out that sample size of milled material can have an effect on NIR spectra. This effect can be minimized by working with second derivative spectra (Norris and Williams 1984). Nevertheless, the mathematical manipulations – derivatization, normalization, and others – cannot substitute reproducible sample preparation and spectral evaluation. For instance, particle size of the milled wood and surface quality of wood are still the most relevant parameters influencing the penetration depth of NIR radiation into the sample and should always be the focus of attention (Zavarin et al. 1990).

Numerous studies have reported the effects of varying wood surfaces on NIR spectra (Tsuchikawa et al. 1992; Gierlinger et al. 2004) and their influence on model performance (Thumm and Meder 2001; Schimleck et al. 2003; Jones et al. 2006). However, *Eucalyptus* wood was seldom included in this type of research. The aim of the present investigation was to close this gap. The influence of the milling procedure, particle size, and solid wood surface quality should be investigated in terms of the prediction of chemical properties of *Eucalyptus urophylla* wood by NIR spectroscopy, whereas the reliable PLS regression approach should be the mathematical model for data reduction and property prediction.

Materials and methods

Sampling and sample preparation

A total of 60 discs in breast height were taken from 14-year-old *Eucalyptus urophylla* S.T. Blake trees established by progeny testing in the Republic of the Congo in the experimental area of research center UR2PI ''Unité de Recherche sur les plantations Industrielles du Congo'' (04°45′ S, 12°00′ E, alt 50 m). The climate is tropical humid with a mean annual temperature of 24°C, a mean annual rainfall of 1200 mm, and a dry season from May to October. The progeny trial was composed of 35 full-sib families produced by controlled pollination. These families were from an incomplete factorial mating design (8×8) with *E. urophylla* (16 genitors originated from two provenances). The families were planted in a randomized design, and density of plantation was 625 trees/ha (4×4 m spacing).

Sample preparations for NIR spectroscopy were as follows: (1) on the solid wood discs, NIR spectra labeled as ''rough'' were taken directly from the transversal surface of the chainsawed and dried (12% equilibrium moisture content, EMC) discs. (2) A clean wedge (knot-free) was cut from each disc and the transverse and radial surfaces were sanded (glass paper grade 0:220 grains cm^{-2}). The planed surfaces were submitted to NIR spectroscopy producing the spectra designated as ''surfaced''. (3) Coarse wood powder was produced from wedges which were ground in a Retsh rotating-knife grinder (SM 100). The particle sizes of wood meals obtained were $<$4.0 mm and were designated ''4.0 mm'' or ''coarse'' for NIRS analysis. (4) Wood powder was re-ground in a Retsh ultra-centrifugal mill (ZM 200). Particle sizes of wood meals were $<$0.5 mm and were designated ''0.5 mm'' or ''fine'' for NIRS analysis, too. This wood meal was not sieved before chemical analysis. All samples (rough and surfaced solid samples and the two milled samples) were kept in a conditioned room with 60% relative humidity and temperature of 20°C before NIRS analysis. Under these conditions, the EMC was 12%.

Wet-lab chemistry

The chemical analyses were conducted by the UMR Biological Chemistry (INRA-Agro ParisTech). All samples were subjected to an exhaustive extraction in a Soxhlet apparatus with toluene/ethanol (2:1, v/v), ethanol, and then water to eliminate all extractives that could interfere with lignin analyses. The klason lignin (KL) and acid soluble lignin (ASL) were determined from the extractive-free dried material (300 mg of ''fine'' powder, particle size $<$0.5 mm) according to a standard method (Dence 1992). The ratio between syringyl (S) and guaiacyl (G) units was performed on the extractive-free dried material by thioacidolysis, using a previously described method (Lapierre et al. 1995). Chemical analyses were performed in duplicate for the 60 samples.

NIR spectroscopy

A Bruker spectrophotometer (model Vector 22/N, Bruker Optik GmbH, Ettlingen, Germany) was used in the diffuse reflectance mode. This FT spectrometer is designed for reflectance analysis of solids with an integrating sphere which measures the diffuse reflected light on a 150 mm^2 spot. The integrating sphere collects light from all angles; thus, the effects of wood texture and other non-homogeneities are minimized. From a practical viewpoint, the sphere is ''upward looking'', with a window on the sphere top. A sintered gold standard was used as background. Spectral analysis was performed within the 12 500–3500 cm^{-1} (800–2850 nm) range at 8 cm^{-1} resolution (each spectrum consisted of 2335 absorption values).

Rough and surfaced NIR spectra (measured on longitudinal surfaces) were respectively taken in tree radial positions from pith to bark (internal, intermediate, and external). For wood meals (4.0 mm and 0.5 mm), NIR spectra were also collected by means of a 50-mm spinning cup module. Each spectrum was obtained with 64 scans, and means were calculated and compared with the standard to obtain the absorption spectrum of the sample. All NIRS measurements were repeated three times and the triplicate NIR spectra were averaged.

Statistical analysis

Partial least squares (PLS) regression analyses were applied to describe the relationship between the data sets obtained from NIR spectra and wood properties. Unscrambler (CAMO AS, Norway) software, version 9.7, was employed. First derivatives (13-point filter and a second order polynomial) or second derivatives (25-point filter and a third order polynomial) were applied on the NIR spectra data by the Savitzky and Golay (1964) algorithm to enhance the quality of the calibrations. The PLS calibrations were performed in full cross-validation mode with a maximum of 12 latent variables (LVs). The final number of LVs adopted for each model corresponded to the first minimal residual variance, and the outlier samples were indentified from the Student residuals and leverage value plot analyses.

The Martens' uncertainty test (Westad and Martens 2000) was used to select the wavenumbers with significant regression coefficients to develop more robust and reliable PLS models. To compare calibration and validation, the following statistics were

Table 1 Chemical properties of 14-year-old *Eucalyptus urophylla* woods from Congo UR2PI.

	Klason lignin (%)	Acid soluble lignin (%)	S/G ratio[a]
Average	28.5	1.4	2.4
Standard deviation	1.37	0.21	0.34
Maximum value	31.9	1.8	3.0
Minimum value	25.4	1.0	1.7
Coefficient of variation (%)	4.8	13.2	14.5
Number of samples	60	60	60

[a]Syringyl-to-guaiacyl ratio obtained by thioacidolysis.

applied: (1) coefficient of determination of calibration (R^2c), (2) coefficient of determination of cross-validation (R^2cv), (3) standard error of calibration (SEC), (4) standard error of cross-validation (SECV), (5) ratio of performance to deviation (RPD), and (6) the number of LVs. Formulas used to estimate the SEC and SECV are given in the paper by Schimleck et al. (2001). These data should be as low as possible, whereas the coefficient of determinations should be high. The RPD value is the ratio of the standard deviation (SD) of the reference data to the SECV. This statistic provides a basis for standardizing the SECV (Williams and Sobering 1993) and makes possible a comparison of different calibration parameters, such as spectral information obtained from different wood surfaces.

Results and discussion

Wet-lab chemistry

The contents of KL, ASL, and the syringyl-to-guaiacyl (S/G) ratios are presented in Table 1. Chemical analyses were performed in duplicate and had good repeatability. The duplicates never showed differences at the 5% significance level. Scattering of these chemical properties was high. This range could be explained by the genetic variability of the genitors which originated from two different provenances, the outcrossing effects, the growth conditions, and the age of trees.

Chemical properties presented in Table 1 are in accordance to properties found by other authors who investigated mature *Eucalyptus* wood and are higher than those reported for juvenile wood. Table 2 presents results of chemical analysis of *Eucalyptus* wood reported in other studies. For instance, Gomide et al. (2005) evaluated clones of *Eucalyptus grandis* and *E. urophylla* (7-year-old) and found lower KL content, higher ASL content, and higher S/G ratios. Brito and Barrichelo (1977) also studied 7-year-old *E. urophylla* from Brazilian plantations and reported lower KL content (23.6%). Similarly, Carvalho and Nahuz (2001) studied hybrid of *E. grandis* and *E. urophylla* (7-year-old) and reported similar average KL content (22.4%). Higher KL contents were reported by Brito and Barrichelo (1977) when they evaluated *E. urophylla* from Timor (11-year-old). Poke et al. (2006) evaluated 13-year-old *E. globulus* and reported lower lignin content and higher ASL content. Alencar et al. (2002) found high lignin content (27.4%) in hybrids of 7-year-old *E. grandis* and *E. urophylla*. The results reported by these authors are comparable to the results of lignin content found in 14-year-old *Eucalyptus* presented in Table 1.

NIR spectra

Averaged raw NIR spectra measured on rough and surface woods and on coarse and fine wood powders are presented in Figure 1a. Fine wood powder (0.5 mm) provides NIR spectra with the lowest absorbance values. Absolute differences among NIR spectra are shown in Figure 1b. Differences were detected among NIR spectra acquired from the four types of sample preparation mainly because averaged NIR spectra measured on solid wood (rough and surfaced) displayed high absorbance values. For this reason, absolute differences between 0.5-rough and 0.5-surface NIR spectra exhibited slightly similar patterns of variation: their absolute differences increased toward the longer wavelength range (2500 nm).

With regard to absolute differences between NIR spectra recorded from 0.5 mm and 4.0 mm particle sizes, their absorbance variation was continuously similar (between -0.04 and -0.06) along the NIR spectral range and no differences in the fine structure of spectra were detected. NIR spectra measured on rough and surfaced wood are influenced by local heterogeneities, whereas milled wood is more homogeneous.

Table 2 Literature data for contents of Klason lignin (KL) and acid-soluble lignin (ASL) and syringyl-to-guaiacyl ratios (S/G) in *Eucalyptus* woods.

Reference	Species	Age (years)	Property	Average	Min	Max
Brito and Barrichelo (1977)	*E. urophylla*	7	KL (%)	23.6	–	–
		11	KL (%)	29.8	–	–
Carvalho and Nahuz (2001)	*E. grandis*× *E. urophylla* hybrids	7	KL (%)	22.4	–	–
Alencar et al. (2002)	*E. grandis*× *E. urophylla* hybrids	7	KL (%)	27.4	–	–
Gomide et al. (2005)	*E. grandis* and	7	KL (%)	24.7	22.4	27.0
	E. urophylla clones	7	ASL (%)	4.1	3.1	5.1
		7	S/G	2.5	2.1	2.8
Poke et al. (2006)	*E. globulus*	13	KL (%)	22.4	19.0	25.0
		13	ASL (%)	6.1	4.4	8.1

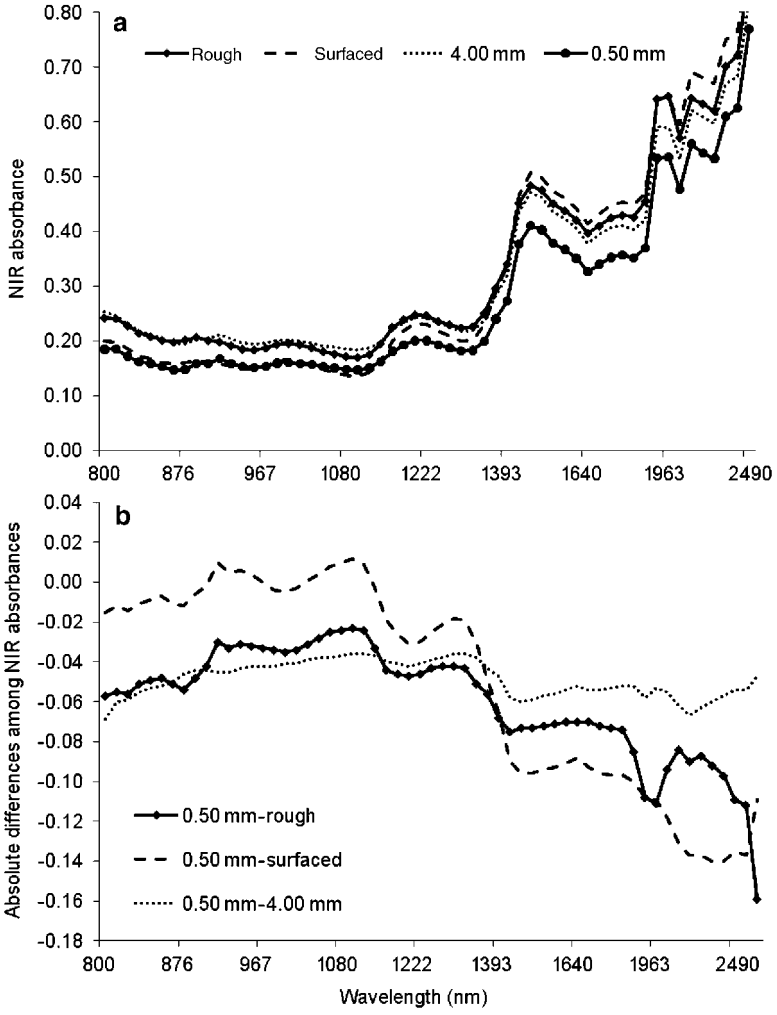

Figure 1 Averaged raw NIR spectrum (a) and absolute differences between averaged raw NIR spectrum for each type of *Eucalyptus urophylla* wood sample preparation (b).

Hence, the absolute difference between solid and powder NIR spectra (0.5 mm/rough or 0.5/surfaced) is higher than the difference between the NIR spectra measured on wood powders (0.5–4.0 mm).

PLS-R calibrations

Statistical summaries of the predictive PLS models are presented in Table 3. PLS-R calibrations for KL content had satisfactory correlations, particularly from the 4.0 mm milled wood, which presented R^2cv of 0.86 and RPD of 2.85. PLS-R models for solid wood are also lower (R^2cv = 0.76 for rough wood); however, they require more LVs. In general, the RPD values of the PLS-R calibrations of both coarse (RPD = 2.85) and fine powders (RPD = 2.58) were satisfactory to predict KL content in *E. urophylla* wood. The standard error of cross-validation of calibrations of coarse powder (SECV = 0.48) was lower than that of fine powder (SECV = 0.53), indicating that calibration based on 4.0 mm NIR spectra is the best to predict KL content in *E. urophylla* wood. Figure 2 shows the plots measured KL content versus NIR predicted KL content.

These predictive PLS models for KL content (Table 3) were comparable to those published by other groups. For instance, Meder et al. (1999) developed models with R^2 values ranging from 0.57 to 0.84 and prediction error of 4.9% to estimate KL content in *Pinus radiata*. Baillères et al. (2002) adjusted models to predict KL content in hybrids of *E. urophylla*×*E. grandis* and reported a R^2 value of 0.87, SECV of 0.37%, and RPD of 2.3 based on eight LVs of PLS regression. Hodge and Woodbridge (2004) studied the lignin contents in *Pinus caribaea*, *P. oocarpa*, and *P. tecunumanii* from progeny testing in Brazil. These authors calibrated models to estimate the lignin content from milled wood spectra and reported coefficients of determination of validation ranging from 0.77 to 0.91 and SECV from 0.38% to 0.49%. Yeh et al. (2004) evaluated lignin content in *Pinus taeda* by NIR spectroscopy and found a R^2 value of 0.72 and standard error of prediction of 0.87% when they based data on an external calibration set to validate their predictive models.

Table 3 Summary of PLS-R models to estimate contents of Klason lignin (KL) and acid-soluble lignin (ASL) and syringyl-to-guaiacyl ratios (S/G) in 14-year-old *Eucalyptus urophylla* woods according to sample preparation.

Chemical properties	Sample preparation	Mathematical manipulation	R^2c	SEC	R^2cv	SECV	LV	Outliers	RPD
Klason lignin	Rough disc	First derivative	0.76	0.63	0.76	0.75	5	1	1.82
	Surfaced wedge	Second derivative	0.69	0.74	0.64	0.80	3	1	1.71
	Milled 4.0 mm	None	0.88	0.44	0.86	0.48	5	2	2.85
	Milled 0.5 mm	None	0.88	0.44	0.85	0.53	6	3	2.58
Acid soluble lignin	Rough disc	None	0.74	0.099	0.58	0.13	9	2	1.68
	Surfaced wedge	Second derivative	0.83	0.088	0.74	0.11	6	–	1.99
	Milled 4.0 mm	First derivative	0.83	0.086	0.72	0.11	6	1	1.99
	Milled 0.5 mm	Second derivative	0.88	0.073	0.77	0.10	6	–	2.12
S/G ratio by thioacidolysis	Rough disc	Second derivative	0.94	0.072	0.74	0.16	12	3	2.16
	Surfaced wedge	Second derivative	0.74	0.167	0.71	0.18	4	3	1.90
	Milled 4.0 mm	Second derivative	0.90	0.097	0.86	0.12	7	3	2.88
	Milled 0.5 mm	Second derivative	0.92	0.099	0.86	0.13	7	3	2.68

R^2cal, coefficient of determination of the calibration model; SEC, standard error of calibration; R^2cv, coefficient of determination of the cross-validation; SECV, standard error of cross-validation; LV, latent variable; RPD, ratio of performance to deviation.

The calibration statistics associated with models to predict ASL content by PLS regression are promising. NIR spectra of surfaced wood and in coarse powder provide similar calibration statistics ($R^2c = 0.83$ and RPD = 1.99) for ASL content by PLS regression. It is visible that SECV decreases from 0.128% (rough solid wood) to 0.101% (fine wood powder) depending on the sample preparation. According to the RPD values, it is obvious that spectra recorded from surfaced wood and milled wood (4.0 and 0.5 mm) are useful to assess ASL content of 14-year-old *E. urophylla*. Figure 3 shows the plots measured data versus NIR predicted data for ASL content of the calibrations presented in Table 3.

PLS regressions to estimate the ratio of S/G units are presented in Figure 4. PLS-R models developed from wood powder show a good fit ($R^2cv = 0.86$) and high RPD value (> 2.5); however, coarse wood powder has a weaker SECV (0.12%) with the same number of LVs and outliers. The R^2cv values of wood powder models were better (0.86).

Statistics of the models to estimate S/G ratio are in principal in agreement with those of other studies. For instance,

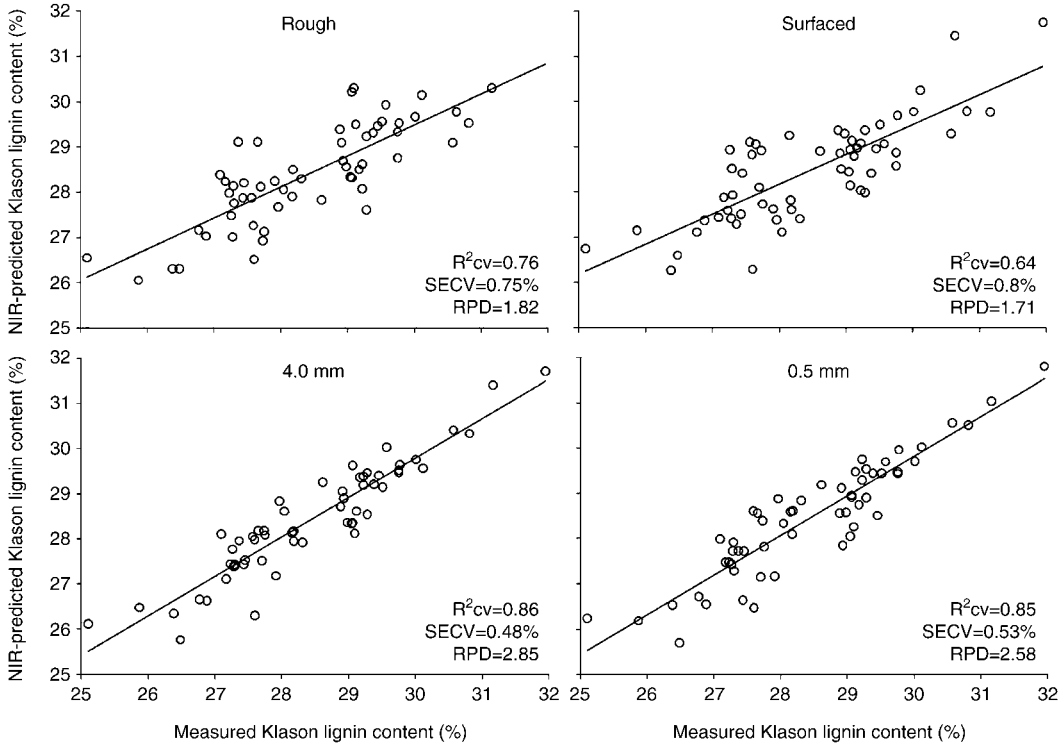

Figure 2 Measured versus NIR predicted plot for Klason lignin content in *Eucalyptus urophylla* wood.

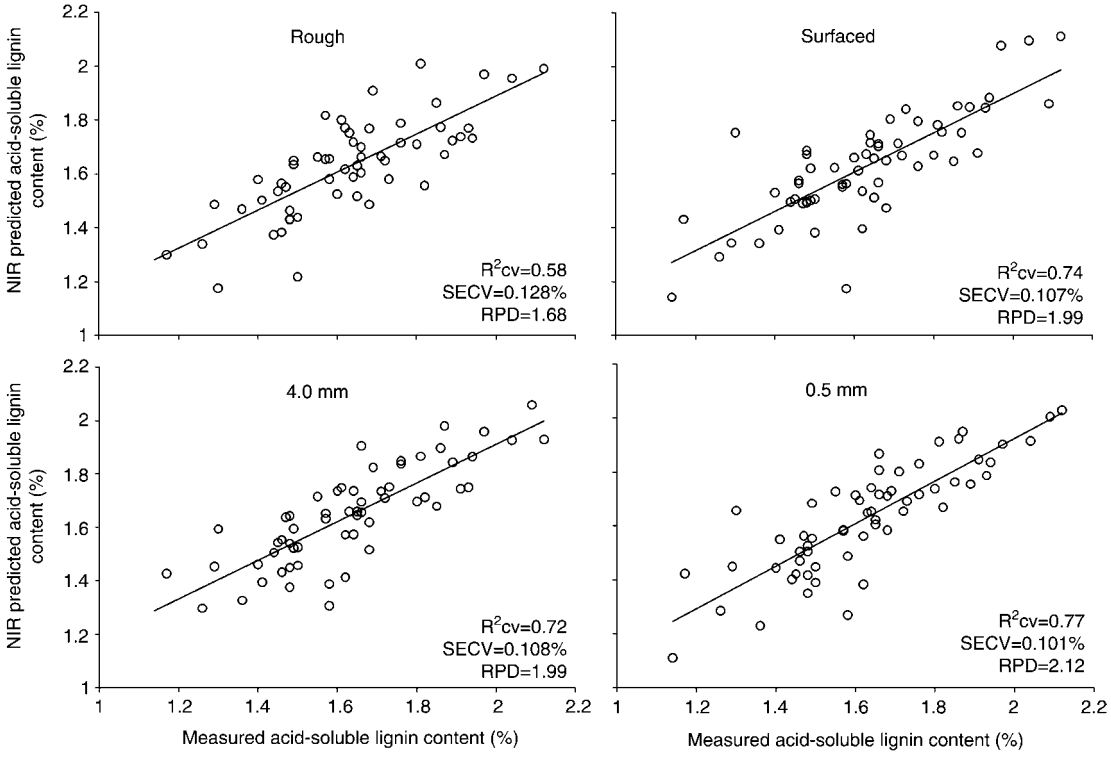

Figure 3 Measured versus NIR predicted plot for acid-soluble lignin content in *Eucalyptus urophylla* wood.

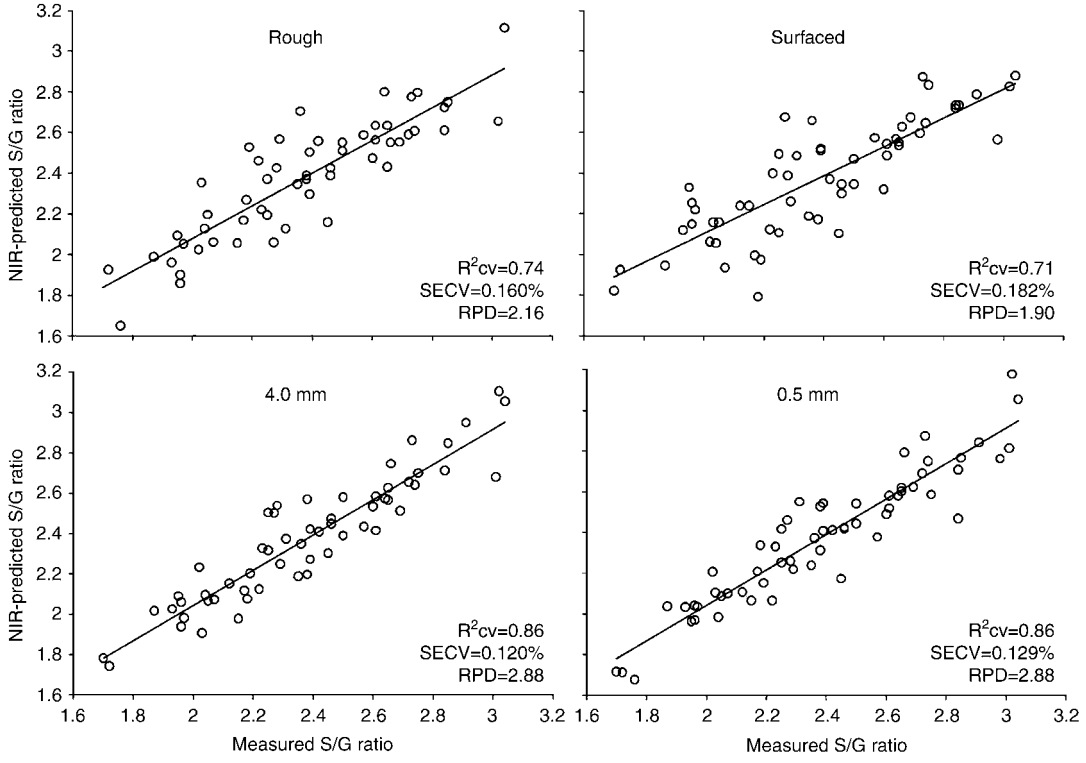

Figure 4 Measured versus NIR predicted plot for syringyl-to-guaiacyl ratio in *Eucalyptus urophylla* wood.

Baillères et al. (2002) reported good PLS-R calibrations ($R^2 = 0.90$, SECV = 0.22, and RPD = 2.4 with 10 LVs) to estimate the S/G ratio in hybrids of *E. urophylla* × *E. grandis* wood. Alves et al. (2006) estimated the *p*-hydroxyphenyl-to-guaiacyl ratio of 68 maritime pines by NIR cross-validations with strong (0.89) coefficient of determination and low RMSE (0.0054). Robinson and Mansfield (2009) evaluated lignin composition in *Populus alba* × *tremula* reporting even better PLS-R cross-validations to separately estimate *p*-hydroxyphenyl ($R^2 = 0.71$ and RMSECV = 0.005), guaiacyl units ($R^2 = 0.96$ and RMSECV = 0.202), and syringyl units ($R^2 = 0.96$ and RMSECV = 0.201).

From the results of the present work, it is obvious that the reduction of particle size from coarse to fine wood powder does not improve PLS-R models to assess KL content and S/G ratio in *E. urophylla* by NIR spectroscopy. For these properties, the difference between NIR spectra taken from solid wood and powdered wood was more important than differences in particle size concerning coarse and fine powder.

Figure 5 shows the general plot of weighted PLS regression coefficients to estimate KL content. These regression coefficients between models and absorbances along NIR spectra bands allow comparison of the loadings of the four types of sample preparations. For all PLS-R calibrations to KL content, the higher loadings were obtained in the NIR spectra range from 1638 nm to 2352 nm. The gray parts indicate the bands where regression coefficient is significantly different to zero according to the Martens' uncertainty tests (Westad and Martens 2000). The PLS-R models based on NIR spectra recorded from wood powders showed similar patterns for loadings presenting the highest regression coefficients at wavelengths of 1672 nm and 2300 nm and lower regression coefficient at 1724 nm. These loadings are in accordance with data of Tsuchikawa and Siesler (2003), who affirm that the wavelength of 1672 nm represents the absorption band of the aromatic groups in lignin (CH stretching in the first overtone). According to these authors, the wavelength of 1724 nm is for the absorption band of the furanose/pyranose units of hemicelluloses. In the present study, the significant regression coefficients obtained at 1724 nm (Figure 5) can be interpreted that the lignin and hemicelluloses have a common absorbance band at this wavelength.

Ability of NIR predictions of chemical properties based on solid wood spectroscopy

Limited information is available in the literature regarding NIR analysis for the prediction of chemical composition of solid wood. Kelley et al. (2004) investigated loblolly pine (*Pinus taeda*) and found satisfactory calibrations and prediction values for lignin, extractives, and contents of glucose, xylose, mannose, and galactose in hydrolysates of solid wood. Yeh et al. (2004) evaluated lignin content with NIR spectra measured on *P. taeda* increment core samples and found high correlations ($R^2 = 0.81$) between lignin related data obtained by wet chemistry and NIR prediction.

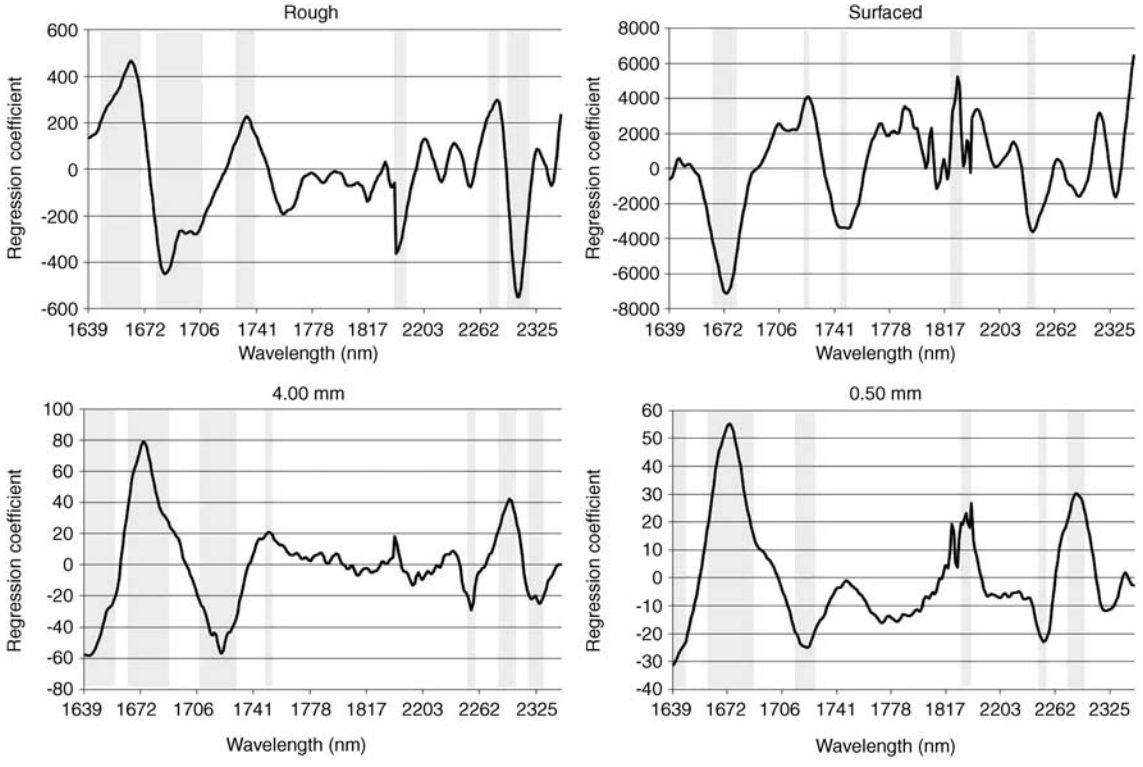

Figure 5 Significant absorption bands according to Martens' uncertainty test and regression coefficients of the PLS-R models to estimate Klason lignin content in *Eucalyptus urophylla* wood.

Poke and Raymond (2006) evaluated NIR calibrations to predict contents of extractives, ASL, and KL in 14-year-old *E. globulus* from Tasmania. The improved model yielded high R^2 values. The ASL and KL contents could be predicted with R^2 values of 0.72 and 0.78, SEC of 0.41% and 1.02% requiring six and four LVs, respectively. Comparing the data of the quoted authors with those presented in Table 3, the R^2c values in Table 3 are superior (0.74 for rough and 0.83 for surfaced), but inferior concerning the SEC values (0.099% for rough and 0.088% for surfaced). Solid wood NIR models for KL content in Table 3 are inferior ($R^2cv = 0.76$ for rough and 0.69 for surfaced wood) and the SECV values are also inferior (0.63% for rough and 0.74% for surfaced wood), and moreover one more LV was needed. These comparisons concern only calibration statistics. With regard to the validations of the calibrations, the data presented in Table 3 are more satisfactory according to criteria proposed by Fujimoto et al. (2008): superior R^2cv and inferior SECV for prediction of ASL and KL contents.

Effect of mathematical treatment on NIR spectra information

NIR spectra measured of rough wood required first derivative to improve the KL model performance, whereas for ASL content prediction based on the original NIR spectra (without mathematical manipulation) was the best choice. Related to the wood powder spectra, first and second derivative spectra were required to develop acceptable models for ASL determination. However, to estimate KL contents from these spectra, raw NIR data provide best adjustment (with higher number of LV). The second derivative improves the modeling fit to predict S/G ratio for all types of sample preparation.

Cross-correlation among predicted values from NIR calibrations

The cross-correlation among NIR predicted values for KL, ASL, and S/G ratio are listed in Table 4. Correlations between predicted values from rough and surfaced spectra were moderate (0.72 and 0.76) for S/G ratio and KL content and weak (0.59) for ASL content. Accordingly, wood surface conditions influence the results. By contrast, correlation between estimated values from coarse and fine powder wood calibrations was strong (from 0.93 to 0.95), indicating that particle size effects are less important. This is also confirmation again that coarse powder produces calibrations as good as fine powder. Baillères et al. (2002) also reported that variations in particle size between 30 and 60 mesh of *Eucalyptus* wood did not have a significant effect on NIR spectra. However, Yeh et al. (2004) evaluated lignin content in *P. taeda* and observed an influence of particle size. The band at 1400 nm of the fine powder was stronger than that of the raw wood meal.

The differences found in the measurements of NIR spectra carried out on powder and solid wood can be attributed to three complementary aspects: (1) the level of interaction between the incidence of the light and the samples. The arrangement of the particles of the powder wood promotes a deeper penetration of light into the material and the path travelled by light in the sample is able to capture more detailed information. In solid wood, the light penetrates the sample with the lowest depth. (2) Wood powder is composed of broken wood fibers and particles of other anatomical elements, such as parenchyma and vessels. The light passes through the particles bringing additional information to the NIR spectrum. (3) The spectrum obtained from both rough and surfaced wood could be influenced by local wood structure, contributing to noise in the calibration.

Table 4 Cross-correlation among chemical properties predicted by PLS-R models based on NIR spectra recorded from 14-year-old *Eucalyptus urophylla* wood samples prepared by different methods.

	Rough disc	Surface wedge	Milled 4.0 mm
Klason lignin			
Surface wedge	0.76		
Milled 4.0 mm	0.79	0.81	
Milled 0.5 mm	0.77	0.82	0.95
Acid soluble lignin			
Surface wedge	0.59		
Milled 4.0 mm	0.69	0.85	
Milled 0.5 mm	0.69	0.87	0.93
S/G ratio			
Surface wedge	0.72		
Milled 4.0 mm	0.79	0.87	
Milled 0.5 mm	0.82	0.83	0.94

Conclusions

The PLS calibrations yielded satisfactory results for estimating contents of KL and ASL and S/G ratios in *E. urophylla* wood by NIR spectroscopy. Needless to say, the higher the RPD value the more reliable the calibration (Fujimoto et al. 2008). Williams and Sobering (1993) claimed that a RPD value >2.5 is considered satisfactory for screening. In the present work, the best calibrations were found based on wood powder (RPD from 1.99 to 2.88), but calibrations obtained from solid samples were below this level (RPD from 1.68 to 2.16). Accordingly, preparation strongly influences the statistics associated with the predictive models.

In the present work, differences were higher between solid and milled wood than between fine and coarse powder. NIR data from solid wood could be sufficient only to rough estimation of the contents of KL and ASL and the S/G ratio. However, milling is strongly recommended for optimum accuracy. NIR spectra acquired from coarse saw mill yielded strong correlations ($RPD = 2.85$ for KL content and $RPD = 2.88$ for S/G ratio), so that the effort required to produce 0.5 mm wood powder is not justified. The results were not uniform concerning mathematical spectral manipulation.

Only for predicting S/G ratios was the second derivative NIR spectra advantageous.

Acknowledgements

The authors thank Pr. Catherine Lapierre and her team from INRA-Agro ParisTech (UMR 206 Chimie Biologique) for chemical measures, UR2PI (Republic of Congo) and the Bureau des Ressources Génétiques (BRG) for providing material, and UPR39 and UPR40 of CIRAD-Montpellier for providing technical support. We thank the National Council of Technological and Scientific Development (CNPq-Brazil) for partially supporting the present work (process no. 200970/2008-9) and particularly to Philippe Rozenberg from INRA (Orleans) for the financial support of the Alfa Gema Project (II-0266-FA) within which this research was conducted. In addition, we thank the referees and the editor-in-chief for their useful comments and suggestions.

References

Alencar, G.S.B., Barrichelo, L.E.G., Júnior, F.G.S.J. (2002) Qualidade da madeira de híbrido de *E. grandis*×*E. urophylla* e seleção precoce. In: 35 Congresso e exposição anual de celulose e papel. ABTCP, São Paulo, Brazil. pp. 1–6.

Alsberg, B.K., Kell, D.B., Goodacre, R. (1998) Variable selection in discriminant partial least squares analysis. Anal. Chem. 70: 4126–4133.

Alves, A., Schwanninger, M., Pereira, H., Rodrigues, J. (2006) Calibration of NIR to assess lignin composition (H/G ratio) in maritime pine wood using analytical pyrolysis as the reference method. Holzforschung 60:29–31.

Alves, A., Santos, A., Perez, D.S., Rodrigues, J.C., Pereira, H., Simões, R., Schwanninger, M. (2007) NIR PLSR model selection for Kappa number prediction of maritime pine Kraft pulps. Wood Sci. Technol. 41:491–499.

Baillères, H., Davrieux, F., Ham-Pichavant, F. (2002) Near infrared analysis as a tool for rapid screening of some major wood characteristics in a Eucalyptus breeding program. Ann. For. Sci. 59:479–490.

Ben-Gera, I., Norris, K. (1968) Direct spectrophotometric determination of fat and moisture in meat products. J. Food Sci. 33:64–67.

Birkett, M.D., Gambino, M.J.T. (1988) Estimation of pulp kappa number with near infrared spectroscopy. Tappi J. 72:193–197.

Brito, J.O., Barrichelo, L.E.G. (1977) Correlações entre características físicas e químicas da madeira e a produção de carvão vegetal: I. densidade e teor de lignina da madeira de eucalipto. IPEF 14:9–20.

Bull, C.R. (1991) Compensation for particle size effects in near infrared reflectance. Analyst 116:781–786.

Burns, D.A., Ciurczak, E.W. Handbook of Near-Infrared Analysis. CRC Press, Boca Raton, FL, 2008.

Campos, A.C.M., Hein, P.R.G., Mendes, R.F., Mendes, L.M., Chaix, G. (2009) Near infrared spectroscopy to evaluate composition of agro-based particleboards. BioResources 4:1058–1069.

Carvalho, A.M., Nahuz, M.A.R. (2001) Valorização da madeira do híbrido *Eucalyptus grandis*×*urophylla* através da produção conjunta de madeira serrada em pequenas dimensões, celulose e lenha. Sci. For. 59:61–76.

Codgill, R.P., Schimleck, L.R., Jones, P.D., Peter, G.F., Daniels, R.F., Clark, A. (2004) Estimation of the physical wood properties of *Pinus taeda* L. radial strips using least squares support vector machines. J. Near Infrared Spec. 12:263–269.

Dence, C.W. (1992) The determination of lignin. In: Methods in Lignin Chemistry. Eds. Lin, S.Y., Dence, C.W. Springer-Verlag, Berlin. pp. 33–61.

Easty, D.B., Berben, S.A., DeThomas, F.A., Brimmer, P.J. (1990) Near-infrared spectroscopy for the analysis of wood pulp: quantifying hardwood-softwood mixtures and estimating lignin content. Tappi J. 73:257–261.

Faix, O., Böttcher, J.H. (1992) The influence of particle size and concentration in transmission and diffuse reflectance spectroscopy of wood. Holz Roh Werkst. 50:221–226.

Fujimoto, T., Kurata, Y., Matsumoto, K., Tsushikawa, S. (2008) Application of near infrared spectroscopy for estimating wood mechanical properties of small clear and full length lumber specimens. J. Near Infrared Spec. 16:529–537.

Ghasemi, J., Niazi, A., Leardi, R. (2003) Genetic-algorithm-based wavelength selection in multicomponent spectrophotometric determination by PLS: application on copper and zinc mixture. Talanta 59:311–317.

Gierlinger, N., Schwanninger, M., Wimmer, R. (2004) Characteristics and classification of Fourier-transform near infrared spectra of heartwood of different larch species (*Larix* sp.). J. Near Infrared Spec. 12:113–119.

Gomide, J.L., Colodette, J.L., Oliveira, R.C., Silva, C.M. (2005) Caracterização tecnológica, para produção de celulose, da nova geração de clones de *Eucalyptus* do Brasil. Árvore 29:129–137.

Hart, J.R., Norris, K.H., Golumbic, C. (1962) Determination of the moisture content of seeds by near-infrared spectrophotometry of their methanol extracts. Cereal Chem. 39:94–99.

Hein, P.R.G., Lima, J.T., Chaix, G. (2009) Robustness of models based on near infrared spectra to predict the basic density in *Eucalyptus urophylla* wood. J. Near Infrared Spec. 17:141–150.

Hodge, G.R., Woodbridge, W.C. (2004) Use of near infrared spectroscopy to predict lignin content in tropical and sub-tropical pines. J. Near Infrared Spec. 12:381–390.

Hoffmeyer, P., Pedersen, J. (1995) Evaluation of density and strength of Norway spruce wood by near infrared spectroscopy. Holz Roh Werkst. 53:165–170.

Jones, P.D., Schimleck, L.R., Peter, G.F., Daniels, R.F., Clark III, A. (2006) Nondestructive estimation of sections of radial wood strips by diffuse reflectance near infrared spectroscopy. Wood Sci. Technol. 40:708–720.

Jones, P.D., Schimleck, L.R., Daniels, R.D., Clark III, A., Purnell, R.C. (2008) Comparison of *Pinus taeda* L. whole-tree wood property calibrations using diffuse reflectance near infrared spectra obtained using a variety of sampling options. Wood Sci. Technol. 42:385–400.

Kelley, S.S., Rials, T.G., Snell, R., Groom, L.H., Sluiter, A. (2004) Use of near infrared spectroscopy to measure the chemical and mechanical properties of solid wood. Wood Sci. Technol. 38: 257–276.

Lapierre, C., Pollet, B., Rolando, C. (1995) New insights into the molecular architecture of hardwood lignins by chemical degradative methods. Res. Chem. Interm. 21:397–412.

Lestander, T.A., Johnsson, B., Grothage, M. (2008) NIR techniques create added values for the pellet and biofuel industry. Bioresource Technol. 100:1589–1594.

Meder, R., Gallagher, S., Mackie, K.L., Böhler, H., Meglen, R.R. (1999) Rapid determination of the chemical composition and density of *Pinus radiata* by PLS modelling of transmission and diffuse reflectance FTIR spectra. Holzforschung 53:261–266.

Mora, C.R., Schimleck, L.R., Isik, F. (2008) Near infrared calibration models for the estimation of wood density in *Pinus taeda* using repeated sample measurements. J. Near Infrared Spec. 16:517–528.

Næs, T., Isaksson, T., Fearn, T., Davies, T. A User-Friendly Guide to Multivariate Calibration and Classification. NIR Publication, Chichester, UK, 2002.

Norris, K.H., Williams, P.C. (1984) Optimization of mathematical treatments of raw near-infrared signal in the measurement of protein in hard red spring wheat. I. Influence of particle size. Cereal Chem. 61:158–165.

Otsuka, M. (2004) Comparative particle size determination of phenacetin bulk powder by using Kubelka-Munk theory and principal component regression analysis based on near-infrared spectroscopy. Powder Technol. 141:244–250.

Pasquini, C. (2003) Near infrared spectroscopy: fundamentals, practical aspects and analytical applications. J. Braz. Chem. Soc. 14:198–219.

Poke, F.S., Raymond, C.A. (2006) Predicting extractives, lignin, and cellulose contents using near infrared spectroscopy on solid wood in *Eucalyptus globulus*. J. Wood Chem. Technol. 26:187–199.

Poke, F.S., Potts, B.M., Vaillancourt, R.E., Raymond, C.A. (2006) Genetic parameters for lignin, extractives and decay in *Eucalyptus globulus*. Ann. For. Sci. 63:813–821.

Robinson, A.R., Mansfield, S.D. (2009) Rapid analysis of poplar lignin monomer composition by a revised thioacidolysis procedure and NIR-based prediction modeling. Plant J. 58: 706–714.

Savitzky, A., Golay, M.J.E. (1964) Smoothing and differentiation of data by simplified least-squares procedures. Anal. Chem. 36: 1627–1639.

Schimleck, L.R., Evans, R. (2004) Estimation of *Pinus radiata* D. Don tracheid morphological characteristics by near infrared spectroscopy. Holzforschung 58:66–73.

Schimleck, L.R., Evans, R., Ilic, J. (2001) Estimation of *Eucalyptus delegatensis* wood properties by near infrared spectroscopy. Can. J. For. Res. 31:1671–1675.

Schimleck, L.R., Doran, J.C., Rimbawanto, A. (2003) Near infrared spectroscopy for cost-effective screening of foliar oil characteristics in a *Melaleuca cajuputi* breeding population. J. Agric. Food Chem. 51:2433–2437.

Schimleck, L.R., Evans, R., Jones, P.D., Daniels, R.F., Peter, G.F., Clark III, A. (2005) Estimation of microfibril angle and stiffness by near infrared spectroscopy using sample sets having limited wood density variation. IAWA J. 26:175–187.

Taylor, A.M., Baek, S.H., Jeong, M.K., Nix, G. (2008) Wood shrinkage prediction using NIR spectroscopy. Wood Fiber Sci. 40:301–307.

Thumm, A., Meder, R. (2001) Stiffness prediction of radiata pine clearwood test pieces using near infrared spectroscopy. J. Near Infrared Spec. 9:117–122.

Tsuchikawa, S. (2007) A review of recent near infrared research for wood and paper. Appl. Spectrosc. Rev. 42:43–71.

Tsuchikawa, S., Siesler, H.W. (2003) Near-infrared spectroscopic monitoring of the diffusion process of deuterium-labeled molecules in wood, Part.1: softwood. Appl. Spectrosc. 57: 667–674.

Tsuchikawa, S., Hayashi, K., Tsutsumi, S. (1992) Application of near infrared spectrophotometry to wood. 1. Effects of the surface-structure. Mokuzai Gakkaishi 38:128–136.

Tyson, J., Schimleck, L., Aguiar, A.M., Muro Abad, J.I., Rezende, G.S.P. (2009) Adjusting near infrared wood property calibrations for central Brazil to predict the wood properties of samples from southern Brazil. Appita J. 62:46–51.

Westad, F., Martens, H. (2000) Variable selection in near infrared spectroscopy based on significance testing in partial least square regression. J. Near Infrared Spec. 8:117–124.

Williams, P.C., Sobering, D.C. (1993) Comparison of commercial near infrared transmittance and reflectance instruments for analysis of whole grains and seeds. J. Near Infrared Spec. 1:25–33.

Wright, J., Birkett, M., Gambino, M. (1990) Prediction of pulp yield and cellulose content from wood using near infrared reflectance spectroscopy. Tappi J. 73:164–166.

Yeh, T.-F., Chang, H.-M., Kadla, J.F. (2004) Rapid prediction of solid wood lignin content using transmittance near-infrared spectroscopy. J. Agric. Food Chem. 52:1435–1439.

Zahri, S., Moubarik, A., Charrier, F., Chaix, G., Baillères, H., Nepveu G., Charrier, B. (2008) Quantitative assessment of total phenol content of European oak (*Quercus petraea* and *Quercus robur*) by diffuse reflectance NIR spectroscopy on solid wood surfaces. Holzforschung 62:679–687.

Zavarin, E., Jones, S.J., Cool, L.G. (1990) Analysis of solid wood surfaces by diffuse reflectance infrared Fourier-transform (DRIFT) spectroscopy. J. Wood Chem. Technol. 10:495–513.

Received April 8, 2009. Accepted July 30, 2009.
Previously published online December 7, 2009.

Paper 5

Authors: Hein, PRG, Lima JT and Chaix G

Title: Robustness of models based on near infrared spectra to predict the basic density in Eucalyptus urophylla wood

Journal: J. Near Infrared Spectrosc, v.17, n.3, p.141-150 (2009)

Received: 18 February 2009 ■ *Revised: 18 May 2009* ■ *Accepted: 22 May 2009* ■ *Publication: 1 June 2009*

JNIRS JOURNAL OF NEAR INFRARED SPECTROSCOPY

Robustness of models based on near infrared spectra to predict the basic density in *Eucalyptus urophylla* wood

Paulo Ricardo Gherardi Hein,[a,*] José Tarcísio Lima[b] and Gilles Chaix[c]

[a]CIRAD—PERSYST Department, 73 rue Jean-François Breton TA B-40/16, 34398 Montpellier Cedex 5, France email: phein1980@gmail.com

[b]Ciência e Tecnologia da Madeira, Departamento de Ciências Florestais, Universidade Federal de Lavras, Campus Universitário, Lavras, Minas Gerais, Brazil, CEP 37200-000

[c]CIRAD—BIOS Department, 73 rue Jean-François Breton TA A-39, 34398 Montpellier Cedex 5, France

Scientific contributions have shown good results by using near infrared (NIR) spectroscopy as a rapid and reliable tool for characterising lignocellulosic materials. Many reports have evaluated the predictive power and the robustness of the NIR models by means of methods known to validate them. However, in most of these investigations, the samples were divided systematically into two non-independent groups: one group was used to build and the other to validate the NIR models. This approach does not adequately simulate a real situation in which the properties of unknown samples should be predicted by established NIR models. Hence, the aim of this paper was to evaluate the robustness of models based on NIR spectroscopy to predict wood basic density in *Eucalyptus urophylla* using two totally independent sample sets. Wood density and NIR spectra were measured in diffuse reflectance mode on transversal, radial and tangential surfaces of wood samples in two data sets. We used one data set to build partial least squares regression (PLS-R) models and another to validate them and *vice versa*. The predictive models developed from the radial surface NIR spectra proved satisfactory with r^2_p varying from 0.79 to 0.85 and *RPD* ranging from 2.3 to 2.7, while the spectra measured on tangential and transversal wood surfaces generated less robust regression models. Our results showed that it is possible to assess wood density in unknown samples by established PLS-R models from solid wood samples preferably using radial surfaces.

Keywords: near infrared spectroscopy, robustness, validation, basic density, wood surface, *Eucalyptus urophylla*

Introduction

Wood density is widely regarded as a key trait in determining whole wood quality because it exhibits a strong correlation with other wood properties.[1] This wood trait varies radially, usually increasing from the pith to the cambium.[2] It also varies with tree height but, in this case, variations are not consistent and depend on species.[3] Hence, variation in wood properties within a species can have a tremendous impact on product quality and tree breeders have known for many years that most wood quality traits are under a high degree of genetic control.[4]

Determination of wood basic density is traditionally done by a volumetric method that is accurate but time-consuming for large-scale sampling. Several methods and instruments, including the Torsiometer,[5] Resistograph,[6-8] microdensitometry[9-11] and pilodyn wood tester[12,13] have been developed to replace the standard method.

Parallel to this, since 1980, several characteristics related to wood chemistry have been estimated by near infrared (NIR) spectroscopy. The NIR analyses rely on developing a calibration that relates NIR spectra of the samples to their known

ISSN: 0967-0335
doi: 10.1255/jnirs.833

chemical constitution, for example, lignin content. This calibration is then used to predict lignin content of further samples based on their NIR spectrum.[14] According to Pasquini,[15] the most common regression method for calibration development is partial least squares (PLS). Birkett and Gambino,[16] Easty *et al*.[17] and Wright *et al*.[18] have initiated studies on the paper industry and they used NIR analysis to investigate some wood properties. The NIR spectroscopic approach has also been extended to assess non-chemical characteristics of solid wood samples and showed that NIR spectroscopy is capable of determining mechanical, anatomical and physical properties, including basic density. Probably the first study involving NIR spectra and wood density values was presented by Thygesen.[19] She used shavings and solid wood of Norway spruce, [*Picea abies* (L.) Karst.] and showed that NIR spectroscopy could be used to estimate the dry matter content and density in this wood. Later, Pedersen and Hoffmeyer[20] used NIR spectroscopy of solid wood samples of the same species to evaluate dry density (dry weight per dry volume); they stated that NIR spectroscopy could be used to predict density, compression and bending strength of dry wood. Currently, NIR spectroscopy is widely used as a tool for rapid screening of wood characteristics in tree breeding programmes[21] and covers a wide range of applications, such as predictions of microfibril angle,[22] mechanical properties,[23] kappa number,[24] wood crystallinity,[25] pulp yield,[26] phenol[27] and oil content,[28] shrinkage[29] and properties of heat-treated wood.[30]

The reliability of the NIR predictions is verified by the validation of models. The best way to test a calibration model, whether quantitative or qualitative, is to have some samples in reserve which are not included among the ones on which the calibration calculations are based and use those samples as "validation samples" (sometimes called "test samples", "prediction samples" or "known" samples).[31,32] A second approach is cross-validation, which removes one sample or a segment of samples from the calibration data set and constructs the model without these data.[15] The sample or samples left out then have their values predicted by the model and the prediction error calculated; this validation procedure is indicated when few samples are available.[32] An interesting application of cross-validation is to use it as a tool to identify outliers and to determine the optimum number of PLS factors to retain in the calibration model. This makes it possible to perform a calibration and validate it with an external set of samples using the information obtained from cross-validation simulation.

Several studies have used independent test sets to validate their calibration models.[23,33–38] These studies were carried out on a sampling systematically divided into two groups and the regressions were performed with one group and validated with the other. These approaches do not adequately simulate a real situation in which the properties of unknown samples may be predicted by established NIR models. Few studies have been addressed to verify the robustness of the predictive models using external and independent sample sets. Souza-Correia *et al*.[28] and Rodrigues *et al*.[39] used independent test sets in their studies in order to investigate this issue.

The main objective of this study was to evaluate the robustness of the PLS-R models for wood basic density analysis in *Eucalyptus urophylla* wood based on NIR spectra using two independent sample sets. We assumed that the data sets were totally independent because there were at least four independent sources of variation: (i) samples taken from different trees, (ii) sample preparation, (iii) wood density measurement and (iv) NIR spectra measurement. Finally, we used one data set to build the PLS-R models and another one to validate them, and vice-versa, bringing insight to the real external validation approach.

Materials and methods

Sample preparation and wood density measurement

Forty (40) breast height wood disks from a 14-year-old *Eucalyptus urophylla* from UR2PI (Republic of Congo) were used in this study. The disks had an average circumference of 53 cm (coefficient of variation = 21.2%) and were divided in diametrical bands by a vertical bandsaw machine. The diametrical bands were cut in 15 mm × 20 mm × 20 mm sized wood samples for NIR spectra and basic density measurements (Figure 1). Each surface of the wood samples was sanded with 300-grit sandpaper for approximately 30 s. Wood basic density was determined by ASTM D2395 procedures.[40] Basic density and the NIR spectral measurements were carried out in two different situations: the first measurement set on wood samples was carried out by technician 1 on the diametrical bands from 20 disks and produced data set 1 represented by 105 samples. Six months later, the second measurement set was carried out on the other wood disks by technician 2 and produced data set 2 with 85 samples. All measurements

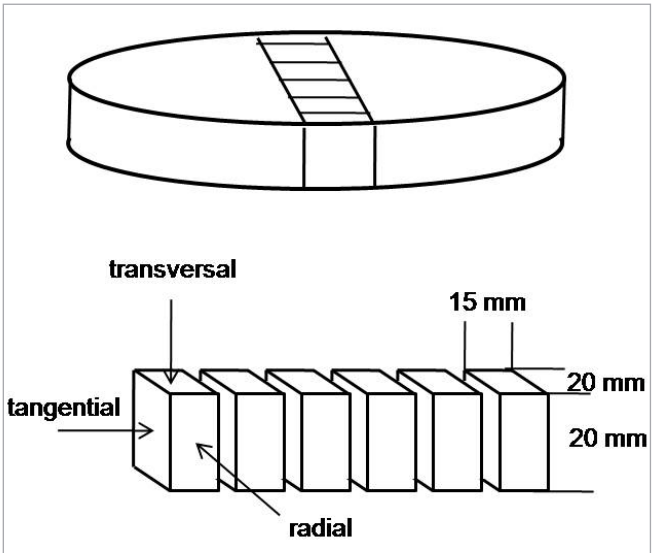

Figure 1. Sample preparation procedure for NIR spectra and wood basic density measurements.

were carried out using the same conditions and equipment and the total data set was composed of 190 samples from 40 disks. A summary of the wood basic density measurements is presented in Table 1.

NIR spectral measurements

NIR spectra were measured in diffuse reflectance mode with a Fourier transform spectrometer (model Vector 22/N, Bruker Optik GmbH, Ettlingen, Germany). This Fourier transform spectrometer is designed for reflectance analysis of solids with an integrating sphere (diameter of measured area = 10 mm). Spectral analysis was performed in the 12,500 cm^{-1} to 3500 cm^{-1} (800 nm to 2850 nm) range at 8 cm^{-1} resolution (each spectrum consisted of 2335 values). A sintered gold standard was used as reference or as background. Thirty-two (32) scans were performed for each measurement and means were calculated and compared to the standard in order to obtain the absorption spectrum of the sample. Spectral acquisitions were carried out on the transversal (transv), radial (radial) and tangential (tang) surface of the wood samples; spectra were acquired in a room with a controlled temperature of around 20°C and relative humidity of around 65%. In these conditions, the moisture content of the wood samples stabilised at 12%.

Statistical analysis

Principal component analysis (PCA) and partial least squares (PLS) regression analyses were performed using The Unscrambler software (CAMO AS, Norway; version 9.8). The PLS regression method was used to correlate the near infrared spectrum readings with the reference basic density of wood. First derivatives (13-point filter and a second order polynomial) and second derivatives (25-point filter and a third order polynomial) were applied on the NIR spectral data using the Savitsky and Golay[41] algorithm.

In a first step, data sets 1 and 2 were merged into data set 1 + 2 and PLS-R calibrations were performed by cross-validation using five segments with 38 samples selected randomly. The number of latent variables (*LV*s) and the outlier samples were identified during the cross-validation process. The Martens' uncertainty test[42] was used to select the wavenumbers with significant regression coefficients for basic density.

In a second step, PLS cross-validations were performed with data set 1 and were validated by data set 2 and vice-versa. We compared cross-validated PLS-R regressions using the complete sample set (no. of samples = 190) with cross-validated PLS-R regressions and independent validations using data set 1 (no. of samples = 105) and 2 (no. of samples = 85).

To evaluate cross-validations and independent validations, the following statistical parameters were used: (i) coefficient of determination of cross-validation (r^2_{cv}); (ii) coefficient of determination of prediction (r^2_p); (iii) standard error of cross-validation (*SECV*); (iv) standard error of prediction (*SEP*); (v) ratio of performance to standard deviation (*RPD*) and (vi) number of *LV*s.

Formulae used to estimate the *SECV* and *SEP* are given in Sykes *et al.*[43] and should be as low as possible while coefficients of determination should be high. The *RPD* value is the ratio of the *SECV* or *SEP* to the standard deviation (*SD*) of the used density values;[44] this parameter provides a basis for standardising the *SECV* or *SEP*[46] to compare regression reliabilities from other reports.[28] The higher the *RPD* value, the more reliable is the calibration.[23] Williams and Sobering[45] claim that an *RPD* greater than 2.5 is considered satisfactory for screening, although it has been shown that an *RPD* of approximately 1.5 indicates that NIR spectroscopy can be used as an initial screening tool.[46]

Results and discussion

NIR spectra from wood samples

At the outset, we assumed that external factors could discriminate data sets 1 and 2, namely (i) basic density measurement; (ii) range of density values; (iii) wood surface quality and (iv) moisture content of the wood samples. With regard to the density measurement procedure, the weight and volume measurements were totally independent and subtle procedural variations, inherent in human activities, could contribute to variations. The difference between the range in density values of data sets can be verified in Table 1. We believe that the first two external factors would have a minimal effect in data set differences, while the last two factors could have a major impact on variability between data set 1 and 2. The cutting operation was carried out using the same machine and the samples were sanded using the same procedures but by different operators. Hence, the surface quality of the wood samples after cutting and

Table 1. Summary of basic density (*BD*) measurements (kg m^{-3}).

	BD_{SET1}	BD_{SET2}	BD_{SET1+2}
Average	526	524	525
SD	80	84	82
Min.	401	338	338
Max.	746	689	746
CV (%)	15.3	16.0	15.6
No. of samples	105	85	190

sanding certainly was not the same. These particularities (for example, speed of cutting, sanding pressure) could have affected the NIR spectra. If these assumptions were true, we would suppose that mathematical treatments on the NIR spectra could minimise these effects. Regarding the last point, uncontrollable humidity variations could occur due to the time lag of six months, despite the samples being kept in the same room at a controlled temperature.

As NIR spectral differences between the samples can be simply realised by the application of PCA,[23] we performed these analyses to verify our preliminary assumptions. Figure 2 shows the results of PCA of the raw NIR spectra obtained from two measurements on radial surfaces of the wood samples. The principal components (PCs) 1 and 2 accounted for 97% of the spectra variability and no clusters were found in the scatter plot of scores for PC1 and PC2 (Figure 2). According to these PCA results, there were no NIR spectral differences between the data sets in spite of the sample set having been prepared by different technicians and at different times. The PCA of the NIR spectra taken from transversal and tangential surfaces (not presented) showed similar scores plots.

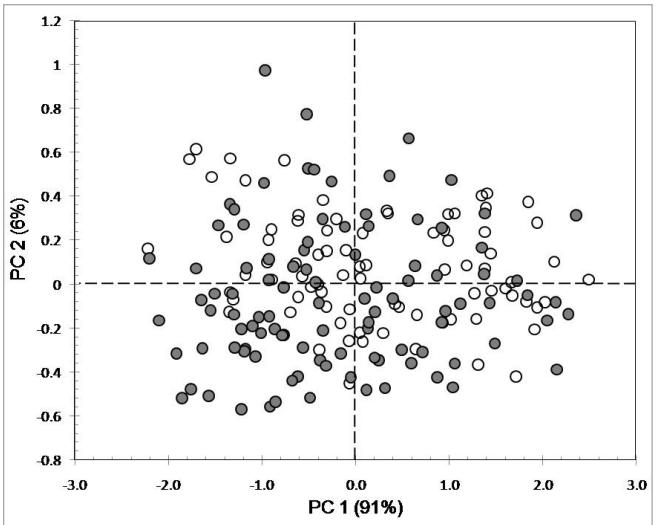

Figure 2. Two-dimensional scatter plot of scores for PC1 and PC2 from principal component analysis (PCA) of the original NIR spectra of data set 1 (grey circles) and data set 2 (white circles).

NIR spectroscopic calibration of wood basic density

Currently, many scientific contributions have shown good results by using NIR spectroscopy as a rapid and reliable tool for characterising lignocellulosic materials. Some works have used cross-validation[27,30,47,48] and others an independent data set for validation[23,33–38] to predict a range of wood properties. However, few studies have used external and independent sample sets in order to verify the robustness of the established predictive models.

In the present study, we tried to simulate a real situation building and validating predictive models with totally independent data sets. First, we merged data sets 1 and 2 into data set 1+2 to perform PLS-R cross-validation with the 190 samples (Table 2) and second, we independently investigated data sets 1 and 2 (Tables 3 and 4). The NIR spectra were taken from transversal, radial and tangential wood surfaces to compare the effect of cross-sections on PLS regressions.

PLS cross-validations for wood density

A statistical summary of the cross-validated PLS-R models developed for the 190 samples is shown in Table 2. The cross-validated PLS regressions from the radial and transversal spectral surfaces provided good coefficients of determination with r^2_{cv} ranging from 0.78 to 0.83 and *RPD* values varying from 2.2 to 2.5. The coefficients of determination from the tangential surface spectra were lower (r^2_{cv} from 0.63 to 0.67 and *RPD* from 1.6 to 1.7). The outliers reported in Table 2

Table 2. Cross-validated PLS-R models for wood basic density (190 samples) according to surface NIR spectra measurement and mathematical treatment.

Surface	Model	Treat.	*LV*	r^2_{cv}	*SECV*	No. of outliers	*RPD*
Transv.	1	no	3	0.83	33	1	2.5
	2	1d	6	0.81	36	3	2.3
	3	2d	7	0.78	38	4	2.2
Radial	4	no	3	0.83	34	1	2.4
	5	1d	3	0.83	33	1	2.5
	6	2d	3	0.81	35	1	2.3
Tang.	7	no	3	0.63	50	2	1.6
	8	1d	3	0.67	47	4	1.7
	9	2d	4	0.66	47	4	1.7

Treat: pre-treatment applied;1d: first derivative; 2d: second derivative; *LV*: number of latent variables; r^2_{cv}: coefficient of determination of cross-validation; *SECV*: standard error of cross-validation (kg m^{-3}) and *RPD*: ratio of performance to deviation

were identified and removed from a visual examination of the student residuals and leverage value scatter influence plot in The Unscrambler software.

For the PLS-R cross-validations from transversal surface NIR spectra, the original spectra provided the least outliers while the first derivative model (1d) required six latent variables and removal of additional samples to present more reasonable statistics. The cross-validations from radial surface spectra required three *LV*s, only one outlier was detected and the *SECV* were quite similar (33–35 kg m^{-3}).

The statistics presented in Table 2 were slightly lower than those shown by other studies. For instance, Mora *et al*.[38] presented a preliminary calibration model fitted to basic density in *Pinus taeda* using raw NIR spectra. They reported a PLS-R model with root mean square error of cross-validation (*RMSECV*) of 31 kg m^{-3}. Gindl *et al*.[47] evaluated 51 samples of *Larix decidua* Mill. obtaining an *r* value of 0.975 (r^2_{cv} = 0.95) and *RMSECV* of 23 kg m^{-3} for their cross-validated NIR calibration.

Independent validations of the PLS-R models for wood density

First, PLS-R models were developed from data set 1 (with 105 samples) and validated by data set 2 (with 85 samples) for transversal, radial and tangential surfaces of the *Eucalyptus urophylla* wood (Table 3).

The calibration to predict wood basic density from the radial wood surface NIR spectra provided the best results. The coefficients of determination of prediction (r^2_p) ranged from 0.81 to 0.85, the *RPD*s from 2.5 to 2.7 and the standard errors of prediction from 30 kg m^{-3} to 33 kg m^{-3}. Model 15 (with second derivative NIR spectra) provided a higher coefficient of determination in the independent data set (r^2_p=0.85) from the NIR spectra measured on radial surfaces. With regard to the radial NIR spectra, these statistics were similar to the cross-validated PLS-R models built with 190 samples (Table 2), although some samples were removed from the data set. The original transversal surface NIR spectra supplied a good PLS regression (model 10) showing similar statistics when using cross-validation method (models 1, 2 and 3 from Table 2). The first and second derivative of the transversal wood surface NIR spectra provided weaker regressions with lower r^2_p (< 0.59) and *RPD* values (1.6) while the treated transversal NIR spectra provided good cross-validated PLS-R models with the merged data set (Table 2). Mora *et al*.[38] compared PLS-R models established for density from raw and treated NIR spectra. In their study, the second derivative of the NIR spectra provided higher r^2_p and lower *RMSEP* than raw spectra while treatments such as multiplicative scatter and orthogonal signal corrections gave weaker relationships between the spectral data and basic density. In the present study, the best PLS regression (model 15) was developed from the second derivative NIR spectra measured on radial wood surface. This PLS regression required three latent variables presenting an *RPD* value of 2.7 in the independent validation set. Figure 3 shows the measured versus NIR predicted values plot for basic density in *Eucalyptus urophylla* wood with cross-validation (grey circles) and independent validation (white circles) for the model 15.

In PLS regression, it is not recommended to extrapolate the data range[31,32] and samples out of the calibrated range should be removed. Based on the range of density values of the data sets 1 and 2 (Table 1), some samples were systematically discarded from the independent validation while in the cross-validations (Table 2) these samples were not classified as outliers.

Table 3. PLS-R cross-validation models based on data set 1 and independent validation with data set 2 for wood basic density according to surface NIR spectra measurement and mathematical treatment.

Surface	Model	Treat	*LV*	Cross-validation (*n* = 105)			*RPD*	Validation (*n* = 85)			*RPD*
				r^2_{cv}	*SECV*	No. of outliers		r^2_p	*SEP*	No. of outliers	
Transv.	10	no	7	0.81	35	0	2.3	0.83	33	5	2.4
	11	1d	5	0.80	36	0	2.2	0.58	49	5	1.6
	12	2d	4	0.80	35	0	2.3	0.59	49	4	1.6
Radial	13	no	3	0.84	32	1	2.5	0.83	32	5	2.5
	14	1d	3	0.87	28	1	2.9	0.81	33	4	2.4
	15	2d	3	0.89	27	1	3.0	0.85	30	4	2.7
Tang.	16	no	3	0.67	46	2	1.7	0.61	48	4	1.7
	17	1d	3	0.70	44	3	1.8	0.62	49	5	1.6
	18	2d	4	0.66	47	3	1.7	0.65	45	5	1.8

Treat: pre-treatment applied; 1d: first derivative; 2d: second derivative; r^2_{cv}: coefficient of determination of cross-validation; r^2_p: coefficient of determination of prediction; *SECV*: standard error of cross-validation (kg m^{-3}); *SEP*: standard error of prediction (kg m^{-3}); *LV*: number of latent variables and *RPD*: ratio of performance to deviation

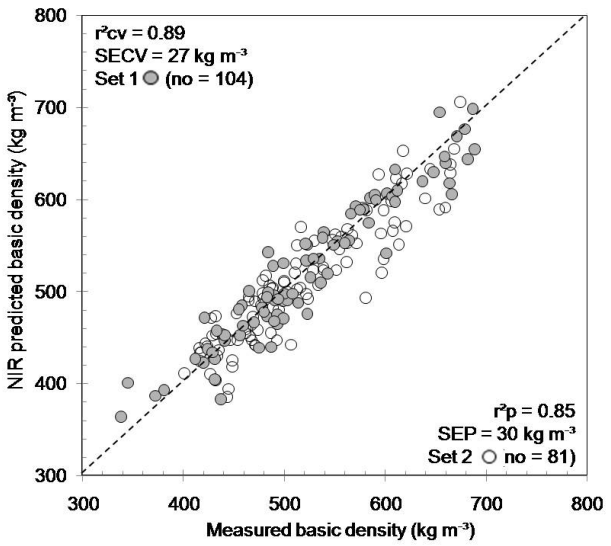

Figure 3. NIR predicted versus measured values for basic density. The original NIR spectra from data set 1 were used for cross-validation and those from data set 2 for independent validation.

Finally, the same procedures for cross-validation and independent validation were repeated by exchanging the data sets. We assumed that this approach simulated a real situation where the wood density values must be predicted on unknown samples by established NIR-based models reliably replacing the reference methods. PLS-R models were cross-validated with 85 samples from data set 2 and were validated with the 105 samples from data set 2. Table 4 presents the results of this second step.

The PLS-R models presented in Table 4 show very similar trends confirming the results presented in Table 3. Models 22, 23 and 24, built from the radial NIR spectra, always showed the strongest correlations and those from tangential faces always showed the weaker correlations (Tables 2, 3 and 4). NIR spectra from the transversal surface of wood gave only good validated models when original spectra were used (model 19 from Table 4 and model 10 from Table 3).

Figure 4 presents the NIR predicted versus measured basic density plot with calibration set samples in white circles and validation set samples in grey circles for model 22. This PLS-R model used three latent variables and, as in the case of model 13 from Table 3, also presented an acceptable *RPD* value (2.5) for screening.

The application of mathematical treatments during modelling is an important procedure to improve the statistics of the PLS regression models.[49] Regarding NIR spectra measured on radial and tangential surfaces, we observed that the first and second derivatives of spectra influenced the statistics of the models in a different manner and no trends could be identified. For instance, when the PLS-R models were validated by data set 2 (Table 3), the best regression (*RPD* = 2.7) was developed from the second derivative of the radial spectra (model 15). On the other hand, for the models validated by data set 1 (Table 4), the raw radial NIR spectra (model 22) provided the higher *RPD* value (*RPD* = 2.5). However, the raw spectra information of the transversal wood surface provides the best results for the established models.

The validation procedure used in this study showed that the PLS-R models to predict wood density in *Eucalyptus urophylla* (models 13, 15 and 22) were robust and had potential to predict this property with reasonable accuracy in unknown wood samples. The regression coefficients of these models

Table 4. PLS-R cross-validation models based on data set 2 and independent validation with data set 1 for wood basic density according to surface NIR spectra measurement and mathematical treatment.

Surface	Model	Treat	*LV*	Cross-validation (*n* = 85)			*RPD*	Validation (*n* = 105)			*RPD*
				r^2_{cv}	*SECV*	No. of outliers		r^2_p	*SEP*	No. of outliers	
Transv.	19	no	5	0.84	33	0	2.4	0.80	33	4	2.5
	20	1d	6	0.74	41	0	2.0	0.69	47	3	1.7
	21	2d	7	0.75	41	1	2.0	0.67	52	3	1.5
Radial	22	no	3	0.87	31	1	2.6	0.79	33	4	2.5
	23	1d	3	0.83	30	1	2.7	0.80	35	5	2.3
	24	2d	3	0.84	30	1	2.7	0.80	34	4	2.4
Tang.	25	no	3	0.67	47	0	1.7	0.56	56	5	1.4
	26	1d	4	0.66	43	2	1.9	0.63	50	5	1.6
	27	2d	3	0.63	46	1	1.7	0.61	52	5	1.5

Treat: pre-treatment applied; 1d: first derivative; 2d: second derivative; r^2_{cv}: coefficient of determination of cross-validation; r^2_p: coefficient of determination of prediction; *SECV*: standard error of the cross-validation (kg m^{-3}); *SEP*: standard error of the prediction (kg m^{-3}); *LV*: number of latent variables and *RPD*: ratio of performance to deviation

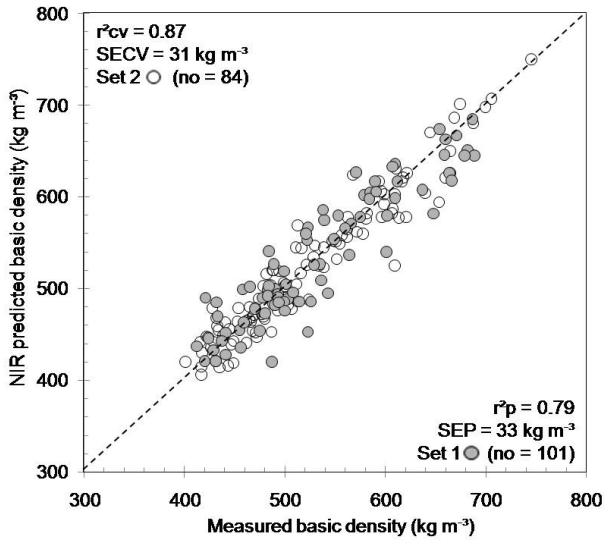

Figure 4. NIR predicted versus measured values for basic density. The original NIR spectra from data set 2 were used for calibration and those from data set 1 for validation.

presented similar patterns; Figure 5 shows the general plot of weighted regression coefficients. The grey rectangles indicate the uncertainty limits from cross-validations using Martens' uncertainty tests.[42]

Although intuitive, an interesting finding of this study was that the models built from a sample set with more samples (Table 3) present better statistics than the models built from a set with fewer samples (Table 4).

The model statistics shown in Tables 3 and 4 were very similar to those presented by other studies that have used external test sets as a validation method to determine the predictive ability of the PLS-R model. For instance, Schimleck *et al.*[33] divided their *Eucalyptus delegatensis* sampling into two groups using 70 samples for calibration and 34 samples for validation. They reported PLS-R models with r^2_p of 0.92 and *SEP* of 31 kg m^{-3}. Schimleck *et al.*[50] have studied eight-year-old *Eucalyptus globulus* Labill. subsp. *globulus* and found wood basic density models with coefficients of determination ranging from 0.63 to 0.80 for second derivative spectra, depending on the number of PLS components applied (four to ten). They used approximately 75% of available samples (random choice) to develop calibration models and 25% to test the predictive ability of the models. Via *et al.*[34] have reported NIR calibrations to predict density in mature, juvenile and pith wood of *Pinus palustris* by multiple linear regression and principal component regression. From a total of 263 available samples, they used approximately 65% for model calibration and 35% for validation, reporting models with $R^2 = 0.75$ and root mean squared error of validation varying from 51.2 kg m^{-3} to 50.7 kg m^{-3}. Cogdill *et al.*[35] used a very large number of samples to develop calibrations for *Pinus taeda* air-dry density. The calibration set contained 489 NIR spectra and the prediction set 240. They reported an R^2 of 0.81 for the calibration model, *SEP* = 42 kg m^{-3} and *RPD* = 2.6 using six PLS components. Via *et al.*[36] verified the ability of NIR spectroscopy to monitor wood air-dry density in ten *Pinus* trees; they used 170 samples to develop the models for density and 93 samples randomly held aside to validate them.

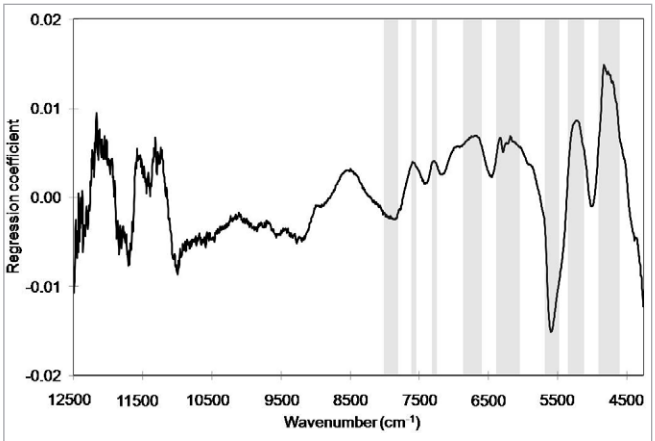

Figure 5. Significant absorption bands according to Martens' uncertainty test and regression coefficients of the PLS-R models to predict basic density.

Our results confirm the above-mentioned studies which showed that it is possible to assess wood density by near infrared spectroscopy from solid wood samples preferably using radial surfaces.

Differences between NIR spectra from wood surfaces

Some papers have shown differences between NIR spectra acquired from wood surfaces. Tsuchikawa *et al.*[51] has studied the effects of surface-structure on near infrared spectra; Thum and Meder[52] related some differences between spectra measured from radial and transversal faces in *Pinus radiata*. Similarly, Gierlinger *et al.*[53] evaluated spectral differences from transversal and radial faces of heartwood in three species of larch to classify these trees. They reported small spectral differences when analysing the second derivative of the spectra and reported that, for spectra acquired from radial surfaces, all three clusters showed high heterogeneity; however, spectra from axial surfaces showed less heterogeneity between larches. Schimleck *et al.*[54] used radial faces to predict physical properties in green *Pinus taeda* and Schimleck *et al.*[55] compared models to predict wood properties based on radial and transversal faces of strips from *Pinus taeda*. Jones *et al.*[56] also used spectra measured from radial faces of wooden strips from *Pinus taeda* to develop models to predict chemical composition. Fujimoto *et al.*[23] reported the same trends with regard to radial and transversal wood faces to predict mechanical properties in samples of hybrid larch. Sykacek *et al.*[57] used an impressive number of samples and spectra showing the differences between calibration results from NIR spectra taken from radial and transversal surfaces.

They attributed the differences between spectra to the chemical and structural properties in larch wood.

The differences in model accuracy for basic density estimation from the wood cross-sections can be explained by the variation of anatomical structures of the different surfaces; however, the relationship between NIR spectra and the wood properties were not clearly understood. Fujimoto *et al*.[23] supplied a good explanation of differences between spectral information from wood surfaces. Particularly for the wood density, this property is a result of the interaction between chemical and anatomical wood properties.[1] Therefore, the variations in wood density are caused by differences in the cell dimensions, interaction and by the amount of extractive components present in the unit of volume. Thus, it is possible to suggest that the higher exposure of parenchyma cells in the radial wood surface in comparison with the tangential surface had a positive influence on the fittings presented in this study with *Eucalyptus* wood.

Additionally, the NIR spectra of the tangential surface do not get an average, because the measurment is carried out mainly on wood formed in one year or a part of one year, whereas on the radial surface, the spectra capture information averaged over years. Thus the spectrum is more representative.

Conclusions

Our results showed that it is possible to assess wood density in unknown samples by established PLS-R models from solid wood samples, preferably using radial surfaces. Radial surface NIR spectra provided the best PLS-R models for wood density predictions and the tangential surface spectra supplied weaker regression statistics. Raw NIR spectra measured on transversal surface also provided acceptable cross-validated PLS-R models. The procedure for model validation used in this investigation ensures the reliability of the use of this tool in routine analysis for basic density in *Eucalyptus* wood. This technique, associated with a motor-driven coring system, allows prediction of basic density in a large dry sample set as required by genetic studies (high throughput phenotyping), since the moisture content of the sample can be stabilised and the core sample is cut parallel to the fibre orientation, allowing the radial face to be measured by the spectrometer. Further studies are required to understand the effects of varying wood moisture content, sample preparation and wood surface qualities on PLS-R models in order to predict wood properties.

Acknowledgements

The authors would like to thank UR2PI (Republic of Congo) and UPR39 and UPR41 of CIRAD for providing the materials and to Ana Carolina Maioli Campos (UFLA) and Fernando Campos de Oliveira (UFPR) for providing the technical support. We would like to thank the National Council of Technological and Scientific Development (CNPq-Brazil) for partially supporting the present work (process no. 200970/2008-9) and particularly to Philippe Rozenberg from INRA (Orleans) for the financial support of the Alfa Gema Project (II-0266-FA) within which this research was conducted. In addition, we would like to thank the referees for theirs useful comments and suggestions.

References

1. A.J. Panshin and C. de Zeeuw, *Textbook of Wood Technology*. McGraw-Hill, New York, USA, p. 722 (1980).
2. B.J. Zobel and J.B. Jett. *Genetics of Wood Production*. Springer-Verlag, Berlin, Germany, p. 352 (1995).
3. B.J. Zobel and H. Van Buijtenen. *Wood Variation: Its Causes and Control*. Springer-Verlag, Berlin, Germany, p. 363 (1989).
4. A.J. Michell and L.R. Schimleck, "Developing a method for the rapid assessment of pulp yield of plantation eucalypt trees beyond the year 2000", *Appita J.* **51,** 428–432 (1998).
5. H. Polge, "Investigation of the use of samples taken with a Pressler borer for studying physical and mechanical properties of wood", *Rev. for. franc.* **X**, 835–853 (1962).
6. F. Rinn, F.H. Schweingruber and E. Schär, "Resistograph and X-ray density charts of wood comparative evaluation of drill resistance profiles and X-ray density charts of different wood species", *Holzforschung* **50,** 303–311 (1996).
7. G. Chantre and P. Rozenberg, "Can drill resistance profiles (Resistograph) lead to within-profile and within-ring density parameters in Douglas-fir wood?" in: *Proceedings of CTIA – IUFRO International Wood Quality Workshop: Timber Management Toward Wood Quality and End-Product Value*, Québec, 18–22 August, pp. 41–47 (1997).
8. L. Bouffier, C. Charlot, A. Raffin, P. Rozenberg and A. Kremer, "Can wood density be efficiently selected at early stage in maritime pine (*Pinus pinaster* Ait.)?", *Ann. For. Sci.* **65,** 106–114 (2008). doi: 10.1051/forest:2007078
9. H. Polge, "Study of wood density variations by densitometric analysis of X-ray negatives of samples taken with a Pressler auger", IUFRO, Section 41, p. 19 (1965).
10. P. Rozenberg, A. Franc and C. Cahalan, "Incorporating wood density in breeding programs for softwoods in Europe: a strategy and associated methods", *Silvae Genet.* **50,** 1–7 (2001).
11. D.S. DeBell, R. Singleton, B.L. Gartner and D.D. Marshall, "Wood density of young-growth western hemlock: relation to ring age, radial growth, stand density and site quality", *Can. J. For. Res.* **34,** 2433–2442 (2004). doi: 10.1139/x04-123
12. C.A. Raymond and A.C. MacDonald, "Where to shoot your pilodyn: within tree variation in basic density in plantation *Eucalyptus globulus* and *E. nitens* in

Tasmania", *New Forests* **15,** 205–221 (1998). doi: 10.1023/A:1006544918632

13. B. Joe and R. Dickson, "Effective non-destructive segregation of *Eucalyptus grandis* logs according to radial and tangential hardness", *Australian Forestry* **69,** 248–256 (2006).

14. C.A. Raymond, "Genetics of *Eucalyptus* wood properties", *Ann. For. Sci.* **59,** 525–531 (2002). doi: 10.1051/forest:2002037

15. C. Pasquini, "Near infrared spectroscopy: fundamentals, practical aspects and analytical applications", *J. Braz. Chem. Soc*. **14,** 198–219 (2003). doi: 10.1590/S0103-50532003000200006

16. M.D. Birkett and M.J.T. Gambino, "Estimation of pulp kappa number with near-infrared spectroscopy", *Tappi J.* **72,** 193–197 (1989).

17. D.B. Easty, S.A. Berben, F.A. DeThomas and P.J. Brimmer, "Near infrared spectroscopy for the analysis of wood pulp-Quantifying hardwood softwood mixtures and estimating lignin content", *Tappi J.* **73,** 257–261 (1990).

18. J.A. Wright, M.D. Birkett and M.J.T. Gambino, "Prediction of pulp yield and cellulose content from wood samples using near-infrared reflectance spectroscopy", *Tappi J.* **73,** 164–166 (1990).

19. L. Thygesen, "Determination of dry matter content basic density of Norway spruce by near infrared reflectance and transmittance spectroscopy", *J. Near Infrared Spectrosc.* **2,** 127–135 (1994). doi: 10.1255/jnirs.39

20. P. Hoffmeyer and J.G. Pedersen, "Evaluation of density and strength of Norway spruce wood by near-infrared reflectance spectroscopy", *Holz Roh Werkst.* **53,** 165-170 (1995). doi: 10.1007/BF02716418

21. H. Baillères, F. Davrieux and F. Ham-Pichavant, "Near infrared analysis as a tool for rapid screening of some major wood characteristics in a *Eucalyptus* breeding program", *Ann. For. Sci.* **59,** 479–490 (2002). doi: 10.1051/forest:2002032

22. L.R. Schimleck, R. Evans, P.D. Jones, R.F. Daniels, G.F Peter and A. Clark, III, "Estimation of microfibril angle and stiffness by near infrared spectroscopy using sample sets having limited wood density variation", *IAWA J.* **26,** 175–187 (2005).

23. T. Fujimoto, Y. Kurata, K. Matsumoto and S. Tsuchikawa, "Application of near infrared spectroscopy for estimating wood mechanical properties of small clear and full length lumber specimens", *J. Near Infrared Spectrosc.* **16,** 529–537 (2008). doi: 10.1255/jnirs.818

24. A. Alves, A. Santos, D. da Silva Perez, J.C. Rodrigues, H. Pereira, R. Simões and M. Schwanninger, "NIR PLSR model selection for Kappa number prediction of maritime pine Kraft pulps", *Wood Sci. Technol.* **41,** 491–499 (2007). doi: 10.1007/s00226-007-0130-0

25. Z-H. Jiang, Z. Yang, C-L. So and C-Y. Hse, "Rapid prediction of wood crystallinity in *Pinus elliotii* plantation wood by near-infrared spectroscopy", *J. Wood Sci.* **53,** 449–453 (2007). doi: 10.1007/s10086-007-0883-y

26. C.R. Mora and L.R. Schimleck, "On the selection of samples for multivariate regression analysis: application to near-infrared (NIR) calibration models for the prediction of pulp yield in *Eucalyptus nitens*", *Can. J. For. Res.* **38,** 2626–2634 (2008). doi: 10.1139/X08-099

27. S. Zahri, A. Moubarik, F. Charrier, G. Chaix, H. Baillères, G. Nepveu and B. Charrier, "Quantitative assessment of total phenols content of European oak (*Quercus petraea* and *Quercus robur*) by diffuse reflectance NIR spectroscopy on solid wood surfaces", *Holzforschung* **62,** 679–687 (2008). doi: 10.1515/HF.2008.114

28. C. Sousa-Correia, A. Alves, J.C. Rodrigues, S. Ferreira-Dias, J.M. Abreu, N. Maxted, B. Ford-Lloyd and M. Schwanninger, "Oil content estimation of individuals kernels of *Quercus ilex* subsp. *rotundifolia* [(Lam) O. Schwarz] acorns by Fourier transform near infrared spectroscopy and partial least squares regression", *J. Near Infrared Spectrosc.* **15,** 247–260 (2007). doi: 10.1255/jnirs.733

29. A.M. Taylor, S.H. Baek, M.K. Jeong and G. Nix, "Wood shrinkage prediction using NIR spectroscopy", *Wood Fiber Sci.* **40,** 301–307 (2008).

30. B. Esteves and H. Pereira, "Quality assessment of heat-treated wood by NIR spectroscopy", *Holz Roh Werkst.* **66,** 323–332 (2008). doi: 10.1007/s00107-008-0262-4

31. H. Mark and J. Workman, *Chemometrics in Spectroscopy*. Academic Press, London, UK, p. 526 (2007).

32. R.G. Brereton, *Chemometrics: Data Analysis for the Laboratory and Chemical Plant*. John Wiley & Sons Ltd, Chichester, West Sussex, UK, p. 489 (2003).

33. L.R. Schimleck, R. Evans and J. Ilic, "Estimation of *Eucalyptus delegatensis* wood properties by near infrared spectroscopy", *Can. J. For. Res.* **31,** 1671–1675 (2001). doi: 10.1139/cjfr-31-10-1671

34. B.K. Via, T.F. Shupe, L.H. Groom, M. Stine and C.L. So, "Multivariate modelling of density, strength and stiffness from near infrared spectra for mature, juvenile and pith wood of longleaf pine (*Pinus palustris*)", *J. Near Infrared Spectrosc*. **11,** 365–378 (2003). doi: 10.1255/jnirs.388

35. R.P. Cogdill, L.R. Schimleck, P.D. Jones, G.F. Peter, R.F. Daniels and A. Clark, "Estimation of the physical wood properties of *Pinus taeda* L. radial strips using least square support vector machines", *J. Near Infrared Spectrosc*. **12,** 263-269 (2004). doi: 10.1255/jnirs.434

36. B.K. Via, C.L. So, T.F. Shupe, M. Stine and L.H. Groom, "Ability of near infrared spectroscopy to monitor air-dry density distribution and variation of wood", *Wood Fiber Sci*. **37,** 394–402 (2005).

37. N. Gierlinger, M. Schwanninger, B. Hinterstoisser and R. Wimmer, "Rapid determination of heartwood extractives in *Larix* sp. by means of Fourier transform near infrared spectroscopy", *J. Near Infrared Spectrosc*. **10,** 203–214 (2002). doi: 10.1255/jnirs.336

38. C.R. Mora, L.R. Schimleck and F. Isik, "Near infrared calibration models for the estimation of wood density

in *Pinus taeda* using repeated sample measurement", *J. Near Infrared Spectrosc.* **16,** 517–528 (2008). doi: 10.1255/jnirs.816

39. J. Rodrigues, A. Alves, H. Pereira, D. da Silva Perez, G. Chantre and M. Schwanninger, "NIR PLSR results obtained by calibration with noisy, low-precision reference values: Are the results acceptable?", *Holzforschung* **60,** 402-–408 (2006). doi: 10.1515/HF.2006.063

40. American Standards and Testing Methods—ASTM, *Standard Test Methods for Specific Gravity of Wood and Wood-Based Materials*, D2395-02. American Standards and Testing Methods, West Conshohocken, PA, USA (2002).

41. A. Savitzky and M.J.E. Golay, "Smoothing and differentiation of data by simplified least-squares procedures", *Anal. Chem.* **36,** 1627–1639 (1964). doi: 10.1021/ac60214a047

42. F. Westad and H. Martens, "Variable selection in near infrared spectroscopy based on significance testing in partial least square regression", *J. Near Infrared Spectrosc.* **8,** 117–124 (2000). doi: 10.1255/jnirs.271

43. R. Sykes, B. Li, G. Hodge, B. Goldfarb, J. Kadla and H.-M. Chang, "Prediction of loblolly pine wood properties using transmittance near-infrared spectroscopy". *Can. J. For. Res.* **35,** 2423-2431 (2005). doi: 10.1139/x05-161

44. *AACC, AACC Method 39-00*. American Association of Cereal Chemists, St Paul, MN, USA, p. 15 (1999).

45. P.C. Williams and D.C. Sobering, "Comparison of commercial near infrared transmittance and reflectance instruments for analysis of whole grains and seeds", *J. Near Infrared Spectrosc.* **1,** 25–33 (1993). doi: 10.1255/jnirs.3

46. L.R. Schimleck, J.C. Doran and A. Rimbawanto, "Near Infrared Spectroscopy for cost-effective screening of foliar oil characteristics in a *Melaleuca cajuputi* breeding population", *J. Agric. Food Chem.* **51,** 2433–2437 (2003). doi: 10.1021/jf020981u

47. W. Gindl, A. Teischinger, M. Schwanninger and B. Hinterstoisser, "The relationship between near infrared spectra of radial wood surfaces and wood mechanical properties", *J. Near Infrared Spectrosc.* **9,** 255–261 (2001). doi: 10.1255/jnirs.311

48. B.K. Via, C.L. So, L.H. Groom, T.F. Shupe, M. Stine and J. Wikaira, "Within tree variation of lignin, extractives, and microfibril angle coupled with the theoretical and near infrared modeling of microfibril angle", *Iawa J.* **28,** 189–209 (2007).

49. S.R. Delwiche and J.B. Reeves, III, "The effect of spectral pre-treatments on the PLS modelling of agricultural products", *J. Near Infrared Spectrosc.* **12**, 177-–182 (2004). doi: 10.1255/jnirs.424

50. L.R. Schimleck, A.J. Michell, C.A. Raymond and A. Muneri, "Estimation of basic density of *Eucalyptus globulus* using near-infrared spectroscopy", *Can. J. For. Res.* **29,** 194–201 (1999). doi: 10.1139/cjfr-29-2-194

51. S. Tsuchikawa, K. Hayashi and S. Tsutsumi, "Application of near infrared spectrophotometry to wood. 1. Efects of the surface-structure", *Mokuzai Gakkaishi*. **38,** 128–136 (1992).

52. A. Thumm and R. Meder, "Stiffness prediction of radiata pine clearwood test pieces using near infrared spectroscopy", *J. Near Infrared Spectrosc.* **9,** 117–122 (2001). doi: 10.1255/jnirs.298

53. N. Gierlinger, M. Schwanninger and R. Wimmer, "Characteristics and classification of Fourier-transform near infrared spectra of the heartwod of different larch species (*Larix* sp.)", *J. Near Infrared Spectrosc.* **12,** 113-119 (2004). doi: 10.1255/jnirs.415

54. L.R. Schimleck, C. Mora and R.F. Daniels, "Estimation of the physical wood properties of green *Pinus taeda* radial samples by near infrared spectroscopy", *Can. J. For. Res.* **33,** 2297–2305 (2003). doi: 10.1139/x03-173

55. L.R. Schimleck, R. Stürzenbecher, C. Mora, P.D. Jones and R.F. Daniel, "Comparison of *Pinus taeda* L. wood property calibrations based on NIR spectra from the radial-longitudinal and radial-transverse faces of wooden strips", *Holzforschung* **59,** 214–218 (2005). doi: 10.1515/HF.2005.034

56. P.D. Jones, L.R. Schimleck, G.F. Peter, R.F. Daniels and A. Clark, III, "Non-destructive estimation of wood chemical composition of sections of radial wood strips by diffuse reflectance near infrared spectroscopy", *Wood Sci. Technol.* **40,** 708–720 (2006). doi: 10.1007/s00226-006-0085-6

57. E. Sykacek, N. Gierlinger, R. Wimmer and M. Schwanninger, "Prediction of natural durability of commercial available European and Siberian larch by near-infrared spectroscopy", *Holzforschung*. **60,** 643–647 (2006). doi: 10.1515/HF.2006.108

Paper 6

Authors: Hein PRG, Clair B, Brancheriau L and Chaix G

Title: Predicting microfibril angle in Eucalyptus wood from different wood faces and surface qualities using near infrared spectra

Journal: J. Near Infrared Spectrosc, v.18, n.6, p.455-464 (2010)

Received: 22 August 2010 ■ *Revised: 25 October 2010* ■ *Accepted: 26 October 2010* ■ *Publication: 4 January 2011*

JNIRS JOURNAL OF NEAR INFRARED SPECTROSCOPY

Special Issue on Wood and Wood Products

Predicting microfibril angle in *Eucalyptus* wood from different wood faces and surface qualities using near infrared spectra

Paulo R.G. Hein,[a,*] Bruno Clair,[b] Loïc Brancheriau[a] and Gilles Chaix[c]

[a]CIRAD–PERSYST Department–Production and Processing of Tropical Woods, 73 rue Jean-François Breton TA B-40/16, 34398 Montpellier, Cedex 5, France. E-mail: phein1980@gmail.com

[b]Laboratoire de Mécanique et Génie Civil, CNRS, Université Montpellier 2, Place E. Bataillon, cc 048, 34095 Montpellier, Cedex 5, France

[c]CIRAD–BIOS Department–Genetic Diversity and Breeding of Forest Species, 73 rue Jean-François Breton TA B-40/16, 34398 Montpellier, Cedex 5, France

The microfibril angle (MFA) of crystalline cellulose in the wood cell wall along the stem axis has major effects on stiffness and longitudinal shrinkage of wood and is of key importance to timber quality. The aims of this study were: (1) to develop partial least square (PLS) regression models for microfibril angle (measured on tangential sections by X-ray diffraction) based on NIR spectra measured on tangential and on radial surfaces; (2) to develop PLS regression models for MFA based on radial NIR spectra collected from wood surfaces of different quality; and (3) to verify the reliability of these PLS-R models by external validations. *T* values were recorded by X-ray diffraction on tangential sections while NIR spectra were taken on tangential and radial wood surfaces. PLS-R calibrations for MFA based on tangential NIR spectra were better (r^2_p=0.72) than those using radial NIR spectra (r^2_p=0.64). The key role of the chemical components and the effect of surface quality of wood on NIR spectroscopy calibrations are discussed. Considering the differences between experimental conditions, these findings showed the potential of the NIR-based models for predicting MFA in *Eucalyptus* wood, even using spectra taken from different wood faces and surface qualities.

Keywords: *Eucalyptus urophylla* S.T. Blake, microfibril angle, NIR calibration, X-ray diffraction, wood phenotyping, surface quality

Introduction

Microfibril angle (MFA) is a property of the cell wall of wood fibres, which is made up of millions of strands of cellulose called microfibrils.[1] This elementary wood trait represents the orientation of crystalline cellulose in the cell wall with respect to the stem axis.[2] It is of particular interest for breeding programmes[3,4] since MFA has major effects on two key properties of wood: its stiffness and longitudinal shrinkage.[5] Among all available techniques, only X-ray diffractometry (XRD) provides quick MFA measurements for a large number of samples;[6,7] however, sample preparation is often time-consuming. XRD has been largely used because of the crystalline arrangement of cellulose microfibrils in the wood cell wall; it allows a study of not only its organisation (such as MFA) but also its apparent crystal size[8] or its mechanical state.[9] Numerous papers have proposed near infrared (NIR) spectroscopy to determine MFA (Table 1). NIR spectroscopy is a rapid method for the determination of many chemical properties which have been successfully related to physico–mechanical properties of wood.[26] One of its main advantages is the possibility of estimating a range of wood traits from the same NIR spectra. To explain the results of these established NIR-based calibrations for MFA, a common assumption is that the supposed correlation that exists between

ISSN: 0967-0335
doi: 10.1255/jnirs.905

density and MFA plays a major role on NIR models. In regard to this pertinent issue, Schimleck *et al.*[16] investigated the importance of density variation on NIR calibrations for MFA using *Pinus radiata* D. Don and *P. taeda* L. wood samples, demonstrating that NIR spectroscopy can provide strong relationships for MFA, even when density variation is limited.

Most studies on MFA prediction using NIR spectroscopy have been based on reference data provided by SilviScan measurements,[7] while calibrations for MFA based on independent XRD and NIR devices are rarely reported (Table 1). Schimleck *et al.*,[4] Kelley *et al.*[24] and Huang *et al.*[25] used softwoods to build their NIR calibrations for MFA based on measurements made on a polyvalent XRD apparatus.

Thus, the aims of this study were: (1) to develop partial least square (PLS) regression models for MFA (measured on tangential sections by XRD) based on NIR spectra measured on tangential sections of *Eucalyptus urophylla*; (2) to develop PLS regression models for MFA based on radial NIR spectra collected from wood surfaces of different quality; and (3) to verify the reliability of these PLS-R models by independent test validations.

We used NIR spectra scanned on tangential and radial wood faces and with different surface qualities (tangential sections were cut with a mini-circular bandsaw while the radial surfaces were cut with a vertical bandsaw and sanded). Using this procedure, we tried to simulate a real situation in which established NIR-based models should be applied to assess wood properties of unknown samples, often prepared with different tools and unpredictable conditions.

Material and methods

Forty breast-height wood disks of 14-year-old *Eucalyptus urophylla* S.T. Blake trees from the Centre de recherche sur la durabilité et la productivité des plantations industrielles (CRDPI) in the Republic of Congo were used in this study. The climate is tropically humid with a mean annual temperature of 24°C, a mean annual rainfall of 1200 mm and a dry season from May to October. The trees were planted in a randomised design and with a stocking density of 625 trees ha^{-1} (4 × 4 m spacing). Trees coming from the same experimental plantation

Table 1. Most important papers on MFA evaluation by NIR spectroscopic models, including the method used as reference, the species, its age (in years), and its range of variation, and the model statistics.

Reference	Method	Species	Age	MFA range	r^2_p	*SEP*	*RPD*
Schimleck *et al.*[10]	SilviScan	*E. delegatensis*	mature	—	0.74	1.73	—
Schimleck *et al.*[10]*	SilviScan	*E. delegatensis*	mature	—	0.78	0.97	—
Schimleck *et al.*[11]	Silviscan	*E. delegatensis*	—	—	0.45–0.61	1.91–2.56	—
Schimleck *et al.*[11]	Silviscan	*P. radiata*	—	—	0.55–0.63	3.05–4.62	—
Schimleck and Evans[12]	Silviscan	*P. radiata*	26	10.7–41.6	0.96–0.98	1–2.5	—
Schimleck *et al.*[13]	SilviScan	*P. taeda*	~20	10.7–36.4	0.76–0.80	3.4–4.0	1.9–2.2
Codgill *et al.*[14]	SilviScan	*P. taeda*	21–26	11–45.2	0.85–0.91	2.9–2.2	2.5–3.3
Schimleck *et al.*[15]	SilviScan	*P. taeda*	21–26	11–45.2	0.88	3.2	2.3
Schimleck *et al.*[16]	SilviScan	*P. radiata*	26	—	0.79–0.99	0.4–1.9	2.2–9.1
Schimleck *et al.*[16]	SilviScan	*P. taeda*	21–26	—	0.41–0.96	1.1–3.4	1.3–4.9
Schimleck *et al.*[17]	SilviScan	*P. taeda*	—	10.7–37.4	0.81–0.89	2.5–3.2	2.3–3
Schimleck *et al.*[18]	SilviScan	*P. taeda*	21–26	11.6–40.7	0.85–0.88	5.2–9.9	0.8–1.5
Jones *et al.*[19]	SilviScan	*P. taeda*	21–26	9.7–45.2	0.80–0.84	3.12–7.22	1.01–2.34
Schimleck *et al.*[20]	SilviScan	*E. globulus* and *E. nitens*	8	12.0–26.8	0.20	2.9	—
Schimleck *et al.*[21]	SilviScan	*P. taeda*	21–26	8.7–51.7	0.79–0.85	2.72–4.92	—
Jones *et al.*[22]	SilviScan	*P. taeda*	21–26	—	0.48–0.84	3.8–6.03	1.21–2.07
Antony *et al.*[23]	SilviScan	*P. taeda*	33	—	0.83	2.4	1.8
Schimleck *et al.*[4]	XRD	*P. taeda*	30–33	—	0.81–0.91	3.89–4.66	2.3–2.4
Huang *et al.*[24]	XRD	*C. lanceloata*	—	—	0.77	—	—
Kelley *et al.*[25]	XRD	*P. taeda*	—	6.5–43	0.31–0.46	6.8–8	—

*Refers to the 100/MFA transformation.

were previously evaluated for wood density[27] and chemical composition.[28]

Sampling preparation

From each disc, a pith to bark radial strip (Figure 1) was removed by a vertical bandsaw and its radial surfaces were sanded with 300-grit sandpaper for approximately 30 s. The radial strips were marked randomly but well distributed from pith to bark to supply tangential sections (thickness of 2 mm), as parallel as possible, to the growth rings for measurements of the MFA [Figure 1(a)]. These wood strips have variable height and length (depending on the circumference and thickness of each wood disc), but their width was fixed at 30 mm. After sectioning, the samples were kept in a climate-controlled room (temperature around 20°C and relative humidity around 65%). Under these conditions, the moisture content of the wood samples stabilised at 12%.

Measurement of the microfibril angle

All X-ray diffraction data were collected on a diffractometer (Gemini-S, Agilent Technologies, Yarnton, UK) with Cu Kα radiation at the Institut Européen des Membranes at the University of Montpellier. Images were integrated between $2\beta = 21.5$ and 23.5 along the whole 360° azimuthal interval to plot the intensity diagram of the (200) plane. An automatic procedure allowed the detection of the 200 peaks and their inflexion points. The *T* parameter is defined by Cave[29] as the measure of the width of the (200) diffraction arc. Thus, the half distance between intersections of tangents at inflection points of the 200 peaks with the baseline was measured and the results are given as the mean of values obtained for the two 200 peaks.

Two methods were applied in order to estimate MFA based on their XRD pattern, namely: (1) MFA_C for the values estimated by the Cave[29] formula and (2) MFA_γ for estimations using the formula proposed by Yamamoto *et al.*[30] These formulae give an estimation of the mean MFA of woods based on their *T* value and are given by:

$$MFA_C = 0.6 \times T \quad (1)$$

and

$$MFA_\gamma = (1.575 \times 10^{-3} \times T^3) - (1.431 \times 10^{-1} \times T^2) + (4.693 \times T) - 36.19 \quad (2)$$

Three XRD profiles were recorded on three points of each sample (Figure 1). The estimated error of the repeatability of the *T* parameter measurements was 3%, on average, for *T* ranging from 14° to 29° which correspond to ±0.6 degrees.

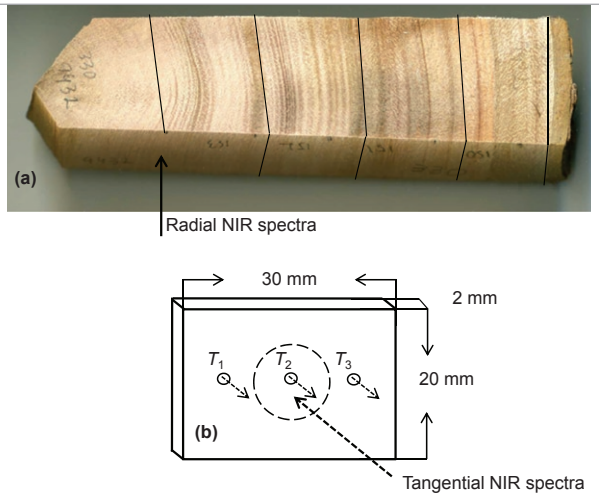

Figure 1. Sampling protocol. Radial strips (a) cut from discs; tangential sections for X-ray diffraction measurement (b). The dotted arrows represent NIR spectra for MFA calibrations.

Measurements of NIR spectra

NIR spectra were measured in diffuse reflectance mode with a Fourier transform spectrometer (model Vector 22/N; Bruker Optik GmbH, Ettlingen, Germany). This spectrometer is designed for reflection mode analysis of solids with an integrating sphere (diameter of measured area = 10 mm). Spectral analysis was performed within the 12,500 cm^{-1} to 3500 cm^{-1} (800–2850 nm) range at 8 cm^{-1} resolution. A sintered "gold standard" was used as the reference or as background. Thirty-two scans were performed and averaged for each measure and compared to the standard in order to obtain the reflectance spectrum of the sample. NIR spectra were acquired in a climate-controlled room with temperature around 20°C and relative humidity around 65%.

NIR spectra were recorded on the radial surface of the two sides of the wood strips on marked points. These records were labelled as "radial NIR spectra" or "rad" in the tables. Subsequently, the radial strips were cut using a mini-circular bandsaw machine in order to produce: (1) 175 tangential sections (thickness of 2 mm) for X-ray diffraction measurement [Figure 1(b)]. The wood samples were kept in the same climatised room to stabilise the moisture content. Thereafter, NIR spectra were acquired directly from tangential sections of the wood samples and were labelled as "tangential NIR spectra" or "tang" in the tables. In Figure 1, the continuous arrow represents radial NIR spectra while the dotted arrow represents tangential NIR spectra for MFA calibrations and the path of the XRD beam used for MFA determinations.

As described above, we used a NIR spectrometer with a window size of 10 mm. Thus, the NIR spectra scanned on tangential sections represent the wood formed at the same time, whereas the NIR radial surface takes into account the property averaged over a variable time period. This is the reason why tangential sections of wood were chosen for evaluating MFA by XRD. We assumed that they could provide more repeatable MFA estimates.

In practice, where a high throughput of samples is expected to screen geneotypes, it is easy to gather wood samples using a motor-driven coring system. It is then easier to record NIR scans from radial strips of wood. If NIR spectra are to support tree breeding programmes the calibrations must be developed

Table 2. Descriptive statistics, including average, standard deviation (*SD*), minimum (Min), maximum (Max) and coefficient of variation (*CV*) for microfibril angle (MFA) measurements in 14-year *Eucalyptus urophylla*.

Parameter	MFA_C (°)	$100/MFA_C$ (°)	MFA_Y (°)	$100/MFA_Y$ (°)
Average	11.9	8.6	12.5	8.2
SD	1.65	1.06	2.14	1.47
Min	9.1	4.9	7.7	5.1
Max	20.2	10.9	19.7	13.0
CV (%)	13.9	12.4	17.1	17.9
No. of samples	175	175	175	175

using precise reference data for important wood traits such as MFA.

Chemometric analysis

Partial least squares (PLS) regression analyses were developed using The Unscrambler software (version 9.8; CAMO AS, Oslo, Norway). The PLS-R method was used to correlate the NIR spectra with referenced microfibril angle and wood density of the samples. First derivatives (13-point filter and a second-order polynomial) and second derivatives (25-point filter and a third-order polynomial) were applied on the NIR spectra data using the Savitsky and Golay[31] algorithm.

The PLS-R models were developed using cross-validation with five segments and 35 samples selected randomly using tangential or radial NIR spectra. The cross-validations were used to identify the following calibration parameters: the best pre-treatments; the number of latent variables; outlier samples and wavelengths with significant regression coefficients. Also, cross-validations were useful to identify which reference values of MFA and its transformations generated the best NIR calibration. Outliers were identified and removed from a visual examination of the student residuals and leverage value scatter plot. The Martens[32] uncertainty test was used to select the wavelengths with regression coefficients significantly different from zero. The models built with the remaining variables improved: the coefficient of determination increased and the root mean of standard errors of validations for MFA decreased.

Based on these established parameters, PLS-R calibrations (using 115 samples) and test set PLS-R validations (using 60 samples) were performed for MFA. To compare cross-validations and independent validations PLS-R regressions for MFA, developed using tangential and radial NIR spectra, the following statistics were used: (1) the coefficient of determination between measured and predicted values (r_p^2) or between measured and cross-validated values (R_{cv}^2); (2) the root mean of standard error of prediction (*RMSEP*) or cross-validation (*RMSECV*); (3) the ratio of performance to deviation (*RPD*); and (4) the number of latent variables (*LV*).

The *RPD* value is the ratio of the standard deviation of the reference values for the *RMSECV* or *RMSEP*.[33] The higher the *RPD* value the more reliable the calibration.[34] In an attempt to improve the calibrations, a simple transformation[10] (100/MFA) was applied and labelled as $100/MFA_C$ and $100/MFA_Y$.

Results and discussion

Measurements of microfibril angle

Each measurement was used as the reference data for NIR calibrations. A summary of the microfibril angle measurements is reported in Table 2. The range of variation in the investigated properties is crucial for NIR calibrations. An increase in variability of the trait as reference data improves the models (R^2, *RMSECV* and *RPD*). According to Mora and Schimleck,[35] calibration models must include all possible sources of variation that can be encountered later in real applications because the goal is to estimate the properties in new samples.

The two approaches for conversion of the X-ray pattern to microfibril angle are based on the same *T* parameter. Hence, as expected, the microfibril angle values estimated by the Cave and Yamamoto formulae presented high correlations ($r = 0.97$).

NIR spectroscopic-based models

In the present study, there was no correlation ($-0.085 < r < -0.112$) between MFA and wood density. Hence, the density of wood, which has been extensively calibrated by NIR spectroscopy,[13,18,27,34] did not play any role on the PLS-R models for MFA presented in this study.

PLS-R cross-validations

A statistical summary of the cross-validated PLS-R models developed for microfibril angle using tangential NIR spectra measured from 1100 nm to 2500 nm are shown in Table 3.

The calibration for MFA_C ($R_{cv}^2 = 0.57$; $RMSECV = 0.88°$) was better (higher *RPD*) than the calibration for MFA_Y ($R_{cv}^2 = 0.60$; $RMSECV = 1.32°$). However, when using the parameter $100/MFA_Y$, the regression (model 4) presented the higher R_{cv}^2 (0.64). The highest *RPD* was reached for the MFA_C model. In general, the models for MFA estimated by Yamamoto's formulae[30] gave the higher *RMSECV*s both for MFA or 100/MFA.

Table 4 presents the cross-validated PLS-R models for MFA using radial NIR spectra. The PLS-R cross-validation for MFA_Y based on radial NIR spectra (model 7) presented the higher R^2_{cv} (0.59) and *RMSECV* (1.36) values. The higher *RPD* value (1.70) was presented again for MFA_C, which also yielded the lowest R^2_{cv} (0.48). The higher *RPD* values of models when using Cave's estimation as reference can be explained by the *RMSECV*: 0.97° for MFA_C against 1.36° for MFA_Y. Similarly, Cave's formula yielded lower *RMSECV* values for MFA or 100/MFA (Table 3).

Validations of the test set

To verify the robustness of these PLS-R models, the complete data set (175 samples) of the present study was split randomly into two sub-groups: a calibration set with

Table 3. Cross-validated PLS-R models for microfibril angle using tangential NIR spectra.

Property	Model	Treat	R^2_c	*RMSEC*(°)	R^2_{cv}	*RMSECV*(°)	*LV*	Outliers	*RPD*
MFA_C	1	First derivative	0.65	0.79	0.57	0.88	6	2	1.85
$100/MFA_C$	2	Second derivative	0.69	0.55	0.57	0.66	6	1	1.62
MFA_Y	3	Second derivative	0.68	1.17	0.60	1.32	5	0	1.62
$100/MFA_Y$	4	Second derivative	0.72	0.73	0.64	0.84	6	3	1.76

R^2_c, coefficient of determination of the calibration model; *RMSEC*, root mean standard error of calibration; r^2_{cv}, coefficient of determination of the cross-validation; *RMSEC*, root mean standard error of cross-validation; *LV*, latent variables; *RPD*, ratio of performance to deviation.

Table 4. Cross-validated PLS-R models for microfibril angle using radial NIR spectra.

Property	Model	Treat	R^2_c	*RMSEC* (°)	R^2_{cv}	*RMSECV*(°)	*LV*	Outliers	*RPD*
MFA_C	5	Second derivative	0.61	0.83	0.48	0.97	5	4	1.70
$100/MFA_C$	6	First derivative	0.64	0.60	0.56	0.67	5	2	1.58
MFA_Y	7	Second derivative	0.66	1.24	0.59	1.36	6	0	1.57
$100/MFA_Y$	8	Second derivative	0.63	0.87	0.56	0.95	5	1	1.55

R^2_c, coefficient of determination of the calibration model; *RMSEC*, root mean standard error of calibration; r^2_{cv}, coefficient of determination of the cross-validation; *RMSEC*, root mean standard error of cross-validation; *LV*, latent variables; *RPD*, ratio of performance to deviation.

Table 5. Descriptive statistics, including average, standard deviation (*SD*), minimum (Min) and maximum (Max) values and coefficient of variation (*CV*) for microfibril angle (MFA_Y) of the calibration and validation data set.

Set	Average	*SD* (°)	Min (°)	Max (°)	*CV* (%)	No. of samples
Calibration	12.3	1.75	7.7	17.3	14.2	115
Validation	12.5	1.82	8.4	16.1	14.5	60

Table 6. PLS-R calibrations and independent validations for microfibril angle according to surface used to collect NIR spectra.

Trait	Model	Surface	Treat	R^2_c	*RMSEC* (°)	r^2_p	*RMSEP* (°)	*LV*	Outlier	*RPD*
MFA_C	9	tang	Second derivative	0.66	1.24	0.60	1.35	6	0	1.59
$100/MFA_C$	10	rad	Second derivative	0.70	0.65	0.63	0.94	6	3	1.60
MFA_Y	11	rad	Second derivative	0.67	1.21	0.64	1.32	6	0	1.63
$100/MFA_Y$	12	tang	Second derivative	0.72	0.64	0.72	0.89	7	3	1.65

tang, tangential NIR spectra; rad, radial NIR spectra; R^2_c, coefficient of determination of the calibration model; *RMSEC*, root mean standard error of calibration; r^2_p, coefficient of determination of the prediction by test set validation; *RMSEP*, root mean standard error of the prediction by test set validation; *LV*, latent variables; *RPD*, ratio of performance to deviation.

115 samples to build new PLS-R models and a test set with 60 samples to validate them. Table 5 presents the descriptive statistics of the calibration and validation data sets. The PLS-R models and independent validations for MFA, according to the surface NIR spectra were collected from, are summarised in Table 6.

The validation of PLS-R models for 100/MFA_γ (model 12) provided an r_p^2 of 0.72 using tangential NIR spectra. For these validations, the *RMSEP* were lower when using MFA estimates by Yamamoto's formula.[30] Model 11, which used MFA_γ and radial NIR spectra, had an r_p^2 value of 0.64 and *RMSEP* of 1.32°. These findings were comparable with those reported by Kelley *et al*.[25] who studied loblolly pine reporting R_c^2 values from 0.52 to 0.72 for MFA. When these models were validated with a test set, the statistics were weaker: r_p^2 from 0.29 to 0.31(for wavelengths from 500 nm to 240 nm). Schimleck *et al*.[4] also measured MFA using XRD on tangential faces sections cut from loblolly pine radial strips and developed NIR calibrations. The measured and NIR-predicted MFA presented a strong r_p^2 (0.81) and *RPD* (2.23). Their results suggested that a better model could have been obtained if the current sampling would have contained a wider range of MFA (the sampling used in Schimleck *et al*.[4] ranged from 7.5 to 60.8° (for *Pinus*) while our MFA range varied from 7.7° to 19.7°; Table 2).

The NIR-predicted versus XRD-measured MFA_γ plot using radial NIR spectra (model 11) is shown in Figure 2 while the NIR predicted versus XRD measured 100/MFA_γ plot using tangential NIR spectra (model 12) is presented in Figure 3.

In comparison with other studies using *Eucalyptus* wood, the r_p^2 presented in Table 6 were slightly lower than those shown by Schimleck *et al*.[10] who evaluated by NIR spectroscopy the density and microfibril angle of *Eucalyptus delegatensis* R.T. Baker. Using MFA estimated on SilviScan-2, Schimleck *et al*.[10] reported good PLS-R models in independent validations with r_p^2=0.74 and *SEP*=1.73° for MFA, and r_p^2=0.78 and *SEP*=0.97° for 100/MFA in *E. delegatensis*. Our PLS-R calibrations for MFA (models 9 and 11) and for 100/MFA (models 10 and 12) had lower coefficients of determination, but our *RMSEP*s were also lower than the Schimleck *et al*.[10] models. These results (Table 6) were slightly better for the model statistics presented by Schimleck *et al*.[11] who used an established mixed species calibration to predict MFA and 100/MFA on a *Eucalyptus delegatensis* sample set. They reported r_p^2 ranging from 0.45° to 0.61° for MFA and r_p^2 varying from 0.58 to 0.66 for 100/MFA. In short, the calibration statistics presented in this work were restricted mainly by the narrow range of MFA variation.

NIR spectroscopy for the assessment of microfibril angle: why it works

Numerous papers have demonstrated that NIR spectroscopy is a suitable tool for quick estimation of several non-chemical wood traits, such as mechanical properties and microstructural features, including MFA. However, it is not explained in the literature how NIR, based on vibrational spectroscopic analysis, could be used to estimate the orientation of cellulose in the secondary layers of the cell wall in vascular plants. In regard to this fundamental issue, an interpretation is proposed, based on

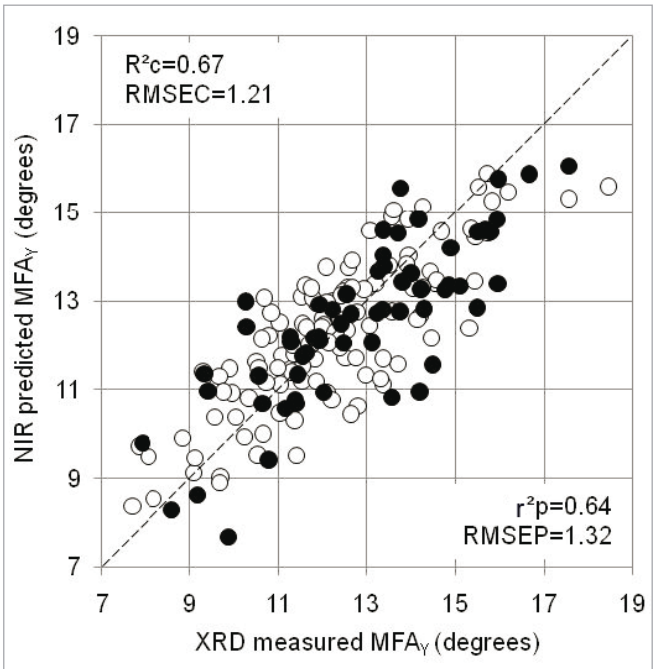

Figure 2. NIR predicted versus measured values for MFA_γ using radial NIR spectra. The calibration set samples are represented by white circles and the validation set samples are represented by black circles.

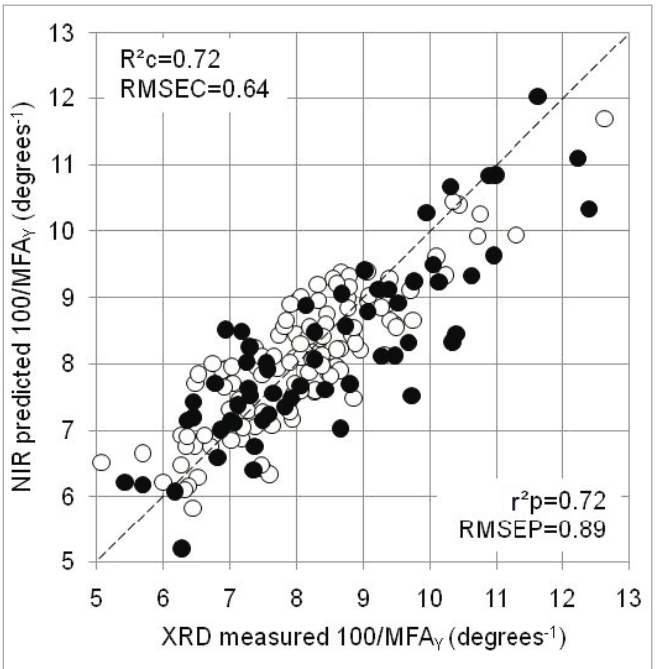

Figure 3. NIR predicted versus measured values for 100/MFAY using tangential NIR spectra. The calibration set samples are represented by white circles and the validation set samples are represented by black circles.

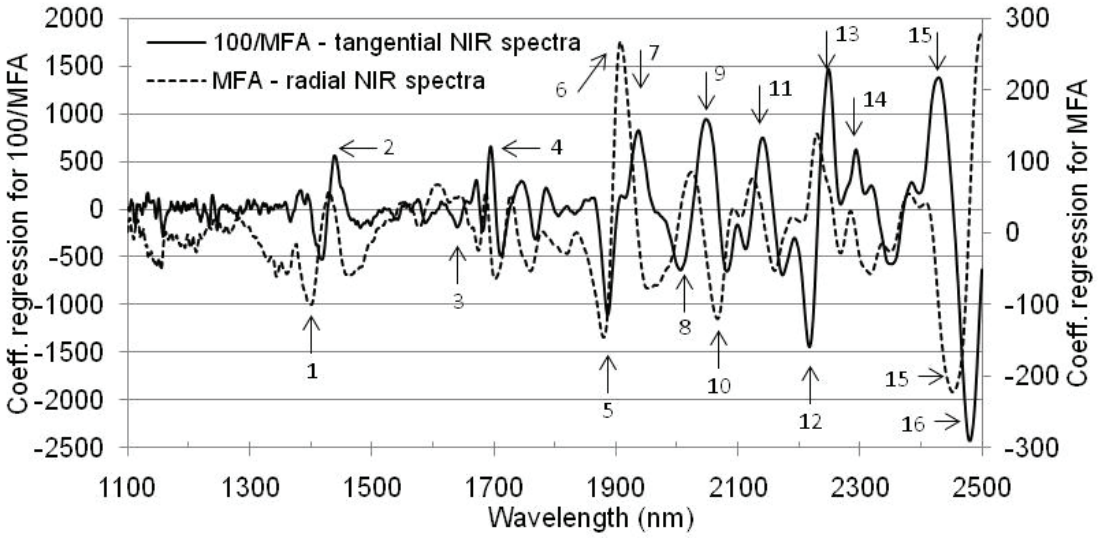

Figure 4. Regression coefficients of the PLS-R models to predict 100/MFA$_Y$ and MFA$_Y$ using tangential and radial NIR spectra. Bands assigned to chemical compounds are represented by numbers and listed in Table 7.

the regression coefficients of the PLS-R models for wood density and MFA and based on chemical properties and MFA links.

Figure 4 shows the plot of weighted regression coefficients for 100/MFA$_Y$ (solid line) using tangential NIR spectra (model 12) and MFA$_Y$ (broken line) using radial NIR spectra (model 11). For the MFA$_Y$ and 100/MFA$_Y$ calibrations, the wavelengths around 1875 nm (index 5); 2050 nm (index 9); 2080 nm (index 10); 2200 nm (index 12); 2270 nm (index 13); 2425 nm (index

Table 7. NIR absorption bands normally associated with the main wood components (cellulose, hemicelluloses, lignin, polysaccharides and water) according to Workman and Weyer.[36]

Index	Wavelength (nm)	Bond vibration	Structure
1	1410	OH stretching first OT lignin or first overtone of an O–H stretching vibration of phenolic hydroxyl groups	Lignin
2	1428	O–H stretching	Amorphous cellulose
3	1672	First overtone CH stretching	Lignin
4	1685	C–H (2v), ArC–H: C–H aromatic associated C–H	Lignin
5	1875	Not assigned	—
6	1916	O–H stretching + OH deformation	Water
7	1930	O–H stretching + HOH bending combination	—
8	2012	N–H/C=O combination	Polyamide
9	2050	N–H/C–N/N–H amide II and III combination	Amides
10	2080	O–H stretching + CH deformation	Semi-crystalline or crystalline regions of cellulose
11	2140	C–H + C–C stretching	Amorphous cellulose
12	2200	C–H stretching and C=O combination	Lignin
13	2270	O–H stretching + C–O stretching combination	Cellulose
14	2280	C–H stretching and CH_2 deformation	Polysaccharides
15	2425	Not assigned	Cellulose
16	2488	C–H stretching and C–C stretching combination	Cellulose

Numbers assigned to the specific bands and regression coefficients are presented in Figure 4.

15) and 2488 nm (index 16) represent high PLS regression coefficients. These important absorption bands are related to the O–H, C–O, C–H and C–C stretching observed in crystalline regions of cellulose, as well as to the C–O stretching and C=O combination observed in aromatic groups of lignin. Moreover, we identified two specific bands which may play a major role in NIR calibrations for MFA and 100/MFA: (1) a minimum at 1875 nm (index 5) and maxima/minima at 2425 nm (index 15). The loadings for MFA and 100/MFA are shown in Figure 4.

Effect of chemical properties on microfibril angle

Based on studies of reaction tissues produced in hardwoods and softwoods to straighten the stem, which possess special features in cell wall composition, one may assume that cellulose MFA and lignin content in the S_2 layer could, generally, be related to each other.[37] In coniferous wood, Via *et al*.[38] showed that MFA and lignin content are associated: the higher the lignin content, the higher the MFA. In hardwoods, this trend has been observed in a range of wood species,[39] both in reaction and normal wood, but some studies have reported no correlations between MFA and chemical components.[37] Baillères *et al*.[40] investigated hybrids of *Eucalyptus* clones from the Republic of Congo demonstrating clearly that decreases in microfibril angles of cellulose are linked to the decrease in lignin content and increase in the syringyl/guaiacyl ratio (S/G). Thus, these findings suggested that the calibrations for MFA can be related to changes in lignin content or S/G ratio, at least partially, since these properties vary simultaneously in most woods and can play a key role in NIR models. On the other hand, Jungnikl *et al*.[37] examinated the correlation between microfibril angle and lignin content in *Picea abies* tissues and did not find any correlation, either for the individual tissue types or for the compiled data of all tissues.

In the present study, MFA showed a low coefficient of correlation with NIR-based predicted lignin content. We used our earlier NIR-based models for Klason lignin content established for trees from the same progeny trial[28] in order to predict Klason lignin content in the 175 tangential sections. The correlation between the NIR-based estimates of lignin content and XRD measured microfibril angle values was 0.4. It is important to note that this lignin model was calibrated from NIR spectra measured on the transverse face of the wood discs (such discs were surfaced using a plane). Despite the low correlation ($r = 0.4$), this finding seems to indicate that the lignin content may play a key role in NIR-based calibrations for microfibril angle.

Challenges of this study

While undertaking this work, several problems and limitations were encountered. These are addressed here. First, the narrow range of microfibril angle of woods (previously discussed) was a restrictive factor in this work. Indeed, the narrow range of the MFA did not represent a limitation for comparing PLS-R calibrations based on tangential and radial NIR spectra, but makes the achievement of stronger calibration/prediction statistics difficult. For NIR calibration purposes, the larger the property variability, the greater the likelihood of obtaining a better coefficient of determination (between references and predicted values) of the predictive model; however, for Eucalypt woods, it is unlikely that the MFA range would be much greater than reported here. For instance, Lima *et al*.[41] found no significant differences in MFA from pith to bark for *E. grandis* × *E. urophylla* clones.

Second, we used a Fourier transform spectrometer which measures the diffuse reflected light through a window size of 10 mm. Hence, the NIR spectra measured on tangential and radial wood surfaces has information averaged over 78.5 mm^2 of wood surface whereas the surface area of the X-ray incident beam was less than 1 mm^2. In order to minimise this problem, three *T* parameters were recorded on each tangential section, but the area scanned for the NIR measurement remained much larger. In regard to this issue, we also used a NIR device equipped with a fibre-optic probe (Labspec Pro; ASD Inc, Boulder, CO, USA) to investigate the supposed scale effect on these tangential sections, but we found quite similar results and decided to work only with the NIR information obtained with the Bruker device.

Finally, an important limitation of the proposed method is the difficulty in cutting tangential sections, which is time-consuming and is not compatible with the high throughout of phenotypes expected for genetic studies.

Despite all challenges we faced, the association of XRD and NIR spectroscopy in evaluating MFA in these woods had two substantial advantages: speed and accuracy; sufficient, at least to distinguish classes in genetic studies. The NIR calibrations for MFA generate estimates with errors (*RMSEP* = 1.32° or 10.5% for radial spectra against 3% of error from the X-ray approach), but they are able to distinguish trees that produce wood with a large range of MFA.

It is important to note that the wood radial surfaces were sanded while the tangential sections were not sanded. The mini-circular bandsaw machine used to produce the tangential sections provided high quality surfaces while the vertical bandsaw machine used to cut the radial strips from the discs provided irregular surfaces which were sanded (300-grit sandpaper for approximately 30 s). Hence, using different wood faces and surface qualities, the attempt was made to simulate a real situation in which established NIR-based models should be applied to predicting such wood properties of unknown samples, frequently prepared under different experimental conditions. Therefore, these PLS-R models showed the potential of the NIR-based validations for MFA (based on X-ray diffraction) from both tangential ($r^2_p = 0.72$) and radial ($r^2_p = 0.64$) wood surfaces, and with different wood quality surfaces.

Conclusions

It was possible to develop PLS-R calibrations for MFA in *Eucalyptus* wood based on reference values recorded on tangential sections by the XRD technique using both radial and tangential NIR spectra. Using a calibration set to build

the models, and a test set to validate them, the PLS-R model for 100/MFA based on tangential NIR spectra presented the best statistics (r^2_p=0.72) while the model based on radial NIR spectra was the best for MFA (r^2_p=0.64). With respect to the models for MFA, the reference data based on the Yamamoto formula generated better statistics.

Considering the differences between experimental conditions, these results showed the NIR models for MFA: NIR spectroscopy was able to predict MFA of *Eucalyptus* wood, using both different wood faces and wood quality surfaces.

Acknowledgements

The authors would like to thank Arie van der Lee from the Institut Européen des Membranes, CNRS, University of Montpellier for assistance with XRD measurements and Joseph Gril from CNRS for comments; to Nina Ognouabi and Emilie Villar from CRDPI (Republic of Congo) and the Bureau des Ressources Génétiques (BRG) project for providing material and funding; especially to Dr Jean Marc Gion and to Dr Philippe Vigneron (coordinators of the BRG project "CCR gene in *Eucalyptus*: a model of functional variability in forest trees") from UPR39 and UPR40 of CIRAD (Montpellier, France) for providing technical support. P.R.G. Hein was supported by the National Council of Technological and Scientific Development (CNPq, Brazil – process no. 200970/2008-9).

References

1. S.-Z. Fang, W.-Z. Yang and Y. Tian, "Clonal and within-tree variation in microfibril angle in poplar clones", *New Forests* **31,** 373 (2006). doi: 10.1007/s11056-005-8679-7

2. S. Andersson, R. Serimaa, M. Torkkeli, T. Paakkari, P. Saranpfifi and E. Pesonen, "Microfibril angle of Norway spruce [*Picea abies* (L.) Karst.] compression wood: comparison of measuring techniques", *J. Wood Sci.* **46,** 343 (2000). doi: 10.1007/BF00776394

3. C.A. Raymond, "Genetics of *Eucalyptus* wood properties", *Ann. For. Sci.* **59,** 525 (2002). doi: 10.1051/forest:2002037

4. L.R. Schimleck, E. Sussenbach, G. Leaf, P.D. Jones and C.L. Huang, "Microfibril angle prediction of *Pinus taeda* wood samples based on tangential face NIR spectra", *IAWA J.* **28,** 1 (2007).

5. L. Donaldson, "Microfibril angle: measurement, variation and relationships—a review", *IAWA J.* **29,** 345 (2008).

6. R. Evans, S.A. Stuart and J. Van der Touw, "Microfibril angle scanning of increment cores by X-ray diffractometry", *Appita J.* **49,** 411 (1996).

7. R. Evans, "A variance approach to the x-ray diffractometric estimation of microfibril angle in wood", *Appita J.* **52,** 283 (1999).

8. R. Washusen and R. Evans, "The association between cellulose crystallite width and tension wood occurrence in *Eucalyptus globulus*", *IAWA J.* **22,** 235 (2001).

9. B. Clair, T. Alméras, H. Yamamoto, T. Okuyama and J. Sugiyama, "Mechanical behaviour of cellulose microfibrils in tension wood, in relation with maturation stress generation", *Biophys. J.* **91,** 1128 (2006). doi: 10.1529/biophysj.105.078485

10. L.R. Schimleck, R. Evans and J. Ilic, "Estimation of *Eucalyptus delegatensis* wood properties by near infrared spectroscopy", *Can. J. For. Res.* **31,** 1671 (2001). doi: 10.1139/cjfr-31-10-1671

11. L.R. Schimleck, R. Evans and J. Ilic, "Application of near infrared spectroscopy to a diverse range of species demonstrating wide density and stiffness variation", *IAWA J.* **22,** 415 (2001).

12. L.R. Schimleck and R. Evans, "Estimation of microfibril angle of increment cores by near infrared spectroscopy", *IAWA J.* **23,** 225 (2002).

13. L.R. Schimleck, C. Mora and R.F. Daniels, "Estimation of the physical wood properties of green *Pinus taeda* radial samples by near infrared spectroscopy", *Can. J. For. Res.* **33,** 2297 (2003). doi: 10.1139/x03-173

14. R.P. Cogdill, L.R. Schimleck, P.D. Jones, G.F. Peter, R.F. Daniels and A. Clark, "Estimation of the physical wood properties of *Pinus taeda* L. radial strips using least square support vector machines", *J. Near Infrared Spectrosc.* **12,** 263 (2004). doi: 10.1255/jnirs.434

15. L.R. Schimleck, R. Stürzenbecher, P.D. Jones and R. Evans, "Development of wood property calibrations using near infrared spectra having different spectral resolutions", *J. Near Infrared Spectrosc.* **12,** 55 (2004). doi: 10.1255/jnirs.407

16. L.R. Schimleck, R. Evans, P.D. Jones, R.F. Daniels, G.F. Peter and A. Clark, III, "Estimation of microfibril angle and stiffness by near infrared spectroscopy using sample sets having limited wood density variation", *IAWA J.* **26,** 175 (2005).

17. L.R. Schimleck, R. Stürzenbecher, C. Mora, P.D. Jones and R.F. Daniel, "Comparison of *Pinus taeda* L. wood property calibrations based on NIR spectra from the radial–longitudinal and radial–transverse faces of wooden strips", *Holzforschung* **59,** 214 (2005). doi: 10.1515/HF.2005.034

18. L.R. Schimleck, P.D. Jones, G.F. Peter, R.F Daniels and A. Clark, III, "Success in using near infrared spectroscopy to estimate wood properties of Pinus taeda radial strips not due to autocorrelation", *J. Near Infrared Spectrosc.* **13,** 47 (2005). doi: 10.1255/jnirs.456

19. P.D. Jones, L.R. Schimleck, G.F. Peter, R.F. Daniels and A. Clark, III, "Nondestructive estimation of *Pinus taeda* L. wood properties for samples from a wide range of sites in Georgia", *Can. J. For. Res.* **35,** 85 (2005). doi: 10.1139/x04-160

20. L.R. Schimleck, G.M. Downes and R. Evans, "Estimation of *Eucalyptus nitens* wood properties by near infrared spectroscopy", *Appita J.* **59,** 136 (2006).

21. L.R. Schimleck, J.A. Tyson, P.D. Jones, G.F. Peter, R.F Daniels and A. Clark, III, "*Pinus taeda* L. wood property

calibrations based on variable numbers of near infrared spectra per core and cores per plantation", *J. Near Infrared Spectrosc.* **15,** 261 (2007). doi: 10.1255/jnirs.738

22. P.D. Jones, L.R. Schimleck, C.-L. So, A. Clark, III and R.F. Daniels, "High resolution scanning of radial strips cut from increment cores by near infrared spectroscopy", *IAWA J.* **28,** 473 (2007).

23. F. Antony, L. Jordan, L.R. Schimleck, R.F. Daniels and A. Clark, III, "The effect of mid-rotation fertilization on the wood properties of loblolly pine (*Pinus taeda*)", *IAWA J.* **30,** 49 (2009).

24. A. Huang, F. Fu, B. Fei and Z. Jiang, "Rapid estimation of microfibril angle of increment cores of Chinese fir by near infrared spectroscopy", *Chin. For. Sci. Technol.* **7,** 52 (2008).

25. S.S. Kelley, T.G. Rials, L.R. Groom and C-L. So, "Use of near infrared spectroscopy to predict the mechanical properties of six softwoods", *Holzforschung* **58,** 252 (2004). doi: 10.1515/HF.2004.039

26. S. Tsuchikawa, "A review of recent near infrared research for wood and paper", *Appl. Spectrosc. Rev.* **42,** 43 (2007). doi: 10.1080/05704920601036707

27. P.R.G. Hein, J.T. Lima and G. Chaix, "Robustness of models based on near infrared spectra to predict the basic density in *Eucalyptus urophylla* wood", *J. Near Infrared Spectrosc.* **17,** 141 (2009). doi: 10.1255/jnirs.833

28. P.R.G. Hein, J.T. Lima and G. Chaix, "Effects of sample preparation on NIR spectroscopic estimation of chemical properties of *Eucalyptus urophylla* S.T. Blake wood", *Holzforschung* **64,** 45 (2010). doi: 10.1515/HF.2010.011

29. I.D. Cave, "Theory of X-ray measurement of microfibril angle in wood", *For. Prod. J.* **16,** 37 (1966).

30. H. Yamamoto, T. Okuyama and M. Yashida, "Method of determining the mean microfibril angle of wood over a wide range by the improved Cave's method", *Mokuzai Gakkaishi* **39,** 118 (1993).

31. A. Savitzky and M.J.E. Golay, "Smoothing and differentiation of data by simplified least-squares procedures", *Anal. Chem.* **36,** 1627 (1964). doi: 10.1021/ac60214a047

32. F. Westad and H. Martens, "Variable selection in near infrared spectroscopy based on significance testing in partial least square regression", *J. Near Infrared Spectrosc.* **8,** 117 (2000). doi: 10.1255/jnirs.271

33. American Association of Cereal Chemists, *AACC Method 39-00*. American Association of Cereal Chemists, p. 15, (1999).

34. T. Fujimoto, Y. Kurata, K. Matsumoto and S. Tsuchikawa, "Application of near infrared spectroscopy for estimating wood mechanical properties of small clear and full length lumber specimens", *J. Near Infrared Spectrosc.* **16,** 529 (2008). doi: 10.1255/jnirs.818

35. C.R. Mora and L.R. Schimleck, "On the selection of samples for multivariate regression analysis: application to near-infrared (NIR) calibration models for the prediction of pulp yield in *Eucalyptus nitens*", *Can. J. For. Res.* **38,** 2626 (2008). doi: 10.1139/X08-099

36. J.J. Workman and L. Weyer, *Practical Guide to Interpretive Near-Infrared Spectroscopy*. CRC Press, Boca Raton, Florida, USA, p. 332 (2007).

37. K. Jungnikl, G. Koch and I. Burgert, "A comprehensive analysis of the relation of cellulose microfibril orientation and lignin content in the S2 layer of different tissue types of spruce wood [*Picea abies* (L.) Karst.]", *Holzforschung* **62,** 475 (2008). doi: 10.1515/HF.2008.079

38. B.K. Via, C.L. So, T.F. Shupe, L.H. Groom and J. Wikaira, "Mechanical response of longleaf pine to variation in microfibril angle, chemistry associated wavelengths, density, and radial position", *Composites: Part A* **40,** 60 (2009). doi: 10.1016/j.compositesa.2008.10.007

39. J.R. Barnett and V.A. Bonham, "Cellulose microfibril angle in the cell wall of wood fibres", *Biol. Rev.* **79,** 461 (2004). doi: 10.1017/S1464793103006377

40. H. Baillères, B. Chanson, M. Fournier, M.T. Tollier and B. Monties, "Structure, composition chimique et retraits de maturation du bois chez les clones d'*Eucalyptus*", *Ann. For. Sci.* **52,** 157 (1995). doi: 10.1051/forest:19950206

41. J.T. Lima, M.C. Breese and C.M Cahalan, "Variation in microfibril angle in *Eucalyptus* clones", *Holzforschung* **58,** 160 (2004). doi: 10.1515/HF.2004.024

Paper 7

Authors: Hein PRG, Brancheriau L, Trugilho PF, Lima JT, Chaix G

Title: Resonance and near infrared spectroscopy for evaluating dynamic wood properties

Journal: J. Near Infrared Spectrosc, v.18, n.6, p.443-454 (2010)

Received: 21 April 2010 ■ *Revised: 24 December 2010* ■ *Accepted: 24 December 2010* ■ *Publication: 11 January 2011*

JNIRS JOURNAL OF NEAR INFRARED SPECTROSCOPY
Special Issue on Wood and Wood Products

Resonance and near infrared spectroscopy for evaluating dynamic wood properties

Paulo Ricardo Gherardi Hein,[a] Loïc Brancheriau,[a] Paulo Fernando Trugilho,[b] José Tarcísio Lima[b] and Gilles Chaix[c]

[a]CIRAD, UPR Tropical Woods, 73 rue Jean-François Breton TA B40/16, 34398 Montpellier Cedex 5, France. E-mail: phein1980@gmail.com

[b]Universidade Federal de Lavras–UFLA–CTM/DCF, 37200-000 Lavras, Minas Gerais, Brazil

[c]CIRAD, UPR Forest Genetics, 73 rue Jean-François Breton TA B40/16, 34398 Montpellier Cedex 5, France

Dynamic longitudinal ($_L$) and transversal ($_T$) tests based on wood resonance were performed on *Eucalyptus* specimens measuring 410 mm × 25 mm × 25 mm to obtain the dynamic elastic modulus (E_L and E_T), the first resonance frequency (f_{1L}), the loss tangent ($\tan\delta_T$) and the specific modulus (E'_L and E'_T). Such dynamic traits and the air-dry density of wood were correlated by partial least squares (PLS) regressions to the near infrared (NIR) spectra measured in the central position of the longitudinal–radial surfaces. The statistics of the validation models for E, E' and f_{1L} ranged from 0.72 to 0.81 while the calibrations for loss tangent presented lower r^2_v (0.38), but promising *RPD* (ratio of performance to deviation) values (1.88). The key role of chemical wood components in the NIR-based calibrations for dynamic properties of wood is discussed. The association of the NIR spectroscopy and resonance techniques appears to be a rapid, low-cost and precise way to evaluate the visco-elastic properties of woods.

Keywords: NIR spectroscopy, resonance, stiffness, dynamic elastic modulus, frequency, loss tangent, specific modulus, *Eucalyptus* wood

Introduction

A number of techniques are available to evaluate the mechanical properties of wood in a non-destructive way. Near infrared (NIR) spectroscopy has been widely used as a tool to evaluate a range of wood and wood-based materials[1] being successfully applied for estimating physical and mechanical properties of wood.[2–9] Especially for modulus of elasticity, most of these studies have established NIR models based on stiffness measured by the SilviScan device[10–16] because, until recently, such precise but expensive equipment was considered to be the only instrument able to rapidly provide stiffness (and MFA). Thus, relatively few studies[17–20] used classical testing equipment to obtain the modulus of elasticity and develop NIR-based calibrations.

The resonance technique is a simple, rapid, precise and low-cost non-destructive technique for characterising the dynamic elastic properties of wood.[21] Several studies have shown a strong linear correlation between dynamic and static modulus of elasticity for a range of wood species, including *Eucalyptus*.[22] Hence, NIR spectroscopy combined with the resonance technique could quickly provide estimates of wood stiffness at relatively low cost. Moreover, other wood properties could be predicted from the same NIR spectral data if calibrations were available. Schimleck *et al.*[12] developed calibrations for stiffness based on the Silviscan-2 device (E_{LSS}) from NIR spectra recorded on the radial–longitudinal face of *Eucalyptus delegatensis* and *Pinus radiata* wood samples. Their estimates yielded good correlations between NIR-estimated E_{LSS} and static elastic modulus (E). Since the E_{LSS} (SilviScan2-based) had good correlations with dynamic E (resonance-based), their findings indicated that information in an NIR spectrum could be used to provide precise estimates of stiffness if correlated directly with resonance measurements.

To our knowledge, NIR calibrations for dynamic elastic properties based on the resonance technique are rarely reported.

ISSN: 0967-0335
doi: 10.1255/jnirs.907

It is likely that Fujimoto *et al.*[23] were the first team to report findings in regard to this issue. They applied a longitudinal vibration test to obtain the dynamic elastic modulus (E_L) in lumber samples and NIR-based calibrations were developed for E_L demonstrating the success of the combination of the two techniques.

Hence, the aim of this study was to build PLS regressions based on NIR spectra and dynamic elastic properties in order to predict elastic mechanical and physical properties of *Eucalyptus* wood.

The dynamic longitudinal ($_L$) and transversal ($_T$) tests based on resonance technique were performed on *Eucalyptus* wood specimens measuring 410 mm × 25 mm × 25 mm to obtain the dynamic elastic modulus (E_L and E_T), the first resonance frequency (f_{1L}), the loss tangent ($\tan\delta_T$) and the specific modulus (E'_L and E'_T). Such dynamic traits measured on entire specimens were correlated by PLS regressions to the NIR spectra which in turn were measured in the centre of the radial–longitudinal wood surface. Considering the remaining issue of the estimates of wood properties of stems or even whole-tree by means of NIR spectra measured on specific points or regions of wood samples (as increment cores, for instance), the challenge of this study was to establish correlations between traits of whole specimens and localised NIR spectra, taking into account the range of variation within the wood samples.

Material and methods

Origin and preparation of wood samples

One hundred and fifty logs of six-year-old *Eucalyptus grandis* x *E. urophylla* hybrids coming from a clonal comparison established in Brazil (19°17' S, 42°23' W, alt 230–500 m) were used in this study. The type of climate is Aw (Tropical savanna climate), according to the classification of Köppen (http://www.ask.com/wiki/Köppen_climate_classification), with mean annual rainfall of 1205 mm. The mean annual temperature is around 25°C and the average annual humidity is 67.3%. The trees were planted in a randomised design and the density of planting was 1667 trees ha^{-1} (3 m × 2 m spacing).

A total of 410 beams with well-defined tangential, radial and transverse faces were cut from central boards which had been removed from the stem base. The beams were trimmed to nominal cross-section of 25 mm × 25 mm using a circular saw machine. Subsequently, 330 small, clean specimens measuring 25 mm × 25 mm × 410 mm were cut from the beams, according to the ASTM D143-94 procedures[24] and submitted to dynamic tests and to NIR spectroscopic analysis.

Before dynamic tests and NIR spectra measurements, the specimens were conditioned in a room set for 20°C and 65% relative humidity to maintain the equilibrium moisture content (EMC) of 14%. The mass and dimension were measured and the air-dry density (D) of each specimen was calculated. The error of measurement was 0.001 g and 0.001 mm for mass and dimension, respectively. Figure 1 shows the procedure of dynamic tests and NIR spectral measurements.

Dynamic tests on specimens

The dynamic tests used to evaluate the elastic properties of these wood samples were described previously in Hein *et al.*[25] The specimens were placed on elastic supports so as to allow free vibrations. An exciting impulse was produced by lightly striking the specimen with an instrumented hammer at the opposite side to that of the output transducer (acoustic microphone). The specimens were submitted to transversal and longitudinal vibration tests. The transverse vibration was induced by an edgewise impact and the longitudinal vibration by an impact along the bound.[26] In transversal vibration, the first four modes of vibration were measured and used for estimating the dynamic transverse modulus of elasticity (E_T) of wood (also called Young's modulus). The loss tangent ($tg\delta_T$, 10^{-3}), also called internal damping, was calculated. In longitudinal vibrations, the first vibration mode was measured and used for estimating the dynamic longitudinal modulus of elasticity (E_L) of the wood. The analysis of the spectral signal, the selection of the peaks of the natural frequency of vibration of the wood samples and the estimates of the E_L, E_T and $tg\delta_T$ were performed using the software BING® (CIRAD, Montpellier, France, version 9.1.3). The maximum relative

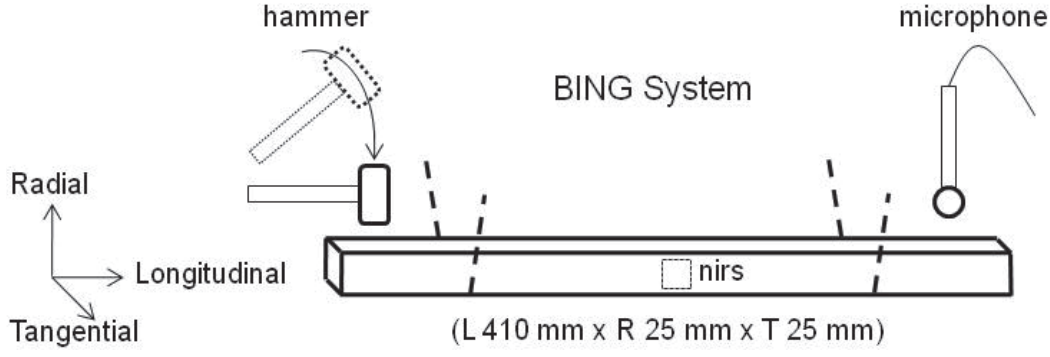

Figure 1. Procedure used for resonance and NIR spectra measurements.

errors for dynamic E_X obtained by means of this system are less than 5%.[21]

Equations of motion

The theoretical model used to describe the motion of a uniform prismatic beam that vibrates transversely was proposed by Timoshenko[27] as follows:

$$E_X I_{Gz}\frac{\partial^4 v}{\partial x^4}-\rho I_{Gz}\left(1+\frac{E_X}{KG_{XY}}\right)\frac{\partial^4 v}{\partial x^2\partial t^2}+\frac{\rho^2 I_{Gz}}{KG_{XY}}\frac{\partial^4 v}{\partial t^4}+\rho A\frac{\partial^2 v}{\partial t^2}=0 \quad (1)$$

where E_X is the Young's modulus, I_{GZ} is the moment of inertia, v is the transverse displacement, ρ is the density, G_{XY} is the shear modulus, K is a constant which depends of the geometry of the section (for rectangular section, K=5/6), x is the distance along the axis of the beam, A, cross-sectional area of the beam, t is the time. Using the Bordonné's solution[28] for this differential equation, the shear effect is taken it account, but the support effects are ignored. The elastic (E_X) was calculated according to the follow equation, described in Brancheriau and Baillères:[21]

$$\frac{E_X}{\rho}-\frac{E_X}{KG_{XY}}\left[QF_2(m)4\pi^2\frac{AL^4}{I_{Gz}}\frac{f_n^2}{P_n}\right]=4\pi^2\frac{AL^4}{I_{Gz}}\frac{f_n^2}{P_n}[1+QF_1(m)] \quad (2)$$

where f_i is the resonance frequency of the order i and P_n is the solution of Bernoulli (rank n). Parameters Q, F_1, F_2, m and θ were calculated as described in Brancheriau and Baillères.[21] In longitudinal vibrations, the first vibration mode can be used in order to estimate its dynamic longitudinal modulus of elasticity (E_L) by means the formula:

$$E_x=4L^2\rho f_1^2 \quad (3)$$

The parametric method of Steiglitz and McBride[29] was used to simultaneously determine the first resonance frequency f_1, the amplitude β_1 and the temporal damping α_1 associated with f_1. Only the first frequency was considered because of its high energy. The internal friction (tgδ, 10^{-3}) was calculated associated with the complex modulus concept with respect to transverse vibrations[30] according to the equation given by Brancheriau *et al.*:[31]

$$tg\delta=\frac{\alpha_1}{\pi f_1} \quad (4)$$

A detailed discussion about different theoretical models of motion, their approximate solutions and their respective hypotheses in longitudinal and flexural vibrations and the effects of the elastic support required by the BING system, has been provided in Brancheriau and Baillères.[21]

NIR spectra acquisition

A Bruker spectrophotometer (model Vector 22/N, Bruker Optik GmbH, Ettlingen, Germany) was used in diffuse reflectance mode. This Fourier transform spectrometer is designed for reflectance analysis of solids with an integrating sphere which measures the diffuse reflected light on a 150 mm^2 spot. The integrating sphere collects light from all angles; thus, the effects of wood texture and other non-homogeneities are minimised. It is also advantageous that the sphere is "upward looking", with a window on top of the sphere. A sintered gold standard was used as a reference. Spectral analysis was performed within the 12,500–3500 cm^{-1} (800–2850 nm) range at 8 cm^{-1} resolution (each spectrum consisted of 2335 reflectance values).

Each NIR spectrum was obtained with 16 scans; means were calculated and compared to the standard to obtain the reflectance spectrum of the sample. NIR spectra were recorded in the centre of the two sides of the longitudinal radial surfaces of each specimen (Figure 1) and averaged. First derivatives (13-point filter and a second order polynomial) and second derivatives (25-point filter and a third order polynomial) were applied on the NIR spectra using the Savitsky and Golay[32] algorithm (Figure 2). Our earlier studies[20,33] showed that these pre-treatments enhance the quality of the information and calibrations in *Eucalyptus* wood.

PLS-R model statistics

PLS regressions were developed to describe the relationship between the wood properties and the NIR spectra by means of the Unscrambler (CAMO AS, Norway, v. 9.7) software.

First, the PLS-R calibrations based on a complete data set (330 specimens) were performed in cross-validation mode with a maximum of 12 latent variables (LV). Martens' uncertainty test[34] was used to select the wavenumbers with significant regression coefficients. Outliers were indentified from the Student residuals and leverage value plot analyses. The number of LVs adopted for each model corresponded to the first minimal residual variance. These first cross-validated PLS-R models were used to pre-define the parameters (such as wavenumbers, number of LVs and outliers) to be used in calibrations for dynamic traits. Thus, PLS-R models were performed based on the pre-defined parameter in samples of a training set and validated by the samples of a test set. The selection of the samples of each subset was made manually as follows. The complete sample set (330 specimens) was ranked in ascending order and split into two uniformly distributed subsets. This procedure allowed close control of the trait variability within each subset.

Selection of the PLS-R models

To compare the PLS-R model validations, the following statistics were used: the coefficient of determination of calibration (R_c^2), cross-validation (r_{cv}^2) and test set-validation (r_v^2); the root mean standard error of calibration (*RMSEC*), cross-validation (*RMSECV*) and test set-validation (*RMSEP*); the number of LV and the ratio of performance to deviation (*RPD*). Root mean standard errors should be as low as possible while the coefficient of determinations should be high. The *RPD* value is the ratio of the root mean standard error to the standard deviation (*SD*) of the reference data.[35] This statistic provides a basis for standardising the *RMSECV* or *RMSEP* and makes possible a comparison between PLS-R calibrations and its validations for different wood traits.[36] According to Fujimoto *et al.*,[23] the higher the *RPD* value, the more reliable are the predictions.

Table 1. Summary of the air-dry density of wood and dynamic properties of the small, clean specimens of *Eucalyptus* wood.

Trait	D	E_L	E'_L	f_{1L}	E_T	E'_T	$\tan\delta_T$
Av.	517.4	13,361	25.7	6,170	12,468	24.0	7.51
SD	58.38	2,528	3.23	396.5	2,332	3.07	1.53
Min	362.5	6,522	17.9	4,919	5,930	14.1	5.18
Max	708.4	21,258	29.8	6,945	18,732	30.6	10.60
CV	11.3	18.9	12.6	6.4	18.7	12.8	20.3
N	327	327	327	327	327	327	147

Abbreviations:
Traits: Density (*D*), dynamic elastic modulus (E_L and E_T), the first resonance frequency (f_{1L}), the loss tangent (tanδT) and the specific modulus (E'_L and E'_T) for longitudinal (L) and transversal (T) tests.
Data: Average (Av.), standard deviation (*SD*), minimum (Min) and maximum (Max) values, coefficient of variation (*CV*) and number of observations (*N*).

Results and discussion

Dynamic tests on woods

Table 1 lists the descriptive statistics for air-dry density (*D*) and dynamic properties of the small, clean specimens of *Eucalyptus* wood, including the dynamic longitudinal modulus of elasticity (E_L), the first resonance frequency (f_{1L}) in longitudinal tests, the dynamic transversal modulus of elasticity (E_T) and the loss tangent ($tg\delta_T$, 10^{-3}), also called internal damping, in transversal tests. E'_L and E'_T are the specific modulus (elastic modulus to air-dry density ratio) for longitudinal and transversal tests, respectively. The range of variation (minimum and maximum values) of these data is very important to develop predictive models.

As the BING software alerts us about imprecise estimations, we used 327 of 330 estimates for the dynamic properties and only 147 values for $tg\delta_T$. Loss tangent is a wood property which is difficult to measure precisely.

NIR spectra of wood

Wood is a complex three-dimensional biopolymer material composed of an interconnected network of cellulose, hemicelluloses and lignin with minor amounts of extractives and inorganics.[37] Hence, NIR spectra comprise of the energy reflected (or captured) by chemical bonds from different wood components, their contents and interactions. Figure 2 illustrates the raw and pre-treated NIR spectra measured directly in two specimens of six-year *Eucalyptus*. The spectra labelled as "A" came from a specimen that presented the highest E_L value while the spectra "B" was from the sample with the lowest stiffness. Table 2 summarises the assignments of NIR absorption bands normally associated with the main wood components. The index (Table 2) refers to the assignments presented in Figure 2 and to regression coefficients of the wood traits presented by Figures 3–6. The chemical components of wood, mainly the cellulose and lignin contents, contributed to the NIR information and played a key role in the PLS-R models for mechanical and physical properties of wood.

NIR-based models

Table 3 lists the mean, minimum and maximum values, coefficient of variation and number of training samples and test sets for air-dry density and dynamic properties of the small, clean specimens of *Eucalyptus* wood. According to Mora and Schimleck[38] the predictive models must include all possible sources of variation that can be encountered later in real applications because the goal is to estimate values in new samples. By selecting the subsets manually we guaranteed that the test set had as extreme values as possible. Thus, the minimum and maximum values of the test set samples were comprehended within the variation range of the training set.

The cross-validation approach was used to develop preliminary PLS-R models (Table 4). The outliers, the selected wavenumbers and the number of LVs to retain in the calibration for each trait were based on these cross-validation models. Thus, PLS-R models were developed taking into account such parameters and used to estimate the air-dry density and dynamic elastic modulus of samples in separate test sets (Table 5).

Cross-validated PLS-R models

PLS-R models were built from the untreated and pre-treated NIR spectra data from 9000 cm^{-1} to 4000 cm^{-1} for D, E_L, E'_L, f_{1L}, E_T, E'_T and $\tan\delta_T$ of *Eucalyptus* wood specimens. Statistical summaries of the cross-validated PLS-R models are presented in Table 4.

While promising model statistics ($r^2_{cv} \geq 0.72$) were obtained for E_L, E_T and f_{1L}, the PLS-R models for E'_T and $\tan\delta_T$ yielded low to moderate coefficients of determination (r^2_{cv} from 0.39 to 0.62) but still acceptable *RPD* values (from 1.61 to 2.01) for screenings.[14] E'_T yielded models with good r^2_{cv}, and low *RPD* values. For air-dry density, the model statistics were weaker ($r^2_{cv} = 0.67$) than those reported in early studies.[2–3,16,33,38–40]

These relatively weaker PLS-R models can be explained by the representativeness of the sampling used in this study. For instance, Hein *et al.*,[33] Mora *et al.*[38] and Meder *et al.*[39] measured the density and the NIR spectra from small samples, which provide the statistical performance of the models. Here,

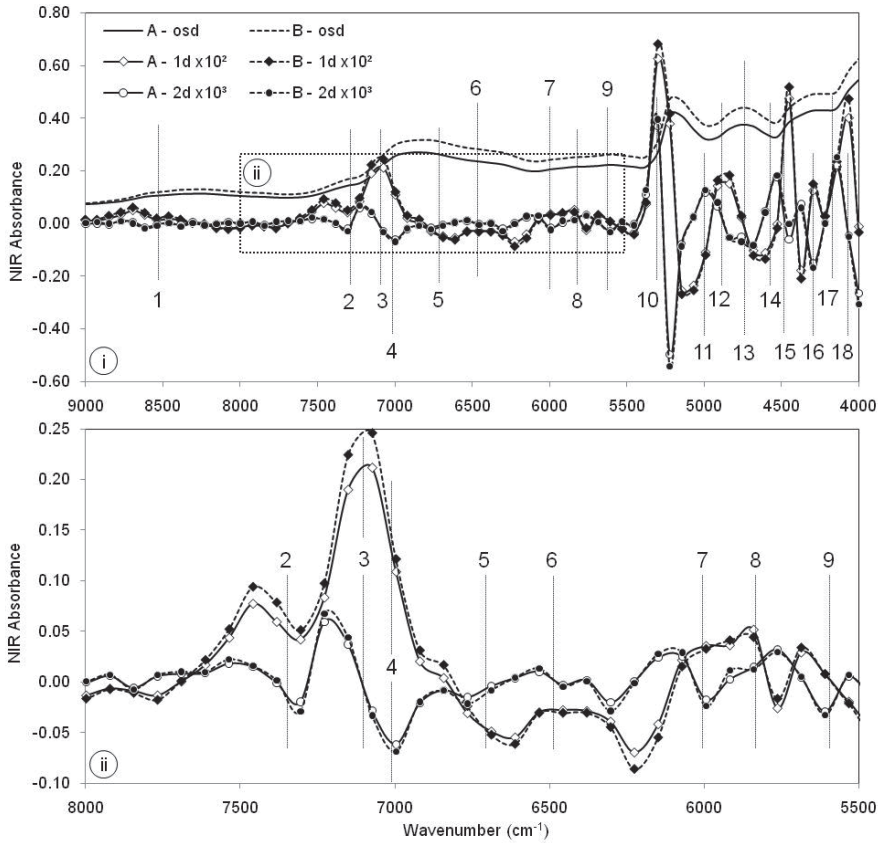

Figure 2. Absorbance versus wavenumber plot for untreated NIR spectra and first and second derivative of the NIR spectra from 9000 cm^{-1} to 4000 cm^{-1} (i) and minutely from 8000 cm^{-1} to 5500 cm^{-1} (ii). A is the NIR spectra of the stiffest sample while B refers to the least stiff sample. The scaling factor for first derivatives was 10^2 and for second derivative was 10^3. Bands assigned to chemical compounds are represented by numbers and listed in Table 2.

the specimen dimension was of 410 mm × 25 mm × 25 mm and only two NIR spectra were recorded on the centre of each longitudinal–radial surface. Moreover, the intra-specimen variability of these 410 mm × 25 mm × 25 mm specimens naturally was higher than of small samples. We used the same localised NIR information to correlate to the wood traits, but the problem of representativeness was stronger for air-dry density, and consequently, for specific modulus. E'_L, E'_T and f_{1L} were less sensitive to the scale effect, providing more robust PLS-R models. Moreover, other possible source of error came from the reference measurement error. For air-dry density, the error of measurement was 0.001 g and 0.001 mm for mass and dimension, respectively, while for the estimates of dynamic wood properties using this system, the estimated error is less than 5%.[21]

Validations by test set

The statistics associated with the PLS-R models validated by test sets (Table 5) were very similar to those cross-validated (Table 4). For air-dry density, cross- and test set-validated models had similar r^2 and slightly higher *RPD* and *RMSEP* (the *SD*s of the density were 56.7 kg m^{-3} and 61 kg m^{-3} for training and test set, respectively). A plot of laboratory-determined air-dry density versus NIR-predicted air-dry density is given in Figure 3. Cross- and test set validations for first frequency resonance of specimens also have similar performance.

For modulus of elasticity and specific modulus, validation by test set yielded slightly higher r^2 and *RPD* than cross-validations, which can be attributed by the selection procedure of subset samples where the samples included in the test set could be predicted with relative higher precision. This trend was expected as the (phenotypic) correlation between E and E' was quite strong (r = 0.82) from both transversal and longitudinal test.

Recently, Fujimoto *et al.*[23] presented NIR calibrations for the dynamic elastic modulus of elasticity. They used their NIR-based calibration (r^2 = 0.72) to estimate the E_L of samples in separate test sets (r^2_p = 0.75) producing a standard error of prediction of 1.32 GPa. Here, PLS-R models were developed for E_L and E_T providing slightly higher r^2_v (0.81 for E_L and 0.77 for E_T) and *RPD* values in test set validations and lower standard error of validation (1.15 GPa) than Fujimoto's models[23] (R^2_c = 0.75, r^2_p = 0.72 and *RPD* = 1.87). Fujimoto *et al.*[23] measured E based on longitudinal vibration. Since the range of variation of dynamic elastic modulus was similar for both studies (from ~7 MPa to ~20 MPa), the

Table 2. NIR absorption bands normally associated with the main wood components (cellulose, hemicellulose lignin, and water) contained in the wood specimens. Index numbers relate to the specific bands indicated in Figure 2 and to regression coefficients identified in Figures 3, 4, 5 and 6.

Index	cm^{-1}	Bond vibration	Structure	Ref.
1	8547	2nd overtone asymmetric stretching CH, HC=CH	Lignin	45
2	7353	CH deformation + CH stretching 2nd overtone	CH_3	46
3	7092	OH stretching 1st OT lignin or first overtone of an O–H stretching vibration of phenolic hydroxyl groups	Lignin	47
3	7057	C-H combination, aromatic associated C–H	Lignin	45
4	7003	1st overtone OH stretching (amorphous region in cellulose)	Cellulose	23
5	6711	1st overtone OH stretching	Cellulose	45,48
6	6460	1st overtone OH stretching (crystalline regions in cellulose)	Cellulose	47
7	5981	1st overtone CH stretching	Lignin	23
7	5934	1st overtone CH stretching (aromatic associated CH)	Lignin	45,48
8	5800	1st overtone CH stretching	Hemicellulose	23
9	5618	1st overtone CH_2 stretching	Cellulose	45,48
10	5250	not assigned		
11	5050	OH stretching + OH deformation combination band	Water	23,45
12	4800	Asymmetric NH stretching + amide III		45
13	4750	not assigned		
14	4545	CH stretching and C=O combination	Lignin	45
15	4490	not assigned		
16	4375	not assigned		
17	4282	CH stretching + CH_2 deformation combination band (and 2nd overtone of CH_2 streching)	Cellulose	45,(47)
17	4261	CH (1st overtone CH_2 symmetric stretching and δ CH_2) combination	Cellulose	45,47
17	4252	CH bending and stretching combination band	Cellulose	45
18	4063	CH stretching + CC stretching	Cellulose	45

Table 3. Statistical summary of the training and test sets for air-dry density and dynamic properties of the small, clean specimens of *Eucalyptus* wood.

Traits	Training set					Test set				
	Av.	Min	Max	*CV*	*N*	Av.	Min	Max	*CV*	*N*
D	517.1	362	708	11.0	196	517.8	375	697	11.8	131
E_L	13,333	6,522	21,258	18.2	195	13,403	6,715	19,475	20.0	131
E'_L	25.6	17.9	29.8	8.2	195	25.6	18.0	29.7	9.0	131
f_{1L}	6170	4919	6945	6.2	195	6171	5014	6916	6.7	131
E_T	12,455	5,930	18,732	18.1	196	12,488	6,035	18,176	19.6	131
E'_T	24.0	14.1	30.6	12.5	196	24.1	15.3	29.8	13.2	131
$\tan\delta_T$	7.52	5.18	10.60	20.9	80	7.51	5.66	10.03	19.7	67

Abbreviations: See Table 1.

Table 4. Cross-validated PLS-R models for air-dry density and dynamic properties of the small, clean specimens of *Eucalyptus* wood.

Traits	Pre-treat.	Outliers	R^2_c	*RMSEC*	r^2_{cv}	*RMSECV*	LV	*RPD*
D	2d	3	0.70	31.3	0.67	32.6	5	1.74
E_L	1d	4	0.79	1153	0.77	1197	4	2.03
E'_L	1d	0	0.75	1.61	0.72	1.70	6	1.24
f_{1L}	2d	0	0.74	202	0.72	211	5	1.83
E_T	2d	2	0.74	1185	0.73	1229	5	1.84
E'_T	2d	1	0.67	1.75	0.62	1.87	6	1.61
$\tan\delta_T$	1d	2	0.47	0.73	0.39	0.78	5	2.01

Abbreviations: See Table 1

Table 5. PLS-R models for air-dry density and dynamic properties of the small, clean specimens of *Eucalyptus* wood validated by test set.

Traits	Pre-treat.	Outliers	R^2_c	*RMSEC*	r^2_v	*RMSEP*	LV	*RPD*
D	2d	3	0.66	31.4	0.67	34.8	4	1.75
E_L	1d	4	0.78	1128	0.81	1149	5	2.34
E'_L	2d	0	0.74	1.59	0.76	1.62	5	1.41
f_{1L}	2d	0	0.77	186	0.72	215	6	1.92
E_T	1d	2	0.71	1211	0.74	1219	4	2.01
E'_T	1d	1	0.62	1.82	0.70	1.69	6	1.88
$\tan\delta_T$	1d	2	0.49	0.71	0.38	0.81	5	1.84

motion equations used in this study can explain, at least partially, the robustness of the statistics associated to the established PLS-R models (Tables 3 and 4) for E_T. The E_T estimates from the resonance technique used in this study were based on improved solutions[28] for the equations of motion,[27] which take into account the shear moduli component. Figure 4 shows the NIR-predicted versus measured values for dynamic longitudinal elastic modulus, the coefficients of regression and the important assignments. Thus, it is easy to find which variables or wood components are important for the established PLS-R models. Cellulose, hemicelluloses and lignin contents played a major role in calibrations.

There was strong agreement between NIR-estimated f_{1L} and laboratory-determined f_{1L} as indicated by high r^2 values (Figure 5). Figure 6 shows the plot of NIR-estimated versus resonance-estimated loss tangent. To our knowledge, PLS-R calibrations based on NIR spectra for first frequency resonance and for loss tangent have not been reported. Indeed, calibration for f_{1L} has no practical application because their estimates are only valid for *Eucalyptus* samples measuring exactly 410 mm × 25 mm × 25 mm and within the density range here. However, it is interesting to see that NIR spectroscopy is able to predict this particular intrinsic wood property. It is known that the first frequency is less influenced by the viscosity of the material; providing, theoretically, the elastic modulus nearest to the static elastic modulus conventionally obtained by a static bending test.[41]

The loss tangent is an important wood characteristic which indicates the quality of wood for manufacturing musical instruments. According to Ono and Norimoto,[42] wood having high specific modulus and low loss tangent is suitable for soundboards. For instance, Buksnowitz *et al.*[43] applied the resonance technique on *Picea abies* wood to evaluate and predict violin makers quality-grading. However, this trait is poorly reported in the literature, especially in *Eucalyptus* wood, due to the difficulty of measurement accuracy.[25] Here, a PLS-R model was established between loss tangent and NIR spectra with low r^2_v (0.38) but promising *RPD* value (1.84). This low r^2_v reflects the difficulty of measuring the loss tangent. To our knowledge, the present study was the first effort to correlate these vibrational properties of wood (f_{1L}, $\tan\delta_T$ and E') with NIR spectroscopy.

NIR interaction with wood

The underlying factors controlling wood properties are essentially the result of its chemical composition at three levels: i) chemical features of the molecules that constitute the cell walls (structural components) and those contained within the cellular structure (extractive components); ii) distribution of the chemical components in the cell structure; and iii) the relative proportions of the different chemical components in the wood cells and tissues. The specific properties of wood may be traced back to a combination of these aspects, and wood utilisation and end-product related quality should thereby link directly to its chemical characteristics.[44] Hence, mechanical,

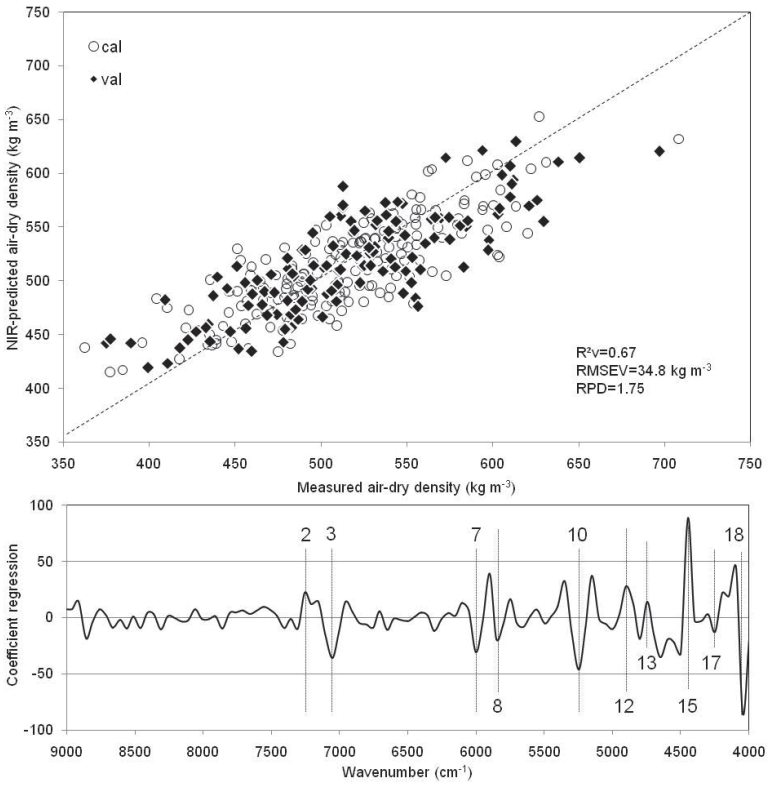

Figure 3. NIR-predicted versus measured values plot for air-dry density (*D*) based on the second derivative of NIR spectra for both training (open circles) and test sets (filled rhombs) and regression coefficients for PLS-R model predicting *D*.

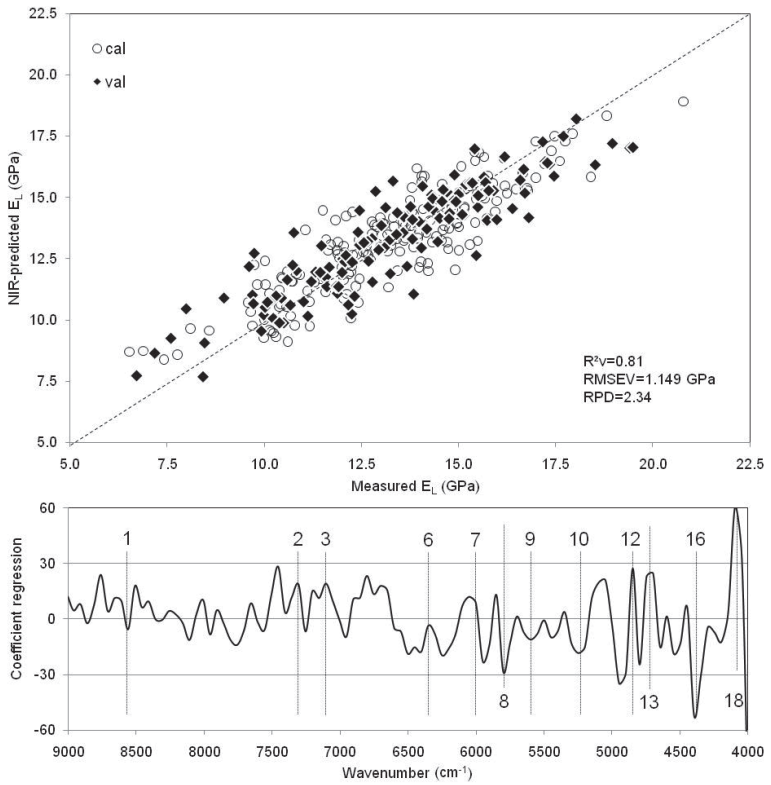

Figure 4. NIR-predicted versus measured values plot for dynamic longitudinal modulus of elasticity (E_L) based on the first derivative of NIR spectra for both training (open circles) and test sets (filled rhombs) and regression coefficients for PLS model predicting E_L.

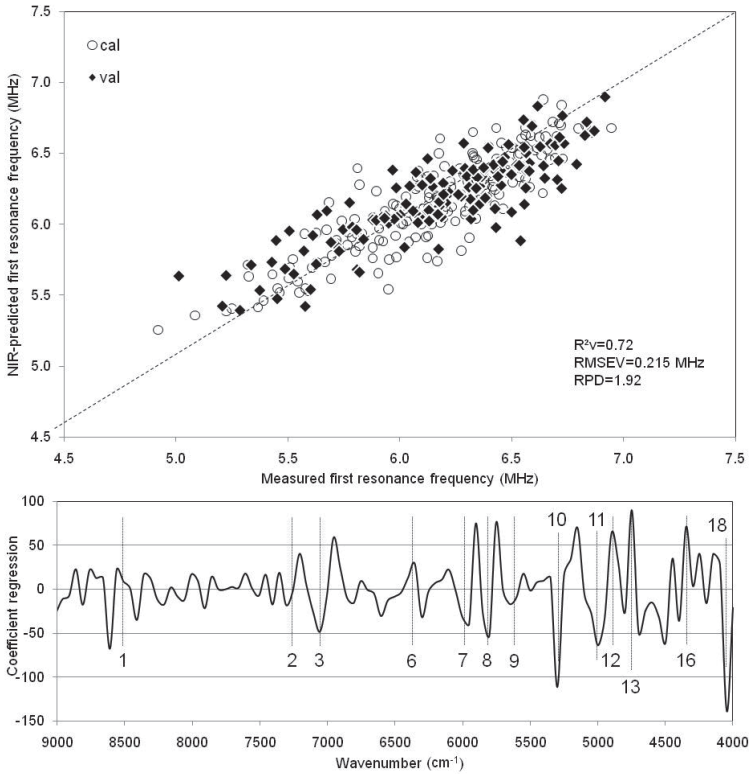

Figure 5. NIR-predicted versus measured values plot for first resonance frequency (f_{1L}) based on the second derivative of NIR spectra for both training (open circles) and test sets (filled rhombs) and regression coefficients for PLS-R model predicting f_{1L}.

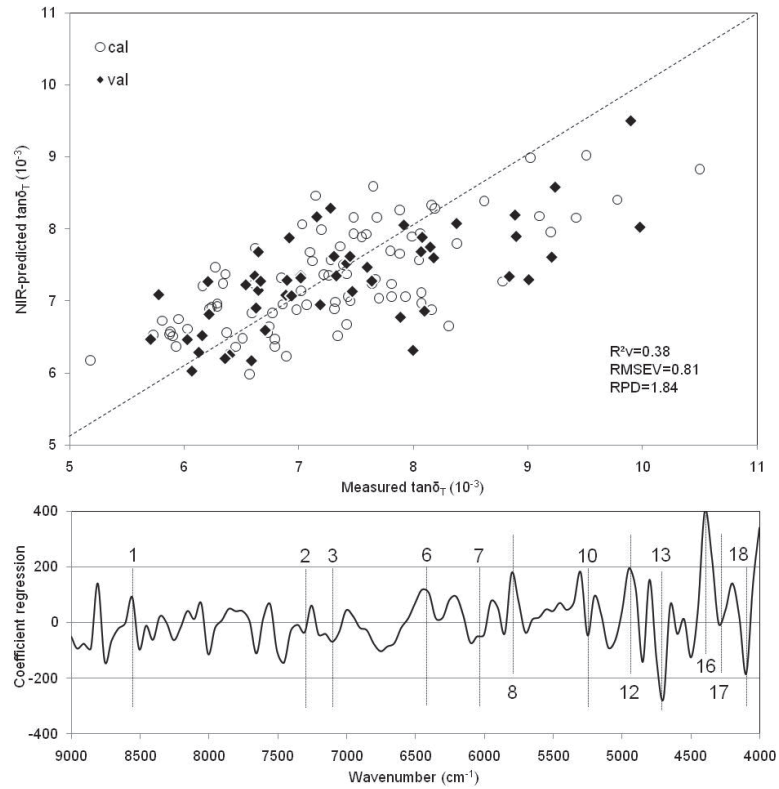

Figure 6. NIR-predicted versus measured values plot for loss tangent ($\tan\delta_T$) based on the first derivative of NIR spectra for both training (open circles) and test sets (filled rhombs) and regression coefficients for PLS model predicting $\tan\delta_T$.

physical and chemical wood traits are often correlated. For instance, it is known that the influence of density on strength and elasticity of wood is strong.[37]

The analysis of the loading plots for each calibration is useful to investigate the underlying relationships that have made the estimation of air-dry density and dynamic elastic properties of wood possible by NIR spectroscopy. The assignments of absorbance bands indicated in Figures 3–6 are useful to identify which wood components were important for the PLS-R models. It helps to understand how NIR spectroscopy can evaluate wood traits based on resonance analysis.

The lignin content of wood was important for air-dry density PLS-R models, as bands at 7092–7057 cm^{-1} (index 3) and 5081–5934 cm^{-1} (index 7) yielded high regression coefficients and were assigned to lignin. The high regression coefficient at 4282 cm^{-1} (index 18) indicates that cellulose content also played an important role on PLS-R models for air-dry density. The band at 4490 cm^{-1} (index 15) also seems to be important for air-dry density calibration. For dynamic elastic models, the bands at 5800 cm^{-1} (index 8), associated with the hemicellulose content; at 4800 cm^{-1} (index 12) and 4750 cm^{-1} (index 13) had a strong regression coefficient, but the bands at 4375 cm^{-1} (index 16) and 4282 cm^{-1} (index 18) appear to be the most important for stiffness. Schimleck *et al.*[13] also reported similar loading plots for air-dry density and for stiffness.

The bands with higher coefficients of regression for first frequency resonance were those associated with hemicelluloses (4750 cm^{-1}) and cellulose (4282 cm^{-1}) contents, and also the bands at 5250 cm^{-1} (index 10) and 4750 cm^{-1} (index 13). Cellulose and hemicellulose contents were also important for PLS-R models for loss tangent. High absorptions occurred at 5800 cm^{-1} (index 8), at 4750 cm^{-1} (index 13), at 4375 cm^{-1} (index 16) and at 4282 cm^{-1} (index 18). In short, combinations of lignin, hemicelluloses and cellulose contents in wood control the elastic properties of wood. The absorbance corresponding to lignin (index 3, 7 and 14), to hemicelluloses (index 8) and to cellulose (index 4, 5, 6, 9, 17 and 18) content were significant to the Martens' uncertainty test[34] for the wood traits, and other important bands (index 10, 13 and 16) seem to be associated or combined with the specific absorptions of the known wood components.

Concluding remarks

In this study, the NIR-based PLS-R models for air-dry density and dynamic properties of wood were validated by cross-validations and independent test sets. The validated PLS-R models by cross-validation and by test set presented similar performance, and acceptable statistics, showing the robustness of the combination of NIR and resonance. The association of resonance and NIR spectroscopy techniques to evaluate mechanical properties of woods has three substantial advantages: speed, accuracy and low-cost. Considering the small area scanned by NIR spectra and the high correlations of elastic properties of entire wood specimens, the scale effect was not a source of substantial error. If the idea behind the proposed approach is to provide a large data set of key elastic–mechanical wood properties, sufficiently representative of the properties in parts of the stem, and sufficiently precise for genetic studies, the association of NIR spectroscopy and resonance technique seems to be an adequate, low-cost tool for estimating such timber traits, from increment cores, for instance.

Here, the established PLS-R models for dynamic traits presented *RPD* > 1.74, except for specific modulus. For genetic approaches, the absolute value of the property is not important. The interesting point is to know the relative value of the characteristic between trees or regions of the stem, its variation or stability within the logs. Since high throughput phenotyping tools are required in genetic studies and breeding programmes, these models can be useful for selection of candidate genotypes or commercial clones from a large wood sampling in the forestry industry.

Acknowledgements

The authors express their special thanks to the CENIBRA (Celulose Nipo-Brasileira) (Antonio Marcos Rosado) for providing trees; to the Department of Wood Science and Technology of the *Universidade Federal de Lavras* (UFLA, Brazil, José Reinaldo Moreira da Silva) for supporting the experimental work and to the *Centre de Cooperation Internationale en Recherche Agronomique pour le Development* (UR39 and UR40 of CIRAD, Montpellier, France) for laboratory facilities. Special thanks to José Francisco de Sousa, Carlos Henrique da Silva, Heber Alvarenga and Hernani Alves (UFLA) for their technical support. This study was funded by CENIBRA, CNPq (Conselho Nacional de Desenvolvimento Científico e Tecnológico, Brazil) and CIRAD (UR40). P.R.G. Hein was supported by CNPq grants (process no. 200970/2008–9).

References

1. S. Tsuchikawa, "A review of recent near infrared research for wood and paper", *Appl. Spectrosc. Rev.* **42,** 43–71 (2007). doi: 10.1080/05704920601036707
2. L.G. Thygesen, "Determination of dry matter content and basic density of Norway spruce by near-infrared reflectance and transmission spectroscopy", *J. Near Infrared Spectrosc.* **2,** 127–135 (1994). doi: 10.1255/jnirs.39
3. P. Hoffmeyer and J.G. Pedersen, "Evaluation of density and strength of Norway spruce wood by near-infrared reflectance spectroscopy", *Holz Roh Werkst.* **53,** 165–170 (1995). doi: 10.1007/BF02716418
4. R. Meder and A. Thumm, "Stiffness prediction of radiata pine clearwood test pieces using near infrared spectroscopy", *J. Near Infrared Spectrosc.* **9,** 117–122 (2001). doi: 10.1255/jnirs.298

5. W. Gindl and A. Teischinger, "The relationship between near infrared spectra of radial wood surfaces and wood mechanical properties", *J. Near Infrared Spectrosc*. **9,** 255–261 (2001). doi: 10.1255/jnirs.311

6. J.B. Hauksson, G. Bergqvist, U. Bergsten, M. Sjostrom and U. Edlund, "Prediction of basic wood properties for Norway spruce. Interpretation of near infrared spectroscopy data using partial least squares regression", *Wood Sci. Technol*. **35,** 475–485 (2001). doi: 10.1007/s00226-001-0123-3

7. L.R. Schimleck and R. Evans, "Estimation of wood stiffness of increment cores by near infrared spectroscopy: The development and application of calibrations based on selected cores", *IAWA J.* **23,** 217–224 (2002).

8. R. Meder, A. Thumm and D. Marston, "Sawmill trial of at-line prediction of recovered lumber stiffness by NIR spectroscopy of *Pinus radiata* cants", *J. Near Infrared Spectrosc*. **11,** 137–143 (2003). doi: 10.1255/jnirs.361

9. S.S. Kelley, T.G. Rials, R. Snell, L.H. Groom and A.D. Sluiter, "Use of near infrared spectroscopy to measure the chemical and mechanical properties of solid wood", *Wood Sci. Technol*. **38,** 257–276 (2004). doi: 10.1007/s00226-003-0213-5

10. L.R. Schimleck, R. Evans and J. Ilic, "Application of near infrared spectroscopy to a diverse range of species demonstrating wide density and stiffness variation", *IAWA J.* **22,** 415–429 (2001).

11. L.R. Schimleck, R. Evans and J. Ilic, "Estimation of *Eucalyptus delegatensis* wood properties by near infrared spectroscopy", *Can. J. For. Res.* **31,** 1671–1675 (2001). doi: 10.1139/cjfr-31-10-1671

12. L.R. Schimleck, R. Evans, J. Ilic and A.C. Matheson, "Estimation of wood stiffness of increment cores by near-infrared spectroscopy", *Can. J. For. Res*. **32,** 129–135 (2002). doi: 10.1139/x01-176

13. L.R. Schimleck, R. Evans and A.C. Matheson, "Estimation of *Pinus radiata* D. Don clear wood properties by near-infrared spectroscopy", *J. Wood Sci.* **48,** 132–137 (2002). doi: 10.1007/BF00767290

14. L.R. Schimleck, C. Mora and R.F. Daniels, "Estimation of the physical wood properties of green *Pinus taeda* radial samples by near infrared spectroscopy", *Can. J. For. Res.* **33,** 2297–2305 (2003). doi: 10.1139/x03-173

15. P.D. Jones, L.R. Schimleck, G.F. Peter, R.F. Daniels and A. Clark III, "Nondestructive estimation of *Pinus taeda* L. wood properties for samples from a wide range of sites in Georgia", *Can. J. For. Res.* **35,** 85–92 (2005). doi: 10.1139/x04-160

16. P.D. Jones, L.R. Schimleck, C.-L. So, A. Clark III and R.F. Daniels, "High resolution scanning of radial strips cut from increment cores by near infrared spectroscopy", *IAWA J.* **28,** 473–484 (2007).

17. B.K. Via, T.F. Shupe, L.H. Groom, M. Stine and C.L. So, "Multivariate modelling of density; strength and stiffness from near infrared spectra for mature, juvenile and pith wood of longleaf pine (*Pinus palustris*)", *J. Near Infrared Spectrosc*. **11,** 365–378 (2003). doi: 10.1255/jnirs.388

18. B.K. Via, C.L. So, T.F. Shupe, L.G. Eckhardt, M. Stine and L.H. Groom, "Prediction of wood mechanical and chemical properties in the presence and absence of blue stain using two near infrared instruments", *J. Near Infrared Spectrosc*. **13,** 201–212 (2005). doi: 10.1255/jnirs.538

19. S. Tsuchikawa, Y. Hirashima, Y. Sasaki and K. Ando, "Near-infrared spectroscopic study of the physical and mechanical properties of wood with meso- and micro-scale anatomical observation", *Appl. Spectrosc*. **59,** 86–93 (2005). doi: 10.1366/0003702052940413

20. P.R.G. Hein, A.C.M. Campos, J.T. Lima, P.F. Trugilho and G. Chaix, "Estimativa da resistência e da elasticidade à compressão paralela às fibras da madeira de *Eucalyptus grandis* e *E. urophylla* usando a espectroscopia no infravermelho próximo", *Scientia Forestalis* **37,** 7–16 (2009).

21. L. Brancheriau and H. Baillères, "Natural vibration analysis of clear wooden beams: a theoretical review", *Wood Sci. Technol*. **36,** 347–365 (2002). doi: 10.1007/s00226-002-0143-7

22. J. Ilic, "Relationship among the dynamic and static elastic properties of air-dry *Eucalyptus delegatensis* R. Baker", *Holz Roh Werkst*. **59,** 169–175 (2001). doi: 10.1007/s001070100198

23. T. Fujimoto, Y. Kurata, K. Matsumoto and S. Tsuchikawa, "Application of near infrared spectroscopy for estimating wood mechanical properties of small clear and full length lumber specimens", *J. Near Infrared Spectrosc.* **16,** 529–537 (2008). doi: 10.1255/jnirs.818

24. American Standards and Testing Methods—ASTM, *Standard methods of testing small, clear specimens of timber*, D143–94. American Standards and Testing Methods, Denver, USA, p. 23–53 (1997).

25. P.R.G. Hein, L. Brancheriau, J.T. Lima, J. Gril and G. Chaix, "Resonance of structural timbers indicates the stiffness even of small specimens of *Eucalyptus*", *J. Wood Sci.* (submitted).

26. L. Brancheriau and H. Baillères, "Use of the partial least squares method with acoustic vibration spectra as a new grading technique for structural timber", *Holzforschung* **57,** 644–652 (2003). doi: 10.1515/HF.2003.097

27. S. Timoshenko, "On the correction for shear of the differential equation for transverse vibrations of prismatic bars", *Phil. Mag. J. Sci. XLI* **6,** 744–746 (1921).

28. P.A. Bordonné, "Module dynamique et frottement intérieur dans le bois, mesures sur poutres flottantes en vibrations naturelles", *Inst. Nat. Polytech. Lorr.* **109** (1989).

29. K. Steiglitz and L.A. McBride, "A technique for the identification of linear systems", *IEEE Trans Automat. Contr.* **10,** 461–464 (1965). doi: 10.1109/TAC.1965.1098181

30. M. Aramaki, H. Baillères, L. Brancheriau, R. Kronland-Martinet and S. Ystad, "Sound quality assessment of wood for xylophone bars", *J. Acoust. Soc. Am*. **121,** 2407–2420 (2007). doi: 10.1121/1.2697154

31. L. Brancheriau, H. Baillères, P. Détienne, J. Gril and R. Kronland-Martinet, "Key signal and wood anatomy parameters related to the acoustic quality of wood for xylophone-type percussion instruments", *J. Wood Sci.* **52,** 270–274 (2006). doi: 10.1007/s10086-005-0755-2

32. A. Savitzky and M.J.E. Golay, "Smoothing and differentiation of data by simplified least-squares procedures", *Anal. Chem.* **36,** 1627–1639 (1964). doi: 10.1021/ac60214a047

33. P.R.G. Hein, J.T. Lima and G. Chaix, "Robustness of models based on near infrared spectra to predict the basic density in *Eucalyptus urophylla* wood", *J. Near Infrared Spectrosc.* **17,** 141–150 (2009). doi: 10.1255/jnirs.833

34. F. Westad and H. Martens, "Variable selection in near infrared spectroscopy based on significance testing in partial least square regression", *J. Near Infrared Spectrosc.* **8,** 117–124 (2000). doi: 10.1255/jnirs.271

35. *AACC Method 39–00*. American Association of Cereal Chemists (AACC) (1999).

36. P.C. Williams and D.C. Sobering, "Comparison of commercial near infrared transmittance and reflectance instruments for analysis of whole grains and seeds", *J. Near Infrared Spectrosc.* **1,** 25–33 (1993). doi: 10.1255/jnirs.3

37. F.F.P. Kollmann and W.A. Côté, *Principles of wood science. I. Solid wood*. Springer, Berlin, Heidelberg, New York (1968).

38. C.R. Mora and L.R. Schimleck, "On the selection of samples for multivariate regression analysis: application to near-infrared (NIR) calibration models for the prediction of pulp yield in *Eucalyptus nitens*", *Can. J. For. Res.* **38,** 2626–2634 (2008). doi: 10.1139/X08-099

39. R. Meder, S. Gallagher, K.L. Macki, H. Böhler and R.R. Meglen, "Rapid determination of the chemical composition and density of *Pinus radiata* by PLS modelling of transmission and diffuse reflectance FTIR spectra", *Holzforschung* **53,** 261–266 (1999). doi: 10.1515/HF.1999.044

40. L.R. Schimleck, A.J. Michell, C.A. Raymond and A. Muneri, "Estimation of basic density of *Eucalyptus globulus* using near-infrared spectroscopy", *Can. J. For. Res.* **29,** 194–201 (1999). doi: 10.1139/cjfr-29-2-194

41. C. Cilas, C. Godin, D. Grenier, C. Montagnon and H. Baillères, "Variability in the rigidity of *Coffea canephora* Pierre stems determined by acoustic analysis", *Trees* **16,** 23–27 (2002). doi: 10.1007/s00468-001-0140-8

42. T. Ono and M. Norimoto, "Study on Young's modulus and internal friction of wood in relation to the evaluation of wood for musical instruments". *Jpn J. Appl. Phys.* **22,** 611–614 (1983). doi: 10.1143/JJAP.22.611

43. C. Buksnowitz, A. Teischinger, U. Muller, A. Pahler and R. Evans, "Resonance wood [*Picea abies* (L.) Karst.]—evaluation and prediction of violin makers quality-grading", *J. Acoust. Soc. Am.* **121,** 2384–2395 (2007). doi: 10.1121/1.2434756

44. H. Pereira, J. Graça and J.C. Rodrigues. "Wood chemistry in relation to quality", in *Wood Quality and its Biological Basis*, Ed by J.R. Barnett and G. Jeronimidis. Blackwell Publishing, Victoria, p. 226 (2003).

45. J.J. Workman and L. Weyer, *Practical Guide to Interpretive Near-Infrared Spectroscopy*. CRC Press, Boca Raton, p. 332 (2007).

46. L.R. Schimleck and R. Evans, "Estimation of *Pinus radiata* D. Don tracheid morphologicalcharacteristics by near infrared spectroscopy", *Holzforschung* **58,** 66–73 (2004). doi: 10.1515/HF.2004.009

47. J.S. Shenk, J.J. Workman and M.O. Westerhaus, "Application of NIR spectroscopy to agricultural products", in *Handbook of Near-Infrared Analysis*, Ed by D.A. Burns and E.W. Ciurczak. Marcel Dekker Inc., New York, p. 419 (2001).

48. L. Schimleck, P.D. Jones, G.F. Peter, R.F. Daniels and A. Clark III, "Nondestructive estimation of tracheid length from sections of radial wood strips by near infrared spectroscopy", *Holzforschung* **58,** 375–381 (2004). doi: 10.1515/HF.2004.057

Paper 8

Authors: Hein PRG, Bouvet JM, Mandrou E, Vigneron P and Chaix G

Title: Genetic control of growth, lignin content, microfibril angle and specific gravity in 14-years Eucalyptus urophylla S.T. Blake wood

Journal: Annals of Forest Science (*submitted*)

Editorial Manager(tm) for Annals of Forest Science
Manuscript Draft

Manuscript Number:

Title: Age trends of microfibril angle inheritance and their genetic and environmental correlations with growth, density and chemical properties in Eucalyptus urophylla S.T. Blake wood

Article Type: Research Paper

Keywords: variance components; MFA; Klason lignin; syringyl to guaiacyl ratio, factorial mating design; wood phenotyping; near infrared spectroscopy.

Corresponding Author: Paulo Ricardo HEIN, M.D.

Corresponding Author's Institution: CIRAD

First Author: Paulo Ricardo HEIN, M.D.

Order of Authors: Paulo Ricardo HEIN, M.D.;Jean Marc Bouvet, PhD;Eric Mandrou, PhD;Philippe Vigneron, PhD;Gilles Chaix, PhD

Abstract: Context: the genetic and environmental control of microfibril angle (MFA) and its genetic correlations with other wood and growth traits are still not well established in Eucalyptus.
Aims: to determine the narrow-sense heritability estimates (h^2) of MFA, wood density (D), Klason lignin (KL) content, syringyl to guaiacyl (S/G) ratio and growth traits, their variation from pith to cambium and their genetic correlations.
Methods: heritability and correlations were assessed in 340 control-pollinated progenies of 14-year-Eucalyptus urophylla S.T. Blake.
Results: high heritability were found for MFA (h^2=0.65), D (h^2=0.61), LK (h^2=0.72) and S/G (h^2=0.71). The genetic control of D and MFA and the genetic and residual correlation chemical and growth traits varied with age. The genetic correlation C x D was always strongly negative (r<-0.88) while the correlation D x MFA remained constant and positive in the juvenile wood (r=0.7), decreasing considerably in the mature wood (r=0.3). These results could be explained by gene pleiotropic effect, low microfibril angle compensating low wood density and fast growth or by linkage disequilibrium induced by sampling. Variations in MFA and KL in the mature wood are also genetically controlled.
Conclusions: these findings allow discussing their impact on breeding strategies for pulpwood, fuelwood and sawntimber production.

Suggested Reviewers: Luis Apiolaza PhD
University of Canterbury
luis.apiolaza@canterbury.ac.nz
He has published many papers on genetics of wood traits and one of the few papers concerning MFA heritability in Eucalyptus

Matthew Hamilton PhD
University of Tasmania
Matthew.Hamilton@utas.edu.au
He has published many papers on genetics of wood traits

Carolyn Raymond PhD
Southern Cross University
carolyn.raymond@scu.edu.au
She has published many papers on genetics of wood traits in Eucalypus

Philippe Rozenberg PhD
INRA
philippe.rozenberg@orleans.inra.fr
He has published many papers on genetics of wood traits

José Tarcísio Lima PhD
Universidade Federal de Lavras
jtlima@dcf.ufla.br
He has published one of the few papers concerning MFA heritability in Eucalyptus

Covering letter

April 21th, 2010

Dear editor Dr. Erwin DREYER,

Please find enclosed a paper entitled "**Age trends of microfibril angle inheritance and their genetic and environmental correlations with growth, density and chemical properties in *Eucalyptus urophylla* S.T. Blake wood**" by Hein et al., we wish to submit it for publication as an original paper in *Annals of Forest Science*. The present study reports the genetic control of microfibril angle (MFA), wood density (D), Klason lignin (LK) content, syringyl to guaiacyl ratio (S/G) and growth traits, and genetic and residual correlations among such traits in full-sib families of 14-year *Eucalyptus urophylla* planted in the Republic of the Congo, Central Africa.

While many papers have reported heritability estimates and correlations among growth and density (or pilodyn penetration) in *Eucalyptus* wood, few studies have addressed the genetic parameters of chemical, mechanical and ultrastructural features of the wood. Moreover, most findings on *Eucalyptus* have been based on open-pollinated progeny or clonally propagated trials. In addition, numerous studies on genetic parameters of *Eucalyptus* wood traits have been based on averaged values per tree. Because MFA and wood density varies radially, assessing averaged values may not be the best option.

The originality of this study was the experimental dispositive we used for assessing the wood and growth traits (control-pollinated progenies), the age of the plantation (169 months) and the wood quality traits we evaluated (MFA, KL, S/G, in addition to the commonly reported traits such as D and growth traits (circumference at breast height and tree height). Here, the genetic parameters of microfibril angle and wood density were assessed in three radial positions (inner heartwood, outer heartwood and sapwood) from calibrations based on near infrared spectroscopy. Genetic and residual correlations among such wood traits are presented and the age trends of these genetic parameters are discussed.

Our findings indicates that trees adapt their wood properties by changing the density and MFA to respond to the specific needs of the stems (like its ever-increasing mass) and that the underlying biological mechanisms involved in such wood adaptation are somewhat regulated by genetic factors. In conclusion, the genetic correlations MFA x D and MFA x KL acting together reveal a smart biological strategy for the survival of the tree.

This paper is original and has not been submitted to another journal.

Looking forward to hearing from you

Yours sincerely,

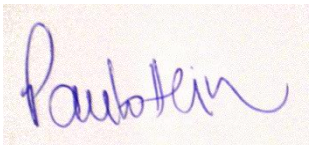

*Title Page

Age trends of microfibril angle inheritance and their genetic and environmental correlations with growth, density and chemical properties in *Eucalyptus urophylla* S.T. Blake wood

Authors:

Paulo Ricardo Gherardi HEIN* (corresponding author)
CIRAD, UPR Bois Tropicaux, F-34398 Montpellier, France
Université Montpellier 2, F-34095 Montpellier, France
Tél: +33 4 67 61 44 51
Fax: +33 4 67 61 65 60
email: phein1980@gmail.com

Jean-Marc BOUVET
CIRAD, UMR AGAP, F-34398 Montpellier, France
email: jean-marc.bouvet@cirad.fr

Eric MANDROU
Centre de recherche Vallourec, CEV, Route de Leval BP 17, Aulnoye Aymeries, France;
CIRAD, UMR AGAP, F-34398 Montpellier, France
INRA, UMR 1202 BIOGECO, 69 route d'Arcachon, Cestas Pierroton, France

Philippe VIGNERON
CIRAD, UMR AGAP, F-34398 Montpellier, France
email: philippe.vigneron@cirad.fr

Gilles CHAIX
CIRAD, UMR AGAP, F-34398 Montpellier, France
email: gilles.chaix@cirad.fr

Short title: Microfibril angle heritability in Eucalyptus

Keywords: variance components; MFA; Klason lignin; syringyl to guaiacyl ratio, factorial mating design; wood phenotyping; NIR spectroscopy.

==========
total number of characters: 39,005
number of tables: 4
number of figures: 2
==========

1 INTRODUCTION

Eucalyptus is one of the most widely cultivated hardwood genera in tropical and subtropical regions of the world. This genus is adapted to a variety of climatic and edaphic conditions and grows at high rates producing raw material adequate for many industrial applications. Wood quality is determined from the combination of intrinsic factors such as stiffness or hardness that depend on microfibril angle (MFA) and density and the contents of its main chemical components (Kollmann and Cote 1986). A range of studies has pointed out the importance of microfibril angle for the wood stiffness and wood products quality in *Eucalyptus* (Evans and Ilic 2001). In general, wood in which the MFA is low presents high rigidity and therefore high economic value. Hence, the determination of the genetic factors contributing to quantitative trait variation of wood properties is essential for tree breeders (Raymond 2002; Apiolaza 2009) allowing the selection of trees with adequate characteristics. Furthermore, adverse genetic and environmental correlations between wood quality and growth traits remain as one of the main constraints in tree breeding programs for pulp and paper, bio-energy or sawnwood industries.

Because growth, cellulose content, and more recently wood density (or pilodyn penetration) are the main traits considered by tree breeders for *Eucalyptus* pulpwood plantations, many papers have reported heritability estimates and correlations among such properties (Greaves et al. 1997; Raymond 2002; Costa e Silva et al. 2009). However the genetic parameters of chemical, mechanical and ultrastructural features are rarely reported in *Eucalyptus*. Moreover, the estimation of genetic parameters presents a large variation according to the peculiarities of each study. For instance, the findings reported by Kube et al. (2001) in *Eucalyptus nitens* and Apiolaza et al. (2005) and Poke et al. (2006) in *Eucalyptus globulus* are contrasting, demonstrating that these parameters are specific to the population and site under investigation but also that they have to be considered with caution due to the low accuracy of their estimation.

With the growing need and interest in establishing plantations for sawlog production, recent studies have focused on the heritability of wood traits controlling its quality, such of MFA (Baltunis et al. 2007). Most of studies dealing with the genetic control of MFA were done on softwoods and the degree to which MFA is heritable and its genetic relationship with other traits are poorly reported for the *Eucalyptus* genus. To our knowledge, there is only one study reporting narrow-sense heritability estimates (h^2) (Apiolaza et al. 2005) and one study providing broad-sense heritability estimates (H^2) for MFA in *Eucalyptus* (Lima et al. 2004). References reporting genetic and environmental correlations among MFA, density, lignin, S/G ratio and growth traits are rare (or unknown) in *Eucalyptus*. The extent to which the microfibril angle is controlled by additive genetic and environmental effects is poorly documented; what is the relationship between MFA and the other wood and growth traits, and how these relationships vary with age are still not established in *Eucalyptus*. Knowledge about these issues would be useful to understanding how trees adapt their wood traits in order to maintain their erect habit even when they are constrained by bending movements in response to wind and gravity.

Therefore, the main aims of this study were: (i) to assess the level of genetic control of MFA, wood density (D), Klason lignin content (KL) and syringyl to guaiacyl ratio (S/G) and growth traits from a control-pollinated progeny test of 14-year-old *Eucalyptus urophylla*; (ii) to determine

the genetic and residual correlations among MFA, D, KL, S/G and growth traits; and (iii) to investigate the age trends of these genetic parameters.

Most studies on genetic parameters of *Eucalyptus* wood traits have been based on averaged values per tree. Because MFA and wood density varies greatly from pith to cambium (Kollmann and Cote 1986) assessing averaged values may not be the best option. In this study, MFA and wood density were assessed in three radial positions namely inner heartwood, outer heartwood and sapwood. Radial variation of genetic parameters and the genetic and residual correlations among such wood traits are presented and the implications for selection are discussed.

2 MATERIAL AND METHODS

2.1 Genetic material

Three hundred and forty breast height wood discs were collected from a 14-year-old *Eucalyptus urophylla* S.T. Blake progeny test stand in Pointe Noire, Republic of Congo in the experimental area of the CRDPI "Centre de Recherche sur la Durabilité et la Productivité des Plantations Industrielles" (04°45'S, 12°00'E, alt 50 m). The climate is tropical humid with a mean annual temperature of 24°C, a mean annual rainfall of 1,200 mm and a dry season from May to October. This progeny trial was composed by 33 full-sib families produced by controlled pollination using an incomplete factorial mating design (ratio 33/64) involving 16 genitors (8 males and 8 females) originated from two provenances (8 from Mont Egon and 8 from Mont Lewotobi of the Flores Island in the Sunda archipelago, 122°-127°E, 8°-10°S). This progeny trial was established in 1992. In 2006, nine to ten trees were selected and harvested from each family, resulting in a total of 348 sample trees. Trees were collected from only one block to limit the environmental effect due to inter block variation and to fit with analysis capacity. The circumference at the breast height (C) and the height (H) of the trees were measured at 169 months, immediately before harvesting. A disc of wood (~30mm tick) was obtained at the breast height of each tree and transported to the CIRAD in Montpellier, France were the analyses were performed.

2.2 Sampling preparation

Wedges (defect free) were cut from the discs and milled using a Retsh knife mill (SM100) and a Retsh ultra-centrifugal mill (ZM 200) in order to produce coarse wood powders with particle sizes lower than 0.5 mm (Figure 1 A) for wet-chemistry analysis. Pith to bark radial strips were removed from the discs using a vertical bandsaw machine at a random position. Then, small wood samples measuring ~15 mm x ~20 mm x ~30 mm (Figure 1 B) and tangential sections (Figure 1 C) measuring ~2 mm x ~20 mm x ~30 mm were cut, as parallel as possible to the growth rings, from each wood strip for wood density and microfibril angle measurements, respectively. The wood powders of 60 samples (well representative of total sampling, selected after Principal Component Analysis based on their Near Infrared spectra) were submitted to chemical analysis. The samples (milled and solid woods) were kept in a conditioned room with 50% relative humidity and temperature of 20°C before analysis. Under these conditions, the equilibrium moisture content was around 10%.

2.3 Wood phenotyping

The Klason lignin (KL) content and ratio between syringyl (S) and guaiacyl (G) of the wood were conducted by the Biological Chemistry Laboratory (INRA-Agro ParisTech, France). The analyses were performed in duplicate for the 60 samples and were previously reported in Hein et al. (2010a). The basic density of wood (D) was determined according to water immersion procedure in 190 small wood samples (~20 mm x 25 mm x 30 mm) cut from radial strips as previously reported in Hein et al. (2009). All X-ray diffraction data were collected on a diffractometer (Xcalibur-I, Oxford Instruments, USA) with CuK α radiation at "Institut Européen des Membranes" of the University of Montpellier, France. Three X-ray diffraction profiles were recorded and averaged for 175 tangential sections (2 mm x 20 mm x 30 mm) cut from radial strips. The error of the measure was estimated at 3%. The procedure for microfibril angle measurements was previously reported in Hein et al. (2010b).

2.4 Near infrared spectroscopy analysis

The wood traits under investigation in this study were based on predictions from near infrared (NIR) spectroscopy calibrations. NIR spectra were recorded using a spectrophotometer (model Vector 22/N, Bruker Optik GmbH, Ettlingen, Germany) on both milled and solid woods. First, NIR spectra were recorded on the radial surface of the wedges (NIR spectra^{1}) at three radial positions (1, 2 and 3) from pith to bark and on the wood powders (NIR spectra^{2}) and, for predictions (Figure 1 A).

Partial Least Square Regressions (PLS-R) were developed from the NIR spectra of the wood powders and the chemical analysis of the 60 samples for Klason lignin (KL) and syringyl to guaiacyl (S/G) ratio. These PLS-R calibrations were previously described in Hein et al. (2010a) providing the estimates of single values of KL content and S/G using the NIR spectra^{2} taken from the wood powders of the 340 trees. The PLS-R model for density (D) was based on 190 small wood samples and their NIR spectra^{3} (Hein et al. 2009) while the PLS-R model for MFA was based on 175 tangential sections and their NIR spectra^{4} (Hein et al. 2010b). These established PLS-R models were applied on the NIR spectra^{1} providing the estimates of MFA and wood density in the inner- and outer-heart wood and in the sapwood. Table 1 presents the statistic associated to the NIR-based models used for phenotyping the woods from this progeny trial.

The point 1 represented the wood formed at the ~3-4th year (hereafter called inner heartwood - HW), the point 2 the wood of the ~6-7th year (outer heartwood - HW) and the point 3 the wood of the ~12-14th year (sapwood - SW). The averaged value per tree for density and microfibril angle are expressed as D and MFA, respectively, while the local D and MFA estimates are expressed as D_1, D_2 and D_3 and MFA_1, MFA_2 and MFA_3, accordingly. A single, averaged value per tree was used for the chemical properties. We considered as outliers the samples which presented estimates with high standard errors, and removed them from the original dataset (Table 2).

2.5 Statistical methods for genetic parameter estimation

Growth, KL, S/G, D and MFA were analyzed independently (univariate analysis) to estimate the variance components by using the following mixed linear model:

$$y = X.b + Z.a + e$$

where *y* is the vector of observations, *b* is the vector of fixed effects (in our case the mean value of the trait in the population), *a* is the vector of genetic effects (individual additive genetic values), *e* is the vector of residuals and *X* and *Z* are the incidence matrices linking observations to the effects.

The random effect fits a normal distribution whose parameters were:

$$E\begin{bmatrix} a \\ e \end{bmatrix} = \begin{bmatrix} 0 \\ 0 \end{bmatrix} \text{ and } \quad Var\begin{bmatrix} a \\ e \end{bmatrix} = \begin{bmatrix} G & 0 \\ 0 & R \end{bmatrix}$$

The variance-covariance matrices were defined as follows:

$$G = A.\sigma^2{}_A \quad \text{and} \quad R = I.\sigma^2{}_e$$

where *A* is the additive genetic relationship matrix computed from a pedigree file that takes into account all the relationships between the individuals, I is the identity matrix, σ^2_A the additive genetic variance and σ^2_e the residual variance. The variances associated to random effects were estimated by restricted maximum likelihood (REML method) using ASReml version 2 (Gilmour et al. 2005). As the variances are assumed to be independent, the total phenotypic variance σ^2_P was calculated as follows:

$$\sigma^2{}_P = \sigma^2{}_A + \sigma^2{}_E$$

The narrow-sense heritability estimates were calculated as follows:

$$h^2 = \frac{\sigma^2{}_A}{\sigma^2{}_P}$$

Variances are not independent of the scale and the mean of the respective traits. Therefore, to compare the genetic and phenotypic variances of the different traits, the genetic (CV_A), residual (CV_E) and phenotypic (CV_P) coefficient of variation were calculated as:

$$CV_{Aj} = \frac{100 \times \sigma_{Aj}}{\bar{x}}$$

$$CV_{Ej} = \frac{100 \times \sigma_{Ej}}{\bar{x}}$$

$$CV_{Pj} = \frac{100 \times \sigma_{Pj}}{\bar{x}}$$

Where σ_{Aj} is the square root of the additive genetic variance for the trait; σ_{Ej} is the square root of the residual variance for the trait, σ_{Pj} is the square root of the phenotypic variance for the trait and x is the population mean for the trait.

The estimate of phenotypic (r_P), residual (r_E) and genetic additive (r_A) correlations between two traits (X and Y), were performed from a bi-variate analysis using the same individual model as for univariate analysis. r_P, r_E and r_A were estimated as follows:

$$r_P = \frac{Cov_P(x,y)}{\sqrt{\sigma^2_{Px}.\sigma^2_{Py}}}$$

$$r_E = \frac{Cov_E(x,y)}{\sqrt{\sigma^2_{Ex}.\sigma^2_{Ey}}}$$

$$r_A = \frac{Cov_A(x,y)}{\sqrt{\sigma^2_{Ax}.\sigma^2_{Ay}}}$$

Standard errors of h^2, σ^2_A, σ^2_P, r_P, r_E and r_A were calculated with ASReml using a standard Taylor series approximation (Gilmour et al. 2005).

3 RESULTS

The descriptive statistics of the wood traits of the 14-year-*Eucalyptus urophylla* are listed in Table 2. As expected for most woods, the MFA were, on average, higher near the pith decreasing towards the bark and an opposite trend was observed for the basic density of wood (Table 2).

The coefficients of variation were similar to those observed in previous studies on *Eucalyptus* in the Congo (Bouvet et al.1999). They were higher for growth than for wood property traits. Their magnitude showed that the sampling used in this study was representative of a breeding population involved in genetic improvement programs in the Congo (Bouvet et al. 2009).

3.1 Variance components and heritability estimates

The additive genetic and residual variance components and narrow-sense heritability estimates for various traits are given in Table 3. Genetic and residual variations were higher for growth traits than for wood traits as shown by CV_A and CV_E. As expected, the narrow-sense h^2 estimates were lower for growth traits: h^2=0.30 for height and h^2=0.14 for circumference while moderate to high levels of heritability (from 0.37 to 0.72) were reported for wood traits.

When the mean values of wood density (D) or MFA per disc were taken into account, higher narrow-sense heritability estimates were observed (h^2>0.60). The high magnitude of these h^2 estimates can be mathematically explained: once the three data per tree is averaged, the phenotypic (and residual) variances are sharply reduced causing an increase in the additive to phenotypic variance ratio.

Patterns in pith to cambium variation of these traits have been known for many years; wood density generally increases while MFA decreases (Kollmann and Cote 1968). The genetic control of the wood density linearly increased from 0.37 to 0.51 towards the bark; however this linear trend should be considered with caution since the standard errors (SE) were elevated (~0.17). The h^2_{MFA} was 0.43 in the inner heartwood (MFA_1), increasing to 0.50 in the outer heartwood (MFA_2),

and decreasing again to 0.44 in the sapwood (MFA_3). Considering the magnitude of SE (0.14-0.17), no specific trend was observed for the heritability estimates of MFA.

3.2 Genetic and residual correlations

Estimates of genetic and residual correlations among growth, KL, S/G ratio and mean MFA and density are shown in Table 4.

As expected, the genetic and residual correlations between growth traits were positive. The genetic correlations between growth and wood traits (MFA, D and KL) were negative. Positive residual correlations were obtained for this same group of correlations. Such patterns are different for S to G ratio. The correlations concerning S/G are of low magnitude considering the standard errors.

The strong genetic correlation between C and D was investigated by means of the residual scattering analysis (not shown). The point dispersions revealed that there was no aberrant point, which could favour (stretching) the correlation. The correlation estimates had large standard errors probably due to the small sample size.

Radial variations of genetic, residual and phenotypic correlations between wood and growth traits are presented Figure 2. The genetic correlation between circumference and wood density remained high during all phases of wood formation. On the other hand, the genetic correlation between circumference and MFA seemed to linearly decrease towards the bark. This trend was also found between MFA and lignin in which there was an increase with age. The genetic correlation between MFA and wood density decreased from juvenile to mature wood.

The residual correlation was of low magnitude, except for the correlation between MFA and D. The phenotypic and additive genetic correlation between C and MFA, and LK and MFA presented the same trends slightly differing in their magnitude. The phenotypic correlation between circumference and wood density was null while the genetic correlation was strong. Similarly, the phenotypic correlation between MFA x D was of low magnitude while the residual and genetic were considerable.

In general, additive genetic correlations presented higher magnitudes when compared with the residual correlations. Moreover, the radial variations of the values of the genetic relationships were stronger than those for residual or phenotypic correlations.

4. DISCUSSION

This study compares the genetic control of wood and growth traits, with special focus on microfibril angle which has been poorly reported in hardwood species. Moreover, genetic and like-environmental correlations among those traits were assessed at different age improving our knowledge on the functional aspects of wood formation in *Eucalyptus*.

4.1 Heritability of MFA and wood traits

A narrow-sense heritability estimate of elevated magnitude was found for MFA ($h^2=0.65\pm0.17$) when calculated from the mean values per disc (Table 3). These narrow-sense heritabilities were higher than those reported in two previous studies. Apiolaza et al. (2005) used increment cores

from 188 open-pollinated progenies of 11-year-old *E. globulus* reporting h^2_{MFA}=0.27±0.24 while Lima et al. (2004) reported mean broad-sense heritability (H^2) of 0.29 in 8-year-old *Eucalyptus* wood. Normally, broad-sense heritability estimates are higher than narrow-sense estimates. The low H^2 estimate of Lima et al. (2004) was expected since they evaluated selected clones of *E. grandis* x *E. urophylla* for pulpwood so the genetic base was narrow. On the other hand, the relatively lower narrow-sense h^2 estimates of Apiolaza et al. (2005) can be attributed to larger environmental variation since their CV_A (8.36%) is close to the CV_A of Table 3 (8%).

Just as the phenotypic values, the genetic control also varied with age. The heritability estimates of the MFA in the inner heartwood (h^2_{MFA1}=0.43±0.16) increased towards the outer heartwood (h^2_{MFA2}=0.50±0.14), decreasing in the sapwood (h^2_{MFA3}=0.44±0.17). However, due to the high standard error no specific trend can be demonstrated. This result was similar to the variation pattern reported by Lima et al (2004) in *Eucalyptus* clones (h^2_{MFA} departing from 0.13, increasing to 0.36 and decreasing to 0.16 towards the cambium).

Comparing these findings requires prudence because the experimental designs were different (open- and controlled-pollinated and clonally propagated tests) and the methods for wood phenotyping were distinct: Apiolaza et al. (2005) estimated the phenotypic MFA values of their study by means of the SilviScan device (based on X-ray diffraction); Lima et al. (2004) used polarised light microscopy technique and, here, we associated X-ray-diffraction and NIR spectroscopy to estimate the MFA. In short, the above studies have reported estimations of MFA and the corresponding estimated genetic parameters.

Considerable genetic control was found for mean wood density (h^2=0.62±0.17) and for wood density measurements at different radial positions. The heritability estimates linearly increased from 0.37±0.16 to 0.51±0.18 towards the sapwood. The slight increment in heritability estimates of density with age might have been due a reduction in environmental variation, which may have been associated with canopy closure in the Congolese conditions. Previous studies on *Eucalyptus* in the environmental conditions of the Congo have shown that before canopy closure, there are large micro-environmental variations between trees while in the following years, tree development depends to a higher magnitude on their genetic potential (Bouvet et al. 2003).

Due its relatively easy and simple measurement, the wood density has been extensively investigated in *Eucalyptus* and the heritability of such trait exhibits variable magnitudes: from H^2=0.51±0.13 (Kube et al. 2001, for all sites) to h^2=0.73 (Greaves et al. 1997, for whole-disc density at 1.3 m across sites) in *E. nitens*; from h^2=0.24±0.26 (Poke et al. 2006) to h^2=0.44±0.22 (Apiolaza et al. 2005) in *E. globulus* and of h^2=0.17±0.12 (Raymond et al. 1998) in *E. regnans*. Most of these studies have shown the high heritability of this trait mainly explained by the low environmental rather than marked genetic variation (see CV's in Table 3); our study reinforces these previous results.

Lignin content and S/G ratio were shown to be under strong genetic control (Table 3). The high narrow-sense heritability of these chemical traits (h^2>0.7±0.2) indicates that genetic gain is possible through breeding. The heritability for lignin (h^2=0.72±0.2) was lower than that reported by Gominho et al. (1997) in *E. globulus* clones (h^2=0.83) and higher than that reported by Vigneron et al. (2004) in *E. urophylla* x *grandis* (individual broad-sense H^2=0.27±0.2), Poke et al.

(2006) in *E. globulus* families (narrow-sense h^2=0.13±0.2 and family means h^2=0.42±0.19). As lignin content and its composition are key traits of *Eucalyptus* breeding programs, especially for pulp, paper and bioenergy production, their high genetic control reported here (Table 3) is critical for tree breeders.

The heritability estimates for growth traits were low (h^2=0.14±0.09; h^2=0.3±0.14 for circumference and height respectively), which are strongly influenced by the environment. These results confirm the trends described in previous studies for other *Eucalyptus* breeding programs (Kube et al. 2001; Costa e Silva et al. 2004; Costa e Silva et al. 2009) and more specifically in the Congo (Bouvet et al. 2003; Bouvet et al. 2009).

Although these estimates are population- and site-specific, these findings are coherent with previous studies and useful for tree breeders since they show that MFA, D, KL and S/G present a high heritability being susceptible to improvement.

4.2 Correlation at mature age

A sizable body of literature exists about genetic correlations between growth traits and wood density; however the findings concerning this issue are inconsistent; see for example Zobel and Van Buijtenen (1989) for a range of wood species. For *Eucalyptus* several studies presented also inconsistent results *(*Hamilton and Potts 2008, Greaves et al. 1997, Wei and Borralho 1999, Kube et al. 2001) probably due to the small sampling size. The conclusion is that correlation between wood density and growth should be low. In addition, some studies have shown that correlations are influenced by site conditions (Wei and Borralho 1999; Muneri and Raymond 2000; Hamilton et al. 2009) outlining the environmental impact.

Our results bring new elements to the understanding of the correlation between wood and growth traits. Here, few additive and residual correlations (C x H; KL x MFA) presented the same sign (Table 4 and Figure 2). This may indicate pleiotropic gene effect (Falconer 1993), implying that these couple of traits are governed by a given locus (Mode and Robinson 1959).

Most of the additive and residual correlations and especially those implying MFA (Table 4) presented an opposite sign. This indicates that linkage disequilibrium (non-random associations of genes) between loci may affect the relationship among different wood traits (Falconer 1993). This means that the genes controlling these traits can be statistically associated, but there is no functional relationship among them. Sampling procedure used in this study could have played a role in linkage disequilibrium, since the 9 or 10 trees of each family were selected among the best ones as to growth and stem straightness. According to Villanueva and Kennedy (1990) selection changes the genetic variance and creates linkage disequilibrium.

4.3 Genetic parameter expression with age

As the tree grows upward, new layers of wood are produced and overlapped in order to withstand the ever-increasing mass of the tree. The variations of the genetic and residual correlations with age may be useful for understanding how the cambial activity and maturation phases are regulated in order to modify the characteristics of the wood making the stem able to support gravity and bending movements caused by winds.

The narrow-sense heritability estimates for wood density seems to increase with age (Table 3), but remains more or less constant for MFA. For density this is explained by a lower impact of environment effect with age (see CV_E in Table 3). For the MFA the absence of trends is due to the increase of CV_A and CV_E with age (Table 2). The genetic correlation C x D is always strongly negative while the correlation D x MFA remained constant in the juvenile wood, decreasing considerably in the mature wood (Figure 2). This could mean that trees with a strong potential to grow fast are genetically programmed to produce low-density woods and also to decrease the microfibril angles for ensuring stiffness (the negative correlation MFA x C). However, the eventual occurrence of linkage disequilibrium within this population leads to consider this functional explanation with caution.

When the tree reaches maturity, the stem becomes especially susceptible to prevailing winds because of the higher heights and inertia moments. It is known that reaction wood is typically formed as the tissues of the periphery are held in "tension" and in many wood species, tension wood is characterised by the presence of a thick and unlignified, inner cell-wall layer that consists of highly crystalline cellulose, in which the MFA is close to zero (Kollmann and Cote 1986). Thus, the low lignin content and MFA of the sapwood is associated to tension wood occurrence (Figure 2). Our results indicate that variations in these wood traits are also genetically controlled since the genetic correlation between MFA and KL increases from 0.4 to 0.74 towards the cambium.

4.4 Implications for selection

Our study allows considering the consequences that these results can have on the genetic improvement strategies. If the studied population is to constitute the first generation of a breeding program, according to the objectives, different points should be taken into account for selecting candidate trees.

In the frame of pulpwood production, the objective is to produce trees with important biomass production (volume and density) and reduced lignin content. The negative r_A between growth traits and lignin content (r_A=-0.61 for height and -0.16 for circumference) and the positive correlation between MFA and KL ($0.4<r_A<0.74$) are favourable for pulp and paper production since the reduction in all of these traits would be simultaneously possible. Lignin is undesirable compound for pulp and paper production, because the delignification process requires energy and reagent consumption

In the frame of bio-energy production, the positive genetic correlation between lignin and density (0.28) is favourable, despite the low magnitude. However, positive additive correlations between MFA and lignin are unfavourable for bioenergy purposes since decreasing MFA, may result in decreasing lignin content. The problem is that, for energy production, the wood may simultaneously have high lignin content and adequate mechanical properties. Charcoal is used in blast furnaces for iron-steel production and has to support the weight load of the iron feedstock during the steps of oxidation-reduction reactions at elevated temperatures (above 1,500°C) without breaking.

In the frame of sawn wood production, the objective is to obtain stiff (low MFA) and dense woods, preferable (at a economic point of view) at high growth rates. Our findings have shown that wood density and MFA were unfavourably genetically correlated with growth. Moreover, selection for increasing density will result in increase of MFA and decrease of wood stiffness, the major wood trait for structural, furniture and flooring uses.

As pointed out by Baltunis et al. (2007), breeders, forest managers and wood producers will have to strike a balance between overall wood and growth traits, and geneticists should develop breeding strategies to deal with such negative, unfavorable genetic correlations. For *Eucalyptus*, developing breeding objectives may be the first step in dealing with these unfavorable genetic correlations between wood and growth traits.

5 ACKNOWLEDGMENTS

The authors would like to thank Arie van der Lee from the Institut Européen des Membranes and B Clair from LMGC-MAB, CNRS, University of Montpellier for assistance with X-ray diffraction measurements; Dr. C Lapierre and her workteam from INRA-Agro ParisTech for chemical measures; N Ognouabi and E Villar from CRDPI (Republic of Congo) and the "Bureau des Ressources Génétiques" (BRG) project for providing material and funding; and especially Dr. JM Gion (coordinator of the BRG project "CCR gene in *Eucalyptus*: a model of functional variability in forest trees") from CIRAD for providing technical support.

6 FUNDING

This study is a part of the project "CCR gene in Eucalyptus: a model of functional variability in forest trees" funded by the "Bureau des Ressources Génétiques" (BRG) The project was also funded by the Centre de Coopération Internationale en Recherche Agronomique pour le Development (CIRAD) in Montpellier, France. The first author was supported by the National Council of Technological and Scientific Development (CNPq, Brazil - process no. 200970/2008-9) during his PhD thesis. He also was supported by the Alfa Gema Project (II-0266-FA) during his master.

7 CONTRIBUTION OF THE DIFFERENT AUTHORS

PRGH is a PhD candidate and this study is a part of his thesis. He was responsible for performing the NIR, X-ray diffraction analysis and wood measurements, for generating the phenotypic data set, analysing the results and the writing of the paper;

JMB was responsible for planning the experimental design and performing the statistical analysis. He provides comments and corrections to the text;

EM was responsible for performing part of the statistical analysis and writing part of the material and methods section.

PV was responsible for planning the experimental design and part of the preliminary analysis and

GC was responsible for planning the measurements and analysing the results. He's co-supervisor of PRGH PhD. He provides comments and corrections to the text.

8 REFERENCES

Apiolaza LA, Raymond CA, Yeo BJ (2005) Genetic Variation of Physical and Chemical Wood Properties of *Eucalyptus globulus*. Silvae Genet 54:4-5

Apiolaza LA (2009) Very early selection for solid wood quality: screening for early winners. Ann Forest Sci 66:601

Balturis BS, Wu HX, Powell MB (2007) Inheritance of density, microfibril angle, and modulus of elasticity in juvenile wood of *Pinus radiata* at two locations in Australia. Can J For Res 37:2164-2174

Bouvet JM, Vigneron P, Gouma R, Saya A (2003) Trends in variances and heritabilities with age for growth traits in Eucalyptus spacing experiments. Silvae Genet 52:3-4

Bouvet JM, Bouillet JP, Vigneron P, Ognouabi N (1999) Genetic and environmental effects on growth and wood basic density with two Eucalyptus hybrids. In: 09/99 Connexion between silviculture and wood quality through modelling approaches and simulation softwares: modelling approaches and simulation softwares. La Londe-Les Maures, France, September, 5-12

Bouvet JM, Saya A, Vigneron P (2009) Trends in additive, dominance and environmental effects with age for growth traits in Eucalyptus hybrid populations. Euphytica 165:35-54

Costa e Silva J, Borralho NMG, Araujo JA, Vaillancourt RE, Potts BM (2009) Genetic parameters for growth, wood density and pulp yield in *Eucalyptus globulus*. Tree Gen and Genom 5:291-305

Costa e Silva J, Hardner C, Potts BM (2004) Genetic variation and parental performance under inbreeding for growth in *Eucalyptus globulus*. Ann Forest Sci 67(6)

Evans R, Ilic J (2001) Rapid prediction of wood stiffness from microfibril angle and density. For Prod J 51:53-57

Falconer DS (1993) Introduction to quantitative genetics. Longman Scientific and Technical, New York

Gilmour AR, Gogel BJ, Cullis BR, Welham SJ, Thompson R (2005) ASReml user guide release 2.0, VSN international Ltd, Hemel Hempstead HP1 1ES, UK

Gominho J, Rodrigues J, Almeida MH, Leal A, Cotterill PP, Pereira H (1997) Assessment of pulp yield and lignin content in a first-generation clonal testing of *Eucalyptus globulus* in Portugal, in: Proceedings of the IUFRO Conference on Silviculture and Improvement of Eucalypts, Salvador, Brazil, August 24-29, 1997, p. 84-89

Greaves BL, Borralho NMG, Raymond CA, Evans R, Whiteman PH (1997a) Age-age correlations and relationships between basic density and growth in *Eucalyptus nitens*. Silvae Genet 46:264-270

Hamilton MG, Potts BM (2008) *Eucalyptus nitens* genetic parameters. N Z J For Sci 38:102-119

403 Hamilton MG, Raymond CA, Harwood E, Potts BM (2009) Genetic variation in *Eucalyptus nitens*
404 pulpwood and wood shrinkage traits. Tree Gen Genom 5:307-316

405 Hein PRG, Lima JT, Chaix G (2009) Robustness of models based on near infrared spectra to
406 predict the basic density in *Eucalyptus urophylla* wood. J Near Infrared Spec 17:141-150

407 Hein PRG, Lima JT, Chaix G (2010a) Effects of sample preparation on NIR spectroscopic
408 estimation of chemical properties of *Eucalyptus urophylla* S.T. Blake wood. Holzforschung 64:45-
409 54

410 Hein PRG, Clair B, Brancheriau L, Chaix G (2010b) Predicting microfibril angle in Eucalyptus
411 wood from different wood faces and surface qualities using near infrared spectra. J Near Infrared
412 Spec 18:455-464

413 Kollmann FR, Coté WA (1968) Principles of Wood science and technology. Springer-Verlag,
414 Berlin

415 Kube PD, Raymond CA, Banham PW (2001) Genetic parameters for diameter, basic density,
416 cellulose content and fibre properties for *Eucalyptus nitens*. For Gen 8:285-294

417 Lande R (1984) The genetic correlation between characters maintained by selection, linkage and
418 inbreeding. Genet Res 44:309-320

419 Lima JT, Breese MC, Cahalan CM (2004) Variation in microfibril angle in Eucalyptus clones.
420 Holzforschung 58:160-166

421 Mode CJ, Robinson HF (1959) Pleiotropism and the genetic variance and covariance. Biometrics
422 15:518-537

423 Muneri A, Raymond CA (2000) Genetic parameters and genotype-by-environment interactions for
424 basic density, pilodyn penetration and stem diameter in *Eucalyptus globulus*. For Gen 7:317-328

425 Poke FS, Potts BM, Vaillancourt RE, Raymond CA (2006) Genetic parameters for lignin,
426 extractives and decay in *Eucalyptus globulus.* Ann Forest Sci 63:813-821

427 Raymond CA, Banham P, MacDonald AC (1998) Within tree variation and genetic control of
428 basic density, fibre length and coarseness in *Eucalyptus regnans* in Tasmania. Appita J 41:299-305

429 Raymond CA (2002) Genetics of Eucalyptus wood properties. Ann Forest Sci 59:525-531

430 Vigneron P, Giordanengo T, Ognouabi N, Gion JM, Chaix G, Baillères H (2004) Genetic
431 components of wood quality traits in *Eucalyptus urophylla* x *E. grandis* full sib families. IUFRO
432 Congress unit 2.08.03 "Eucalyptus in a Changing World", Aveiro, Portugal, October, 11-15

433 Villanueva B, Kennedy BW (1990) Effect of selection on genetic parameters of correlated traits.
434 Theor Appl Gen 80:746-752

435 Wei X, Borralho NMG (1999) Objectives and selection criteria for pulp production of *Eucalyptus*
436 *urophylla* plantation in south east China. For Gen 6:181-190

437 Zobel BJ, Van Buijtenen JP (1989) Wood Variation - Its Causes and Control. Springer-Verlag,
438 Berlin

9 TABLES

Table 1 - Partial least square regression models for estimating the microfibril angle (MFA), wood density (D), Klason lignin (KL) content and syringyl to guaiacyl ratio (S/G) from NIR spectra of *E. urophylla* wood

Trait	R^2_c	RMSEC	R^2_p	RMSEP	RPD
MFA (degrees)	0.72	0.73	0.64	0.84	1.76
D (kg m^{-3})	0.89	27.0	0.85	30.0	2.70
KL (%)	0.88	0.44	0.85	0.55	2.58
S to G ratio	0.92	0.01	0.86	0.13	2.68

R^2_c: coefficient of determination of calibration; R^2_p: coefficient of determination of validation; RMSEC: root mean standard error of calibration; RMSEP: root mean standard error of validation and RPD: ratio of performance to deviation.

Table 2 - Mean, minimum and maximum values, coefficient of variation (CV) and number of observations (N) for growth (Circumference, C and Height, H), chemical properties (Klason lignin , KL and syringyl to guaiacyl ratio, S/G), wood density (D) and microfibril angle (MFA) of the 14-year-old *Eucalyptus urophylla* population

Trait	Unit	N	Mean	Minimum	Maximum	CV_P (%)
C	cm	340	52.7	24.0	84.0	21.2
H	m	340	21.2	7.8	29.6	17.3
KL	%	321	28.0	25.1	31.7	4.4
S/G	-	321	2.3	1.5	3.5	13.5
D_1	kg m^{-3}	274	443	330	607	10.2
D_2	kg m^{-3}	274	522	391	698	8.4
D_3	kg m^{-3}	274	615	480	761	8.1
D	kg m^{-3}	274	526	423	654	7.2
MFA_1	degrees	274	18.1	12.7	23.9	10.2
MFA_2	degrees	274	15.3	10.0	21.1	12.4
MFA_3	degrees	274	13.3	7.2	19.5	13.9
MFA	degrees	274	15.6	11.0	20	9.8

453 Table 3 - Additive genetic and residual variance components, genetic and residual coefficient of
454 variance and narrow-sense heritability estimates for Circumference (C), Height (H), Klason lignin
455 (KL), syringyl to guaiacyl ratio (S/G), wood density (D), and microfibril angle (MFA)

Trait	Additive genetic variance			Residual variance			Genetic control	
	σ^2_A	SE σ^2_A	CV_A	σ^2_E	SE σ^2_E	CV_E	h^2	SE h^2
C	13.62	9.44	7.0	85.61	8.59	17.6	0.14	0.09
H	3.27	1.69	8.6	7.63	6.37	13.1	0.30	0.14
KL	1.11	0.47	3.8	0.43	1.72	2.3	0.72	0.20
SG	0.068	0.069	11.4	0.027	1.77	7.2	0.71	0.20
D_1	8.16	4.11	6.4	13.54	4.95	8.3	0.37	0.16
D_2	8.90	4.02	5.7	11.40	4.40	6.5	0.44	0.17
D_3	13.44	6.12	6.0	12.89	3.67	5.8	0.51	0.18
D	9.22	3.69	5.8	5.51	2.35	4.5	0.61	0.17
MFA_1	1.47	0.68	6.7	1.96	4.75	7.7	0.43	0.16
MFA_2	1.88	0.82	8.9	1.88	3.70	8.9	0.50	0.14
MFA_3	1.58	0.74	9.5	1.96	4.27	10.5	0.44	0.17
MFA	1.57	0.60	8.0	0.84	2.25	5.9	0.65	0.15

456 σ^2_A - additive genetic variance component; σ^2_E - residual variance component; h^2 - narrow-sense
457 heritability estimates and SE - standard errors. For D and MFA the index correspond to radial
458 position, 1 is close the pith. The phenotypic values of wood density were divided by 10 for
459 estimating its variance components.

460

461 Table 4 - Estimated additive genetic (r_A, below the diagonal) and residual (r_E, above the diagonal)
462 correlations for Circumference (C), Height (H), microfibril angle (MFA), wood density (D),
463 Klason lignin (KL), and syringyl to guaiacyl ratio (S/G). Standard errors are shown in parentheses.

	C	H	MFA	D	KL	SG
C		0.80 (0.05)	0.07 (0.15)	0.48 (0.27)	0.30 (0.18)	-0.20 (0.17)
H	0.46 (0.32)		0.16 (0.22)	0.41 (0.24)	0.35 (0.29)	-0.41 (0.27)
MFA	-0.50 (0.33)	-0.70 (0.21)		-0.87 (0.00)	0.22 (0.34)	0.63 (0.49)
D	-0.99 (0.18)	-0.56 (0.26)	0.48 (0.16)		-0.35 (0.44)	0.10 (0.43)
KL	-0.16 (0.39)	-0.61 (0.24)	0.58 (0.20)	0.28 (0.28)		-0.24 (0.39)
SG	0.18 (0.39)	0.37 (0.30)	-0.27 (0.28)	-0.65 (0.18)	-0.16 (0.29)	

464

465

10 CAPTIONS OF FIGURES

Figure 1 - Procedure of sample preparation for wood characterization. Wedges (A) and radial strips were cut from discs; small wood samples (B) and tangential sections (C) were cut for density and microfibril angle measurements. Near Infrared (NIR) spectra were obtained from the solid wood (index 1, 3 and 4). The wedges were ground for wet-chemistry analysis and NIR spectra were measured from the powders (index 2).

Figure 2 - Variation with age of phenotypic, residual and additive genetic correlations of density (D) with Circumference (C), and Microfibril angle (MFA) with C, Klason Lignin (KL) and D and representation of standard error of estimation.

476 **11 FIGURES**

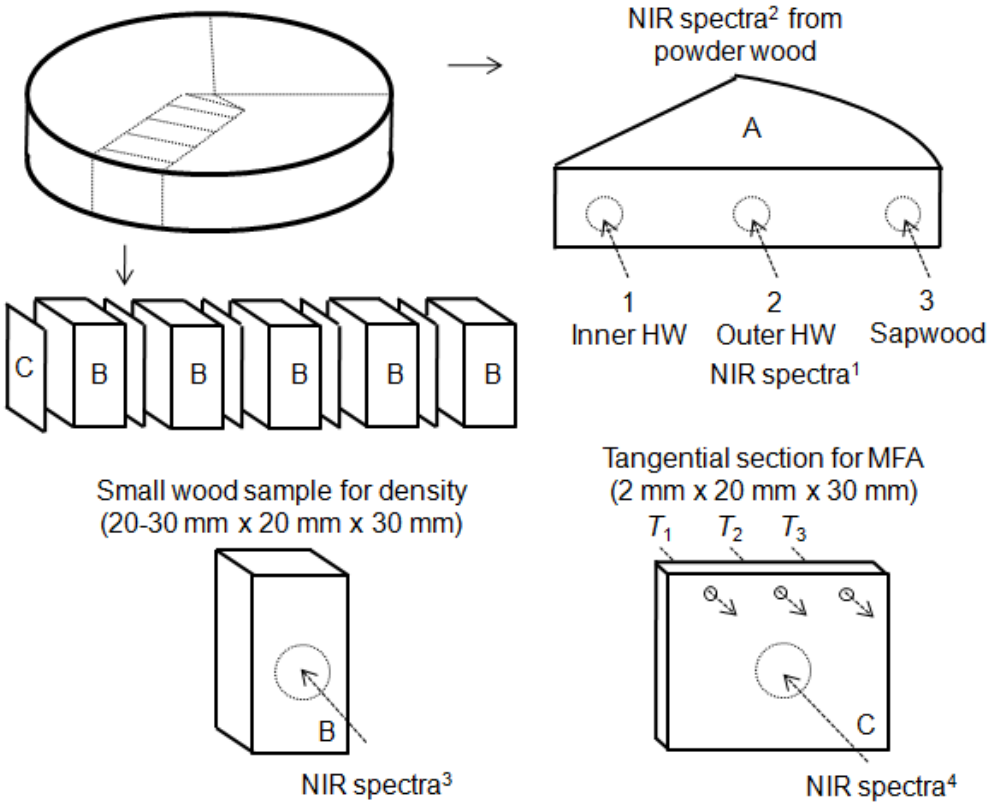

477

478 Figure 1

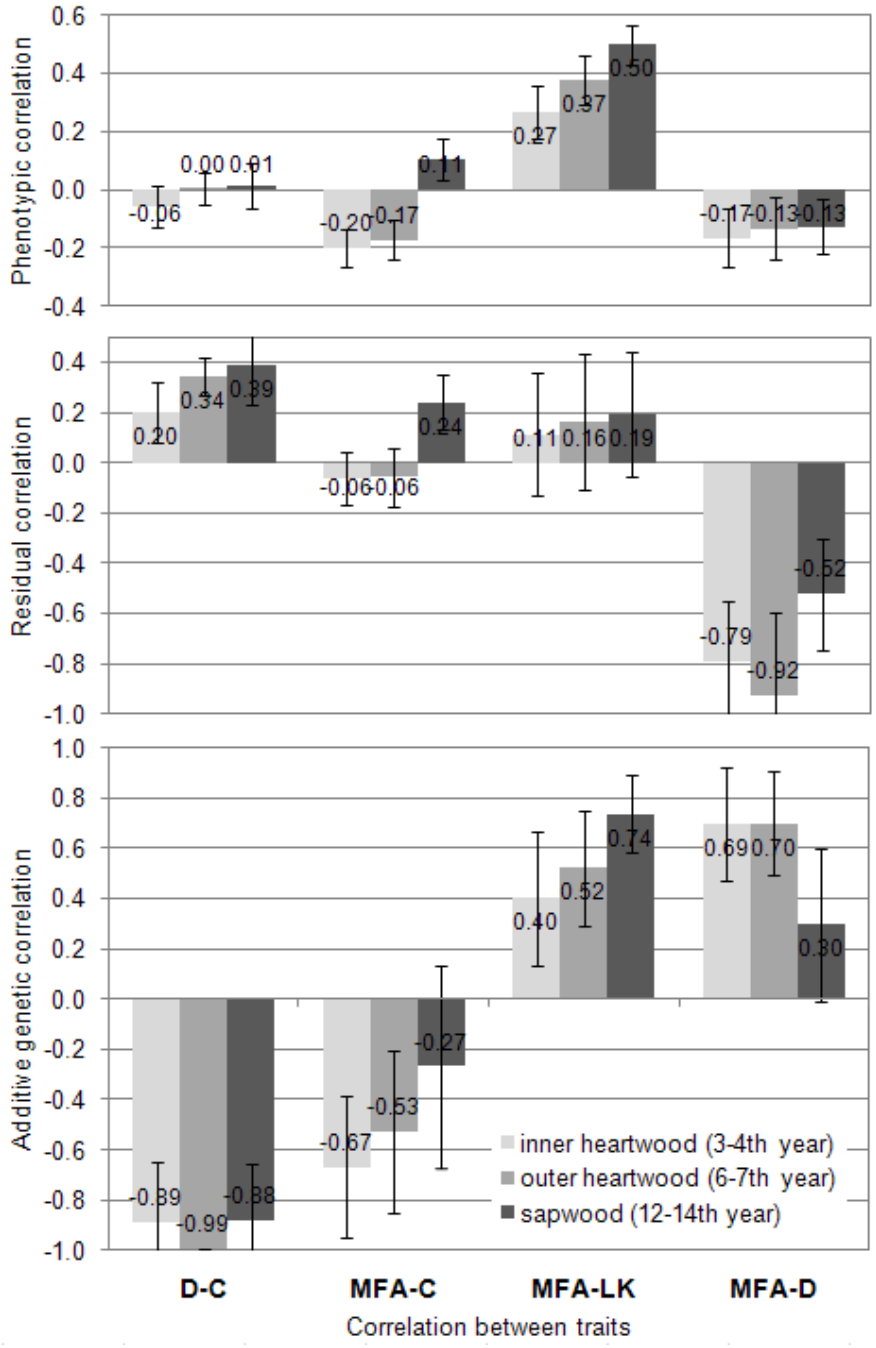
Phenotypic correlation
0.6
0.4
0.2
0.0
-0.2
-0.4
-0.06
0.00
0.01
-0.20
-0.17
0.11
0.27
0.37
0.50
-0.17
-0.13
-0.13
Residual correlation
0.4
0.2
0.0
-0.2
-0.4
-0.6
-0.8
-1.0
0.20
0.34
0.39
-0.06
-0.06
0.24
0.11
0.16
0.19
-0.79
-0.92
-0.52
Additive genetic correlation
1.0
0.8
0.6
0.4
0.2
0.0
-0.2
-0.4
-0.6
-0.8
-1.0
-0.89
-0.99
-0.88
-0.67
-0.53
-0.27
0.40
0.52
0.74
0.69
0.70
0.30
inner heartwood (3-4th year)
outer heartwood (6-7th year)
sapwood (12-14th year)
D-C
MFA-C
MFA-LK
MFA-D
Correlation between traits

Figure 2

Paper 9

Authors: Hein PRG, Brancheriau L, Lima JT, Rosado AM, Gril J and Chaix G

Title: Clonal and environmental variation of structural timbers of Eucalyptus for growth, density, and dynamic properties

Journal: Cerne, v.16, p.74-81 (2010)

CLONAL AND ENVIRONMENTAL VARIATION OF STRUCTURAL TIMBERS OF *Eucalyptus* FOR GROWTH, DENSITY, AND DYNAMIC PROPERTIES

Paulo Ricardo Gherardi Hein[1], Loic Brancheriau[2], José Tarcísio Lima[3], Antônio Marcos Rosado[4], Joseph Gril[5], Gilles Chaix[6]

ABSTRACT: The main objective of *Eucalyptus* breeding programs for the pulp and paper industry is to produce varieties of trees with high levels of cellulose with the least possible amount of lignin. However, trees with these characteristics can be a major problem in the field, because of their fragility that makes them susceptible to breaking. The aim of this study was to investigate the clonal and environmental variation of the growth, wood density, and dynamic properties on large pieces of *Eucalyptus* wood by means of resonance technique. Here, we demonstrated that no other non-destructive technique is able to characterize the mechanical properties of wood so simply and rapidly at such low cost. The resonance technique provided a large, accurate data set of the key mechanical traits (such as the Young, the shear modulus and the loss tangent) of the wood even in lumber containing knots, small cracks and also slightly damaged areas. There were significant differences between clones and sites for height and circumference, and density of the trees. Using the dynamic elastic estimates, significant differences were detected between clones for all traits; however, no significant differences between sites were detected for dynamic modulus of elasticity. There were significant effect of interaction clone x site for circumference, height, density and shear modulus. These findings can be useful for screenings, classifications, or preliminary selections in breeding programs of *Eucalyptus*.

Key words: Acoustic, resonance, elastic properties, wood, lumber, hardwood.

VARIAÇÃO CLONAL E AMBIENTAL DE VIGAS DE *Eucalyptus* PARA CRESCIMENTO, DENSIDADE E PROPRIEDADES DINÂMICAS

***RESUMO**: O objetivo principal dos programas de melhoramento genético de Eucalyptus para a indústria de celulose e papel é produzir variedades de árvores com níveis elevados de celulose e com a menor quantidade de lignina possível. No entanto, as árvores com estas características podem ser um grande problema em campo, devido à sua fragilidade que as torna suscetíveis à quebra. Este estudo foi realizado com o objetivo de investigar a variação do crescimento, da densidade da madeira e das propriedades dinâmicas por meio da técnica de ressonância em vigas de Eucalyptus em função dos clones e do ambiente. Os resultados mostram que nenhuma outra técnica não-destrutiva é capaz de caracterizar as propriedades mecânicas da madeira de forma tão simples, rápida e a baixo custo. A técnica de ressonância é capaz de estimar características mecânicas (como o módulo de elasticidade e de cisalhamento e o amortecimento interno) em grandes amostragens de madeira, mesmo com presença de nós, pequenas fissuras e também com áreas ligeiramente danificadas. Houve diferenças significativas entre os clones e os sítios para altura, circunferência e densidade da madeira das árvores. A partir das estimativas dinâmico-elásticas, foram detectadas diferenças significativas entre os clones para todas as características, no entanto, não houve diferenças significativas entre os sítios, para o módulo de elasticidade dinâmico. Houve efeito significativo da interação clone x site para a circunferência, altura, densidade e módulo de cisalhamento. Estes resultados podem ser úteis para a classificação ou a seleção preliminares em programas de melhoramento de Eucalyptus.*

Palavras-chave: Acústica, ressonância, propriedades elásticas, madeira, lenho, folhosas.

1 INTRODUCTION

The main objective of *Eucalyptus* breeding programs for the pulp and paper industry is to produce varieties of trees with high levels of cellulose with the least possible amount of lignin. However, trees with these characteristics can be a major problem in the field, because of their fragility that makes them susceptible to breaking.

[1]PhD Candidate at University of Montpellier 2. CIRAD – PERSYST Department – TA A-40/16 – Production and Processing of Tropical Woods, 73 rue Jean-François Breton – 34398 – Montpellier, France – phein1980@gmail.com

[2]Researcher of CIRAD – PERSYST Department – TA A-40/16 – Production and Processing of Tropical Woods, 73 rue Jean-François Breton – 34398 – Montpellier, France – loic.brancheriau@cirad.fr

[3]Lecturer at Departamento de Ciências Florestais/DCF – Universidade Federal de Lavras/UFLA – Cx. P. 3037 – 37200-000 – Lavras, MG – jtlima@ufla.br

[4]PhD, Forest Engineer, Celulose Nipo-Brasileira S.A – Rodovia BR 381, Km 172 – 35196-000 – Belo Oriente, MG – antonio.rosado@cenibra.com.br

[5]Lecturer at University of Montpellier 2 – Research Director of CNRS – Place E. Bataillon, cc 048 – 34095 – Montpellier, France – jgril@lmgc.univ-montp2.fr

[6]Researcher of CIRAD – BIOS Department – TA A-39 – Genetic diversity and breeding of forest species, 73 rue Jean-François Breton – 34398 – Montpellier, France – gilles.chaix@cirad.fr

Natural vibration analysis is a simple and efficient way of characterizing the mechanical properties of many materials, including wood (BRANCHERIAU; BAILLERES, 2002; BUCUR, 1995). Using various species of wood, sample dimensions and growth conditions, several studies have shown a strong linear correlation between dynamic and static modulus of elasticity (ROSS et al., 1999; WANG et al., 2001; GREEN et al., 2004; BIBLIS et al., 2004).

Dynamic tests based on the resonance frequency have been applied successfully in order to analyze among other elastic properties, the dynamic modulus of elasticity of structural timber (HAINES; LEBAN; HERBE, 1996; BURDZIAK; NKWERA, 2002; OUIS, 1999; JIANG et al., 2010). To our knowledge, few studies were conducted in order to evaluate genetics aspects of the timber on the basis of their dynamic elastic properties. Thus, the aim of this study was to investigate the clonal and environmental variation of the dynamic properties on large pieces of *Eucalyptus* wood by means of resonance technique.

Here, we performed longitudinal and transversal dynamic tests on scantlings of clones of *Eucalyptus grandis* x *urophylla* hybrids from three contrasting clonal tests. The estimates of elastic traits based on resonance technique, in addition to the growth and density information for each tree, were used to assess the clonal and environmental variation of these traits.

2 MATERIAL AND METHODS

2.1 Wood sampling

In this study we evaluated 5 individuals of 10 clones (A, B, C… and J) of 6-years old *Eucalyptus grandis* x *urophylla* hybrids coming from three contrasting clonal tests (1, 2 and 3) established in Brazil (19°17' S, 42°23' W, alt 230-500 m), totalizing 150 trees. The main difference between clonal tests was the inclination of the plantations: the clonal test 1 had a slope of 40°, the clonal test 2 had a slope of 20° and clonal test 3 was plane (0°). The type of climate is Aw (Tropical savanna climate), according to the classification of Köppen (PEEL; FINLAYSON; MCMAHON, 2007), with mean annual rainfall of 1,205 mm. The mean annual temperature is around 25°C and the average annual humidity is 67.3%. The trees were planted in a randomized design and density of plantation was 1,667 trees/ha (3 m x 2 m spacing). Circumference at breast height (C) and commercial height (H) were measured before harvesting. Breast height wood disk was obtained from each tree and transported to the University of Lavras in Lavras, Minas Gerais State, Brazil. The commercial height was considered when the diameter measured 7 cm.

A total of 410 pieces of wood with nominal sizes of 45 mm x 60 mm x 2,100 mm (hereafter referred to as 'scantlings') were taken from 150 central boards. Subsequently, the scantlings were kiln-dried at 14% (nominal) of moisture content under soft condition during two weeks. After the drying process the scantlings presented defects such as small cracks, checks and splits in their ends and, therefore, were trimmed to variable dimensions, depending of the extension of their defects. The clean scantlings had, in average, 1.54 meters of length, varying from 0.645 m to 2.080 m (CV=16.9%) and the averaged width and thickness were, 60 mm and 43 mm, respectively, fluctuating slightly (CV=5.7% for width and CV=2.8% for thickness). Thus, all pieces were free of large fissures, biological affections, defects produced in the saw mill as severe reduction of width or thickness, but they presented knots and small cracks as well.

2.2 Dynamic tests on woods

The scantlings were submitted to transversal and longitudinal vibration tests. In transversal vibration, the first four modes of vibration were measured and used for estimating the dynamic transversal modulus of elasticity (E_T) of wood (also called modulus of Young), which represents its stiffness under bending stress, and the dynamic shear modulus (G). In longitudinal vibrations, the first vibration mode was measured and used for estimating the dynamic longitudinal modulus of elasticity (E_L) of wood, which represents its stiffness under compressive stress, and the loss tangent (tg δ), also called internal damping. The theoretical models of motion and their solutions used to estimate such elastic properties were deeply detailed in Brancheriau and Baillères (2002). These authors also provided a discussion about different theoretical models of motion; theirs approximate solutions and their respective hypotheses in longitudinal and transversal vibrations; and the effects of the elastic support required by BING system. The mass and the dimensions of each scantling were measured at the moment of the dynamic tests providing the weight density (ρ) of the wood samples. The error of measure was 0.1 g and 0.1 mm for mass and dimension, respectively. Figure 1 sums up the procedure of sample preparation and acoustic measurements.

2.3 Procedure of dynamic tests

The scantlings were placed on elastic supports so as to generate free vibrations. An exciting impulse was

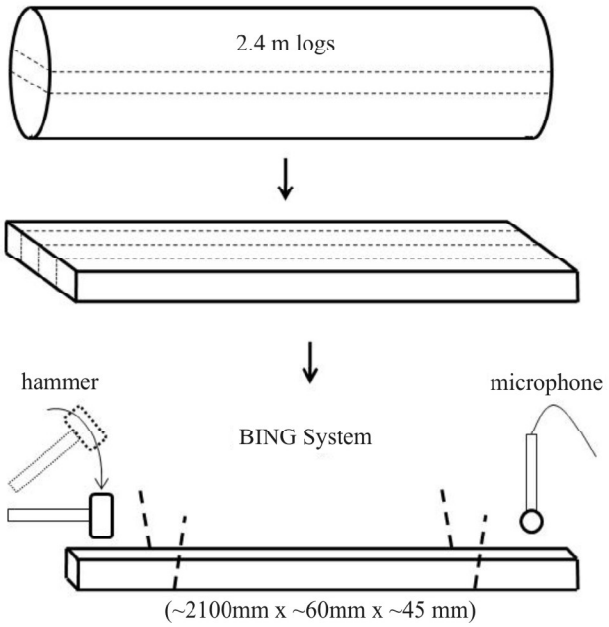

Figure 1 – Procedure of sample preparation and acoustic measurements.

Figura 1 – *Procedimento de preparação de amostras e de medições acústicas.*

produced by lightly striking the scantlings with an instrumented hammer at the opposite side of the output transducer (acoustic microphone). The transverse vibration was induced by an edgewise impact and the longitudinal vibration by an impact along the bound. The input and output signals were transmitted via a low-pass filter to an acquisition card on a computer and recorded as described in Brancheriau and Baillères (2003).

2.4 Parameter of dynamic tests

The analysis of the spectral signal, the selection of the peaks of the natural frequency of vibration of the wood samples and the estimates of the E_T, G, E_T and tg ä were performed using the software BING ® (CIRAD, Montpelier, France, version 9.1.3). The sampling frequencies of the signal were 78,125 Hz and 39,062 Hz for longitudinal and transversal vibration, respectively. The spectral acquisition was carried out by using 32,768 points for each test.

2.5 Statistic analysis

Analyses of variance for all observed values were performed according to the models in Eq. 1 using the general linear model (GLM) procedure of the Statistical Analysis System (SAS INSTITUTE, 1990):

$$Y_{ij} = \mu + C_i + S_j + CS_{ij} + \varepsilon_{ij} \quad (1)$$

where Y_{ij} is the measurement of property ij, ì is the general mean, C_i is the fixed effect of Clone i, S_j is the fixed effect of Site j, CS_{ij} is the random effect of Clone i with Site j, and $å_{ij}$ is the error. The model assumes that the random factors are distributed normally with expectation zero.

3 RESULTS AND DISCUSSION

3.1 Dynamic properties and densities of the scantlings

Table 1 lists the descriptive statistics of the density and the dynamic elastic properties of scantlings of *Eucalyptus grandis* x *urophylla* wood. Based on early studies on dynamic tests of wood (HEARMON, 1948; ILIC, 2001; ILIC, 2003), we expected to find longitudinal elastic properties higher than the transversal ones. However, there was no statistically significant difference between averages of elastic modulus (Table 1). Some key factors affecting the transverse vibration were reported by Murphy (2000). In addition to these factors, according to Burdzik and Nkwera (2002) no method of elasticity measurement leads to the calculation of pure modulus of elasticity in bending, due to the presence of a shear component in the deflection of the specimen. We assume that the transversal vibrations are more sensible at the presence of knots and small cracks in the scantlings than longitudinal vibrations, especially for air-dried scantlings. The loss tangent values of the specimens were calculated from longitudinal test. As the software alerts us about imprecise estimations, we used only 328 values for tg $ä_L$ and 378 for shear modulus.

3.2 Correlations among scantlings properties

The correlations among growth, physical and elastic properties of 395 scantlings are listed in Table 2. Fifteen samples were considered as outliers, because their estimates yielded anomalous values. Circumference and height had a good correlation (0.83). Correlations between longitudinal and transversal dynamic elastic modulus were strong (0.953). It is well know that values of the modulus of elasticity increased with increasing wood density (KOLLMANN; COTÉ, 1968). According to the Table 2, the density of the scantlings showed good correlation with theirs elastic properties: 0.80 for E_L and 0.765 for E_T.

The E_L presented higher correlations with density than the E_T (Table 2). The main reason for this trend is the

Table 1 – Descriptive statistics of the density (ρ, kg m^{-3}) and the dynamic elastic properties of the scantlings of *Eucalyptus grandis* x *urophylla*, including first resonant frequency (*f*, Hz), dynamic elastic modulus (E, MPa), specific modulus (E', MPa m^3 kg^{-1}), loss tangent (tg δ, 10^{-3}) and shear modulus (G, MPa) estimated by longitudinal ($_L$) and transversal ($_T$) vibration tests.

Tabela 1 – *Estatística descritiva da densidade (ρ, kg m^{-3}) e das propriedades dinâmico-elásticas das vigas de* Eucalyptus grandis *x* urophylla*, incluindo a freqüência do primeiro modo de ressonância, (f, Hz), modulo de elasticidade dinâmica (E, MPa), módulo específico (E', MPa m^3 kg^{-1}), atrito interno (tg δ, 10^{-3}) e módulo de cisalhamento (G, MPa) estimados por testes longitudinais ($_L$) e transversais ($_T$).*

	ρ	f_L	E_L	E'_L	tg δ_L	f_T	E_T	E'_T	G_T
Average	547	1,618	12,825	23.43	7.74	98.27	13,278	24.3	693.69
Sd	65.8	346	2,565	2.98	1.74	49.04	2740	3.32	207.6
Min	383	1,027	7432	15.6	4.45	42.9	6,555	13.8	123
Max	776	3,414	21236	32.5	18.7	441.1	23,941	35.5	1,833
CV(%)	12	21.4	20	12.7	22.4	49.9	20.6	13.7	29.9
N	410	410	410	410	328	410	410	410	378

Table 2 – Correlations among growth, physical and dynamic elastic properties of the scantlings of *Eucalyptus grandis* x *urophylla* wood. The probability level for all relationships was <0.0001.

Tabela 2 – *Correlações entre crescimento e propriedades físicas e dinâmicas das vigas de* Eucalyptus grandis x urophylla*. O nível de probabilidade das correlações foi menor que 0,0001.*

	C	H	ρ	E_L	E'_L	tg δ	E_T	E'_T
H	0.83	1						
ρ	-0.23	-0.14	1					
E_L	-0.03	-0.01	0.80	1				
E'_L	0.14	0.09	0.02	0.82	1			
tg δ	-0.07	-0.08	0.06	-0.18	-0.34	1		
E_T	-0.06	-0.01	0.76	0.95	0.78	-0.20	1	
E'_T	0.096	0.05	-0.13	0.14	0.57	-0.14	0.82	1
G	-0.09	-0.08	0.35	0.28	0.14	0.03	0.18	0.10

lower uncertainty of measurement for longitudinal test. The higher correlations with density for E_L are in accordance to the findings of Ilic (2001), who tested small samples of *Eucalyptus delegatensis* R. Baker and found good correlations between air-dried density and longitudinal (0.83) and transversal (0.81) dynamic elastic modulus.

3.3 Genetic studies on wood quality

Analysis of variance (GLM) was performed to study clonal and environmental variation of a range of wood traits. Results of the analyses of variance are presented in Table 3. Significant differences between clones were detected for all traits. No significant differences between sites were detected for dynamic modulus of elasticity. There were significant effects of interaction clone x site for circumference, height, density and shear modulus.

Figure 2 A presents the circumference at breast height (C) of the clones by the clonal tests 1, 2 and 3. The circumference of all clones increased from sites 1 to 3, except for the clone F, which had the lowest circumference in the site 3. The environmental negative effect on growth was stronger for clone C in the site 2, which produced the trees with small diameters (>60 cm), but the highest circumference for site 1 and 3.

Figure 2 B shows the mean wood density of clones by clonal test. The trees from site 1 produced the denser woods (573 kg m^{-3}) while the clones from site 3 had the lowest wood density (518 kg m^{-3}). Clearly, the trees that grow faster produce wood with lowest densities. The clones from test 1 had higher densities, except for clones C, D and

Table 3 – Analyses of variance (GLM) for growth, wood density and dynamic elastic properties of the scantlings of *Eucalyptus grandis* x *urophylla*.

Table 3 – *Análise de variância (GLM) para o crescimento, densidade da madeira e propriedades dinâmico-elásticas das vigas de* Eucalyptus grandis x urophylla.

	C (0.68)	H (0.51)	ρ (0.40)	E_L (0.22)	tg δ (0.18)	E_T (0.21)	G (0.16)
site	**	**	**	ns	**	ns	*
clone	**	**	**	**	**	**	**
interaction	**	**	**	ns	ns	ns	*

(* significative at 0.05 and ** significative at 0.001)

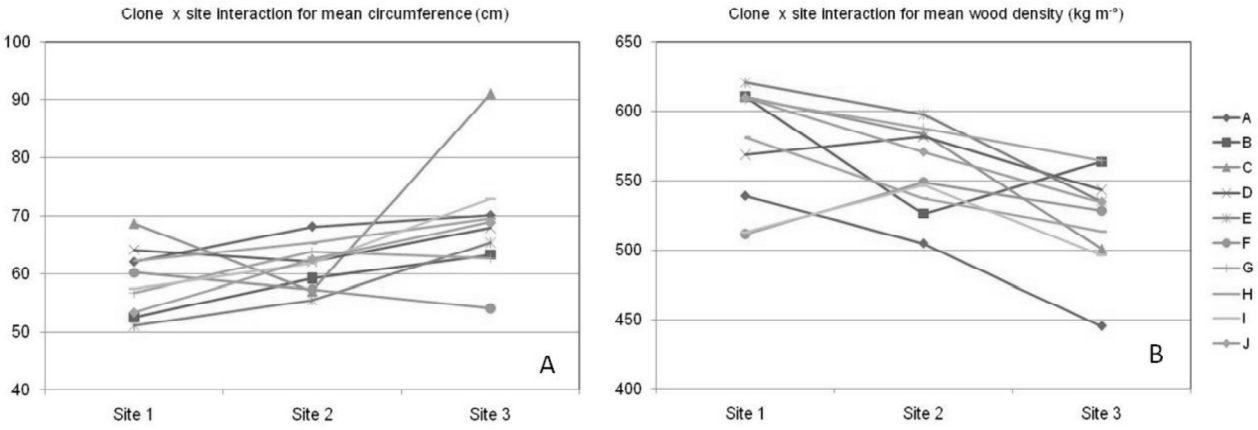

Figure 2 – Clone x site interaction for mean circumference (A) and for wood density (B).

Figura 2 – *Interação clone x sítio para circunferência média (A) e para densidade (B).*

F. Figure 3 A shows the dynamic modulus of elasticity in longitudinal test of the clones by clonal test (sites).

Table 3 shows that there was no environmental effect, but there were significant differences between clones for modulus of elasticity. For E_L and E_T (not shown) the clones presented stability between clonal tests, excepting the clones A, B, E and F which presented high variations. The differences between clones and clonal tests for dynamic modulus of shear are showed by Figure 3 B. The shear modulus of the clones was high (700 MPa) in the site 1, except for the clones B, D and I. Tukey (HSD) multiple range tests for growth, wood density and dynamic elastic properties of the scantlings by clone and by site are presented in Table 4.

3.4 Advantages for breeding selection

The early studies on genetics of *Eucalyptus* concentrated on tree growth, survival, stem straightness and branch quality. As breeding programs progressed the range of traits assessed increased to include fitness, which relate to the ability of trees to survive environmental threats, and to quality, of which those pertaining to wood quality are amongst the most important (GREAVES, BORRALHO; RAYMOND, 1997). In addition, the traditional methods of assessment for wood quality traits are expensive and restrict the numbers of samples that can be processed (RAYMOND, 2002). Here, we demonstrated that no other non-destructive technique is able to characterize the mechanical properties of wood so simply and rapidly at such low cost. The resonance technique enabled us to rapidly estimate key mechanical properties (such as the Young, the shear modulus and the loss tangent) of the wood even in lumber containing knots, small cracks and also slightly damaged areas.

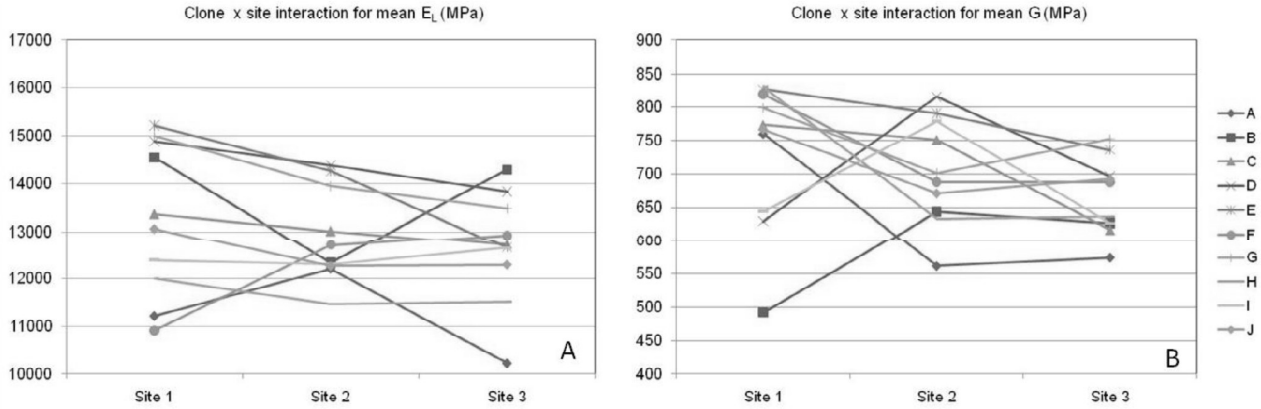

Figure 3 – Clone x site interaction for dynamic modulus of elasticity in longitudinal test (A) and for dynamic modulus of shear in transversal test (B).

Figura 3 – *Interação clone x sítio para módulo de elasticidade dinâmico médio (A) e para módulo de cisalhamento (B).*

Table 4 – Tukey (HSD) multiple range tests for growth, density and dynamic elastic properties of the *Eucalyptus* scantlings.

Tabela 4 – *Teste de média de (Tukey, HSD) para crescimento, densidade e propriedades dinâmico-elásticas de vigas de* Eucalyptus.

Clone	C (cm)	H (m)	ρ (kg m^{-3})	E_L (MPa)	tg δ (10^{-3})	E_T (MPa)	G (MPa)
A	66.8 B	23.6 CB	496.6 FE	11254 D	7.25 ABC	11801 D	625.6 B
B	59.2 D	21.7 ED	560.2 ABCD	13636 ABC	8.16 ABC	14906 A	599.3 B
C	77.8 A	26.0 A	546.9 BCDE	12934 ABCD	7.82 ABC	13301 BDC	680.0 AB
D	64.7 BC	23.3 CBD	564.7 ABCD	14272 A	7.96 ABC	14639 AB	728.5 AB
E	58.3 D	21.1 E	578.4 AB	13877 AB	7.07 BC	14269 BC	778.1 A
F	57.7 D	21.8 ED	528.8 DEF	11959 CD	8.37 AB	12421 C	742.8 AB
G	61.5 CD	22.2 CDE	586.5 A	14131 AB	7.88 ABC	14515 AB	741.5 AB
H	66.1 BC	22.8 CBD	540.2 CDE	11638 D	8.55 A	12114 D	689.6 AB
I	64.5 BC	24.1 B	518.3 FE	12451 BCD	6.95 C	12593 C	678.2 AB
J	62.3 BCD	22.9 CBD	568.5 ABC	12490 BCD	7.58 ABC	12833 BC	705.2 AB
Site	C (cm)	H (m)	ρ (kg m^{-3})	E_L (MPa)	tg δ (10^{-3})	E_T (MPa)	G (MPa)
1	59.8 B	21.2 B	573.4 A	13044 A	8.38 A	13355 A	742.2 A
2	61.6 B	23.7 A	558.5 A	12930 A	7.56 B	13528 A	700.1 AB
3	72.0 A	24.3 A	518.0 B	12610 A	7.45 B	13042 A	653.3 B

4 CONCLUSION

There were significant differences between clones and sites for height and circumference, and for density of the trees. Using the dynamic elastic estimates, significant differences were detected between clones for all traits. No significant differences between sites were detected for dynamic modulus of elasticity. There were significant effects of interaction clone x site for circumference, height, density and shear modulus. In short, the BING system rapidly provided a large accurate data set of mechanical wood properties as required for high-throughput phenotyping of genetic approaches. These results can be useful for initial classifications, screenings or preliminary selections in breeding programs of *Eucalyptus*. As reported by Burdzik and Nkwera (2002), this method proved to be

fast, highly repeatable and does not require heavy equipment, making it the ideal method for on-site determining of MOE at the sawmill.

5 ACKNOWLEDGEMENT

The authors express their special thanks to the CENIBRA for providing vegetal material; to the Department of Wood Science and Technology of the Universidade Federal de Lavras (UFLA, Brazil) for supporting the experimental work. We thanks particularly to José Francisco de Sousa, Carlos Henrique da Silva, Heber Alvarenga, and Hernani Alves for their technical support. This project was funded by CENIBRA (Celulose Nipo-Brasileira), CNPq (Conselho Nacional de Desenvolvimento Científico e Tecnológico, Brazil) and CIRAD (UR40). P.R.G. Hein was supported by CNPq (process no. 200970/2008-9).

6 BIBLIOGRAPHICAL REFERENCES

BIBLIS, E. J.; MELDAHL, R.; PITT, D. Predicting flexural properties of dimension lumber from 40-year-old loblolly pine plantation stands. **Forest Products Journal**, Madison, v. 54, p. 109-113, 2004.

BRANCHERIAU, L.; BAILLÈRES, H. Natural vibration analysis of clear wooden beams: a theoretical review. **Wood Science and Technology**, New York, v. 36, n. 4, p. 347-365, 2002.

BRANCHERIAU, L.; BAILLÈRES, H. Use of the partial least squares method with acoustic vibration spectra as a new grading technique for structural timber. **Holzforschung,** Berlin, v. 57, n. 6, p. 644-652, June 2003.

BUCUR, V. **Acoustics of wood**. Boca Raton: CRC, 1995. 284 p.

BURDZIK, W. M. G.; NKWERA, P. D. Transverse vibration tests for prediction of stiffness and strength properties of full size *Eucalyptus grandis*. **Forest Products Journal,** Madison, v. 52, n. 6, p. 63-67, June 2002.

GREAVES, B. L.; BORRALHO, N. M. G.; RAYMOND, C. A. Breeding objective for plantation eucalypts grown for production of kraft pulp. **Forest Science**, Lawrence, v. 43, n. 4, p.465-472, Nov. 1997.

GREEN, D. W. et al. Improved grading system for structural logs for log homes. **Forest Products Journal,** Madison, v. 54, n. 9, p. 59-62, Sept. 2004.

HAINES, D. W.; LEBAN, J. M.; HERBE, C. Determination of Young's modulus for spruce, fir and isotropic materials by the resonance flexure method with comparisons to static flexure and other dynamic methods. **Wood Science and Technology,** New York, v. 30, n. 4, p. 253-263, Aug. 1996.

HEARMON, R. F. S. **An introduction to applied anisotropic elasticity.** Oxford: Oxford University, 1961. 136 p.

ILIC, J. Dynamic MOE of 55 species using small wood beams. **Holz als Roh und Werkstoff,** Berlin, v. 61, n. 3, p. 167-172, Mar. 2003.

ILIC, J. Relationship among the dynamic and static elastic properties of air-dry *Eucalyptus delegatensis* R. Baker. **Holz als Roh und Werkstoff**, Berlin, v. 59, n. 3, p. 169-175, June 2001.

JIANG, J. et al. Predicting the flexural properties of Chinese fir (*Cunninghamia lanceolata*) plantation dimension lumber from growth ring width. **Journal of Wood Science,** Madison**,** v. 56, n. 1, p. 15-18, Feb. 2010.

KOLLMANN, F. R.; COTÉ, W. A. **Principles of wood science and technology**. Berlin: Springer/Verlag, 1968. 592 p.

MURPHY, J. F. **Commentary on factors affecting transverse vibration using an idealized theoretical equation**. Madison: U.S. Department of Agriculture, 2000. (Forest Products Laboratory, 276).

OUIS, D. Vibrational and acoustical experiments on logs of spruce. **Wood Science and Technology,** New York, v. 33, n. 2, p. 151-184, 1999.

PEEL, M. C.; FINLAYSON, B. L.; MCMAHON, T. A. World map of the Köppen-Geiger climate classification updated. **Hydrology and Earth System Sciences,** Katlenburg-Lindau, v. 11, n. 5, p. 1633-1644, 2007.

RAYMOND, C. A. Genetics of *Eucalyptus* wood properties. **Annals of Forest Science**, Les Ulis, v. 59, n. 8, p. 525-531, Dec. 2002.

ROSS, R. J. et al. **Transverse vibration nondestructive testing using a personal computer.** Madison: U. S. Department of Agriculture, 1991. (Forest Products Laboratory, 502).

SAS INSTITUTE. **SAS/STAT:** user's guide, version 6. 4. ed. Cary, 1990. v. 2.

WANG, X. et al. **Several nondestructive evaluation techniques for assessing stiffness and MOE of small-diameter logs**. Madison: U. S. Department of Agriculture, 2001. (General Technical Report FPL-RP-600).